10th AIVC Conference

Progress and trends in air infiltration and ventilation research

(held at Hotel Dipoli,Espoo, Finland
25-28 September 1989)

Proceedings

Volume 1

CONTENTS (i)

Volume 1

International Energy Agency

The International Energy Agency (IEA) was established in 1974 within the framework of the Organisation for Economic Co-operation and Development (OECD) to implement an International Energy Programme. A basic aim of the IEA is to foster co-operation among the twenty-one IEA Participating Countries to increase energy security through energy conservation, development of alternative energy sources and energy research development and demonstration (RD&D). This is achieved in part through a programme of collaborative RD&D consisting of forty-two Implementing Agreements, containing a total of over eighty separate energy RD&D projects. This publication forms one element of this programme.

Energy Conservation in Buildings and Community Systems

The IEA sponsors research and development in a number of areas related to energy. In one of these areas, energy conservation in buildings, the IEA is sponsoring various exercises to predict more accurately the energy use of buildings, including comparison of existing computer programs, building monitoring, comparison of calculation methods, as well as air quality and studies of occupancy. Seventeen countries have elected to participate in this area and have designated contracting parties to the Implementing Agreement covering collaborative research in this area. The designation by governments of a number of private organisations, as well as universities and government laboratories, as contracting parties, has provided a broader range of expertise to tackle the projects in the different technology areas than would have been the case if participation was restricted to governments. The importance of associating industry with government sponsored energy research and development is recognized in the IEA, and every effort is made to encourage this trend.

The Executive Committee

Overall control of the programme is maintained by an Executive Committee, which not only monitors existing projects but identifies new areas where collaborative effort may be beneficial. The Executive Committee ensures that all projects fit into a pre-determined strategy, without unnecessary overlap or duplication but with effective liaison and communication. The Executive Committee has initiated the following projects to date (completed projects are identified by *):

I Load Energy Determination of Buildings * II Ekistics and Advanced Community Energy Systems * III Energy Conservation in Residential Buildings *
IV Glasgow Commercial Building Monitoring * V Air Infiltration and Ventilation Centre
VI Energy Systems and Design of Communities * VII Local Government Energy Planning * VIII Inhabitant Behaviour with Regard to Ventilation *
IX Minimum Ventilation Rates * X Building HVAC Systems Simulation
XI Energy Auditing * XII Windows and Fenestration * XIII Energy Management in Hospitals * XIV Condensation XV Energy Efficiency in Schools
XVI BEMS - 1: Energy Management Procedures
XVII BEMS - 2: Evaluation and Emulation Techniques
XVIII Demand Controlled Ventilating Systems XIX Low Slope Roof Systems
XX Air Flow Patterns within Buildings
XXI Energy Efficient Communities XXII Thermal Modelling

Annex V Air Infiltration and Ventilation Centre

The IEA Executive Committee (Building and Community Systems) has highlighted areas where the level of knowledge is unsatisfactory and there was unanimous agreement that infiltration was the area about which least was known. An infiltration group was formed drawing experts from most progressive countries, their long term aim to encourage joint international research and increase the world pool of knowledge on infiltration and ventilation. Much valuable but sporadic and uncoordinated research was already taking place and after some initial groundwork the experts group recommended to their executive the formation of an Air Infiltration and Ventilation Centre. This recommendation was accepted and proposals for its establishment were invited internationally.

The aims of the Centre are the standardisation of techniques, the validation of models, the catalogue and transfer of information, and the encouragement of research. It is intended to be a review body for current world research, to ensure full dissemination of this research and based on a knowledge of work already done to give direction and firm basis for future research in the Participating Countries.

The Participants in this task are Belgium, Canada, Denmark, Federal Republic of Germany, Finland, Italy, Netherlands, New Zealand, Norway, Sweden, Switzerland, United Kingdom and the United States of America.

PROGRESS AND TRENDS IN AIR INFILTRATION AND VENTILATION RESEARCH

10th AIVC Conference, Dipoli, Finland
25-28 September, 1989

KEYNOTE SPEECH

KARI RAHKAMO

Chairman of the City Council of Helsinki
and
Chairman of the Finnish Association of Heating Piping and Air-conditioning Societies.

AIVC 10th Annual Conference

Keynote address
Mr Kari Rahkamo
Chairman of the City Council of Helsinki
and
Chairman of the Finnish Association of Heating Piping
and Air-conditioning Societies

Ladies and Gentlemen, Mrs Chairman,
It is with pleasure that I have accepted the offer to open today the first working session of the 10th Conference of the Air Infiltration and Ventilation Centre of the International Energy Agency. As the chairman of the Finnish Association of Heating, Piping and Air-conditioning Societies it is also an honour to have the opportunity to do it.

The Nordic location of our country places high demands on building techniques, where ventilation, air infiltration and energy economy play a significant part. We are, therefore, very pleased to have in Finland a conference, which deals with developments in the area of ventilation during the past ten years and also focuses the future trends. I find this conference a most necessary and useful forum for researchers from different countries to exchange information on the research work they have done and also to get fresh ideas for further developments.

The funding of energy research in our country has nearly preserved its volume during the last few years, so the situation in that respect is good. National research has been programmed into various research programmes, which enable long-term research activities.

One of these national programmes, HVAC-2000, was started in the year 1988. The objectives of this programme is to find ways of introducing technical solutions at the systems level which enchance the effectiveness of energy use and improve indoor climate control features in future buildings. Besides the future buildings also systems and methods for retrofitting and renovation operations are being considered.

International cooperation is closely articulated with national interests and it is taken care of within each particular research programme. The significance of international cooperation for a national research programme is highly emphasized - it is even considered as an advantage when applying for the funding. International Energy Agency makes an excellent forum for this cooperation. Finland has participated in the activities of IEA since the year 1984 and is also actively taking part in several other IEA annexes besides AIVC. Participation in the international research programmes has proved to be very fruitful for our national research and development work.

We hope that on going home everyone of you could find these four days worthwhile; that you have created new valuable contacts and got a lot of innovative ideas to bring along home. We have made efforts to encourage new contacts and discussions between participants by placing poster demonstrations and discussions in the programme. The programme also includes a review on the present situation of ventilation research in each of the fourteen member countries of AIVC.

The tight schedule of the conference sessions hopefully allows you some time to see around the district of our capital city and to enjoy the colourful Finnish autumn nature - hopefully also the weather will favour us!

Ladies and Gentlemen, Mrs Chairman, I wish the conference every success!

PROGRESS AND TRENDS IN AIR INFILTRATION AND VENTILATION RESEARCH

10th AIVC Conference, Dipoli, Finland
25-28 September, 1989

Paper 1

ANNEX 14 - CONDENSATION AND ENERGY

H. HENS

KULeuven,
Laboratory of Building Physics
Arenbergkasteel
B-3030 Leuven
BELGIUM

1. INTRODUCTION: MOTIVATIONS FOR THE ANNEX

Annex 14 -Condensation and Energy- started in April 1987, with a take of meeting in Utrecht, The Netherlands. The annex itself was born after a moisture-workshop in September 1985 at the Laboratory of Building Physics, KULeuven, Belgium.

Motivations from the beginning were a widespread feeling that badly balanced energy conservation actions in the seventies and early eighties had increased the number of moderate to severe mould complaints in dwellings, with all possible nuisance, health and financial consequences, the fear that this could enhance each energy conservation policy, and the conviction that the mould reality was socially inacceptable, especially because of the problem being most pronounced in the low income housing sector.

Nevertheless, a convincing argument for the first motivation was and is difficult to find. A Belgian enquiry of 1986 in 5000 social dwellings showed a mould problems level of some 20% [1]. The Netherlands reported ± a same percentage in the subsidised building market [2]. The U.K. spoke of ± 25 to 30 % of dwellings affected in the low income, rented housing [3]. Only this year, a more convincing argument was advanced by the U.K., where a new enquiry showed a net increase in mould and a clear growth in severe mould problems (Oral information at the Leuven meeting, may 1989). But still here, the question remains if that isn't a result of 10 years conservative government, with a lower interest in overall social policy, rather then of a conscious but badly balanced energy conservation policy.

The paper starts with focusing on the so called first order surface condensation theory. Then a short shift to the energetical links follows. After that, the organisation and progress of the work is explained, and we end with an overview of the results.

2. A FIRST ORDER THEORETICAL APPROACH [4],[5]

Surface condensation starts when the relative humidity (RH) on a surface reaches 100%, t.m.,when the vapour pressure p in the air against the surface equals or becomes higher then the saturation pressure p' on it:

$$p \geq p' \qquad (1)$$

Introducing the hypothesis of ideal mixing of the air in each zone (= a simplification of reality), the vapour pressure against the surface doesn't differ from the overall value in the zone and (1) can be reformulated as:

$$pi \geq p' \qquad (2),$$

the vapour pressure in the zone (pi) equal to or higher then the saturation pressure on the surface, or:

$$Td \geq Ts \qquad (3),$$

the zonal inside dewpoint (Td) equal to or bigger then the surface temperature (Ts).

The condition for **mould growth** is much more complicated. As a first order rule, we accept mould becomes possible when the relative humidity (= the water activity) on a surface remains higher then a threshold value a. Accepting ideal mixing of the zonal air, this condition simplifies to:

$$pi \geq a*p'/100 \qquad (4)$$

The saturation pressure on a surface is exponentially linked to the **surface temperature** Ts, given by:

$$Ts = Te + \tau * (Ti-Te) \qquad (5)$$

with τ the temperature ratio of the surface, Ti the inside reference temperature and Te the sol-air outside temperature.

For a flat wall in steady state thermal conditions (= mean thermal situation), τ equals:

$$\tau = 1 - U/hi \qquad (6)$$

with U the thermal transmittance of the wall and hi the thermal film coefficient against the surface.

In non steady state, the temperature ratio becomes a time function, dependant of the course of the in- and outside temperature, of the film coefficient and of the thermal inertia of the wall.

For two- and three-dimensional configurations (= thermal bridges) the temperature ratio can only be calculated, using a suitable software package.

The mean **inside vapour pressure** pi is related to the outside vapour pressure pe, the moisture production φp, and the ventilation rate ß, according to the formula:

$$pi = pe + [R*(Ti+273.16)]* \varphi p / (ß*V) \qquad (7)$$

with R the gas constant of vapour (462 J/K) and V the zonal volume.
This simple relation only holds for a 1-zonal situation, if no surface condensation is taking place. It also supposes ideal

mixing of the zonal air.

The simple formulas (2) to (7), combined with statistical data on the outside climate and the relation inside temperature-outside temperature, enable to study, for a given case and outside climate, the relations 'outside temperature-temperature ratio-maximum inside R.H.- minimum ventilation rate'for different levels of the inside moisture production, so, that mould problems or surface condensation should be prevented.

Figure 1 shows the results for a sleeping room (V= 35 m3, φp= .96 kg/d), figure 2 for a day-zone (V= 100 m3, φp= 3.6 kg/d) (Calculations done with as mould condition: a= 0.85).
Both figures indicate that the ventilation rate needed to prevent mould germination and growth is significantly higher in mean-season as it is during cold winter periods. They also show that the overall relation is not a linear one.

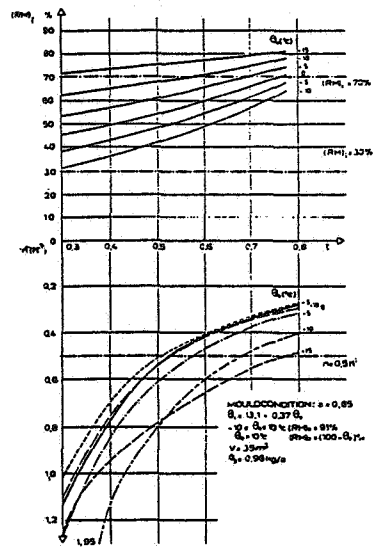

fig. 1: SLEEPING ROOM
RELATION $(RH)_i - \tau - \theta_e - n$

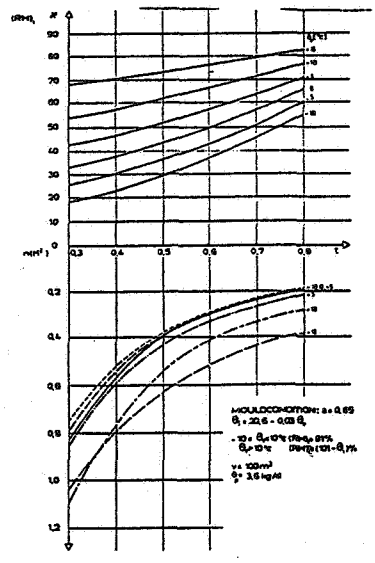

fig. 2: LIVING ROOM + KITCHEN
RELATION $(RH)_i - \tau - \theta_e - n$

In general, the chance on mould/ surface condensation heightens, the lower the surface temperature Ts and the higher the inside vapour pressure pi

The first order theory now im- and explicitly learns that both conditions depends of:

- the outside climate

the temperature: the lower Te, the more probable mould and surface condensation...
the vapour pressure: the lower pe, the more probable ...
A low temperature and a high vapour pressure are mutually conflicting: they cannot occur together

the wind: the lower the wind velocity, the lower for natural ventilation the ventilation rate ß.
The lower ß, the more probable...

- the building fabric

the volume: the smaller, the more probable ...
the thermal quality: the lower the temperature ratio, the more probable ... A low temperature ratio is directly linked to high U-values and low film coefficients hi, t.m. a poor heat flow to the surface by convection and radiation
the airtightness: the lower ß, the more probable .. Specifically the basic ventilation rate is a direct result of the airtightness of the fabric
the inside environmental temperature: is a weighted combination of the air and the radiative temperature. The last is to a significant amount influenced by the overall thermal quality of the fabric and the 'outside wall surface-total wall surface'-ratio,in the sense of:the worsen the thermal quality and the higher that ratio,the lower the radiative temperature and the more probable..
Also the air temperature is coupled to the fabric: if badly insulated, maintaining a high enough air temperature may turn out being too energy consuming and through that too expensive. The lower the air temperature, the more probable...
the vapour production: the higher φp, the more probable .. A high vapour production may be a consequence of other moisture problems
the internal finishing: some materials, paints, wall papers are more sensitive to mould then others. Through that, the threshold relative humidity a can be lowered by the choice of the finishing...

- the inhabitants behaviour

the inside environmental temperature: depends on heating habits. The less heating, the lower Ti and the more probable..
the ventilation rate: the lower ß, the more probable..Inhabitants have a substantial effect on excess ventilation
the moisture production: the higher φp, the more probable..Living in and using a dwelling inevitably means moisture production. Using it in a non adapted way, may result in too much vapour ...

These rather complicated and interrelated influencing parameters are summarised in figure 3. This figure doesn't give any qualitative information on how important the respective parameters are.

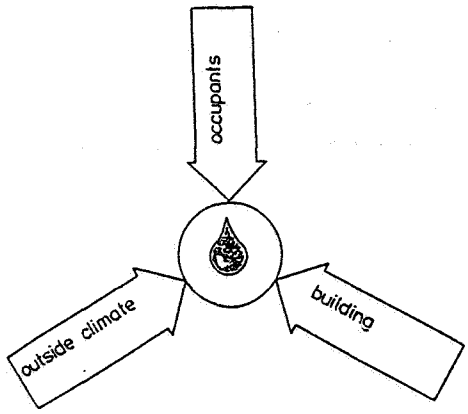

Fig.3: influencing factors

3. LINKS WITH ENERGY DEMAND AND USE FOR HEATING

From the review of parameters, it may be clear that mould and surface condensation are most likely in non-insulated dwellings, t.m. in houses with a high basic energy demand.
More, avoiding mould in these energetical ruins, asks for a substantial ventilation rate, especially when, because of intensive use, the moisture production is high. This counts for an important extra increase in energy demand.
Also, the possible heating economy by lowering the mean inside temperature is partly counteracted by a compelling necessity for more ventilation, the lower this inside temperature.

Insulated houses give complaints as far as problematic thermal bridges are left. These have a net energetical impact, heightening in negative cases the conductive heat losses through the envelope as much as 30 %.
At the same time, to avoid mould on these spots with low temperature ratio, a substantial ventilation is requested, pushing on its turn the energy demand for heating to still higher levels.

To illustrate the importance of these effects, the results of some energy demand calculations on a small house are summarised in table 1 and figure 4:

Assumptions:

house= 1 thermal zone
intensive use (φp = 12 kg/day),
inside temperature= 16.9+ 0.17*Te (a)
13.5+ 0.17*Te (b)
energetical year for Belgium.

lowest temperature ratio:

non-insulated	(Um=1.7 W/(m2K)	: 0.3 (1)
insulated, thermal bridges	(Um=0.56 W/(m2K)	: 0.5 (2)

insulated, no thermal bridges (Um=0.44 W/(m2K) : 0.7 (3)

(1) behind cupboards against outside walls
(2) lintels, thresholds ...
(3) design value

Results:

Table 1

	Um W/(m2K)	τ -	En avoiding mould kWh/y	En n=0.5h-1 kWh/y
Ti=(a)	1.7	0.3	45670	39360
(b)	1.7	0.3	36620	25040
Ti=(a)	0.56	0.5	15430	14810
Ti=(a)	0.44	0.7	10620	11990

or, no insulation or, an insulation with thermal bridging, are triple punished: higher to high conductive losses, more ventilation losses, less economy when maintaining lower inside temperatures.

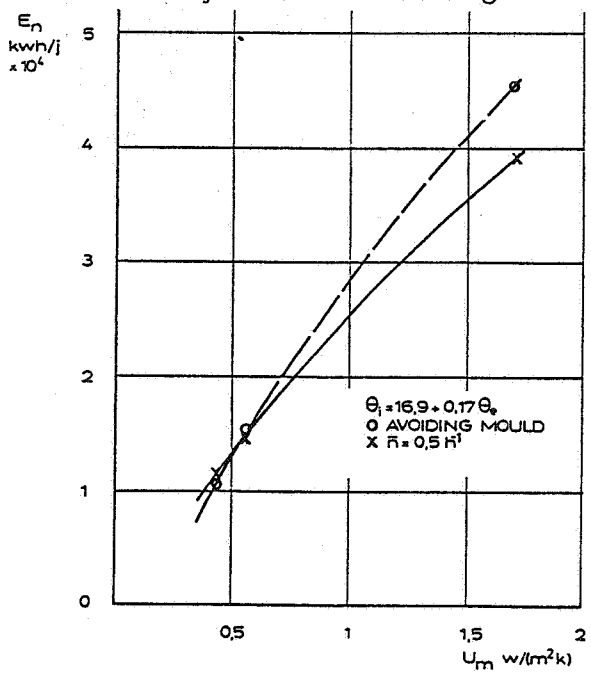

fig. 4: ENERGY DEMAND FOR HEATING
. $\bar{n} = 0,5\ h^{-1}$
. $\bar{n}$ = NEEDED TO AVOID MOULD (a = 0,85)

There is only one disturbing element in this straight on 'energy demand-mould'-relation: the role of the inside surface coefficient. The lower hi,the lower the temperature ratio of that surface but the better the insulation value, t.m. the lower the conductive losses!
This is illustrated in fig 4 for a badly insulated cavity wall.

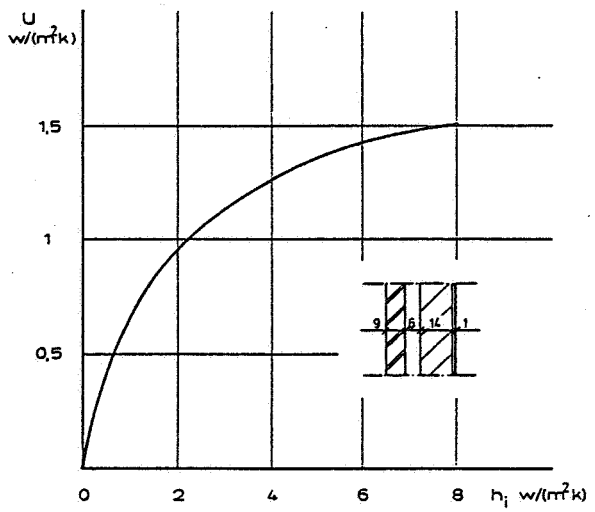

fig. 5: U-VALUE OF A NON-INCULATED CAVITY WALL AS FUNCTION OF THE INSIDE FILM COEFFICIENT h_i

4. THE WORK IN THE ANNEX

4.1 Principles and scope

From the start, the principles backing the international cooperative effort, called Annex 14, were:

not - to set up basic work in the field of the biology of mould;
- to develop new overall calculation models on the heat-air-moisture transfer in buildings, introducing as boundary conditions the avoidance of mould;
- to streamline and push all national programs on mould, surface condensation and moisture transfer in a well defined direction, with the danger of killing much creative and fundamental research,

but - to gather as much as possible existing information: mould, material properties, case studies a.o.
- to apply the knowledge on heat- air- and moisture transport on the complex phenomenon of mould and surface condensation, with the specific aim of broadening the understandings of the static and dynamic physical context. This may include limited modelling;
- to develop a common experience by exchanging information, running case studies and performing common exercises;
- to inspire national research.

Scope is to produce a source book on mould, surface condensation and energy, including data on mould and materials, the physics involved, case studies and performance formulations for practice.

4.2 Organisation

The work was structured in 3 major parts:

- gathering data;
- studying models and confronting them with case studies;
- search for solutions

These 3 parts were split in 9 steps, each of them being the responsibility of one, two or all participating countries:

Table 2

STEPS		NL	FRG	UK	I	B
DATA	1. material properties					
	2. mould					
MODELS	3. thermal aspects					
	4. hygric aspects					
	5. combined heat-air-moisture					
	6. boundary conditions					
CASE STUDIES	7. monitored case studies					
	8. common exercises					
SOLUTIONS	9. practice					
	practice source book					

Being in charge of a step includ

- taking the initiative of gathering information;
- drafting that part of the final report.

The cooperation was materialised in working meetings.

The first 3-days meetings had a more scientific aim, promoting an exchange of past research and case studies, focusing on a specific key-note address, creating time to present fresh papers and presenting progress reports on the case studies.
The last ones were more concerned with the joint project, discussing the results of the common exercises, reading the drafts of the specific chapters of the final source book, and looking to practice.
Place, date and major topic of the meetings:

PAST

Utrecht, NL,	6-7 apr 87	take of state of the art in the 5 countries

		elaboration of the working scheme of table 2
Stuttgart, FRG,	12-14 oct 87	case studies
Glasgow, UK,	11-13 apr 88	mould analyses
Torino, I,	17-19 oct 88	modelling 1 first common exercise
Leuven, B,	8-10 may 89	modelling 2 second common exercise first drafts of the source book
FUTURE		
Den Haag, NL,	23-25 oct 89	case studies: final reports second drafts of the source book practice
?		
Rotterdam, NL,	3-6 sept 90	international CIB-symposium Energy, moisture, climate Presentation of the source book

5. PRELIMINARY RESULTS

5.1 Material properties (B)

Array of properties

All physical properties of materials, of importance in mould and surface condensation analysis, have been putted in an array code, referring to the fundamental difference between capacitive properties, transfer properties, combined properties with a specific physical meaning and properties, being a consequence of..:table 3
This array is far more complete than the lists, found in national codes or standards.
For each property, also the influencing material linked and environmental parameters have been defined and brought together.

Table 3

	1.CAPACITIVE	2.TRANSFER	3.COMBINED	4.CONSEQUENCE
T. THERMAL				
H. HYGRIC				
A. AIR				

f.e. T.2. thermal conductivity
H.1. hygroscopic curve, capillar moisture content...
A.2. air permeance...

data

Most numerical values were measured at the labs, involved in the annex or are taken from literature.

catalogue

The catalogue proposes calculation values. These coincide, if enough data available, with the 5 or 95% limit of the measured values. Otherwise, the few results are averaged or standard list information is used. If known, parametric relations between the property and the most important influencing parameters are also given.

5.2 Mould (UK, NL, B, FRG)

- the number of mould species is enormous and their biology, with the germination, linear growth and sporulation phases, rather complicated. Nevertheless, as far as building mould problems are concerned, it seems reasonable to focus on aspergillus, penicillium and cladosporium and their germination conditions;

- as part of these conditions, temperature and free water activity (= RH) are of mayor importance. They are interrelated in that sense that a lower or too high temperature asks for a higher RH, with the optimal combination (lowest RH) around 25 degC;

- most experimental data on germination and growth rates are gained from cultivation on special substrates. The resulting 'temp.-RH'-couples seem too pessimistic for use as design values for mould germination on finishing layers present in buildings;

- a realistic 'temp-RH'- formula could be:

$$RH = 5.3E\text{-}2 * T^2 - 2.7 * T + 113 \quad (\%)$$

or

$$a = 5.3E\text{-}4 * T^2 - 2.7E\text{-}2 * T + 1.13$$

Against a wall, RH is the local relative humidity value and T the wall's surface temperature.

This result strengthens the fact that mould germination is a moderate cold, wet weather problem (autumn, springtime)

5.3 Modelling

THERMAL ASPECTS (NL, FRG, I, B)

- with the software available on the market, calculating the temperature field in and heat flow densities in and through thermal bridges is no longer a problem. Nevertheless, the result depends strongly on subtile section specification differences and on the thermal conductivity values used, but, especially and by far the most on the inside surface film coefficient;

- the choice of a representative couple 'surface film coefficient -reference temperature' remains a difficult question.
  In fact, surface heat transfer is the result of joined convection and radiation. Convection is linked to the local air temperature, radiation to the so called radiative temperature of the surroundings, as seen by the surface involved. Both differ from point to point, and, in non steady state, from moment to moment.

  In energy calculations, so called overall mean standard values

  f.e. vertical surfaces : hi= 8 W/(m2K)
  horizontal surfaces, : hi= 6 W/(m2K)

  have been introduced, linked to the air or the comfort temperature. There, that seems a reasonable way of handling the problem.

  To predict mould and surface condensation, they are useless.
  In fact, here, we have to know the correct local values.

  The problem can be solved:
  or by calculating for each case as precise as possible the surface heat transfer using the theory of convection and radiation Calculations in that sense have been performed by Belgium;
  or by accepting a so called reference temperature and searching design values of hi for critical situations (by calculation or measurement).

Until now,different methodologies for the last possibility have been proposed. All show, independent of the choice of the reference temperature, surface film coefficients, much lower then 8 W/(m2K), to a great amount influenced by the number of outside walls (the more, the lower hi) and decreasing with a better insulation.
The Netherlands go as low as 2 W/(m2K) for outside wall surfaces, against which cupboards could be postioned.

At least one guess remains: the value of the convective surface film coefficient.

HYGRIC ASPECTS (NL, FRG, B)

The most important achievement here is a better understanding of the hygroscopic influences. This has been realised by measurements and calculations:

- hygroscopicity dampens and shifts the inside RH- fluctuations. On daily basis, only the first mm of all inside surfaces are active (t.m. the wallpaper and a thin layer of plaster). On yearly basis, the whole envelope has some influence;

- furniture, books, draperies, carpets have a mayor influence on the hygroscopic inertia. Indeed, they often or always are made of very hygroscopic materials and have a very high specific surface in contact with the air;

- because of the hygroscopic inertia, the RH against a surface becomes to some extend uncoupled from the vapour pressure in the room and from the surface temperature. In fact, it turns to be more dependant from the surface materials RH, self coupled to the surface layers hygroscopic moisture content.
This results in a non response to short RH-peaks in the air and may explain why, as long as no surface condensation exists, these don't cause mould problems.

- hygroscopic inertia also strongly reduces the positive effect of peak ventilation, except if this coincides with peaks in moisture production. Otherwise, as soon as the ventilation stops, the inside RH returns to his pre-peak level...

- hygroscopic moistening of wall paper goes on 2 to 3 times quicker then hygroscopic drying. Once moist, a surface seems to persist in being moist. This experimental fact sustains the opinion that the real important thing is to maintain a mean relative humidity, low enough to avoid mould germination!

HEAT-AIR-MOISTURE TRANSFER (NL, B)

Apart of a detailed study on the air-moisture balance in a single and multiple zone situation with ideal zonal mixing, experimental

work on the spread of vapour,produced locally, in a room, between rooms and in dwellings has been performed.
The development of a vapour front clearly reflects the convective air circulation and exchanges: in a room from the bottom up to the ceiling and back to the floor, between rooms from downstairs to upstairs locations.

BOUNDARY CONDITIONS (FRG)

Information has been gathered and ordered on:

- vapour production in dwellings;
- climatic data;
- ventilation rates;
- heating habits.

5.4 Case studies, common exercises

CASE STUDIES

As case studies have run/ are running:

COUNTRY	CASE	SPECIFIC ELEMENTS
B	Zolder	miners estate, build shortly after world war 2, retrofitted in the early eighties. Since,very severe mould problems. Causes: poor ventilation possibilities,ruinous thermal design Monitoring before and after remedial treatment (air dryers, ventilation system, in- and outside insulation, loft space insulation (or, or)) Monitoring results used as input for the first common exercise.
NL	Pijnacker case	end of a row one-family dwelling Insulated, but, with thermal bridges left. Moderate mould growth. The monitoring gave no conclusive information on the cause of the mould presence. It seemed as if past circumstances were responsible..
	Alexander Polder	appartment block, not insulated. Diffuse mould growth in a first floor flat. The monitoring gave no conclusive information on the cause of the mould presence. It seemed as if past

		circumstances were responsible.. The case generated a discussion on the monitoring difficulties. It was used as input for the second common exercise.
I	Leuman villagge	brick made flathouses, build 1896-1925, retrofitted 1978-1980. Severe moisture and mould problems The monitoring revealed wet basement walls (t.m. extra moisture production) and a poor ventilation.
	IACP-building	a 10-storied flat building, not insulated, single glazed. Widespread mould problems. The monitoring revealed as causes a poor ventilation and thermal bridging
U.K.	Edingburg	large scale investigation on the relation between damp houses and lower respiratory symptoms in children, living in these. Confusing results in the sense that a parents survey gave a strong relation but a monitoring campaign a less convincing relation.

COMMON EXERCISES

- the first common exercise was focused on calculated predictions of mould and surface condensation situations, using the Zolder case study as input.
  The results revealed a widespread ability of handling the problems but major differences in the quantitative aspects. Causes have to be sought in material property values, in the use of other film coefficient values, in the sophistication of the models a.o.;

- the second common exercise looked to the diagnostic abilities. Starting point was the Alexander Polder case study,a damage exemple without clear cut cause. This was reflected in the diagnostics offered, some being a too slavish application of national codes, others really focusing on the specific case. Perhaps the most important result was the commonly accepted conclusion that mould growth may have two distinct causes:

  . a long lasting too high relative humidity on a surface (cfr the a-value);
  . short periods of surface condensation, alternating with dry-

ing in such a frequency, that the wetted surface remains wet enough to unable mould germination.

6. REFERENCES AND LITERATURE

1. WTCB/CSTC Enquete 5000
   Results, discussed at the Den Haag meeting

2. Oral information

3. Oral information

4. Tammes E., Vos B.H., vochttransport in bouwconstructies, Kluwer Technische boeken NV, Deventer-Antwerpen 1980

5. Hens H., Bouwfysica 2, Warmte en Vocht, praktische problemen en toepassingen, Acco, Leuven 1982

6. List of IEA-Annex 14 reports: see add. 1

7. ACKNOWLEDGMENT

This interesting international cooperation on condensation and energy has been possible thanks to the enthousiasm, knowledge and experience of:

I	Politecnico di Torino Dipartimento di Energetica	prof. C. Lombardi
FRG	Fraunhofer Institut fuer Bauphysik, Stuttgart	dipl.ing. H. Erhorn
	Dornier Systeme gmbh	
UK	BRE, Scottish Laboratory	dr C. Sanders
NL	Rijksgebouwendienst	ir. P. Van der Laan
B	KULeuven, Laboratorium Bouwfysica	ir. E. Senave
	Physibel adviesbureau	

IEA ANNEX XIV
CONDENSATION AND ENERGY

LIST OF IEA - ANNEX XIV REPORTS update: 01/06/89

---

1. Material properties

B-T1-01/1988 : Material Properties: first text proposal
B-T2-02/1988 : Material Properties: additions to the first text proposal

2. Mould

NL-T2-04/1988 : Summary of mould research
B-T2-05/1988 : Summary of mould research
UK-T2-06/1988 : Summary and bibliography of UK research on conditions for growth of moulds and control strategies
UK-T2-07/1989 : Mould: First text proposal

3. Thermal modelling

B-T3-01/1988 : Combined conduction-convection-radiation in a room
D-T3-02/1988 : Basic discussion text topic 3.2
D-T3-03/1988 : Wärme und Feuchteübergangskoeffizienten in Außenwand ecken von wohn bauten
B-T3-04/1989 : Combined conduction-convection-radiation in a room Final Report
D-T3-05/1989 : First text proposal topic 3.2
I-T3-06/1989 : First Text Proposal topic 3.1
NL-T3-07/1989 : Surface Heat Transfer Coefficients - related to calculation systems and measurements

4. Hygric modelling

B-T4-01/1988 : First text proposal: Modelling: some hygric aspects
NL-T4-02/1988 : A Second Order Model for the Prediction of Indoor Air Humidity
B-T4-03/1989 : Second text proposal

5. HMA modelling

NL-T5-01/1988 : Vapour distribution in dwellings
D-T5-02/1988 : Building energy and hygric analysis simulation model (BEHAS)
NL-T5-03/1988 : Inventory of models for intra and interroom moisture transfer
NL-T5-04/1989 : Extended Content Proposal
NL-T5-05/1989 : Inventory of models for the distribution of water vapour in buildings: Final Report.

6. Boundary conditions

D-T6-01/1988 : Basic Discussion text
D-T6-02/1989 : First text proposal

7. Case studies

B-T7-01/1987 : Generalities
B-T7-02/1987 : Review of 3 previous case studies
D-T7-06/1987 : Review of previous case studies
UK-T7-07/1987 : Review of previous case studies
UK-T7-08/1987 : Questionnaire forms
B-T7-09/1987 : First results of the Zolder case study
B-T7-15/1988 : Subsequent results of the case study at Zolder
B-T7-16/1988 : Mould research in Zolder
NL-T7-17/1988 : Case study Pijnacker TNO/IBBC
NL-T7-18/1988 : Case study Cauberg Huygen
I-T7-19/1988 : Case study 1: Leumann Village
I-T7-20/1988 : Case study 2: IACP Torino
UK-T7-21/1988 : UK case study: first report
NL-T7-22/1988 : Review of previous case studies
NL-T7-23/1988 : Case Study Pijnacker: 2nd report
NL-T7-24/1988 : Mould and surface condensation in Dutch dwellings, a case study (Cauberg-Huygen): Final Report
NL-T7-25/1988 : Study of methods for measuring atmospheric humidity
D-T7-26/1988 : Case study of mould growth in a bathroom
I-T7-27/1988 : Case study 2: IAPC Building: thermal bridges
UK-T7-28/1988 : UK case study: second report
B-T7-29/1988 : Case Study Zolder: Planned measurements and measures
UK-T7-30/1988 : Zolder, condensation case study
NL-T7-31/1988 : Working Paper Case Studies
▸ NL-T7-32/1989 : Case Study Pijnacker: Investigation on the causes of moisture and mould problems: Final Report
NL-T7-33/1989 : Case Study Alexanderpolder: Final Report

8. Organisation

B-OR-01/1987	: distribution/classification system
B-OR-02/1987	: list of standard symbols
B-OR-03/1988	: working paper for the Glasgow Meeting
B-OR-04/1988	: First integration exercise
NL-OR-05/1988	: Annual report 1987
NL-OR-06/1988	: Projectdescriptions / Reporting format
B-OR-09/1988	: Working paper for the Torino Meeting
I-OR-10/1988	: Solution for the first integration exercise
B-OR-11/1988	: Solution for the first integration exercise
NL-OR-12/1988	: Solution for the first integration exercise
UK-OR-14/1988	: Solution for the first integration exercise
NL-OR-15/1988	: Second Integration Exercise
B-OR-16/1988	: Project desciptions : International : First Report
B-OR-17/1988	: Results of the first integration exercise
NL-OR-18/1989	: Dutch Project Descriptions: Second report
B-OR-19/1989	: Solution for the second integration exercise
NL-OR-20/1989	: Solution for the second integration exercise
D-OR-21/1989	: Solution for the second integration exercise
I-OR-22/1989	: Solution for the second integration exercise
UK-OR-23/1989	: Solution for the second integration exercise
NL-OR-24/1989	: Results of the second integration exercise
B-OR-25/1989	: Project desciptions : International : Second Report
NL-OR-26/1989	: Description of Annex XIV database : concept
D-OR-25/1989	: German Contribution to the Leuven Meeting (*)

9. Proceedings

NL-PR-01/1987	: Utrecht T.O.-meeting (6-7 April 1987)
B-PR-02/1987	: Stuttgart meeting (12-14 October 1987)
B-PR-03/1988	: UK meeting (11-13 April 1988)
B-PR-04/1988	: Torino meeting (17-19 October 1988)
B-PR-05/1989	: Leuven meeting (8-10 may 1889)

(*) Out of this report (handed at the Leuven meeting) we distillated 2 other reports:

D-T3-05/1989	: First text proposal topic 3.2
D-T6-02/1989	: First text proposal

PROGRESS AND TRENDS IN AIR INFILTRATION RESEARCH

10th AIVC Conference, Espoo, Finland
25-28 September 1989.

Paper 2

ANNEX 18

DEMAND CONTROLLED VENTILATING SYSTEMS

LARS-GORAN MANSSON

LGM CONSULT AB
Adler Salvius vag 87
S-146 00 Tullinge
SWEDEN

SYNOPSIS

The IEA Annex 18 Demand Controlled Ventilating Systems-(DCV-Systems) with 9 participants are just in the middle of the work. Reviews are indicating energy conservation possibilities in the range of 8 - 40 % in experiments and even more in theoretical studies. Most of the case studies will start this autumn with sensor tests, test room studies, and trials in occupied spaces. In the test rooms will be simulated the conditions in dwellings and offices with various ventilating systems. Almost 30 occupied buildings will be involved in tests in dwellings, offices, auditoria, and schools. The final report will be given in a source book planned to be printed at the end of 1991.

1. BACKGROUND

Many IEA countries have an increasing problem with the indoor air quality and studies are undertaken concerning outgasing from building material, human habits, odour, threshold limits etc. Such energy conservation measures as tightening of the building envelop and increased use of return air has in many cases been accused to be the main reasons of the indoor air quality problems. The experiences from all these indoor air quality studies may result in a demand for an increased outdoor air volume.

Variations in the number of occupants and their activities will lead to the possibility to control the supply and exhaust air volume according to the demand.

We are spending almost 90 % of our time indoors at home or at work. However the problem is to predict the number of people in a room, a dwelling, a building etc. These circumstances can lead to overventilation and unnecessary use of energy.

The problem is that there is always more or less uncertainty in the assumption of how many occupants there are or can be in a room. Each room or building then need a certain air flow to extract pollutant from outgasing of materials to an acceptable level. Before and after a space has been used it can also be necessary to run the ventilation system in order to remove the pollutant from the material and the occupants. If we can find ventilating systems which can be controlled to above mentioned conditions good enough sensors, the use of outdoor air will be more effective and also give a good possibility to save energy.

2. INTRODUCTION

In the IEA Annex 9 Minimum Ventilation Rates results are given to meet the requirement of air flow rates based on human needs. The discussion started on how to use the knowledge with the purpose to minimize the waste of energy.

When the basic needs were given it was obvious that the results could be used in a new Annex focusing on how to control the ventilation following the occupants' demand.

The objective of the Annex 18 is to develop guidelines for Demand Controlled Ventilating System (DCV systems) based on state of the art analyses and case studies for different users in different types of domestic, office, and school buildings.

The work in the Annex is divided into three Subtasks.

Subtask A: Review of existing technology

Subtask B: Case studies
1. Sensor tests
2. Trials in unoccupied test buildings.
3. Trials in occupied spaces.

Subtask C: Design and operation of DCV systems

Participants in the Annex are:

Canada	Lead Country Subtask B
Denmark	
Fed. Rep. of Germany	Lead Country Subtask A
Finland	
Italy	Lead Country Subtask B2
The Netherlands	
Norway	
Switzerland	
Sweden	Operating Agent and Lead Country Subtask B1 and C

Observers:

AIVC
Belgium

3. SUBTASK A - REVIEW OF EXISTING TECHNOLOGY

This subtask is now to be completed as a report with the title "Demand Controlled Ventilating System - State of the Art Review". The result is used in the work in the Annex by choice of sensors, making the case studies comparable, and focusing on questions not yet sufficiently answered in the already finished case studies.

The chapters in the report are the following subheadings 3.1 - 3.5.

3.1. Review of contaminant concentrations in occupied spaces.

The information about average and peak concentrations can be found but not easily if the measurements were carried out in projects with no connection to any research work. The participants have gathered information from both research projects and other reliable measurements often with the purpose to find a solution of an indoor air quality problem.

In table 1 is summarized data about carbon dioxide and in table 2 about hydrocarbons. Information about humidity is found in the results from Annex 14 - Condensation and mostly from measurements in dwellings. Not many studies are reported about humidity in countries with cold climate.

3.2. Review of international standards

The threshold values of indoor air pollutant are given for humidity, carbon dioxide, carbon monoxide, nitrogen dioxide, formaldehyde, and hydro carbons. These standards were reported at the 9th AIVC conference in Gent, 1988.

3.3. Sensors

The function principles of sensors are given for humidity, carbon dioxide, and mixed gases. The sensor market review reports complete devices distributed on:

Humidity	17
Carbon dioxide	6
Carbon monoxide	7
Air quality sensor	6

A detailed report on sensors and sensor market is given in the proceedings from the 9th AIVC conference.

3.4. Review of measured results and knowledge about DCV systems

The last 10 years case studies and experiences with regard to DCV systems have been reviewed.

Out of totally 32 reports was found that nearly all (29 reports) were discussing CO_2 sensors and CO_2 as the controlling pollutant. In some of the reports were also discussed humidity (5 reports) and mixed gases (7 reports) to be the controlling pollutants. Totally 23 reports are from real experiments with

DCV-systems and the other papers are reports on monitoring studies and theoretical analyses. Two examples of reviewed papers will be given.

The first example is a CO_2-controlled air conditioning system in a bank i Pasco, WA U.S.A. The objective was to save energy without sacrificing the indoor quality. In figure 1 is compared normal temperature control with CO_2-control. The experiment was run both during winter and summer conditions. Energy savings was reported to be 8 % and the pay-back time was 2 - 3 years.

The second example is an office in Otaniemi, Finland. Also here the objective was to save energy in an air conditioned building. Three different modes were studied and the energy savings were compared to normal designed control strategy.

A) CO_2 set point 700 ppm gives 40 % savings
B) CO_2 set point 650 ppm gives 10 % savings
C) Time-related control case with the air flow close to A) above gives 30 % savings

Figure 2 gives the air flow rates during a working day in the three studied modes.

3.5. Conclusions

Most of the studies were about application of DCV-systems in offices and public buildings and only 3 studies were about dwellings. The choice of building is probably depending on the expectation that public or office buildings easier can stand the investment and handle larger air flows per installed DCV-unit.

The sensors used in the reviewed projects were to control on CO_2, humidity, and odour.

The location of the sensors are generally chosen to be in two places. One is in the exhaust duct close to the return duct and controlling the mixing of return air and outdoor air. The other is to locate the sensor close to temperature control in the room. No detailed study has been carried out on the sensor location. But yet ventilation efficiency has been studied in some tests giving an idea if the location of the sensor in the room was a good choice according to the air distribution pattern.

Reported energy savings vary from between 8 % to 40 % in projects based on measurement and from 30 % to 60 % in theoretical studies. A general remark is that the percentage of the energy savings depend on many factors e.g. total energy consumption, air flow, climate, basic standard of the system.

The design of a DCV system will very much depend on climate, building type, occupancy pattern, and the general design of the ventilating system. Therefore, energy savings coming from the use of a DCV system should be reported in relation to a defined reference system, for which air quality levels are well known. Energy savings and air quality achieved can then be put in a calculus where investment is compared to energy savings and life cycle costs. If a method for comparing human performance as a function of air quality can be found, also that parameter can be included in the life cycle cost.

4. SUBTASK B - CASE STUDIES

Some of the case studies have already started but most of them will start during this autumn and winter. Here is given a short description of the various tests. See also in the Appendix and in the matrix giving the distribution of the work amongst the participants.

4.1. Sensor test

A fundamental prerequisite for demand controlled ventilation system is the possibility to find a measurable "indicator" of the air quality. Another prerequisite is the existence of commercially available sensors for the measurand which have acceptable sensitivity, accuracy, long term characteristics and price level.

15 sensors for the following types of indicators will be tested:

* water vapour (RH, WBT, DPT)	7 sensors
* carbon dioxide	3 sensors
* unoxidized gases (H_mC_n, CO, etc. also called mixed gase sensor)	5 sensors

The tests will consist of 2 main parts. In part 1 one specimen of each sensor type is extensively laboratory tested. In part 2 three specimens of each sensor type is exposed to normal indoor climate conditions (in an office building).

The laboratory test procedure will consist of 4 main parts including

* data sheet evaluation
* performance of new sensors
* cross-sensitivity
* environmental tests.

The field test procedure will consist of 4 main parts including

* performance of new sensors
* a building status control
* exposure to ambient conditions
* renewed performance control

The Federal Republic of Germany and Sweden (lead country) are the participants.

4.2. Trials in unoccupied test buildings

The main aims with the experiments in unoccupied test buildings are to study how different ventilating systems can be made controllable. Most of the trials will be concerning pollutants in dwellings and systems applicable there. In one trial is going to be studied simulated normal conditions an office.

In general the countries with cold climate have equipped the test facilities with balanced ventilation systems and the countries with milder and more humid climate are testing natural and exhaust ventilating systems. The location of sensors, and supply and exhaust terminal devices will be studied with regard to the concentration of the measured pollutant from simulated occupants. Energy savings potential will be calculated based on the measured results.

Some of the factors to be studied are:

- Set point or acceptable level of chosen pollutant
- Source strength
- Distribution of sources in the room(s) or the system
- Character of source
- Air distribution pattern
- Choice of sensor type and control strategy
- Various time constants of the system

In the appendix is summarized the experiments in the five countries involved in test room studies. An example of a test room study is given in figure 3. The participating countries are Belgium, The Federal Republic of Germany, Finland, Italy (lead country), and Sweden.

4.3. Trials in occupied spaces

The main purpose with trials in occupied spaces is to study the energy conservation possibilities without sacrificing the indoor air quality.

Under real conditions DCV-systems will be evaluated. Different control strategies in different ventilation systems are applied in various buildings such as residentials, auditoria, offices, schools.

In a few months approximately 30 buildings are involved in tests in the participating countries. The plans are to measure in the following building types:

Residential		14 buildings
single family houses	11 bldgs	
blocks of flats	3 bldgs	
Offices		6 buildings
Auditoria		3 buildings
Schools, day nurseries		3 buildings

Details about the distribution of the work will be found in the appendix.

An example of a trial is illustrated in figure 4. The measurements and evaluation will cover:

- Regulating/controlling function
- Dynamic behaviour of the room and system
- Air quality
- Energy savings

The performance of the ventilation system will be checked in accordance to the Swedish guide "Inspection and performance checking of ventilation systems".

The participating countries are Belgium, Canada (lead country), Italy, Norway, Sweden and Switzerland.

5. SUBTASK C - DESIGN AND OPERATION OF DCV-SYSTEMS

In the subtask will be summarized the knowledge concerning DCV-systems based on the experiments in subtask B and results from now already finished work. Conclusions and recommendations will be given in a source book which can be translated to national languages and then used as a hand book.

SUMMARY

The results from subtask A indicates a broad range of how much energy that is possible to save. Finished experiments in occupied spaces reports that between 8 % to 40 % of energy consumptions could be saved.

The first sensor tests will be carried out on 15 sensors exposed in laboratory and in ventilation systems in an office. Test room studies about air

distribution will give us better knowledge of optimal sensor location and if the ventilation systems can be made controllable.

In occupied rooms or houses of various use will be studied DCV-systems with different control strategy. Conclusions, recommendations and results from the trials will be given in a source book. The work is planned to be finish in June 1991 and a printed report late 1991.

References

1. Raatschen W. Market Analysis of sensors for the use in demand controlled ventilating systems 9th AIVC conference 1988.
2. Demand Controlled ventilating Systems - State of the art Review - working document IEA - Annex 18 Subtask A

Table 1. Measured CO_2 concentrations some examples

Ventilation System	Building use	Air exchange rate (h^{-1})	CO_2 conc [ppm] Min	Max	Mean	Comments
Natural	Day nurseries	0.5 - 1.5	1000	2500	1500	
	schools	0.5 - 4	1000	7500	3000	
	schools			5500	1500	
	dwellings		500	1900	1400	closed doors max 2800 ppm
	school			4500		
Exhaust	Day nurseries	1 - 8	600	1000	800	
	dwellings		800	1700	1400	closed doors max 3700 ppm
	school				900	
Supply Exhaust	day nurseries	2 - 9	400	800	600	
	auditorium		700[1]	1700[2]		
	dwellings		800	1600	1400	closed doors 1400-2900 ppm
	cinema				900	
	day nursery[4]	8	1300	1600		
	nursery[4]	4	1300	1600		
Supply Exhaust Return Air	school		600	1000		
	office		700	1200		humidified air
	office	3)		1000	700	
VAV System	school			2600	1000	
	auditorium				800	DCV-System

1) Air flow rate 2 l/s,person
2) Air flow rate 16 l/s,person
3) 0.1 ach/h during night
4) Two cases: a) supply and exhaust devices located at the ceiling
b) supply devices located at the floor and exhaust at the ceiling

Table 2. Volatile organic compounds (VOC) of which the main parts are hydrocarbons.

Reference	VOC-concentration [ug/m^3]
1. Mølhave, Møller	
Dwellings, new houses	6200
Dwellings, old houses	400
2. Johansson et al.	
Day nurseries	290 - 500
3. Berglund et al.	
New day nursery	300
4. De Bortoli et al.	range 200 - 10000
Dwellings, offices	mean 3000
5. Lebret et al.	no smoker mean 210
Dwellings	smoker mean 350
6. Mølhave, Lundqvist	range 30 - 5500
Dwellings, unoccupied	mean 4600
7. Krause et al.	range 70 -2700
Dwellings	mean 400
8. Hawtorne et al.	
Dwellings	mean 240

Normal concentration is below 1000 ug/m^3

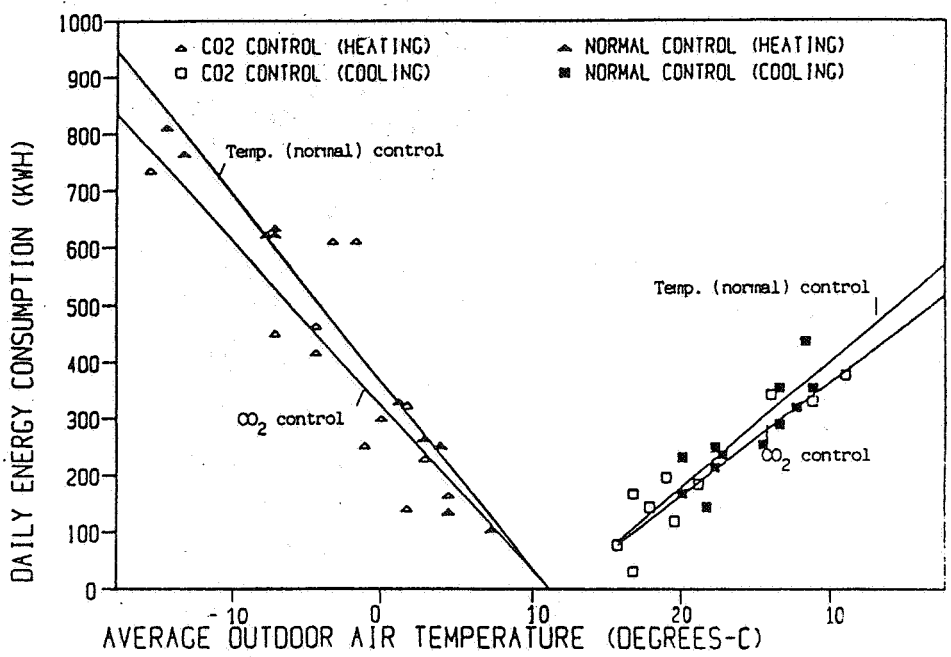

Figure 1. Energy consumption in a bank, Pasco, WA, U.S.A. CO_2 control mode compared to temperature (normal) control mode. Energy savings 8 %. Ref. Gabel S.D; Janssen J.E. et al. Carbon Dioxide based ventilation Control System Demonstration DOE BPA. April 1986. AIVC # 2333

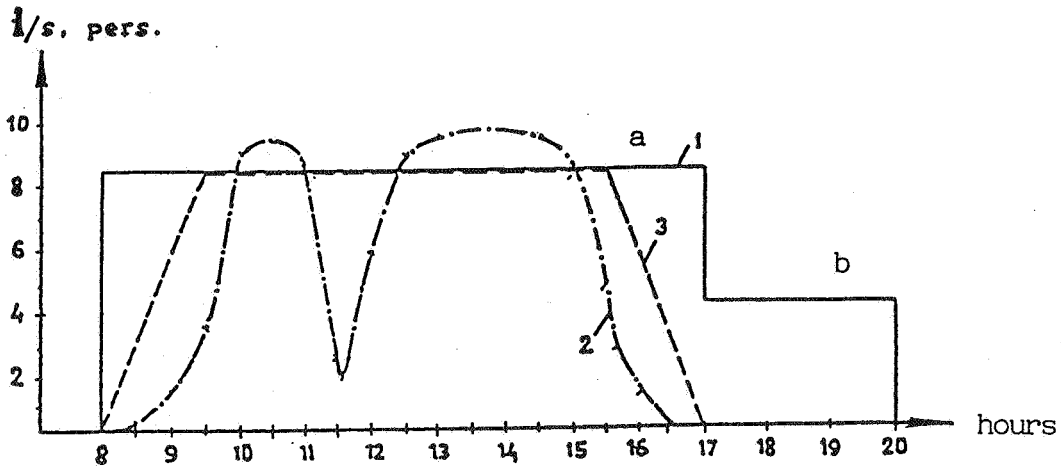

Figure 2. Office in Otaniemi, Finland. Outdoor air flow rates during a working day. Control modes: 1 Constant flow a) working hours b) evening c) during night - only return air. 2 CO_2 control. 3 Time control. Ref. Södergren, D; Punttila, A. A CO_2-controlled ventilation system. Swedish Council for Building Research D7:1983. AIVC # 1218

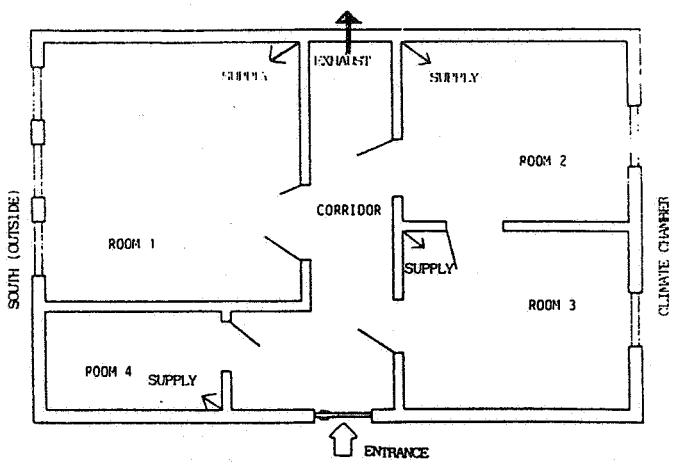

Figure 3. Test rooms at the Swedish National Institute for Building Research. An office space is simulated. Various tests will be run with people and also simulated by heat and CO_2. The number of simulated occupants in each room will vary from 0 - 2.

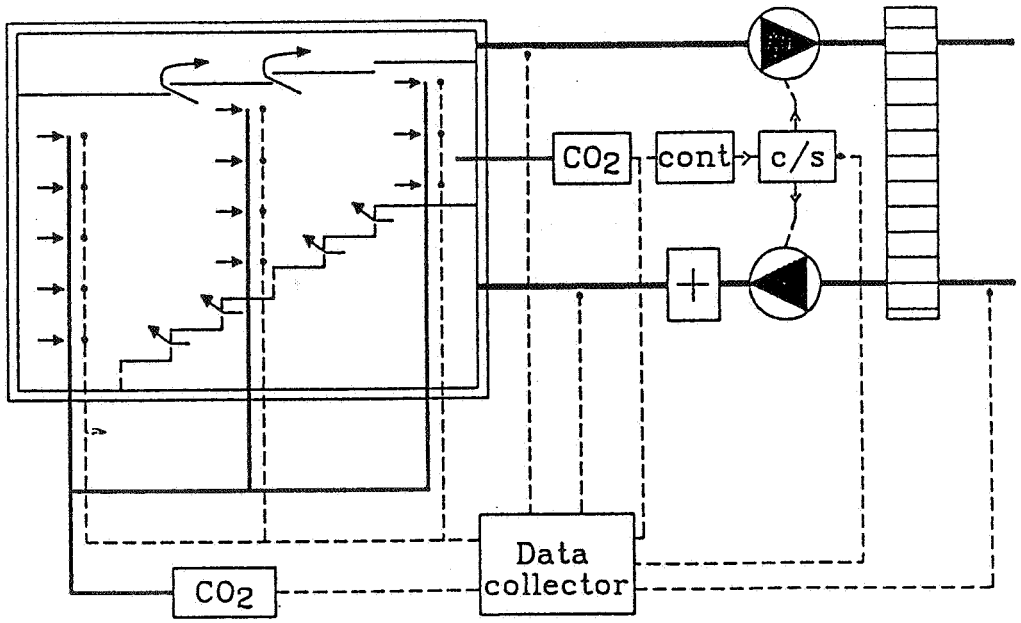

Figure 4. An auditorium in Trondheim, Norway, equiped with temperature and CO_2-controlled air flow. Sketch of the ventilation system, the controller unit, and the data acquisition system. Displacement ventilation with air inlets under the seats and outlets in the ceiling. CO_2 set point 900 ppm.

SUBTASK B - CASE STUDIES

Short description of the tests.

Belgium:

B 2 Unoccupied test houses

In flats will be used DCV systems with humidity and CO_2 sensors and also manual controlled systems. Different locations of the supply and exhaust devices will be studied. One school will be equipped with manual, humidity, and CO_2 controlled natural ventilation.

B 3 Occupied buildings

1. One school with CO_2 controlled system.

2. 2 blocks of flats with natural ventilation have been selected. 10 flats in each block are equipped with humidity and manual controlled systems. During 5 weeks each season measurement will be carried out in bathroom, kitchen, livingroom and in the extract air.

3. Single family houses with natural and exhaust air ventilation will be controlled by CO_2 and humidity sensors also manual and time controlled.

Canada:

B 3 Occupied buildings

1. In the R-2000 program run by Energy Mines and Resources development of single family houses are going on to find energy efficient homes with good indoor air quality. Experiments are ongoing measuring in balanced ventilated houses with humidity control.

2. In an office building a CO_2-sensor is located in the return air shaft. The building is divided in two zones one with CO_2-sensor controlling half of the building and the other half normal temperature controlled.

3. In meeting-rooms the ventilation system will be controlled by CO_2 and humidity sensors and compared to manual and temperature controlled ventilation.

4. Canada Mortgage & Housing Corporation (CMHC) have selected 5 houses. One house will be equipped with a system that can change the supply air according to the number of persons in the house. One house is equipped with humidity control in exhaust and supply devices. One

that will be designed this winter. Two houses will be used more or less as references and equipped with balanced ventilation system and heat recovery, one with and one without reciculating air.

Denmark:

B 3 Occupied buildings
In two existing day nurseries will be installed ventilation system with supply and exhaust air. Humidity and CO_2 sensors will be used to control the air flow.

Federal Republic of Germany:

B 2 Unoccupied test houses

The main objective is energy conservation but also to attain good indoor air quality. Different habits in dwellings are simulated and the pollutant levels are studied while using different ventilating systems and using different control strategies. Ongoing measurement.

Finland:

B 2 Unoccupied test houses

In a standard single family house is installed a supply and exhaust ventilation systems. The research work is in three steps

a) Loading profile, simulation and calculations.

b) Testing the systems when simulating control by the occupants.

c) Interaction ventilation and heating.

Italy:

B 3 Occupied buildings

In a new block of flats with exhaust ventilation is installed humidity controlled supply air grilles in bedrooms and living rooms. The main objective is to avoid moisture damaging the structure.

Netherlands:

B 3 Occupied buildings

1. Tests have been carried out in humidity controlled houses.

2. The objective is to find a cheap and practical system to be used in dwellings. It could be a balanced ventilation system with heat recovery and controlled by a sensor.

The plans are to install DCV system with CO_2, humidity, and odour sensors. Energy consumption will be checked. Humidity set point will be changed according to outdoor temperature. Sensors will be located in the exhaust air duct and in the living room. The systems will be evaluated during 6 weeks with each location of the sensors.

Norway:

B 3 Occupied buildings

Measurements have started in a lecture hall at the University in Trondheim. CO_2 sensor is located in the hall with the set point at 900 ppm.

The system is alternate run with a week with thermal control and a week with CO_2-control. Tests have been done with the same number of students in the hall. Supply air devices are located under the seats and exhaust devices are located in the ceiling and no return air. Measure: CO_2, temperature, relative humidity, air velocity.

Sweden:

B 1 Long term tests of sensors

Sensors for humidity, CO_2 and mixed gases will be tested in laboratory and in field.

B 2 Unoccupied test rooms

A test unit of 4 unoccupied office rooms will be used. A balanced supply and exhaust ventilation system is installed. Air will be supplied in the rooms and exhausted in the corridor. The test unit will be simulated to be occupied. Air movement and the distribution of the pollutants will be studied for the cases of:

- different locations of the controlling sensor

- different locations of supply-air devices.

B 3 Occupied buildings

1. Tests will be carried out in a meeting room with max. capacity of 25 persons. Different sensors will be used when controlling the supply air flow.

   The number of persons in the meeting-room can easily be controlled and the duration of the meetings.

2. In an office building tests will be done in a meeting-room for 15 persons and two open areas with a great variety in the number of persons.

   A VAV-system was installed from the beginning in the

2 year old building . The system controlled by CO_2-sensor will be compared to the original controlled by temperature.

3. A school which today has an exhaust air system will be equipped with a new supply and exhaust air system. The classrooms are nearly always used in the same way and with the same number of occupants present.

Occupied classroom: air flow rate	250 l/s
Unoccupied classroom: air flow rate	28 l/s

This will give 9 - 7,5 l/s, p and a calculated CO_2 level of 1000 ppm with 30 pupils and 900 ppm with 25 pupils. The supply principles will be "mixing" in 5 classrooms and "displacement" in 1 classroom. In 5 classrooms the air flow rate is controlled by an acoustic presence sensor and in 1 classroom controlled by a CO_2-sensor with the set point at 900 ppm.

4. In an office under construction a DCV system will be installed in the VAV-system. The building will be completed in Oct. 1989. Total area is 4500 m^2 and 185 office rooms. Measurements on volatile organic compounds, particles, CO_2, and humidity will indicate what pollutant that can be the controlling one. The measurement will also indicate when it is possible to control on activities coupled to the occupants and not on emission from building material.

Switzerland:

B 3 Occupied buildings

Two auditoria (70 persons in each) will be used at ETH in Zürich. The ventilation systems will be controlled by temperature in both systems. In one of the auditoria the indoor air is controlled by a CO_2-sensor. The supply, exhaust, and return air system is designed to give constant air flow with 750 ppm as a set point.

Table DISTRIBUTION OF THE WORK

Various test in unoccupied houses (B2) and occupied houses (B3)
the controlstrategies, and the various ventilation systems.

Control Strategy	Building category																						
	Residential												Auditoria Theatres				Offices				Schools		
	Single								Flats								meet rooms	whole bldg		small rooms			
	unocc B2				occ B3				unocc B2		occ B3		occ B3				occ B3	occ B3		unocc B2	unocc B2	occ B2	
	Na	E	SE	SEE	Na	E	SE	SEE	SE	SEE	Na	E	E	SE	SER	VAV	VAV	SE	VAV	VAV	Na	E	SE
Manual	D B	D B	SF		B	B	NL	CAN	SF		B	I					CAN				B		
Time Control	D	D			B	B									CH	N		CAN					
Presence	D	D																					S
Temperature (reference)															CH	N	S CAN		CAN	S			
Humidity	D B	D B			B	B	NL	CAN			B	I					CAN				B		DK[1]
Pollution CO_2	D B	D B			B	B									CH	N	CAN S		CAN	S	B	B	S DK[1]
Odour	D	D					NL										S						
C_mH_n																	S						
others								CAN									S						

1) Pressure diff B = Belgium, CAN = Canada, CH = Switzerland, D = Fed. Rep of Germany, I = Italy, N = Norway, NL = Netherlands, S = Sweden, SF = Finland.
Na = Natural vent., E = Exhaust vent, SE = Supply and exhaust, SEE = Supply and exhaust and extra exhaust fan, SER = Supply exhaust and return
VAV = Variable air volume

DK = Denmark 1) Day nursery

Discussion
Paper 2

Willem de Gids (TNO, Netherlands)

Was the booster fan also controlled by a sensor, and if so what type of sensor was used?

Lars Goran Mansson (LGM Consult AB, Sweden)

In ongoing projects in Canada single family houses have supply and exhaust ventilation systems. When needed the air flow is increased by a booster fan which is controlled by a humidity sensor.

Mike Holmes (Ove Arup, London UK)

Your example to demonstrate the potential savings due to the use of a CO_2 detector used working day and night-time ventilation rates of 8 and 4.2 l/s/person. The CO_2 detector model which showed savings of 40% was without any nighttime ventilation. Surely the same result would be achieved without using a detector and turning the system off at night?

Lars Goran Mansson (LGM Consult AB, Sweden)

The control mode 1, see Figure 1, shows the normal designed control of a constant air flow system in the Nordic countries. With the time clocked control mode giving an air flow more like the CO_2 control mode indicates that the potential saving is more like it is in the other example, Figure 1.

PROGRESS AND TRENDS IN AIR INFILTRATION
AND VENTILATION RESEARCH

10th AIVC Conference, Dipoli, Finland
25-28 September, 1989

Paper 3

TRENDS IN AIRFLOW DESIGN AND MANAGEMENT, - CONTRIBUTIONS BY IEA ANNEX 20

ALFRED MOSER

Operating Agent IEA Annex 20,
Energy Systems Laboratory
Inst. für Energietechnik ML
ETH - Zentrum
CH-8092 Zurich, SWITZERLAND

SYNOPSIS

What does the designer of a future energy-efficient building ask of the air flow specialist? - Static predictions of air flow patterns and optimization of thermal comfort and indoor air quality at design conditions will not be enough for him.

The paper suggests that time-dependent air flow simulation is imperative to respond to tomorrow's design needs. Different physical time scales for air flow patterns in spaces will be discussed. Heat capacity by components, different types of heat transfer, varying occupancy, control inputs etc. give rise to disparate time scales. The trend toward occupant controlled ventilation will continue. Air flow will interactively be adjusted to changing needs in each room. The IEA Annex 20 examines tools to predict steady air flow patterns within buildings. The dynamic management of air flows will require new methods that build on Annex 20 work.

1. INTRODUCTION

The air flow in a building is not stationary: People move around or enter rooms, ventilation is turned on or off, sudden sunshine triggers a thermal updraft, or a window is opened. In addition, new ventilation designs allow the occupant to interact with the system and to control location and volume of fresh air supply. Advanced air heating systems distribute hot air with a rotating nozzle and innovative schemes "shoot" lumps of fresh air as vortex rings at the occupant [1]. From the point of view of HVAC control, the indoor air, including supply and return flows, is a component of a dynamic system.

These examples suggest that the air flow pattern in a building is unsteady and that only transient computer simulation is suitable for its prediction.

Why do many of today's methods still simulate steady flow fields only? In particular some of the more complex numerical models for single room or multi-zone air flows aim at steady-state solutions.

Here are two possible answers:

(1) Numerical complexities of time-dependent simulation

(2) The phenomenon of interest can often be considered steady after a careful comparison of the relevant time scales of the actual problem.

The first answer applies to applications that are already complicated in their static description and require a great amount of computer time and resources. A single-room air flow pattern may easily require a 20x20x20 spatial resolution resulting in 8000 memory locations for each variable. If in addition the information for a few hundred time steps must be calculated and stored, along with time-dependent boundary conditions, the amount of data becomes overwhelming.

The same is true for multi-cell simulations where the solution of a large system of coupled equations to determine the steady-state pressure at each of, say, a hundred nodes (i.e., rooms or zones of rooms) is already a delicate task.

Many numerical methods take advantage of a time-marching procedure to asymptotically reach a steady-state solution from an arbitrary initial guess. However, during this process of convergence the boundary conditions are kept constant, and very often the transient solutions at finite times are not of interest.

With regard to explanation (2) above, experience has shown that many air flow patterns of practical interest can be analyzed by just looking at steady solutions at much reduced expense of computer resources. But this approach requires prior knowledge of the relevant time scales of the problem.

This is illustrated by the following example: At time t = 0 the air in a room of dimensions L is at rest. How long does it take to get the air moving when it is driven by the momentum of a jet of velocity u_o and mass flow $\dot{m}$ entering through a nozzle of diameter h ?

Several simplifications will be made: Instead of accounting for friction, a relation proposed by Nielsen [2] is used to estimate the final (steady-state) air velocity in the occupied zone,

$$u_r = K\, u_o \sqrt{h/L}$$

where K depends on the inlet geometry and Reynolds number.

Further, linear acceleration of the air mass is assumed and the constant, c < 1, accounts for the fact that the air in the center circulates at lower speed. The air mass m accelerates as (Newton's law)

$$c\, m \frac{du}{dt} = \dot{m}\, u_o = \text{jet momentum}$$

If n expresses air changes per hour (ach) and if a time constant τ is defined by

$$\frac{u_r}{\tau} = \frac{du}{dt}$$

The time scale for the acceleration of the room air by jet entrainment becomes

$$\tau = 3600\ cK \frac{1}{n} \sqrt{h/L}$$

Thus, in a room with L = 4 m and a jet inlet diameter h = 0.2 m at an air change rate of 6 per hour, the time constant is roughly 134 s when cK is of order unity.

What does this mean? - When we are interested in the air flow pattern in an office building as it exists during the early afternoon, i.e., some average flow field over an hour or two, we do not care about the transient response of the room air caused by a sudden change of jet momentum. On the other hand, we also neglect the slow drifting of certain temperatures resulting from the effect of the day-night temperature variation on the building thermal inertia.

Thus a first conclusion with regard to simulation of flows under conditions which are unsteady in reality could be formulated as:

> If we want to predict, in a generally unsteady situation, a phenomenon that has a characteristic duration sufficiently above the next lower and below the next higher natural time scale of the overall physical problem, then a **steady-state** simulation is adequate.

This paper will review a few different time scales applicable to air flow in buildings in the next section. A further section is devoted to the rate of growth of one-dimensional natural convection boundary layers on vertical surfaces. Then trends for time-dependent air flow simulation are discussed along with a critical overview of the IEA Annex 20 objectives and an appraisal of its intended impact on the future development of flow field prediction. Annex 20 is entitled "Air flow patterns within buildings" and deals with simulation techniques for single- and multi-zone air and contaminant flow.

2. PHYSICAL TIME SCALES IN BUILDING AIR FLOW

Time scales can only be estimated after the physics of the problem have been analyzed and the relevant mechanisms identified. Often, time constants are very sensitive to geometric dimensions and proportions. This becomes apparent in the following example of the heating of the room-air by a radiator.

The air in a cubical room of length L has an initial temperature of T_0. This air is uniformly heated by a radiator with an effective surface of h^2 and a temperature $T_1 = T_0 + \Delta T$. It is assumed that the convective heat transfer coefficient, u, is constant.

The heat balance for the room air (with temperature T) yields:

$$c_p m \frac{dT}{dt} = u(T_1 - T)\, h^2$$

The time constant τ is defined by the initial rate of heating

$$\frac{\Delta T}{\tau} = \frac{dT}{dt}(t=0)$$

And the time scale for convective heating (of the air) becomes

$$\tau = \frac{c_p \rho L}{u} \left(\frac{L}{h}\right)^2$$

and is independent of ΔT.

If an entire wall is heated, h = L, and for L = 4 m, u = 5 W/m^2K, ρ = 1.2 kg/m^3, and c_p = 1000 J/kg K, this thermal time scale is τ = 960 s, or about one quarter of an hour. Of course, if the radiator does not cover a full wall, this time constant becomes much larger and grows with the second power of L/h.

The non-dimensional combinations in τ, above, also could have been obtained by dimensional analysis, but not the power of (L/h). The convection time scale is more sensitive to (L/h) than the air acceleration scale discussed in the introduction.

2.1 Transient air movements

A variety of time scales characterizing **steady** airflow have been identified by Hammond [3]. Also, the "age" of air used to quantify ventilation effectiveness [4 5 6] is a time scale defined mainly for stationary flow fields. The present discussion is not concerned with time constants of steady flows.

There is another class of flow situations in which unsteady signals are recorded during experiments, although the velocity field is steady: That is when the concentration field (of a neutrally buoyant tracer) is unsteady in an otherwise steady flow. Recirculating clouds of tracer gas may produce a nearly periodic signal at a fixed location with a frequency of the order of u/L, where u and L are typical air velocities and room dimensions, respectively. A tracer gas step-input results in an aperiodic response.

We will turn our attention to truly time-dependent flows that require time-derivative terms in the governing transport equations. Again, we can distinguish between time-dependent flows with steady and with unsteady boundary conditions.

2.2 Time-dependent flows with stationary boundary conditions

If a circular cylinder of diameter d is placed in a incompressible, uniform flow at velocity u, vortices separate from the cylinder surface at a frequency of about 0.2 u/d. A Karman trail develops in the wake of the obstacle. A blunt body under constant boundary conditions may give rise to an unsteady, periodic flow field if there is a feedback from the potential flow pressure field to the boundary layer separation mechanism.

Will oscillations of this type develop in room air flows? - The engineer doing numerical flow simulations would welcome a clear answer to this question. When he attempts to compute a flow with an inherent unsteadiness by a set of equations without transient terms, he will perhaps never reach a steady-state solution. In the case of the cylinder, the steady solution would be unstable except at very low Reynolds numbers.

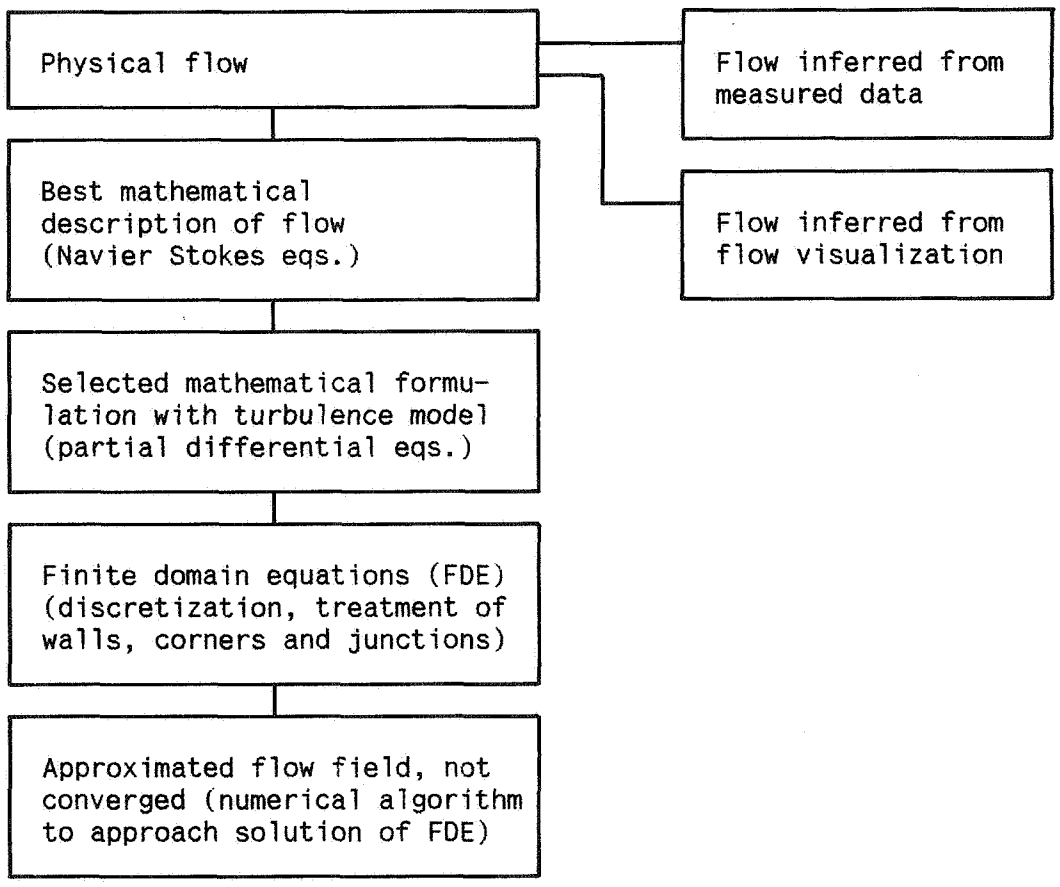

Figure 1 The simulation of flow fields involves a chain of representations where oscillations can develop. Information on the actual physical flow is available only as measured data and through flow visualization.

However, an oscillation during the numerical iteration process does not necessarily point to an unsteady physical flow. And Fig. 1 illustrates that the set of equations for which we seek a solution is merely a highly simplified representation of the actual flow. The source of oscillations can be rooted in the numerical solution algorithm, in the finite domain equations, or in the set of partial differential equations of the model.

Low frequency fluctuations seem to develop sometimes [7] in flows involving natural convection. Since there is an increasing need to simulate such flows, careful studies are needed to learn more about these unsteady phenomena. Parallel tests and calculations by different methods of identical cases, such as conducted by the IEA Annex 20 participants, should shed some light on these problems and help to pinpoint the source and confirm the existence of unsteadiness.

2.3 Time-dependent flows driven by time-dependent boundary conditions

Energy conservation is improved if fresh air is provided only where and when its needed. Demand controlled ventilation systems react to signals from specialized sensors. User-activated control offers the potential of maintaining energy efficiency while improving user satisfaction, because the occupant can adjust the local climate to his individual needs.

Time-dependent air flow predictions are needed to calculate the response of the air flow pattern to such control inputs. With more powerful computers there will be a trend from steady-state calculations to simulation of transient flow fields. Of course, the computation of the dynamic response of a complete air flow pattern requires that static flows are handled routinely and with confidence.

Applications for transient air flow codes:

- Some designs for the house of the future envisage comfort systems in which unoccupied rooms are kept at a temperature and ventilation level far below what is used today (winter situation). When people enter the room, a high-powered system brings the air quality to the required level in a relatively short time. How much power is needed, how much fresh air, and how long does this warm-up take? - These are questions the designer must be equipped to answer.

- A fire starts in a large building. How do hot or toxic gases spread through the building? Can the smoke be removed and escape routes be cleared of toxic gas by the existing ventilation system without feeding the fire with fresh oxygen? These are typical transient problems involving convection of heat and species, buoyancy, and radiation. Some multi-zone smoke control models are reviewed in [8].

- o Sudden sunshine through the glazing of an atrium may heat up one of the inside surfaces and cause a drastic change of the internal air flow pattern and temperature distribution. Also a problem for a transient natural convection flow field code.

It is hypothesized that in future ventilation systems the air flow is not just maintained but dynamically "managed" and adjusted to instantaneous needs in the same way as an aircraft is operated and piloted along an optimum trajectory.

When transient simulation codes are applied, a number of different time scales should be considered. Some are shown in Fig. 2 along a logarithmic time axis. These time constants might also be of relevance when the numerical time steps in a transient simulation are selected. Slow processes should allow larger computational time increments.

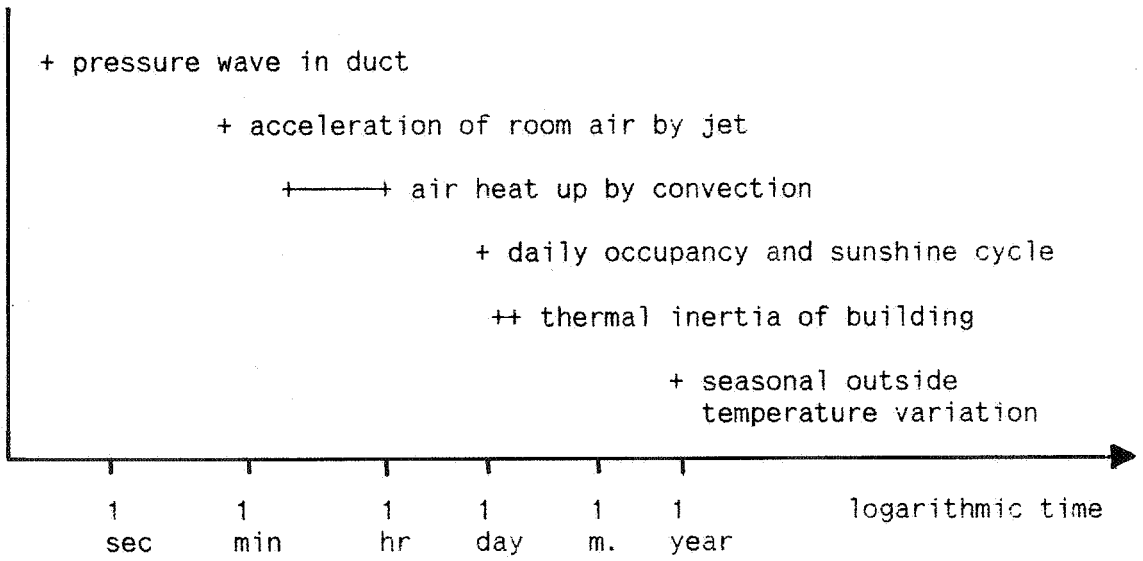

Figure 2 Units of time along a logarithmic scale with approximate ranges of various physical time scales.

In multi-zone air flow in buildings, a number of methods are available today to simulate the transient exchange of air, contaminants, and energy between rooms and with the outside. The intermittent ventilation of a room by opening a window at intervals, for instance, is investigated in subtask 2 of the IEA Annex 20. Initial measurements [9] show that two different time scales are of importance: An initial gravity wave of cold air fills the lower part of the room within the first few minutes after the window is opened, then heat is transferred from the inside walls, and a slow drift of inside air temperature continues for approximately 10 hours depending on the heat capacity of the building structure.

Dynamic simulations of single-room flow fields may also be required to assess the performance of ventilating systems that operate in a pulsed, revolving or intermittent mode. The ability of these systems to mix air masses in a space is discussed in the next section.

3. VENTILATION SYSTEMS THAT GENERATE UNSTEADY FLOW FIELDS

Some novel ventilating systems incorporate schemes for introducing fresh air in a periodic or intermittent[1] way. The technical designs of these systems are not reviewed here, just one aspect of their operation will be discussed: The effectiveness of mixing air in the ventilated room.

A fundamental difference between steady and unsteady flow was demonstrated by J. M. Ottino[10] for applications related to chemical engineering. He has shown experimentally that mixing of different fluids is much more effective in an unsteady flow field than in a stationary flow.

When a blob of ink is introduced in a **steady** flow of a fluid, it will stretch and move and essentially trace a particle path. If the experiment is then reversed with respect to time, the fluid should "unmix" (if molecular diffusion and turbulence are disregarded) and the initial blob should reappear. The convection of a dye in a steady-state flow ideally is a reversible process where errors grow linearly, and the initial state can approximately be recovered.

In a **unsteady** flow the situation is quite different. This is illustrated by the flow visualization recorded by Ottino[10] and sketched in Fig. 3. The unsteady flow between two rotating eccentric cylinders that move periodically in opposite senses effects a thorough mixing of two fluids. Here, the error in reproducing the motion in reverse grows exponentially. Already after a few periods it is practically impossible to undo the mixing.

The experiments suggest that this efficient mixing is accomplished by repeated stretching and folding of fluid filaments, which is typical for unsteady flow with periodic kinematic boundary conditions.

Returning to the ventilating system, we first should decide on the type of ventilation. Is a uniform mixing desired without any pockets of stale air or hot (cold) spots? Or is one-hundred-percent fresh air required near the occupant as in displacement ventilation, where temperature stratification and non-uniform contaminant concentrations are intended? In the latter case, mixing of fresh air with polluted air should certainly be avoided.

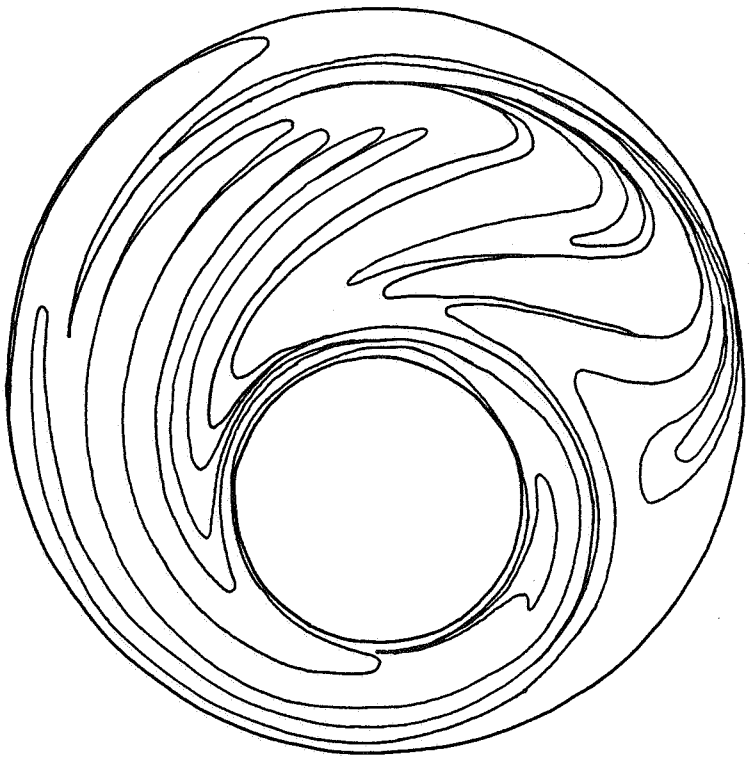

Figure 3 Mixing in unsteady flow: Two eccentric cylinders rotate periodically in opposite directions. The pattern of the mixing liquids after about 10 periods is sketched after a flow visualization photo taken by P. D. Swanson and J-. M. Ottino[1].

It can be concluded that intermittent or periodic (i.e., unsteady) ventilation systems should not be employed if mixing of air masses is not desired; however, these systems can be beneficial if high rates of mixing are wanted.

4. GROWTH RATE OF A VERTICAL ONE-DIMENSIONAL LAMINAR NATURAL CONVECTION BOUNDARY LAYER

Correct simulation of free convection on vertical surfaces is of crucial importance in single-room air flow prediction. In an attempt to better understand free convection boundary layers, we have looked for simple analytical solutions. So far we mainly found studies of steady flow along flat plates, where the boundary layer development, as a function of the streamwise distance from the leading edge, is of interest. But the inside walls of rooms start at the floor junction and do not have real leading edges.

Is there a general but simple model for the local behavior of a free convection layer somewhere on a large vertical surface? - Not for steady flow, where the shear layer develops along a streamwise distance. But the velocity and temperature profiles that develop somewhere on a wall in an **unsteady** situation, e.g., after a sudden change of surface temperature, can locally be determined.

It is this transient buildup of a boundary layer that we studied in order to find its relevant time scales. The solution process of numerical simulation often starts with the room air at rest adjacent to walls of different temperatures. Is it possible to consider the growth of the shear layer as a locally one-dimensional problem? - To find out, we have devised an idealized problem resembling Stokes' first problem[11], where a self-similar laminar shear layer is driven by a moving wall. In the present example, the air is initially at rest and has a uniform temperature T_o. The vertical wall has a constant temperature T_w.

Under the hypothesis of a one-dimensional physical process (direction "y" normal to vertical wall) the governing equations for x-momentum and energy were derived under these assumptions:

- Prandtl's boundary layer approximations
- laminar flow, constant viscosity
- density independent of pressure
- Boussinesq approximation for density/temperature relation
- No frictional or compressive heating

In dimensionless form the equation for vertical momentum is:

$$\frac{\partial u}{\partial t} - \frac{\partial^2 u}{\partial y^2} = \theta$$

and the energy equation:

$$\frac{\partial \theta}{\partial t} - \frac{1}{Pr}\frac{\partial^2 \theta}{\partial y^2} = 0$$

With the initial conditions

$u = 0$ $\quad \theta = 0$ $\quad$ at $\quad t = 0$ and $y > 0$

and boundary conditions

$u = 0$ $\quad \theta = 1$ $\quad$ at $\quad t > 0$ and $y = 0$

$u \to 0$ $\quad \theta \to 0$ $\quad$ as $y \to \infty$

The problem lacks natural length and time scales. The only possible combinations of physical parameters with dimensions [length] and [time] are L and τ, expressed in terms of kinetic viscosity, ν, and gravity, g:

$$L^3 = \nu^2 / g \quad \text{and} \quad \tau^3 = \nu / g^2$$

Non-dimensional temperature is defined by $\theta = (T - T_o)/(T_w - T_o)$

The other variables are (with primes on physical quantities):

$$y = y'/L \qquad t = t'/\tau \qquad u = u'\tau/\{L\beta(T_w - T_o)\}$$

The coefficient of thermal expansion, β, is kept constant.

The above system is relatively simple and can be solved analytically. However, the author is not aware of a solution in this context. In contrast to Stokes' problem, this system does not have a self-similar solution. The energy equation can be integrated directly because it is free of the other dependent variable, u(y,t). The temperature development alone can be expressed in similarity form and is identical to the solution of related heat conduction problems:

$$\theta = \mathrm{erfc}(0.5\, y \sqrt{Pr/t}\,)$$

The momentum equation is driven by the temperature term (buoyancy). Its solution, therefore, also depends on the Prandtl number and is a function of both independent variables:

$$u = f(Pr, y, t)$$

Note that the thermal expansion term, $\beta(T_w - T_o)$, has been incorporated in the definition of u and affects the physical velocity linearly.

This derivation[12] will not be taken any further here. For illustration, a few temperature profiles are shown in Fig. 4 for Pr = 0.7 and ν = 15E-6 m^2/s. After 100 seconds, for instance, the air at a distance of 44 mm from the wall is heated to one-half of the total temperature difference $T_w - T_o$.

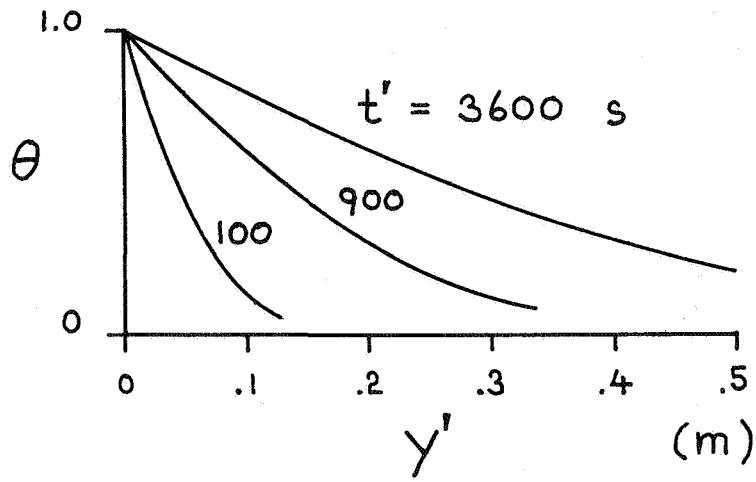

Figure 4 Exact solution for non-dimensional temperature in free convection along hot vertical wall as function of physical normal distance y' [m] and time t' [s] in air.

5. PREDICTION OF STEADY AND TRANSIENT AIR FLOW PATTERNS IN ANNEX 20

The IEA research program on "Energy Conservation in Buildings and Community Systems" sponsors a number of projects (Annexes) that aim at reducing energy consumption of buildings by optimizing the air flow and ventilation systems. The newest air flow project is the Annex 20, "**Air Flow Patterns within Buildings.**"

The task-sharing Annex 20 started in May 1988 for a period of 3 1/2 years. Its main objective is to evaluate the performance of single- and multi-zone air and contaminant flow simulation techniques and to establish their viability as design tools.

The **subtask-1** researchers evaluate flow field simulation programs for the prediction of velocity, turbulence, temperature, and concentration distributions in spaces. Numerical exercises are carried out for clearly defined test cases and the results compared with measurements obtained in identical test chambers by different participating countries.

Five typical test cases have been selected for this study:

b) Forced convection, isothermal flow with wall diffuser,
c) mixed convection, warm-air heating,
d) free convection with radiator and cold window inner surface,
e) mixed convection, summer cooling, warm window surface, and
f) forced convection, isothermal, as in b), with contaminants.

In **subtask 2**, the air, energy, and contaminant flow between rooms and infiltration from the outside are investigated. New algorithms are being developed and evaluated for:

- Flow through large openings
- Inhabitant behavior
- Air flow driven contaminants
- Multi-room ventilation efficiency

Mathematical descriptions of these models will be produced. But the actual implementation in a computerized multi-zone infiltration model is not within the scope of this annex.

The new algorithms will be experimentally verified, and some advanced measurement techniques will be necessary. Improved methods for

- multi-zone airflow measurements and
- enhanced leakage measurements

are developed for that purpose and documented. Validation data sets and physical parameter data bases will be made available on a data bank for later use.

5.1. Need for unsteady simulation

In the near future, design methods will routinely employ infiltration models and flow field prediction tools, and powerful computers will be available in the consultant's office at reasonable cost. Complex flow field simulation codes will calculate the air flow pattern in concert halls, but simplified methods could be more efficient to predict the flow in an office. No doubt, time-dependent flows must also be mastered with confidence.

Today, the researchers participating in Annex 20 strive to advance the state of the art in **steady-state** flow prediction. Engineers of many countries cooperate to learn how to apply modern computational fluid dynamics to building air flow. They share ideas on measurement techniques and, together, interpret experimental and numerical results.

The Annex-20 experts decided early to concentrate on **steady-state** air flow patterns (with a few exceptions in subtask-2 algorithms). As illustrated in Fig. 5, complex flow field simulation is scrutinized under static conditions only, i.e., in the shaded space-coordinate plane of the figure.

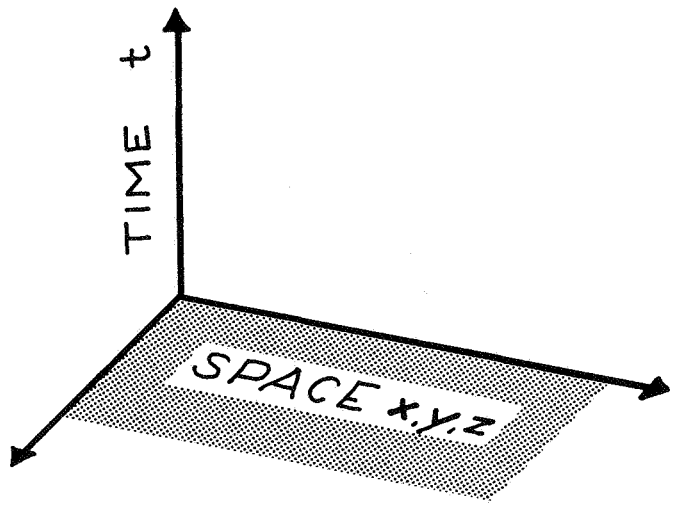

Figure 5 Space and time: Annex 20 aims at preparing a solid basis in the domain of **steady** air flow simulation, as indicated by the shaded "space"-plane.

New ventilation designs and control strategies make future **dynamical** simulation expertise mandatory. The trend toward transient prediction is clear, and the development of new methods will perhaps build on Annex-20 experience.

6. CONCLUSIONS

The goals of the "Air Flow Pattern" Annex are formulated in anticipation of future trends in air infiltration and ventilation. A solid groundwork in numerical and experimental techniques for steady-state building aerodynamics shall be provided. New methods for transient airflow can later be based on this foundation.

A summary of conclusions follows:

- Steady-state simulation is often less expensive and may be adequate for flows that undergo changes of large time scale compared to the observation period of interest. Also, transient behavior with time scales much shorter than this period may be neglected.

- Time scales are sensitive to geometric dimensions and proportions.

- Unsteadiness is observed in different situations:
  - when the concentration of a tracer varies along streamlines of a steady flow field (clouds of tracer gas),
  - periodic shifting of separation points under stationary boundary conditions (Karman vortex trail),
  - oscillations in un-converged numerical solutions, sometimes resulting from problems with the solution algorithm,
  - low-frequency fluctuations in real flows with natural convection or thermal plumes, and
  - fully time-dependent flows with unsteady boundary conditions.

- Low-frequency fluctuations, as observed in experiments with thermal flows, should be carefully investigated.

- Competence in accurate prediction of transient flow fields is required for air flow management in advanced ventilation control systems, in smoke control, or in large spaces with changing thermal loads (atria, lecture theaters).

- Two fluids mix better in unsteady flow. If no mixing is desired, as in displacement ventilation, fresh air should be supplied at constant rate.

- The growth of a one-dimensional laminar free convection boundary layer can be estimated by an analytical formula.

ACKNOWLEDGMENTS

This work was supported by the Swiss Federal Office of Energy (BEW).

REFERENCES

1. GOTTSCHALK, G.
"The adaptive air diffusion for variable air volume systems," ROOMVENT'87, Stockholm, Sweden, 10-12 June 1987, Vol. 2b.

2. NIELSEN, P. V.
"Numerical prediction of air distribution in rooms, - status and potentials," Presented at the Kick-Off Meeting of IEA Annex 20, Winterthur, 1988. Indoor Environmental Technology Paper No. 5, University of Aalborg Rpt. R8823, September 1988.

3. HAMMOND, G. P.
"Convective time-scales and other parameters governing air movement within building spaces," International Seminar of Air Flow Patterns in Ventilated Spaces, Liège, Belgium, Feb. 9, 1989.

4. SANDBERG, M.
"What is ventilation efficiency," Building and Environment, Vol-. 16, No. 2, pp. 123-135, 1981.

5. RAATSCHEN, W.
"Was ist Lüftungseffektivität ?" KI, Klima Kälte Heizung, Hefte 5, 6, 7, and 8, May, June, and July, 1988

6. LIDDAMENT, M. W.
"A review and bibliography of ventilation effectiveness - definitions, measurement, design and calculation," Technical Note AIVC 21, IEA Energy Conservation in Buildings, Annex 5, July 1987.

7. Private communication

8. SAID, M. Nady A.
"A review of smoke control models," ASHRAE Journal, pp. 36-40, April 1988.

9. VAN DER MAAS, J., ROULET, C.-A., HERTIG, J.-A.
"Some aspects of gravity-driven air flow through large apertures in buildings," presented at the ASHRAE Annual Meeting, Vancouver, June 1989, - ASHRAE Transactions 1989, Vol. 95, Part 2.

10. OTTINO, J. M.
"The mixing of fluids," Scientific American, Vol. 260, No.1, pp. 40-49, January 1989.

11. SCHLICHTING, H.
"Boundary Layer Theory," 7th edition, McGraw-Hill 1979.

12. MOSER, A.
Manuscript in preparation.

PROGRESS AND TRENDS IN AIR INFILTRATION
AND VENTILATION RESEARCH

10th AIVC Conference, Dipoli, Finland
25-28 September, 1989

Paper 4

AIR INFILTRATION MEASUREMENT TECHNIQUES

M.H.Sherman

Energy Performance of Buildings Group
Applied Science Division
Lawrence Berkeley Laboratory
University of California
Berkeley, California 94720
USA

Tracer gas techniques have become widely used to measure the ventilation rates in buildings. The basic principle involved is that of conservation of mass (of tracer gas) as expressed in the continuity equation; by monitoring the injection and concentration of the tracer, one can infer the exchange of air. Although there is only one continuity equation, there are many different experimental injection strategies and analytical approaches. These different techniques may result in different estimates of infiltration due to uncertainties and biases of the procedures. This report will summarize the techniques and the relevant error analyses.

As more detailed information is required for both energy and indoor air quality purposes, researchers are turning to complex, multizone tracer strategies. Both single gas and multiple gas techniques are being utilized, but only multigas are capable of uniquely determining the entire matrix of air flows. This report will also review the current effort in multizone infiltration measurement techniques.

Keywords: Ventilation, Infiltration, Tracer Gas, Multizone Measurement Techniques, Error Analysis, Uncertainty

NOMENCLATURE

C	Instantaneous tracer gas concentration [kg/m^3]
$\mathbf{C}$	Multizone tracer gas concentration matrix [kg/m^3]
C_T	Target concentration of tracer [kg/m^3]
F	Instantaneous injection of tracer gas [kg/h]
$\mathbf{F}$	Multizone tracer injection matrix [kg/h]
λ	Air Change rate [h^{-1}]
$\boldsymbol{\lambda}$	Air change rate matrix [h^{-1}]
N	Number of zones [-]
Q	Ventilation [m^3/h]
$\mathbf{Q}$	Ventilation matrix [m^3/h]
t	Time [h]
T	Length of measurement period [h]
V	Volume [m^3]
$\mathbf{V}$	Zone volume matrix [m^3]
ρ	Density of air in a zone [kg/m^3]
δX	Uncertainty in quantity X (e.g. concentration, injection, etc.)
$\overline{X}$	Time average of quantity X over measurement period T
$\dot{X}$	Time rate of change of quantity X
X_R	Indicates X is a parameter found from a regression.
X_I	Indicates X is found using an integral technique.

INTRODUCTION

The purpose of this report is to review the approaches to the use of tracer gasses in the determination of infiltration (i.e. total outside air exchange). A decade ago the author presented work on this same topic;[1] a summary of earlier work has been done by others as well.[2,3] Although the continuity equation has not changed, the tracer techniques now being used have developed in the interim. Both this report and the prior one consider both single-zone and multizone solutions, steady-state and transient methods, and potential sources of bias.

The issue of mixing (which is a rubric for phenomena such as short-circuiting, apparent flow delay, and effective volume,) was stressed heavily in the original work. Mixing must always be a serious concern in tracer gas experiments, The subject of non-tracer measurement techniques (i.e. modeling) was discussed in the original report, but, as modeling has become a topic of extensive effort, it is being reviewed by others,[4] but will not be explicitly treated, herein.

Background

Tracer gasses are used for a wide range of diagnostic techniques including leak detection[5,6] and atmospheric tracing.[7] One application which has had a resurgence in the last decade is the use of tracer gasses to measure ventilation (i.e., air flow) in buildings.[8] Ventilation is an important process in buildings because of its impact on both energy requirements and indoor air quality—both of which are topics of concern to society. Measurement of the tracer gas combined with conservation laws allows a quantitative determination of the tracer transport mechanism (i.e., a measurement of the air flow).

The vast majority of the ventilation measurements made to date have involved a single-tracer gas deployed in a single zone. This technique has proven very useful for building which may treated as a single zone (e.g., houses) and for more complex buildings in which there are isolatable sub-sections. However, as the need to understand more complex buildings has grown, tracer techniques that are able to treat multiple zones have been developed.[9] Multizone techniques recognize that not only does air flow between the outside and the test space, but there are air flows between different parts (i.e., zones) of the test space and, in the complete case, they are able to measure these flows.

As in any experimental techniques, there are uncertainties associated with the fundamental measurements and these errors propagate to become uncertainties in the determination of air flows. Some work on the optimization of the single zone problem has been done. For example, Heidt[10] has demonstrated that optimal precision in tracer decay measurement is on the order of the inverse air-change rate; and D'Ottavio[11] has shown a decrease in precision when a two-zone building is treated as a single zone.

Mixing and Ventilation Efficiency

This report summarizes tracer gas methods for determining air flows between zones, but not within them. For our purposes, zones are statistically treated as having the same concentration of tracer anywhere within a zone. We call the time it takes a zone to reach this effectively homogeneous state the mixing time. As will be discussed in following sections, techniques in which the concentration changes quickly compared to the mixing time, may be subject to significant errors.

The zonal assumption is necessary when there is no knowledge about the size and location of the inlet and exhaust flows to each zone. In cases, (e.g. mechanically ventilated rooms) in which these quantities are known, tracer gasses can be used to measure the ventilation efficiency *within* the zone. *Age of air* concepts are often used to describe spatial variation of ventilation. Sandberg[12] summarizes the definitions and some of the tracer techniques for determining the efficiency (by seeding inlet streams or monitoring exhaust streams). In this language, our mixing assumption can be stated as "the mean age of air is equal to the nominal ventilation time."

Because they are usually concerned with the highly controlled environment of mechanically ventilated buildings, those looking at age of air concepts do not normally consider the time variation of the ventilation. Conversely, the simple zonal approach assumed herein, ignores spatial variations within nominal zones. There is some preliminary modeling work[13] on combining these two approaches using more complex transfer functions for the zones. Further discussion of intrazonal air flows is beyond the scope of this report.

SINGLE ZONE VENTILATION

All tracer gas methods rely on the solution of the continuity equation to infer the ventilation from measurements of the concentrations and injected tracer flow rate. The continuity equation is as follows:

$$V \cdot \dot{C}(t) + Q(t) \cdot C(t) = F(t) \tag{1.1}$$

which can be directly solved for the ventilation:

$$Q(t) = \frac{F(t) - V \cdot \dot{C}(t)}{C(t)} \tag{1.2}$$

Equivalently, we can solve the continuity equation to predict the concentration as a function of time given all of the other quantities:

$$C(t) = \int_{-\infty}^{t} \frac{F(t')}{V} e^{\int_{t}^{t'} \lambda(t'')\,dt''} dt' \tag{1.3}$$

The common definition of air change rate, λ, is used above:

$$\lambda(t) \equiv \frac{Q(t)}{V} \tag{2}$$

As Roulet[14] points out, the continuity equation is a *mass* balance equation and serious errors can result if it is used as a *volume* balance equation unless proper precautions are taken. Accordingly, the concentrations are expressed in mass of tracer per unit volume to assure correctness even when the density of air varies from zone to zone (e.g., if the zones are at different temperatures).

If it were possible to solve eq. 1 on an instantaneous basis to find the ventilation, most of the rest of this report would be not be needed. However, because of measurement problem including mixing issues, the determination of an instantaneous ventilation value is practically impossible. Therefore it becomes necessary to use time-series data to reduce the uncertainties to make the analysis possible. The rest of this report details some of the approaches being used to overcome these measurement limitations.

The exact analytical technique for inverting the measured data to find the ventilation depends on both the experimental technique, the assumption made about the system, and the quantity of interest. The following sections develop the analysis for techniques currently in use. Virtually all of the widely used techniques assume that the ventilation is constant over the measurement period. Although this assumption is often violated, these techniques will be discussed in detail below.

GENERAL SOLUTIONS

The three versions of eq. 1 suggest three different approaches for the determination of the infiltration from the data. The term general here is used to indicated that there are no particular assumptions made about the injections or concentration other than the continuity equation itself. In following sections specific solutions which assume a particular control strategy (e.g. constant injection) will be considered.

Regression Techniques

Regression techniques use eq. 1.3 and assume that the infiltration is constant over the regression period ($0 \leq t \leq T$) and then find the best set of parameters that fit the concentration and injection data to the following equation:

$$C(t) = C_R e^{-\lambda_R t} + \int_0^t \frac{F(t')}{V_R} e^{-\lambda_R (t-t')} dt' \qquad (3)$$

The parameters C_R and λ_R are always treated as unknowns in the regression. The effective volume, V_R, may be treated as either a known or an unknown. The *precision* of the estimate of infiltration can usually be extracted from the details of the regression.

The regression will result in the best single estimate of infiltration to match the data. If the air change is constant, the regression estimate will result in an unbiased estimate of the true infiltration. If the infiltration is not constant, however, the regression will result in a biased estimate of the average air change.

Integral Techniques

Integral techniques make use of the fact that it is often easier to obtain integrals (or, equivalently, averages) of the measured data (i.e. injection and concentration) than it is to get a complete time history of both. In integral techniques the flows and concentrations are integrated from the *initial* time (i.e. t=0) to the final time (i.e. t=T). Thus, these techniques integrate eq. 1.1, assuming the infiltration is constant over the integral period:

$$Q_I = \frac{\int_0^T F(t)dt + V\left(C_{initial} - C_{final}\right)}{\int_0^T C(t)dt} \tag{4.1}$$

or, equivalently, in terms of averages:

$$Q_I = \frac{\bar{F} - V\bar{C}}{\bar{C}} \tag{4.2}$$

where the average concentration is given by

$$\bar{C} = \frac{1}{\mathrm{T}} \int_{initial}^{final} C(t)dt \tag{5.1}$$

the average accumulation is given by,

$$\bar{\bar{C}} = \frac{C_{final} - C_{initial}}{\mathrm{T}} \tag{5.2}$$

and the average injection is the total volume of injected tracer divided by the length of the measurement period:

$$\bar{F} = \frac{1}{\mathrm{T}} \int_0^{\mathrm{T}} F(t)dt \tag{5.3}$$

The uncertainty in this estimate of the infiltration is as follows:

$$\delta Q_I^2 = \frac{\delta\bar{F}^2 + \bar{\bar{C}}^2\delta V^2 + V^2\delta\bar{\bar{C}}^2 + Q_I^2\,\delta\bar{C}^2}{\bar{C}^2} \tag{6.1}$$

$$\delta\lambda_I^2 = \frac{\delta\bar{F}^2}{\bar{C}^2V^2} + \frac{\bar{F}^2}{\bar{C}^2V^2}\frac{\delta V^2}{V^2} + \frac{\delta\bar{\bar{C}}^2}{\bar{C}^2} + \lambda_I^2\frac{\delta\bar{C}^2}{\bar{C}^2} \tag{6.2}$$

where

$$\delta\bar{\bar{C}}^2 \equiv \frac{\delta C(0)^2 + \delta C(\mathrm{T})^2}{\mathrm{T}^2} \tag{7}$$

In the absence of measurement error one can show, as Axley[15] has done for the pulse technique, that the infiltration value calculated with an integral technique must have occurred sometime during the measurement period. Such an *existence proof* may be sufficient if it is exogenously determined that the ventilation moves within a narrow band. For most other purposes one wishes to know the *average ventilation* over the measurement period. If the measurement period, T, is known to be smaller than the characteristic time over which the infiltration changes, then the integral approach will give a good estimate of the average infiltration; otherwise, averaging techniques may be preferable.

Averaging Techniques

The techniques discussed so far all have assumed that the ventilation does not vary over the measurement period. The validity of this assumption will depend, of course, upon the physical situation being measured and the technique being used. If the ventilation is not actually constant over the measurement period it is not always clear what the previous techniques are actually calculating. This kind of error is qualitatively different from the types of error associated with uncertainties in the measured concentrations and flows. Average techniques are those which yield unbiased estimates of the average infiltration over the measurement period.

Although eq. 1.2 cannot practically be used to determine the instantaneous ventilation, it can be averaged over a measurement period in order to get the *average ventilation*:

$$\bar{Q} = \overline{\left(\frac{F}{C}\right)} - \frac{V}{T}\ln\left(\frac{C_{final}}{C_{initial}}\right) \tag{8}$$

This general expression can now be used to determine the average ventilation and its uncertainty for the different experimental approaches previously discussed.

The uncertainty in the estimate of the average infiltration can be estimated the following equations:

$$\delta\bar{Q}^2 = \left(\overline{\left(\frac{1}{C}\right)}\right)^2 \delta\bar{F}^2 + \left(\overline{\left(\frac{F}{C^2}\right)}\right)^2 \delta\bar{C}^2 + \ln^2\left(\frac{C_{final}}{C_{initial}}\right)\frac{\delta V^2}{T^2} + \frac{V^2}{T^2}\left(\frac{\delta C^2_{final}}{C^2_{final}} + \frac{\delta C^2_{initial}}{C^2_{inital}}\right) \tag{9.1}$$

$$\delta\bar{\lambda}^2 = \left(\overline{\left(\frac{1}{C}\right)}\right)^2 \frac{\delta\bar{F}^2}{V^2} + \left(\overline{\left(\frac{F}{C}\right)}\right)^2 \frac{\delta\bar{C}^2}{V^2} + \left(\overline{\left(\frac{F}{C}\right)}\right)^2 \frac{\delta V^2}{V^2} + \frac{\delta C^2_{initial}}{T^2 C^2_{initial}} + \frac{\delta C^2_{final}}{T^2 C^2_{final}} \tag{9.2}$$

SPECIFIC TECHNIQUES

The general techniques cited above can be simplified by controlling the injection of tracer gas in certain well-behaved ways. Different groups have used different techniques depending on practical limitations. A rather complete listing of the groups using various techniques has been compiled by the Air Infiltration and Ventilation Centre[16] and will not be repeated herein.

Steady-State Techniques

Specific techniques tend to fall into two categories: *steady-state* techniques, which measure Q and tend to minimize the effect of the accumulation of tracer in the test volume. In all steady-state techniques the experiment is so arranged that

$$\bar{c} << \frac{\bar{F}}{V} \tag{10}$$

and the accumulation can be ignored in all the steady-state techniques. which implies that

Since the steady-state techniques measure Q, an estimate of λ will have an increased error.

$$\frac{\delta\lambda^2}{\lambda^2} = \frac{\delta Q^2}{Q^2} + \frac{\delta V^2}{V^2} \tag{11}$$

Transient Techniques

Transient techniques tend to emphasize the change in tracer gas concentration in the room and measure λ; inequality 10 is never true. Although Q and λ are simply related by the volume, the building volume the participates in air exchange is usually not known very precisely and the precision of the result may depend on which of the two types of approaches is used. Because the decay techniques are transient techniques and measure λ, the error in Q is increased by the uncertainty in the volume:

$$\frac{\delta Q^2}{Q^2} = \frac{\delta\lambda^2}{\lambda^2} + \frac{\delta V^2}{V^2} \tag{12}$$

TRACER DECAY

The most widely used type of tracer measurement is that of a tracer decay. In a tracer decay test the test space is initially charged up to a concentration of tracer gas appropriate to the instrumentation and then shut-off and allowed to decay. The analysis in all decay techniques is simplified because the terms in both the infiltration and uncertainty equations, involving the injection rate vanish.

The concentration is monitored during the period of zero injection and then used to infer the infiltration rate, λ. There are three different approaches to analyzing a tracer decay, all of which are transient approaches:

Decay Regression

If there is no tracer injection and the concentration is allowed to decay from some initial value, the integral for eq. 3 vanishes and we are left with the decay equation:

$$C(t) = C_R e^{-\lambda_R t} \tag{13}$$

This equation can be fit to the measured data using regression methods. The parameters of the fit are C_R and λ_R. An estimate of the precision can be made from the regression.

The normal method of analysis uses a linear regression on the log of the concentration. This technique is extremely sensitive to zero drift and tends to overweight the contribution of lowest concentration values to the fit. A detailed error analysis of this kind of regression is beyond the scope of this report, but the uncertainty analysis from the other decay techniques can be used to give a reasonable estimate of the *precision* of this technique.

Integral Decay

If over the measurement period there is no injection of tracer, eq. 4 simplifies to the following:

$$Q_I = - \frac{V\bar{C}}{\bar{C}} \tag{14.1}$$

or, equivalently,

$$\lambda_I = \frac{C_{initial} - C_{final}}{T\bar{C}} \tag{14.2}$$

The uncertainty in these quantities can be calculated from the uncertainties in the concentrations.

$$\frac{\delta\lambda_I^2}{\lambda_I^2} = \frac{\delta\bar{C}^2}{\bar{C}^2} + \frac{\delta C_{initial}^2 + \delta C_{final}^2}{\left(C_{initial} - C_{final}\right)^2} \tag{15}$$

Two-Point Decay

For a decay test the term involving the flow and concentration becomes identically zero and the average ventilation can be determined from the initial and final concentrations:

$$\bar{Q} = \frac{V}{T} \ln\left(\frac{C_{initial}}{C_{final}}\right) \tag{16}$$

This analysis technique has been used in what is known as the **container method.**[17] If the air change rate varies over the measurement period, this technique assures an unbiased estimate of the average; it is, however, a less precise technique than the others.

The uncertainty in the ventilation can be calculated from this expression:

$$\delta\lambda^2 = \frac{1}{T^2}\left(\frac{\delta C_{initial}^2}{C_{initial}^2} + \frac{\delta C_{final}^2}{C_{final}^2}\right) \tag{17}$$

Assuming the initial and final concentration can be measured equally well,

$$\delta\bar{\lambda} \approx \frac{\sqrt{1+e^{2\bar{\lambda}T}}}{T} \frac{\delta C}{C_{initial}} \tag{18}$$

the uncertainty is minimized by making the measurement time about the same at the decay time, $T_{opt} \approx \frac{1}{\bar{\lambda}}$. Thus

$$\frac{\delta\bar{\lambda}}{\bar{\lambda}} \geq 3\frac{\delta C}{C_{initial}} \tag{19}$$

Note that this limit is inferior to the precision possible with the integral decay; such is the price of having an unbiased measurement.

PULSE TECHNIQUE

The **pulse** technique is a steady-state variant on the integral decay technique.[18] Unlike the decay techniques the measurement period begins *before* the tracer is injected and then waiting until the concentration decays. Also unlike decay techniques, the total volume of tracer gas injected into the space must be known. When the concentration has decayed sufficiently that the inequality of eq. 10 has been satisfied, the measurement can be terminated and the infiltration can be estimates as follows:

$$Q_I = \frac{\overline{F}}{\overline{C}} \tag{20}$$

The uncertainty in this estimate is as follows:

$$\frac{\delta Q_I^2}{Q_I^2} = \frac{\delta\overline{C}^2}{\overline{C}^2} + \frac{(\overline{C}^2 + \delta\overline{C}^2)V^2}{\overline{F}^2} + \frac{\delta V^2\overline{C}^2}{\overline{F}^2} + \frac{\delta\overline{F}^2}{\overline{F}^2} \tag{21}$$

Since it takes infinitely long to decay to zero the accumulation term and its uncertainty must be considered, even though it does not contribute to the estimate of the infiltration. Because the injection is usually known quite precisely and the accumulation term is made small, the last two terms can usually be neglected.

Care must be taken not to wait too long or the concentration errors could increase because of the low average value.* The concentration-term error will increase as the square root of the measurement time and the accumulation-term error will decrease exponentially as does the instantaneous concentration. The optimum time will occur when these two terms are approximately equal.

$$e^{-\lambda T} << 1 \tag{22}$$

Since the total amount of tracer injected can be known quite well, the uncertainty only depends on the ability the measure the average concentration well and the measurement time:

$$\frac{\delta Q^2}{Q^2} \approx \frac{\delta\overline{C}^2}{\overline{C}^2} + e^{-2\lambda T} \tag{23}$$

Charge Up

If the pulse is injected quickly and the mixing in the test space if quite good. The rise in concentration due to the pulse of tracer gas can be used to determine the effective volume of the test space. However, care must be taken to insure that good mixing is present and that the air change rate is not too high, before this volume measurement technique should be considered.

*A possible improvement on this technique would be to use a non-zero starting and stopping value by pre-injecting a small amount of tracer before beginning the experiment; thus allowing the accumulation term to be made smaller without needing such a long integration time. Such a technique approaches a modified *constant concentration* method, which is discussed in a later section.

CONSTANT INJECTION

If the tracer injection is non-zero, but constant the integral in eq. 3 can be simply evaluated:

$$C(t) = \frac{F}{Q_R} + \left(C_R - \frac{F}{Q_R}\right)e^{-\lambda_R t} \tag{24}$$

Although some researchers[1,19] have fit this curve directly using non-linear methods to find the ventilation and the effective volume, most use of this method has been to wait until **steady state** has been reached and then the data is fit to the steady state equation:

$$Q_R = \frac{F}{C(t)} \qquad \text{for } e^{-\lambda t} \ll 1 \tag{25}$$

Regression techniques in this instance are equivalent to an average. Multiple independent measurements of the ventilation can be used to increase the precision accordingly. Again, it should be noted that if the infiltration is not constant during the measurement period the result may be biased. The result will not be biased, however, if the following condition is met:

$$\left|\ln\left(\frac{C_{final}}{C_{initial}}\right)\right| \ll \bar{\lambda}T \tag{26}$$

Often, however, an average concentration is used in the denominator; such an approach is actually an integral approach (See the long-term average technique):

$$Q_I = \frac{F}{\bar{C}} \tag{27}$$

This approach will be biased, but not in the same way as above. As long the accumulation term remains small:

$$Q_I \leq Q_R \approx \bar{Q} \tag{28}$$

Thus, Q_R is preferable to Q_I.

Charge Up

As noted above constant injection is usually done after steady-state has been achieved. However, if the mixing is good, it may be possible to use the period of tracer accumulation (i.e. $\lambda t \approx 1$) to determine λ (or, alternatively, the effective volume). Although the mixing constraints are not as severe as in the pulse charge-up technique, similar care must be taken.

LONG-TERM INTEGRAL

The **long-term integral** method—sometimes called the long-term (concentration) average method—is a steady-state approach in which the accumulation term is minimized by using a continuous injection and averaging long enough for the T in the denominator of the accumulation term to make the term arbitrarily small. Eq. 4.2 then becomes the following:

$$Q_I = \frac{\overline{F}}{\overline{C}} \qquad \text{for} \lambda T >> 1 \tag{29}$$

Note that although this technique is usually used with constant injection, any injection pattern could be used. (When done with constant injection, this technique is sometimes referred to as the *passive ventilation measurement* technique most typically used with PerFluorocarbon Tracer.)[20] Non-constant injection is a potential source of bias in the determination of the average infiltration.

If we assume that the accumulation term is sufficiently small so that errors attributable to the accumulation term are negligible, the uncertainty is this steady-state result is simply,

$$\frac{\delta Q^2}{Q^2} = \frac{\delta \overline{C}^2}{\overline{C}^2} + \frac{\delta \overline{F}^2}{\overline{F}^2} \tag{30}$$

One potential problem with this technique is that is requires a measurement time very long compared to the decay time, but it also assumes that ventilation is constant over that time. It has been shown.[21] that even if the injection is constant, this technique always leads to a negative bias in the estimation of the ventilation unless the ventilation is quite constant. This technique is *not* recommended for use in determining the *average ventilation* in buildings.

The average ventilation is not always the quantity of interest in making tracer gas measurements. It has been shown[22] that the quantity of interest for determining the amount of pollutant dilution provided by ventilation is not the average ventilation, but a quantity called the *effective ventilation.* The passive ventilation technique directly measures the effective ventilation and so may be the technique of choice for determining pollutant dilution.

CONSTANT CONCENTRATION

In the constant concentration technique is a steady-state technique in which an active control system is used to change the amount of injected tracer to maintain the concentration of tracer at some target level, C_T. With that assumption the accumulation term is identically zero and eq. 8 can used to calculate the average ventilation from the average injection:

$$\overline{Q} = \frac{\overline{F}}{C_T} \tag{31}$$

Although it does not enter the estimate of the ventilation the accumulation term can effect the uncertainty, if the control is not perfect:

$$\frac{\delta Q^2}{Q^2} = \frac{\delta \overline{F}^2}{\overline{F}^2} + \frac{\delta \overline{C}_T^2}{C_T^2} + \frac{V^2 \delta \overline{C}^2}{\overline{F}^2} \tag{32}$$

The last term is due to the uncertainty in the accumulation term. The error in the second term comes from the difference between the average concentration during the period and the target.

EXAMPLE ERROR ANALYSES

In this section a few examples of how various techniques might be used in specific situations and what kind of uncertainties could be expected. For the purposes of these examples, it will be assumed that a single concentration measurement can be made with a 10% uncertainty scaled to the initial concentration. Although almost all analyzers have better accuracy than 10%, the vagaries of sampling and mixing make 10% a reasonable number. In any case, the calculated uncertainties will scale with this number. It will also be assumed that it is possible to make 10 measurements/hr.

The volume of the example zone will be assumed to be $100m^3$. For the decay methods only λ will be calculated and for the steady-state methods only Q will be calculated so that the uncertainty in the volume will not enter. However, (effective) it should be kept in mind that zone volumes are rarely known to better than 20% so that the additional error could be significant.

Average Decay

UNCERTAINTIES FOR AN AVERAGE DECAY				
$\delta\lambda$	$\bar{\lambda}[h^{-1}]$			
T	0.25	0.5	1	2
20 min	0.443 (**177%**)	0.464 (**93%**)	0.515 (**52%**)	0.657 (**33%**)
1 hour	0.163 (**65%**)	0.193 (**39%**)	0.290 (**29%**)	0.746 (**37%**)
3 hours	0.078 (**31%**)	0.153 (**31%**)	0.670 (**67%**)	13.4 (**672%**)
8 hours	0.093 (**37%**)	0.683 (**137%**)	37. (**3726%**)	∞

The last row should never be used in a real experiment, but it serves to demonstrate what can happen to the precision if the decay goes on too long.

Integral Decay

As can be seen from the average-decay uncertainty analysis, the uncertainties begin to increase for long measurement times and high air exchange rates. This increase is due to the fact that the final concentration begins to get quite low and, hence, quite uncertain. The alternative decay procedures do not suffer from this and can give better precision in this range—*provided the air change rate can be assumed to be constant.*

UNCERTAINTIES FOR AN INTEGRAL DECAY				
$\delta\lambda$	$\lambda[h^{-1}]$			
T	0.25	0.5	1	2
20 min	0.442 (**177%**)	0.462 (**92%**)	0.503 (**50%**)	0.607 (**30%**)
1 hour	0.160 (**64%**)	0.181 (**36%**)	0.229 (**23%**)	0.356 (**18%**)
3 hours	0.067 (**27%**)	0.093 (**19%**)	0.160 (**16%**)	0.359 (**18%**)
8 hours	0.041 (**17%**)	0.076 (**15%**)	0.167 (**17%**)	0.456 (**23%**)

The last row of this table suggests that good precision can be achieved for longer measurement periods with an integral decay. However, an eight hour measurement period may only be justified if the infiltration were known to be constant. It should be noted that this technique is quite sensitive to errors caused by offsets in the concentration measurement. If there is no zero offset (and if the concentration measurement is still random at low values), the integral method has the potential for greater precision than the general decay method; the cost for this is potential bias if the infiltration is not constant.

If the weighting is done correctly, the regression decay has the potential for the same level of error as the integral decay. However, if the standard method is used, the regression decay will give unreliable results when the concentration is allowed to decay too far.

Pulse Method

For the pulse method it is assumed that the amount of injected tracer is known to better than 1% and can be neglected in the error analysis.

UNCERTAINTIES FOR THE PULSE METHOD				
δQ	$\bar{Q}[m^3h^{-1}]$			
T	25	50	100	200
20 min	23 (92%)	42 (85%)	72 (72%)	103 (51%)
1 hour	19 (78%)	30 (61%)	37 (37%)	30 (15%)
3 hours	11 (47%)	11 (23%)	8 (8%)	22 (11%)
8 hours	3 (14%)	2 (5%)	9 (9%)	36 (18%)

As in the decay methods, an eight hour measurement period may only be justified if the infiltration were known to be constant. Also like the decay methods, this technique is sensitive to zero offsets.

Because of the trade-off between additional measurement points, accumulation term, and low average concentration, the pulse technique's precision behavior is complex. However, there is an optimal measurement time for any given experimental set of conditions, which tends to be longer than for the decays.

Constant Concentration

The constant concentration method will be used as an example of the general steady-state method. It is assumed that the control is unbiased (i.e. that there is no difference between the *mean* concentration and the target. It is also assumed that the average flow can be determined to 1% precision; not all constant concentration systems can achieve this, but many can. With these assumptions and for the example values chosen, the error is dominated by the uncertainty in the accumulation term:

UNCERTAINTIES FOR CONSTANT CONCENTRATION				
δQ	$\bar{Q}[m^3h^{-1}]$			
T	25	50	100	200
20 min	42 (**170%**)	43 (**85%**)	43 (**43%**)	44 (**22%**)
1 hour	14 (**57%**)	14 (**28%**)	15 (**15%**)	16 (**8%**)
3 hours	5 (**19%**)	5 (**10%**)	5 (**5%**)	6 (**3%**)
8 hours	2 (**7%**)	2 (**4%**)	2 (**2%**)	3 (**2%**)

The absolute error in the table does not depend much on the infiltration, but on the measurement time. (This result is a consequence of the high measurement rate and the small injection error.) If the measurement time were extended, this trend would change.

DISCUSSION OF SINGLE-ZONE METHODS

SUMMARY OF MEASURMENT METHODS			
NAME	*MEASUREMENT TYPE*	*FLOW CONTROL*	*BIASED AVERAGE?*
TRANSIENT METHODS (measure λ)			
(Simple) Decay	Regression	Decay	Yes
Two-Point Decay	Average	Decay	No
Integral Decay	Integral	Decay	Yes
Charge Up	Regression	Const. Inj./Pulse	*
STEADY-STATE METHODS (measure Q)			
Pulse	Integral	Pulse	Yes
Constant Injection	Regression	Constant Injection	No
Long-Term Integral	Integral	Any	Yes
Constant Concentration	Average	Constant Concentration	No
* Usually used with other methods to ascertain effective volume.			

The choice of method to use in a given situation will depend on the practical details of the experiment as well as the reason for measuring the air change in the first place.

Decay and pulse methods require the least time and usually the least preparation. With the exception of the two-point method, all of these give biased estimates of the average air change rate. In most circumstances, however, the biases will be negligible as long as the measurement period is limited to times on the order of the air change time. Although unbiased, the two-point method may yield unacceptably large uncertainties in the air change rate, unless the precision in the measurement of those two concentrations can be made quite high.

Like the pulse technique, the long-term integral technique may yield a biased estimate of the average infiltration. Because of the much longer measurement period, however, the bias may not be negligible. Although the long-term technique may prove unacceptable for determining average infiltration, it can

nevertheless provide an unbiased estimate of the effective air change rate.

The constant concentration technique can be both accurate and precise, but it requires the most equipment as well as sophisticated control systems and real-time data acquisition. The constant injecting technique (without charge-up) can be considered a somewhat simplier version of the constant concentration technique, in that no active control of the injection rate is needed. Rather segments of data which meet eq. 26 are used to determine the average infiltration. If this condition is not met eq. 8 must be used to analyze the data.

MULTIZONE MEASUREMENT TECHNIQUES

Single-zone (single-gas) measurement techniques have been used extensively in a wide variety of situations and by a large number of different people. Field experience has yielded a significant amount of practical knowledge about the limitations of the techniques. For complex buildings (i.e. those whose interiors are not a simple, well-mixed zone) cannot be easily described by a single-zone infiltration measurement. Thus, one might wish to determine flows to and from multiple zones in the building to better understand it. Although multizone techniques have been utilized and discussed for over a decade[1,23,24] there has not been the same level of investigation or use.

To develop a multizone infiltration measurement technique, a *matrix* form of the continuity equation must be used:

$$\mathbf{V}\cdot\dot{\mathbf{C}}(t) + \mathbf{Q}(t)\cdot\mathbf{C}(t) = \mathbf{F}(t) \tag{33.1}$$

For every zone of the system there will be a row in both the concentration and injection matrices. For every unique tracer there will be a column in those matrices. If there are N zones, the volume and air flow matrices will be square matrices of order N and the continuity equation can be rewritten with explicit indices:

$$\sum_{j=1}^{N}\left[V_{ij}\dot{C}_{jk}(t) + Q_{ij}(t)C_{jk}(t)\right] = F_{ik}(t) \tag{33.2}$$

If there are as many tracer species as there are zones, the problem is called *complete* and there will be an exact answer. Incomplete techniques, however, may still contain useful information and will be discussed at the end of the report.

The measured data are the flows and concentrations of each tracer gas in each zone. Specifically, $\dot{C}_{ij}$, C_{ij}, and S_{ij} all represent the respective value of the jth tracer gas in the ith zone. The volume matrix can either assumed to be independently determined or derived from the measured data. For most practical purposes the volume matrix can be assumed diagonal with the individual zone volumes as the entries. If, however, there is *short circuiting* of the injected tracer from one zone to another, it can manifest itself as an off-diagonal volume element, but the sum of each column must be equal to the (effective) physical volume of the zone.

The interpretation of the air flow matrix requires a bit more explanation. The diagonal elements, Q_{ii}, represent the total flow out of that zone to all other zones and should have positive sign. The off-diagonal elements represent the flows between zones; specifically, $-Q_{ij}$ is flow from the jth zone to the ith zone. Since

the flow from the jth zone to the ith zone can be different from the flow from the ith zone to the jth zone, this matrix will in general not be symmetric.

The flow matrix explicitly contains information about flows between measured zones and the total flow. If there are flows to zones other than those being measured (e.g., outside), the sum of some rows and columns of the flow matrix will be positive; and system is said to be *open.* If all zones of the building are monitored these flows to "elsewhere" are attributed to air exchange with the outside.

Conceptually, the three types of techniques (integral, regression, and averaging) can be applied for the multizone case as well as the single-zone case. For each approach, there are complications that arise due to the multizone nature of the problem The integral technique is the most straightforward generalization of the three approaches:

$$\mathbf{Q}_I = \left(\overline{\mathbf{F}} - \mathbf{V}\cdot\overline{\mathbf{C}}\right)\cdot\left(\overline{\mathbf{C}}\right)^{-1} \tag{34}$$

Like the single-zone case, there can be significant bias in the estimate—if the measurement period is too long. Because of the many air flows involved, the requirement is even more stringent in the multizone case. Furthermore, it is *not* necessary true that the result of this technique ever occurred during the measurement period.

The single-zone regression and averaging techniques rely on the integration of a simple first order differential equation in the concentration to get analytic solutions. The matrix nature of the multizone problem increases the practical difficulty of this significantly to the point where no general solution can be profitably presented. Specific solutions, however, will be presented below

The uncertainty analysis associated with multizone ventilation is sufficiently detailed that it will not be repeated here. The reader is referred to the literature.[25]

MULTIZONE DECAYS

For a decay technique the continuity equation becomes a set of coupled homogeneous, linear differential equations, whose solutions are linear combinations of decaying exponentials.

$$\lambda(t)\cdot\mathbf{C}(t) = -\dot{\mathbf{C}}(t) \tag{35}$$

Thus as the early work by Sinden[26] has demonstrated it can be reduced to an *eigenvalue* problem. From the eigenvalues and eigenvectors, the infiltration matrix can be recomposed.

Although this technique has been under academic study,[27,28] the constraints on the mixing time and data capture rate are so extreme that it may not be generally practicable. Because the coupled equations are solved by decoupling them into a set of higher order simple differential equations, uncertainties in the concentration can lead to very large uncertainties in the eigenvalues and thus in all of the terms of the matrix. Thus, the ability of the analysis to extract the flow rates will be limited as the number of zones increased.

In considering the analysis of their multizone decay data, Enai[29] has demonstrated that the optimal analysis period is between the mixing time and the longest time constant of the system. Eigenvalues far from the analysis time will, thus, be poorly determined. In this same report, mixed decay and constant injection strategies were employed, but no improvement in the analysis were found.

Integral Decay

Although it may contain an integral bias, the integral decay method is much more robust for the multizone decay than is an eigenvalue decomposition, and thus is usually superior:

$$\lambda_I = -\bar{\dot{C}} \cdot \bar{C}^{-1} \tag{36}$$

If a unique tracer gas is injected into each zone both matrices on the right-hand side will tend to be well-conditioned.

MULTIZONE STEADY-STATE

The difficulty of the analysis and the high degree of potential uncertainty make transient multizone techniques less attractive. The steady-state techniques, however, do not suffer from the same problems. The condition of steady-state can be summarized as follows:

$$\overline{\left(F(t) \cdot C(t)^{-1}\right)} >> \overline{\left(V \cdot \dot{C}(t) \cdot C(t)^{-1}\right)} \tag{37.1}$$

which is usually equivalent to

$$\bar{\dot{C}} << \bar{\lambda} \cdot \bar{C} \tag{37.2}$$

and will always be satisfied if

$$\bar{\dot{C}} << V^{-1} \cdot \bar{F} \tag{37.3}$$

where the comparisons are done element-by-element and are independent of sign.

Thus the average infiltration is as follows:

$$\bar{Q} = \overline{\left(F(t) \cdot C(t)^{-1}\right)} \tag{38}$$

Multizone Integral

In the multizone long-term integral method is analogous to the single-zone method:

$$Q_I = \bar{F} \cdot \left(\bar{C}\right)^{-1} \tag{39}$$

in that it uses the average injections and concentrations and it has at least the same potential for bias. Thus, it might be more accurate to use a *multizone pulse* technique[15], than to use a *long-term multizone* concentration integral technique).[30]

MULTITRACER MEASUREMENT SYSTEM

An intermediate technique currently in use by the author is called the multitracer measurement system (MTMS),[31] in which the concentration of tracer gasses are held in reasonably narrow ranges and the analysis is an integral analysis over a short time period (i.e. T≈½*h*):

$$Q = \left(\overline{F} - V \cdot \overline{C}\right) \cdot \left(\overline{C}\right)^{-1} \tag{40}$$

The ostensibly large uncertainty reduced by using a high data rate and physical limits on the infiltration values.[32]

MULTIZONE CONSTANT CONCENTRATION

The MTMS technique does not control the concentrations of all gasses in all zones and, hence, could not be a true constant concentration system. There are currently no systems that do control all gasses in all zones, and unless a reasonable method exists for effectively injecting *negative* amounts of tracer gas, there will be no *complete* multizone constant concentration system practical.

Although complete multizone constant concentration systems are not in use, there are single-gas multizone ones in operation.[33,34] Such single-gas systems cannot measure any of the zone-to-zone air flows, but they attempt to measure the infiltration from outside to each zone. Without some knowledge of the interzonal air flows, however, it is impossible to estimate the uncertainty of these infiltrations[25]. However, with reasonable control[35] and low interzonal air flows, the precision can be acceptable.

Other Incomplete Approaches

If there are an insufficient number of tracer gasses available for a complete analysis, there are various other approaches for determining the infiltration matrix (e.g. in this conference).[36] Almost all of these approaches use multiple sets of data taken at different times (e.g. using constant emission[24] or multiple decay tests) Thus the columns in the concentration and flow matrices are not different tracers taken simultaneously, but some tracer taken at different times. Various control strategies such as charge-up, decay, rotating injection, etc. can be used in these approaches. For example, a general, regression, pulse technique is being used,[37] to measure both the air flow rates and effective volumes using a single-tracer gas. All of these approaches must assume that the air flows do not change over the time of the entire measurements; regardless of the analysis approach used the measurement time will be significantly longer than if multiple tracers were used.

Another method of extracting useful information in an incomplete system is to use a second gas an an erstwhile single-gas constant concentration system .[38] In such a system one of the interzonal flows (and all of the infiltrations from outside) can be measured at a time.

DISCUSSION OF MULTIZONE METHODS

Single-gas constant-concentration systems are increasing in use and provide a bridge between single-zone techniques and a complete multizone technique. This technique is ideal for zones that are not well-connected and for which the outside air infiltration is the quantity of interest. As indoor air quality concerns increase, multigas systems may become more popular.

The only multigas technique in common usage is the long-term integral technique using PFTs. However, care must be taken in interpreting these numbers as averages under varying conditions.

Incomplete techniques that require sequential measurements (e.g. repeated single-gas decays) like the long-term concentration average method suffer from sensitivity to variations in the air flows. These techniques should not be used if the air flow changes significantly (with respect to the uncertainty of the estimates) over the course of the complete experiment.

The short-term integral techniques (i.e. decay and pulse) show great promise for relatively simple determination of multizone air flows and may be the technique of choice for spot measurements.

Real-time systems such as MTMS offer a complete solution, although they are much more complex and cumbersome. Constant injection techniques with appropriate (i.e. inverse) concentration averaging is also a technique worth considering for continuous operation.

There are far fewer multizone measurement techniques in use compared with the single-zone ones, so it is far too early to do a complete summary, but there will undoubtedly be more to summarize in ten years.

REFERENCES

1. Sherman, M.H., Grimsrud D.T., Condon, P.E., Smith B.V., "Air Infiltration Measurement Techniques" Proceedings 1st AIC Conference *Air Infiltration Instrumentation and Measuring Techniques*", Air Infiltration and Ventilation Centre, Coventry, UK, (1980)
   Lawrence Berkeley Laboratory LBL-10705, 1980

2. Hunt, C.M., "Air Infiltration: A Review of Existing Measurement Techniques and Data," *Building Air Change Rate and Infiltration Measurements*, ASTM STP 719, pp. 3, American Society for Testing and Materials, Philadelphia PA (1980).

3. Lagus, P.L., "Air Leakage Measurements by the Tracer Dilution Method — A Review," *Building Air Change Rate and Infiltration Measurements*, ASTM STP 719, pp. 3e, American Society for Testing and Materials, Philadelphia PA (1980).

4. Feustel, H.E., "Mathematical Modeling of Infiltration and Ventilation," Proceedings 10th AIVC Conference *Progress and Trends in Air Infiltration Research*, Air Infiltration and Ventilation Centre, (1989).

5. Singer, P.H., "Helium Leak Detection in Vacuum Systems and IC Packages", *Semicond. Int.* **10 (11),** pp. 51-5 (1987).

6. McCullough, R., "Leak Testing", *ASTM Standardization News,* **10 (11),** pp. 32-3 (1982).

7. Ferber, G.J., Telegadas, K., Heffter, J.L., et al., "Demonstrations of a Long-Range Atmospheric Tracer System Using Perfluorocarbons," BNL-33846, Brookhaven National Laboratory (1983).

8. Lagus P., Persily, A.K., "A Review of Tracer Gas Techniques for Measuring Airflows in Buildings," *ASHRAE Transaction* **91**(IIB) p1075-1087 (1985).

9. Harrje, D.T., Dutt, G.S., Bohac, D.L., "Documenting Air Movements and Infiltration in Multicell Buildings Using Various Tracer-gas Techniques," *ASHRAE Transaction,* **91(II) (1985).**

10. Heidt, F.D. and Werner, H., "Microcomputer-aided Measurement of Air Change Rates", *Energy and Buildings,* **9**, pp 313-320 (1986).

11. D'Ottavio, T.W., Dietz, R.N., "Errors resulting from the use of single zone ventilation models on multi-zone buildings: implications for energy conservation and indoor air quality studies," *ASHRAE Transaction* **91**(II) (1985).

12. Sandberg, M., Sjoberg, M., "The use of moments for assessing air quality in ventilated rooms," *Building & Environment,* **18**, pp181(1983)

13. Axley J., "Multi-zone contaminant dispersal analysis using an element assembly approach," Proceedings 9th AIVC Conference *Effective Ventilation* II pp. 157. (1988)

14. Roulet, C.A., Compagnon, R, "Multizone Tracer Gas Infiltration Measurements Interpretation Algorithms for Non Isothermal Cases, In press *Building & Environment,* **24** 1989.

15. Axley J., Persily, A., "Integral mass balance and pulse injection tracer-techniques," Proceedings 9th AIVC Conference *Effective Ventilation* I pp. 125. (1988)

16. Charlesworth, P.S., "Air Exchange Rate and Airtightness Measurement Techniques — An Applications Guide, Air Infiltration and Ventilation Centre, (1988)

17. -, "Standard Test Method for Determination Air Leakage Rate by Tracer Dilution", *ASTM E 741-83,* Annual Book of Standards, American Society of Testing and Materials, **04.07**, 1988.

18. Axley J., Persily, A., "Measuring Air Flow Rates with Pulse Tracer Techniques," in ASTM STP 1067 *Air Change Rate and Air Tightness in Buildings,* M. Sherman Ed. American Society of Testing and Materials Philadelphia, (1989)

19. Blomsterberg, A.K., Modera, M.P., Grimsrud, "The Mobile Infiltration Test Unit — Its Design and Capabilities", Lawrence Berkeley Laboratory, LBL-12259, 1981

20. Dietz, R.N. et al., "Detailed Description and Performance of a Passive Perfluorocarbon Tracer System for Building Ventilation and Air Exchange Measurements," in *Measured Air Leakage of Buildings* ASTM STP 904, Trechsel/Lagus Ed., American Society of Testing and Materials, 1986.

21. Sherman, M.H., "Analysis of Errors Associated with the Passive Ventilation Measurement Technique," *Building & Environment* **24**(2), pp. 131-139,(1989). Lawrence Berkeley Laboratory Report LBL-23088 (1988)

22. Sherman M.H., Wilson D.J., "Relating Actual and Effective Ventilation in Determining Indoor Air Quality", *Building & Environment* **21**, pp.135-144, (1986).

23. Condon, P.E., et al., "An Automated Controlled-Flow Air Infiltration Measurement System", *Building Air Change Rate and Infiltration Measurements,* ASTM STP 719, pp. 60, American Society for Testing and Materials, Philadelphia PA (1980).

24. Grimsrud, D.T. et al., "Infiltration-Pressurization Correlations: Detailed Measurements on a California House," *ASHRAE Transaction* **85**(I), (1979).

25. Sherman M.H., "Uncertainty of Air Flow Calculations Using Tracer Gas Measurements," *Building & Environment* (1989)

26. Sinden, F.W., "Multichamber Theory of Air Infiltration", *Building & Environment* **13**, pp 21, (1978)

27. Irwin, C, "A method of Measuring Air Movements in Compartmentalized Buildings," Ph.D. dissertation, University of Manchester, UK (1985)

28. Prior, J.J., "A New Multitracer Gas Technique for Measuring Interzonal Air Flows in Buildings," Ph.D. dissertation, Polytechnic of Central London, UK, (1985)

29. Enai, M. Shaw, C.Y., Reardon, J.T., "On the Multiple Tracer Gas Techniques for Measuring Interzonal Airflows in Buildings," *ASHRAE Transaction* (In Review), 1990.

30. Sateri, J. et al. "The Performance of the Passive Perfluorocarbon

Method," Proceedings 10th AIVC Conference *Progress and Trends in Air Infiltration Research*, Air Infiltration and Ventilation Centre, (1989).

31. Sherman, M.H., Dickerhoff, D.J. "A Multigas Tracer System for Multizone Air Flow Measurements" To be published in *Proceedings* Thermal Performance of Exterior Envelopes of Buildings, IV Conference [Orlando FL, Dec. 1989], *ASHRAE*

32. Sherman M.H., "On Estimation of Multizone Ventilation Rates from Tracer-Gas Measurements," *Building & Environment* (1989)

33. Kvisgaard, B., Collet,. P.F. and Kur, J. "Research on Fresh-air Change Rate: 1", Rpt. Tech. Inst. of Copenhagen, ISBN 87-5711-460-7 (1985).

34. Bohac, D.L., "The Use of a Constant Concentration Tracer Gas System to Measure Ventilation in Buildings," *PU/CEES Rpt.* **No. 205**, Princeton University (1986).

35. Comapgnon, R., et al., "Development of an efficient control algorithm for a multizone constant concentration tracer gas air infiltration measurement system," Proceeding 9th AIVC Conference *Effective Ventilation* II pp. 103. (1988)

36. Edwards, R.E., Irwin, C., "A Comparison of Different Methods of Calculating Interzonal Airflows from Multiple Tracer Gas Decay Tests," Proceedings 10th AIVC Conference *Progress and Trends in Air Infiltration Research*, Air Infiltration and Ventilation Centre, (1989).

37. O'Neil, P.J., Crawford, R.R., "Multizone Flow Analysis and Zone Selection using a New Pulsed Tracer Gas Technique," Proceeding 10th AIVC Conference *Progress and Trends in Air Infiltration Research*, Air Infiltration and Ventilation Centre, (1989).

38. Kvisgarrd B, Collet, P, "Constant Concentration Measurement with 2 Tracers," Proceedings 9th AIVC Conference *Effective Ventilation* I pp. 183. (1988)

Discussion

Paper 4

Bjorn Hedin (Lund Institute of Technology, Sweden)

On page 20, under the subheading "other incomplete approaches" you mention the single gas method in paper 5 due to O'Neill and Crawford. But in my opinion this method does indeed look very "complete" since both the entire flow matrix and the effective volume can be determined. What is "incomplete" referring to?

Max Sherman (LBL, USA)

It is not that incomplete systems such as the one suggested by O'Neill and Crawford are absolutely incapable of determining all of the flows; rather, incomplete systems are incapable of resolving all of the flows simultaneously. Thus some strong assumption is necessary in order to infer the complete system from incomplete data. In this case it is necessary to assume that all the airflows are constant over the measurement period. In a real situation the flows may vary significantly, but no estimates are usually given for the sensitivity of the results to such variation.

To get meaningful results in a field situation inverse methods and system identification techniques must be robust. Incomplete techniques are necessarily less robust than complete techniques, but that does not necessarily mean they are unusable. Careful analysis of the uncertainties and sensibilities to the assumptions need to be made. From those it can be determined whether or not a specific technique is suitable in a specific situation for a specific purpose.

Rodger Edwards (UMIST, UK)

My apologies for not forwarding a copy of our conference contribution as requested, but I was extremely late in submitting the paper (as witnessed by its absence from the book of proceedings!).

Your paper was a most informative piece of work. However, I should point out that the UMIST multiple tracer gas technique operates (and indeed always has operated) on the basis of one tracer gas per zone.

Max Sherman (LBL, USA)

Thank you for correcting my misclassification of your system.

David Harrje (Princeton University)

Under topic "multizone constant concentration" you state "Such single gas systems cannot measure any of the zone-to-zone air flows, but they attempt to measure the infiltration from outside to each zone - - - without interzone air flows it is impossible to estimate the uncertainty of these infiltrations ". This places a completely false impression in the mind of the reader. Using close control of tracer concentration in each zone, accurate infiltration values are provided. Removing tracer gas to individual zones, Bohac et al in AIVC Conference 8 demonstrated how interzone flows can also be measured with a single gas using the constant concentration system under stable ventilation conditions. Low interzonal air flows are not necessary for a CCTG system to provide suitable zone ventilation measurements and the section should be corrected.

Max Sherman (LBL, USA)

The text is correct but may be incomplete. It is of course true that the better the control, the smaller the uncertainty, but the suitability of the results for some purpose can only be determined by using an estimate of the error in the results. While it is not possible to calculate the uncertainty without an estimate of the interzonal flows, it may be possible to set upper limits on the uncertainty - if bounds on these flows can be estimated exogenously. I have found no published procedure for setting these bounds, but I am aware of efforts by Richard Grot at the National Institute of Standards and Technology to estimate upper limits for constant concentration techniques.

PROGRESS AND TRENDS IN AIR INFILTRATION AND VENTILATION RESEARCH

10th AIVC Conference, Dipoli, Finland
25-28 September, 1989

Paper 5

THE PERFORMANCE OF THE PASSIVE PERFLUOROCARBON METHOD

J. SATERI[1], P. JYSKE[2], A. MAJANEN[1], AND O. SEPPANEN[1]

[1]Helsinki University of Technology
02150 Espoo
Finland

[2]University of Helsinki
Division of Analytical Chemistry
00100 Helsinki
Finland

SYNOPSIS

The use of passive perfluorocarbon technique for air flow measurements has been developed and tested. The building and testing of the system took approximately one year. The reproducibility of the analysis was tested during the period. The results show that the relative standard deviation of the analysis for parallel samples is less than 7 % for each tracer in most of the cases. A drift of calibration was noticed, but it can be allowed for by using reference samples with known amounts of tracers.

The accuracy of the method was tested in controlled laboratory conditions. The results reveal some rather high differences from the reference, though the results are distributed evenly on both sides of the zero line. With few exceptions, the inaccuracy of the PFT-method can be estimated to be approximately ±20 %, when PMCP or PMCH are used. For PDCH the inaccuracy is somewhat higher. Improving the calibration procedure and allowing for the drift of calibration should improve the accuracy of the method. The test in a duct flow implies that the use of the method should be limited to room flow conditions until further research has been done.

The mixing was tested in laboratory and field conditions. The results of the laboratory measurements show that the mixing was good, the relative standard deviation being generally below 10%. No stratification could be found. Field measurements were made in 50 typical Finnish homes. When the interior doors within the zone were kept open during the measurement, the concentration distribution was uniform. The standard deviations of concentration varied from 1% to approximately 25%.

The technique is best suited for studies concentrating on the health and comfort of the people living in the house. If the energy use of ventilation is studied, the use of an integrating technique should be limited to cases with little temporal variation. The technique is applicable to large field surveys of ventilation. Anyhow, the complexity of room ventilation limits the number of potential users of the method. It is important to have enough knowledge of room ventilation in order to be able to conduct the measurements properly and to interpret the results correctly.

1 INTRODUCTION

The aim of this study was to develop the use of the passive perfluorocarbon tracer gas method applicable to field measurements in a large number of homes. The use of the passive multi–tracer technique solves many of the problems normally involved in inexpensive and simple field measurements. There are,however, some important problems to be solved. The project was divided into two tasks: building and testing of the analysis system and testing of the reliability of the method.

This paper describes the applied ventilation measurement model and the research done on the testing of the method. The performance of the sources, samplers and the analysis system is discussed. The measurements made to test the accuracy of the method are described. The mixing of tracers in zones was tested with laboratory tests and field measurements in 50 homes. The results are also discussed.

2 DESCRIPTION OF THE APPLIED PFT-TECHNIQUE

2.1 The principle of the measurement

The passive perfluorocarbon air infiltration measurement technique is based on the principles presented by Dr. Dietz at Brookhaven National Laboratory[1]. It is a constant emission technique with passive adsorption sampling of tracers. Each individual ventilation zone of the building is traced with separate gas. The gas emission is achieved with passive permeation sources giving a constant tracer flow. The (quasi–) equilibrium concentration is monitored with a passive adsorption tube sampler. The typical measurement period can vary from few days to several weeks. The samples are analysed in a laboratory using a gas chromatograph with an electron capture detector. The passive tracer sources and adsorption samplers were supplied by Dr. Dietz. The analysis system is a copy of the system used by Dr. Harrje at Princeton University[2]. At the moment three different tracer gases are used.

2.2 The ventilation measurement model

The model is based on the multi–zone models presented by Sandberg[3] and Sherman[4]. A building consists of zones with uniform and instantaneous internal mixing such as that in Fig. 1. The air flows within the multi–zone system can be presented in matrix form:

$$\mathbf{Q} = \begin{pmatrix} Q_{11} & -Q_{12} & \cdots & -Q_{1N} \\ -Q_{21} & Q_{22} & \cdots & -Q_{2N} \\ \vdots & \vdots & \ddots & \vdots \\ -Q_{N1} & -Q_{N2} & \cdots & Q_{NN} \end{pmatrix} \qquad (1)$$

In the flow matrix Q the first index denotes the destination and the second index the origin. N is the number of zones in the system. The row sum of the flow matrix is equal to the total flow rate of outdoor air direct to zone

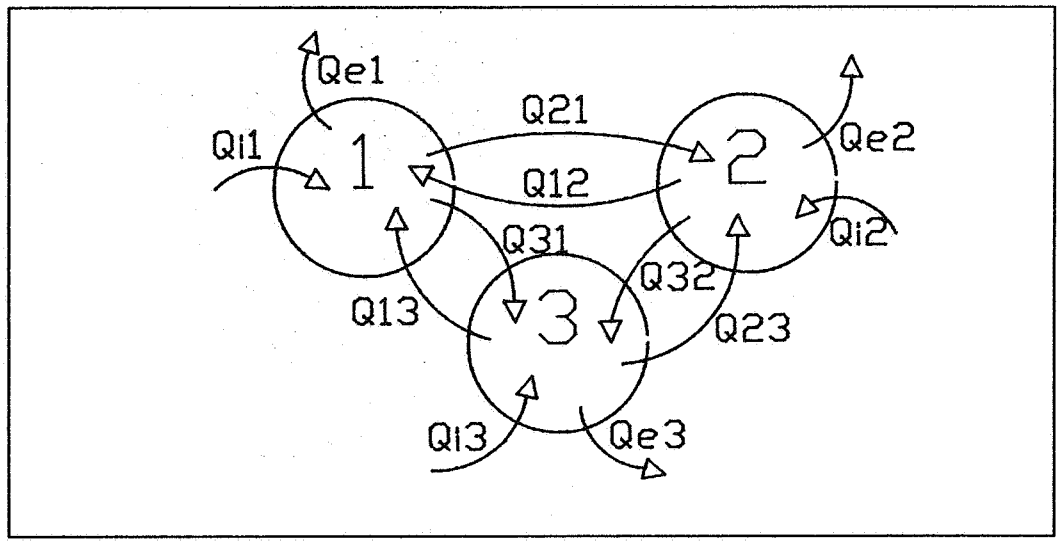

Figure 1: A multi–zone system

i and the column sum of the flow matrix indicates the total flow rate of air transferred outdoors from zone j. In the passive perfluorocarbon method a tracer gas is supplied at a constant rate to each zone. The diagonal source matrix S is composed of the emission volume rates. Constant emission and constant air flows yield a steady–state concentration of tracers in each zone. The concentration is monitored with passive adsorption samplers and a gas chromatograph. The concentration matrix C is composed analogously to the flow matrix. It can be shown[3] that the steady–state flow rates in the system can be solved from a set of linear differential equations written in matrix form:

$$\mathbf{Q} = \mathbf{S} \times \mathbf{C}^{-1} \tag{2}$$

This approach can be used only when measuring relatively constant air flows. With temporally varying air flows there will be a bias due to the lower efficiency of a varying air flow[4]. A quantity that better describes the performance of the ventilation system with temporally varying air flows is the age of contaminants in the exhaust, the turn–over–time. It can be shown that the turn–over–time matrix, which shall be denoted as $\mathcal{T}_t$, can be calculated from the following equation:

$$\mathcal{T}_t = \bar{\mathbf{C}} \times (\mathbf{V}^{-1} \times \mathbf{S})^{-1} \tag{3}$$

In Eqn. 2 the matrix $\bar{\mathbf{C}}$ consists of the (time–) average concentrations measured with integrating sampling. The turn–over–time is directly related to the human respiratory exposure to indoor air pollutants and can thus be used in examining the effects of ventilation on the health of the people living in the house. If the air flow rates are constant with time and there is uniform and instantaneous internal mixing in the system, the turn–over–time is equal to the nominal time–constant.

Table 1: The calibration of the tracer sources (22.0 ^oC)

Lot	PMCP			PMCH			PDCH		
	Man. Code	Emis. nl/min	std %	Man. Code	Emis. nl/min	std %	Man. Code	Emis. nl/min	std %
1	B	38.48	2.8	C	25.34	4.4	C	16.72	8.9[a]
2	F	31.44	1.2	F	22.20	0.6	F	15.07	0.8
3[b]	G	31.65	1.4	G	22.94	1.8	H	12.25	2.8

[a]Reduced to 5.0 % after excluding 4 outliers differing over 10% from the average
[b]Calibration temperature 22.6 ^oC

3 THE PERFORMANCE OF THE INSTRUMENTS

3.1 The passive tracer sources

In the tracer source liquid perfluorocarbon tracer is sealed with a silicone rubber cap in an aluminium capsule. The gas flow is determined by the differences of the vapour pressure of the tracer over the rubber cap and the permeability of the cap material. The emission varies for two main reasons: the unreproducibility of manufacturing and the temperature of the liquid. In order to estimate the effects of these deviations the sources were calibrated individually. The sources were kept in a constant temperature for two weeks. After that the sources were weighed using a precision balance twice at a week's interval. The volume emission of each tracer was calculated from the change of mass over the weighing interval using the ideal gas law. The emissions were corrected with the purities of the liquids given by the manufacturer. Three main lots of sources were used. The results of the calibrations are presented in table 1.

The effect of temperature on the emission rate was tested by splitting the lot of 40 sources into six different calibration temperatures. The weighing procedure was as described earlier. The results of these measurements are shown in Fig.1.

The results show that there is no need to use an individual emission rate for each source—one rate for each manufacturing lot is enough. Due to the existence of outliers (as in Lot 1,PDCH) all sources should be checked at least once before use.

The effect of temperature on the emission rate correlated well with the data given by the manufacturer[5]. A change in temperature of one degree changes the emission by 3–5 %. Thus it is very important to know the source temperature during the field measurement.

3.2 The samplers and the analysis system

The sampling is based on Ficks diffusion in a glass tube. On the open end of the tube is the equilibrium concentration produced by the emission and air flows. Packed inside the tube is charcoal-like adsorbent, which has, due

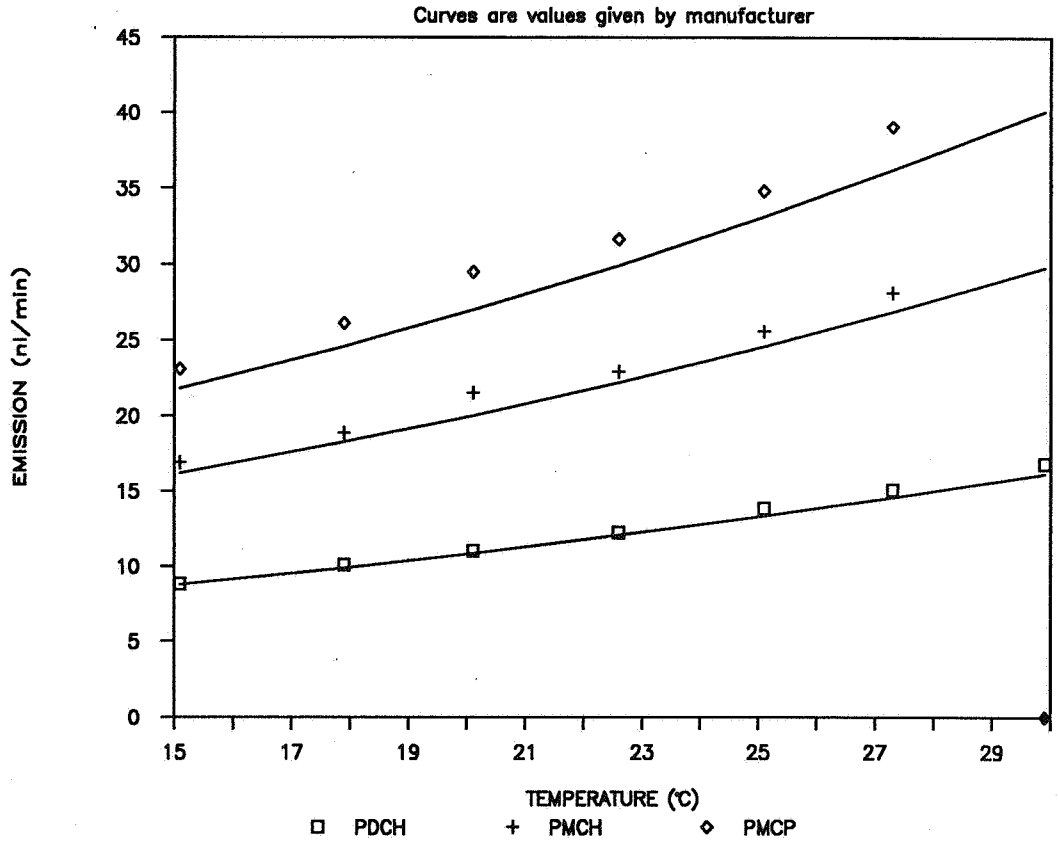

Figure 2: The effect of temperature on the emission rate

to its large surface area, practically zero concentration. The theoretically calculated sampling rates for this situation are applied in the measurements. In normal measuring conditions (sampling in a room, low concentrations) the main causes of deviations are manufacturing tolerances. In the analysis system there are several potential causes for deviation. The most important ones to overcome have been the desorption of samples in a 23–port rack, desorption from the re–concentration trap and the timing of the system. The deviations in the sampling and in the analysis were studied with several tests. The principle of the tests was to make several parallel samples and to analyse the samples with the system. Some of the samples were made in a test room or draught cabin using the permeation sources and others were made by loading the samplers with the calibration gas. The measured volumes varied from 5 to 250 pl. The results of these tests are presented in tables 2 and 3. The relative standard deviation of the samples represents the errors caused by the deviations in the sample rate and in the analysis. It is calculated from the peak height (pkhgt) or from the measured volume (vol.)—or both. The differences between these two are caused by the calibration.

The reproducibility of sampling and normal analysis (splitter on) is for PMCP 0.5–2.2 %,for PMCH 0.4–2.8 %, for PDCH:B 0.8–7.3 % and for PDCH:C 0.9–6.9 %. These results are derived from the latest tests in spring 1989. The calibration seems to give a small increase in these values, but in most of the cases the relative standard deviation is under 7 % for each tracer. In field

Table 2: The summary of the reproducibility tests (winter -89)

Date	Num. of Samp.	The Relative Standard Deviation of the Samples (%) PMCP pkhgt	PMCP vol.	PMCH pkhgt	PMCH vol.	PDCH:B pkhgt	PDCH:B vol.	PDCH:C pkhgt	PDCH:C vol.
3.10.88	6	3.2	4.6	3.2	4.7	6.7	12.4	6.8	8.6
21.10.88	4	4.3	–	4.1	–	4.6	–	4.5	–
28.10.88	4	0.9	–	3.2	–	3.8	–	4.7	–
28.10.88	3	0.5	–	0.3	–	2.6	–	2.6	–
2.11.88	12	–	7.0	–	11.6	–	6.4	–	6.7
7.11.88	5	3.1	–	6.2	–	4.5	–	4.8	–
11.11.88	7[a]	5.5	–	4.8	–	2.8	–	9.7	–
11.11.88	6	1.9	–	2.4	–	5.2	–	5.2	–
1.12.88	10	5.0	–	10.8	–	11.1	–	11.3	–
2.12.88	10	4.2	–	7.1	–	10.4	–	10.5	–
16.12.88	10	4.6	11.9	6.7	5.3	8.4	7.6	6.9	6.3
21.12.88	9	2.8	8.3	3.9	7.4	6.5	5.7	7.2	6.5
21.12.88	9[b]	7.3	–	6.5	–	6.7	–	12.7	–
4. 1.89	10	5.6	–	8.6	–	12.5	–	13.9	–
6. 1.89	15	5.2	–	8.1	–	16.3	–	17.4	–

[a]No Splitter
[b]Peak Area Measured with Integrator

Table 3: The summary of the reproducibility tests (spring -89)

Date	Num. of Samp.	The Relative Standard Deviation of the Samples (%) PMCP pkhgt	PMCP vol.	PMCH pkhgt	PMCH vol.	PDCH:B pkhgt	PDCH:B vol.	PDCH:C pkhgt	PDCH:C vol.
12.4.89	5	2.2	6.5	2.8	4.0	7.3	2.4	6.9	2.8
13.4.89	5	1.3	4.2	1.5	2.8	3.9	1.6	3.9	1.5
14.4.89	5	1.1	3.4	1.1	2.0	3.3	1.2	3.5	1.5
17.4.89	5	0.5	1.6	0.9	2.2	4.7	2.1	4.8	2.5
3.5.89	5	1.6	6.5	0.4	1.1	5.2	2.5	3.9	2.1
21.4.89	5[a]	6.0	–	3.9	–	1.1	–	1.2	–
24.4.89	5[a]	1.6	–	1.0	–	0.4	–	0.5	–
25.4.89	5[a]	3.6	–	2.7	–	0.8	–	0.9	–
26.4.89	5[a]	9.3	–	6.1	–	1.6	–	1.6	–
27.4.89	5[a]	3.2	–	2.2	–	1.1	–	1.1	–
3.5.89	5[a]	4.2	–	2.8	–	1.7	–	1.6	–
5.5.89	10	1.7	–	0.6	–	1.0	–	0.9	–
5.5.89	10	1.9	–	0.8	–	1.1	–	0.9	–
8.5.89	10	1.0	–	0.5	–	0.8	–	0.9	–

[a]No Splitter

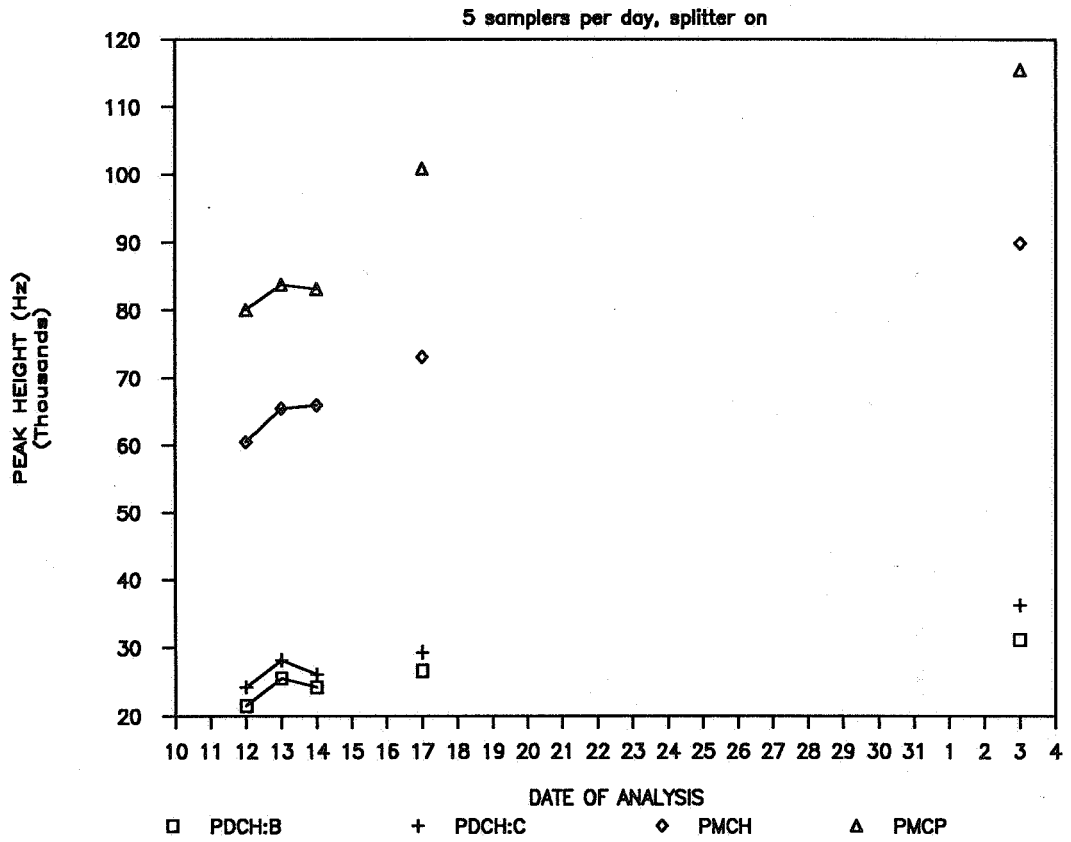

Figure 3: The drift of the analysis system

measurements the effect of poor tracer mixing within a zone must be added to this deviation.

The analysis system is calibrated done by loading samplers with known amounts of calibration gas and analysing the samples. The calibration curve is composed of measured peak heights plotted versus the amounts of loaded gas. A fourth degree polynomial is fitted to this curve. The main problem in the calibration was to determine the concentration of the calibration gas delivered with the system. This was done in the following manner. The permeation sources were used to create equilibrium concentration in a small flask. The flask was kept in a constant temperature. Pure nitrogen was released through a glass heat– exchanger to the flask. The dilution was led to a sample loop in the gas chromatograph. The contents of the loop were flushed with carrier gas to the samplers. Five samplers on five different levels were made. The samplers were analysed without using the splitter. The concentration on the calibration gas cylinder was determined by comparing the gas with this calibration.

The drift of the calibration was studied by making parallel samplers which were analysed on different dates. The analysis was done normally. An example of the results is shown in figure 3. It can be seen that there is a positive drift. The drift seems to be a function of time or the number of analysed samples.

The temperature of the carrier gas can also have an effect on the drift. The effect of this drift can be allowed for by using reference samplers with known amounts of tracers in each run.

4 THE ACCURACY OF THE PFT-METHOD

4.1 The test procedures

The accuracy of the applied PFT-technique was studied in controlled laboratory conditions. Several tests were made during the research project. The principle of the test was always the same: the PFT-method was compared to (in most cases continuous) air flow measurement. The air flows were kept as constant as possible and internal mixing fans were used in all tests except test set IV. Individual tests were arranged as follows:

I The tests were carried out in September 1986 in test chamber 2. The air flows and temperatures during the test were recorded using a data–logger. The air flow rates were checked with the tracer gas decay method before and after the tests. The samplers were analysed by Brookhaven National Laboratory.

II The tests were carried out in September 1987 in test chamber 1. The air flows were set before the measurements and the situation was checked regularly. The air flows were measured after the test set with the tracer gas decay method.The temperatures were measured using a recorder. This test set consists of one situation with five different measurement periods.

III The tests were made in December 1987 in test chamber 1. The air flows and temperatures were measured as in test set II. Differents tests had different combinations of tracer sources and concentration levels.

IV This set was carried out in February 1989 in a test apartment with two rooms and a hall between the rooms. The temperatures and air flows were recorded using a data–logger. The air flow measurement was made with an orifice tube and precision manometer. The first test was a single zone case with the samplers in one place in the middle of the hall. The other tests were two zone cases with samplers placed at 23 points in the apartment. The air flows are calculated from the third tracer emitted in both zones.

V The purpose of this test was to study the method in measuring air flows in a duct. The sources were places in a mixing chamber from which the air was exhausted to the duct. The samplers were placed perpendicular to the flow on two sides of an orifice plate. The caps on one end of the sampler caused the samplers to tilt approximately four degrees. The air flow was measured with a vortex meter and recorded with a data–logger. The test took place in February 1989.

Table 4: The summary of the accuracy tests

Set	Test	Num. of Samp.	Reference Air Flow		Measured Air Flow PMCP		PMCH		PDCH	
			l/s	std%	l/s	std%	l/s	std%	l/s	std%
I	1	2	19.5	10.0	19.7	5.90	–	–	–	–
	2	1	19.5	10.0	20.8	–	–	–	–	–
II	1	5	9.0	15.0	9.60	4.70	9.90	2.50	3.0	5.40
	2	2	9.0	15.0	10.1	1.30	10.3	4.90	6.0	11.3
	3	2	9.0	15.0	9.90	4.20	8.50	11.7	6.20	27.7
	4	3	9.0	15.0	9.70	8.80	10.9	9.50	12.3	16.3
	5	5	9.0	15.0	6.80	4.90	11.8	4.40	–	–
III	1	8	8.0	10.0	6.50	4.90	6.30	3.30	6.80	6.80
	2	7	8.0	10.0	12.2	8.90	8.40	15.0	10.8	12.4
	3	9	8.0	10.0	8.10	5.10	5.50	2.90	7.60	7.90
	4	9	8.0	10.0	4.0	7.0	7.30	5.30	5.30	12.3
	5	8	8.0	10.0	6.80	6.0	7.30	7.80	3.60	8.70
IV	1	29	10.4	10.0	10.7	8.70	11.1	2.60	15.7	4.20
	2a	23[a]	6.0	10.0	4.0	30.2	–	–	–	–
	2b	23	6.0	10.0	8.30	27.0	–	–	–	–
	3	47	6.0	10.0	–	–	–	–	7.30	10.6
V	1	6[b]	27.9	3.0	7.80	2.70	5.40	5.30	16.1	3.80
	2	5[c]	27.9	3.0	6.10	8.70	3.80	15.0	11.9	16.8
VI	1	5	18.4	2.50	18.3	9.40	21.7	1.40	21.3	3.40
	2	15	18.6	2.50	21.1	2.70	20.8	4.60	19.9	3.60

[a]The parallel samplers at the 23 points in the flat were analysed in two runs (2a and 2b). The system was calibrated between the runs.
[b]Samplers before the orifice plate
[c]Samplers after the orifice plate

VI This test was made in May 1989 in the test apartment. The sources were placed in the rooms and the samplers in one place in the hall. The air flows were measured as in Set V. 20 samplers were split into two lots after three days, otherwise tests 1 and 2 are similar.

The samples were analysed during the building and testing period of the analysis system. The concentration of the calibration gas was allowed for afterwards for sets I–V. The drift of calibration was not taken into account.

4.2 The results of the measurements

The results of the accuracy tests are presented in table 4 and figure 4.

As Fig.4 reveals. there are some rather high differences from the reference.In particular PDCH seems to give a few unreliable results. While studying the results one should bear in mind that the analyses were made during

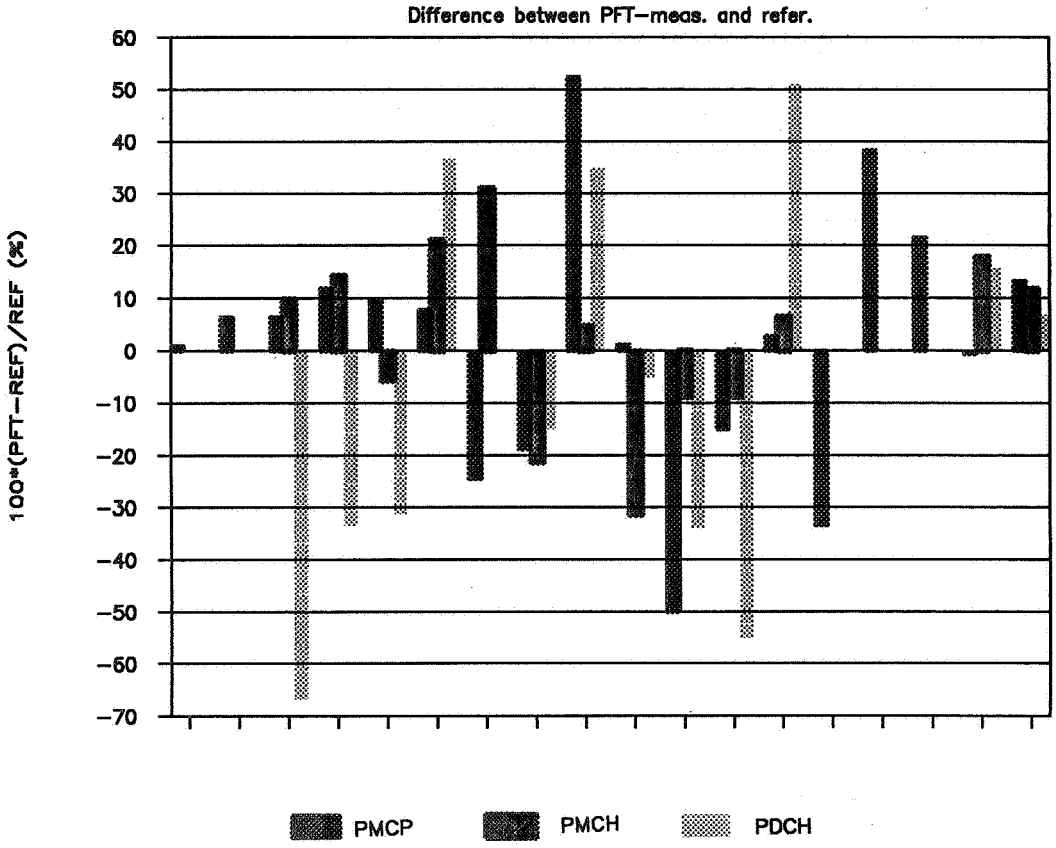

Figure 4: Summary of the accuracy tests in chambers

the building and testing of the system. The best results are gained with the BNL–system, but the system of our laboratory also gives betters results towards the end of the testing. It should also be noticed that the air flow rates were quite low, which easily increases the relative differences. Considering also the confidence limits for both PFT– and reference measurement, the relative errors become more acceptable. The results are distributed evenly on both sides of the zero line. Thus, with few exceptions, the inaccuracy of the PFT-method can be estimated to be approximately ±20 %, when PMCP or PMCH are used. For PDCH the inaccuracy is somewhat higher. Improving the calibration procedure and allowing for the drift of calibration should improve the accuracy of the method. This was indicated by the last test set (VI), where the inaccuracies vary from -0,5 % to +17,9%.

Test V is markedly different from the other measurements. It seems that the sampling rate in a duct increases. This gives higher concentrations and lower air flow rates. The increase in the sampling rate can be due to the dynamic pressure of the flow. The difference between simultaneous tests 1 and 2 is explained by the tilting of the samplers. The samplers in test 1 were tilted so that their opening was on the leeward side of the flow, while the openings of the other samplers were on the windward side. The samplers in test 1 had a lower dynamic pressure on their opening than the other samplers, which gave lower concentrations and thus higher air flow rates. This test implies that the use of the method should be limited to room flow conditions

Table 5: The mixing of tracers in test 1

Tracer in:	Measured volume in: Room 1		Hall		Room 2	
	pl	std-%	*pl*	std-%	*pl*	std-%
Room 1	177.3	3.9	112.4	10.4	99.2	5.4
Room 2	26.9	3.9	79.4	7.4	94.5	9.2
Both	111.1	2.7	126.6	5.4	134.2	6.6

Table 6: The mixing of tracers in test 2

Tracer in:	Measured volume in: Room 1		Hall		Room 2	
	pl	std-%	*pl*	std-%	*pl*	std-%
Room 1	173.2	20.4	153.6	8.6	169.3	11.8
Room 2	2.9	8.1	294.4	11.1	574.5	7.4
Both	254.4	10.4	482.9	3.2	346.8	7.1

until further research has been done.

5 THE MIXING OF TRACERS WITHIN ZONES

5.1 The measurements in the laboratory

The measurement model assumes that there is instantaneous uniform mixing within each zone. In field measurements this assumption is almost never fullfilled. Poor mixing will cause high deviations in the concentrations, which can yield an ill–conditioned system with unacceptably high errors[6]. The best available estimate of the room concentration is the room average concentration. Sandberg and Stymne[7] have shown that the use of the average concentration can also cause severe errors in the results, but the errors can be minimized with correct placement of sources and samplers.

The mixing within zones was studied with field and laboratory measurements. The laboratory measurements were carried out in February and March 1989 in the test flat of Helsinki University of Technology. Two different tests were made. In the first test there was only mechanical exhaust from the hall and room 2. In the second test the air was supplied to room 1 and exhausted from room 2. There was one–directional air flow between the rooms. In both tests three tracers were used, one in each room and the third in both rooms. The door between room 1 and the hall was closed but had a 60 cm^2 opening at the top. Other interior doors were open. The concentrations were measured at 23 points in the apartment. The supply and exhaust air flows, pressure differences and temperatures were recorded using a data–logger system. The results of these tests are presented in tables 5 and 6 and figures 5 and 6.

The results show that the mixing was good, the relative standard deviation

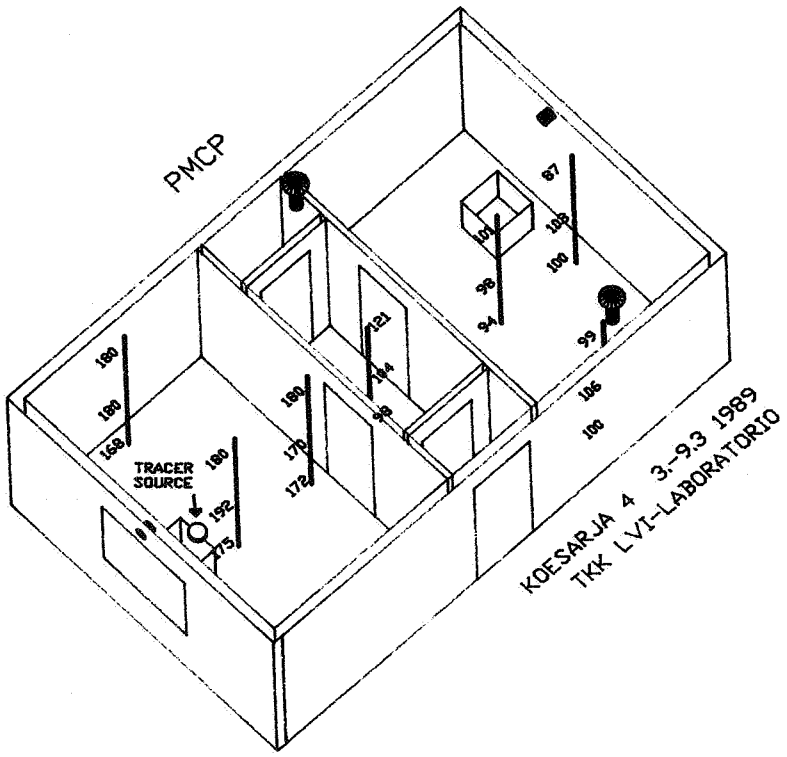

Figure 5: An example of mixing in test 1

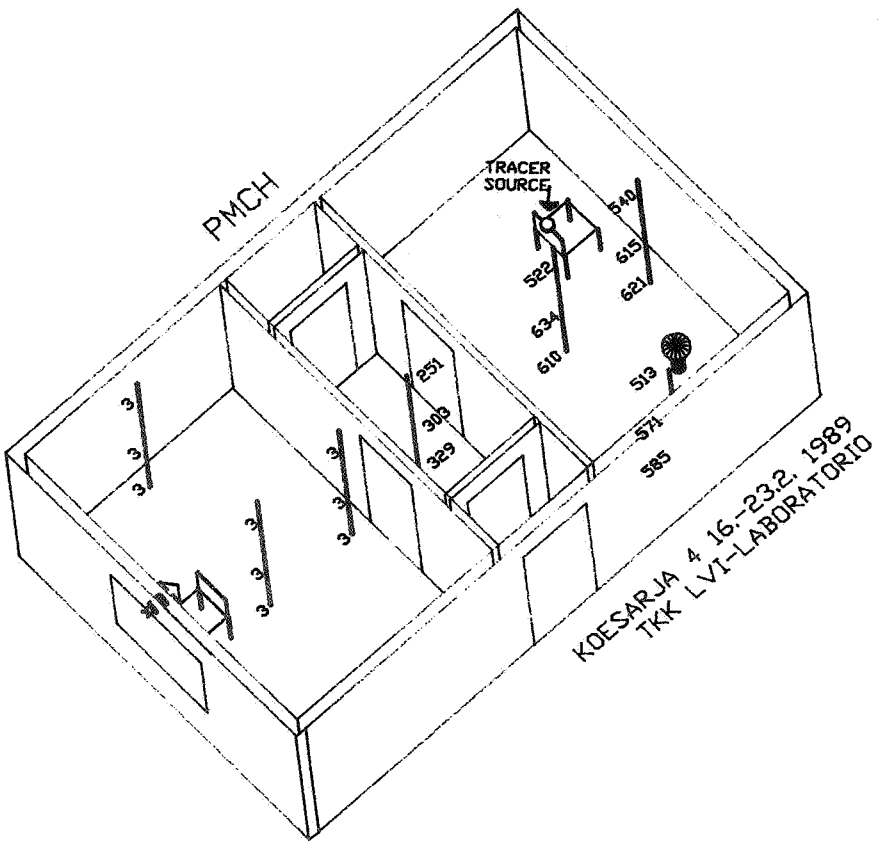

Figure 6: An example of mixing in test 2

Table 7: The distribution of measured homes

	natural ventilation	mechanical exhaust	balanced ventilation	total
single–family	1	1	4	6
semi–detached	7	9	6	22
flat	7	8	7	22
total	15	18	17	50

being generally below 10%. The higher values are caused by samplers placed too close (less than 1 m) to the source. Regardless of the fact that the samples were taken from extreme points in the room, no stratification could be found. The location of the samplers in respect to the sources and the air flows gives a reasonable explanation for the deviations.

5.2 Field measurements

Field measurements were made in typical Finnish homes during the heating season of 1987–1988. The study included 50 homes, the distribution of which is shown in table 7. Ventilation measurements using the passive perfluorocarbon technique were carried out twice during the spring of 1988. The first measurement was in January and the second was in April, the measurement period being two weeks. The buildings were divided into one to three ventilation zones according to the following main principles:

- different floors are different zones
- the sauna section, the door of which is closed most of the time, is one zone
- the master bedroom, the door of which is closed during the night, is one zone

The instructions given by Brookhaven National Laboratory[8] were applied in the placement of sources and samplers. In the second field measurement period several samplers were placed in zones larger than one room. The standard deviations of the concentrations were calculated in order to see how well the assumption of uniform internal mixing was fullfilled.The results of these measurements are shown in figure 7.

When the interior doors within the zone were kept open during the measurement, the concentration distribution was uniform. The standard deviations of concentration varied from 1% to approximately 25%. The deviations caused by the adsorption rate of samplers and the reproducibility of the analysis system are included. The estimated deviation of 10% gives a fairly good estimate of the errors due to non–homogeneous mixing. The case was more complicated when some of the interior doors within the zone were closed. When a sampler was placed in the same room as the source and the door

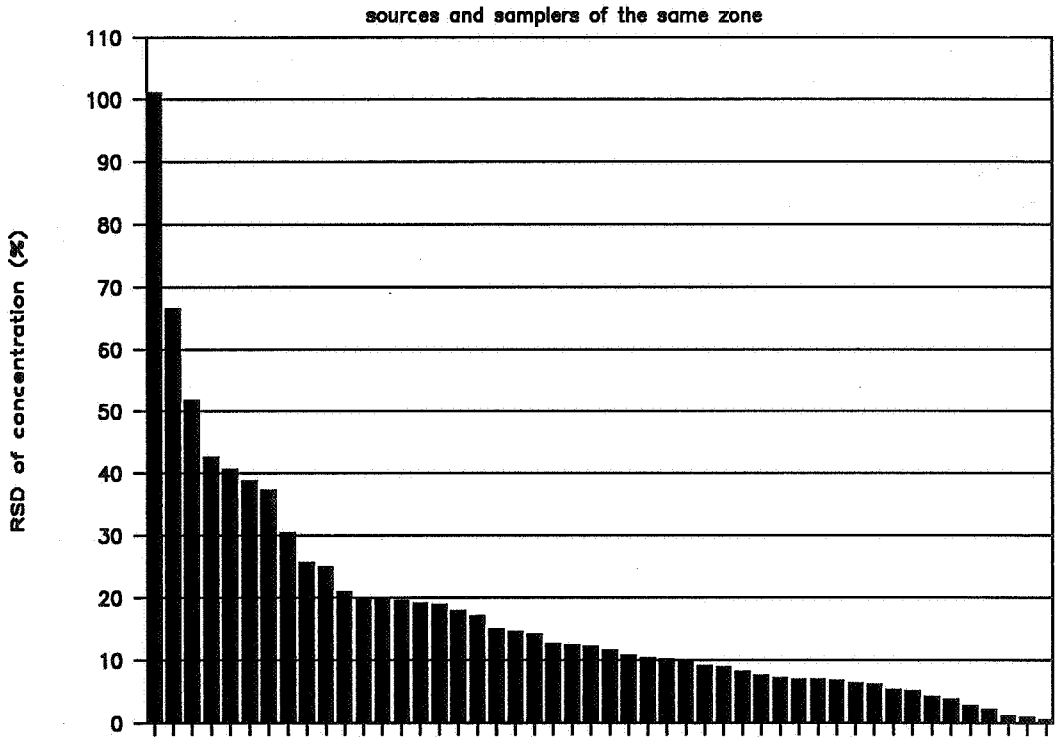

Figure 7: The relative standard deviation of concentration

was closed, the concentration in that sampler was, of course, higher than in other samplers in the same zone.The same problem occurred when a sampler was placed in a small closed space. In these cases the standard deviations of concentration varied from 25% to 100%. The solution to these problems is usually found by modifying the measurement model, but each dwelling is an individual case,so it is difficult to give general instructions.

6 DISCUSSION

The use of passive perfluorocarbon technique for air flow measurements has been developed and tested. The project was divided into two tasks: building and testing of the analysis system and testing of the reliability of the method. Building the system demanded quite lot of work, because complete, working systems were not commonly available. Each system is an individual, which has its own demands. Building and testing the system took approximately one year. The most difficult problems were the desorption of samples in the rack, desorption from the re–concentration trap and the timing of the system. Once these problems had been overcome and the system calibrated the reproducibility of the analysis was tested. The results show that the relative standard deviation of the analysis for parallel samples is less than 7 % for each tracer in most of the cases. The calibration procedure of the system was found to be sensitive to errors, because determination of the curve was based

on only one sample per point. In future the number of samples per point will be increased in order to decrease the uncertainties. A drift of calibration was noticed, but the drift can be allowed for by using reference samples with known amounts of tracers.

The accuracy of the method was tested in controlled laboratory conditions. The results reveal some rather high differences from the reference. Some explanation can be made. It should be noted that most of the analyses were made during the building and testing of the system. If the confidence limits for both PFT– and reference measurement are considered, the relative errors are more acceptable. The results are distributed evenly on both sides of the zero line. Thus, with few exceptions, the inaccuracy of the PFT-method can be estimated to be approximately ±20 %, when PMCP or PMCH are used. For PDCH the inaccuracy is somewhat higher. Improving the calibration procedure and allowing for the drift of calibration should improve the accuracy of the method.

The test made in a duct flow is markedly different from the other measurements. It seems that the sampling rate in a duct increases. The increase in the sampling rate can be due to the dynamic pressure of the flow. This test implies that the use of the method should be limited to room flow conditions until further research has been done.

The mixing of tracer within zones is crucial to the accuracy of the model. The mixing was tested in laboratory and field conditions. The results of the laboratory measurements show that the mixing was good, the relative standard deviation being generally below 10%. The higher values are caused by samplers placed too close (less than 1 m) to the source. Regardless of the fact that the samples were taken from extreme points in the room, no stratification could be found.

Field measurements were made in typical Finnish homes during the heating season of 1987–1988. The study included 50 homes. The instructions given by Brookhaven National Laboratory were applied in the placement of sources and samplers. When the interior doors within the zone were kept open during the measurement, the concentration distribution was uniform. The standard deviations of concentration varied from 1% to approximately 25%. The case was more complicated when some of the interior doors within the zone were closed. In these cases the standard deviations of concentration varied from 25% to 100%. The solution to these problems is usually found by modifying the measurement model.

In spite of the problems, the PFT-technique can be used to study the ventilation of dwellings. The technique is best suited to studies concentrating on the health and comfort of the people living in the house. If the energy use of ventilation is studied, the use of an integrating technique should be limited to cases with little temporal variation. Further research is needed on the temporal efficiency of air flows before the PFT-technique can reliably be applied in all cases.

The technique is applicable to large field surveys of ventilation. The restrictions mentioned above should be noticed. Anyhow, the complexity of

room ventilation limits the number of potential users of the method. It is imporant to have enough knowledge of room ventilation in order to be able to conduct the measurements properly and to interpret the results correctly. This holds true for any ventilation measurement method, of course.

7 REFERENCES

1. R.N.Dietz, R.W.Goodrich, E.A.Cote, and R.F.Wieser. *Detailed Description and Performance of a Passive Perfluorocarbon Tracer System for Building Ventilation and Air Exchange Measurements.* Technical Report BNL-36327, Brookhaven National Laboratory, 1985.

2. D.Bohac, D.Harrje, and G.Horner. Field study comparisons of constant concentration and PFT infiltration measurements. In *Supplement to Proceedings of the 8th AIVC Conference*, 1987.

3. Mats Sandberg. The Multi-chamber Theory Reconsidered from the Viewpoint of Air Quality Studies.*Building and Environment*,19(4):221–233,1984.

4. M.H.Sherman.*Analysis of Errors Associated with Passive Ventilation Measurement Techniques.* Technical Report LBL-23088. Applied Science Division, Lawrence Berkeley Laboratory, Berkeley,CA,U.S.A.,1987.

5. B.P.Leaderer, L.Schaap, and R.N.Dietz. Evaluation of the perfluorocarbon tracer technique for determining infiltration rates in residences. *Environmental Science Technology*, 19(12):1225–1232, December 1985.

6. J.Säteri, A.Majanen and P.Jyske. The evaluation of field measurements of ventilation parameters made using the passive perfluorocarbon method. In *Proceedings of CLIMA2000 Conference*, Sarajevo, 1989

7. M.Sandberg and H.Stymne. The Constant Tracer Flow Technique. Preprint from *Building and Environment*, 1988.

8. R.N.Dietz.Instructions.Brookhaven Air Infiltration Measurement System. In *Proceedings of the AIVC Measurement Techniques Workshop.* Technical Note AIVC 24,1988

Discussion
Paper 5

N. Bergsoe (Danish Building Research Inst.)

How often do you calibrate your instrument?

J. Sateri (Helsinki University of Technology)

The system is calibrated for every new lot of samples, and/or every two weeks.

N. Bergsoe (Danish Building Research Inst.)

The rubber cap on the sampler may collect tracer gas during a measurement and release it to the adsorption material in the tube later - i.e. if the tube is stored for some time before analysis. This effect may contribute to the positive drift of the calibration.

J. Sateri (Helsinki University of Technology)

Yes, this requires further research.

Saffa Riffat (Loughborough University, UK)

Did you have any problems with the use of PFT's as tracer gases?

J. Sateri (Helsinki University of Technology)

The problems caused by small amounts of analysed tracers and thus danger of contamination were minimised by taking appropriate precautions in the transport and handling of the equipment. The most difficult problems existed with the calibration gases and the determination of the concentration of the gas standard.

PROGRESS AND TRENDS IN AIR INFILTRATION
AND VENTILATION RESEARCH

10th AIVC Conference, Dipoli, Finland
25-28 September, 1989

Paper 6

EXPERIMENTAL STUDY OF AIR FLOW PATTERNS IN A THREE BEDROOM HOUSE

B. Fleury, A. Gadilhe

Laboratoire des Sciences de l'habitat
ENTPE-LASH Rue Audin
69518 Vaulx en Velin Cedex
France

ABSTRACT

This paper describes a set of experiments conducted in a three bedroom house in order to identify the leakage distribution of the building and the air flow rate through the on-purpose designed opening of the interior doors. Starting from the depressurization test in every zone, we were unable to track all the flow equation of every specific identified connection. We therefore propose to characterize the leakage between two zones by a unique general connection. Its flow behavior (K,n) is determined by an optmization under constraints of the results of the various tests. In the second phase, we study the aeraulic behavior of a slot, usually included in French doors and then we replace the existing interior doors by tight doors with a calibrated duct having a similar areaulic behavior $f(Q,\Delta P)=0$. In the absence of wind and temperature difference, we measure the air flow rate through the interior doors for differents mechanical extraction rates and compare them to the results of a pressure model simulation.

1. INTRODUCTION

In order to reduce the energy losses in buildings due to ventilation, innovative HVAC systems have been designed to satisfy the minimum air change rate at every instant according to weather and indoor conditions (humidity, temperature, concentration). A global ACH of 0.1-0.2 can be encountered. However, if we do not want to face some disorders such as air quality, condensation meldew problems, the optimum theoritical air flow path between the different rooms in the apartment should be respected. Our main question is to know if we can control the air pattern at such low air extraction rate. The answer to this question is conditionned by the building overall permeability and the leakage distribution between the various components including interior partitions. The first part of our study is devoted to identify the flow behavior of the air paths. Many studies have focused on enveloppe components but almost no research refers to interior ones. Unfortunately, the air flow pattern within the building can be largely modified in presence of leaky interior components. In the second phase of our study, we compare the experimental air flow rate through on purpose designed connections with the numerical air flow rate.

2. BUILDING PERMEABILITY

2.1 Experiment

Experiments are conducted on a new semi-detached house which respects the French building regulations. The reference building is a three bedroom house of 100 square meters, located in the suburbs of Lyon, France, on a well sheltered site. It has never been occupied and is equipped with a mechanical ventilation system. Automatic air inlets are casted in the frame of windows of the living room and bedrooms. Air Extraction takes place in the toilets, bathrooms and kitchen with a proportion of 1/5, 1/5, 3/5. The total mechanical extraction rate can be varied from 50 to 300 m3/h.

In order to characterize the leakage distribution of the house, a series of depressurization tests in the entiere building and in every aeraulic zone are realized. During the experiments, the wind speed is lower than 2 m/s and no temperature difference is notified between the outside and inside and within the interior zones. Otherwise, the test is rejected.

Some of the air connections : air inlet, shutter chest, window frame, light switch, wall-floor link, pipes,... are identified. After sealing of some of these detectable air paths, we reconduct some tests in order to analyse their specific behavior and their role.

2.2 Analysis

The results of the experiments are presented in Figure 1. We notice the major contribution of undectectable connections on the infiltration. The tighness of the house could have been drastically improved with a good quality of construction and adequate choice of building components. For example, the high quality window frame is associated with a poor shutter chest. No sealing joint between the interior partition and the floor of the bedroom has been installed. Some care seems to have been brought to the kitcken. At the opposite, the bathroom, the toilets and the hall present large undetectable infiltration in comparison with their volume. Running waterpipes and electrical wiring may represent some privilegeous air paths. Bedrooms have a similar behavior, bedroom $\neq$ 2 has a reduced surface of exterior enveloppe and is less leaky. The living room with the stairwell represents a large volume with important infiltration. However, the air flow rate per unit of volume is in the average of the building.

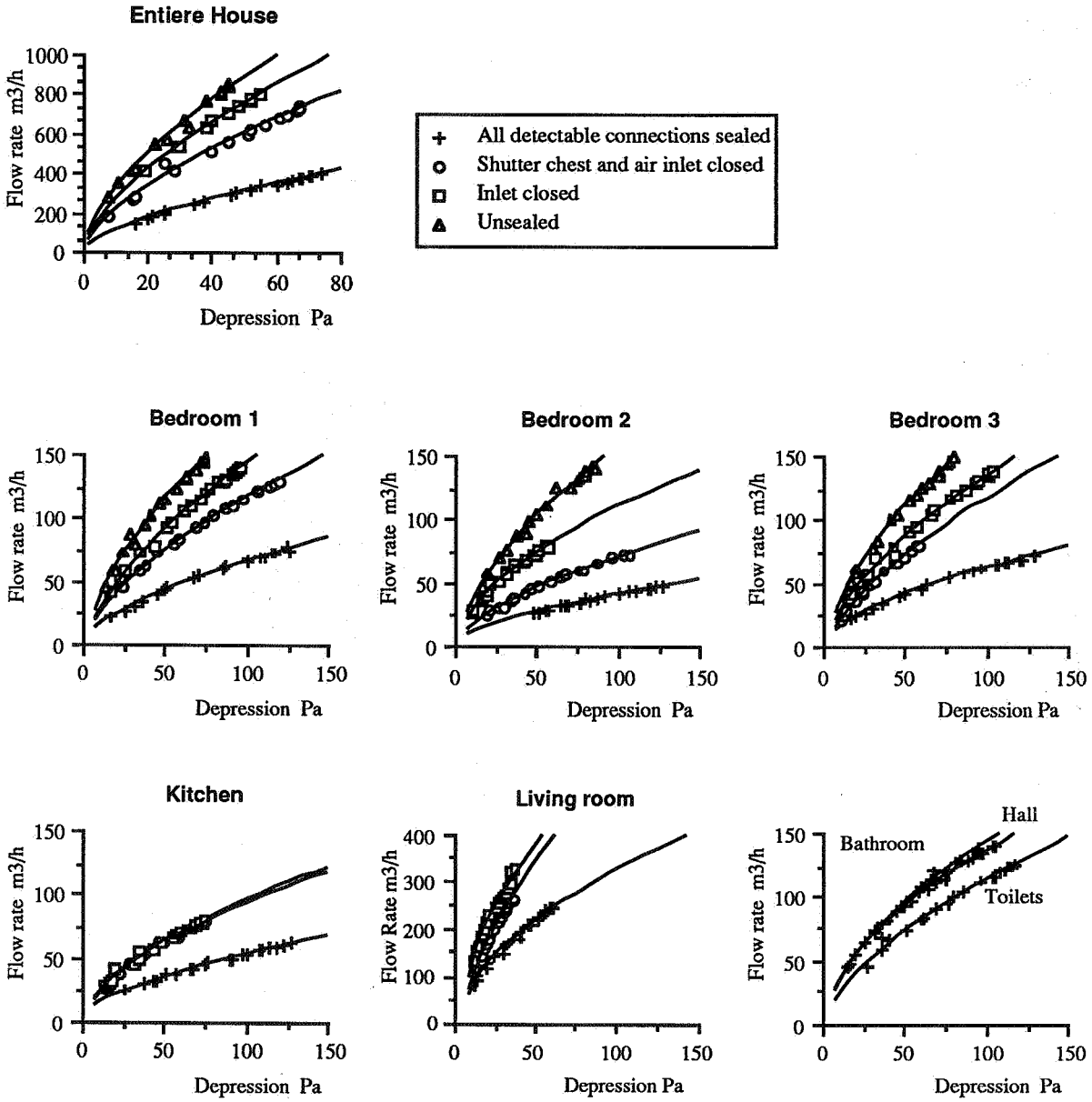

Figure 1: Results of depressurization tests

The leakage characteristic of this house is representative of new built houses in France. At 1 Pascal, the air flow rate per unit of volume is equal to 0.24 in the 0.24-0.48 range (table 1) which is the result of an extensive survey on 70 houses in France[1].

On purpose designed air inlet do not represent the major source of incoming air.

	massive buildings exterior insulation		massive buildings interiorinsulation		light building	wood frame building
	simple	multi-family	simple	multi-family	simple	multi-family
Average	0.25	0.11	0.36	0.17	0.39	0.74
Variance	0.08	0.10	0.12	0.15	0.18	0.38
Number of Houses tested	6	20	54	21	15	19

Table 1 : Permeability per unit of volume at 1 Pascal[1]

3. Leakage distribution

Many of the pressure models require a precise description of the air connections between the different zones. For example, in ESPAIR, the geometry of the connection (width, length, area) should be mentionned as well as its type : crack, opening or large opening. The methodology adopted in the experiment was conceived to identify the behavior of detectable air paths by making the connection inactive and then active. Let us identify the aeraulic behavior of some components.

3.1 Power Law

In the same buiding configuration, let us take two depressurization tests : one with the connection A sealed and the other unsealed.

From test 1 (resp 2), we get a series of couples ($\Delta P1, Q1$) (resp ($\Delta P2, Q2$)).

If we suppose that the connection A follows a power law, we have different possible methods to identify it :

. Look for tests at same depression ΔP and fit a power curve through the points (ΔP,Q1-Q2)

. Suppose the test 1 and 2 follow a power law : $Q1 = K1\ \Delta P^{n1}$ and $Q2 = K2\ \Delta P^{n2}$ then identify $Q = Q1 - Q2 = K\ \Delta P^{n}$

. Suppose that the zone with all detectable connections sealed follows a law of type $Q = K\ \Delta P^{n}$. Then, suppose that the unsealing of a connection adds a new power law. For a specific building configuration, the depressurization test can be expressed in the following way :

$$Q_{old} = \Sigma\ Ki\ \Delta P^{ni}$$

If we unseal a new connection j, $Q_{new} = Q_{old} + Kj\ \Delta P^{nj}$.

(Kj,nj) are determined by a curve fit of the data ($Q_{new}-Q_{old}$,ΔP_{new}).

Due to the limited number of tests at the same depression, method 1 has limited applications and the results are really sensible to the quality of the few measurements. Methods 2 and 3 give better results because of the higher number of measured points.

	Undetectable Permeability		Wall-Floor link		Shutter chest		Air inlet	
	K	n	K	n	K	n	K	n
bedroom 3	3.32 *3.32*	0.622 *0.622*	1.07 *1.20*	0.723 *0.689*	1.49 *3.26*	0.586 *0.500*	1.78	0.651
bedroom 1	2.93 *2.93*	0.662 *0.662*	 *1.63*	 *0.695*	2.42	0.530	3.30 *3.30*	0.500 *0.500*

Table 2 : Behavior law of some connections determined by:
- Method 1 - *Method 3*

We note that the results are not convergent. It appears such a large discrepancy between the impact of the various connections that determining the behavior of small connections is almost impossible. We can also point out that the shutter chest are really leaky. Their theoritical value suggested by the French standard is ten times less that the measured one. The identical air inlets do not present the same behavior. Moreover, many laws for specific components are unrealistic :
- n is lower than .5
- the unsealing of a connection decreases the flow rate at the same ΔP.

The couple (K,n) is so sensitive to the measurements that any perturbation (a sudden wind, a solar spot,...) may induce an unrealistic (K,n). Moreover, the accuracy of the equipment is limited in the low ΔP range. It is surprising to note that the depressurization test facility is not well appropriate at low depression which is the usual situation in buildings. Some improvements should be brought in the selection of the equipment such as accurate flow meter, precise manometer, stable extraction rate, ... Then, instead of verifying that the wind speed is lower that 2 m/s, it would be preferable to measure the pressure difference between two facades.

Then, the progressive unsealing of components is not an appropriate methodology because a poor intermediate test implies poor following tests. The influence of any connection should be evaluated with a reference test even at the cost of a lengthly procedure.

However, an identification of each component behavior does not seem to be promoted to a large success: air paths are difficult to identify, control of experimental conditions is limited, the behavior of minor connections is really sensitive to perturbations and obscured by the finite accuracy of the equipment. We propose a more global approach to take benefit of depressurization tests.

3.2 Optimization under constraints

We divide the building in zones where the pressure and temperature are uniform as it is common in pressure models. Then, we suppose that the air paths between two adjacent zones can be gathered and modeled in a unique law of type $Q = \Delta P^n$. The physical connections between two zones may be of different types : small or large cracks, small openings, smouth or rough surfaces,.... Moreover, they are usually difficult to identify. This method represents a global approach that may simplify the building description.

Now, the problem is to identify the couple (K,n) for every global connection.

Let us take the building configuration when all the detectable connections are sealed.

For every zone i, we have made k(i) tests which should respect the following equation.

$$\sum_{j=1}^{nzones} m_{ij} \left(K_{ij} \Delta P_{ik}^{n_{ij}} - Q_{ik} \right) = 0$$

with $m_{ij} = 1$ if zones i and j are adjacent
$= 0$ otherwise
$(\Delta P_{ik}, Q_{ik})$ results of the depressurization test k in zone i

K_{ij} permeability coefficient of the connection between zones i and j
n_{ij} exponent coefficient between zones i and j
nzones total number of zones

Therefore, we get $M = \sum_{j=1}^{nzones} k(j)$ equations with $N = \sum_{i=1,nzones}^{i>j} m_{ij}$ unknowns.

For our specific configuration, $M \simeq 200$ and $N \simeq 60$. The non linear system is overdetermined. Moreover, the unknowns should respect some constraints such as:

$$K_{ij} > 0 \text{ and } 0.5 < n_{ij} < 1.$$

The problem can be reformulated as a minimization problem with constraint and Kühn and Tücker theorem is usually applied to solve it. However, the programming is quite lenghtly. Lau[2] has suggested a new approach to solve this kind of problem. The principle is based on the Monte Carlo method : a simple random search technique. (See appendex 1)

This method is straightforward programming but is time consuming and has been applied to our problem. A reduced and confident interval for the constraints improve the convergence speed and the quality of the results. A more detailed study is necessary to access the pertinence of this method. However, it looks promising.

Figure 2 shows the perfect matching between the pressurization test and the numerical results. Figure 3 illustrates the flow rate under a 10 Pascals pressure difference in every connection. As mentionned before, we notice interconnection between toilets, hall and bathroom due mainly to ducts. The living room presents an important leakage area.

In a second stage, we use the Lau's method to determine the behavior law of the air path when no connection are sealed. We get the same good matching than in the first stage.

We therefore conclude to the feasibility of the proposed method. From individual depressurization tests, we can identify the flow behavior of global components separating two zones. According to the values of (K,n), we can comment on the permeabilty of the connections and the type of the defaults. Now, we should be able to visualize the air flow pattern within the house under various conditions.

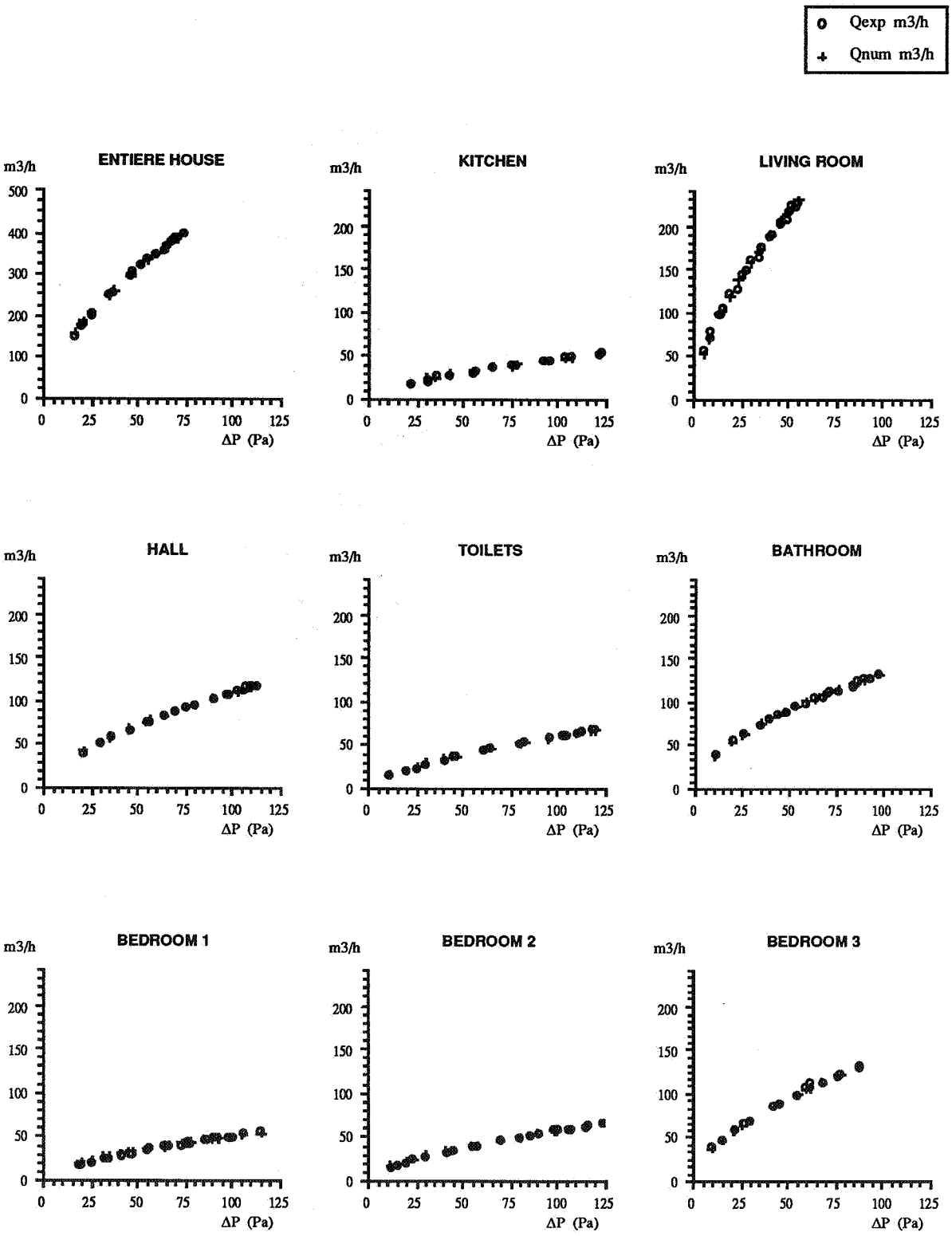

Figure 2: *Results of depressuration Test in every room. Comparaison with numerical results obtained by Lau's determination.*
- All detectable air paths Sealed.

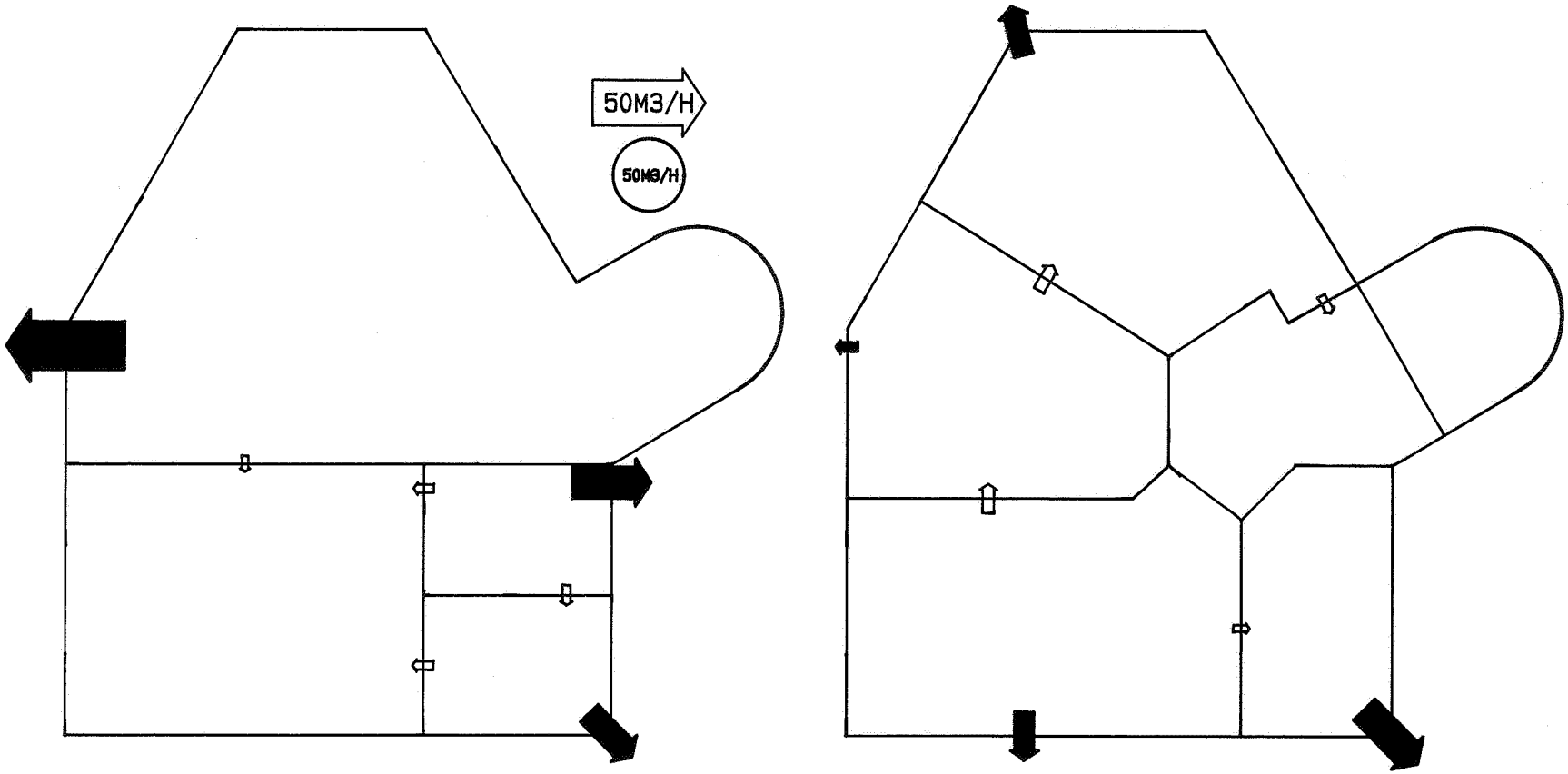

Figure 3: Illustration of the Flow rate under every global connection at 10 Pa pressure difference

3. Interior doors

In the previous tests, interior doors are substituted by tight door with a mounted fan that creates the depression. Therefore, the influence of this element is not included in the general laws and should be evaluated.

Even when closed, interior doors should be designed to facilate the air transfer between the various zones of a house. They can be equipped with a grille, a shaft or a void at the lower level. At the extreme, we trust on the poor tightness of this building component to represent the least air resistance path. Usually, these origins combine each other to offer a priveligeous track for the air.

In the second phase of our study, our objective is to identify under real conditions how much air transit through the doors at various extraction flow rates. Unfortunately, it is almost impossible to measure the flow rate through a typical door. So, we propose to substitute the existing door by an airtight door with a calibrated pipe which has the same aeraulic behavior. Moreover, it is easier to evaluate the volume flow rate in a pipe. Our approach can be divided in three phases :

- identifying the behavior of a slot of various depths and width encountered under interior French doors
- selecting the diameter of the pipe to be representative of an interior door
- measuring the flow rate through the pipe.

3.1 Behavior of a slot

In am airtigth box (figure 4), we have tested cracks of 200 mm length with various width, 3 mm to 10 mm, and various depth, 4.7 mm to 34.7 mm. Our results are presented in term of a power law as it is usual (figure 5). We note that the permeability, K, at 1 Pa increases linearly with the width (figure 6) bus it almost constant with the depth (figure 7). The flow exponent is almost constant with the depth and a width superior to 3 mm (figure 8 and 9).

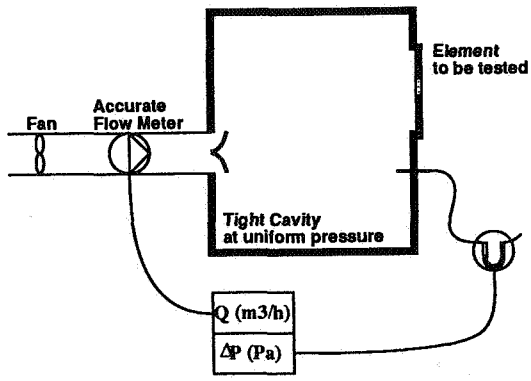

Figure 4: Test Facility to characterize the flow behavior of typical elements

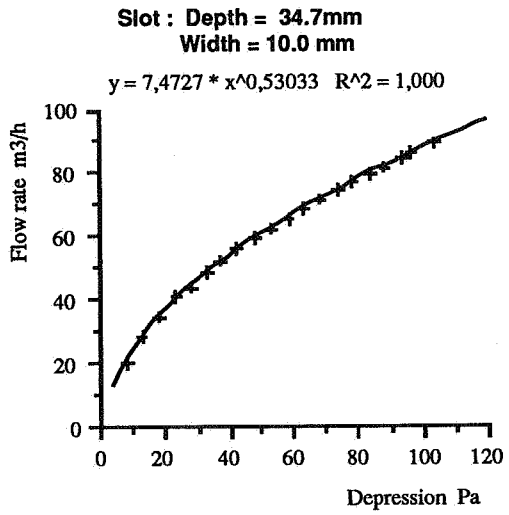

Figure 5: Behavior law of a slot

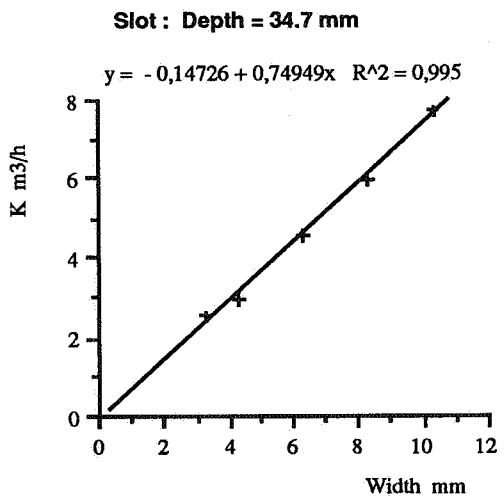

Figure 6: Variation of the permeability at 1 Pa with the width

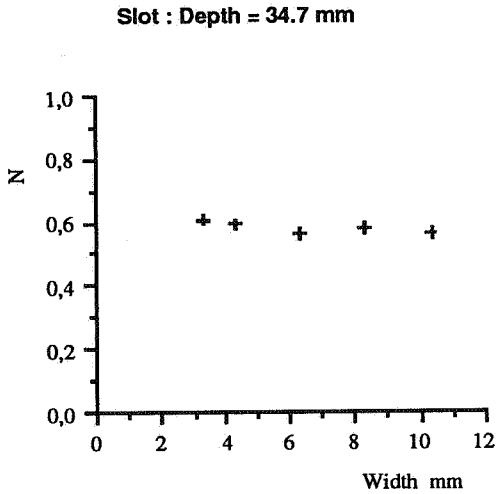

Figure 7: Variation of the flow exponent with the width

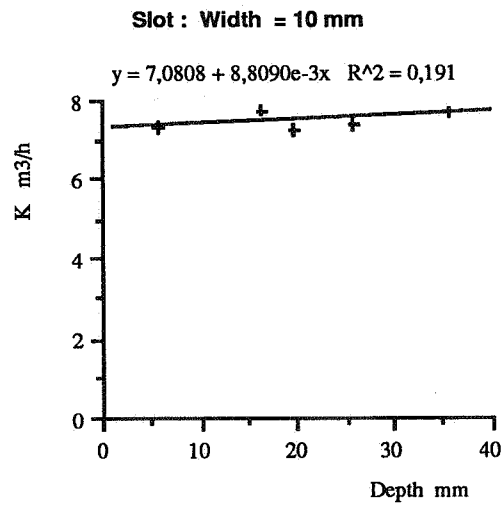

Figure 8: Variation of the permeability at 1 Pa with the width

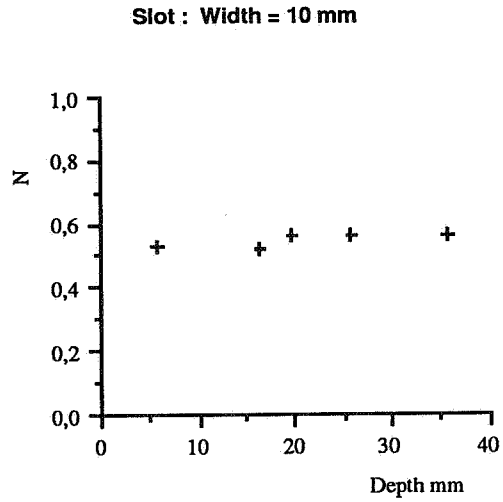

Figure 9: Variation of the flow exponent with the width

3.2 Behavior of a pipe

The depression through a closed door in a house is often around 10 Pa. So, we compare the behavior of a 104 mm diameter pipe and an 800 mm length crack of 10 mm width in the range of 0 to 10 Pa. We notice that the flow exponent and the permeability are quasi identical. The curves of the pipe and the crack are situated between the curves of an interior door without an opening at the bottom and an interior door with an 10 mm opening (figure 10). We conclude that the suggested pipe is representative of French interior doors. All interior doors are substituded by an airtight door with the calibrated pipe.

3.3 Determination of the flow rate through a pipe

In the laboratory, we verify that the velocity distribution is uniform over the outlet section of the pipe. Thus, the flow rate is equal to the product of the velocity by the section area. The measured and the calculated flowrate are in a good agreement (figure 11).

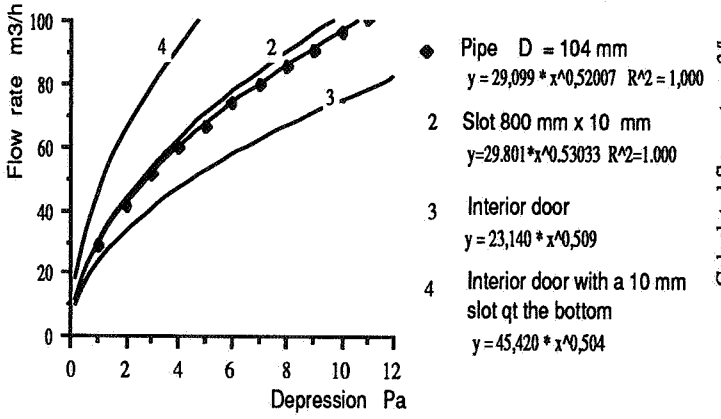

Figure 10 : Comparison of the behavior law of pipe crack and doors

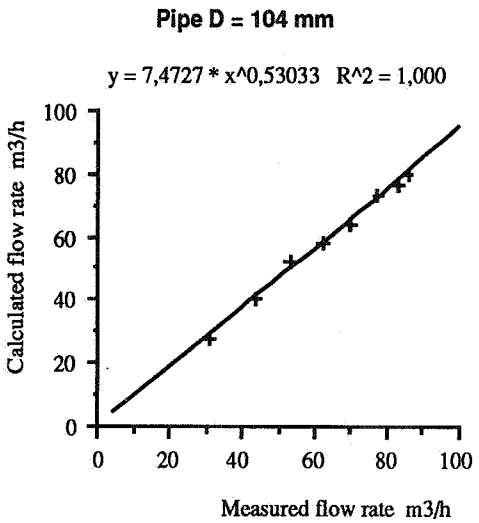

Figure 11 : Comparison of the measured and calculated flow rate in a pipe

4. MULTIZONE AIR MOVEMENT

4.1 Experiment

For different total extraction rates and building configurations, we measure the flow rate through interior doors in the absence of wind and temperature differences. This gives us an image of the flow pattern within the house. In an ideal flow diagram, all the air should transit through the on purpose designed opening in the interior door. Figure 12 illustrates that when the infiltrations of a room are high, controlling the air flow pattern become tricky.

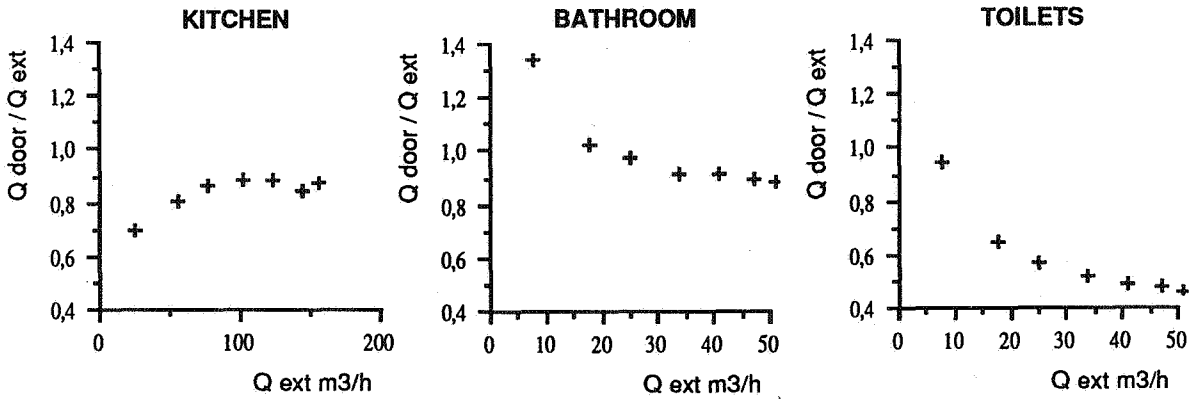

Figure 12: Evolution of the flow rate through the door / extracted flow rate in the room

4.2 Comparisons with numerical results

Using a modified version of ESPAIR, we calculate the air flow pattern with the house for various extraction rate, supposing the behavior laws of the connections determined by Lau's method. For every experiment, we compare the measured and the simulated flow rate through the interior doors. We get a good agreement for the interior doors located at the ground floor even for the toilets that are really leaky. For the first floor, the results are in a poor agreement. Limited air flow rates and air moving downward the stairs may explain it. Moreover, any temperature difference may induce a strong convective flow that is not taken in account in our numerical approach.

Figure 13 represents the air flow pattern for a total extraction rate of 250 m3/h. We note that the ideal flow diagram for a ventilation system is quite well respected. However, this is a strong short circuiting in the bathroom and in the toilets. Permeability of interior components has a limited effect on the flow paterns because of a reduced pressure difference between interior zones in comparaison with the pression difference between inside and outside.

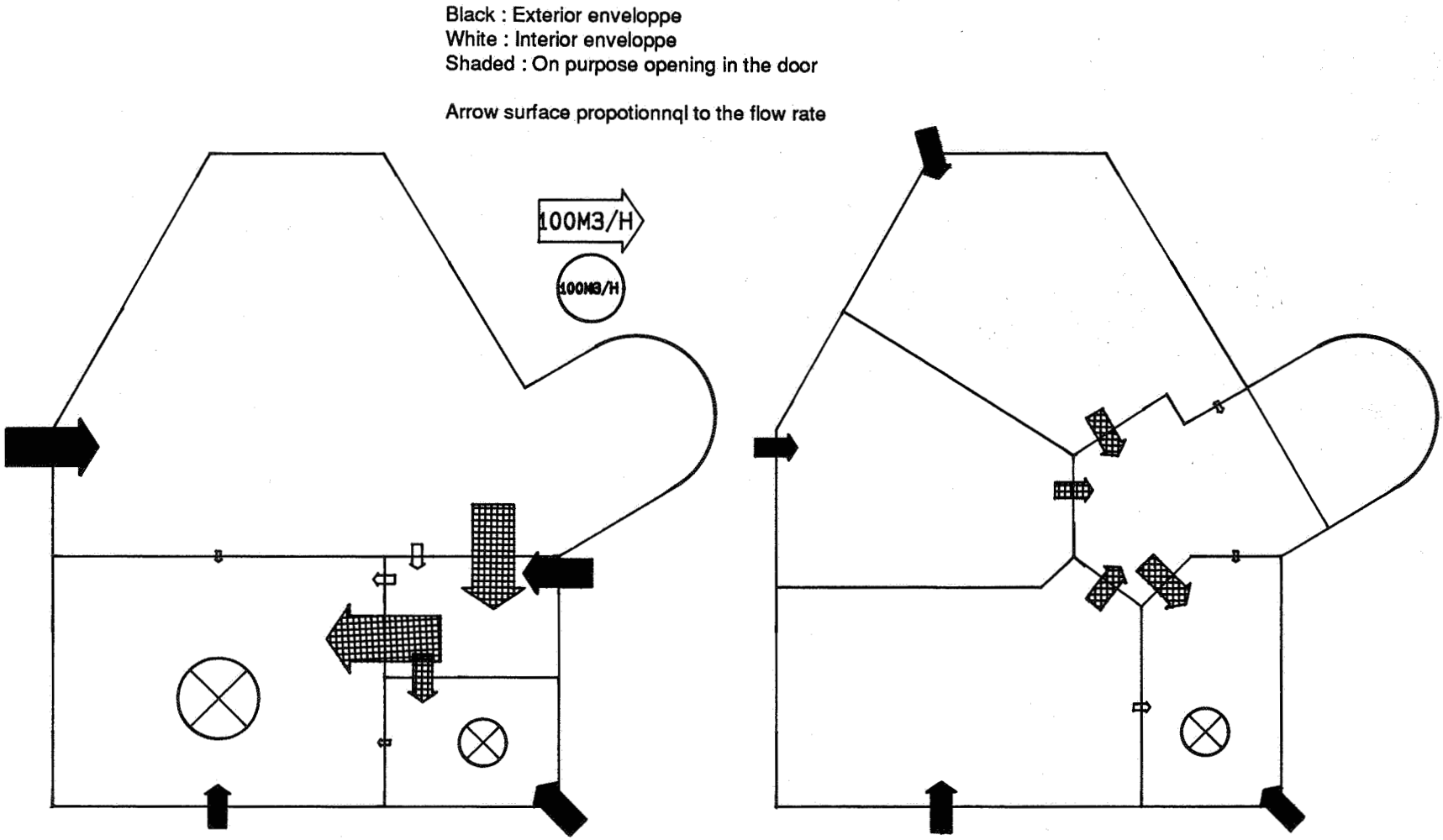

Figure 13 : Air flow pattern within the building

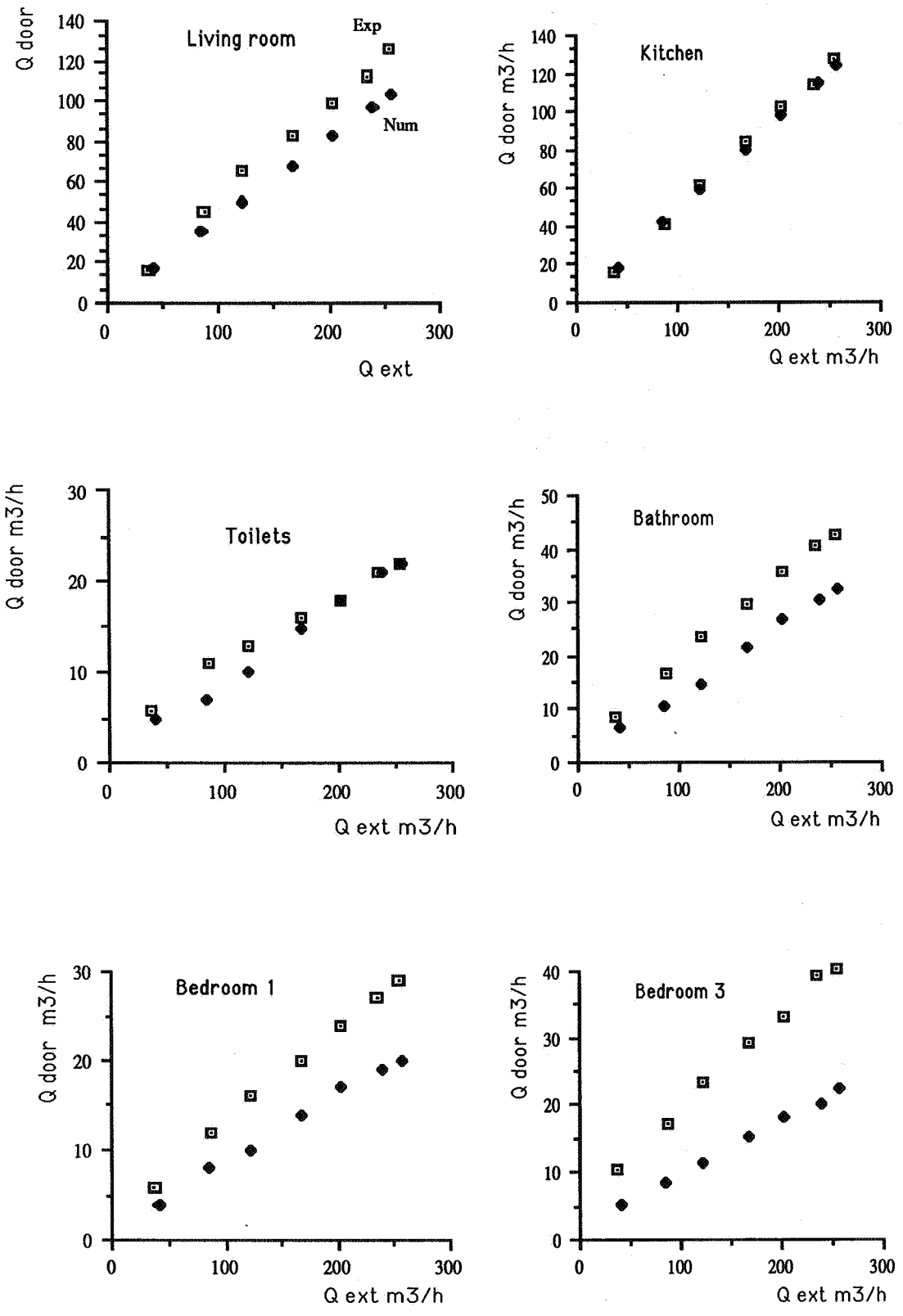

Figure 14 : Air flow rate through the interior doors

5. CONCLUSIONS

This study allows us to characterize the permeability of global components from depressurization tests by using an innovative numerical approach. After identification of the flow behavior of a typical interior door and their substitution by an equivalent pipe, we study the air flow pattern within the building under various extraction rates. The initial flow diagram is respected but less air than expected transits through the interior doors because of the poor level of tightness of the exterior enveloppe. A reduced ventilation rate results in the living room and in the bedrooms. More work is needed to take benefit of all the experiments and to fully characterize the building from a ventilation point of view.

6. APPENDIX

Reformulated Problem :

$$\text{minimize} \quad \sum_{i=1}^{nzones} \sum_{k=1}^{k(i)} \left| \sum_{j=1}^{nzones} m_{ij} (K_{ij} \, \Delta P_{ik}^{n_{ij}} - Q_{ik}) \right|$$

Subject to :

$$S_{ij} \leq K_{ij} \leq T_{ij}$$
$$Q_{ij} \leq n_{ij} \leq R_{ij}$$

Lau's method:

Step 1

- For each variable K_{ij}, n_{ij}, generate a random number in a given interval of constraints.Evaluate the objective function.

Step 2

- Repeat step 1 i1 times and memorize the best random vector that minimizes the objective function.

Step 3

- Shrink the constraint interval around the best random vector.
- Go to step 2 until step 3 has been applied i2 times. Then, the final solutionis the best random vector.

7. ACKNOWLEDGEMENTS

The work described in this paper was funded by the French Energy Agency (AFME) and the French Department of Construction. We would like to thank M. Kilberger and V. Richalet from CETE-France for conducting the on-site experiments.

8. REFERENCES

1. LAU, H.T.
"On solving systems of nonlinear equations by simulation"
Mathematics and Computers in Simulation, Vol 30, 1988, pp253-256

2. KILBERGER, M., GIBERT, J.P.
"Etanchéité à l'air des batiments"
CETE Report, 1985

Discussion
Paper 6

Peter Wouters, (Belgian Building Research Institute, Belgium)

I agree with you. But our objective was to measure the flow rate through on purpose openings (grille of the interior doors). On the second point of your question, a compensated flow meter would have been more appropriate. However, simultaneous measurements would require seven of them, and I suppose you know the price of each of them?

B. Fleury (ENTPE LASH, France)

The measurement of internal leakages with your pipe technique doesn't allow to estimate the leakages through the walls or between walls and doors. A compensated flow meter might be more accurate and quicker.

PROGRESS AND TRENDS IN AIR INFILTRATION
AND VENTILATION RESEARCH

10th AIVC Conference, Dipoli, Finland
25-28 September, 1989

Paper 7

MULTIZONE FLOW ANALYSIS AND ZONE SELECTION USING A NEW PULSED TRACER GAS TECHNIQUE

Patrick J. O'Neill and Roy R. Crawford

Department of Mechanical and Industrial Engineering
University of Illinois
Urbana, Illinois 61801
USA

NOMENCLATURE

$\mathbf{A}$ = discrete-time system matrix
$\mathbf{B}$ = discrete-time input matrix
$\mathbf{c}$ = vector of tracer gas concentrations
$\mathbf{D}$ = output matrix
$\mathbf{F}$ = matrix of interzonal flows
$\mathbf{G}$ = matrix used to represent $\mathbf{V}^{-1}\mathbf{F}$ during discrete to continuous inversion
$\mathbf{g}$ = vector of applied inputs
$\mathbf{I}$ = identity matrix
$\mathbf{L}$ = least-squares gain matrix
$\mathbf{M}$ = matrix whose columns are the eigenvectors of $\mathbf{A}$
$\mathbf{P}$ = matrix used during recursive least-squares algorithm
$\mathbf{R}$ = matrix used to calculate $\mathbf{V}$-- formed from infinite series
$\mathbf{v}$ = vector containing unmeasured system disturbances
$\mathbf{V}$ = matrix containing effective volumes of zones
$\mathbf{W}$ = transfer function matrix
$\mathbf{y}$ = least-squares output vector
$\boldsymbol{\phi}$ = least-squares regression vector
$\boldsymbol{\theta}$ = least-squares parameter matrix
$\hat{\boldsymbol{\theta}}(N)$ = least-squares estimate of $\boldsymbol{\theta}$ based upon N observations
a_{ij} = parameter appearing in input-output system formulation
b_{hq} = parameter appearing in input-output system formulation
c'_i = tracer concentration in zone i
$\dot{c}'_i$ = time derivative of tracer concentration in zone i
c_i = (concentration of tracer in zone i) - (outdoor tracer concentration)
Δc = concentration difference in two-zone system after impulse is applied
F_{ij} = flow from zone i to j
F' = interzonal airflows of equal magnitude in a two zone system
g_i = tracer input in zone i
h,i,j,k,q = indices used for sequences or series
n = total number of zones
N = number of data points
p_{ij} = parameter appearing in input-output system formulation
Q_i = total flow into or out of zone i
$S(\theta)$ = total sum of the squared error using the indicated parameter matrix
s = complex frequency variable defined in context of Laplace transform
T = sampling interval
t = time
T* = $T/(V/F_0)$; F_0 defined as total flow into a reduced order model
t* = $t/(V/F_0)$; F_0 defined as total flow into a reduced order model
V_i = effective volume of zone i
$y_{i,act}$ = ith actual measured output
$y^n_{i,pred}$ = ith output predicted by an ARMA model of order n
z = complex frequency variable defined in context of z transform
α = constant used to set initial condition of $\mathbf{P}$
β = used during least-squares analysis to apply varying weights to the data
δ_{ij} = Dirac delta function ($\delta_{ij} = 0$ for $i \neq j$; $\delta_{ij} = 1$ for $i=j$)
Δ = constant used to bound maximum sampling interval
ε = $\Delta c(t)/\Delta c(0)$
λ = forgetting factor
μ = eigenvalue of $\mathbf{V}^{-1}\mathbf{F}$
ν_i = eigenvector of $\mathbf{A}$
σ^2 = variance
τ = time constant for tracer decay
ω_i = eigenvalue of $\mathbf{A}$

1. SUMMARY

This paper presents and evaluates a new method, based upon tracer gas techniques, for determining interzonal airflows and effective volumes in a multizone enclosure. Presently used tracer gas techniques have a number of drawbacks including the need for multiple tracers when analyzing a multizone structure. Also, traditional techniques cannot be used to independently determine flows and volumes in the multizone case. The method described in this paper eliminates some of the problems introduced by multiple tracers and allows the independent determination of both flows and volumes.

The proposed method uses a single tracer gas to disturb the zones. A state-space formulation is used to model the multizone system. The concentration data are used in combination with a recursive least-squares identification algorithm to determine all of the interzonal airflows and effective volumes. A number of simulations are then used to validate the method The simulations show that there are important considerations to keep in mind when selecting the type of input applied to each zone. They also indicate that the proper choice of sampling interval is critical for accurate identification.

The recursive least-squares formulation is readily adapted to the case where the system parameters are varying. A number of simulations show that this method can be used to track varying interzonal flows and effective volumes provided they are changing slowly with time.

Finally, a method for determining the number of interconnected zones in a system is introduced. The method uses a single impulse applied to one of the zones. The tracer concentration in that zone is then monitored. The data are fit to an auto-regressive moving-average model and the residuals are analyzed using Akaike's AIC criterion which provides an indication of the order of the system.

2. INTRODUCTION

In recent years, increasing emphasis has been placed upon reducing overall building energy usage, while still maintaining acceptable levels of indoor air quality. As a tool in analyzing potential indoor air quality problem areas, tracer gas techniques have been employed with varying degrees of success (Harrje[1], Afonso[2], Jensen[3], Axley[4], Charlesworth[5]). Proper application of these techniques, whether based upon single or multiple tracers, can yield quantitative knowledge of the internal air circulation patterns.

If an accurate dynamic model of a building with respect to energy or mass transport is desired, the airflow measurement technique must determine the airflow rates, F, between zones and the effective volumes, V, of the zones as shown in Figure 1.

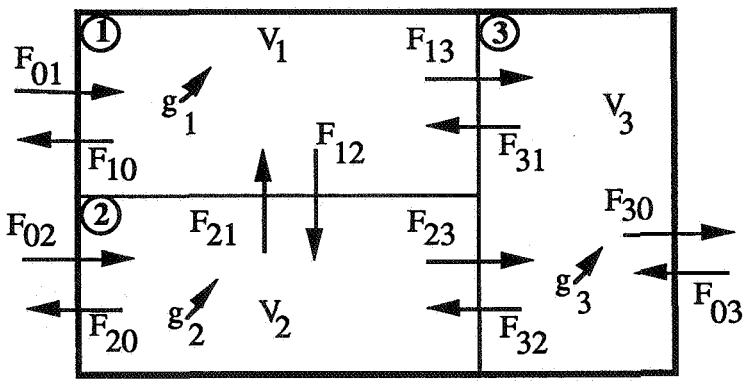

Figure 1. Three-Zone Airflow and Volume Model

The flows between zones can be the result of either mechanical (forced ventilation system) or natural convection (open doors or windows). Many buildings contain some combination of these two and most tracer gas techniques do not differentiate between them.

The effective volume is the volume of the interior of a zone in which complete mixing occurs (Allen[6]). In order to determine interzonal airflows, most tracer techniques assume that the effective volume is known a priori. For example, the effective volume might be assumed to be nearly equal to the unfilled volume of a room. However, if dead zones or ventilation system short circuiting occurs, the results of these techniques may be completely erroneous. Accurate determination of the effective volume will ensure not only robust control of indoor air quality and human comfort but will also indicate areas where improvements are needed.

This paper further evaluates a new method (O'Neill[7]), based upon tracer gas techniques, for determining interzonal airflows and effective volumes in a multizone enclosure. The method uses inputs of a single tracer gas to disturb each of the zones. A state-space formulation is used to model the multizone system and the concentration data were used in combination with a least-squares identification algorithm to determine all of the interzonal airflows and effective volumes.

Several issues which arise during the implementation of this and other tracer gas techniques are also addressed. These include:

- required length of test
- sampling period based upon:
  - numerical stability of identification algorithm
  - system dynamics
- input requirements
- identifying the number differentiable zones
- varying flows and/or effective volumes

3. MULTIZONE MODEL FORMULATION

For a multizone system as shown in Figure 1, conservation of mass for the tracer gas in a single zone, i, can be written as (Sinden[8])

$$V_i(t)\,\dot{c}'_i(t) = \sum_{j=0}^{n}(1-\delta_{ij})F_{ji}(t)c'_j(t) - c'_i(t)\sum_{j=0}^{n}(1-\delta_{ij})F_{ij}(t) + g_i(t) \qquad (3.1)$$

where

$g_i(t)$ = tracer input into zone i (mass/time)
$V_i(t)$ = effective volume of zone i
$c'_i(t)$ = tracer concentration in zone i (mass/volume)
$\dot{c}'_i(t)$ = time derivative of tracer concentration in zone i (mass/volume•time)
$F_{ij}(t)$ = flow from zone i to j (volume/time)
δ_{ij} = Dirac delta function ($\delta_{ij} = 0$ for $i \neq j$; $\delta_{ij} = 1$ for $i = j$)
n = total number of zones

The subscript "0" represents outdoor air. For the remaining theoretical analysis and simulations to follow, units will be omitted from the numerical results. These numbers may either be considered dimensionless or have units consistent with those defined in Equation (3.1). Also, for the remainder of the analysis, the concentration of tracer in the outdoors will be considered constant or relatively slowly changing. If this approximation is made, the outdoor concentration, c'_0, can be eliminated from Equation (3.1) by defining the other concentration terms to be the difference between the actual zone concentration and the outdoor value

$$c_i \equiv c'_i - c'_0 \qquad (3.2)$$

Equation (3.1) represents n first-order simultaneous differential equations for the multizone system. For the case where n = 3, Equation (3.1) could be written in state-space form as

$$\begin{bmatrix} V_1(t) & 0 & 0 \\ 0 & V_2(t) & 0 \\ 0 & 0 & V_3(t) \end{bmatrix} \begin{bmatrix} \dot{C}_1(t) \\ \dot{C}_2(t) \\ \dot{C}_3(t) \end{bmatrix} = \begin{bmatrix} -Q_1(t) & F_{21}(t) & F_{31}(t) \\ F_{12}(t) & -Q_2(t) & F_{32}(t) \\ F_{13}(t) & F_{23}(t) & -Q_3(t) \end{bmatrix} \begin{bmatrix} C_1(t) \\ C_2(t) \\ C_3(t) \end{bmatrix} + \begin{bmatrix} g_1(t) \\ g_2(t) \\ g_3(t) \end{bmatrix} \qquad (3.3a)$$

where

$$Q_i(t) = \sum_{j=0}^{n}(1-\delta_{ij})F_{ij}(t) = \sum_{j=0}^{n}(1-\delta_{ij})F_{ji}(t) \qquad (3.3b)$$

In Equation (3.3) the term $Q_i(t)$ represents the total flow into or out of zone i.

Equation (3.3) can be represented more compactly in matrix form as

$$\mathbf{V}(t)\,\dot{\mathbf{c}}(t) = \mathbf{F}(t)\,\mathbf{c}(t) + \mathbf{g}(t) \qquad (3.4)$$

or multiplying through by $\mathbf{V}^{-1}(t)$

$$\dot{\mathbf{c}}(t) = \mathbf{V}^{-1}(t)\mathbf{F}(t)\,\mathbf{c}(t) + \mathbf{V}^{-1}(t)\mathbf{g}(t) \qquad (3.5)$$

Equation (3.5) is known as the time varying state-space representation of the system of linear differential equations described by Equation (3.1). At this point, it is not

necessary to assume that the matrices $\mathbf{V}(t)$ and $\mathbf{F}(t)$ are constant for the entire duration of the tracer gas test.

The least-squares algorithm described below requires that the system be represented in discrete form. If it is assumed that the flows, $\mathbf{F}(t)$, volumes, $\mathbf{V}(t)$, and input, $\mathbf{g}(t)$, are held constant during the sampling interval, T, Equation (3.5) can be written as (Kuo[9])

$$\mathbf{c}[(k+1)T] = \mathbf{A}\,\mathbf{c}(kT) + \mathbf{B}\,\mathbf{g}(kT) \tag{3.6}$$

where $\mathbf{A}$ and $\mathbf{B}$ are defined as

$$\mathbf{A} = \exp[(\mathbf{V}^{-1}\mathbf{F})T] = \mathbf{I} + (\mathbf{V}^{-1}\mathbf{F})T + \frac{[(\mathbf{V}^{-1}\mathbf{F})T]^2}{2!} + \frac{[(\mathbf{V}^{-1}\mathbf{F})T]^3}{3!} + \cdots \tag{3.7}$$

$$\mathbf{B} = \int_0^T \exp[(\mathbf{V}^{-1}\mathbf{F})t]\mathbf{V}^{-1}dt = \left[\mathbf{I}T + \frac{(\mathbf{V}^{-1}\mathbf{F})T^2}{2!} + \frac{(\mathbf{V}^{-1}\mathbf{F})^2T^3}{3!} + \cdots\right]\mathbf{V}^{-1} \tag{3.8}$$

with $\mathbf{V}^{-1}$ and $\mathbf{F}$ defined as the values of $\mathbf{V}^{-1}(t)$ and $\mathbf{F}(t)$ on the interval (kT, [k+1]T). Equation (3.6) is the linear discrete-time state-space formulation of the system described in Equation (3.1) with k = t/T.

4. RECURSIVE LEAST-SQUARES IDENTIFICATION ALGORITHM

The problem of parameter identification has been studied extensively in many fields as a necessary first step in any type of system analysis (Ljung[10], Eykhoff[11], Kudva[12], Ossman[13]). One well known procedure used in parameter estimation is known as the method of least-squares. In this method, a model form containing one or more unknown parameters is assumed to describe the system. One or more tests are then run in which known inputs are applied and the outputs of the system are measured. These data are then used to select the best combination of parameters with respect to minimizing the sum of the squared error between the actual data and the predicted value.

To formulate the least-squares estimate of the system parameters, Equation (3.6) is rewritten in a slightly different form

$$y[k] = \theta^T\phi(k-1) + v(k-1) \tag{4.1}$$

where y[k] is a vector containing the measured tracer concentrations in each zone at time step k. The symbol, θ, is used to denote the parameter matrix,

$$\theta = [\,\mathbf{A}\;\;\mathbf{B}]^T \tag{4.2}$$

and contains the unknown parameters of interest. The variable, $\phi(k-1)$, is the regression vector whose components are comprised of past observations of the inputs and outputs of the system (regression variables)

$$\phi(k-1) = [c_1(k-1)\;\; c_2(k-1)...c_n(k-1)\;\; g_1(k-1)\;\; g_2(k-1)...g_n(k-1)]^T \tag{4.3}$$

The vector, v(k-1), contains unknown and unmeasurable disturbances to the system (eg. measurement noise).

The method of least-squares is described by the criterion function

$$S(\theta) = \sum_{k=1}^{N} \beta(k)\left\{ [y^T[k]-\phi^T(k-1)\theta] [y[k]-\theta^T\phi(k-1)] \right\} \quad (4.4a)$$

$$= \sum_{k=0}^{N-1} \beta(k)v^T(k)v(k) \quad (4.4b)$$

assuming v(k) is a sequence of random variables with zero mean (white noise). In Equation (4.4), the term, N, is the number of data points collected and $\beta(k)$ is a sequence which can be used to give varying weights to different data. The optimal choice of the parameter vector is that vector which minimizes $S(\theta)$–producing the smallest summation of the squared errors. Since Equation (4.4) is quadratic in θ, it is straightforward to solve analytically. This gives

$$\hat{\theta}(N) = \left[\sum_{k=1}^{N} \beta(k)\phi(k-1)\phi^T(k-1) \right]^{-1} \sum_{k=1}^{N} \beta(k)\phi(k-1)y^T(k-1) \quad (4.5)$$

$\hat{\theta}(N)$ is the least-squares estimate, based upon N observations, of the actual parameter matrix θ.

The method of determining the unknown system parameters by first collecting all of the data and then calculating $\hat{\theta}(N)$ using Equation (4.5) is known as the batch method. The batch method is useful for systems which are well understood and prior knowledge about when to apply the inputs is known. However, it is often more useful to represent Equation (4.5) in a recursive fashion. With a recursive identification algorithm, the unknown parameters can be calculated as each new data point is recorded.

While the derivation of the recursive form of Equation (4.5) is straightforward, it is somewhat algebraically involved (See Ljung[10] or Eykhoff[11]). Therefore, just the results will be presented here. The recursive least-squares algorithm is simple in concept. Using this procedure, the new estimate of the parameter matrix, $\hat{\theta}(k)$, is equal to the old estimate, $\hat{\theta}(k-1)$, plus some gain matrix, L(k), times the error between the predicted and actual values of the output(s). The algorithm is thus,

$$\hat{\theta}(k) = \hat{\theta}(k-1) + L(k)[y^T[k]-\phi^T(k-1)\hat{\theta}(k-1)] \quad (4.6a)$$

where

$$L(k) = \frac{P(k-1)\phi(k-1)}{1/\beta(k-1) + \phi^T(k-1)P(k-1)\phi(k-1)} \quad (4.6b)$$

$$\mathbf{P}(k) = \mathbf{P}(k-1) - \frac{\mathbf{P}(k-1)\phi(k-1)\phi^T(k-1)\mathbf{P}(k-1)}{1/\beta(k-1) + \phi^T(k-1)\mathbf{P}(k-1)\phi(k-1)} \tag{4.6c}$$

Therefore, the most computationally involved part of the algorithm comes in computing the gain matrix, $\mathbf{L}(k)$.

Examination of Equation (4.6) leaves the question of initial conditions of the matrices $\hat{\theta}(k_0)$ and $\mathbf{P}(k_0)$ as yet unresolved. As $N \rightarrow \infty$ the effect of the initial values disappears. In practice however, even for a small number of data points, the effect of initial conditions is negligible. Thus, common choices for the initial values of $\mathbf{P}(k_0)$ and $\hat{\theta}(k_0)$ are $\mathbf{P}(k_0) = \alpha\mathbf{I}$ and $\hat{\theta}(k_0) = \mathbf{0}$, where α is some large constant. However, if an 'exact' initial guess is desired or only a few data points are available, the following values of $\mathbf{P}(k_0)$ and $\hat{\theta}(k_0)$ should be used

$$\mathbf{P}(k_0) = \left[\sum_{k=1}^{k_0} \beta(k)\phi(k-1)\phi^T(k-1) \right]^{-1} \tag{4.7a}$$

$$\hat{\theta}(k_0) = \mathbf{P}(k_0) \sum_{k=1}^{k_0} \beta(k)\phi(k-1)y(k-1) \tag{4.7b}$$

The value of k_0 in Equations (4.7a) and (4.7b) should be chosen such that the required matrix inversion is possible.

The recursive least-squares method allows one to examine, in real time, the response of the system parameters to the applied inputs and determine when (and possibly where) new inputs should be applied. For example, if one or more inputs have been applied in the past and the parameters of interest are no longer changing appreciably with each new data point collected, then it is appropriate to apply an additional input or terminate the test.

5. INVERSION FROM A AND B TO V AND F

Before evaluating the least-squares algorithm described above, some discussion is necessary on how to interpret the values of the flows, **F**, and effective volumes, **V**, from the matrices **A** and **B**. In the development of Equation (3.6), it was not necessary to approximate the differentials appearing in Equation (3.5). Thus, the values of **A** and **B** obtained during the least-squares analysis are not affected by any such approximations. However, when going in the opposite direction, that is, calculating **F** and **V** from **A** and **B** it is not as simple.

Depending upon the length of the sampling interval, different approaches may be necessary. If the sampling period is short, relative to the system eigenvalues, then an Euler approximation (forward differencing) may be adequate. For example, if the Euler approximation is made, the differential is written as

$$\dot{c}(t) = \frac{c([k+1]T) - c(kT)}{T} \tag{5.1}$$

and Equation (3.6) becomes

$$\mathbf{c}[(k+1)] = (\mathbf{I}+T\mathbf{V}^{-1}\mathbf{F})\,\mathbf{c}(k) + T\mathbf{V}^{-1}\,\mathbf{g}(k) \tag{5.2}$$

thus,

$$\mathbf{V} = T\mathbf{B}^{-1} \tag{5.3a}$$

$$\mathbf{F} = \mathbf{V}(\mathbf{A} - \mathbf{I})/T \tag{5.3b}$$

Examination of Equations (3.7) and (3.8) show that the Euler approximation is equivalent to using the first two terms of the infinite series for **A** and the first term in the infinite series for **B**. Tustin's and other higher order approximations are obtained in a similar manner. In practice, it has been found that using the first several terms from each series is adequate in most cases.

When larger sampling intervals are used however, the higher order terms in the series remain significant. Here, the simple approximations described above may not prove adequate. One method for circumventing difficulties associated with larger sampling intervals uses properties of eigenvalues and eigenvectors in the calculation of the exponential of a matrix (Sinha[14]).

If the eigenvalues, $\omega_1, \omega_2,\ldots,\omega_n$ are distinct the eigenvectors $\nu_1,\nu_2,\ldots,\nu_n$ of the matrix **A** can be calculated (In case of multiple eigenvalues, the eigenspace must have equal multiplicity) then it is possible to form the matrix **M**

$$\mathbf{M} = [\nu_1\ \nu_2\ \ldots\ \nu_n] \tag{5.4}$$

which will diagonalize **A**. The quantity $\mathbf{V}^{-1}\mathbf{F}$ is given by forming the following equality

$$\mathbf{V}^{-1}\mathbf{F} = \mathbf{G} = \left\{\mathbf{M}\ \mathbf{diag}\left[\frac{1}{T}\ln\omega_1\ \ \frac{1}{T}\ln\omega_2\ \ldots\ \frac{1}{T}\ln\omega_3\right]\mathbf{M}^{-1}\right\} \tag{5.5}$$

If **A** has negative eigenvalues, the logarithms in Equation (5.5) become undefined. This problem is eliminated by proper selection of sampling interval and will be discussed in a following section. Finally, the matrix **V** is given by

$$\mathbf{V} = \mathbf{B}^{-1}\mathbf{R} \tag{5.6}$$

where the matrix **R** is defined as

$$\mathbf{R} = \mathbf{I}T + \frac{\mathbf{G}T^2}{2!} + \frac{\mathbf{G}^2T^3}{3!} + \cdots \tag{5.7}$$

6. SIMULATIONS USING THE LEAST-SQUARES ALGORITHM

The algorithm described by Equation (4.6) was tested on various multizone systems using computer generated data, $\beta(k)=1$. The interzonal flows and volumes were picked arbitrarily and chosen so that the system was asymmetric. The algorithm

was tested for systems with one, two, and three-zones. Table 1 shows the results of these simulations for the case of clean data (no noise) and also for cases of data with low and moderate measurement noise. The noise added to the simulation data were random variables with a maximum value equal to a fixed percentage of the zones initial concentration. The maximum values of the noise used in the simulations were 5 and 10% and resulted in variances of $\sigma^2 = 0.002$ and 0.008.

Table 1. Identification of Flows and Effective Volumes using Least-Squares Algorithm

# of Zones	Noise σ^2	V_1	V_2	V_3	F_{01}	F_{10}	F_{02}	F_{20}	F_{03}	F_{30}	F_{12}	F_{13}	F_{21}	F_{23}	F_{31}	F_{32}
1	0.00	1006	-	-	.20	.20	-	-	-	-	-	-	-	-	-	-
1	0.002	998	-	-	.21	.21	-	-	-	-	-	-	-	-	-	-
1	0.008	986	-	-	.21	.21	-	-	-	-	-	-	-	-	-	-
Actual	-	1000	-	-	.20	.20	-	-	-	-	-	-	-	-	-	-
2	0.00	1023	2031	-	.10	.29	.50	.31	-	-	.21	-	.41	-	-	-
2	0.002	1010	1970	-	.11	.27	.53	.28	-	-	.25	-	.43	-	-	-
2	0.008	964	2107	-	.09	.35	.55	.31	-	-	.23	-	.48	-	-	-
Actual	-	1000	2000	-	.10	.30	.50	.30	-	-	.20	-	.40	-	-	-
3	0.00	1006	2017	3021	.00	.10	.31	.00	.00	.21	.42	.00	.52	.21	.00	.00
3	0.002	1003	2015	2973	.01	.09	.30	-.02	.01	.18	.43	.00	.53	.18	-.01	.00
3	0.008	935	2086	3126	.01	.11	.34	.02	-.04	.31	.58	.04	.60	.27	.05	-.04
Actual	-	1000	2000	3000	.00	.10	.30	.00	.00	.20	.40	.00	.50	.20	.00	.00

The total time for all the identification runs listed in Table 1 was 10,000. The sampling interval was 100–a total of 100 samples each. The table shows that in most cases, the identification procedure was able to estimate all the flows and volumes to within ± 20%. As the amplitude of the noise increases, the system parameters are identified less accurately. If the noise is increased significantly beyond that shown ($\sigma^2 > 0.008$) , the algorithm is unable to adequately identify any of the parameters and becomes unstable. For the case of no noise, the identification algorithm was able to predict the system parameters to within ± 10% in all cases and usually much closer. For all of the simulations, the inputs were assumed to be impulses which mixed instantaneously with all of the air within the zone.

Figures 2 thru 7 show the 'real time' estimation of the parameters for the three-zone case. Figures 2 thru 4 indicate that when there is little noise in the data, the estimated parameters converge to steady-state values shortly after the impulses. Also, the parameters converge to their final, correct values, only after all of the zones have been pulsed. This is because all of the modes of the system are not suitably excited by the impulses unless they are applied to all of the zones.

Figures 5 thru 7 indicate that when there is significant noise ($\sigma^2 = 0.002$) associated with the data, the character of the least-squares solution changes considerably. The noise has the effect of slowing the convergence of the solution. Between the impulses, there is a considerable amount of random oscillation before the parameters settle down and approach steady values. Figure 7 indicates that the calculation of the effective volumes of the zones is much less sensitive to noise than that of the flows. The figure also indicates that the effective volume of each zone is determined immediately after the pulse and varies little thereafter.

All the figures show that the identified parameters steady-out sometime shortly after the previous pulse. Thus, when all of the parameters are changing only slightly with each new sample, then it is appropriate to apply an input to another zone. Also,

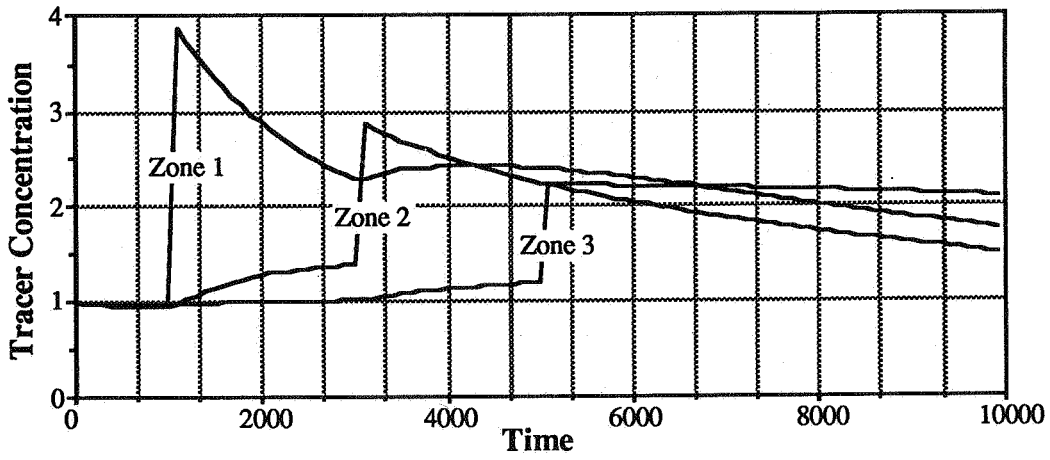

Figure 2. Tracer Concentrations for Three-Zone Simulation (No Noise)

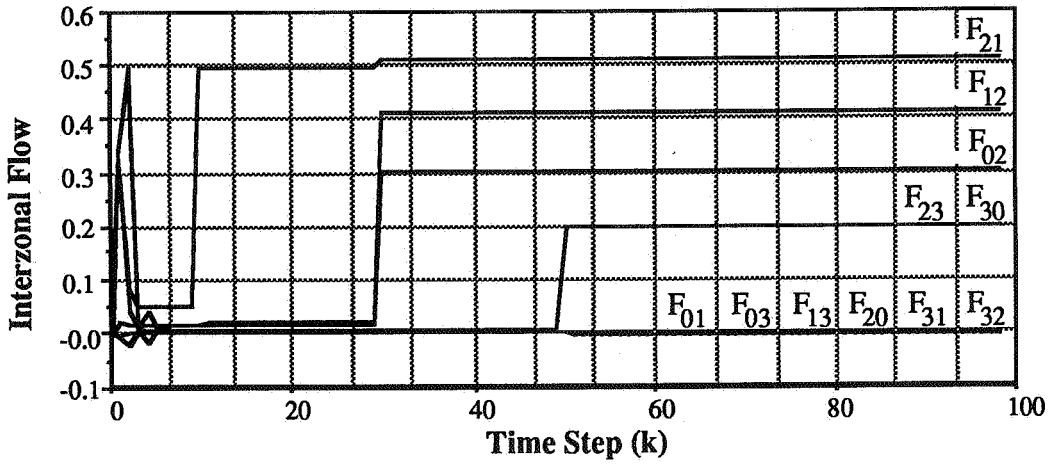

Figure 3. Interzonal Airflows Calculated using Recursive Least-Squares (No Noise)

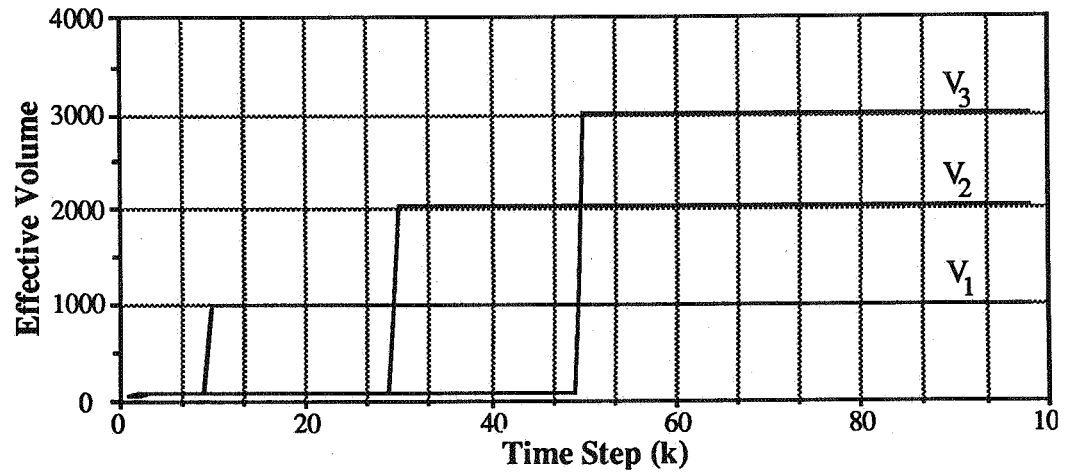

Figure 4. Effective Volumes Calculated using Recursive Least-Squares (No Noise)

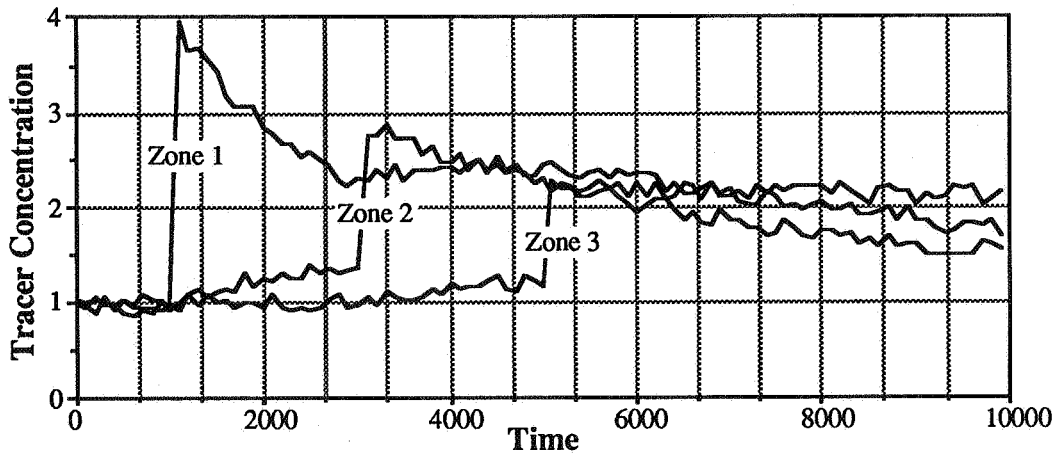

Figure 5. Tracer Concentrations for Three-Zone Simulation ($\sigma^2 = 0.002$)

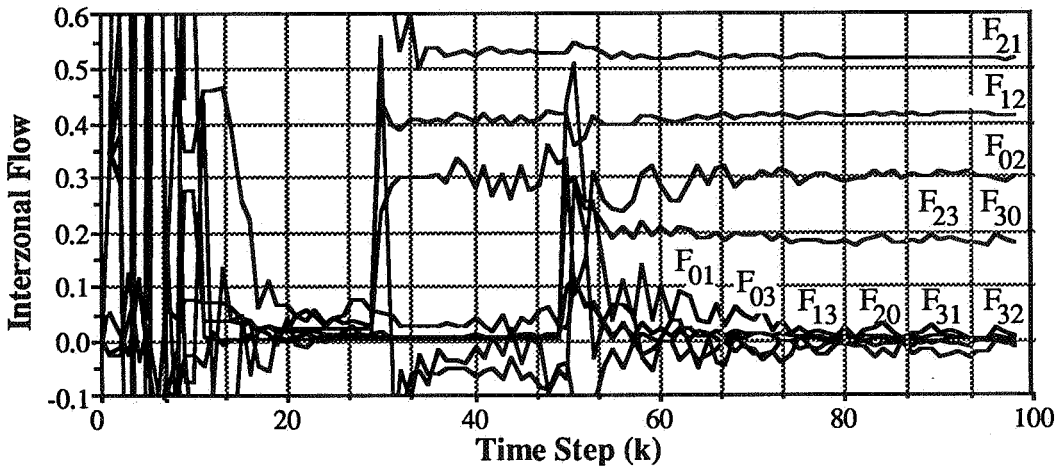

Figure 6. Interzonal Airflows Calculated using Recursive Least-Squares (σ^2 =0.002)

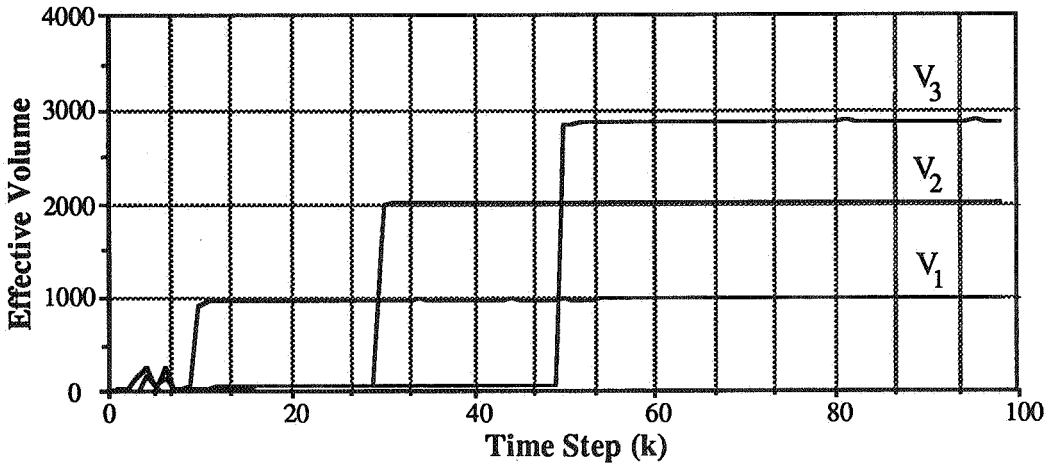

Figure 7. Effective Volumes Calculated using Recursive Least-Squares ($\sigma^2 = 0.002$)

as described above, a sampling interval of 100 was used in all of the identification runs listed in Table 1. This interval proved adequate for the cases shown. However, as the unmeasured disturbances to the system and the number of zones increases, the selection of the sampling interval becomes more important. Choosing a sampling interval which is either too small or too large can result in incorrect parameter estimation or instability of the identification algorithm

7. INPUT REQUIREMENTS FOR COMPLETE IDENTIFICATION

The identification of a dynamic system using the least-squares technique requires that the input which is applied to the system provide sufficient excitation. Another way of stating this is that the input must independently activate all of the modes of the system. In most control systems literature, an input which is often used to ensure that this condition is satisfied is a pseudorandom binary sequence (Jensen[3]) Unfortunately, to apply this type of input requires well regulated and calibrated equipment capable of providing real time readings of the flow rate of tracer into each zone at each sampling interval.

The identification runs described in the preceding section used inputs which were rapid injections (impulses). This type of input proved to be adequate for complete identification of the systems in question. It is also believed that an impulse type injection is practical to implement. A near impulse injection could be achieved by the rapid discharge of a pressurized cylinder or bursting a balloon filled with a known amount of tracer.

The simulations indicate that as each additional pulse is applied to the system, more parameters are identified. The simulations also reveal that all of the unknown flows and effective volumes are not determined until after an impulse has been applied to each zone. Thus, the conclusion can be drawn that for the impulse type input, sufficient excitation for complete system identifiability is achieved only by applying an impulse to all of the zones. Also, as will be discussed in the next section, if system parameters are varying, multiple impulses over time are required to track the parameters.

It was mentioned in the previous section that a new input should be applied as soon as possible after the preceding one. The natural question to ask is how close the inputs can be applied to one another and still result in satisfactory identification of the system parameters. To test this, the identification algorithm was run for the two-zone system examined in the previous section ($\sigma^2 = 0.002$) . Two different input intervals were examined. In the first case, the impulse inputs were applied simultaneously (Figure 8). Both of the inputs were applied at t = 2000.

Figure 9 shows how the least-squares algorithm responded to the applied inputs. The figure indicates that the calculated flows take a considerable amount of time to approach their correct values–doing so only after an additional 100+ time steps following the applied inputs. Figure 8 also indicates that the tracer concentration in Zones one and two was considerably different after the two were pulsed with tracer. Further simulations have shown that as this difference is reduced, the identification algorithm becomes ill conditioned. It was also noticed that noise affects the identification procedure more significantly for the case of simultaneously applied inputs.

Figures 10 and 11 show the results of a nearly identical simulation. The only difference is that the inputs applied to the two zones are separated by 10 sample periods. Examination of Figure 11 indicates that the effect of this slight separation is to significantly improve the conditioning of the identification procedure. The inputs are applied to the zones at time steps 20 and 30. The figure also indicates that the identification is essentially complete by time step 40. This is a significant improvement over the simultaneous pulse results. Thus, while it appears possible to apply simultaneous inputs to each zone and still identify the parameters of interest,

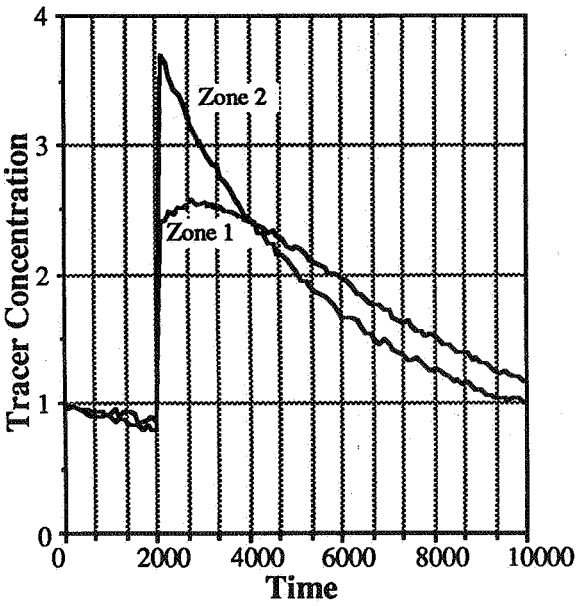

Figure 8. Data for Simultaneous Impulse Injection Input

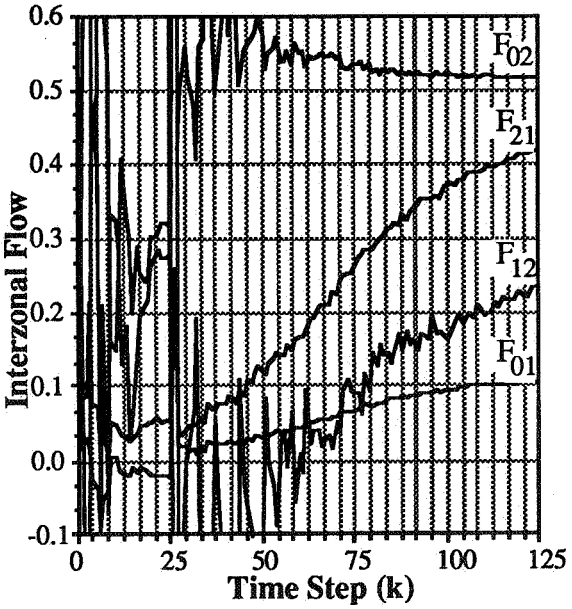

Figure 9. Calculated Flows for Simultaneous Impulse Injection Input

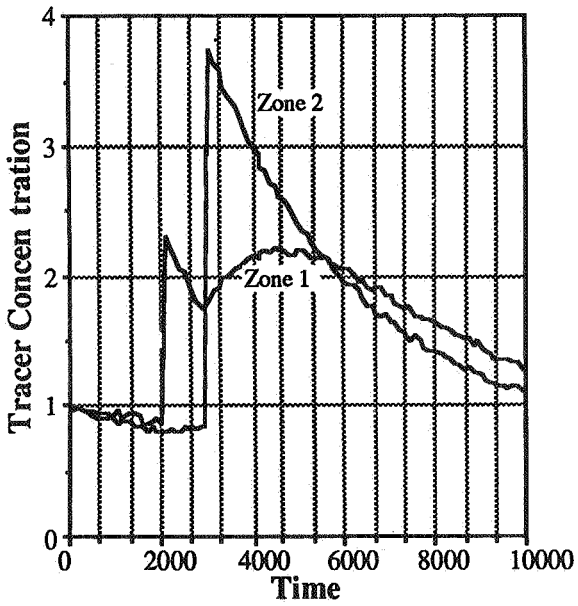

Figure 10. Data for Separated Impulse Injection Input

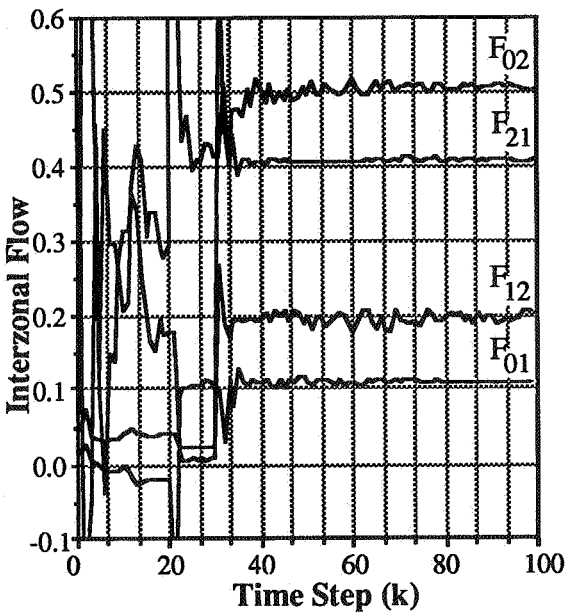

Figure 11. Calculated Flows for Separated Impulse Injection Input

the recursive least-squares algorithm is much more robust if the inputs are separated by several sample periods.

It should be noted that as the level of noise associated with the data is reduced toward zero (ie. the system becomes deterministic), the least-squares algorithm is able to identify the parameters much more rapidly. For simultaneous impulse inputs and clean data, the system is completely identified within 20 time steps following the inputs. However, even for clean data, separation of the inputs by a few time steps speeds the convergence of the least-squares algorithm.

8. VARYING FLOWS AND EFFECTIVE VOLUMES

The flows and effective volumes calculated using Equation (4.6) with $\beta(k) = 1$ are assumed to be constant for the duration of the test. If this assumption is not valid, the system parameters calculated by the least-squares analysis will be those which give the best overall fit of the data to the assumed system model and not necessarily the true values. If the system parameters are varying, then a slightly different approach must be followed when using the identification algorithm.

One of the primary purposes of obtaining the recursive formulation of the least-squares algorithm is for tracking the parameters in a system which is varying slowly with time. It should be noted that the approach presented below is not suited for identification of a system with high frequency parameter fluctuations. The variation in the parameters must be slow enough to allow the algorithm to 'catch' up with the new values before they change again significantly. If this condition is not satisfied, then the procedure will not work.

Equation (4.4) included the parameters, $\beta(k)$, and it was indicated that these parameters were a sequence which could give different weighting to the data during the recursive calculations. For example, proper selection of this sequence can reduce start-up transients which may pose problems if the data were very noisy. However, if $\beta(k)$ is assumed to have the form (Ljung[10], Goodwin[15])

$$\beta(k) = \lambda^{N-k} \tag{8.1}$$

where $0<\lambda<1$ then the algorithm is said to employ exponential forgetting of the data. The parameter, λ, is referred to as the forgetting factor. While in general, λ may also vary in time, in the following discussion, it is assumed a constant. The addition of this term effectively reduces the importance of data which were collected in the past and gives increasing weight to new data as they are recorded. Hence, if the flows and volumes are varying slowly, then this method can be used to track that variation in time.

This form of $\beta(k)$ also results in a slight modification of Equation (4.6). The recursive least-squares algorithm becomes

$$\hat{\theta}(k) = \hat{\theta}(k-1) + L(k)[y^T[k]-\phi^T(k-1)\hat{\theta}(k-1)] \tag{8.2a}$$

$$L(k) = \frac{P(k-1)\phi(k-1)}{\lambda + \phi^T(k-1)P(k-1)\phi(k-1)} \tag{8.2b}$$

$$P(k) = \frac{1}{\lambda}\left[P(k-1) - \frac{P(k-1)\phi(k-1)\phi^T(k-1)P(k-1)}{\lambda + \phi^T(k-1)P(k-1)\phi(k-1)} \right] \tag{8.2c}$$

Examination of Equation (8.2c) shows that the addition of exponential forgetting effectively keeps P(k) from approaching zero, thus keeping the algorithm robust with respect to tracking.

The selection of the forgetting factor will have a substantial influence on the identification algorithm. Using a relatively small value of λ ($\lambda < 0.9$) will have the effect of discounting all but the last few data points. However, if substantial noise is associated with the data, the identification procedure will perform poorly and may become unstable. As λ approaches 1, the algorithm approaches that of the standard least-squares and all data are weighted equally. Thus, there exists a trade-off between noise considerations and the ability of the procedure to track varying parameters.

The use of the forgetting factor is shown in Figures 12 and 13 for the two-zone system described previously. Initially, the system is identical to that described in Table 1. However, at t = 5000, several of the system parameters associated with the second zone change: V_2 increases from 2000 to 3000, F_{02} drops from 0.5 to 0.3 and F_{20} decreases from 0.3 to 0.0. The data were noisy ($\sigma^2 = 0.002$) and a forgetting factor of 0.97 was used during the identification.

The inputs are applied to Zone 1 at t = 1000 and 6000 and applied to Zone 2 at t = 2500 and 7500. Figure 12 shows that the algorithm is able to follow the flow parameters reasonably well with some fluctuation occurring around the times of the impulses. Figure 13 indicates that the algorithm is able to follow the effective volumes but only after the zone in which the volume changed is pulsed a second time.

In simulations using clean data, the algorithm was able to respond in a manner similar to that shown in Figure 3. The new values of the system parameters were all accurately identified (with little fluctuation) a few time steps after the conclusion of the second round of impulses. As might be expected, a more exciting input is required for identification of the time varying system parameters. If an impulse type input is being used as the excitation, it has been found that each zone must receive multiple inputs.

One final note on the selection of the value of the forgetting factor, λ. If the system is noisy, a value of λ less than 0.95 is usually not satisfactory for the cases studied. The algorithm becomes too sensitive to the random fluctuations induced by the unmeasured disturbances and does a poor job in tracking the system parameters. However, if very clean data are available, it is possible to use forgetting factors of 0.95 or slightly less.

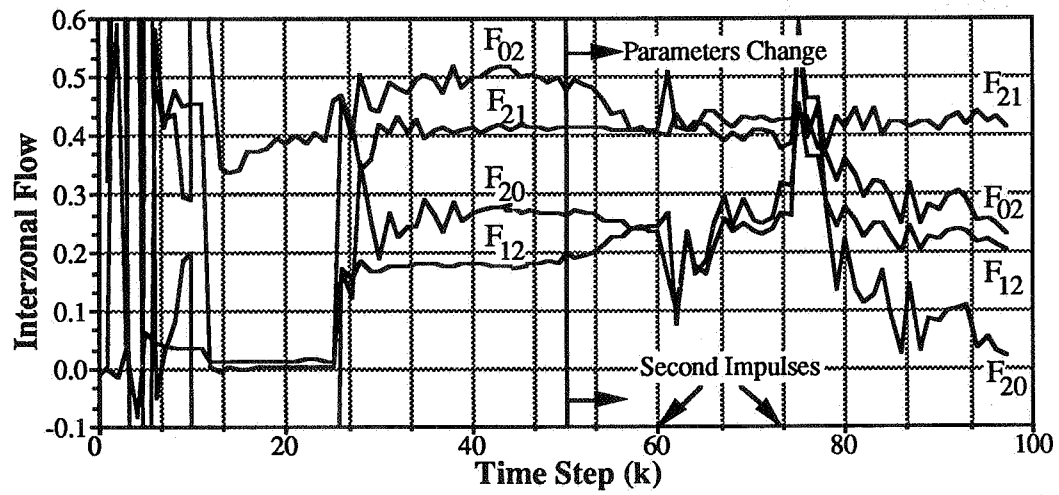

Figure 12. Interzonal Airflows Calculated using a Forgetting Factor ($\lambda = 0.97$)

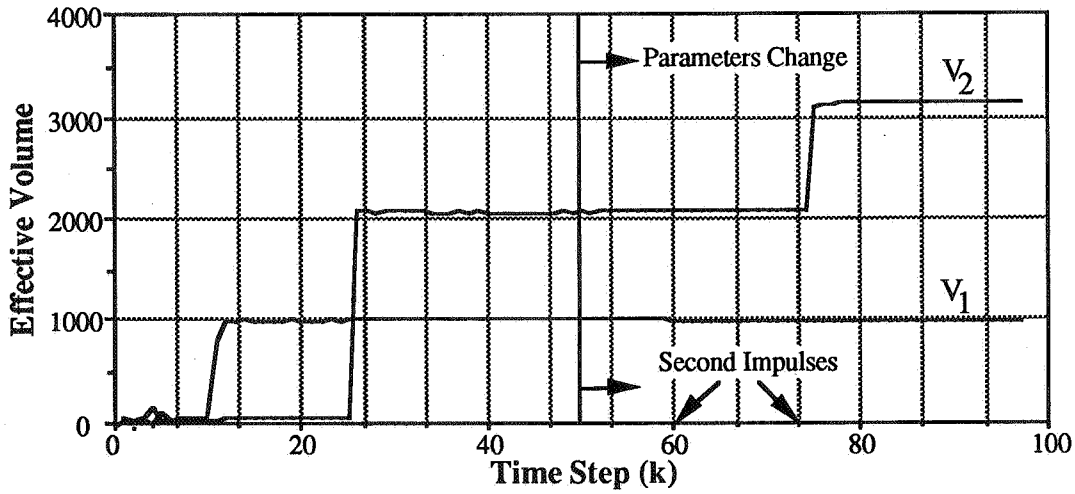

Figure 13. Effective Volumes Calculated using a Forgetting Factor ($\lambda = 0.97$)

9. SAMPLING INTERVAL

In the past several sections little mention was made as to how the sampling interval was chosen. However, selecting the correct sampling interval can make the difference between successful identification of the unknown system parameters or complete failure. Either the least-squares algorithm produces erroneous results or becomes unstable.

In choosing some 'optimal' (optimal in the sense that the system is accurately identified) sampling interval, there are two different though related considerations which must be addressed. First, the sampling interval must be rapid enough to capture the fastest dynamics of importance within the system. Sampling too slowly, with respect to the fastest system eigenvalue, will result in poor identification of the overall system. Second, the sampling interval must be slow enough to allow adequate mixing of the inputs between the injection and the first sample following it.

9.1 Sampling Interval and Eigenvalue Locations

The question of selecting an optimal sampling interval with respect to capturing important system dynamics has been studied by several researchers (Sinha[16], Sinha[17], Puthenpura[18]). A rule of thumb which is often mentioned by these authors is that the sampling interval should be chosen such that

$$|\mu T| \leq \Delta \tag{9.1}$$

where μ is the eigenvalue with the largest magnitude (fastest) in the continous-time system. The value of Δ is usually in the range $0 < \Delta \leq 0.5$. In examining the criterion presented in Equation (9.1) two questions come to mind. First, since an unknown system is being identified and the fastest eigenvalue is not a priori information, how can an appropriate sampling period be chosen? Second, why not sample as fast as possible to ensure that the criterion will be satisfied? The answer to both of these questions can be found by examining the transformation of the system eigenvalues when mapped from continuous-time to discrete-time.

Since the flow systems under study must be stable, (no unmeasured tracer is injected) all of the eigenvalues are located on the left side of the Im sT axis as shown in Figure (14). If it is further assumed that the sampling criterion of Equation (9.1) is satisfied, then the eigenvalues of the continuous-time system must lie within the shaded regions in the sT-plane. Recall from Equation (3.7) that in going from the continuous time system to its discrete equivalent, the system matrix becomes

$$\mathbf{A} = \exp[(\mathbf{V}^{-1}\mathbf{F})T] \tag{9.2}$$

If μ is an eigenvalue of $\mathbf{V}^{-1}\mathbf{F}$ then $\omega = \exp(\mu T)$ is an eigenvalue of A. The figure also indicates that the consequence of this mapping is that the region in the sT-plane containing the eigenvalues of $\mathbf{V}^{-1}\mathbf{F}$ are compressed into the lens shaped region in the z-plane when the system is discretized.

The z-plane figure reveals a problem which can arise if the sampling interval is chosen to be too small. As smaller values of T are chosen, the region in which all of the discrete-time eigenvalues are located becomes smaller and moves closer to the point $1 + j0$ ($j = \sqrt{-1}$). The eigenvalues found outside of the circle with radius $r = 1$ are unstable. If there is appreciable noise associated with the data then the identification algorithm may calculate values of the A matrix which have unstable eigenvalues. This will result in poor conditioning of the least-squares identification algorithm.

A number of identification runs were conducted to determine the best value of Δ for an impulse type input. Table 2 shows the results for the one, two, and three-zone systems described in Section 6. The table indicates that the sampling interval has a significant impact upon the accuracy of the identification algorithm. With no noise in the data, it is possible to use very small values of the sampling interval. This results in a very accurate estimate of the unknown flows and volumes. However, the accuracy appears to deteriorate as the sampling interval is raised past $\mu T \approx 0.1$.

As noise is added to the data ($\sigma^2 = 0.002$), the behavior of the least-squares algorithm changes. Table 2 shows that selection of a sampling interval which is too small decreases the accuracy of the identification procedure and can, in some cases, result in numerical instability. However, if the 'correct' sampling interval is chosen,

the accuracy of the identified parameters for the case of noisy data is similar to the corresponding case without noise.

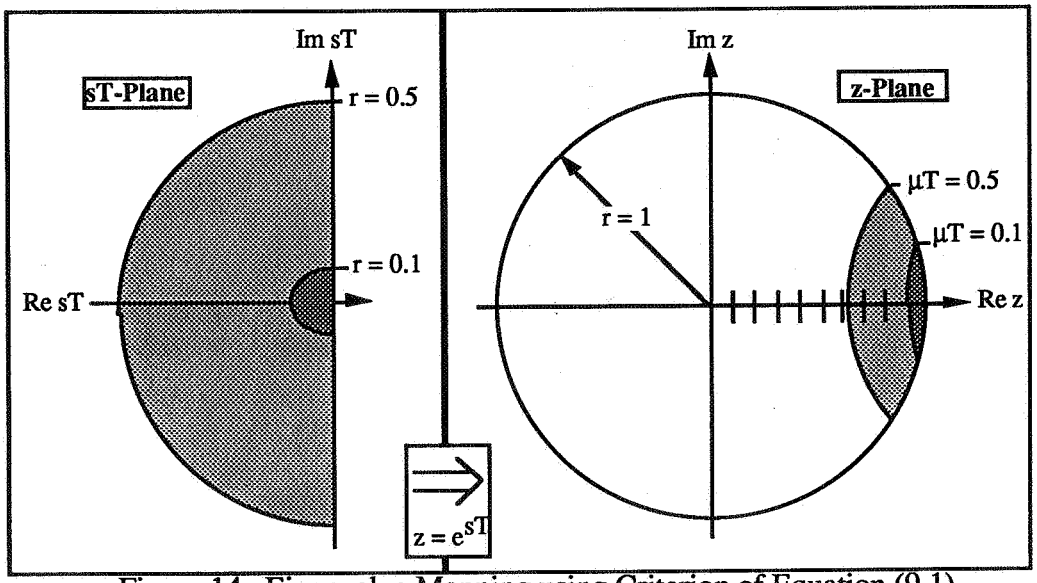

Figure 14. Eigenvalue Mapping using Criterion of Equation (9.1)

Table 2. Accuracy of Identification Algorithm with Different Sampling Intervals

# Zones	ω_{max}	ω_{min}	$\lvert \mu_{max} T \rvert$	Max. Error in Calculated Parameters(%) Without Noise	Max. Error in Calculated Parameters(%) With Noise
1	-	0.998	0.002	0.1	10
	-	0.940	0.06	5	5
	-	0.900	0.10	5	5
	-	0.821	0.20	11	12
	-	0.552	0.60	40	42
2	0.997	0.996	0.004	0.2	30
	0.979	0.938	0.06	10	24
	0.959	0.880	0.13	15	16
	0.900	0.731	0.30	51	50
	0.810	0.527	0.60	110	124
3	0.999	0.995	0.005	0.2	Unstable
	0.993	0.928	0.07	2.5	16
	0.991	0.900	0.10	4.0	9
	0.987	0.861	0.15	11	18
	0.967	0.687	0.40	22	211

Thus, proper selection of the sampling interval is critical for accurate identification of system parameters. A criterion for this selection can be established by examining the second, third, and fourth columns of Table 2. For very small values of the sampling interval, the eigenvalues of the discrete-time system are close to one another and to the point 1 + j0. This is a point of potential instability in the algorithm. Fortunately, as the sampling interval is increased, the eigenvalues of the discrete-time system spread out and shift toward the left. As these eigenvalues change, the accuracy of the identified parameters improves up to the point where the smallest eigenvalue is in the range $0.88 < \omega < 0.92$. This corresponds to selection of the

value of μT such that $0.083 < |\mu T| < 0.13$. Therefore, for the simulations shown, a value of $\Delta \approx 0.1$ should be used when following the criterion for sampling interval selection described by Equation (9.1).

9.2 Sampling Interval and Effective Volumes

The effective volume that the analysis predicts for each zone also depends upon how well the impulse is dispersed between the time that it is injected into the zone and the first sampling of the concentration in that zone after the impulse (O'Neill[7]). In an attempt to better understand this relationship, it is useful to determine the conditions for which a two-zone system can be adequately represented as a single zone as shown in Figure 15. In the two-zone model shown on the left, if the interzonal flows (F ') are sufficiently high relative to the external flows (F_o), then an impulse of tracer gas into either zone should be quickly dispersed throughout both zones and the concentrations in each should approach each other rapidly.

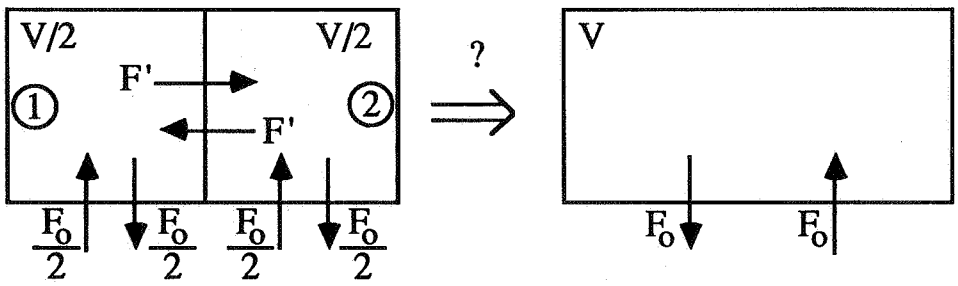

Figure 15. Two-Zone versus One-Zone Model for Least-Squares Analysis

The response of both zones to a single impulse of tracer gas (g_1) to Zone 1 can be determined by analytically solving Equation (3.3) for two zones to give an expression for the difference in zone concentrations (Δc) as a function of time, volume, and airflow rates as shown below.

$$\Delta c(t) = c_1(t) - c_2(t) = \left(\frac{2g_1}{V}\right) e^{-t(F_o+4F')/V} \quad (9.3a)$$

$$= \Delta c(0)\, e^{-t(1+4F'/F_o)/(V/F_o)} \quad (9.3b)$$

The term, $\Delta c(0)$, is the difference between the zone concentrations immediately after Zone 1 is pulsed. This equation shows that the concentration difference decays exponentially with time as the two zones mix. If the definitions, $\varepsilon = \Delta c(t)/\Delta c(0)$ and $t^* = t/(V/F_o)$, are made, Equation (9.3) can be rewritten as

$$\frac{F'}{F_o} = -0.25 \left(\frac{\ln \varepsilon}{t^*} - 1\right) \quad (9.4)$$

The term, ε, indicates the difference in zone concentrations relative to the pulse disturbance and the term, t^*, is a nondimensional time based on the external air exchange rate of the zones. A criteria for uniform mixing can be defined by requiring that the concentration difference due to an impulse input (ε) must decay to certain value within a prescribed period of time (t^*). By specifying values for ε and t^*,

Equation (9.4) can be used to determine the required relative interzonal airflow rate (F'/F_o) to assure uniform mixing. Figure 16 graphically relates the relationship given by Equation (9.4).

This figure indicates, for example, that a flow ratio of $F'/F_o \approx 5$ is required to reduce ε to 0.1 within time $t^* = 0.1$. The simulation model was applied to a case where V=1000, F_o= 0.1, and F'= 0.5 (F'/F_o= 5) with an impulse of tracer gas injected into Zone 1. Figure 17 shows how the concentration varies within the two zones as a function of $t^* = t/(10000)$ for a single impulse in Zone 1. The figure shows that, as expected, the difference in concentrations between the two zones decays to within 10% of the maximum value at $t^* \approx 0.1$.

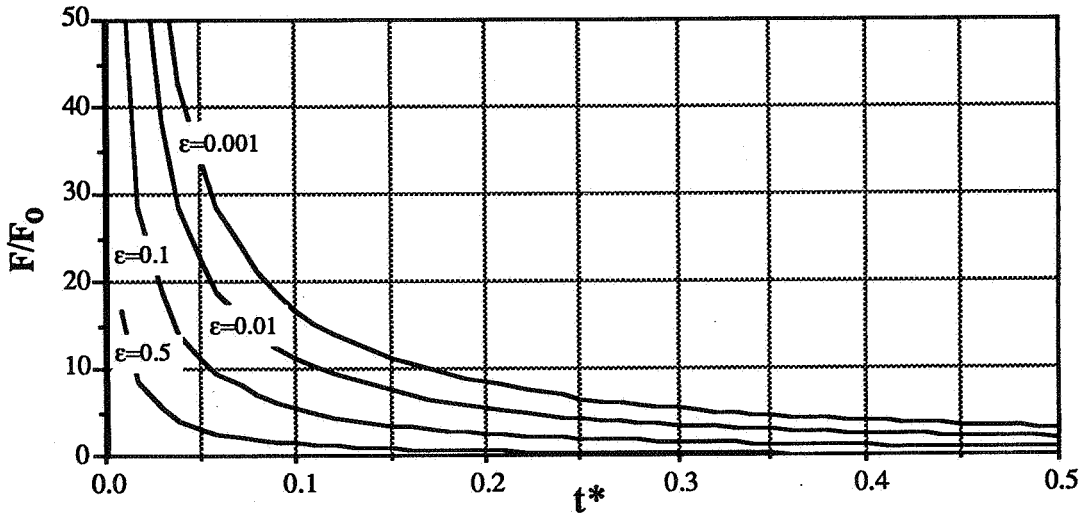

Figure 16. Ratio of F'/F_o as a Function of t^* and ε

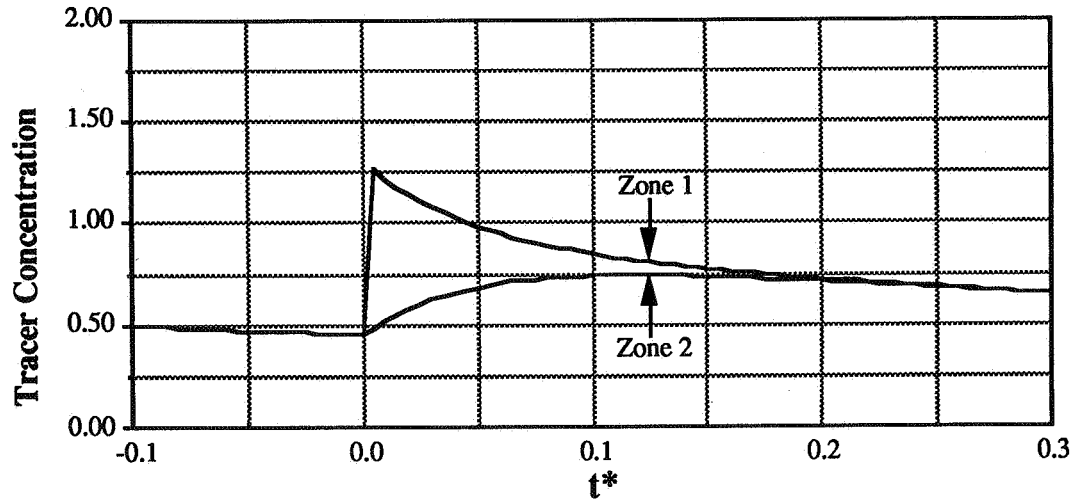

Figure 17. Tracer Concentration versus t* For a Two-Zone System

The two-zone simulation model was used to generate data for several additional cases where Zone 1 is pulsed with a tracer gas and the recursive least-squares identification algorithm was used to determine the total effective volume, V, and external airflow rate, F_o, for a corresponding single zone system based on the concentration data for Zone 1. The results are shown in Table 3 for various airflow rates and sampling intervals, $T^* = T/(V/F_o)$. For F/F_o less than 5, a single zone

approximation is unsatisfactory. However, as F/F_0 is increased to 5, a single zone approximation produces a flow and volume within 20% of the correct values of 0.1 and 1000 provided the appropriate sampling interval is chosen ($T^* = 0.1$). Numerous tests of the algorithm have indicated an approximate relationship between T^*, t^*, and ε. Using Equation (9.4), for a given F/Fo, if one assumes $t^* \approx \varepsilon$, the sampling period, T^* should be in the interval $0.1 < T^* \leq 0.2$.

Table 3. Single Zone Predictions for a Simulated Two-Zone System

	2 Zone (Actual)			1 Zone (Predicted)		
F/F_0	V	F'	F_0	T*	V	F_0
0.5	1000	0.05	0.10	0.005	501	0.08
1	1000	0.1	0.10	0.005	503	0.10
5	1000	0.5	0.10	0.005	521	0.15
5	1000	0.5	0.10	0.020	587	0.14
5	1000	0.5	0.10	0.100	901	0.12
10	1000	1.00	0.10	0.100	1023	0.11
115	1000	11.5	0.10	0.100	1004	0.10

Once it has been established that a single zone approximation of an actual two-zone system is possible under appropriate flow conditions, it is natural to wonder whether an extension to a three-zone system is possible. Here, the question considered is when can an actual three-zone system be modeled by a simplified two-zone approximation. In this case, the interzonal flows between zone 2 and 3 are varied relative to the outdoor flows (Figure 1). In the simulated three-zone system, $F_{02} = F_{03} = F_{20} = F_{30} = F_{21} = F_{31} = F_{12} = F_{13} = 0.5F_0$ ($F_0 = 0.1$), $F_{01} = F_{10} = 0.1$, $V_1 = 2V_2 = 2V_3 = 500$, and $F' = F_{23}=F_{32}$. The results of various simulations are summarized in Table 4. If the three-zone system is perfectly modeled as a two-zone system with Zones 2 and 3 behaving as a single zone (2), the following parameters would be predicted: $V_1 = V_2 = 500$ and $F_{12} = F_{21} = F_{01} = F_{10} = F_{02} = F_{20} = 0.10$. The table indicates that a two-zone approximation is valid provided the interzonal flows F_{23} and F_{32} are approximately ten times larger than F_0. The simulations also indicate that the guidelines for sampling period described above have changed slightly. For the two-zone case, the sampling period should be based upon the characteristic time of the faster of the two zones. Then, using Equation (9.4), for a given F'/F_0, if one assumes $t^* \approx \varepsilon$, then the sampling period, T^*, should be in the interval $0.1 < T^* \leq 0.2$.

Table 4. Two-Zone Modeling of an Actual Three-Zone System

Three-Zone (Simulated)					Two-Zone (Predicted)						
V_1	$V_{2,3}$	F'	F_0	F'/F_0	T*	V_1	V_2	F_{12}	F_{21}	F_{01}	F_{02}
500	250	0.01	0.01	1.0	0.020	504	255	0.007	0.009	0.012	0.008
500	250	0.05	0.01	5.0	0.020	504	271	0.009	0.016	0.011	0.011
500	250	0.05	0.01	5.0	0.100	525	371	0.010	0.014	0.011	0.011
500	250	0.05	0.01	5.0	0.400	632	610	0.015	0.015	0.011	0.011
500	250	0.10	0.01	10.0	0.020	504	293	0.009	0.018	0.010	0.012
500	250	0.10	0.01	10.0	0.100	531	458	0.011	0.012	0.010	0.011
500	250	0.10	0.01	10.0	0.200	565	539	0.012	0.012	0.011	0.011
500	250	1.00	0.01	100.0	0.004	501	336	0.010	0.021	0.010	0.018
500	250	1.00	0.01	100.0	0.010	502	443	0.010	0.012	0.010	0.011
500	250	1.00	0.01	100.0	0.020	505	495	0.010	0.010	0.010	0.010
500	250	1.00	0.01	100.0	0.040	510	512	0.011	0.011	0.010	0.011

At first glance, it may appear that we have developed two separate criteria for determination of sampling interval which may not be compatible. However, it turns out that satisfying the criterion established in Section 9.1 usually results in an acceptable 'mixing interval' for the input between the impulse and the first sample following it. For example, the continuous-time eigenvalue of interest for the two-zone system (with high interzonal airflows) described in Table 3 is $\mu = -(F_0/V) = -0.0001$. Satisfying the criterion established in Equation (9.1) requires that the sampling interval be $T = 1000$ ($|\mu T| = 0.1$). This results in a value of $T^* = 0.1$. For the purpose of system identification, Section 9.2 indicates that these two zones will be adequately described by a single zone if the concentration ratio between them is reduced to 0.1 within $t^* = 0.1$ ($t = 1000$).

10. IDENTIFYING THE NUMBER OF INTERCONNECTED ZONES

Before a successful tracer gas experiment can be undertaken, one of the most important parameters which must be determined is the total number of zones. Often, the physical characteristics of a building aid in this process. For example, individual rooms separated by doorways or corridors are often obvious choices for separate zones. However, there are other situations in which determining the number of zones is not as easy. For example, deciding whether a very large room is best modeled as one, two, or even three zones is often not a simple matter. Another difficulty might be in determining whether to combine a series of small well connected rooms into a fewer number of larger zones.

Thus, a method for determining the number of zones in a system would be useful to the analyst conducting tracer gas studies. Such information would be of particular interest in determining whether to break a larger zone up into smaller zones or combine a series of smaller zones into fewer larger ones. This would greatly increase the accuracy of the identification process which is, the goal of most tracer gas studies.

Consider again the system of discrete-time difference equations represented by Equation (3.6)

$$\mathbf{c}(k+1) = \mathbf{A}\,\mathbf{c}(k) + \mathbf{B}\,\mathbf{g}(k) \qquad (10.1)$$

If an output equation is defined as

$$\mathbf{y}(k) = \mathbf{D}\,\mathbf{c}(k) \qquad (10.2)$$

then the system of equations can be transformed from the state-space system of equations to an input-output formulation (Kuo[9]). Taking the z-transforms of Equations (10.1) and (10.2) and combining them produces

$$\mathbf{y}[z] = \mathbf{D}\,(z\mathbf{I}-\mathbf{A})^{-1}\,\mathbf{B}\,\mathbf{g}(z) = \mathbf{W}(z)\,\mathbf{g}(z) \qquad (10.3)$$

assuming **D**, **A**, and **B** are constant. The matrix $\mathbf{W}(z)$ is known as the transfer function matrix and is the complex frequency matrix which 'filters' the inputs as they travel through the system. If **D** is assumed to be the identity matrix–that is, each output, $y_i(k)$ is simply equal to the concentration of tracer in that zone at time step k,

then Equation (10.3) can be inverted back into the discrete-time domain. This results in the formation of n discrete-time input-output equations

$$y_i(k) = \sum_{j=1}^{n} p_{ij} y_i(k-j) + \sum_{j=1}^{n} a_{ij} g_i(k-j) + \sum_{h=1}^{n} \sum_{q=2}^{n} (1-\delta_{ih}) b_{hq} g_h(k-q) \quad \{i = 1... n\} \quad (10.4)$$

If a single input is applied to the zones, the double summation drops out and Equation (10.4) takes the form of the well known auto-regressive moving-average system (ARMA). ARMA systems appear often in control system theory and signal processing. A great deal of study has gone into methods for determining the order of an ARMA process by simply observing the input-output sequence (Akaike[19], Bhansali[20], Soderstrom[21], and Chen[22]). Many of these methods rely upon a statistical test of the residuals of the least-squares fit of the parameters to the data.

A method known as the AIC criterion (Information Criterion–A), first introduced by Akaike[19], has been found to produce consistent estimates of the order of multizone airflow systems using a single impulse input into one of the zones as the excitation. Let S[n] be the sum of the squared error between the actual output and the output predicted by an ARMA model of order n

$$S[n] = \sum_{k=1}^{Ndata} (y_{i,act}(k) - y^n_{i,pred}(k))^2 \quad (10.5)$$

The AIC criterion for selection of model order is based upon maximizing the following function

$$AIC = 2 \ln\{ L(S[n])\} - 2p \qquad \{ n = 1... \text{ max. order}\} \quad (10.6)$$

where p is the number of parameters associated with the chosen model order (p=2n). The term L(S[n]) is the maximum likelihood function. For the case where the noise superimposed upon the data is white the first term in Equation (10.6) is given by

$$2 \ln\{L(S[n])\} = -\frac{N}{2}(1+\ln 2\pi + \ln\{S[n]/N\}) \quad (10.7)$$

Thus, the appropriate order of the system is given by the n which maximizes the AIC function.

Before describing the results of a number of computer simulations to verify the performance of the AIC criterion, it is necessary to describe the fundamental concepts of controllability and observability of a system from a prescribed input-output pair. In simplified terms, a multizone system which is completely controllable from an input $g_i(k)$ is one in which the concentration of tracer in any zone can be raised or lowered to any prescribed level by a judicious choice of $g_i(k)$ within a finite time interval. In a similar manner, a multizone system which is completely observable from an output $y_i(k)$ is one in which a change in tracer concentration in any of the zones will have some effect upon the value of the output, $y_i(k)$. Figure 18 illustrates the concepts of controllability and observability for a simple two-zone system. A number of tests exist for determining controllability and observability of a system from an input-output pair. However, these tests require a priori knowledge of the A matrix which is not available in the identification procedure.

The results of simulations conducted to test the AIC criterion are shown in Table 5. Simulations of actual one, two, and three-zone systems were run. In each case, the input was applied to Zone 1 a few time steps into the simulation and the output was the tracer concentration of Zone 1. and The data were then fit to Equation (10.4) for models up to fourth order and the resulting sums of the squared error were computed for each. Equation (10.6) was then used to calculate the AIC. For the two-zone case, the flows were varied to determine the effect that interzonal flows have upon the predicted model order. The results shown indicate that decreasing the flows between the two zones relative to the total flow reduces the likelihood of correctly predicting the order of the system.

For the three-zone case, the effective volumes of the zones were varied. Table 5 indicates that if all interzonal flows are equal, the effective volumes of all three zones must be substantially different before the AIC criterion is able to discern the presence of three different zones. It should also be noted that changing some or all of the interzonal airflows and/or initial tracer concentrations can have a similar effect.

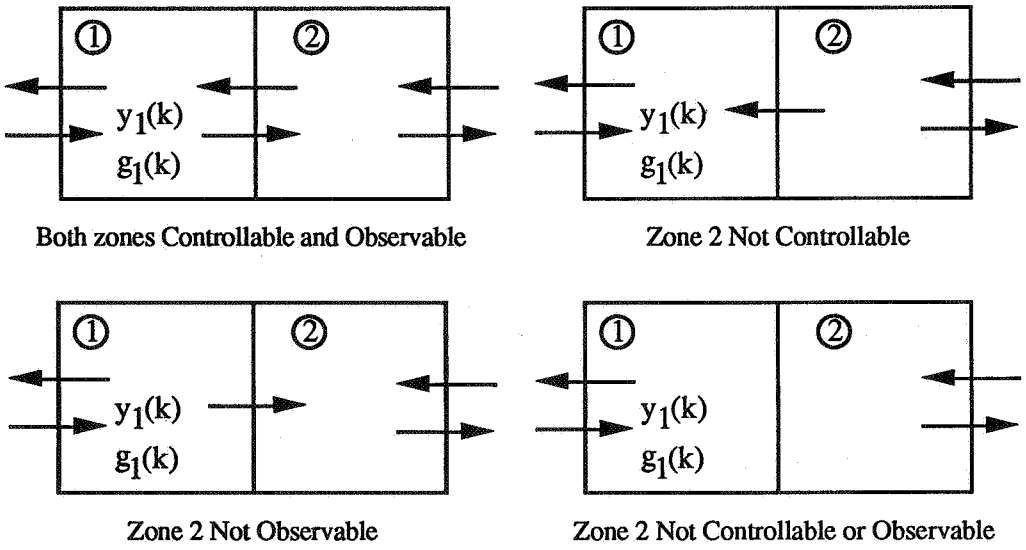

Figure 18. Examples Showing Conditions Under Which a Two-Zone is Controllable and Observable from Input-Output Pair [$g_1(k)$ $y_1(k)$]

Table 5. Determination of Model Order Using AIC Criterion

Actual Number of Zones	Effective Volumes of Zones 1/2/3	Interzonal Airflows (all = 0.1 unless otherwise noted)	AIC Criterion Number of Zones 1	2	3	4
1	1000	0.1	**158**	150	138	128
2	1000/1000	0.1	106	**132**	130	120
2	1000/1000	$F_{12}=F_{21}=0.5$	88	**118**	114	104
2	1000/1000	$F_{12}=F_{21}=0.02$	**155**	148	138	129
3	1000/1000/1000	0.1	78	**132**	131	120
3	1000/500/250	0.1	75	**132**	**132**	121
3	1000/500/100	0.1	67	129	**131**	120

Table 5 shows that under certain conditions, the AIC criterion will result in a correct prediction of the number of zones, n, in a multizone flow system. However, this number should be interpreted as only the minimum possible number of zones

which are required to adequately model the system. There may be more zones within the system which the procedure was not able to identify. There are two possible reasons for this. First, some of the zones may not be controllable or observable (or only weakly controllable and observable) from the input-output pair selected. In such a case, the dynamics of the system will not be completely captured using that choice of input-output pair. Second, as the number of actual zones is increased past 2, symmetries within the system make it difficult to separate the effect that different zones have upon the output. Thus, the more asymmetric a system is, with respect to effective volumes and interzonal flows, the more likely that the AIC criterion will identify a larger number of zones. If it is suspected that more zones may exist, it may be advisable to change locations of the input (impulse) and/or output (sensor), and repeat the test.

The AIC criterion is also sensitive to the sampling rate. As the sampling interval is decreased, the number of data points increases. This results in a larger sum of the squared error. When the number of data points becomes large, even with low noise, increasing the order of the model has only a slight effect upon the sum of the squared error and the AIC criterion predicts a lower number of zones. In the case of an extremely small sampling interval, increasing the model order will have little or no effect upon the sum of the squared error.

Conversely, using only a small number of data points (a large sampling interval) in conjunction with the AIC criterion will also produce erroneous results. In this case, increasing the order of the system will have a disproportionate effect upon the sum of the squared error. The AIC criterion will predict a larger number of zones than exist in the actual system. In the extreme case where the number of data points equals the number of model parameters, the sum of the squared error will be zero and the AIC criterion blows up.

Simulations have shown that the AIC criterion performs most accurately when a sampling interval of $T \approx 0.1\tau$ is used. The time constant, $\tau = (t_2 - t_1)$, is the time it takes for the zone tracer concentration to decay from the initial concentration following the impulse input, $c(t_1)$, to a concentration $c(t_2) = c(t_1)e^{-1}$. The total test time, t_{tot} should be approximately 2τ.

Once again, a guideline has been established for selection of the proper sampling interval. While this criterion may seem new, it is closely related to that established in Section 9.1 where the discrete-time eigenvalues were used to select an appropriate sampling interval. Unfortunately, when the system is transformed to an input-output representation, the eigenvalues become less accessible. In this case, it becomes necessary to look at the actual tracer decay curve to obtain an indication of the system eigenvalues and thus, obtain the sampling interval.

11. CONCLUSIONS

The recursive least-squares identification algorithm presented in this paper provides a method for accurate prediction all of the interzonal airflow rates and effective volumes of a multizone system. The algorithm requires that an input of tracer gas be applied to each zone of interest and uses the concentration data for each to calculate the unknown system parameters. In addition, this method shows potential for tracking flows and effective volumes in time varying systems.

The sampling period has also been shown to greatly affect the accuracy of the results. Careful selection of the sampling period is important both to the stability of the identification algorithm and to ensure proper mixing of the inputs between samples.

A method has also been introduced for determining the order of the system to be identified. This method, which uses the residuals of least-squares parameter fits of various model orders, can accurately predict the true system order under the appropriate conditions.

Work is underway on the construction of an experimental facility to verify some of these results. It should be noted that the conclusions and results reported above are limited to the specific cases examined in this paper and are not necessarily general. More work is needed to prove their applicability to more general cases and make refinements as necessary.

12. REFERENCES

1. Harrje, D. T. et. al. "Documenting Air Movements and Infiltration in Multicell Buildings Using Various Tracer-Gas Techniques". ASHRAE Technical Data Bulletin, Vol. 1, No. 2, 1985.
2. Afonso, C.F.A., Maldonado, E.A.B., Skaret, E.A. "Single Tracer-gas Method to Characterize Multi-room Air Exchanges". Energy and Buildings, 9, p. 273-80, 1986.
3. Jensen, L. "Determination of Flows and Volumes in Multiple Cell Systems". Proceedings of RoomVent-87, June 1988, Stockholm Sweden.
4. Axley, J., Persily, A. "Integral Mass Balances and Pulse Injection Tracer Techniques".U.S. Department of Commerce, NISTIR 88-3855, October, 1988.
5. Charlesworth, P. S. "Air Exchange Rate and Airtightness Measurement Techniques- An Applications Guide". AIVC Document AIC-AG-2-88, 1988.
6. Carolyn Allen. AIRGLOSS: Air Infiltration Glossary . AIC Technical Note 5, December, 1981.
7. O'Neill, P.J. and R. R. Crawford. "Development of an Interzonal Airflow Measurement Technique Using a Pulsed Tracer Gas".Transactions of Clima 2000. Sarajevo, Yugoslavia. August 27-September 1, 1989.
8. Sinden, F. W. Multi-Chamber Theory of Air Infiltration. Building and Environment, Vol. 13, 1978.
9. Kuo, B. C. Digital Control Systems. Holt, Rinehart, and Winston, Inc., New York, 1980.
10. Ljung, L.,Soderstrom, T. Theory and Practice of Recursive Identification. The MIT Press, Cambridge, 1983
11. Eykhoff, P. Ed. Trends and Progress in System Identification. Pergamon Press, New York, 1981.
12. Kudva, P., Narendra, K. S. "An Identification Procedure for Discrete Multivariable Systems". IEEE Transactions on Automatic Control, pp. 549-52, October, 1974.
13. Ossman, K. A.,Kamen, E. W.,"Adaptive Regulation of MIMO Linear Discrete -Time Systems Without Requiring a Persistent Excitation". IEEE Transactions on Automatic Control, Vol. AC-32, No. 5, May 1987

14. Sinha, N. K., Lastman, G. J."Identification of Continuous-Time Multivariable Systems from Sampled Data". International Journal of Control, Vol. 35, No. 1, pp. 117-126, 1982
15. Goodwin, G. C., Sin, K. S. Adaptive Filtering Prediction and Control. Prentice-Hall, Inc., New Jersey, 1984
16. Sinha, N. K., Lastman, G. J., Zhou, Q. J., "On the Choice of the Sampling Interval for the Identification of Continuous-Time Systems from Sampled Data". Proceedings of the 25th Midwest Symposium on Circuits and Systems (Houghton, MI) pp. 328-32 1982.
17. Sinha, N. K., Kuszta, B. Modeling and Identification of Dynamic Systems. Van Nostrand Reinhold Company, New York, 1983.
18. Puthenpura, S., Sinha, N. K. "A Procedure for Determining the Optimal Sampling Interval for System Identification Using a Digital Computer". Canadian Electrical Engineering Journal, Vol. 10, No. 4, pp. 152-7, 1985
19. Akaike, H., "A New Look at the Statistical Model Identification". IEEE Transactions on Automatic Control, Vol. AC-19, No. 6, pp. 716-23, 1974.
20. Bhansali, R. J., Downham, D. Y. "Some Properties of the Order of an Autoregressive Model Selected by a Generalization of Akaike's EPF Criterion". Biometrika, Vol. 64, No. 3, pp. 547-51, 1977.
21. Soderstrom, T. "On Model Structure Testing in System Identification". International Journal of Control, Vol. 26, No. 1, pp. 1-18 , 1977.
22. Chen, H-F.,Guo, L. "Consistent Estimation of the Order of Stochastic Control Systems". IEEE Transactions on Automatic Control, Vol. AC-32, No. 6, June 1987.

Discussion
Paper 7

Mike Holmes (Ove Arup, London UK)

Can the method be used to look at the general mixing in a single zone? For example the distribution of pollutants?

Patrick O'Neil, Roy R. Crawford (University of Illinois, USA)

Yes, we believe that a zone's response to the impulse type input is closely related to the internal mixing characteristics of that zone. An integral part of our ongoing research effort is to analyze systems in which it takes a significant amount of time for the inputs to mix within the zone(s). By simply analyzing the impulse response of a zone, we hope to be able to characterize, in some sense, the mixing characteristics of that zone.

Bjorn Hedin (Lund Institute of Technology, Sweden)

There are some advantages of using the PRBS input: by theory, the discrete time description (3.6) requires that the input is constant during the sample period. The PRBS fulfils this demand, but a short impulse injection doesn't, i.e. such impulses will violate the sampling theorem. This can lead to extra estimation errors. The PRBS input will neither violate the assumption of ideal mixing as obviously as the short impulse. Do you want to comment on these things?

Patrick O'Neil, Roy R. Crawford (University of Illinois, USA)

Certainly. As you mentioned, the impulse type input, as described in this paper, may not satisfy the criterion of constant inputs between sample periods. However, the simulations which we have run indicate that this should not be a significant problem. If necessary, you could assume that the impulse was evenly distributed over a single sample interval. In addition to the fact that an impulse input is easier to apply to a zone, we also believe that it gives you additional information on the mixing characteristics of the zone.

Bjorn Hedin (Lund Institute of Technology, Sweden)

Why do you use the recursive least-square (LS) method? You don't have use of the advantage which is a short execution time, but suffer from the disadvantage of higher sensitivity to noise (or even breakdown at higher noise levels). The common or batch LS method can never be unstable, it's fast enough, and it's easy to use "forgetting factors" in this method as well.

Patrick O'Neil, Roy R. Crawford (University of Illinois, USA)

If the recursive method causes difficulty during the data analysis, then one can certainly fall back upon the batch method which I have described. However, depending upon the computing power available, there may be utility in using the recursive method when analyzing very "fast" systems.

Bjorn Hedin (Lund Institute of Technology, Sweden)

The volume matrix V is calculated as $V = B^{-1}R$ (eg. 5.6,page 9).

But the chance to receive a diagonal volume matrix from multiplication of two filled matrices doesn't seem to be very big, especially not when the estimations of B and R are disturbed by noise. How do you interpret the non-zero off-diagonal elements in $V = B^{-1}R$? Can they be ignored?

Patrick O'Neil, Roy R. Crawford (University of Illinois, USA)

In most of the simulations, the off-diagonal elements have been 1 or 2 orders of magnitude smaller than the diagonal elements. Consequently, these elements were ignored. However, if noise and/or mixing problems result in volume matrices with significant off-diagonal elements, then using methods which constrain them may become necessary.

Max Sherman (LBL, California, USA)

The linear least squares technique used - which is a standard control theory approach - has some severe limitations as presented. You have linearized the exponential solution which requires a short time step in the analysis, however, at a small time step the concentration is highly autocorrelated and cannot be simply regressed. You must take into account the (non-diagonal) covariance matrix. Since this is a physical system (cf a control system), a chi-squared analysis system with the real covariance matrix is a more appropriate approach.

Patrick O'Neil, Roy R. Crawford (University of Illinois, USA)

Our next step is to validate the proposed method using a three-zone experimental facility which we are developing. We will look at these types of issues as they arise.

Max Sherman (LBL, California, USA)

The multizone, single gas technique you propose is biased unless one has a constant flow rate over the analysis. Thus it is not well suited for time vary systems unless you use a series of pulses and analyze different sets of pulses separately. The relaxation model you propose is not appropriate for this kind of system.

Patrick O'Neil, Roy R. Crawford (University of Illinois, USA)

No indirect method (as all tracer techniques are) for analyzing flows within buildings is well suited for tracking rapidly varying flows. However, if the flows are varying slowly, we believe this method is as appropriate as any.

Max Sherman (LBL, California, USA)

When using real data (as opposed to simulated) you will find that the noise in the concentration is far from "white". One's analysis technique must be quite robust to handle this. Furthermore, all of the parameters are intrinsically and experimentally correlated. It is, therefore, quite important to do a complete error analysis. I look forward to seeing this next year with measured data.

Patrick O'Neil, Roy R. Crawford (University of Illinois, USA)

Again, as we collect experimental data, we will look more closely at these issues.

PROGRESS AND TRENDS IN AIR INFILTRATION
AND VENTILATION RESEARCH

10th AIVC Conference, Dipoli, Finland
25-28 September, 1989

Paper 8

MATHEMATICAL MODELLING OF INFILTRATION AND VENTILATION

Helmut E. Feustel

Energy Performance of Buildings Group
Indoor Environment Program
Lawrence Berkeley Laboratory
University of California
Berkeley, CA 94720
USA

1. SYNOPSIS

It is particularly important to be aware of the air flow pattern in a building when determining indoor air quality problems or calculating space conditioning loads for energy consumption. Correct sizing of space conditioning equipment is also dependent upon accurate air flow information. A number of infiltration models have been developed to calculate infiltration-related energy losses and the resulting air flow distribution in both, single-zone and multizone buildings. International infiltration research has been conducted since the early twenties -- infiltration modeling, however, is a relatively new task. Most of the modeling effort has taken place during the last 15 years, during part of which time the Air Infiltration and Ventilation Centre has been in operation. This paper gives an overview of the development of infiltration models.

2. INTRODUCTION

The annual heat loss due to infiltration, unlike the equivalent for conduction, is dependent not only on the temperature difference between the inside and the outside of the building, but also upon shielding, terrain, wind speed and direction and on the design of the building. High wind speeds often occur at higher outdoor temperatures and may result in higher infiltration rates than those calculated for in the design.

Awareness of infiltration as a major factor in the overall conditioning load of a building has led to tighter construction of both, building components and the overall building shell. This has decreased the infiltration rate and its related ventilation heat loss but has sometimes created another problem with regard to indoor air quality.

The air-mass flow distribution in a given building is caused by pressure differences evoked by wind, thermal buoyancy, mechanical ventilation systems or a combination of these. Air flow is also influenced by the distribution of openings in the building shell and by the inner pathways. Actions by the occupants can also lead to significant differences in pressure distribution inside a building. Figure 1 shows various influences on air-mass flow distribution.

Wind pressure distribution depends on the velocity and direction of the wind, the terrain surrounding of the building and its shape. Differences in air density, due to differences between outside and inside air temperatures, cause further vertical pressures which, in turn, influence the air-mass flow. Mechanical ventilation also introduces a pressure field on the building.

There are two fundamental approaches in determining the infiltration rate in buildings. The most straightforward method is to measure infiltration directly, e.g., by using the tracer gas technique. Multizone tracer gas techniques can be used to determine either the air flows between the inside and the outside of the building only, or in addition, the interzonal air flows. It is necessary to understand the latter so as to determine the impact of infiltration on indoor air quality.

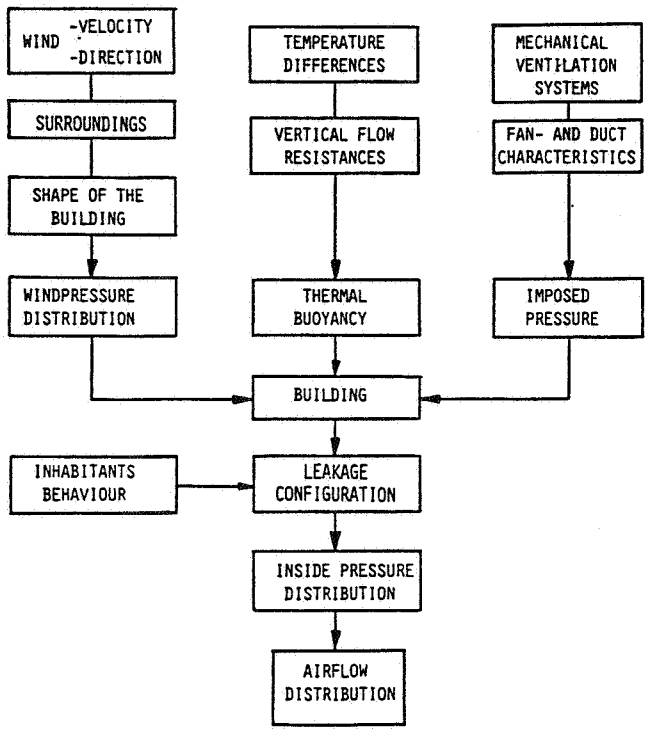

Fig. 1: *Influences on Air Flow Distribution in Buildings*

Tracer gas measurements give a value for infiltration only under prevailing leakage and weather conditions, but a second technique can be used to determine values of infiltration for all leakage and weather combinations. This method uses mathematical models (see Fig. 2).

The Air Infiltration and Ventilation Centre (AIVC) has published a comprehensive handbook, *Air Infiltration Calculation Techniques - an Applications Guide* [1]. This, and a second AIVC publication [2] are valuable tools for obtaining an overview of available techniques in calculating air infiltration.

Infiltration models can be divided into two main categories, single-zone models and multizone models (see Fig. 3). Single-zone models assume that the structure can be described by a single, well-mixed zone. The major application for this model type is the single-story, single-family house with no internal partitions (e.g., all internal doors are open). As a large number of buildings, however, have floor plans that would characterize them more accurately as multizone structures, more detailed models, taking internal partitions into account, have been developed.

Besides the static models described in this paper some models have been developed to determine ventilation rates under dynamic conditions. As these become more important when large openings are present the IEA Annex VIII "Inhabitants' behaviour with regard to ventilation" has investigated these patterns.

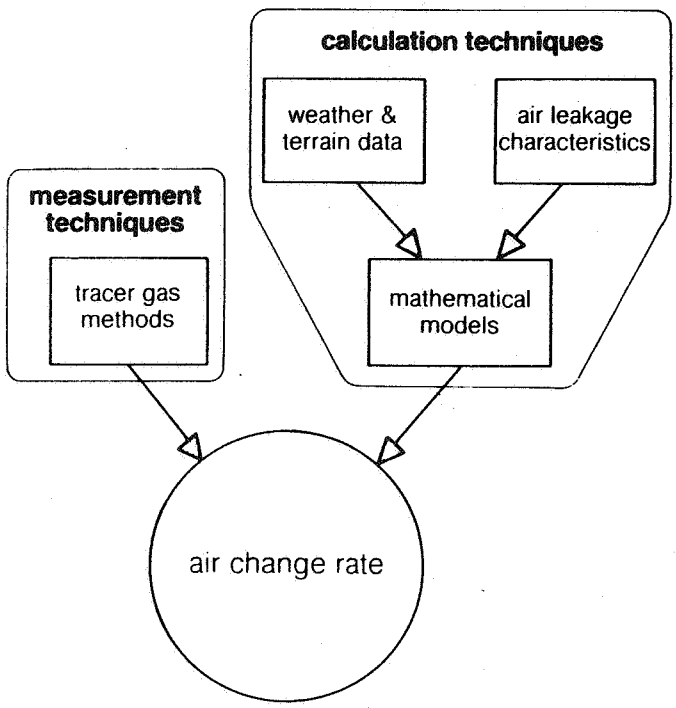

Fig. 2: *Alternative Ways of Determining Infiltration [1]*

A report giving some rules of thumb for estimating air flow rates through open windows has been published by AIVC [3].

3. SINGLE-ZONE MODELS

3.1 General

Single zone models are usually used in determining infiltration rates for single-family buildings. A zone is defined as a fully mixed volume with a constant concentration level of the enclosed gas mixture. Therefore, single-zone buildings do not exist in reality. However, smaller buildings without internal partitions or at least with open internal doors can be simulated with reasonable accuracy by single-zone models (see Fig. 4). Often, however, the limits of the single-zone models are obviously violated by using them for multizonal applications.

Single-zone models can be characterized as either empirical or physical models.

3.2 Empirical Models

Empirical infiltration models are the simplest infiltration models available being based solely on the knowledge obtained from infiltration measurements. Models can be as simple as assuming a constant infiltration rate based on no flow properties of the building; or dividing the leakage obtained by pressurization tests by a

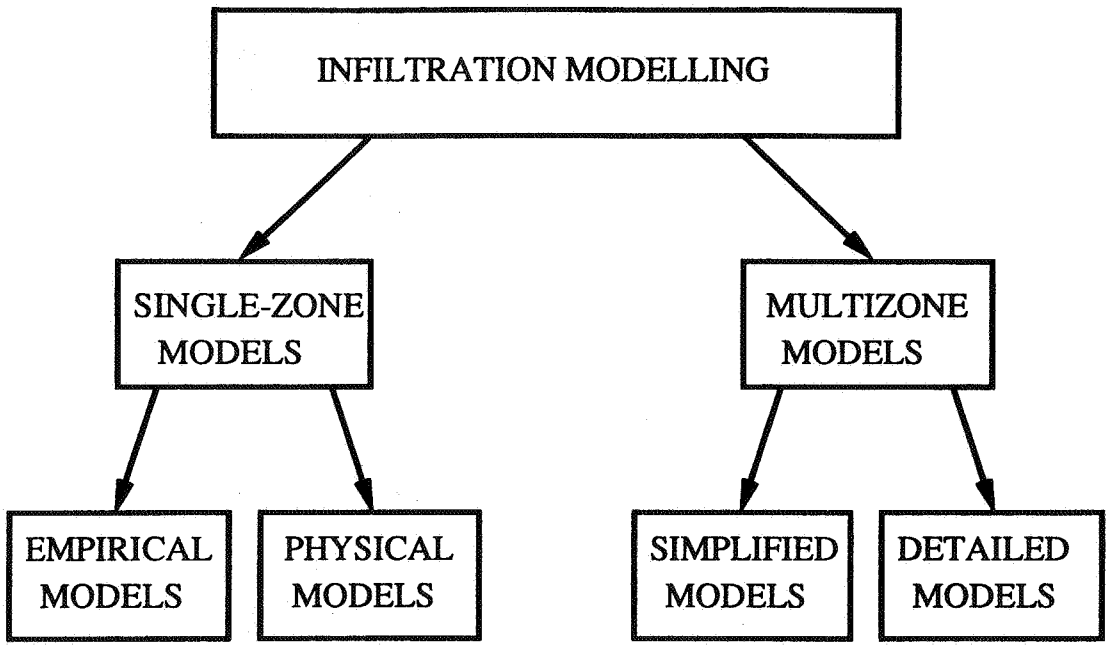

Fig. 3: *Categorizing Infiltration Models*

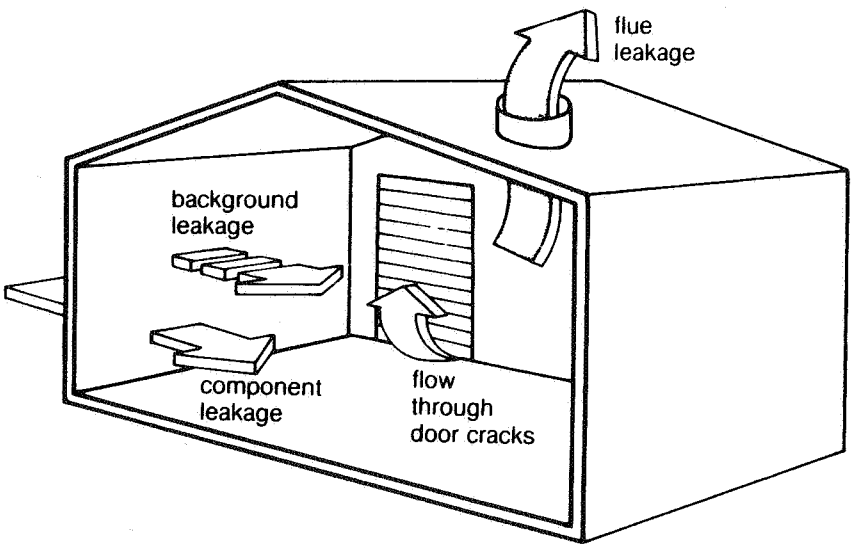

Fig. 4: *Example of a Single-Zone Building [1]*

constant number. Other models must take into account information about wind speed and temperature differences between the inside and the outside of the building.

The **constant rate model** assumes a constant infiltration rate for the whole building irrespective of the factors influencing the amount of air movement between the inside and outside of the building. This kind of model is still included in some of the building simulation programs used to calculate energy requirements for space conditioning but it is an abuse to use it for multizone applications. A more advanced version of the constant rate model determines infiltration as a function of the air flow obtained by pressurization tests. This method gives some indication of the magnitude of average infiltration and so provides some "rule of thumb" for the practitioner.

The **regression method** has been used for some time in order to fit in the enormous amounts of data obtained from tracer gas measurements. The modeling procedure utilizes two weather parameters as the sole weather-related potential for infiltration --the indoor/outdoor dry-bulb temperature difference and wind velocity. Because the regression coefficients reflect structural characteristics as well as shielding effects and occupant behaviour, variances of 20:1 have been found in individual regression coefficients when comparing similar structures [4].

$$Q = A + B\ \Delta T^{\alpha} + C\ v^{\gamma} \qquad (1)$$

with:

Q	infiltration rate
A,B,C	regression coefficients
ΔT	temperature difference
v	wind speed
α, γ	exponents (usually $1.0 \leq \alpha \leq 2.0$; $0.5 \leq \gamma \leq 1.0$)

Based on statistical analysis of field data and the assumption that the air permeability of the envelope is uniformly distributed, wind direction is usually not taken into account.

3.3 Physical Models

Once pressurization measurement techniques for building components or whole buildings existed, physical models became possible. The crack model, which uses the flow characteristics of building components, was probably the first physical model for single zone applications. A second group of models uses information from whole building pressurization tests.

The air permeability of the building's envelope depends on the number and size of cracks, windows, doors and gaps between building components. In addition to these visually observable flow paths leakage is caused by the porosity of building material.

The **crack model** is the first real attempt to estimate leakage of the building's envelope. This method assumes that infiltration is proportional to the product of crack coefficient and crack length and can be expressed by the empirically power law function.

$$Q = a\ l\ \Delta p^n = C\ \Delta p^n \tag{2}$$

with:

Q	infiltration rate
a	crack flow coefficient
l	crack length
C	flow coefficient
Δp	design pressure drop
n	flow exponent

Values for the exponent range between n = 0.5 for fully turbulent jets or turbulent flow and n = 1.0 for fully laminar flow. However, due to the head losses which are directly dependent on the square of the velocity, n = 1.0 cannot be reached in reality. The exponent for calculating infiltration by the crack method is usually set at $n = 2/3$. A comparison of air leakage measurements conducted by means of the blower door technique in 196 houses showed, in respect of the whole house, a mean value for the exponent of 0.66 [5]. This is in good agreement with the measured flow characteristics of building components.

The flow coefficient is determined by the measured crack length of each building component and its specific crack flow coefficient. The latter are published in various handbooks and infiltration standards [6,7].

Single-zone network models are based on the mass balance equation taking any number of flow paths between the outside and the internal zone into account. Essential input data are flow path distribution, flow path characteristics, weather data, shielding and terrain roughness conditions, and the characteristics of the mechanical ventilation system. For a structure with k flow paths the mass flow balance is given by:

$$0 = \sum_{j=0}^{k} \left\{ \rho\, C_j \left| p_{o_j} - p_i \right|^n \left(\frac{p_{o_j} - p_i}{\left| p_{o_j} - p_i \right|} \right) \right\} \tag{3}$$

with:

ρ	density of air
C_j	flow coefficient for flow path j
p_{o_j}	external pressure for flow path j
p_i	internal pressure
n	flow exponent

The latter term determines the flow direction which would otherwise have been lost in the previous term.

Examples of models based on the network idea are ENCORE [8] from the Norwegian Building Research Institute and INFIL [9] from GRI.

The principal disadvantage of the single-zone network approach is its data requirements. This has led to the development of **simplified single-zone models.** These models usually work on the basis of an assumption, which can be obtained from pressurization tests about the distribution of whole house leakage. Wind-induced infiltration and stack-induced infiltration are calculated separately and superimposed later.

The most widely used simplified single-zone model is probably the LBL-model [10]. Airport weather data is converted into local wind conditions with shielding and local terrain also taken into account. The height of the building and the assumed distribution of leakage over its envelope are sufficient, along with the weather data, to calculate the air flow. The LBL-model assumes infiltration to be proportional to the square root of the applied pressure.

$$Q = A \sqrt{\frac{2}{\rho} \Delta p} \tag{4}$$

with:

A effective leakage area

Infiltration due to wind and stack action is calculated separately and later combined. The wind-induced infiltration calculates to:

$$Q_{wind} = f_{wind} A v \tag{5}$$

and the stack-induced infiltration can be expressed by:

$$Q_{stack} = f_{stack} A \sqrt{g H \frac{\Delta T}{T}} \tag{6}$$

with

f_w function describing the wind influence

f_{stack} function describing the stack effect

As a consequence of the flow assumption the flows due to wind and stack driven pressures are combined by summing the results in quadrature.

$$Q_{total} = (Q_{wind}^2 + Q_{stack}^2)^{1/2} \tag{7}$$

As the LBL-model is an easy to use tool further work has been done to improve its performance (mainly when wind and stack effect have the same magnitude) and to adjust the model to the more realistic flow characteristics found in field measurements [11].

Based on the results of a detailed multizone infiltration model the NRCC model [12] uses the following equation for the superimposition of flows:

$$Q = Q_{large}\left[1 + 0.24\left[\frac{Q_{small}}{Q_{large}}\right]^{3.3}\right] \tag{8}$$

with:

Q_{small} smaller of Q_{wind} and Q_{stack}
Q_{large} larger of Q_{wind} and Q_{stack}

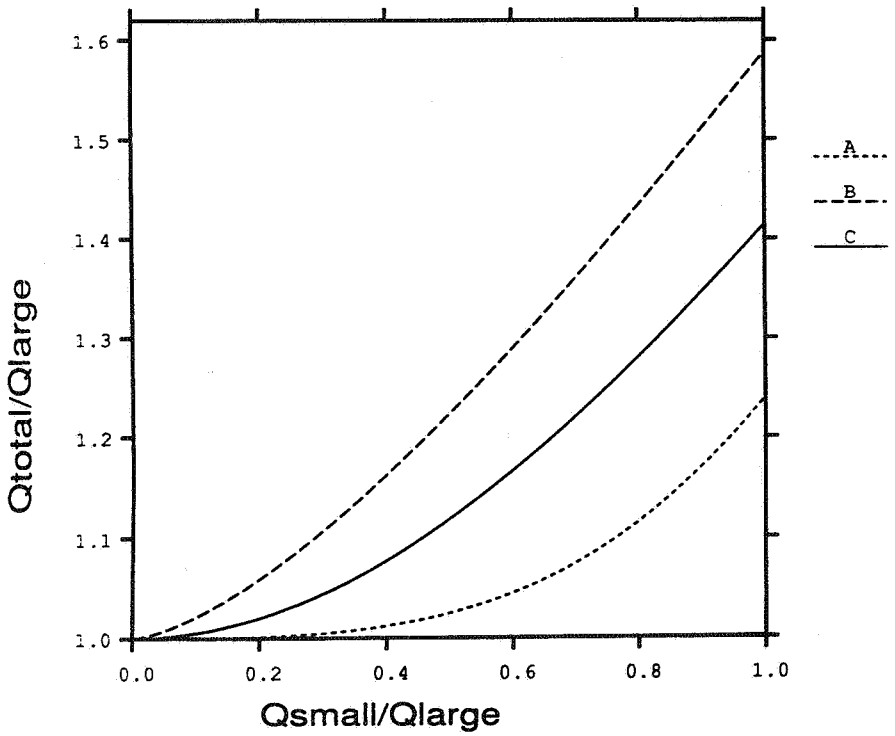

Fig. 5: *Superimposition of Flows [curve a) Eq. 8; curve b) Eq. 7 based on flow exponent n = 2/3; curve c) Eq. 7 based on flow exponent n = 1/2]*

In order to calculate the infiltration rate for one zone the BRE-model [13] relates to the air flow determined at a pressurization test. Air movement under ambient conditions is described by the power law equation.

$$Q = Q_{ref}\left[\frac{\rho v^2}{\Delta p_{ref}}\right]^n F_v\left[Ar, \phi\right] \tag{9}$$

with:

Q_{ref} air flow at pressurization mode
Δp_{ref} reference pressure difference ($10\,Pa \le \Delta p_{ref} \le 60\,Pa$)
F_v infiltration rate function, including the effects of weather dependent parameters
v wind speed at ridge height

This equation can be reduced to wind only and stack effect only action.

As with the LBL-model the BRE model assumes that the air leakage is uniformly distributed across each face and that the exponent n applies to all flow paths.

Several models have been developed to calculate the natural ventilation when ventilation shafts are present. Ertl et al. [14] not only developed and validated an algorithm which allows the performance of ventilation shafts to be evaluated but also published a review of the algorithms used for this purpose.

4. MULTIZONE MODELS

4.1 General

Multizone models are required when there are internal partitions in a building, or in the case of inhomogeneous concentration in the space. Multizone buildings can be either single-room structures (e.g., airplane hangars) single family houses or large building complexes. Fig. 6 shows an example of a very simple multizone building.

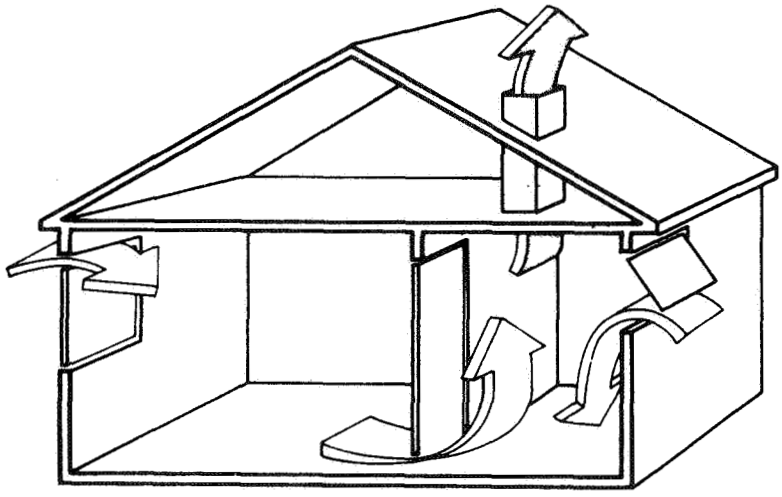

Fig. 6: *Example of a simple Multizone Structure [1]*

A number of infiltration programs have been developed to calculate air flows penetrating the building's envelope and travelling through the different zones of a multizone structure. Besides being able to simulate infiltration in larger buildings these models are able to calculate mass flow interactions between the different zones.

Knowing about the air-mass flow in buildings is important for several reasons:

- exchanging of outside air with the air inside the building is necessary for its ventilation
- energy is consumed to heat or cool incoming air to inside comfort temperature
- air is needed in different zones for combustion in open fireplaces and the exhaust of gasses
- airborne particles and germs are transported by air flow in buildings.
- air flow determines smoke distribution in case of fire.

The necessary information can be obtained either by multizone infiltration network models or by simplified multizone models.

In terms of air-mass flow buildings represent complicated interlacing systems of flow paths. In this grid-system the joints represent the rooms of the building and the connections between the joints simulate flow paths. These include the flow resistances caused by open or closed doors and windows and air leakage through the walls. The boundary conditions for the pressure can be described by grid points outside the building. Wind pressure distribution depends on the velocity and the direction of the wind, the surrounding terrain of the building and the shape of the building. If the physical interrelationship between flow resistance and the air flow is known for all flow paths the air flow distribution for the building can be calculated --as long as there is no temperature difference between outside and inside air. Differences in density of the air due to differences between outside and inside air temperatures, cause further vertical pressures while also influence the air-mass flow.

Mechanical ventilation can be included in this network, the duct system being treated like the other flow paths in the building. The advantage for calculating the air flow distribution effects of mechanical ventilation systems is that the duct pathways, as well as their connections with the building, are known. In the case of mechanical ventilation systems the fan can be described as the source of pressure differences, lifting the pressure level between two joints according to the characteristic curve of the fan.

4.2 Multizone Infiltration Network Models

Multizone infiltration network models deal with the complexity of flows in a building by recognizing the effects of internal flow restrictions. They require extensive information about flow characteristics and pressure distributions and, in many cases, are too complex to justify their use in predicting flow for simple structures such as single-family residences [15].

As for their single-zone counterparts these models are based on the mass balanced equation:

$$0 = \sum_{l=0}^{m} \left\{ \sum_{j=0}^{k} \left[\rho\, C_{j,l} \left| p_{o_{j,l}} - p_i \right|^{n_{j,l}} \left(\frac{p_{o_{j,l}} - p_i}{\left| p_{o_{j,l}} - p_i \right|} \right) \right] \right\} \tag{10}$$

with:

ρ	density of air
$C_{j,l}$	flow coefficient for flow path j of zone l
$p_{o_{j,l}}$	external pressure for flow path j of zone l
p_i	internal pressure
$n_{j,l}$	flow exponent for flow path j of zone l

Unlike the single-zone approach, where there is only one internal pressure to be determined, in the case of the multizone model one pressure for each of the zones must be determined. This adds considerably to the complexity of the numerical solving algorithm, but by the same token, the multizone approach offers wide potential in analyzing infiltration and ventilation air flow distribution.

A literature review undertaken in 1984 [16] revealed 26 papers describing 15 different multizone infiltration models which had been developed in eight separate countries. A review currently under way is producing additional information about the status of network models. One of the first we found was Jackman's model "LEAK" [17] which was published in 1970. In 1974 it was followed by the NRCC model [18], which was the first one available for use by interested parties. Indeed, this numerical tool is probably still the most widely used multizone infiltration model.

Several multizone models were developed in the aftermath of the oil price crises. Between 1975 and 1977 a series of steps were taken at TU Berlin to develop such a model. This resulted in the program STROM [19] which was later extended to handle HVAC-systems and has recently been rewritten to improve the solver and to be combined with a thermal model [20]. Concurrent with STROM, ELA 4 [21] has been developed. The models VENT 1 and VENT 2 [22] as well as BREEZE [23] were developed in the late 70s by researchers from British Gas and the Building Research Establishment. In the early 80s, first versions of Nantka's INFILTRATION & VENTILATION [24], Walton's AIRNET [25] and Herrlin's MOVECOMP [26] appeared. The latter two programs were the first to address the mathematical problem of solving the set of non-linear equations for zones with very different leakage characteristics. Open doorways in otherwise tight constructions are the main cause of significant problems in convergence. This has been solved in both cases by introducing under-relaxation factors to the well known Newton method.

By focusing on the work done in AIVC-member countries, we have neglected extensive program developments undertaken in Japan, France and Brazil. KGVCP from Hayakawa dates back to 1979 [27]. More recent work done in Japan has been published by Ishida and Udagowo [28] as well as Hayashi and Urano [29], Sasaki [30], Okuyama [31] and Matsumoto et al. [32].

France, as a possible future AIVC member, has also developed several multizone models; the recent review unveiled models from CSTB, INSA [33] and EDF. From Brazil, Melo's model FLOW2 [34] has been detected.

The latest development in infiltration modeling is the COMIS model [35]. In a twelve month period ten scientists from nine countries developed a reliable, well-running multizone model on a modular base. Because of its modular structure COMIS is designed to expand its capability to simulate buildings. To accomplish a "user-friendly" program special emphasis was given to the input routines. Support of the international group, working together at Lawrence Berkeley Laboratory, by IEA's Air Infiltration and Ventilation Centre will be likely to help the wide distribution of this model to all interested parties. COMIS can be used as a stand-alone infiltration model with input and output features or as an infiltration module for thermal building simulation programs. It also serves as a module library.

We discovered from the two reviews of the literature above that most of the models described by program authors use the FORTRAN (75%) programming language, followed in order of use, by BASIC, HPL and in one case each by PASCAL and C. As most of the programs represent research tools developed at universities they run on main frame or work station type computers (56%).

Because of the nonlinear dependency of the volume flow rate on the pressure difference, the pressure distribution for a building can only be calculated by using a method of iterations. Multizone network models were developed to deal either with simple structures of only a few zones or with buildings, having arbitrary floor plans, allowing an unlimited number of zones (limited only by the computer to be used). Many models have been developed which simulate a specific structure only, so allowing for the use of simple solving routines. Models which deal with arbitrarily chosen building types use either a great deal of CPU-space or are equipped with very sophisticated mathematical routines to reduce the storage need.

Large computer storage was necessary in the past, when calculating the air flow distribution of more complicated buildings. Nowadays, however, most programs use solver modules which reduce the space requirement, e.g., by band matrices or the skyline method. The Newton method is the most common tool used to solve the set of non-linear equations.

Although most models have been developed in FORTRAN on main frame computers, many use interactive mode to input the necessary data. Only one of the models, however, allows CAD-input. Three-dimensional building description and schedules for climatic data and occupants are more common today than they were

Table 1: Review of Multizone Infiltration Network Models		
Program Language:	FORTRAN BASIC PASCAL C HPL	33 6 1 1 3
Computer Type:	Main Frame Computer Personal Computer	23 18
Solver:	Newton others	22 8
Input Features:	interactive input CAD-input weather data from weather files 3-D building description schedules (e.g. occupants)	10 1 18 8 14
Output Features:	file of arrays used by the model graphical output statistical functions	23 7
Miscellaneous:	combined with thermal model combined with pollution model	12 8
Program Available?	yes no yes, but	7 11 11

five years ago but a comprehensive way of designing the output seems still to be a problem. Most of the models use the file of arrays to present the calculated result --not really a user-friendly method. Few models use the capabilities of personal computers to show the air flow distribution in two-dimensional graphs.

Twelve of the infiltration models are combined with a thermal model and eight feature a further combination with a pollutant transport model. For seven out of twenty-nine models the authors specify their product as "available to third parties". Eleven authors believe that, lacking user-friendliness, their models would be of no use for third parties. The remainder do not wish to make their tools available to others.

The multizone models investigated were, in regard to the equations used, very similar to each other. The flow equation used to describe the air flow characteristics of the buildings is similar to the one describing measured results for air flow through building components (see Eq. 2). Most programs use an empirical power-law expression type of equation, even though the pressure exponent may differ from 0.5 to 1.0, depending on the nature of flow. Only few models consider

wind dynamics.

The programs still differ markedly in their ability to simulate mechanical ventilation systems. Twenty of them are able to simulate forced ventilation systems by means of fan and duct characteristics. This is a tremendous change from the last review.

The difficulty of measuring infiltration in buildings under controlled boundary conditions means that none of the models has been validated properly, if at all. The possibility of doing piecemeal validations of certain algorithms has been considered; e.g., the algorithms for air flow through open doorways or air flow through cracks have been tested separately [36]. Measuring a few cells of the whole structure could still provide a severe test for existing models.

These data are important not only for validation purposes but also as a means of further understanding air movement in large multizoned buildings. We need to identify the critical variables in different building types in order to develop more accurate input data and, ultimately, more accurate models. Wind pressure coefficients, for example, represent a factor that needs further study, and the collating of existing data should help our efforts in simplifying data requirements.

4.3 Simplified Multizone Infiltration Models

Most multicellular models in use at present are not available to the public or are written as research tools, rather than for professional engineers or architects. There is an obvious need for a simplified multichamber infiltration model capable of providing the same accuracy as the established single-cell models.

The extended **crack model** is the simplest multizone model. It is used to design conditioning loads and size the conditioning equipment [37]. The method is based on the single-zone crack model and has been refined to multizone applications by also taking into consideration the crack flow through internal partitions. Buildings are characterized according to their cross flow and stack flow capabilities.

The stack pressures of the core zones for multistory structures are pre-calculated for design weather conditions and published in look-up tables. Together with pressures due to the effect of wind and permeability distribution this enables a user to calculate the infiltration for each of the outside zones.

$$\dot{Q}_{shaft} = \left[\varepsilon_{shaft,wind} \sum(a\ l)_{wind} + \varepsilon_{shaft,lee} \sum(a\ l)_{lee}\right] H\ r\ (T_i - T_o) \qquad (11)$$

$$\dot{Q}_{story} = \varepsilon_{story,wind} \sum(a\ l)_{wind} H\ r\ (T_i - T_o) \qquad (12)$$

with:

$\dot{Q}_{shaft}$	infiltration heat loss for a zone in a shaft-type building
$\dot{Q}_{story}$	infiltration heat loss for a zone in a story-type building
$(a\ l)_{wind}$	crack permeability windward side
$(a\ l)_{lee}$	crack permeability leeward side
ε	coefficient, depending on wind speed and vertical location of the zone in the building
H	coefficient, depending on building type
r	coefficient, depending on permeability distribution of the zone

The **Simplified Multizone Infiltration Model** [38] developed at LBL is able to calculate the air flow distribution for arbitrary structures in any given weather conditions. The basic idea is to determine the flow network and to calculate the effective air permeability of a zone from the combination of flow paths arranged in series and/or parallel. The use of these equations assumes that all permeabilities have the same flow characteristics and, therefore, the same exponent, n (see Eq. 2).

Air flows caused by separate mechanisms (such as wind and thermal buoyancy) are not able to be added because the flow rates are not linearly proportional to the pressure differences. To superimpose the flows, it is necessary to add the pressures.

To describe the air flow distribution inside a building we introduced several lumped parameters reflecting the different permeability distributions of the building's envelope and the flow resistances inside the building; the envelope permeability ratio (epr) which describes the cross-ventilation of the building, the vertical permeability ratio (vpr) to determine the stack influence and the resultant permeability ratio (rpr). The latter describes the removal of the incoming air flow for each zone.

$$epr(\phi) = \frac{D_{lee,envelope}}{D_{total,envelope}} \tag{13}$$

$$vpr = \frac{D_{shaft}}{D_{total,envelope} + D_{shaft}} \tag{14}$$

$$rpr(\phi) = \frac{D_{res,zone,lee}}{D_{res,zone,total}} \tag{15}$$

with:

epr	envelope permeability ratio
vpr	vertical permeability ratio
rpr	resultant permeability ratio
$D_{lee,envelope}$	permeability of the leeward side of the building
$D_{total,envelope}$	permeability of the whole envelope
D_{shaft}	permeability from the shaft to the story
$D_{res,zone,lee}$	leeward resultant permeability of the zone
$D_{res,zone,total}$	resultant permeability of the zone

The resultant permeability ratio (rpr) is the ratio of the resultant permeability of the downstream side to all resultant permeabilities of this particular zone. To keep the model simple no mass balance equation is used to predict the air flows. Because of the pre-calculation of the simplified network the model gives a comprehensive understanding of the flow characteristics of the structure under investigation. The model is simple to use and requires only simple mathematical tools, e.g., pocket calculator.

5. SUMMARY

Traditionally, models of residential buildings were based on the regression analysis of measured data for infiltration and the driving weather forces. As the regression coefficients for these empirical models reflected structural characteristics as well as shielding effects and occupant behaviour, the regression coefficients between similar residences have varied tremendously. These models may therefore not be appropriate for use as a design tool for building energy analysis.

The next step in residential infiltration modeling was the development of physical single-zone models. The amount of information required for single-zone network models led to the development of simplified models. Their development has been justified by their widespread use. These models are based on the physical phenomena of air flow through the building envelope by assuming a certain distribution of air permeability. Shielding effects and local vertical wind profiles are taken into account for calculating the infiltration rate. Measured data for a large number of houses are used to fine-tune, still further, especially the effects of shielding.

Following the analysis of an enormous number of measured ventilation rates in the case of houses for which the leakage characteristics have been determined by pressurization tests, a very simple model has been introduced --in which the air change rate measured at a given pressure differential, is divided by a constant number. This model does not take weather influence or leakage distribution into account.

Even before the development of physical single-zone models took place a number of computer models had been developed to calculate the air flow distribution in multizone buildings. The building is described by a set of zones interconnected by flow paths. Each node represents a space with uniform pressure conditions inside or outside the building and the interconnections correspond to impediments to air flow. The network models are usually based on the conservation of mass in each of the zones in the building. The first of these models to be developed was probably the BSRIA-model "LEAKS" which was published in 1970. Since that time, many more models have been developed but most of them have been written as research tools and are not available to third parties. As a consequence they are difficult to use and are, at the best, "user-tolerant" rather than "user-friendly".

The first very simple multizone model for equipment design calculation for low-rise buildings was introduced with the crack model. This model was later refined to cover high-rise buildings. A simplified approach was followed in the development of LBL's infiltration model, which allows the calculation of all interzonal air flows by means of a pocket calculator.

While multizone infiltration models have existed for the last two decades some of the thermal building simulation models are still working with constant rate models. Now that energy conservation and indoor air quality have become important issues this type of model is inadequate.

6. FUTURE OUTLOOK

Except for the fine-tuning of existing models, the development of single-zone models seems to be completed. As multizone models offer much more potential for further investigation, work will probably go on for some time to suit models to specific needs.

The development of multizone infiltration and ventilation models shows a relatively slow evolution. Lack of exchange of information, restricted distribution of models and the lack of a flexible structure are probably the reasons why models developed in the early seventies are not very different from those developed in the late eighties.

Although several of the models discovered during this review serve a particular purpose they could have been developed using existing models. The COMIS workshop is trying to overcome these problems by creating a multizone infiltration model with a modular structure which will allow modules to be changed easily. The availability of the program together with the international authorship should help to establish COMIS as an infiltration standard on which specific applications can be built.

Along with stand-alone infiltration models, network models will also now finally find their way into thermal building simulation models. With the expected advances in the development of the next generation of building simulation programs infiltration modules will be needed for implementation in the program

libraries.

Future tasks include the development of methods to determine the required input parameters, especially the wind pressure distribution. Further work must be done through sensitivity studies to reduce the input requirement and to increase user-friendliness by using the output features of the PC's.

Validation of the models is another essential task. In order to understand physical phenomena related to transport mechanism in buildings and to develop numerical descriptions, measurements must first be performed under steady state conditions. It is necessary, in order to measure mass flow transport mechanism accurately, to be able to control the pressure level and its fluctuation for each of the outside walls. This is only possible if the building is itself located in a building. Such a test facility would not only validate air flow models as a whole but would also help to validate the tracer gas techniques to be used to validate infiltration models in field experiments.

7. ACKNOWLEDGEMENTS

This work was supported by the Assistant Secretary for Conservation and Renewable Energy, Office of Building and Community Systems, Building Systems Division of the U.S. Department of Energy under Contract No. DE-AC03-76SF00098.

8. REFERENCES

1. Liddament, M.W.: "Air Infiltration Calculation Techniques - an Applications Guide", Air Infiltration and Ventilation Centre, Bracknell, 1986

2. Liddament, M.W. and C. Allen: "The Validation and Comparison of Mathematical Models of Air Infiltration" Air Infiltration Centre, Technical Note AIC 11, 1983

3. Wouters, P., W.F. de Gids, P.R. Warren, and P.J. Jackman: " Ventilation Rates and Energy Losses due to Window Opening Behaviour", in Proceedings, 8th AIVC Conference "Ventilation technology - Research and Application", Ueberlingen, 1987

4. Ross, H. and D.T. Grimsrud: "Air Infiltration in Buildings: Literature Survey and Proposed Research Agenda", Lawrence Berkeley Laboratory, LBL-7822, 1978

5. Sherman M. H., D. J. Wilson and D. E. Kiel: "Variability in Residential Air Leakage", in Proceedings, ASTM-Symposium on Measured Air Leakage Performance of Buildings, Philadelphia, 1984

6. German Standard DIN 4701: "Regeln fuer die Berechnung des Waermebedarfs von Gebaeuden", Beuth Verlag Berlin, 1959

7. Reinhold, C. and R. Sonderegger: "Component Leakage Areas in Residential Buildings" Lawrence Berkeley Laboratory, LBL-16221, 1983

8. Larsen, B.T.: "Energy Consumption of Residential Buildings. The Computer Program ENCORE", Norwegian Building Research Institute, 1977

9. Cole, J.T., J.A. Kinast, T.S. Zawacki, R.H. Elkins, and R.A. Macris: "Development and Field Verification of a Model of House Air Infiltration for Single Family Residences", Gas Research Institute, Final Report, 1981

10. Sherman, M.H.: "Air Infiltration in Buildings", Lawrence Berkeley Laboratory, LBL-10712, 1980

11. Wilson, D.: personal communication at Lawrence Berkeley Laboratory, May 1989

12. Shaw, C.Y. and G.T. Tamura: "The Calculation of Air Infiltration Rates caused by Wind and Stack Action for Tall Buildings", ASHRAE-Transactions 83, Part II, 1977

13. Warren, P.R. and B.C. Webb: "The relationship of tracer gas and pressurization techniques in dwellings", AIC Conference "Instrumentation and Measuring Techniques", Windsor, UK, 1980

14. Ertl, H., A. Fail and E. Panzhauser: "Natuerliche Schachtentlueftungsanlagen, Messung - Beurteilung - Planung" Wohnhabitat, Archivum Oecologiae Hominis, Wien 1987

15. ASHRAE 1985 Handbook of Fundamentals, Chapter 22, American Society of Heating, Refrigerating and Air-Conditioning Engineers, Atlanta, GA, 1985

16. Feustel, H.E. and V.M. Kendon: "Infiltration Models for Multicellular Structures: A Literature Review", *Energy and Buildings*, Vol. 8, No. 2, 1985

17. Jackman, P.J.: "A Study of Natural Ventilation of Tall Office Buildings", Inst. Heat Vent. Eng., Vol 38, 1970

18. Sander, D.M. "FORTRAN IV Program to calculate Air Infiltration in Buildings", DBR Computer Program No. 37, National Research Council Canada, 1984

19. Feustel, H.E.: "Entwicklung eines FORTRAN Programms zur Bestimmung der Luftstromverteilung in Gebaeuden", Diplomarbeit, Technische Universitaet Berlin, 1977

20. Jianxiong Guo: "Weiterentwicklung des Programms mit dem Ergebnis einer Beruecksichtigung thermischer Druckdifferenzen auch innerhalb eines Geschosses und einer spuerbaren Verringerung der Rechenzeiten", Interner Institutsbericht, Technische Universitaet Berlin, 1988

21. de Gids, W.F.: "Calculation Method for the Natural Ventilation of Buildings", TNO Research Institute for Environmental Hygiene, Delft, 1977

22. Etheridge, D.W. and D.K. Alexander: "The British Gas Multi-Cell Model for Calculating Ventilation", ASHRAE Transactions, Vol. 86, Part II, 1980

23. Evers, E. and A. Waterhouse: "A Computer Model for Analysing Smoke Movement in Buildings", Building Research Establishment, 1978

24. Nantka, M.: "A Numerical Method for Air Change Rate of Buildings Calculated" in Proceedings, 5th International Conference on HVAC, Praha, 1981

25. Walton, G.N.: "Thermal Analysis Research Program Reference Manual", NBSIR 83-2655, U.S. Department of Commerce, 1983

26. Herrlin, M.K.: "MOVECOMP: A static Multicell Air Flow Model", ASHRAE Transactions, Vol 91, Part 2B, 1985

27. Hayakawa, S and S. Togari: "Flow Rate Variation of Air Conditioning Systems due to Stack Effect and opening a Window", Kajima Institute of Construction Technology, Japan, Report Nr. 30, 1979

28. Ishida, K. and M. Udagowo: "Validation of the Ventilation Net Work Model for the Estimation of Room Temperatures and Heat Load of Residential Buildings with Measured Data", Transactions of the Architectural Institute of Japan, 1988

29. Hayashi, T., Y. Urano, T. Watanabe and Y. Ryu: "Passive System Simulation Program PSSP and its Applications", in Proceedings, "Building Energy Simulation Conference 1985, Seattle, 1985

30. Sasaki, T.: "Der Lueftungszustand von der Luftschicht durch Wind-Unruhe", Transactions of the Architectural Institute of Japan, No. 372, 1987.

31. Okuyama, H.: "Network Numerical Analysis Method for Heat Transfer and Air Flow in Buildings", in Proceedings, 17th Symposium by the Committee of Building Heat Transfer, Building Environment Committee of Architectural Institute of Japan, 1987

32. Matsumoto, M. and H. Yoshino: "A Calculation Method for Predicting Air Pollution in Multi-Celled Buildings", The Meeting of the Tohoku Branch of the Architectural Institute of Japan, 1988

33. Cacavelli, D., J.J. Roux; and F. Allard: "A simplified Approach of Air Infiltration in Multizone Buildings", in Proceedings, "9th AIVC Conference, Gent, 1988

34. Melo, C.: "FLOW - An Algorithm for Calculating Air Infiltration into Buildings", in Proceedings, ICBEM'87 International Congress on Building Energy Management, Lausanne, 1987

35. Feustel, H.E., F. Allard, V.B. Dorer, M. Grosso, M. Herrlin, M. Liu, J.C. Phaff, Y. Utsumi, and H. Yoshino: "The COMIS Infiltration Model", in Proceedings, "Building Simulation '89, The International Building Performance Simulation Association", Vancouver, 1989.

36. Shaw B. H. and W. Whyte: "Air Movement through Doorways - the Influence of Temperature and its Control by Forced Air Flow", BSE 42 (1974), No. 12, pp. 210-218

37. German Standard DIN 4701: "Regeln fuer die Berechnung des Waermebedarfs von Gebaeuden", Teil 1: Grundlagen der Berechnung Teil 2: Tabellen, Bilder, Algorithmen Beuth Verlag Berlin, Berlin, 1983

38. Feustel, H.E. and M.H. Sherman: "A Simplified Model for Predicting Air Flow in Multizone Structures", Energy and Buildings, Vol 13, No. 3, 1989

PROGRESS AND TRENDS IN AIR INFILTRATION
AND VENTILATION RESEARCH

10th AIVC Conference, Dipoli, Finland
25-28 September, 1989

Paper 9

WIND AND PRESSURE REQUIREMENTS FOR THE VALIDATION OF A MULTIZONE AIR INFILTRATION PROGRAM

J-M Furbringer, R. Compagnon, C-A Roulet

Laboratoire d'Energie Solaire et de Physique due
Batiment LESO-PB, Ecole Polytechnique Federale de
Lausanne EPFL
CH-1015 Lausanne, Switzerland

A. Gadilhe

Laboratoire des Sciences de l'Habitat, ENTPE
F-69518 Vaulx-en-Velin
France

ABSTRACT

The validation process of FLOW, a multizone air infiltration program, has given plenty of information on which we report in this paper.

The methodology of validation is exposed and we describe specific problems which have been met and solutions which are proposed for most of them. The three first stages of a validation process are discussed : analytical verification, inter-model comparison and empirical validation.

A simple situation for a single cell has been calculated analytically and compared with the numerical FLOW simulation. A sensitivity test was applied for some parameters as wind speed, temperature, pressure for both FLOW and another program ESP-AIR, the results showing a very similar behavior.

The confrontation with full scale measurements has just started. But even if it is not yet possible to draw conclusions about the validity of FLOW, the work has learned us a lot to care of in future validations. It is shown that a new method should be used to log the wind data and that the Cp-values found in the litterature are not always suitable for the air infiltration calculation programs.

1. INTRODUCTION

In order to validate computer programs simulating air flows in multizone buildings we have collected data which are being organized in a data set [1].

We have tried to validate the program FLOW [2] which computes the air flows for a static situation in a multizone building modelled with a cubic network. This work has demonstrated all the complexity of the validation process in this domain.

In this paper, we present the many kinds of problems we have met and the solutions we propose.

We have not pushed the validation of FLOW to its end because this program is today obsolete and we prefer to validate the new program COMIS, now under development at the LBL [3].

2. THE VALIDATION PROCESS

2.1 Methodology

Following the ideas developed for the validation of thermal models by Judkoff and al. [4] in the USA as well as by Bowman and Lomas [5] in the UK a coherent validation methodology can be structured as it appears in figure 1.

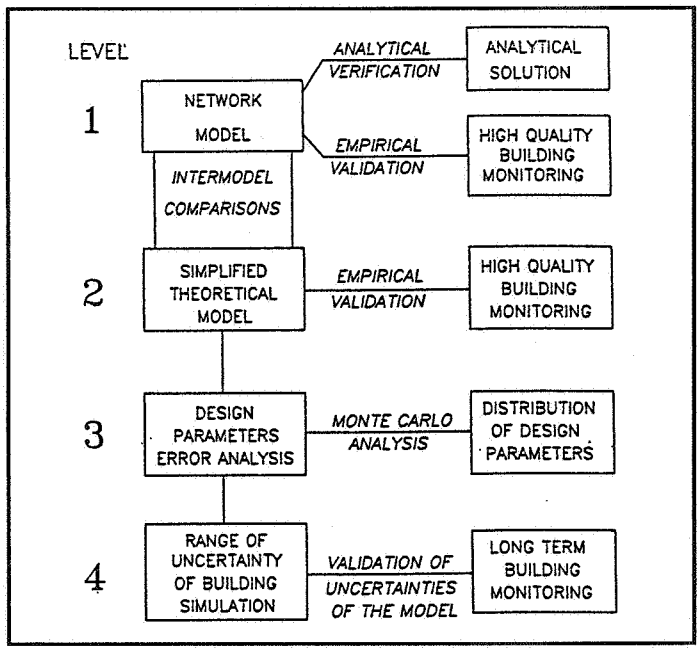

Figure 1 : Validation methodology for network models and simplified theoretical models [6].

The validation steps addressed in this work are :

1) the analytical verification
2) the inter-model comparison
3) the empirical validation.

In the analytical verification the calculation of a simple case is compared with program results.

The inter-model comparison is used to compare the advantages of various models or to appreciate the precision of a simplified model with respect to a more sophisticated one.

In the empirical validation measurements made "in situ" are compared to the computed results. On this level, many errors may influence the results and only a right error analysis can guarantee that the conclusion of the validation is reliable and not a piece of luck.

2.2 Error analysis in a validation process

The errors occurring in a validation process can be of two types :

1) internal errors
2) external errors

The internal errors issue from inaccuracies occurring in modelling the physical phenomena, writing the code, or in the numerical technique. The aim of the validation is to find these internal errors and to correct them. The external errors are contained in the data or coming from a bad use of the program and are to be avoided during the process of finding the internal errors.

Table 2 presents a comprehensive list of external error sources. It is an adaptation for the air flow model of the study of Bowman et al. [5].

Model Input Data	Climatic Data	• Some (or all) climatic data coming from a remote site • Frequency of measurement too low to define the variable (especially for the wind data) • Limited accuracy of measurements
	Site Data	• Cp imprecision problem
	Building Data	• Inadequate description of building geometry and construction • Uncertain workmanship • Use of handbook rather than measured physical properties • Temperature and permeability of adjacent unmodelled zones not defined • Limited accuracy of measured values
	Occupancy	• Interference with the building system • Badly defined occupancy profile • Uncertainty in modelling HVAC
	User Interface	• Blunders when entering data • Interpretation of poorly documented input data • Assuming values to replace missing data • Modification to the building description so that it can be modelled • Amended program coding so that the building can be modelled
Building Response Data	Data Logging	• Noisy, missing or spurious data • Frequency of measurement insufficient to define variable • Finite accuracy of probes and recording system
	Interference	• Internal features of structures altered by monitoring equipment
Comparison procedure	Data Comparison	• Transcription of measured data from charts, etc. • Differences between measured and predicted parameters • The location of the measurement and the prediction differ

Table 2 : External sources of errors occurring in a validation process.

2.3 Problems met and solutions

2.3.1 Frequency of wind data measurements

In the following we assume that wind data are available on site, either by a procedure of transferring meteo data from the remote station [18] or by measurements on site.

The air infiltration model calculates the air change rates averaged over fixed time intervals (here 15 minutes). In order to do so, wind data must be converted into pressures. The averaging of wind pressures over a particular time interval, is a problem.

Indeed, weather data measurement installation set up for building thermal auditing are often not able to collect measurements in a time interval shorter than 15 minutes.

Under these conditions the wind measurements are often of poor quality. On one hand, instantaneous measurements every 15 minutes are insufficient to model the air flows in buildings and on the other hand mean values have no physical meaning. As an example, we imagine the situation where the wind blows half of the time interval from the south and half from the north, then the following situations are possible :

1. The averaging process handling separately the wind speed, V(t) and its direction, $\theta(t)$, results in an average direction which is east or west, and an average speed which is non zero.

   $\{\theta(t_i),\ V(t_i)\} \rightarrow \overline{V}\ ,\ \overline{\theta}$

2. The averaging process computing the vectorial sum gives an average vectorial wind close to zero.

   $\{\vec{V}(t_i)\} \rightarrow <\vec{V}>$

In each case the average wind is of no use to calculate the surface pressures and to simulate air flows reliably. To avoid this problem, an appropriate technique has been developed at the LESO.

But before explaining it, it is necessary to define the two kinds of time intervals occurring in a weather data logging process.

1. The sampling period is the time between two measurements of the same variable (typically 1 minute or equal to the recording period).

2. The recording period is the time after which the averaged, integrated or instantaneous measurement is recorded on the data logger tape (typically 15 to 30 minutes).

Usually the sampling period is equal to the recording period for the slowly varying observables (e.g. temperature) and the sampling period is shorter than the recording period for the quickly varying variables as wind speed or wind direction.

In such conditions, the appropriate technique to have satisfactory wind data consists of :

- Measuring the wind speed V(t) and direction $\theta(t)$ at the highest possible sampling frequency.

- Summing the wind speed V(t) sorted on the wind direction sectors (commonly eight sectors of 45°). As shown in the Annex 1, we shall compute :

$$V_{Jk} = \left(\sum_{\{\theta_J \le \theta(t_{ik}) < \theta_{J+1}\}} [V(t_{ik})]^{2n} \right)^{1/2n} \quad (1)$$

with

J = 1, 2, ..., 8 (sectors)
k = 1, 2, ..., K (recording time)
i = 1, 2, ..., I (sampling time)

and

V_{Jk} : geometrical average wind speed in the sector J for the recording period k, [ms^{-1}]

θ_J : limit angle between the sector J-1 and J

$V(t_{ik})$: instantaneous wind speed at the sampling time i of the recording period k, [ms^{-1}]

$\theta(t_{ik})$: instantaneous wind direction at the sampling time i of the recording period k.

The geometrical average is justifiable by the fact that the pressure on the façade is proportional to the square of the wind speed and the flow to the power n of the pressure difference (n = .65 is taken). Therefore :

if $$Q = C \left(Cp \frac{1}{2} \rho V^2 \right)^n \quad (2)$$

then $$\langle Q \rangle = C \left(Cp \frac{1}{2} \rho \right)^n \langle V^{2n} \rangle \quad (3)$$

- recording the V_{Jk} every recording time

- modelling the flows in accordance with the measurements

$$Q_{lm} = \frac{1}{I} \sum_{J=1}^{8} C_{lm} \left(Cp(\theta_j) \frac{1}{2} \rho V_j^2 \right)^n \quad (4)$$

Q_{lm} : the flow between the nodes l and m, [$m^3\ h^{-1}$]
C_{lm} : the permeability coefficient between the nodes l and m, [$m^3\ h^{-1}\ Pa^{-n}$]
$Cp\ (\theta_j)$: the pressure coefficient for the sector J representing the pressure difference between l and m, [-]

$$Cp = \frac{\Delta P_{lm}}{q}$$

2.3.2 The pressure coefficients

Getting satisfactory pressure coefficients (shape factors) is a very complex problem. The authors do not have the pretension to solve it, but summarize the specific problems for air infiltration codes validation.

Figure 3 gives the air flows, for the eight wind directions, in a room of the LESO building for two sets of Cp-values. The first set was measured in a wind tunnel at the LBL and the second is the default set of the FLOW program. Q_{in} is the flow entering the room from the inside of the building while Q_{out} is the flow entering from the outside. The dramatic discrepancy between the two sets of computed air flows is obvious. This example gives all its importance to the following discussion.

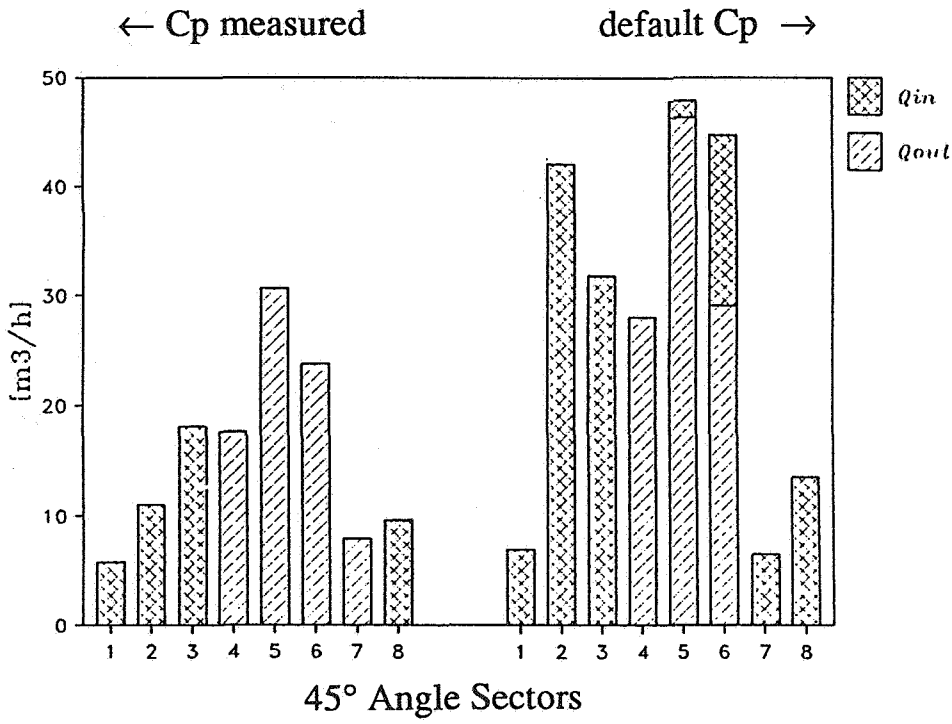

Figure 3 : Calculated air flows entering a room of the LESO building for a wind of 10 [m s^{-1}] for eight wind directions and two sets (right - left) of Cp-values.

The items to be discussed are definitions of the Cp-values, sources of Cp-values, representative location of the Cp-values and representativity of the Cp-values themselves.

The definitions of the Cp - values

Several definitions exist for the pressure coefficients depending on their use, the geometry of the building and the habits of the professionals in a given country.

The Cp is always the ratio of a local pressure p to a dynamic pressure q :

$$q = 0.5\ \rho\ V^2 \quad (5)$$

$$p = Cp\ q \quad (6)$$

where ρ is the air density, [kg m^{-3}], and V is the wind speed, [m s^{-1}].

The definitions differ by the use of different extreme or average values for p and q [7] and, because the high sensitivity of the nodal air flow simulation program to them, it is a very critical point in the validation process. The two most common definitions are presented and commented below.

Cp used with one reference dynamic pressure

The dynamic pressure q is taken at a reference point

$$p(x, y, z) = Cp\ \ q(x_0, y_0, z_0) \quad (7)$$

where z_0 : the reference height.

Definition (7) is better adapted to low rise buildings simulated with a constant wind profile. This profile can be used when the wind flow is driven down by the building. In this case (fig. 4) it is possible to observe, at low level, winds as fast as at roof level.

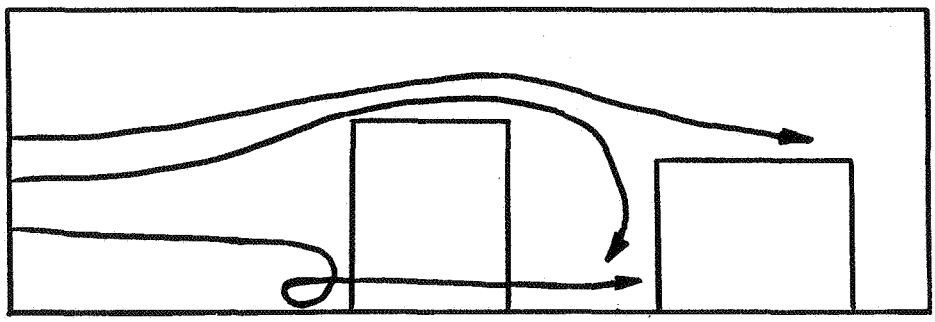

Figure 4 : The wind flow driven down by the building.

The reference point may be placed in various locations, each having advantages and disadvantages as discussed in reference [19]. Various positions on the roof or upstream are possible choices.

Cp used with dynamic measure profile

The dynamic pressure q is considered at the same height as the pressure p (fig. 5).

$$p(x, y, z) = Cp \quad q(z) \tag{8}$$

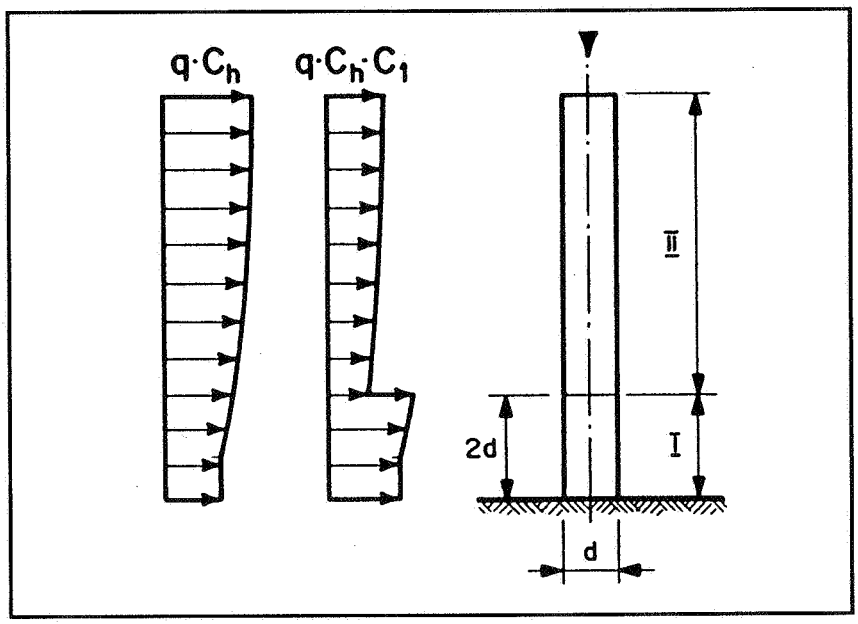

Figure 5 : Dynamic pressure q profile for a high-rise chimney [12].

The wind at the height z is calculated from the exponential law (9)

$$\frac{V(z)}{V(z_0)} = \frac{z^{\alpha}}{z_0{}^{\alpha}} \tag{9}$$

with the exponent α depending on the terrain roughness [8] so that

	0.18	in flat open land
$\alpha \approx$	0.23	in country
	0.36	in urban centers

These exponents are taken from reference [9], but it seems that every author has his own values.

Definition (8) is adapted to high rise buildings when the difference in the wind speed between the basement and the roof is important [10]. But aerodynamicians know a lot of details, which can have their weight in the choice of the appropriate Cp [11]. It would be a gain of time to have a decision tree (an algorithm) to choose the right definition and to avoid subjective screening.

Sources of Cp-values

As sources of Cp-values it is possible to use handbooks [12], simulation codes and wind tunnel measurements. Usually the handbook values are measured in wind tunnels, and sometime on site (full-scale measurements). The numerical codes which simulate tri-dimensional flows are still in development.

When picking Cp-values from a handbook care shall then be taken of which definition, which reference point and which safety margin have been used to obtain those results. In addition the buildings presented in handbooks are measured in open land situation and the influences of adjacent obstructions present in the real situation have to be estimated.

The adaptations of the values from handbooks to those expected by the computer program are theoretically possible if the information is precise enough, but it is better to ask help from a specialist, since for some locations in a building, the Cp values are calculated using special methods which are not explicitly mentioned in handbooks.

Without taking these precautions, every effort to obtain high quality results can be ruined by one or two badly estimated pressure coefficients [7].

For the wind tunnel measurements care should be taken of the correct simulation of the wind as a turbulent boundary layer. Because of the non-stationarity of the wind, its simulation should reproduce carefully the speed and direction profile, the turbulence intensity and the turbulence spectrum.

Representative location of a Cp-value

When a façade is submitted to a pressure field the resulting air flows depend on the permeability distribution.

To illustrate this problem, figure 6 presents different zones on a façade of a cube with respect to Cp-values.

Many typical situations are possible as a portion of the untight element may belong to one zone or another. This point emphasizes the advantage of programs which model the façades element by element.

In addition, the areal average shall be studied in agreement with the pressure distribution on the façade. For example the interpolation of Cp-values between two points is not possible because the pressure field on the building is not monotonic. Indeed, Cp-values vary more strongly horizontally than vertically, especially for high-rise buildings. Moreover, values given in handbooks are often calculated for civil engineering purpose. Therefore they are not representative of an average but more often only valid at a particular location [11]. In order to obtain Cp-values which serve as areal coefficients it is better to measure them as such. Reference [9] gives an example of a scale model built to perform areal and pneumatic averages.

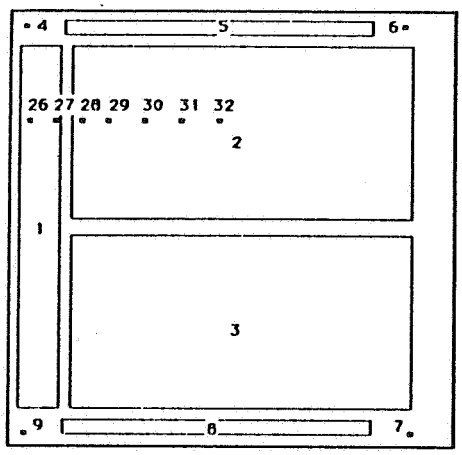

Figure 6 : Areal partition of the leeward side of a cube for wind pressure distribution. The numbers correspond to the probes [9].

Representativity of the Cp for the air flow simulation of buildings

The decisive proof of the quality of a theory is the confrontation with the reality. And here is the critical point for the Cp-values. Full scale and wind tunnel measurements agree only for windy and open, flat, situations for simply shaped buildings [13].

Usually the results for full scale measurements have so large confidence intervals (they can reach the magnitude of the value itself) that any conclusion can be taken [14]. Some specialists doubt the possibility to represent the pressure on a façade by a single value [15].

The reason for such a situation comes from the problem of the pressure measurement and also from the fact that in the low wind situation, which is most frequent in Switzerland, buoyancy induced airflow around the building can be similar to the wind effect.

Annex 2 presents a simplified calculation where it is demonstrated that in a middle sized building (three floors) a temperature difference of 3° C between two façades, caused by radiation from the sun, induces a convective flow of about 1 m/s.

In conclusion the Cp-values, if they are the right ones, probably allow the calculation of the wind effect on the building but not the effective pressure in the most frequent situation when the wind velocity is low and the sun shines.

3. THE PROGRAM FLOW

The program FLOW was developed by H.E. Feustel at the LBL [2] and was available to us when COMIS [3] started. FLOW is constituted by a FORTRAN code and data files as shown in figure 7.

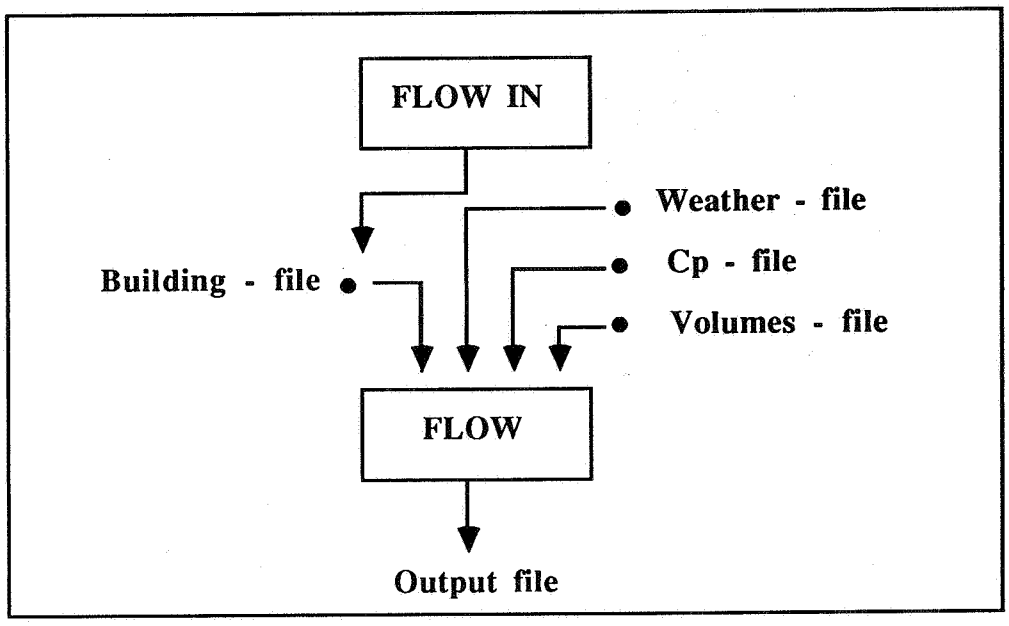

Figure 7 : The file structure of FLOW.

The main program computes the flows by a Newton algorithm for a cubic network of permeabilities connecting the nodes which correspond to the rooms and the outside.

The weather file contains outside temperature, wind speed and wind direction at the reference point for every time step. These values are taken into account as boundary conditions by the program which computes these static situations one after the other.

The output file contains basically the flows between every node and its six neighbors.

4. THE VALIDATION OF THE PROGRAM "FLOW"

The first three levels specified in figure 1 have been taken into account.

4.1 The analytical verification

For this level, the results of the code are compared with an analytical solution for a few simple cases. The test cases have to be chosen in order to be able to test all the algorithms in the code both separately and interacting with one another. Every case which can be handled by the program should be investigated.

For this study the two air flow driving processes were investigated separately :

1. The infiltration due to wind
2. The infiltration due to the stack effect

Each can be investigated in different situations, where different parts of the code are used. This method has allowed us to find many programming bugs. It is very important to begin with these very simple cases because it is easier to find the problematic points that way.

Annex 3 presents the calculation of a simple case of wind induced infiltration.

In table 8 analytical results are compared with computed ones, after correction of the program.

Parameters and variables		Analytical	Computed	Remark
$C_{windward}$ $C_{leeward}$	[m^3 h^{-1} Pa^{-n}] [m^3 h^{-1} Pa^{-n}]	20 40		given
T_{ext} T_{int}	[°C] [°C]	0 0		given
ρ_{ext} ρ_{int}	[kg m^{-3}] [kg m^{-3}]	1.293 1.293	1.27 1.2	FLOW assumes special ρ
Wind speed P_{static}	[m/s] [Pa]	8.8 50	8.87 50	adapted to have the same P_{stat} $\frac{1}{2} \rho V^2$
P_{int} m Q	[Pa] [kg / h] [m^3 / h]	2.8 266.48 209.83	2.80 266.33 221.94	

Table 8 : Comparisons between analytical solution and the computed results for wind induced infiltration.

The principal remark concerns the air density calculation. The program runs with two air densities :

Outside the building : $\rho_{ext}(T) = 1.27 - 0.05\ T$ (10)

and inside : $\rho_{int}(T) = 1.2$ (11)

It is very important to give this kind of information in the instructions for use, otherwise there is a huge loss of time in debugging the program and finding clues to interpret the differences between the computed and the analytical results.

At first it was not obvious that the difference in volume flows was only due to the differences in assumed densities. Such a detail cannot be found in an empirical validation process, because it is hidden under the large amount of possible causes.

4.2 Inter-model comparison

The inter-model comparison was made between the programs FLOW and ESP-AIR [16]. The simulated building is a cube. Its parameters are presented in the table 9 and the table 10 gives the weather data.

Side	Permeability C [$m^3\ h^{-1}\ Pa^{-n}$]	Permeability n [-]	Cp (0°)
South	1	1	β
East	1	1	- 1/3 β
North	1	1	- 1/3 β
West	1	1	- 1/3 β
Roof	0	-	0

Table 9 : Building parameters for the inter-model comparison.

Run -	Wind speed [$m\ s^{-1}$]	Wind dir.	T_{int} [°C]	T_{ext} [°C]	β
1	20	South	20	20	1.5
2	20	South	20	0	.5
3	1	South	20	20	.5
4	1	South	20	0	1.5
5	14	South	20	10	1.0

Table 10 : Weather data parameters for the inter-model comparison and sensitivity study.

The weather data parameters have been chosen to explore regularly the experimental space and perform an optimum sensitivity test with a minimum of runs. The parameter β is artificial and serves to modify the magnitude of the pressure coefficients. Table 11 presents the results.

These results are similar and follow the same variations. A more detailed study would be necessary to explain the differences and define a confidence interval for each result.

Run	FLOW		ESP-AIR	
	[m^3 / h]	[kg / h]	[m^3 / h]	[kg / h]
1	342	410	360	413
2	132	158	127	156
3	.28	.34	.30	.35
4	.99	1.19	.95	1.17
5	123	148	120	143

Table 11 : Results from FLOW and ESP-AIR.

The parametric study has shown that the two programs are most sensitive to the wind speed. Fitting a polynomial on the four first runs, the following relative coefficients were found :

Constant	:	1
Windspeed	:	1
Temperature	:	0.44
β (Cp)	:	0.44

In the constant are hidden non-studied parameters including the permeability distribution and the pressure distribution.

The influence of the wind speed is very large and this is an argument to take into account when considering the quality of the wind measurements (see chapter 2.3).

This inter-model comparison should be continued further, with other situations. We intend to do it with the COMIS program [3]. However, this level of the validation allows us anyway to study the sensitivities of the programs to several variables.

5. CONCLUSIONS

The validation process of the multizone air infiltration programs FLOW and ESP-AIR has shown a high sensitivity of this kind of nodal model to the wind and hence to the pressure coefficients Cp. Available wind data are in general not adapted to the requirements of air infiltration modelling. A new scheme for the measurement and simulation of wind data is proposed suggesting that considerable progress in wind simulation is possible.

Cp-values available in the literature are not adapted to the purpose of air infiltration calculation. They generally do not give an areal average pressure coefficient in a realistic situation, including boundary layer flow, natural convection flow and surroundings.

Before comparing full scale measurements and computed results, we submitted the code to analytical validation in many very simple situations. It was found an easy way to debug the code.

Future research should include the coupling effects of wind and buoyancy on air infiltration.

A few remarks. It is felt that time can be gained by joining the authors of the program, the measuring staff and the validators in a same place during the program validation.

It seems to be scientifically advantageous that the program author and the validator are two different persons. The review will be more censorious that way and the result will be better.

Finally and obviously, it is very important to remember that the validation of a program is a hard and very time consuming work.

6. APPENDICES

ANNEX 1 - A SATISFACTORY AVERAGING METHOD FOR WIND DATA

The mean flow Q_k between two nodes at the limit of the network during the period k is modelled by a sum on 8 sectors of the mean flows Q_{Jk}

$$Q_k = \frac{1}{I} \sum_{J=1}^{8} Q_{Jk} \qquad \text{(A1)}$$

The demonstration is done by showing that this model is equal to the sum (A7) of the instantaneous flows $Q(t_{ik})$. The flow Q_{Jk} is defined so that :

$$Q_k = \frac{1}{I} \sum_{J=1}^{8} C \ [Cp(\theta_J) \frac{1}{2} \rho \ (V_{Jk})^2]^n \qquad \text{(A2)}$$

where

Q_k	:	average flow during the period k, [$m^3 h^{-1}$]
I	:	number of measurements during the period k (recording period)
C	:	permeability coefficient, [$m^3 h^{-1} Pa^{-n}$]
n	:	exponent, [-]
$Cp(\theta_J)$	:	pressure coefficient for the sector J, [-]
ρ	:	air density, [kg m^{-3}]
V_{Jk}	:	integrated wind speed for the sector J during the period k
Q_{Jk}	:	integrated flow during the period k for the sector J.

Let us define

$$(V_{JK})^2 = \left[\sum_{\{\theta_J \le \theta(t_{ik}) < \theta_{J+1}\}} (V(t_{ik}))^{2n} \right]^{1/n} \quad \text{(A3)}$$

which is the averaging method compatible with the model (A2), as shown below. Placing (A3) in (A2) we obtain :

$$Q_k = \frac{1}{I} \sum_{J=1}^{8} \sum_{\{\theta_J \le \theta_{ik} < \theta_{J+1}\}} \left(C \left(Cp(\theta(t_{ik})) \frac{1}{2}\rho \right)^n (V(t_{ik})^{2n}) \right) \quad \text{(A4)}$$

recomposing the two sums

$$Q_k = \frac{1}{I} \sum_{i=1}^{I} C \left[Cp(\theta(t_{ik})) \frac{1}{2}\rho (V(t_{ik}))^2 \right]^n \quad \text{(A5)}$$

$$Q_k = \frac{1}{I} \sum_{i=1}^{I} Q(t_{ik}) \quad \text{(A6)}$$

The precision between the real flow and the modelled one depends on the number of measurements. The greater is I, the more accurate will be the simulation.

ANNEX 2 - THERMAL WIND AROUND A BUILDING

The scope of this calculation is to estimate the magnitude of the air flow between two façades at different temperatures.

This difference can be caused by the radiation on one façade (front façade subscript F) and the shadow on the other (back façade subscript B). We imagine the building in the form of a parallelepiped of height h. From the Bernoulli equation, it is possible to write :

$$P_B + \frac{1}{2} \rho_B V_B^2 = P_F + \frac{1}{2} \rho_F V_F^2 \quad \text{(A7)}$$

to simplify the problem let us assume that V_B is close to zero. Then

$$\Delta P = \frac{1}{2} \rho_F V_F^2 \quad \text{(A8)}$$

and for two colums of air at different temperatures the maximum pressure difference is :

$$\Delta P = h\ g\ \Delta\rho \quad \text{(A9)}$$

then it is possible to estimate the velocity V so that :

$$V = \sqrt{\frac{\Delta\rho}{\rho} g h} = \sqrt{\frac{\Delta T}{T} g h} \qquad \text{(A10)}$$

As a numerical example, ΔT is 3 [°C] and h = 10 [m] would give

$$V = \sqrt{(3/300)\ 9.81\ \cdot 10\ )} = 1 \text{ [m/s]} \qquad \text{(A11)}$$

that means that for a wind velocity of 5 m/s, a value of Cp = 1 can be affected by up to 20 % and a Cp = 0.2 by up to 100 %.

It is interesting to recall that the same characteristic velocity is found by recognizing that the internal Froude number must be close to unity (i.e. buoyancy forces are in equilibrium with the inertial forces) [17]; this is a restatement of equation (A10).

ANNEX 3 - CALCULATION OF THE SIMPLE CASE OF WIND INDUCED INFILTRATION FOR THE ANALYTICAL VALIDATION

A3.1 The building

The monozone building is described as follows :

C_W	:	windward exfiltration coefficient [$m^3\ h^{-1}\ Pa^{-n}$]
C_L	:	leeward exfiltration coefficient [$m^3\ h^{-1}\ Pa^{-n}$]
Cp_W	:	windward pressure coefficient
Cp_L	:	leeward pressure coefficient
n	:	exponent coefficient
V	:	wind speed [$m\ s^{-1}$]
P_W	:	windward pressure, [Pa]
P_L	:	leeward pressure, [Pa]
P_I	:	internal pressure, [Pa]

Figure 12 gives a schematic view of the building-test 1

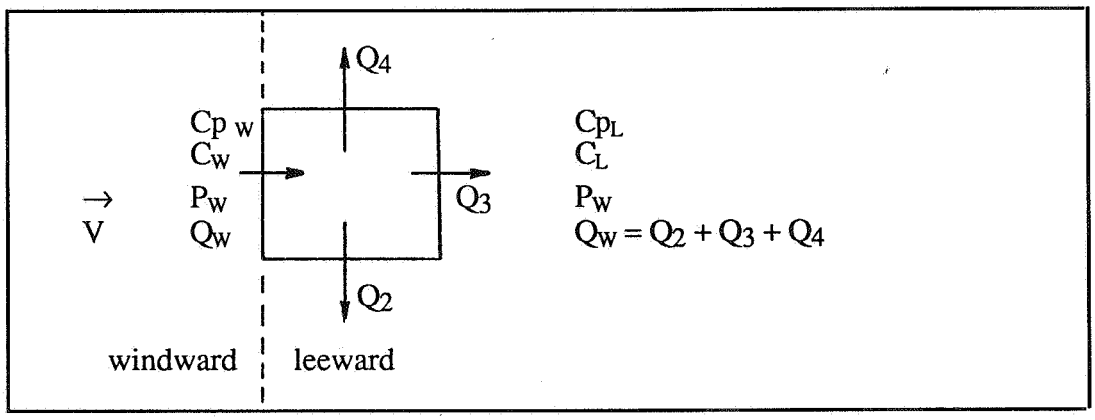

Figure 12 : A schematic view of the building-test 1.

A 3.2 Analytical solution

The wind induced infiltration process is represented by the following equations :

- Exfiltration law

$$Q_W = C_W (P_W - P_I)^n \quad \text{with } 0.5 < n < 1 \qquad \text{(A12)}$$

$$Q_L = C_L (P_I - P_L)^n \qquad \text{(A13)}$$

- Wind induced pressure

$$P_W = C_{pw}\, q \qquad \text{(A14)}$$

$$P_L = C_{pL}\, q \qquad \text{(A15)}$$

- Static pressure

$$q = 0.5\, \rho\, V^2 \qquad \text{(A16)}$$

- Mass conservation

$$\rho\, Q_W = \rho\, Q_L \qquad \text{(A17)}$$

from 6 it is trivial to obtain by (A12) and (A13)

$$C_W (P_W - P_I)^n = C_L (P_I - P_L)^n \qquad (P_W > P_I > P_L) \qquad \text{(A18)}$$

by raising (A18) to the power $\frac{1}{n}$

$$(C_W)^{1/n} (P_W - P_I) = C_L{}^{1/n} (P_I - P_L) \qquad \text{(A19)}$$

and we get

$$P_I = \frac{(C_W)^{1/n} P_W + (C_L)^{1/n} P_L}{C_W{}^{1/n} + C_L{}^{1/n}} \qquad \text{(A20)}$$

$$P_I = q\, \frac{C_{pw} (C_W)^{1/n} + C_{pL} (C_V)^{1/n}}{C_W{}^{1/n} + C_L{}^{1/n}} \qquad \text{(A21)}$$

and finally we get

$$Q_L = Q_W = C_W C_L \frac{(P_W - P_L)^n}{(C_W{}^{1/n} + C_L{}^{1/n})^n} = C_{eq} (P_W - P_L)^n \qquad \text{(A22)}$$

A 3.3 Numerical results

The following data are used :

$C_W = 20$ [m^3/h Pa^n]
$C_L = 40$ [m^3/h Pa^n]
$n = 0.65$
$C_{pw} = 0.8 \rightarrow P_W = 40$ [Pa]

Cp_L = 0.2 $\rightarrow$ P_L = - 10 [Pa]
V = 8.8 [m/s]
ρ = 1.2929 (T = 0 [°C]) (kg / m^3)
q = 1/2 ρ V^2 = 50 [Pa]

The use of equation (A21) gives :

$$P_{int} = 50 \left(\frac{0.8\ (20)^{1/.65} - 0.2\ (40)^{1/.65}}{20^{1/.65} + 40^{1/.65}} \right) = 2.8 \text{ [Pa]} \qquad \text{(A23)}$$

The flows are now obtained from equation (A22)

$$Q_W = 20\ (40 - 2.8)^n = 209.83 \text{ [m}^3\text{/h]} \qquad \text{(A24)}$$

$$Q_L = 40\ (- 10 - 2.8)^n = 209.82 \text{ [m}^3\text{/h]} \qquad \text{(A25)}$$

7. ACKNOWLEDGEMENTS

The authors will express their thankfulness to B. Fleury (LASH-ENTPE), J. van der Maas (LESO-EPFL) and J.-A. Hertig (LASEN-EPFL) for their comments and their help.

The National Energy Research Fondation (NEFF) supports this validation study as a task of the ERL-Project (Energierelevanteluftströmungen in Gebäuden), (credit N° 339.1).

8. BIBLIOGRAPHY

[1] J.-M. Fürbringer, R. Compagnon
"Weather and aeraulic data set for validation - The LESO Building, Part. 1 Content of the data set" internal report, LESO, EPFL, Lausanne, Switzerland (1989).

[2] H.E. Feustel
"Beitrag zur theoretischen Beschreibung der Druck und Luftmassen stromverteilung in natürlisch und maschinell gelüfteten Gebäuden". Forschritt-Berichte der VDI-Zeitschriften, 1984, Reihe 6, Nr 151.

[3] International Workshop COMIS. 1988, 1989
Conjunction of Multizone Infiltration Specialists at Lawrence Berkeley Laboratory.

[4] R. Judkoff and al.
"A methodology for validating building energy analysis simulations", draft report, SERI / TR-254-1508 Golden, CO, USA (1983).

[5] N.T. Bowman and K.J. Lomas
"Empirical validation of dynamic thermal computer models of buildings", Building Services Engineering Research and Technology, Vol. 6 (4). pp. 153 - 162, London, UK (1985).

[6] J.-L. Scartezzini, J.-M. Fürbringer, C.-A. Roulet, H.E. Feustel,
"Data needs for purpose of air infiltration computer code validation" proc. 8th AIVC Conference, Ueberlingen (1987).

[7] G. Barnaud
"Effets locaux-pression interne" in "Aerodynamique", CSTB editor, REFF Vol. II, France.

[8] A.G. Davenport
"The relationship of wind structure to wind loading" in proc. "Wind effects on buildings and structures" National Physical Laboratory, Teddington, UK (1963).

[9] J.A. Hertig et al.
"Essai en soufflerie à couche limite en vue de mesurer les coefficients de pression pour les tableaux de la norme SIA 160 révision 1988" (LASEN, EPFL, Lausanne, Switzerland (1989).

[10] Y. Lee et al.
"Distribution of wind - and temperature - induced pressure differences across the walls of a twenty-storey compartementalised building" Jour. of Wind Eng. and Ind. Aerody. 10 (1982) Amsterdam, Netherlands.

[11] Private discussion with J.-A. Hertig, Lasen, EPFL, Lausanne, Switzerland.

[12] SIA Standard 160 "Action sur les structures porteuses". Ed. SIA, Zurich, Switzerland, (1989).

[13] J. Gusten
"Full-scale wind pressure measurements on low-rise buildings"
in proc. "1984 Wind pressure workshop" TN AIC 13.1.

[14] A. Gadilhe
Intermediate thesis report, LASH, Lyon, France (March 1989).

[15] Private discussion with H. Phaff, TNO, Delft (NL).

[16] J. Clarke, D. McLean, Abacus
"ESP. A building and plant energy simulation system" Version 5, release 3
University of Strathclyde, Glasgow, UK, (1986).

[17] J.S. Turner
"Buoyancy effects in fluids", Cambridge University Press, UK (1973).

[18] J.A. Hertig, J. Ehinger
"Analysis of the influence of topography on the exposure of buildings"
proc. 10th AIVC Conference, Gent (1988).

[19] Carolyn Allen
"Wind pressure data requirements for air infiltration calculations"
TN AIC 12, UK (1984).

PROGRESS AND TRENDS IN AIR INFILTRATION AND VENTILATION RESEARCH

10th AIVC conference, Dipoli, Finland
25-28 September, 1989

Paper 10

AIRFLOW SIMULATION TECHNIQUES - PROGRESS AND TRENDS

PETER V. NIELSEN

University of Aalborg
Sohngardsholmsvej 57
DK-9000 Aalborg
Denmark

SYNOPSIS

The paper describes the development in airflow simulations in rooms. The research is, as other areas of flow research, influenced by the decreasing cost of computation which seems to indicate an increased use of airflow simulation in the coming years.

It is shown that velocity and temperature distribution can be predicted in small rooms of simple geometry as well as in large areas with a complicated geometry, such as theatres, atriums and covered shopping centres. It is also possible to predict variables which are rather difficult to measure as contaminant and humidity concentration, local age and purging flow rate, heat transfer coefficients, etc.

Airflow simulation has been used for the prediction of air movement in mixing ventilation, and new research shows that it might also be used for predicting air distribution in displacement ventilation.

The paper shows that some development work is necessary to give practical descriptions of air terminal devices. It also shows that it may be necessary to develop a turbulent model which deals with low turbulent flow.

LIST OF SYMBOLS

Ar	Archimedes' number
c_{oc}	Mean concentration in the occupied zone
c_R	Concentration in return opening
h	Slot height of air terminal device
H	Height of room
k	Turbulent kinetic energy
L	Length of room
n	Air change rate
Re	Reynolds number
T	Air temperature
T_o	Supply temperature
T_{oc}	Mean temperature in the occupied zone

T_R	Return temperature
u	Mean velocity
u_o	Supply velocity
u_{tot}	Mean velocity in vertical plane
u_{rm}	Maximum velocity in the occupied zone
u', v' and w'	Velocity fluctuations in the three coordinate directions
y	Vertical coordinate
Δt^*	Dimensionless time step
ε	Ventilation efficiency
ϵ	Dissipation of turbulent kinetic energy

1. INTRODUCTION

The ventilation of rooms may be achieved by different types of air distribution systems. A commonly used system is a mixing system where inlet air is supplied from diffusers in the wall or in the ceiling. The supplied air forms wall jets below the ceiling which are easy to describe in terms of velocity distribution, entrainment, etc. The jets deflect at the wall facing the supply openings, and the resultant flow in the lower part of the room - the occupied zone - has a rather complicated structure. It is possible to predict the air distribution in the whole room including the occupied zone by solving differential equations for the flow using a computer-based numerical method. The method has been explained in a number of publications during the last 15 years, as shown e.g. by Nielsen[1] in an early paper, but it is not generally used by the ventilation industry.

Ventilation with vertical displacement flow is another air distribution method. The air is supplied directly into the occupied zone at low velocity from wall mounted or floor mounted diffusers. The flow is in general driven by buoyancy force, and Davidson[2] has shown that airflow simulation can also be used for predicting the air distribution in this case.

The air distribution in radiator heated rooms may also be analysed by air flow simulation as shown for example by Rheinländer[3].

This paper will review the research on airflow simulations in rooms using computer-based numerical methods and further it will show some trends and new developments.

2. FULL-SCALE EXPERIMENTS AND COMPUTER SIMULATION

Full-scale experiments will produce measurements which can be of very high quality but they are time consuming. The cost of a single experiment is in the range 3,000 US$ to 20,000 US$. More expensive full-scale experiments may involve actual decorating, furnishing and interior fittings so that the owner, architect and consultants can experience the environment at a very early stage as discussed by Lärkfeldt[4]. This is of course an extra advantage of full-scale experiments, and furthermore, it will also ensure an acccurate determination of the flow in the occupied zone and give information of the influence from different shapes in the interior such as lamps, technical installations, etc. Full-scale experiments in the cheaper end of the price scale are made in rooms which can be built in a module system with moveable walls and ceiling.

An alternative possibility are model experiments which are necessary for very large installations. Model experiments are difficult to perform, due to problems with similarity. They are also expensive because they require much elaboration of such details as supply openings, etc.

The practical use of flow simulation for room air distribution is a question of the price level as well as the quality of predictions. The cost of a simulation now correspond to that of a full-scale experiment. Chen[5] has shown that 80 CPU minutes on an IBM 3083 - JX1 are used for predicting different flow situations, and Davidson[2] has to use up to 80 CPU hours on a VAX 2000 to simulate the displacement ventilation created by buoyancy driven flow.

Airflow simulations will increase in importance in the coming years due to the economics. Chapman[6] shows how the relative computation cost is decreasing every year, and this trend will continue in the coming years. The reason is that computer speed and storage have increased much more rapidly than computer costs, and figure 1 shows that the cost of performing a given calculation has been reduced by a factor of 10 every 8 years.

Another trend is the movement from large main frame computers in computer centres to work stations located close to the user. This change in the use of a computer will make more people familiar with standard software packets as programs for airflow simulation.

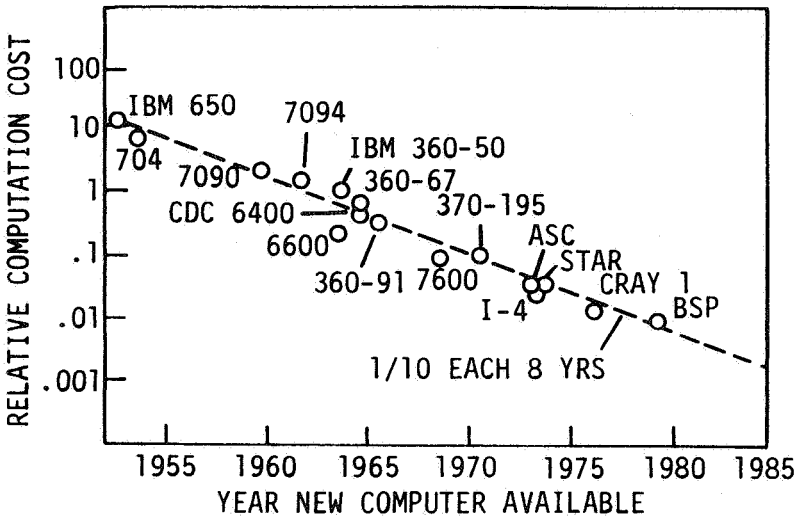

Figure 1. Trend of relative computation cost for a given flow and algorithm.

The increasing internal storage capacity is another important trend. Multi-equations turbulence models, LES-models and other new developments necessitates large computers. Large computer capacity will in general make it possible to make predictions of a high quality in complex situations as for example complicated supply arrangements, complicated room geometry or buoyancy driven flow with more plumes.

3. AIRFLOW SIMULATIONS IN ROOMS WITH DIFFERENT VENTILATION SYSTEMS

This chapter will show some results and discuss the potentials of the numerical method. It is divided into mixing ventilation in small rooms, displacement ventilation, and air movement in large areas.

3.1 Mixing ventilation

Figure 2 shows the results for a room with two-dimensional flow and mixing ventilation. The results are typical for the flow in a room with a heat source at the floor simulating e.g. solar radiator. The supply velocity u_o is 2.2 m/s and the velocity in the wall jet decreases to 0.15 m/s in the area where the cold jet leaves the ceiling, and the recirculating flow is accelerated to 0.2 m/s in a larger part of the occupied zone. It is seen that there is a fairly good agreement between

measurements and calculations for the general flow and for the maximum air velocity in the occupied zone.

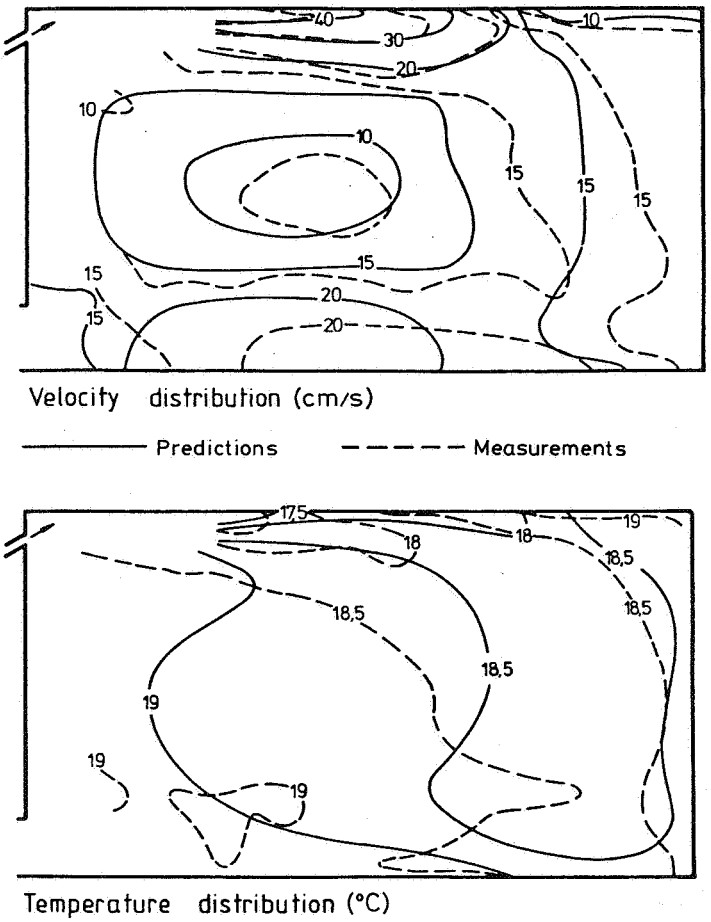

Figure 2. Isovels and isotherms in a room with two-dimensional thermal flow. The tests are made by Hestad[7] and the calculations are made by Nielsen et al.[8]. h/H = 0.003, L/H = 1.9 and Ar = $5.5 \cdot 10^{-4}$.

The air distribution in a small room of simple geometry, as the one shown in figure 2 is well understood, and it is fairly easy to make a full-scale test for the study of velocity and temperature distribution. If other parameters as for example the humidity distribution are to be examined much more complicated measurements are necessary. Schmitz and Renz[9] have studied the airflow and humidity transport in a swimming bath, and it is demonstrated that airflow simulation is an effective means to optimize an air distribution system compared to a large number of full-scale or model scale tests with humidity experiments. This situation is also obvious when

we want to work with parameters as the age distribution and local purging flow rate, quantities which are difficult to measure, but which are interesting in connection with calculation of air exchange efficiency. Davidson and Olsson[10] have shown some numerical predictions of these quantities in a room with mixing ventilation.

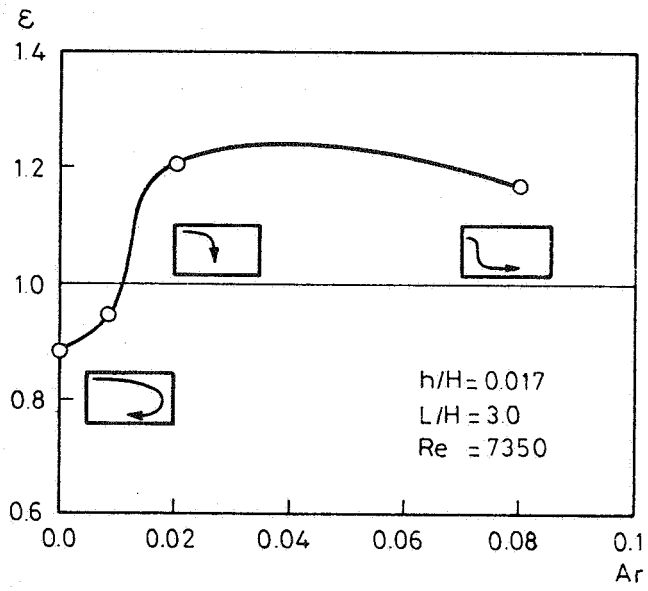

Figure 3. Ventilation efficiency versus Archimedes' number in a room with two-dimensional flow.

Figure 3 shows the ventilation efficiency ε in a room with two-dimensional flow at different Archimedes' numbers Ar. The ventilation efficiency is defined as c_R/c_{OC} where c_R is the concentration in the return opening, and c_{OC} is the mean concentration in the occupied zone. (In this case c_{OC} is the mean value of concentrations at the height 0.35 H above the floor). The contaminant source and heat source are evenly distributed along the floor. The figure shows a high ventilation efficiency in the case when the jet penetrates half of the room length, and this may also be the flow pattern which is optimum for thermal comfort, taking into account that the heat load had to be removed from the room. The results in figure 3 are calculated by airflow simulation, and it is obvious that it would be a time consuming job to perform the necessary concentration measurings although the geometry involved is rather simple.

Chen and Kooi[11] have shown a very interesting combination of airflow simulations in rooms and cooling load calculations for buildings. Cooling load computer programs are normally based on an one-air-point model which means that the values of the whole temperature field in a room are assumed to be uniform, see figure 4. If this model applies to an air-conditioned room with a low ventilation rate or with natural convection or to large industrial halls or theatres it will result in a significant error in the energy comsumption due to the presence of temperature gradients in the room air.

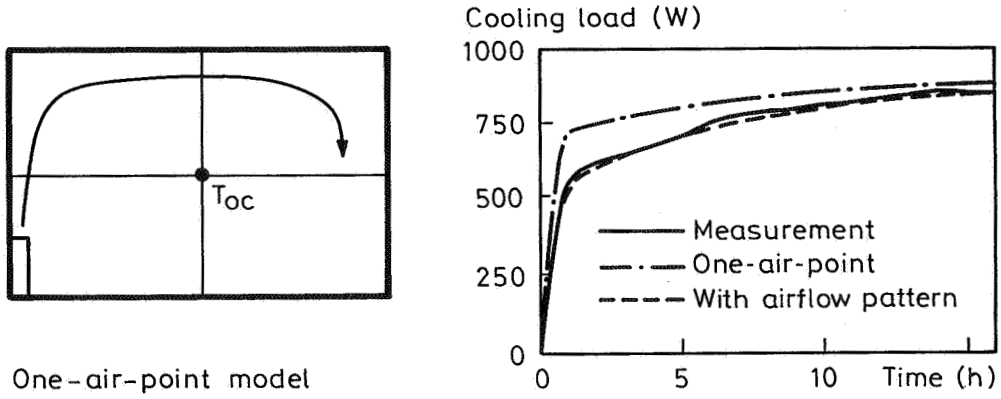

Figure 4. One-air-point model. Time dependent cooling load of a room. Predictions and measurements by Chen and Kooi[11].

Chen and Kooi use results from airflow simulation in the room to correct the cooling load program. It is too expensive to calculate the time-dependent air flow and temperature distribution of a room from an airflow program at each time step in the cooling load program. A data base with velocity distribution for different Archimedes' numbers is precalculated and used at each time step, and it is only necessary to calculate the energy equation to get the correct temperature distribution. Figure 4 shows the measured and the calculated cooling load in a room where 950 W is applied as a step function. The cooling load is obtained from flow rate and temperature difference between return and supply. An one-air-point model does not take account of the vertical temperature gradient and thus the excessive heat transferred into the ceiling, while a cooling load model with airflow pattern is able to handle this effect and results are in this case in good agreement with measurements.

3.2 Displacement ventilation

Figure 5 shows the principle in displacement flow. The air is supplied directly into the occupied zone at low velocity from a wall mounted diffuser. The plume from the heat source creates a natural convective flow upward in the room and a stratification takes place at a height where the plume entrains an airflow equivalent to the supply flow.

The displacement flow systems have two advantages compared with traditional mixing systems. It is possible to remove exhaust air from the room where the temperature is several degrees above the temperature in the occupied zone, and the vertical temperature gradient implies that fresh air and contaminant air are separated, the fresh air being located in the occupied zone.

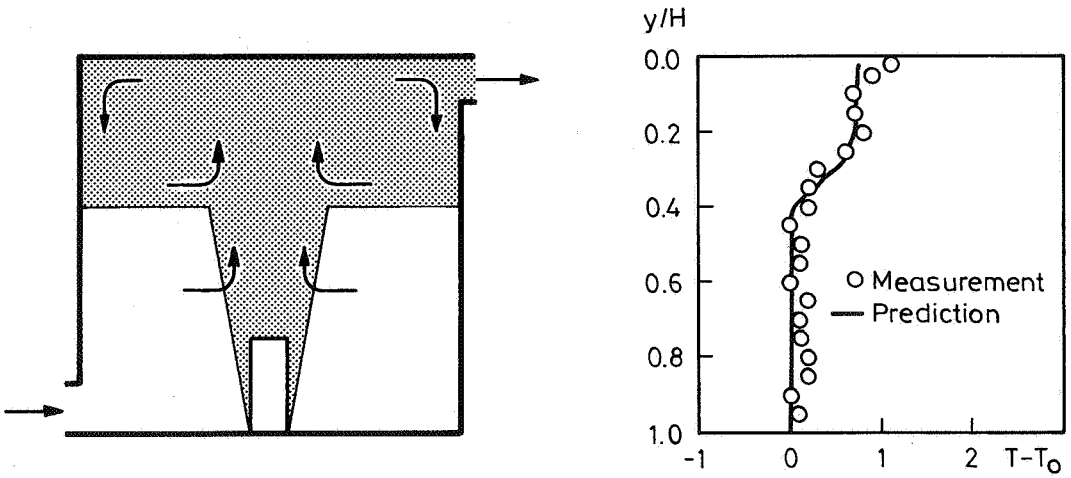

Figure 5. Flow in a room with displacement ventilation and vertical temperature gradient. Predictions are made by Davidson[2] and measurements by Sandberg[12].

The vertical temperature distribution in figure 5 shows the predicted values by Davidson[2]. The comparisons with measured values in a water model show good agreement with respect to temperature distribution and height of the stratification level. As pointed out by Davidson thermal radiation plays an important role in displacement ventilation, and for example Nielsen et al.[13] have shown that the floor temperature is often close to $T - T_o \sim 0.4\ (T_R - T_o)$ instead of $T - T_o \sim 0$ measured and predicted in a water model without radiation (T_o and T_R are supply and return temperature, respectively).

This increase in floor temperature is due to thermal radiation from the ceiling. Some predictions of displacement flow made by Chen[5] take account of radiation by calculating the temperature distribution at surfaces from a cooling load program.

The buoyancy driven flow in displacement ventilation involves elements which could be described by parabolic flow equations. The flow in the plume and cold downdraught are examples, and it might be possible to handle these areas separately using a box method, a prescribed velocity method or direct calculation in the same way as described by Nielsen[14] for the representation of boundary conditions at supply openings.

3.3 Airflow simulation in large areas

Experiments in large areas with complicated geometry can only be made as model experiments. It is also difficult to use the simplified design procedures which can be applied to small rooms as e.g. the room shown in figure 2. Airflow simulation is therefore an alternative possibility and some examples will be discussed in the following.

Figure 6 shows some predictions made by Ehle and Scholz[15]. The experiments were made in a large theatre and the streaklines shown in the upper figure were visualized by smoke. Heat load was simulated by a high number of 60 W light bulbs at the chairs and the volume flow to the main part of the theatre was 67,400 m^3/h.

The experiments show that the flow in the left-hand side of the theatre was rather independent of the main flow pattern and the area was omitted in the numerical predictions. Figure 6 shows good agreement between measurements and predictions, and it is further shown by Ehle and Scholz that there is good agreement between measured and calculated velocities in the occupied zone as well as measured and calculated temperature distribution in the room. The calculations are made as two-dimensional flow.

Waters[16] has worked with airflow simulation for a 13 storey high atrium in Lloyds building in London. The roof and the south elevation of the atrium from seventh to twelfth gallery are completely glazed and in contact with the outside environment. The simulation of cold downdraught on a winter day shows velocities up to 1 m/s at higher levels, but it is destroyed at low level in the atrium by the effect of heat transfer and conditioned air from the offices around the atrium. The downdraught does not disturb the three lower galleries and the ground

floor which are directly open to the atrium. The measured air movement pattern corresponds to the predictions showing that airflow simulation can be used also in a case with buoyancy driven flow and larger dimensions.

Different examples of the use of airflow simulation in rooms are reviewed by Whittle[17].

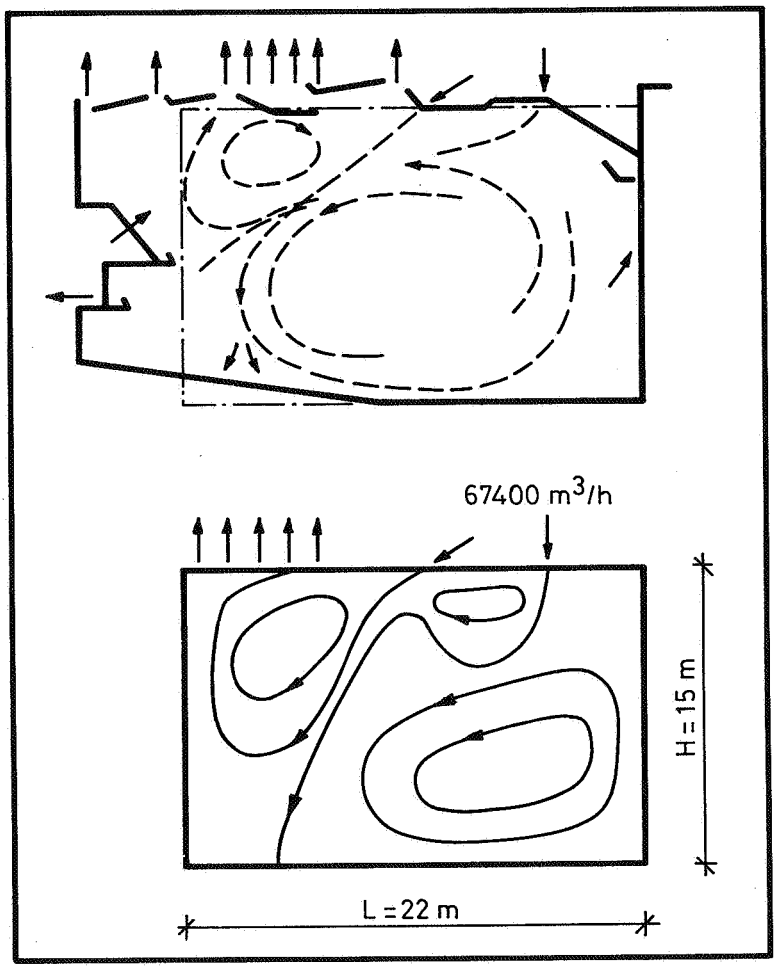

Figure 6. The upper figure shows the flow in a large theatre and the dotted line indicates the area of the flow which is subject to airflow simulation. The lower figure shows the calculated streamline pattern made by Ehle and Scholz[15].

4. DEVELOPMENTS IN THE NUMERICAL METHOD FOR AIRFLOW SIMULATION IN ROOMS

This section will deal with some developments in the numerical method which will make airflow simulation

applicable in practice. An improved handling of boundary values such as air terminal devices, handling of low-turbulence effect and large eddy simulations will be mentioned. Other developments and trends in airflow simulation in rooms, as for example influence from furniture and people and representation of the comfort level are discussed by Nielsen[18].

4.1 Representation of boundary conditions at supply openings

An air terminal device is represented by velocity and temperature profiles as well as profiles for turbulent kinetic energy k and dissipation of turbulent kinetic energy ϵ. The velocity distribution close to a diffuser can be very complicated with variations in level as well as direction, and therefore, it will be difficult to measure in detail. Some ceiling mounted diffusers even have areas with return flow for induction inside the diffuser which is a further complication, and it is especially difficult to obtain the distribution of k and ϵ close to the diffuser. The flow from the diffuser will develop into a free jet or a wall jet in the room. It is therefore practical to move the boundary values a short distance from the opening and give them in the form of normalized free jet or normalized wall jet profiles. The procedure will reduce the necessary measurements on the diffuser and it will also save grid points and computation time. Different methods such as the box method and the prescribed velocity method are given by Nielsen[14].

4.2 Turbulence models

Airflow simulation is normally based on the averaged momentum equations, the continuity equation and the energy equation. The averaged momentum equations contain Reynolds stress terms which are modelled by the eddy viscosity concept. The eddy viscosity is further predicted from a k - ϵ turbulence model consisting of two transport equations for turbulent kinetic energy k and dissipation of turbulent kinetic energy ϵ. The object of the k and ϵ equations is rather to close the equation system, so it is possible to predict for example the mean velocity distribution, than to give a prediction of the turbulence.

Fanger et al.[19] have shown that the thermal comfort is influenced by turbulence. The turbulence is given as a single-directional turbulence intensity by the expression $\sqrt{\overline{u'^2}}/u$, when u is the mean velocity and u' is an instantaneous deviation from the mean velocity. It is difficult to compare results from the k and ϵ calculations with the measured turbulence intensity and it is therefore difficult to predict the influence of turbulence

on thermal comfort.

A rough comparison between predicted and measured turbulence can be made in mixing ventilation where the recirculating flow is rather similar to a wall jet. The normal stresses $\overline{v'^2}$ and $\overline{w'^2}$ in a two-dimensional wall jet are more or less equivalent to 0.6 $\overline{u'^2}$ and 0.8 $\overline{u'^2}$ as shown by Nelson[20]. This means that $\sqrt{k} \sim 1.1\ \sqrt{\overline{u'^2}}$, and figure 7 show measurements and predictions of $\sqrt{\overline{u'^2}}$ and $\sqrt{k}$, respectively, made by Nielsen[21] which confirms this connection.

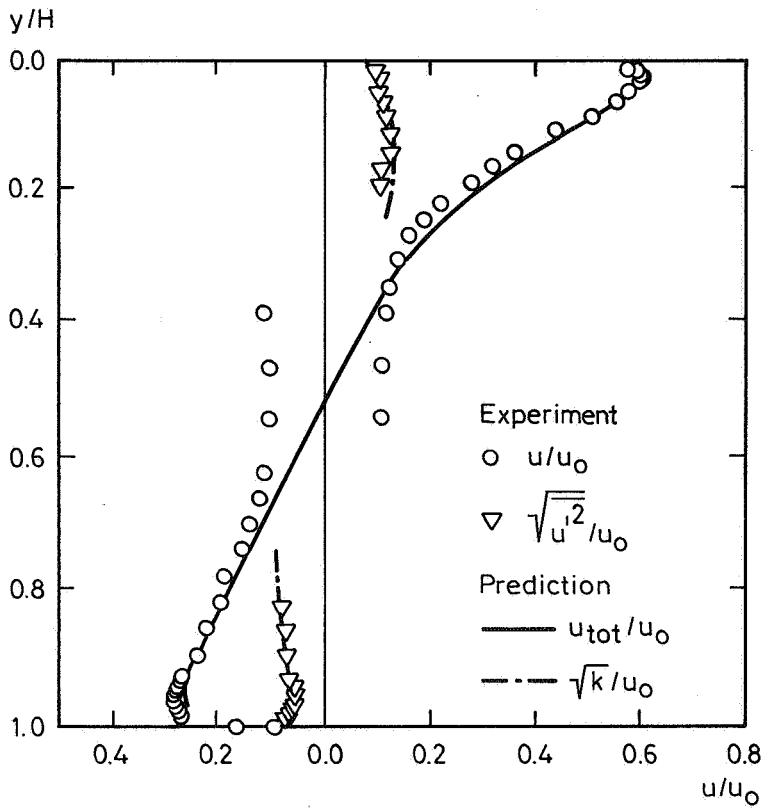

Figure 7. Predicted and measured velocity and turbulence profiles in a room with mixing ventilation. h/H = 0.056, and L/H = 3.0.

It is interesting to note in figure 7 that it is impossible to measure the velocity in a large inner area of the room with hot wire anemometry, and only airflow simulation can show the mean velocity in that area.

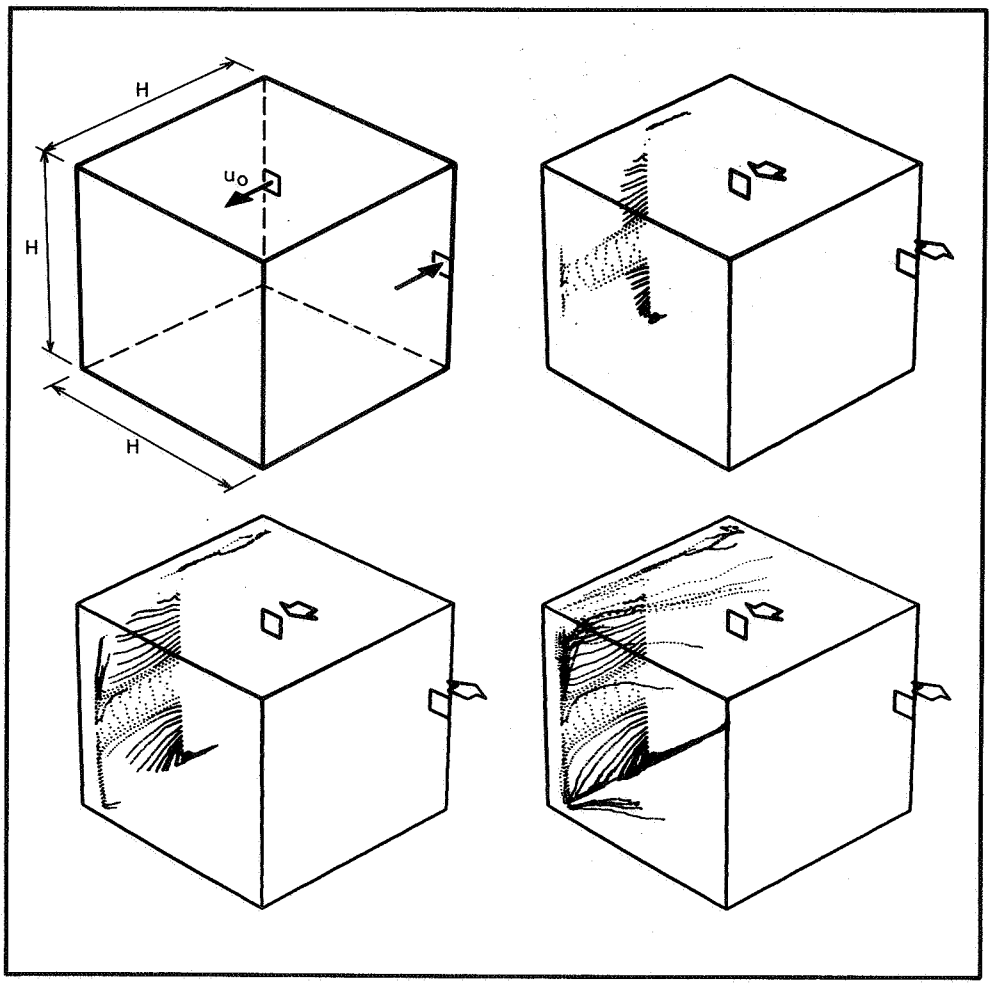

Figure 8. Geometry of a room and three-dimensional streaklines from a vertical line source at three different time steps, $\Delta t^* = 10$, 20 and 50. The calculation and the computer graphic are made by Murakami[22].

Numerical prediction of airflow can also be performed by Large Eddy Simulation (LES). The LES method is based on Navier-Stokes equations, the continuity equation and the energy equation, all filtered with respect to grid space, but not with respect to time. The equation system is closed by an expression for subgrid scale (SGS) Reynolds stresses. The turbulence is represented as the time dependent solution of this equation system, and it is important that the grid spacing is fine enough to allow a description of the energy containing eddies. If mean flow quantities have to be predicted, transient calculation must be conducted over a time which is sufficient to obtain the average values. It is obvious that

output from predictions made by the LES method contains much information, and it is possible to predict the parameters in turbulence which can also be measured, as for example $\sqrt{\overline{u'^2}}$.

The high contents of information in the output makes flow analysis possible in a room by means of computer graphics. Murakami[22] has shown this with streaklines, timelines and high-speed animation of turbulent flow field. Figure 8 shows an example of some computer graphics for the flow in a room. Streaklines are produced from a vertical line source in front of the supply opening, and each time step shows the development in the lines. Δt^* is the time from the start, non-dimensionalized by H and u_o.

4.3 Low-turbulent flow

Turbulence models used for the present calculations assume a fully developed turbulence and, consequently, a self-similar flow that is independent of the Reynolds number (a slight influence from the wall functions is disregarded). This indicates that an air velocity at a given point is proportional with the air change rate in the case of isothermal flow.

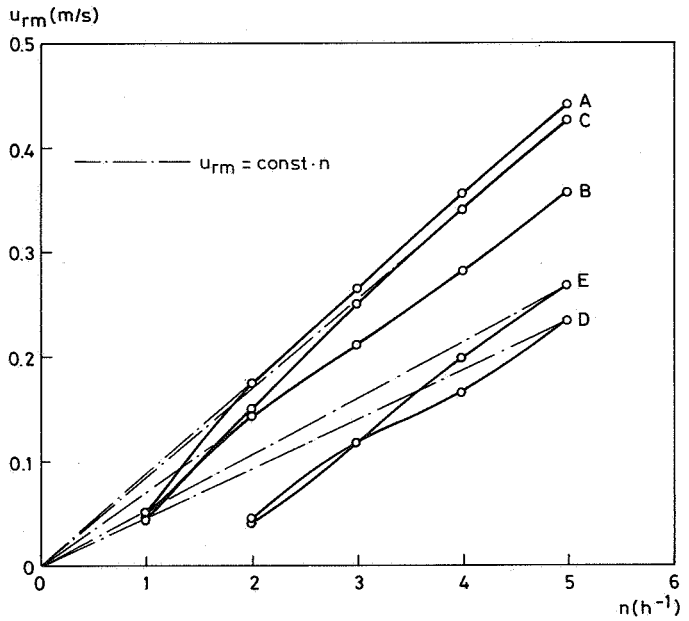

Figure 9. Maximum velocity in the occupied zone as a function of the air change rate n. The tests were performed for five different air terminal devices (A to D).

Figure 9 shows the maximum air velocity in the occupied zone u_{rm} as a function of the air change rate n for five different air terminal devices measured by Heiselberg and Nielsen[23]. The different air terminal devices are of the following types

A. Nozzle

B. Grille

C. Grille with blades adjusted for high diffusion

D. Wall mounted diffuser

E. Ceiling mounted diffuser

It is seen from figure 9 that u_{rm} is proportional with the air change rate n at high airflow rates while there are deviations at low airflow rates. Figure 9 also shows that the low airflow rates have practical relevance (u_{rm} ~ 0.1 - 0.15 m/s). It is evident that there are some low-turbulent effect in this situation, which is especially noticeable for air terminal devices D and E. Part of the low-turbulent effect will be found in the air terminal device and therefore, it can be included in the boundary values of an air terminal device if it has been measured in advance. However, there is still a need for a turbulence model capable of treating flow conditions that do not have a fully developed turbulence level, as shown by Nielsen[18].

5. CONCLUSIONS

Airflow simulation i rooms has taken place as research projects for some years. The development of computation cost indicates an increased use of airflow simulation in practice in the coming years.

Air velocity and temperature distribution in a room are important for the evaluation of thermal comfort, and they are main variables in the prediction method as well as in full-scale experiments. The prediction method can be used to get information of variables which are rather difficult to measure, such as contaminant and humidity distribution, local age and purging flow rate, heat transfer coefficients, etc. and this may be an important use of airflow simulation in the future.

Airflow simulation has been successfully used for the prediction of flow in mixing ventilation for some years, and new results indicate that the method will also be useful for the prediction of flow in displacement ventilation and flow in radiator heated rooms.

Airflow simulation in large areas as for example thea-

atres, atriums and covered shopping centres is an important application, especially because model scale experiments or experience from other projects are the only possibility present.

Development work is necessary to give a practical description of air terminal devices, and it may be necessary to develop a turbulence model which deals with low-turbulent flow in the case of low flow rates in the room.

6. REFERENCES

1. NIELSEN, P.V.
"Berechnung der Luftbewegung in einem zwangsbelüfteten Raum"
Gesundheits-Ingenieur, 94, no. 10, 1973

2. DAVIDSON, L.
"Numerical Simulation of Turbulent Flow in Ventilated Rooms"
Ph.D.-thesis, Chalmers University of Technology, Sweden, 1989

3. RHEINLÄNDER, J.
"Numerische Berechnung von vorwiegend durch die Schwerkraft angetriebenen Raumströmungen"
Forschr.-Ber. VDI-Z, Reihe 7, no. 60, 1981, ISSN 0341-1753

4. LÄRKFELDT, B.
"Full-Scale Tests for Determining Air Movements and Temperature Distributions"
Room Vent 87, International conference on air distribution in ventilated spaces, Stockholm, 1987

5. CHEN, Q.
"Indoor Airflow, Air Quality and Energy Consumption of Buildings"
Ph.D.-thesis, Delft University of Technology, The Netherlands, 1989

6. CHAPMAN, D.R.
"Computational Aerodynamics Development and Outlook"
AIAA J., vol. 17, pp 1293-1313, 1979

7. HESTAD, T.
Private communication
Farex Fabrikker A/S, Norway, 1974

8. NIELSEN, P.V., and RESTIVO, A. and WHITELAW, J.H.
"Buoyancy-Affected Flows in Ventilated Rooms"
Numerical Heat Transfer, vol. 2, 1979

9. SCHMITZ, R.M. and RENZ, U.
"Berechnung Turbulenter Raumluftströmungen bei Gekoppeltem Impuls-, Wärme und Stoffaustausch"
Clima 2000, World Congress on Heating, Ventilating and Air-Conditioning, Copenhagen, 1985

10. DAVIDSON, L. and OLSSON, E.
"Calculation of Age and Local Purging Flow Rate in Rooms"
Building and Environment, vol. 22, no. 2, pp 111-127, 1987

11. CHEN, Q. and KOOI, J.
"ACCURACY - a Program for Combined Problems of Energy Analysis, Indoor Airflow, and Air Quality"
ASHRAE Transactions, vol. 94, part 2, pp 196 - 214, 1988

12. SANDBERG, M.
Private communication (in reference 2)
National Swedish Institute for Building Research, Gävle, Sweden, 1988

13. NIELSEN, P.V., HOFF, L. and PEDERSEN, L.G.
"Displacement Ventilation by Different Types of Diffusers"
9th AIVC Conference on Effective Ventilation, Gent, Belgium, 1988

14. NIELSEN, P.V.
"Representation of Boundary Conditions at Supply Openings"
Internal report for IEA Annex 20, University of Aalborg, 1988, ISSN 0902-7513 R8902

15. EHLE, A. and SCHOLZ, R.
"Beispiele für die numerische Berechnung von zweidimensionalen Geschwindigkeits - und Temperaturfeldern in Räumen"
Luft- und Kältetechnik, no. 4, pp 192 - 194, 1984

16. WATERS, R.
"Prediction of the Environment Inside a 13 Storey Atrium"
Air Conditioning: Impact on the Build Environment, edited by A.F.C. Sherratt, Hutchinson, 1987

17. WHITTLE, G.E.
"Computation of Air Movement and Convective Heat Transfer Within Buildings"
Int. Journal of Ambient Energy, vol. 7, no. 3, pp 151 - 164, 1986

18. NIELSEN, P.V.
"Numerical Prediction of Air Distribution in Rooms - Status and Potentials"
Internal report for IEA Annex 20, University of Aalborg, 1988, ISSN 0902-7513 R8823

19. FANGER, P.O., MELIKOV, A.K., HANZAWA, H. and RING, J.
"Air Turbulence and Sensation of Draught"
Energy and Buildings, 12, 1988

20. NELSON, J.L.
"An Experimental Investigation of the Turbulent and Mean Flow Properties of a Plane Two-Dimensional Turbulent Wall Jet"
Dissertation, University of Tennessee, Dep. of Chem. Eng., 1969

21. NIELSEN, P.V.
"flow in Air Conditioned Rooms"
(English translation of Ph.D.-thesis from the technical University of Denmark, 1974) Danfoss A/S, 1976

22. MURAKAMI, S.
"Visualization of Turbulent Flowfield Generated by Numerical Simulation"
Proc. Int. Symposium on Refined Flow Modelling and Turbulence Measurements, Tokyo, 1988

23. HEISELBERG, P. and NIELSEN, P.V.
"The Contaminant Distribution in a Ventilated Room with Different Air Terminal Devices"
Room Vent 87, International conference on air distribution in ventilated spaces, Stockholm, 1987.

Discussion

Paper 10

R. Mokhtarzadeh (Brunel University, UK)

Most calculations presented here or published describe flows in empty rooms. What are the effects of obstructions/obstacles (e.g. furniture) on the calculations, and how can they be accounted for?

P.V. Nielsen (University of Aalborg, Denmark)

Some measurements on flow in rooms with furniture and people are shown in reference (18) in the paper. Furniture may both give a slight increase and a slight decrease of the velocity level in the occupied zone. It might be possible to do some predictions with additional therms in the floor equations, in the occupied zone, as shown in: Scholz, R. and Hanel, B., Compütorgestütze Berechnung der Raumluftströmung, Rühe Luft- und Kältetechnik, VEB Verlag Technik, Berlin, 1988.

B. Fleury (ENTPE LASH, France)

What are the priorities for you?

- developing a computer graphics package to visualize 3D dynamic flow in buildings for an extensive use of existing detailed air flow models.
- developing existing or new models of turbulence leveling to building air flow configuration?

P.V. Nielsen (University of Aalborg, Denmark)

I think both areas are important but the development of computer graphics do take place in the coming years. The development of a model for low-turbulent flow is very important for airflow simulation in rooms.

PROGRESS AND TRENDS IN AIR INFILTRATION
AND VENTILATION RESEARCH
10th AIVC Conference, Dipoli, Finland
25-28 September, 1989

Paper 11

COUPLED AIR FLOW AND HEAT CONDUCTION MODEL FOR MECHANICALLY VENTILATED FOUNDATIONS

Carl-Eric Hagentoft and Lars-Erik Harderup

Department of Building Technology,
Lund Institute of Technology
Box 118, S-221 00 Lund
Sweden

1. SYNOPSIS

Rising moisture from the ground has caused quite a lot of damage on foundations of Swedish buildings. It is in some constructions possible to prevent this by mechanical ventilation below the floor or below the concrete slab.

This paper will present a model for coupled air flow and heat conduction for mechanically ventilated foundations.

The presented model uses analytical expressions for the air flow in an air-permeable layer below a rectangular building. Analytical double-periodic functions of elliptic type are used.

The ground temperature is simulated by using a time-dependent finite difference method.

2. LIST OF SYMBOLS

h=height of air gap under the floor, m
L=length of building, m
B=width of building, m
K_+=conductance between the ventilated layer and the indoor air, W/m^2 °C
K_-=conductance between the ventilated layer and the ground surface, W/m^2 °C
$\vec{q}_a$= air flow rate, m$_a^3$/m^{2}s (m$_a^3$=m^3 of air)
Q_a= total air flow through a ventilation pipe, m$_a^3$/s
r= radius, m
$\hat{r}$= unit vector pointing in the radial direction
T_a=air temperature in the foundation, °C
T_0=annual average outdoor air temperature, °C
T_+=indoor temperature or temperature above the floor, °C
T_-=ground temperature immediately below the ventilated layer, °C
x=horizontal coordinate, m
y=horizontal coordinate, m
z=complex plane, (x+iy)
Φ=potential function for one or more air point sources in an infinite media, m^2/s
Φ^0=basic potential function from an air point source in an infinite media, m^2/s
Φ_c=complex-valued potential function for one or more air point sources in an infinite media, m^2/s
Φ_c^0=complex-valued basic potential function for an air point source in an infinite media, m^2/s
λ=thermal conductivity of the ground, W/m°C
$\rho_a c_a$=volumetric heat capacity of the air, J/m^3 °C
ϑ_1=Theta function

3. INTRODUCTION

Moisture coming from the ground is a serious problem for some types of Swedish foundations, especially slab on the ground built in the 1970th and at the beginning of the 80's. These houses were often built with the thermal insulation above the concrete slab and without any vapour barrier in the foundation. In another type of slab on the ground the thermal insulation layer is made of a lightweight expanded clay aggregate, placed below the concrete. Unfortunately this layer did not prevent capillary rising water from penetrating into the concrete slab.

If we can prevent the moisture supply from the ground to penetrate the concrete slab or remove the moisture directly above the concrete, and thereby prevent contact between water and organic material in the foundation, the construction will dry out and mould growth and odours will diminish.

One way to remove the moisture supply from the ground is by mechanical ventilation of the foundation, see Figure 1. By such methods the moisture will be transported out from the foundation by the moving air, as long as the air is unsaturated. These methods requires that there is an air-permeable layer below the concrete slab. In a joist floor construction it is often possible, and cheaper, to ventilate above the concrete slab in the floor construction.

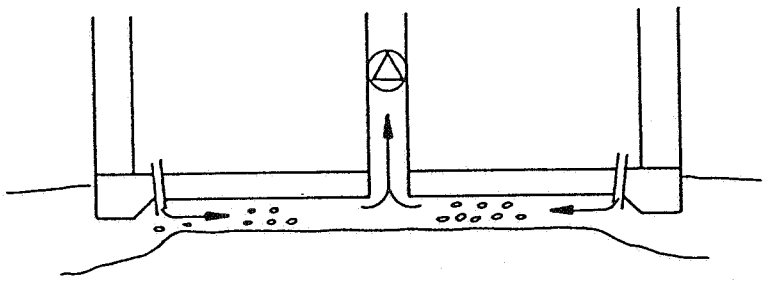

Figure 1: Mechanical ventilation of the foundation

If these methods are going to be successful, certain general conditions must be fulfilled: There has to be a horizontal air gap or an air permeable layer in the construction. The air that is sucked, or pumped into the layer, has to be relatively dry and have a high temperature in order to reduce the risk for condensation. All unventilated connections between the ground and other parts of the building must be as air tight as possible in order to prevent unwanted air leakage.

Because of the condensation risk, it is of great importance to know the temperatures in the ventilated layer, so that condensation can be avoided by using an appropriate air flow intensity.

With the model presented in this paper it is possible to study foundations with two-dimensional air flow coupled to a three-dimensional temperature field below and around the building. The air flow is given by elliptic, complex-valued, double-periodic functions. The three-dimensional temperature field and the energy balance for the air channels are solved by a computer program for time-variable heat conduction based on an explicit finite forward difference method. With this coupled model between air flow and temperature we obtain the temperature distribution below a rectangular building at different depths. The model makes it also possible to investigate how thickness of the thermal insulation, extra insulation outside the outer wall corners, air flow intensity, climate and size of the building influences the temperature distribution in the foundation and in the ground. It is also possible to investigate how positions of the air inlet and air outlet to the vertical rectangular area below a building influence the temperature distribution in the foundation. Figure 2 illustrates two different solutions for a quadratic building. Air inlets, i.e. points where the air are going down into the foundation, are marked $\star$, while air outlets, i.e. points with air leaving from the foundation are marked $\bullet$. In the first case three of the walls are open to air flow. At the middle of the fourth wall, which is closed (air tight), there is an air outlet. In the second case we have a centrally placed air outlet in the building with air inlets near each corner.

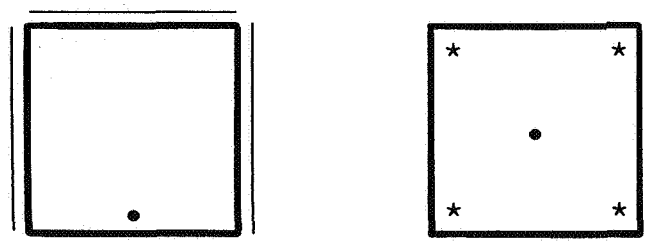

Figure 2: Two different cases for mechanical ventilation of the foundation of a building

These two cases and a third reference case without ventilation of the foundation will be discussed further in Section 6.

Further information about mechanical ventilation of concrete slabs on the ground damaged by moisture, is going to be published in a thesis later this year, by Harderup. General information about repairing methods for concrete slabs on the ground damaged by moisture can be found in Harderup[2,4] and Tobin[6].

4. CALCULATION OF THE AIR FLOW PATTERN

For the considered foundations we will assume that we have an air gap,or a porous layer, of constant height h and constant permeability for flow resistance. The width of the ventilation pipes are assumed to be much smaller than the dimensions of the building. Air inlets to the foundation will be approximated by point sources.

4.1 Radial air flow in an infinite medium

The air flow rate induced by a single air point source in a layer of infinite extension will be studied first. This will give a basic solution that will be used below. Consider an air source located at the origin of coordinates and with the total air flow rate Q_a (m_a^3/s). At the distance r (m) from the center of the air source we get the following air flow rate:

$$\vec{q}_a(r) = \frac{Q_a}{2\pi r}\frac{1}{h}\hat{r} \tag{1}$$

Using the relation

$$\frac{\hat{r}}{r} = \nabla \ln(r), \tag{2}$$

we can write (1) as:

$$\vec{q}_a(r) = \frac{Q_a}{2\pi h}\nabla \ln(r) = \nabla\left\{\frac{Q_a}{2\pi h}\ln(r)\right\} \tag{3}$$

The function in the bracket can be treated as a potential. We introduce the potential of a single air point source in an infinite region:

$$\Phi^0 = \frac{Q_a}{2\pi h}\ln(r) \tag{4}$$

The air flow $\vec{q}_a$ must satisfy the mass balance equation. Using (3) we have:

$$\nabla \cdot \vec{q}_a = 0 \quad \Rightarrow \quad \nabla^2\Phi^0(r) = 0 \qquad r \neq 0 \tag{5}$$

Here $\nabla\cdot$ denotes the divergence operator and ∇^2 denotes the Laplace operator. This Laplace equation for Φ^0 is the same as for steady-state heat transfer problems and electrostatic problems. All results from potential theory are thereby applicable.

4.2 Superpositions of air point sources

For the case with a number of air point sources and sinks located at different places, superposition can be used.

Consider an air point source located at the position (x_n, y_n). The air flow rate at the point (x, y) due to this source becomes:

$$\vec{q}_{a,n}(r) = \nabla\Phi^0(r_n)$$

$$\Phi^0(r_n) = \frac{Q_{a,n}}{2\pi h}\nabla \ln(r_n) \qquad r_n = \sqrt{(x-x_n)^2 + (y-y_n)^2} \tag{6}$$

Here r_n is the distance between the air source and the point (x, y), and $\vec{q}_{a,n}$ is the heat flow rate at the point due to air source number n.

The total air flow rate $\vec{q}_a$ becomes:

$$\vec{q}_a = \sum_{n=1}^{N} \vec{q}_{a,n} = \nabla \left\{ \sum_{n=1}^{N} \Phi^0(r_n) \right\} \tag{7}$$

The foundations we are interested in are of course of finite extension. However, by the use of superposition and the method of images, it is possible to obtain solutions for our cases.

Figure 3 shows the simple case with the superposition of two air point sources of the same air flow rate. Due to the symmetry around the vertical line we obtain a boundary of zero air flow rate.

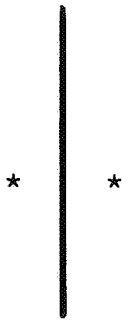

Figure 3: Superposition of two air point sources in order to create a vertical boundary line of zero air flow rate.

To obtain the same result for a rectangular boundary we have to superimpose an infinite number of air point source images of equal air flow rate. Consider the case with a source at the coordinates (x_0, y_0) inside a rectangle with the length L and width B, see Figure 4.

The total potential Φ for the rectangular case with air tight boundaries become:

$$\Phi = \sum_{m=-\infty}^{+\infty} \sum_{n=-\infty}^{+\infty} \Phi^0(r_{1mn}) + \Phi^0(r_{2mn}) + \Phi^0(r_{3mn}) + \Phi^0(r_{4mn}) \tag{8}$$

$$r_{1mn} = \sqrt{(x - (x_0 + m \cdot 2L))^2 + (y - (y_0 + n \cdot 2B))^2}$$

$$r_{2mn} = \sqrt{(x - (x_0 + m \cdot 2L))^2 + (y - (2B - y_0 + n \cdot 2B))^2}$$

$$r_{3mn} = \sqrt{(x - (2L - x_0 + m \cdot 2L))^2 + (y - (2B - y_0 + n \cdot 2B))^2}$$

$$r_{4mn} = \sqrt{(x - (2L - x_0 + m \cdot 2L))^2 + (y - (y_0 + n \cdot 2B))^2}$$

For this case we have used sources only. For the cases of physical interest we must have a balanced ventilation, that is the net air flow rate into the foundation must be equal to zero. It should be noted that expression (8) is divergent.

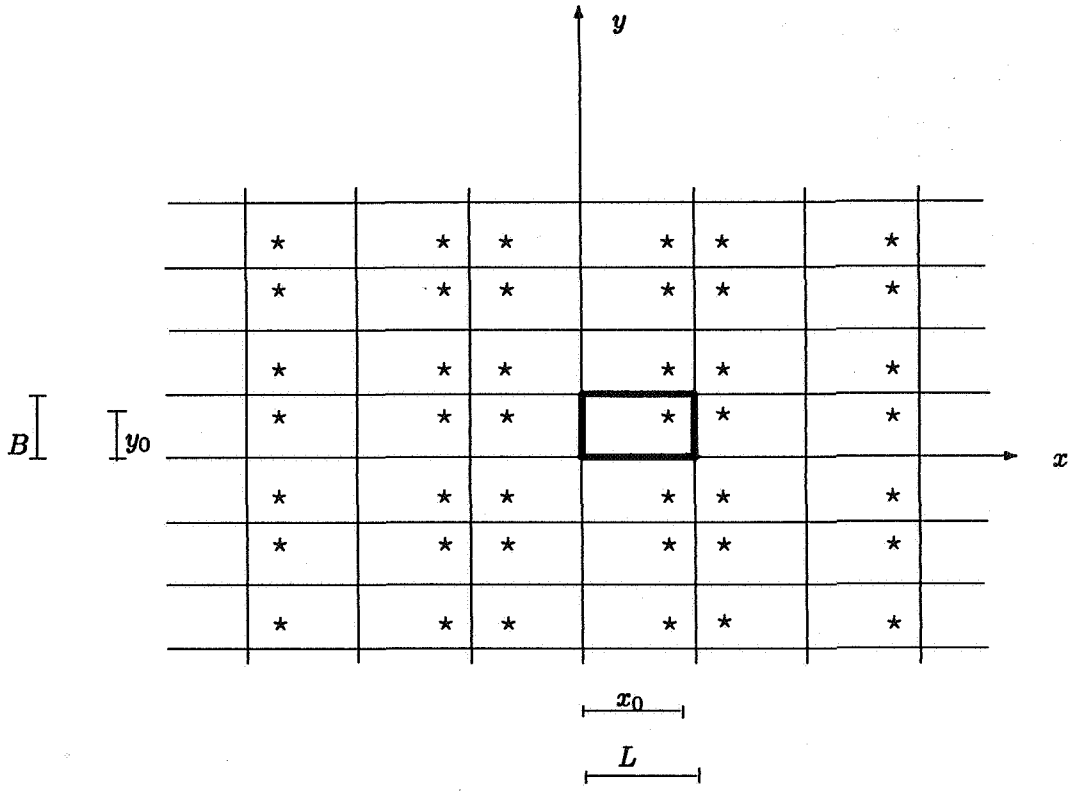

Figure 4: Superposition of an infinite array of point sources in order to obtain zero air flow rate at the rectangular boundary.

The sum of (8) and a corresponding expression for balancing sinks will together converge properly.

Cases with open boundaries, that is boundaries with a constant potential, may also be treated by superposition technique. For these cases it is not necessary to have balanced ventilation, since the net positive air flow rate will flow out through the boundaries. However, the theory for cases with open boundaries will not be dealt with in this paper.

4.3 Complex-valued formulation of the potential functions. Introduction of the theta function

The basic potential function Φ^0 (4) can be expressed as the real part of a complex-valued analytical function:

$$\Phi_c^0(z) = \frac{Q_a}{2\pi h} \ln(z) \qquad z = x + i \cdot y \tag{9}$$

Here we have used the notation c to mark that the function is complex-valued. Formula (8) then becomes:

$$\Phi_c = \sum_{m=-\infty}^{+\infty} \sum_{n=-\infty}^{+\infty} \Phi_c^0(z - z_{1mn}) + \Phi_c^0(z - z_{2mn}) + \Phi_c^0(z - z_{3mn}) + \Phi_c^0(z - z_{4mn})$$

$$\begin{aligned} z_{1mn} &= (x_0 + m \cdot 2L) + i(y_0 + n \cdot 2B) \\ z_{2mn} &= (x_0 + m \cdot 2L) + i(2B - y_0 + n \cdot 2B) \\ z_{3mn} &= (2L - x_0 + m \cdot 2L) + i(2B - y_0 + n \cdot 2B) \\ z_{4mn} &= (2L - x_0 + m \cdot 2L) + i(y_0 + n \cdot 2B) \end{aligned} \tag{10}$$

Here we have used the notation Φ_c for the total complex-valued potential function.

Double-periodic arrays of sinks and sources, and the associated Theta functions are studied in Oberhettinger,Magnus[5] and Whittaker,Watson[7]. These analytical quasi double-periodic functions of z have very interesting properties. The Theta function ϑ_1 is defined by the series:

$$\vartheta_1(z,\tau) = 2\sum_{n=0}^{+\infty}(-1)^n q^{(n+1/2)^2} \sin((2n+1)\pi z) \qquad q = e^{i\pi\tau} \quad \Im(\tau) > 0 \tag{11}$$

As we can see, the convergence of the series are very rapid. The function has zeroes at the points:

$$z_{zero} = n + m \cdot \tau \qquad m, n \text{ integers} \tag{12}$$

A Taylor series of the logarithm of ϑ_1 around any of these points shows that it tends to zero as:

$$\ln(\vartheta_1(z,\tau)) \to \ln(z - z_{zero}) + \text{constant} \qquad z \to z_{zero} \tag{13}$$

The real part of the logarithm of the Theta function satisfies the potential equation (5) at all points in the plane, since ϑ_1 is an analytical function of z. At the zeroes of the Theta function, the logarithm $\ln(\vartheta_1)$ has the same behaviour as the basic complex-valued potential Φ_c^0 around $z = 0$. Thus the real part of the logarithmic expression gives air sources at all zeroes of ϑ_1 in the plane. It is therefore possible to give a closed expression for Φ_c by using the Theta function.

Figure 5 shows the case with a source and a sink inside a rectangular boarder. The source is located at $x_0 + iy_0$ and the sink at $x_1 + iy_1$. The total potential function becomes:

$$\Phi_c \cdot \frac{2\pi h}{Q_a} = \ln\left\{\frac{\vartheta_1((z - (x_0 + iy_0))/2L)}{\vartheta_1((z - (x_1 + iy_1))/2L)}\right\} + \ln\left\{\frac{\vartheta_1((z - (x_0 + i(2B - y_0)))/2L)}{\vartheta_1((z - (x_1 + i(2B - y_1)))/2L)}\right\} +$$

$$\ln\left\{\frac{\vartheta_1((z - (2L - x_0 + i(2B - y_0)))/2L)}{\vartheta_1((z - (2L - x_1 + i(2B - y_1)))/2L)}\right\} + \ln\left\{\frac{\vartheta_1((z - (2L - x_0 + iy_0))/2L)}{\vartheta_1((z - (2L - x_1 + iy_1))/2L)}\right\}$$

$$\tau = iB/L \tag{14}$$

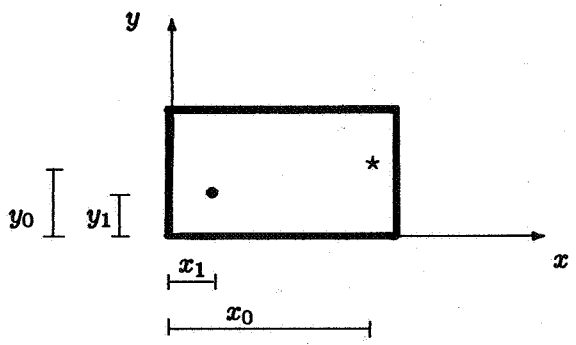

Figure 5: One air point source and one air point sink inside a rectangular boundary of zero air flow rate.

5. COUPLED AIR FLOW AND HEAT TRANSFER FROM THE GROUND

5.1 Balance equation for the air along a stream line

The air flow pattern from the air sources to the sinks is given in Section 4. The air flows in a number of well-defined stream tubes with height h and delimited in the horizontal plane by two stream lines.

Figure 6 shows an air stream tube. The length coordinate along one stream line is denoted by s (m). The width of the stream tube at s is denoted by $b(s)$ (m). The product $q_a \cdot b$ is constant along a stream tube. It gives the air flow rate m_a^3/s in the stream tube. The air temperature is denoted by $T_a(s,t)$. The convective-diffusive heat balance for the air between s and $s+ds$ is:

$$b \cdot ds \cdot K_+(T_+ - T_a) + b \cdot ds \cdot K_-(T_- - T_a) - \rho_a c_a q_a \cdot hb \cdot \frac{\partial T_a}{\partial s} \cdot ds = 0 \quad (15)$$

Here K_+ (W/m^2 °C) is the conductance per unit area, between the indoor temperature T_+ and the air, and K_- the conductance to the center of the first cell in the ground with the temperature T_-. These conductance may be variable along the stream tube. We neglect horizontal heat conduction in the air and the capacity term $(\rho_a c_a \cdot hb \cdot ds \cdot \partial T_a/\partial t)$.

The temperature field in the ground is calculated for time-step after time-step. At each step, equation (15) is solved analytically for every stream tube in the following way. We introduce the average temperature T_m and the length l for the considered section of the stream tube:

$$T_m = \frac{K_+T_+ + K_-T_-}{K_+ + K_-} \quad (16)$$

$$l = \frac{\rho_a c_a q_a hb}{b(K_+ + K_-)} \quad (17)$$

Equation (15) becomes:

$$\frac{\partial T_a}{\partial s} = -\frac{1}{l}(T_a - T_m) \tag{18}$$

For each stream tube we get the same equation as (4) in Harderup,Claesson,-Hagentoft[3]. The stream tube is divided into a number of cells. Cell number i is defined by the area in the stream tube between $s = s_i$ and $s = s_{i+1}$. The quantities l and T_m are piece-wise constant for each cell, $s_i \leq s < s_{i+1}$. The temperature along the stream tube cell becomes:

$$T_a(s,t) = T_{m,i} + (T_a(s_i,t) - T_{m,i})e^{-(s-s_i)/l_i} \tag{19}$$

The air temperature at the air source is given. The outlet temperature becomes the inlet temperature to the next cell, and so on.

When the air temperatures in all air stream tubes are calculated, these will become boundary temperatures for the ground temperature at the next time-step.

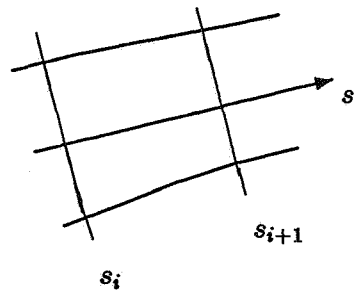

Figure 6: Air stream tube between two stream lines.

In the general case, the stream tube cell is coupled with more than one computational cell in the ground with its rectangular mesh. For this case K_- is the mean conductance between the air and the cells below, and T_- is a weighted ground temperature.

A more detailed treatment of general convective heat flow problems is given in Claesson,Bennet[1].

6. EXAMPLES

The three-dimensional computer program handles time-dependent boundary temperatures and air flows. However, for simplicity we will only show some results from steady-state calculations. All calculations have been performed on an IBM PS/2 386/25 with *87 math co-processer. For the ground we have used a rectangular mesh with 9240 cells. The minimum cell is a cube with the side length 0.2 m. The quadratic building in Figure 2 is used in the calculations.

We have the following data:

$T_+ = 20$ °C	L=10.4 m	$K_+ = 0.6$ W/m^2°C
$T_a(0,t) = 20$ °C	B=10.4 m	$K_- = 4.6$ W/m^2°C
$T_0 = 6.7$ °C	Q_a=100.0 m^3_a/h	$K_w = 0.5$ W/m^2°C
$\lambda = 1.5$ W/m°C		

During the calculations we have constant indoor temperature T_+. The temperature of the air entering into the foundation, $T_a(0,t)$, has the same value as the indoor air. Outside the building the temperature is T_0, which is the annual average outdoor temperature in Stockholm. The dimensions of the building is $L \times B$, and Q_a is the total air flow sucked out from the foundation. Below the outer walls there are thermally insulated foundation walls, with a depth of 0.6 m. The corresponding conductance is denoted K_w. The thermal conductivity for the soil is denoted by λ.

In the example to the right in Figure 7, (A), three of the outer walls are open to air flow from the inside of the building. At the middle of the fourth wall, which is airtight, the air outlet is an exhaust air fan connected to the floor.

In the example to the left, (B), we have a centrally placed exhaust air fan combined with air supply devices (air inlets) at the outer corners. The inlet to the exhaust air fan tube is placed in the ventilated layer below or above the concrete slab. The air supply devices are in direct contact with the indoor air. All connections between the walls and the floor is assumed to be airtight.

A third case, (C), has also been calculated, as a reference. In this case there is no mechanical ventilation of the foundation.

In Figure 7, the streamlines to the exhaust air fan are shown. In the first case, with three open boundaries, the ventilation intensity is poor at the two corners opposite to the airtight wall. For the second case, with air supply devices only at the outer corners, the mid regions near the outer walls are poorly ventilated.

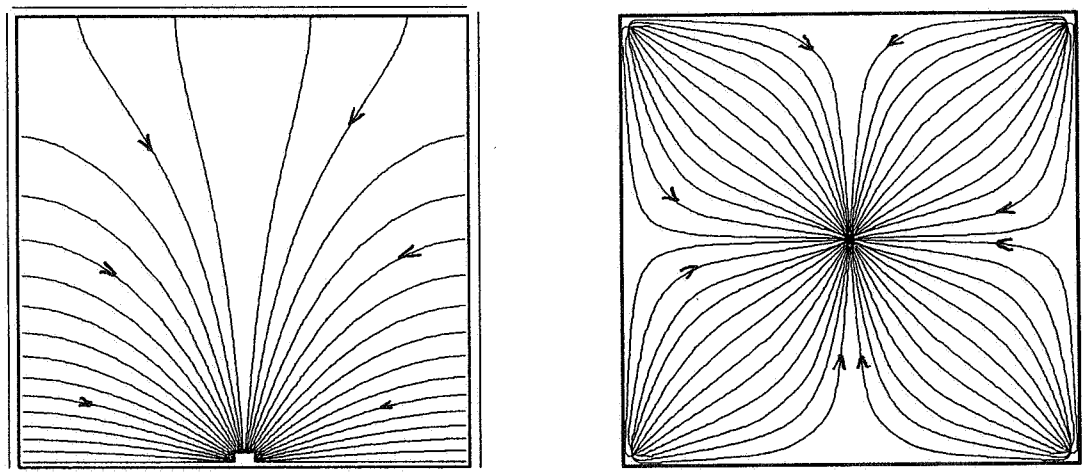

Figure 7: Air stream lines for two types of ventilated foundations. The first building (A), left, has open boundaries at three sides and an exhaust air fan in the middle of the fourth side. The second one (B), right, has air supply devices at the corners and an exhaust air fan in the middle.

Point	Surface temperatures °C		
	Case		
	A	B	C
1	11.9	11.7	11.5
2	10.5	18.1	10.1
3	16.0	11.7	11.5
4	16.9	18.1	10.1
5	13.0	11.7	11.5
6	14.4	14.1	14.2

Table 1: Surface temperatures in six discrete points from steady-state calculations

The influence of the air flow, on the steady state temperature at some discrete points (1-6) is shown in Table 1. These points are marked in Figure 8. The presented values are the temperatures at the surface of a layer immediately below the ventilated horizontal layer.

Low ventilation intensity, near the outer walls, results in small temperature differences between the unventilated case and a ventilated case. From Table 1 it can be seen that the surface temperatures near the outer walls are strongly dependent on how the system is designed. In the undisturbed case (C) without ventilation, the temperature is lowest near the corners. With a ventilation system of type (B), the annual average temperature increased by 8 °C in the corners, points 2 and 4. From the studied cases it can also be seen that the temperature increase, at the middle of the outer walls, is greatest for case (A). It should be noted that temperatures below the center of the building is very stable, see point 6.

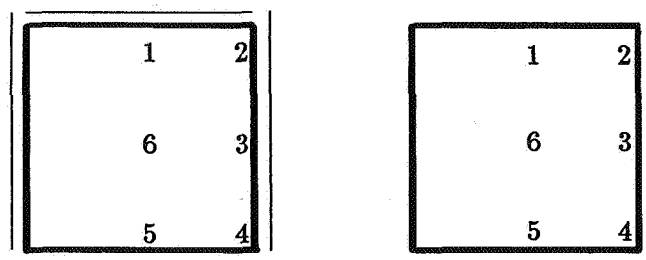

Figure 8: Locations of calculated temperatures given in Table 1.

For a certain building with a certain air flow pattern the surface temperatures can be raised by higher air flow intensity or by thermal insulation in the ground, near the outer walls outside the building.

Before an installation of such a mechanical ventilation system is made, the program can be used to investigate how different locations of the supply air devices and exhaust air devices will influence the temperature at a certain point in the foundation, or immediately outside the building.

7. ACKNOWLEDGEMENTS

This theoretical work has been initiated by Dr. Johan Claesson at the Department of Building Technology in Lund. The computer programming has been carried out by Johan Bennet at the Department of Mathematical Physics in Lund. Their support has been of great value.

The support by the Swedish Council for Building Research is gratefully acknowledged.

8. REFERENCES

1. J. Claesson and J. Bennet. Thermohydraulics of Conformal Groundwater Flow. Departments of Building Technology and Mathematical Physics, Lund. Preliminary version 1987.

2. Fuktgruppens verksamhet 1984-87. Information from the Moisture Research Group in Lund, (Swedish). Departments of Building Technology and Building Science, Lund, 1987:1.

3. Harderup,Claesson and Hagentoft. Prevention of moisture damage by ventilation of the foundation. Contribution to the 8th AIVC Conference, Überlingen, Federal Republic of Germany, September 21-24 1987. The Air Infiltration and Ventilation Centre, Great Britain. Document AIC-PROC-8-87.

4. Harderup. Repairing methods for concrete slabs on the ground damaged by moisture. Contribution to Symposium and Day of Building Physics in Lund, Sweden, August 24-27 1987. Swedish Council for Building Research, D13:1988.

5. F. Oberhettinger und W. Magnus. Anwendung der elliptischen funktionen in physik und technik. Springer-Verlag, 1949.

6. Tobin. Measures against moisture and mould growth in a ground structure. Swedish National Testing Institute. Report 1988:55, (Swedish).

7. Whittaker and Watson. Modern analysis. Cambridge University Press, 1946.

Discussion
Paper 11

Frank D. Heidt (University of Siegen, FRG)

a) Did you consider the effect of evaporating water on air and surface temperatures?
b) There should be an influence due to latent heat transfer.

Carl-Eric Hagentoft (Building Technology, Lund, Sweden)

In the presented model with a two-dimensional air-flow coupled to a three-dimensional temperature field we do not take the effects of evaporating water and latent heat into account. In a similar model with one-dimensional air-flow coupled to a two-dimensional temperature field the effect of evaporating water and latent heat are taken into account. In this model the vapour concentration in the outdoor air, the moisture supply from the ground and the moisture supply to the inside air are accounted for. With this model we can calculate the relative humidity and the temperature along the ventilated layer. All facilities in the model with one-dimensional air flow are going to be incorporated in the other model too.

Mike Holmes (Ove Arup, London, UK)

Temperature predictions require knowledge of heat transfer coefficient. Could you say what values were used for the surface convection coefficient, and if radiant exchange within the cavity was considered to be important?

Carl-Eric Hagentoft (Building Technology, Lund, Sweden)

We assume a constant temperature within the stream tubes and thereby neglect the radiation. The surface resistances are usually small compared with the overall resistance between the air in the stream tube and the ground/indoor temperature. So we have just used standard values if I remember it right.

$1/\alpha$ in the tube is around 0.1 m^2U/m for the examples I have shown.

Alfred Moser (ETH, Switzerland)

For potential flow in a cavity potential lines are not lines of constant pressure in general. (They are in special cases such as radial flow from a single source in infinite space).

Carl-Eric Hagentoft (Building Technology, Lund, Sweden)

In forced convection we neglect the temperature influence on the air flow pattern. We have the following assumption:

$q_a \sim \nabla p$

q_a = *air flow rate*

p = *pressure*

This is the same definition as for our potential discussed in the paper. This means that the pressure will become proportional to the potential function: $p \sim \phi$.

PROGRESS AND TRENDS IN AIR INFILTRATION
AND VENTILATION RESEARCH

10th AIVC Conference, Dipoli, Finland
25-28 September, 1989

Paper 12

MINIMUM VENTILATION RATES TO PREVENT CONDENSATION: A CASE STUDY

C. AGHEMO, C. LOMBARDI, M. MASOERO

Dipartimento di Energetica - Politecnico di Torino
Corso Duca degli Abruzzi 24 - 10129 Torino (Italy)

SYNOPSIS

Moisture and mould in buildings have become fairly common problems in Italy, particularly since regulations aimed at energy conservation have been enforced in the seventies.

Results of a case study conducted within IEA Annex XIV are presented in this paper. Two flats belonging to the same building (one with and the other without moisture problems) have been monitored during the winter 1987-88. Indoor temperature and air humidity, wall surface temperature and weather parameters were recorded for several weeks using two automatic data loggers. Airchange rates were measured using the tracer gas technique.

Processing of the experimental data indicates that the moisture problems in one of the flats are probably due to insufficient airchange rates in a building which presents some noticeable thermal bridges. Differences between the two flats can be attributed primarily to occupants' behaviour (airing habits, retrofits performed on the windows, etc.) and, to a lesser extent, to orientation.

The paper also shows that a good insight on condensation phenomena can be derived from fairly straightforward simplified analyses of temperature and humidity data.

The importance of incorporating guidelines on thermal bridge correction and ventilation strategies into building codes is pointed out.

LIST OF SYMBOLS

D = Indoor water vapour production (kg/h)
h_i = Inside surface heat transfer coefficient (W/m^2K)
N = Airchange rate (1/h)
RH_i = Indoor air relative humidity (%)
RH_e = Outdoor air relative humidity (%)
T_i = Indoor air temperature (°C)
T_e = Outdoor air temperature (°C)
T_s = Inside wall surface temperature (°C)
U = Thermal transmittance of the wall (W/m^2K)
X_i = Indoor humidity ratio (g/kg)
X_e = Outdoor humidity ratio (g/kg)
τ = Temperature factor of the wall (-)

1. INTRODUCTION

During the second half of the past decade, compulsory regulations were introduced in Italy, aimed at promoting energy conservation with regards to space heating, primarily in residential buildings [1].

At that time, the dependence of the Italian energy market on imported oil was extremely high. Oil, in fact, represented almost two thirds of the total primary energy use of the country. Furthermore, a significant percentage of oil consumption was due to space heating, which was the primary consumer within the building sector (accounting, as a whole, for about 30% of global consumption).

Limitation of heating energy consumption, in order to reduce dependence on oil imports, was therefore a high priority goal for the legislator.

The code for energy conservation in space heating, which came into effect in 1977, is based on the following approach. For any new building, as well as for buildings undergoing major renovation work, a maximum permissible *heat loss coefficient* is calculated. Such coefficient is the sum of two terms, one related to envelope thermal losses, the other to air infiltration and ventilation.

In practice, the code poses a limit on the installed power of the heating plant, by setting requirements concerning minimum thermal insulation levels and ventilation strategies. With respect to ventilation, the code makes a distinction between naturally- and mechanically-ventilated buildings:

- For mechanically-ventilated buildings, airchange rates are specified by the designer, but heat recovery is required if the fresh air flow rate, or the number of annual hours of operation of the ventilation system, exceed a threshold value depending on local climate.

- For naturally-ventilated buildings, the code states that the air infiltration heating load must be computed assuming an ACH value which, for residential buildings, is conventionally taken equal to 0.5.

The main limit of such regulation is that no guidelines are specified concerning either envelope airtightness, or provision for mechanical ventilation. Another limit is that minimum insulation levels are specified, but no indication is given on how to avoid thermal bridges.

Changes in construction practice which took place in response to these regulations have often had negative effects on the quality of the internal environment, particularly with respect to condensation and mould growth problems. The occurrence of such problems can be attributed primarily to incorrect thermal insulation solutions, coupled to a lack of ventilation.

In traditional, pre-energy crisis buildings, moisture was usually not a problem because buildings were quite leaky (windows had no weatherstripping) and walls were poorly insulated. Infiltration rates were normally sufficient to prevent condensation, even in the most critical areas of Northern Italy, where winters are fairly cold, humid, and almost windless.

New constructions, on the contrary, were based on different design criteria. The adoption of a national code on air permeability rating of windows [2] allowed the designers to select the appropriate class of window according to building height and windiness of the area. Airtight windows became popular because designers feared that otherwise excessive ventilation heat loads would cause boiler undersizing; however, the absence of controllable air inlets and of effective mechanical ventilation systems was often cause of insufficient airchange rates.

Insulation of walls and roofs was imposed by law, but lack of experience was often the origin of serious thermal bridge problems, particularly in buildings with prefabricated or site-constructed concrete bearing walls.

The final consequence was that moisture problems became very common in new residential buildings, such as the one which is the object of this case study.

2. OBJECT AND GOAL OF THE CASE STUDY

Within the framework of IEA Annex XIV "*Condensation and Energy*", an experimental survey was conducted on a ten-storey, tower-shaped block of flats, owned by Istituto Autonomo Case Popolari (IACP) of Turin [3].

The building, which was constructed in the seventies, is a good example of social housing of the period. Even if its construction is traditional (i.e.: concrete structure, uninsulated masonry cavity walls, metal frame single-glazed windows), moisture and mould growth problems of varying intensity are evident in some of the dwellings, as a consequence of different orientation and occupants' habits.

The floor plan of the building is shown in Fig. 1. In the measurement campaign, attention was concentrated on two flats located at the fifth floor. The two flats are identical in size, but have opposite orientations and a totally different situation with respect to moisture problems: the flat oriented towards NE/NW, which will be identified as "IACP One", showed serious moisture and mould related decay, while the flat oriented towards SE/SW ("IACP Two") revealed no problems at all.
All flats in the building have individual gas-fired boilers for space heating and service hot water; none has mechanical ventilation. Windows weatherstripping and insulation of the rolling shutter box was performed by the inhabitants of IACP One.

Primary aim of the case study was to get a better understanding of moisture-related problems which are fairly common in recently constructed low-cost housing. In particular, the following issues were addressed:

- to identify and quantify the main causes of moisture and mould problems in the North oriented "IACP One" flat;
- to understand why two flats, almost identical in size and occupation pattern, are in such different condition;
- to evaluate the reliability of the experimental procedure.

3. EXPERIMENTAL PROCEDURE

Experimental data were collected using two programmable multi-channel data loggers; the first unit was installed in the flat being monitored, the second was located on the roof of a nearby three-storey building to gather weather data. The following quantities were measured [4]:

- indoor air temperature in each room
- indoor air relative humidity in each room
- inside wall surface temperature at selected locations
- outdoor dry-bulb temperature
- outdoor air relative humidity
- global horizontal solar radiation flux
- wind speed and direction.

Data were collected every two minutes; time trends and hourly average values were stored on magnetic tape for subsequent processing. Altogether, 55 days of measurements were performed for IACP One, and 10 days for IACP Two during the period November 1987 to February 1988.

Two tracer gas measurements of airchange rate were performed in IACP One, using the decay technique and N_2O as the tracer. Values of 0.32 and 0.47 ach were obtained. Such values are consistent with theoretical estimates and are comparable with other experimental data obtained in similar buildings in the Turin area.

A mycological analysis was also performed, in order to characterise the type of mould formation that occured in the dwelling [5].

4. DATA ANALYSIS

Condensation of moisture and mould development in buildings are caused by excessive air humidity levels in the vicinity of the wall surface. In fact, mycological studies quoted in the literature [6] have revealed that spore germination and growth is likely to develop when relative humidity exceeds the values of 70% and 80% respectively.

High relative humidity at the wall surface, in turns, is due to the combined effect of high indoor air moisture content and low surface temperatures: the former phenomenon is normally due to high indoor vapour production or infiltration of warm-moist air, coupled to insufficient ventilation with dry outdoor air, while the latter is usually caused by localised cold spots in the building structure (thermal bridges).

4.1 Air moisture content

Starting from the measured values of air temperature, T_i, relative humidity, RH_i, and wall surface temperature, T_s, the time trend of relative humidity at the wall surface, RH_s, was computed assuming that the partial pressure of water vapour in the air is uniform within the room. Such hypothesis is reasonable within the approximation of the study [7]. A sample of RH_s trend is shown in Fig. 2.

Figure 3 shows the frequency of occurrence of RH_s exceeding the threshold values of 70% and 80%, or reaching 100%, for the various rooms of IACP One; on the contrary, the 70% threshold was never exceeded in IACP Two.

In order to understand how the humidity values measured in IACP One can be rated, a comparison was made with a set of experimental data collected in Belgium. In the graph of Fig. 4, the difference between indoor and outdoor humidity ratio (X_i-X_e) is plotted versus outdoor temperature T_e: the data points indicate the weekly average values measured in each room of IACP One, while the solid line represents the 95th percentile of weekly average data according to the Belgian survey [8]. This result indicates that the situation in IACP One is indeed quite exceptional.

4.2 Surface temperatures

The value of indoor surface temperature of a given wall, T_s, is linked to air temperature outdoors, T_e, and indoors, T_i, by a parameter called the "temperature factor" of the surface τ [7]:

$$\tau = \frac{T_s - T_e}{T_i - T_e} \qquad (1)$$

For one-dimensional, steady-state conditions, τ would be a constant given by the equation:

$$\tau = 1 - U/h_i \qquad (2)$$

where U is the thermal transmittance of the wall and h_i is the indoor surface heat transfer coefficient.

In reality, τ varies in space and time for a number of reasons, such as the presence of two- or three- dimensional heat fluxes in the building structure, or time varying conduction, convection and radiation heat transfer within the wall and at the wall boundaries. A sample of time trend of τ is shown in Fig. 5.

Nevertheless, if values averaged over a sufficiently long period of temperature difference (T_s - T_e) are plotted against (T_i - T_e), a linear correlation between the data points can still be detected, as indicated in Fig. 6. Such result is very useful beacause the slope of the regression line gives a estimate of the mean value of the

temperature factor at a given point of the wall surface.

For IACP One, values on the order of 0.7 (the minimum suggested value according to Belgian recommendations [8]) were found for the bathroom and one of the bedrooms.

4.3 Airchange rates

The indoor humidity ratio, X_i, can be related to outdoor humidity ratio, X_e, indoor vapour production, D, and airchange rate, N, by writing a steady-state water vapour mass balance equation for the room. The resulting expression can be more or less complicated, depending on whether condensation on cold surfaces occurs [8].

In our case, time trends of X_i and X_e are known, while airchange rates can be estimated on the basis of the tracer gas measurements. Moisture production is virtually impossible to measure, but can be derived from the mass balance equations if X_i, X_e and N are known; alternatively, D can be estimated on the basis of literature values.

Assuming a constant airchange rate of 0.4 ach (the average of the two experimental values), the maximum vapour production rate for IACP One was estimated on the order of 1 kg/h, a reasonable value for the type of occupancy of the flat.

As a further step, the minimum ventilation rate necessary to prevent condensation (i.e., to keep RH at the wall surface below 95%) was computed for each hour of the survey. Results for one bedroom of IACP One are shown in Fig. 7; values exceeding 0.4 ach (corresponding to 83.5 m^3, i.e. the assumed value of airchange rate) only are shown in the graph.

These results indicate that for about 30% of the time of the survey, the airchange rate was probably insufficient to prevent condensation in that specific room, thus explaining the occurrence of serious moisture and mould problems.

5. CONCLUSIONS

Some general remarks can be made as a final comment to the case study.

Firstly, the methodology adopted in the case study, based on continuous field measurements of temperatures and relative humidities, provided reasonable results within the accuracy limits of the model describing the physics of the problem.

Secondly, a building like the one that was examined in the case study has a limited "safety margin" with respect to condensation and mould growth, partly because of two specific reasons: the external envelope has a large extension compared to the volume, because of building shape (square plan) and height, and the number of

occupants is high (six) in relation to floor area (100 m^2).

In the presence of thermal bridges, which tend to reduce the temperature ratio of the external walls, fairly high airchange rates (of the order of 0.7 ach) are necessary to avoid the risk of condensation. Such an airchange rate cannot be guaranteed by natural ventilation in a climate characterised by very low wind speed, and would be unacceptable in terms of heat losses. Mechanical ventilation, possibly with humidity-actuated regulation of outdoor air flow rate, would probably solve the problem.

The fact that the occupants of IACP One have retrofitted the windows indicates that comfort conditions in the flat were probably unsatisfactory. This may not have been the case in IACP Two, which has a better orientation (SE/SW instead of NE/NW). Care should therefore be taken in order to achieve a draught-free outdoor air inlet.

These comments suggest that more precise guidelines with respect to thermal bridges correction and ventilation requirements should be specified in the building codes, in order to reconcile the apparently conflicting goals of achieving comfort and acceptable indoor air quality in an energy-wise manner.

REFERENCES

1. Legge 30-04-76
   "Norme per il contenimento dei consumi energetici per usi termici negli edifici".

2. Norma UNI 7979
   "Edilizia - Serramenti esterni verticali - Classificazione in base alla permeabilità all'aria, tenuta all'acqua e resistenza al vento".

3. C. Lombardi et al.
   "A case study: IACP Torino"
   Report n. PT-DE-FT 139, Dipartimento di Energetica del Politecnico di Torino, 1988.

4. Aghemo, C. and Lombardi, C.
   "Condensation and mold: a case study"
   Proc. ASHRAE-DOE-BTECC Conference Thermal Performance of Exterior Envelopes of Buildings IV, Orlando (Florida), December 1989.

5. Sampò, S. and Luppi Mosca, A.M.
   "Fungi from the walls of a flat in Turin"
   Allionia 28, 1987/88, pp 175-184.

6. Magan, H. and Lacey, I.
   "Effect of temperature abd RH on water relations of field and storage fungi"
   Trans. British Mycological Society *82*, pp71-78.

7. Hens, H.
   "Annex XIV - Condensation and Energy"
   Proc. 10th AIVC Conference, Espoo (Finland), September 1989.

8. Centre Scientifique et Technique de la Construction
"Problèmes d'humidité dans les bâtiments"
Note d'information technique 153, 1984.

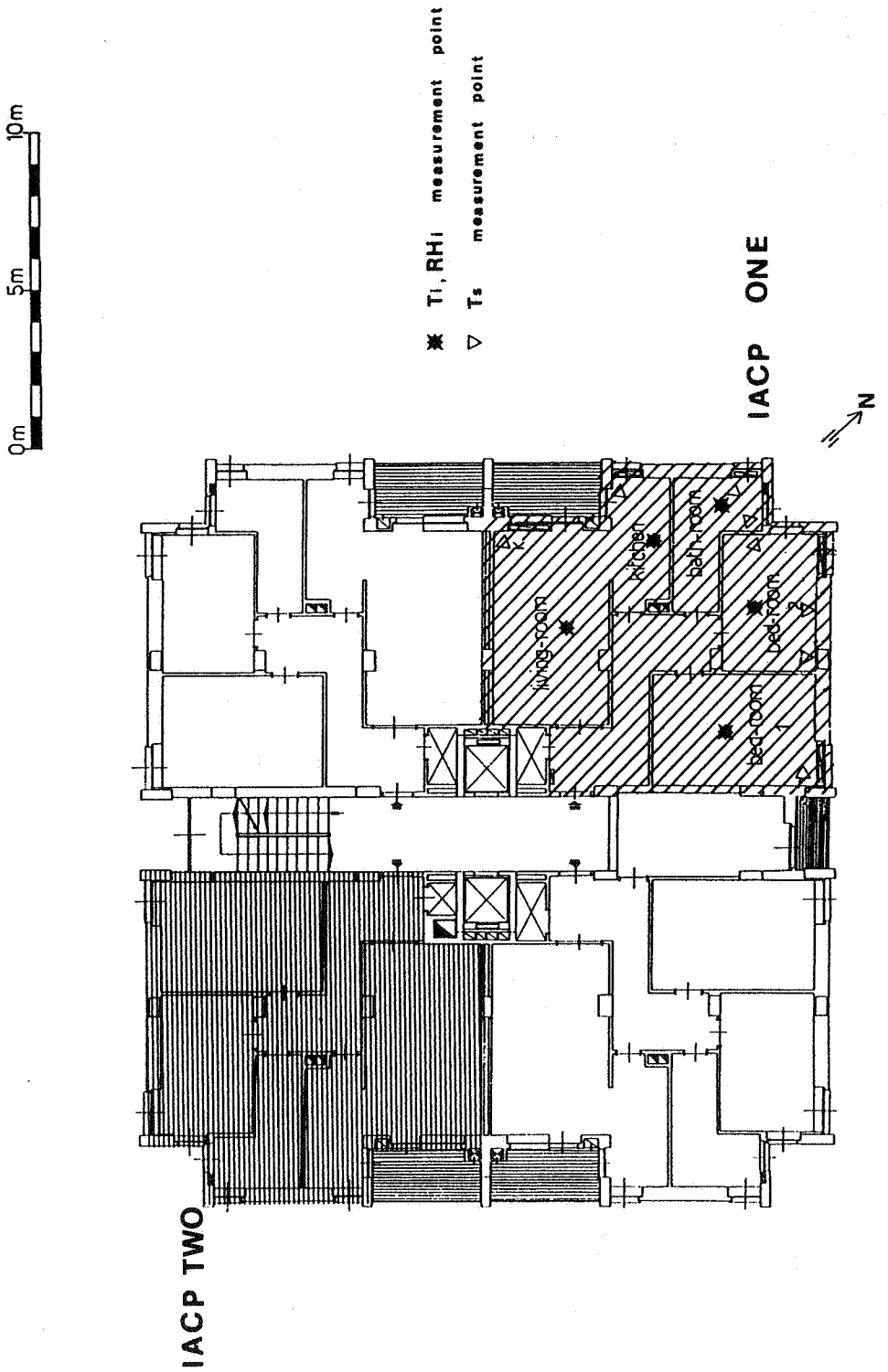

Fig. 1 - Floor plan of the building

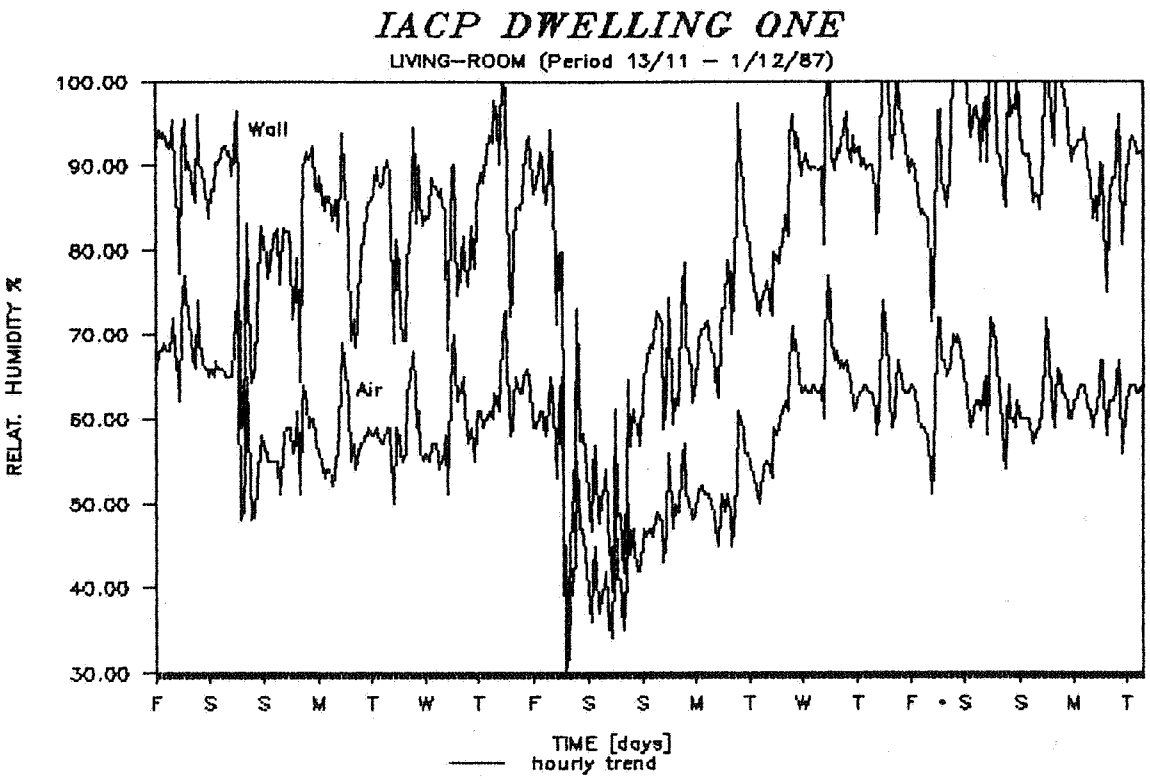

Fig. 2 - Relative humidity (RH) trends in indoor air and at the wall surface.

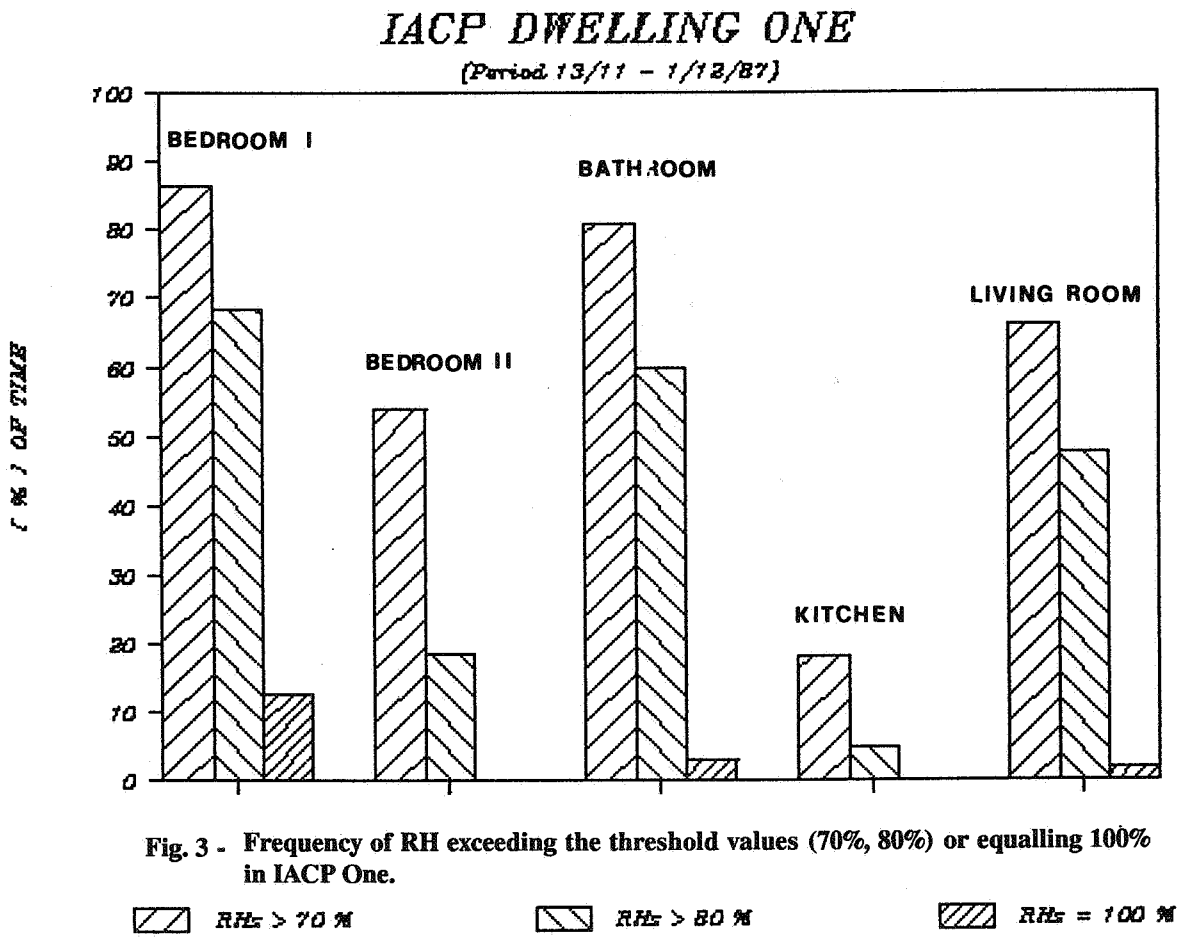

Fig. 3 - Frequency of RH exceeding the threshold values (70%, 80%) or equalling 100% in IACP One.

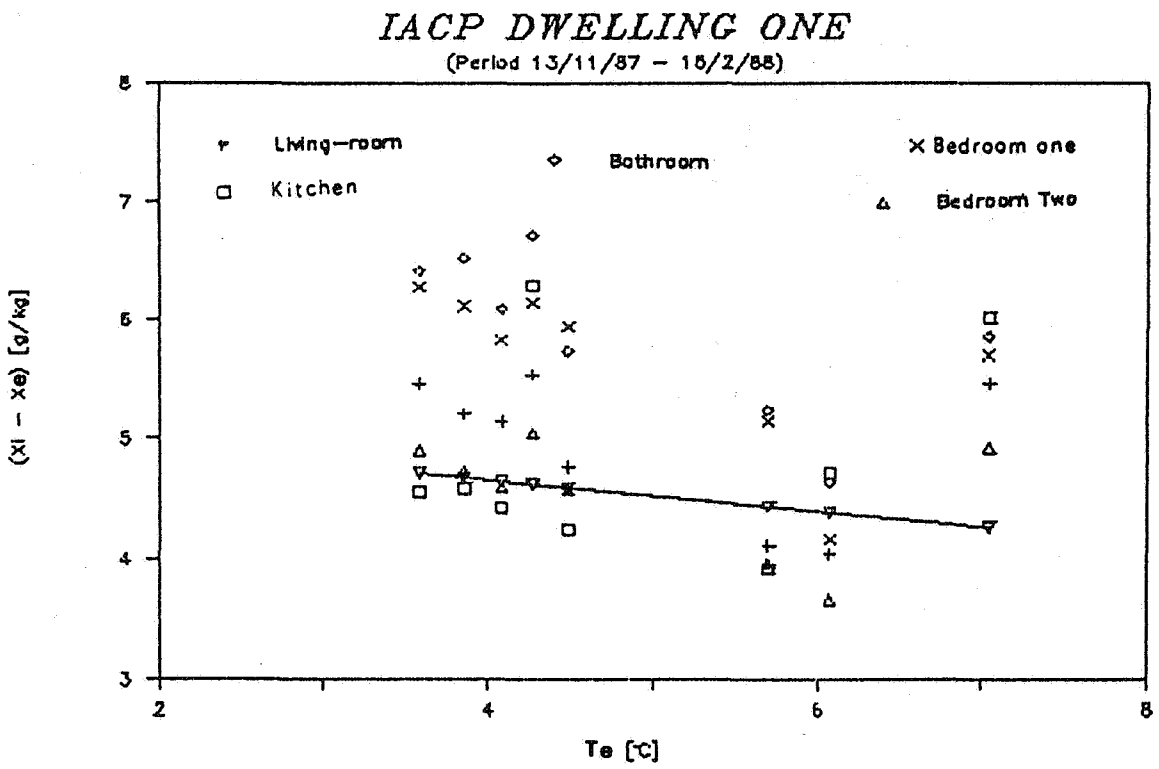

Fig. 4 - Indoor - outdoor humidity ratio vs. outdoor temp.
Comparison of experimental values with statistical data collected in Belgium (solid line indicates the 95th percentile of weekly average data in Belgium).

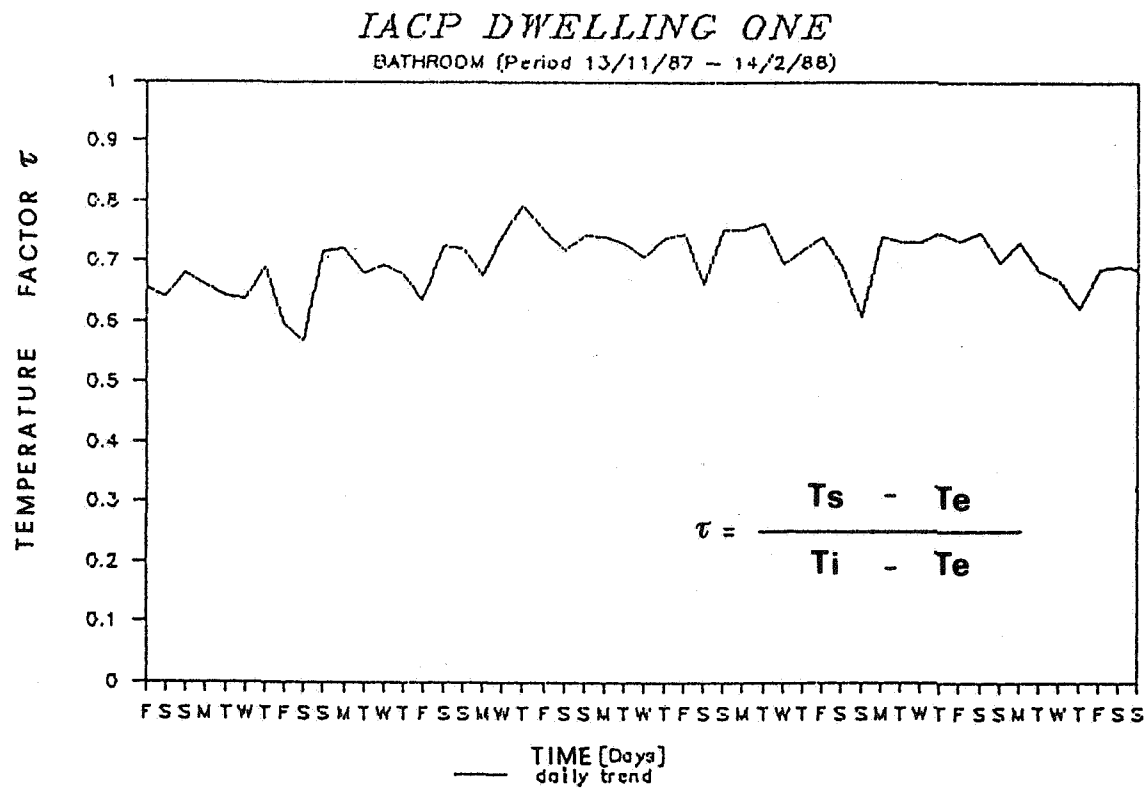

Fig. 5 - Daily average values of wall temperature ratio .

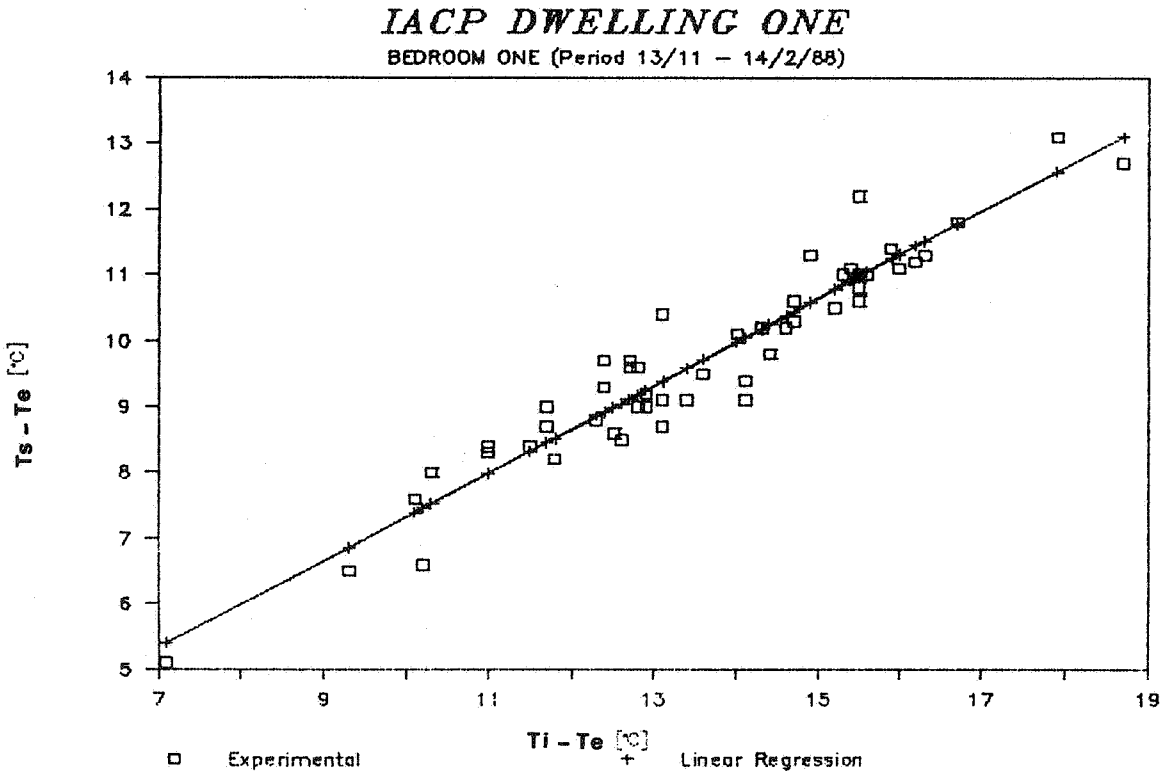

Fig. 6 - Linear regression between daily average values of (T_s - T_e) and (T_i - T_e).

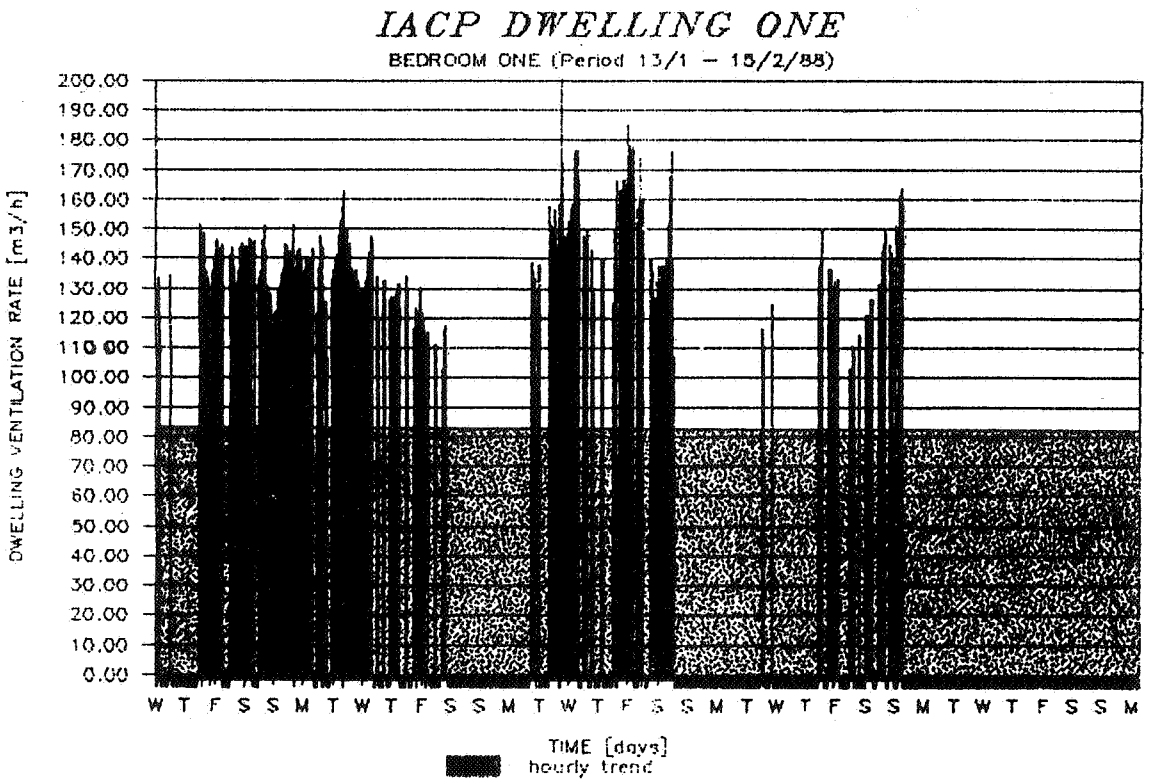

Fig. 7 - Minimum airchange rate to prevent condensation.

PROGRESS AND TRENDS IN AIR INFILTRATION
AND VENTILATION RESEARCH

10th AIVC Conference, Dipoli, Finland
25-28 September, 1989

Paper 13

EXPERIMENTAL METHOD TO MEASURE 3D AIR VELOCITY

G. Gottschalk, Z. Revesz, P. Suter and P. Tanner

Swiss Federal Institute of Technology
Energy Systems Laboratory
ETH-Zentrum, CH-8092 Zurich
Switzerland

EXPERIMENTAL METHOD TO MEASURE 3D AIR VELOCITY

Gregory Gottschalk, Zsolt Revesz, Peter Suter and Peter Tanner

Swiss Federal Institute of Technology, Energy Systems Laboratory
ETH-Zentrum, CH-8092 Zurich, Switzerland

ABSTRACT

A method is being developed for visualization of air flow with application to the indoor problems of heating, ventilating and air conditioning. Photographic images of the soap bubbles seeded in space reveal features of the flow which can be quantified by the digitizing operations. Determination of the velocity vector field from the experimentally recorded images is possible.

air flow visualization; digital image pocessing; soap bubble tracer

1. EXPERIMENTAL PROCEDURE

1.1 Method (Fig. 1)

The investigated space is seeded with the soap bubbles of diameter 3 - 4 mm. They are being transported with the air streams resulting from jets or convective sources. To make the phenomena not only visible but also adapted for recording , the space is darkened and illuminated by the well defined light sheet. By this mean only the bubbles which are actually crossing the light plane become contrastly visible on the dark background. the photographic camera is placed perpendiculary to the light sheet. The long exposed film is integrating the time position dependence resulting in the trajectory images. Applying the three color lighting and the time marking the features of the velocity vector are coded into the bubble track images. Automated digitizing and image treatment are used to extract the quantified flow field from the experimental photographs. Method is orientated to be used not necessarily in laboratory chambers but also in the real spaces. The necessary condition is darkening of the room.

1.2 Soap bubbles

The soap bubbles used for seeding the flow are produced by the standard generator from Sage Action Inc.,(USA). The batch of the bubbles passes through the selector for eliminating those which are too heavy. The homogeneous population of bubbles performing the settling velocity in the still air of about 5 cm/s (diameter 3 - 4 mm) is transferred to the experimental space. The average life time of a bubble amounts to several minutes .

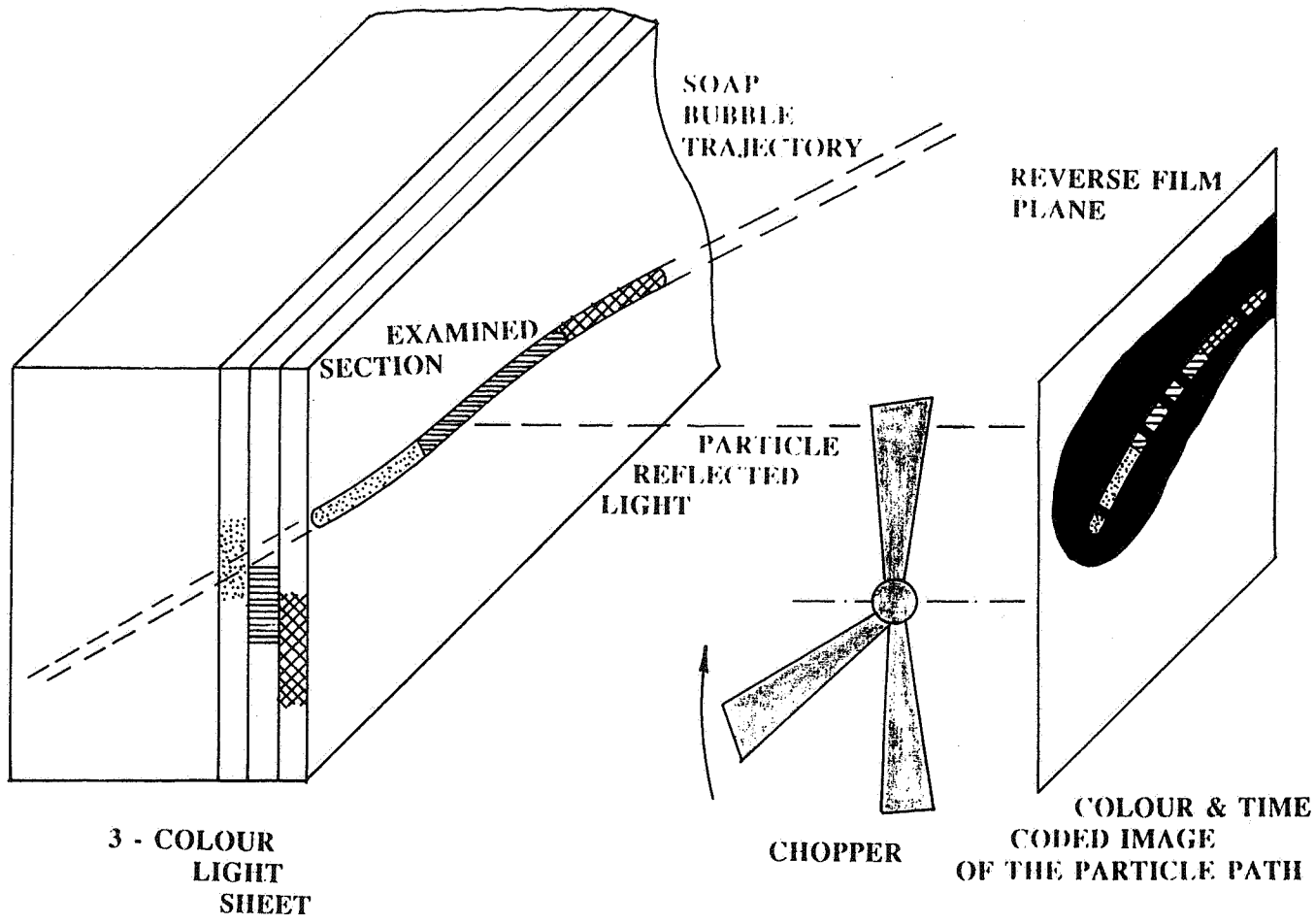

Fig. 1 The scheme of the experiment

The helium filling option foreseen by the manufacturer is not used. Helium is strongly influencing the selection process : even the thick - wall bubbles (i.e. too heavy) arrive to survive in the gravitational selector and get into the experimental space. There, the rapidly diffusing helium (small molecular weight) is decreasing the buoancy and bubbles fall down rapidly.
The neighbourhood of the air outlets and other areas of higher speed (e.g. convective sources) are the places suitable for introducing the tracer.
The comparison had been made between the indications of the omnidirectional DANTEC Flow Velocity Analyzer Type 54N50 and the photographic recording of the bubbles. The experiment was run in the chamber of stabilized horizontal flow (Fig. 2).

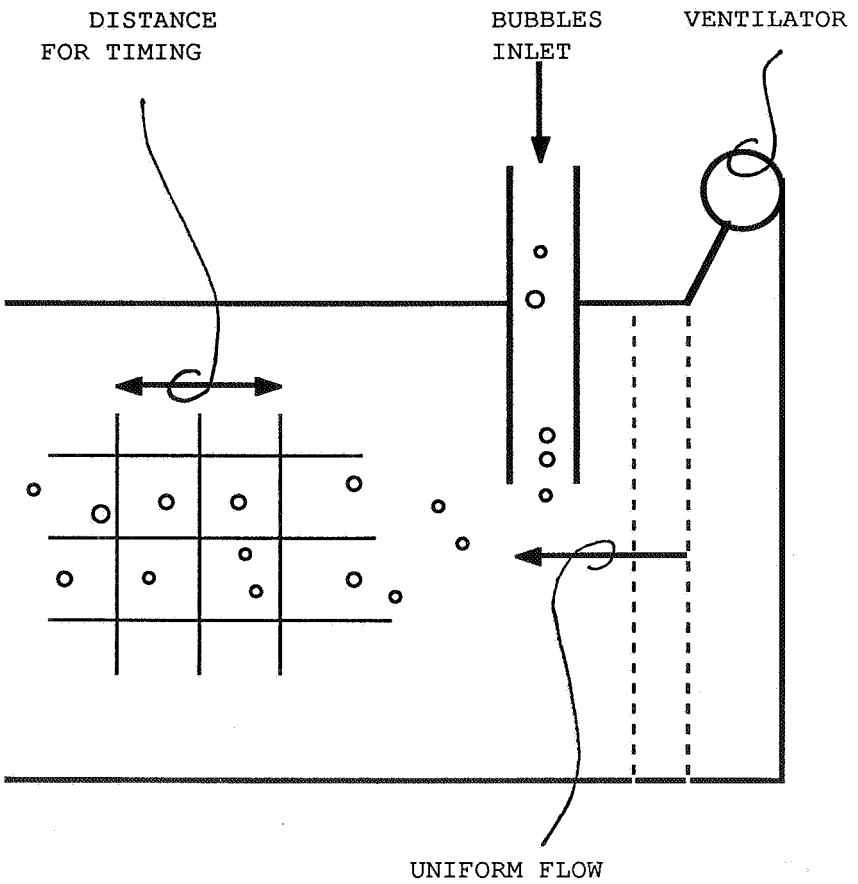

Fig. 2 Flow Visualization vs. Anemometer

The simultaneous measurements arrived to be impossible to realize : the presence of the anemometer strongly perturbated the movement of the bubbles passing at the proximity of the protection cage or holder and those which were close to the sensor were too rare and presenting danger to be deposited on the sensor itself. In this situation velocity was measured before and after series of photographs.

Table 1. Comparison of the anemometer indications vs. photographic recordings.

				Mean
Measured velocity BEFORE				
RMS = 0.8 Tu = 0.04 U 5% = 18 U95% = 21.5				19.6 cm/s
Photo # 1	Track # 1		U1 = 22.0 cm/s	
	2		U2 = 22.0	
	3		U3 = 22.0	
	4		U4 = 22.4	
	5		U5 = 23.2	
	6		U6 = 19.7	
Photo # 2	Track # 1		U1 = 23.6	
	2		U2 = 18.9	
	3		U3 = 23.0	
	4		U4 = 23.0	
Photo # 3	Track # 1		U1 = 23.0	
	2		U2 = 22.5	
	3		U3 = 22.0	
	4		U4 = 22.8	
	5		U5 = 23.4	
Photo # 4	Track # 1		U1 = 23.0	
	2		U2 = 24.8	
	3		U3 = 24.0	22.5 cm/s
Measured velocity AFTER				
RMS = 0.6 Tu = 0.02 U5% = 19.2 U95% = 21.1				20.1 cm/s
Measured velocity BEFORE				
RMS = 1.0 Tu = 0.07 U5% = 11.3 U95% = 14.9				13.1 cm/s
Photo # 1	Track # 1		U1 = 15.0 cm/s	
	2		U2 = 15.0	
	3		U3 = 15.0	
	4		U4 = 16.4	
Photo # 2	Track # 1		U1 = 15.0	
	2		U2 = 16.0	
	3		U3 = 15.5	
Photo # 3	Track # 1		U1 = 16.1	
	2		U2 = 16.5	
	3		U3 = 12.1	
	4		U4 = 17.0	
Photo # 4	Track # 1		U1 = 16.0	

	2	U2 = 14.0	
	3	U3 = 15.0	
Photo # 5	Track # 1	U1 = 15.0	
	2	U2 = 14.8	
	3	U3 = 14.3	
	4	U4 = 13.8	15.1 cm/s
Measured velocity AFTER			
RMS = 1.0 Tu = 0.07	U 5% = 10.9	U95% = 14.5	12.8 cm/s

The anemometer presents a systematic negative off-set. The quantifying of this effect calls for new calibration and examination of the velocity field (uniformity) in the chamber.
The recorded trajectories from the flow in the above experiment as well from the flow the real rooms have smooth character indicating a damping effect (like a low pass filter). Contrary to the hot wire recording the turbulence spectrum is not detectable.

1.2 Lighting

The light sheet is consisting of the 3 distinctly separated colours. By that mean the trajectories which are not parallel to the light sheet (ditto observation plane) are resulting in tracks of coloured sequence. Color change is marking the movement of the tracer perpendicular to the observation plane.
The point light source (halogen metal vapour arc lamp) of the equivalent temperature 5600 deg C is used. The thickness of the light sheet is to be related to the density of tracer distribution in space : if it were too narrow the probability to illuminate the sufficient number of the tracer particles in one shot would be very low. The thickness of 4 cm revealed to be optimal for the middle plane (the red colour) which serves as a depth indicator for the third dimension.

1.3 The Photographic Technique

Standard reflex camera 24 x 36 mm is used. The images are taken on the colour reversal film 1600 ASA. The high equivalent temperature of the light source allows to use the daylight emulsion without any filter corrections.
The shutter is opened for relatively long time (typically 1-2 s) but the effective exposure in that laps of time is shortly interrupted by the rotating chopper ahead of camera lenses. The moment of opening / closing the shutter is synchronized with the position of the distinct arm of the chopper just passing by before the lenses. Due to that the recording of the not complete chopper turns is reduced (i.e. images contain less tracks which must be rejected while treatment as being not integrally exposed).
The non - symetry of the chopper is marking the time evolution on the photographed image otherwise speaking allows detection if the tracer was moving e.g from left to right or vice versa.

1.4 The Third Dimension

In the observation plane (xy) the real distances are scaled to the image using the physical marks in the experiment or by superposing the experimental images with the reference grid from the test shot.
The depth (3rd dimension: along ' z ', perpendicular to xy) is controlled by the thickness of the middle light plane (red colour) On the experimental images the movement of the tracer along ' z ' is resulting in colour changes , e.g. from blue - to - red and red - to - green.
The colour selectivity of the illumination is essential to recognize the 3D flow. Nevertheless the precision of measure the velocity component perpendicular to the observation plane (V z) is lower than for the x - y plane (V x , V y).

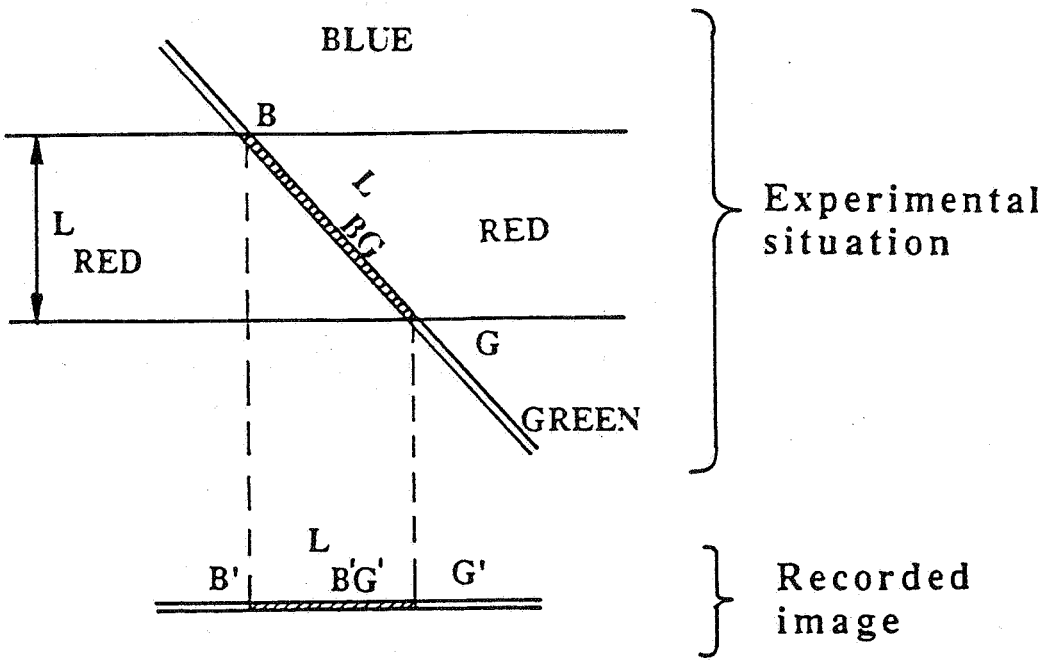

Fig. 3 The reconstruction of the 3rd dimension

The reconstruction of the real depth situation is possible according to Fig. 3:

$$L_{BG} = \sqrt{L^2_{B'G'} + L^2_{RED}}$$

EVALUATION OF THE TRAJECTORIES

When photographing, the camera shutter is opened relatively long so that the chopper completes several rotations during the exposition time. This results in "cutting" the tracer trajectories into segments each consisting three lines, a long one, a shorter and the shortest one. Knowing the sense of rotation of the chopper the direction of the tracer displacement can be determined.

In the observation plane (xy) the real distances are scaled to the image using the physical marks in the experiment. The depth information (the z coordinate) is defined by the colour of the picture, knowing the thickness of the light plane. The intervals on the trajectory image are time marked according to the chopper geometry and the speed of rotation. Taking the sequence of segments in the scanned picture the magnitudes of the velocity vector can be calculated. The opening and closing time has been defined so, that at constant velocity along a straight line the distances between the first and second points equal to the distances between the second and sixth points. This allows a futher control in the trajectory evaluation process.
At the present arrangement the camera and the chopper are not synchronized so that the first and the last recorded track length contains no reliable information.

The colour in the trajectory image is related to depth. The purity of the colours is essential. Each of the colours is associated with a gray scale value determined by light filtering when scanning the photograph.

Colour control is performed on the each level of the procedure. First, the light source temperature is known . Then, the filters used to produce the colour in the light sheets are adapted to the colour reverse film sensitivity. Finally, digitizing is performed adapting filter settings for the best colour distinction after electronic conversion.

DIGITAL IMAGE PROCESSING

The slides are digitized three times (once for each colour) with a CCD-sensor). For every colour, information is stored in the computer,that means per slide one obtains three different matrices in the computer.

Figures 2 and 3 show an electronic image, a 50 x 50 array cut out from a picture for detailed investigation.

Using such arrays the different tracks can be visualized in a number of steps steps. A segment of the original matrix may look like Figure 2.

The original matrix can be modified e.g. by the "Roberts-operator" as follows:

$$b(i,j) = [\ (a(i,j)-a(i+1,j+1))^2 + (a(i+1,j)-a(i,j+1))^2\ ]^{0.5}$$

where a (i,j) is the value at the pixel position i,j before and b(i,j) the value at the same position after transformation. The effect of

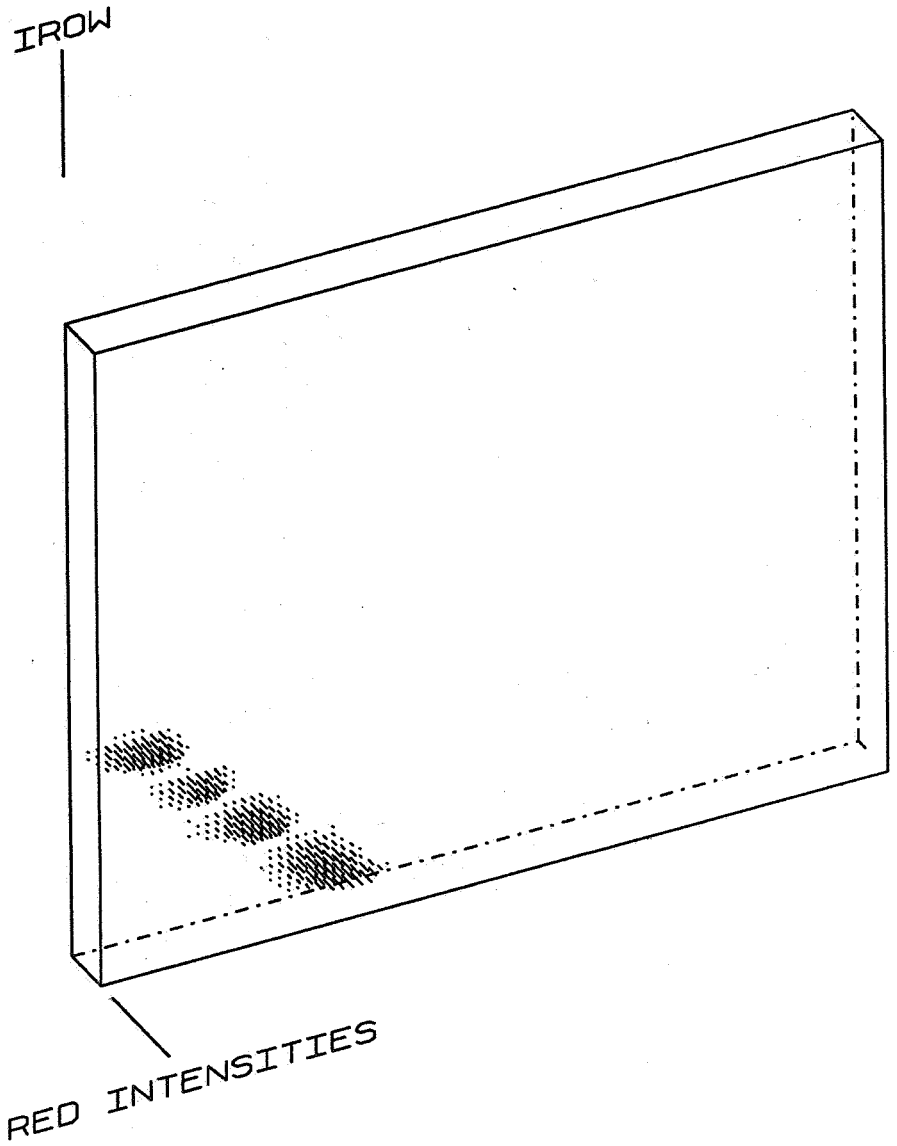

Figure 2. A red intensiy array as scanned

this transformation (in connection with the array shown in Figure 2) is illustrated in Figure 3.

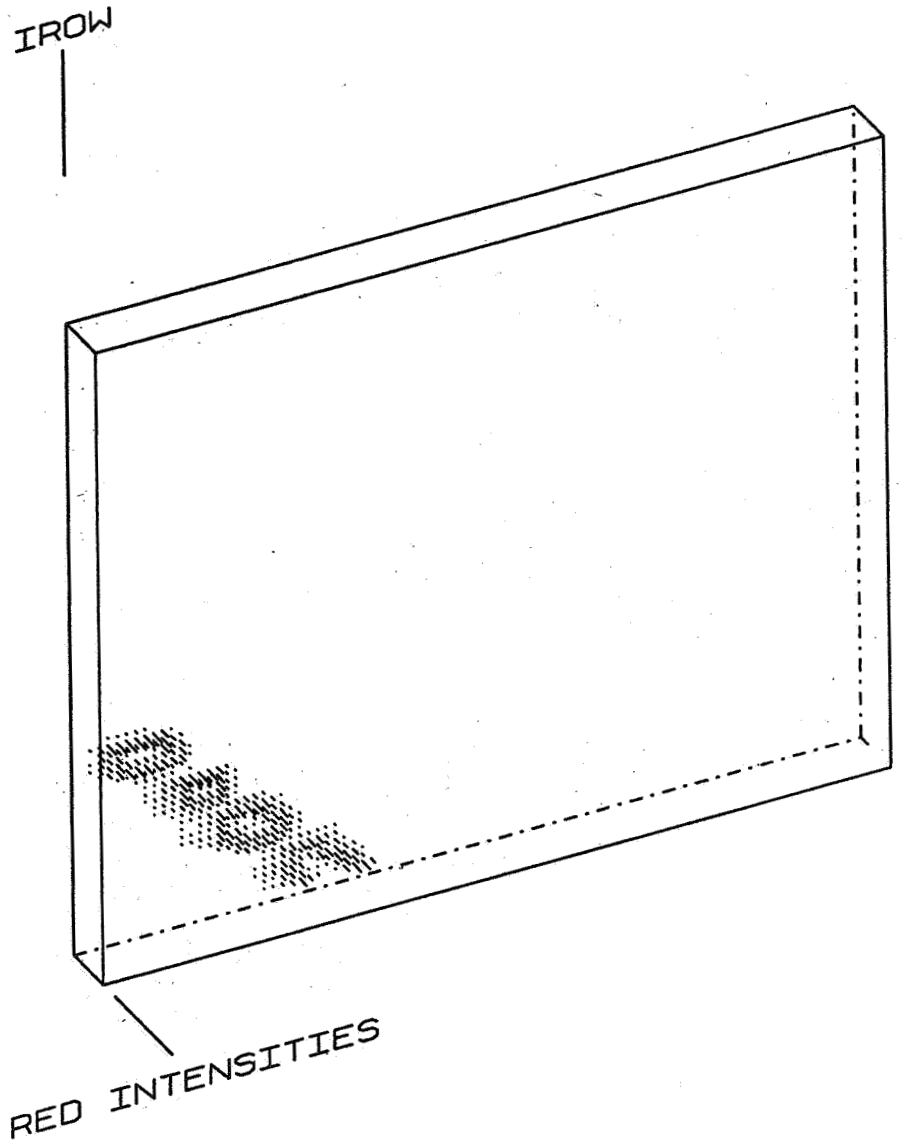

Figure 3. A modified array

This example shows a way to make image edges became "visible" for further recognition operations. Length and orientation determination of the tracks in x,y,z-space is a tedious but straightforward procedure:

Interpretating the sub-sections of the tracks as being tangential to the streamlines, the instantaneous direction of the velocity vector can be computed. This corresponds to an Eulerian type of description.

Longer sequences of the tracer positions (i.e. longer sections of the trajectories) cannot be associated with any one point of observation. Magnitude of the velocity still must be calculated from the time marked sections of the trajectory. When evaluating the magnitude of the velocity, a Lagrangian type of description is used.

It is the resolution (in space and time) and also the interpolation technique which determine which one of the descriptions is taking over.

A series of operations has to be done to achieve good results. This series, at present time, cannot always be predefined, therefore this instrument is at present time rather a research and development tool, than for field application as a routine task.

The velocity vector field is different from what is calculated using only the information stored in the trajectories. To quantify the difference between the air flow field and the vector field constructed from the tracer trajectories (caused by inertia, buoyancy, drag, gravity, centrifugal force, lift, diffusion, etc.) is a further step, still to be done. However, these are second order effects and do not essentially influence neither the above presented results, nor the statement about the applicability of the method.

CONCLUSIONS

Quantitative identification and visualization of the low-speed air streams in ventilated/heated spaces using solid tracers is today feasible. The air flow pattern can be studied using reconstructed velocity vector.

The progress in many associated areas (such as particle tracking in water, colour CCD-cameras, digital image processing software, colour photography, vectorized high speed computing,etc.) keeps fostering development of the presented method. Therefore it is highly probable that this method will soon become a convenient engineering tool, suitable also for field applications.

ACKNOWLEDGEMENT

The authors gratefully acknowledge "Schweizerischer Nationalfonds zur Foerderung der wissenschaftlichen Forschung" for supporting the project (NF: Nr. 2000-5333).

REFERENCES

/1/ Popovich M. M., Weinberg F. J.: Laser Optical Methods for the Study of Very Large Phase Objects, Experiments in Fluids 1, 169-178 (1983)

/2/ Kobayashi T., Saga T., Segawa S.: Some Considerations on Automated Image Processing of Pathline Photographs, 4th International Symposium on Flow Visualization, Paris 1986

/3/ Gonzalez R. C., Wintz P.: Digital Image Processing, Addison-Wesley Publishing Company, 1987

/4/ Richards J. A.: Remote Sensing Digital Image Analysis, Springer-Verlag 1986

/5/ Merzkirch W.: Flow Visualization, Academic Press, Inc.,1987

/6/ Meynart R.: Instantaneous velocity field measurement..., Applied Optics, No.4 Vol.22 (1983)

/7/ Utami T., Ueno T.: Visualization and picture processing of turbulent flow, Experiments in Fluids 2, 25-32 (1984)

/8/ Gottschalk G., Tanner P.A., Suter P.: The Large Area Visualization Method of Air Streams, A I V C 's 9th Annual Conference , Gent (Belgium), 12-15 Sept 1988

Discussion
Paper 13

E. Olsson (Chalmers University, Sweden)

What are the size of bubbles?

G. Gottschalk (ETH-Zentrum, Switzerland)

3 - 4 mm

PROGRESS AND TRENDS IN AIR INFILTRATION
AND VENTILATION RESEARCH

10TH AIVC Conference, Dipoli, Finland
25-28 September 1989

Paper 14

AIRFLOW MEASUREMENT TECHNIQUES APPLIED TO RADON MITIGATION PROBLEMS

DAVID T. HARRJE AND KENNETH J. GADSBY

Center for Energy and Environmental Studies
The Engineering Quadrangle
Princeton University
Princeton
NJ 08544
USA

SYNOPSIS

During the past decade a multitude of diagnostic procedures associated with the evaluation of air infiltration and air leakage sites have been developed. The spirit of international cooperation and exchange of ideas within the AIC-AIVC conferences has greatly facilitated the adoption and use of these measurement techniques in the countries participating in Annex V. But wide application of such diagnostic methods are not limited to air infiltration alone. The subject of this paper concerns the ways to evaluate and improve radon reduction in buildings using diagnostic methods directly related to developments familiar to the AIVC.

Radon problems are certainly not unique to the United States, and the methods described here have to a degree been applied by researchers of other countries faced with similar problems. The radon problem involves more than a harmful pollutant of the living spaces of our buildings -- it also involves energy to operate radon removal equipment and the loss of interior conditioned air as a direct result. The techniques used for air infiltration evaluation will be shown to be very useful in dealing with the radon mitigation challenge.

1.0 RADON BACKGROUND INFORMATION

Although it has been stated many times before, in numerous publications on radon [1-3], it needs to be restated here that the primary source of radon is soil gas. Building materials and radon in water supplies can be important sources in specific countries or localities, but the problem of soil gas carrying radon is by far the most common cause of high radon levels in our buildings. Standards and guidelines have been set in a number of countries. In the United States the Environmental Protection Agency guideline has been set at 4 pCi/L (148 B/m^3). This guideline has been interpreted very exactly in some regions of the United States, i.e., a level of 4.1 pCi/L and you fail the test and steps must be taken to reduce the radon level prior to the sale of that house. These interpretations come from local health officials and in some cases the real estate firms involved in home sales who refuse to take any responsibility that the buyer could claim damages from them for future health problems. In many areas of the U.S. more than 30% of the houses fail to meet the guideline of 4 pCi/L. In New Jersey 64% of those houses mitigated failed to stay below the guideline value considering both professional and homeowner mitigation installations[4]. Therefore, evaluating mitigation system durability is an important subject of current research. The latest legislation would limit radon levels inside to ambient levels outside[5], making radon mitigation even a greater challenge.

Returning to the subject of radon entry with the soil gas, and the subsequent air movement through the house, the driving mechanism for these events is the stack effect. The higher the differential indoor-outdoor temperature (with possible influence of local wind effects) the greater the pressure difference between the substructures of the house and the soil that draws soil gas into basement, crawlspace, or through the floor slab. The looser the substructure construction the easier the path from the soil into the building. Unfortunately the opening

need not be very large, as pointed out at the Radon Diagnostics Workshop[6], a substructure hole of only one square centimeter can result in almost all the radon gas still entering the building. Given the desire to add drains, sump holes, piping and electrical systems in our house designs, it is not hard to imagine easy entry paths for radon.

The proper perspective to always keep in mind is that radon source strength is far more important than the relative tightness of the structure. Air infiltration will normally vary only about half an order of magnitude, but source strength can vary by many orders of magnitude. We have observed soil radon levels as high as 150,000 pCi/L (5,550,000 B/m^3). High source strength coupled with good soil transport is a combination one would like to avoid.

Methods to mitigate radon-plagued buildings tend to use three strategies: pollutant source control, local exhaust near the pollutant source, and dilution via ventilation once the radon has entered the building. Because the primary health danger lies in the radon progeny, rather than the radon gas itself, one could consider another mitigation strategy of filtering out the radon progeny which consist of tiny particles of size range of a fraction of a micron. However, particle removal has all sorts of problems and other implications; first the particles are very small and not easy to filter, filtering does not remove radon gas hence any newly generated progeny have no particles to adhere to and thus can be directly ingested into the human lungs. Dosimetric models indicate that unattached progeny are largely responsible for the radiation dose (Chapter 7, Ref. 2, A.James, Lung Dosimetry).

The most popular mitigation systems seeks to remove the radon prior to house entry[7]. As shown in Figure 1, a fan, preferable placed in the attic or outside, depressurizes the volume beneath the floor slab. That subslab location hopefully is well connected by permeable soil, or the air gaps in the gravel layer (or possibly the gap between slab and soil). By mechanically depressurizing this volume not only does soil gas no longer move upwards through the slab but even soil gas penetrating the hollow block walls may be flushed away via the mitigation system[6].

2.0 DIAGNOSTIC TECHNIQUES THAT ARE APPLICABLE

Given the circumstances for radon entry into buildings and the methods applicable for radon removal, it is easy to see where many similarities exist between these circumstances and the study of air infiltration, for example:

- Below grade entry of the radon gas implies leak site detection. Where these sites are located could imply the use of methods similar to above grade site detection methods as outlined in ASTM-1186-87 Standard Practices for Air Leakage Site Detection in Building Envelopes[8]. Those methods include: combined building depressurization (or the use of pressurization) and infrared scanning; building pressurization (or depressurization) and smoke tracers; building depressurization (or pressurization) and airflow measurement devices; generated sound and sound detection to locate air leakage sites; and detection of tracer gas concentration after adding tracer gas upstream of the leakage sites.

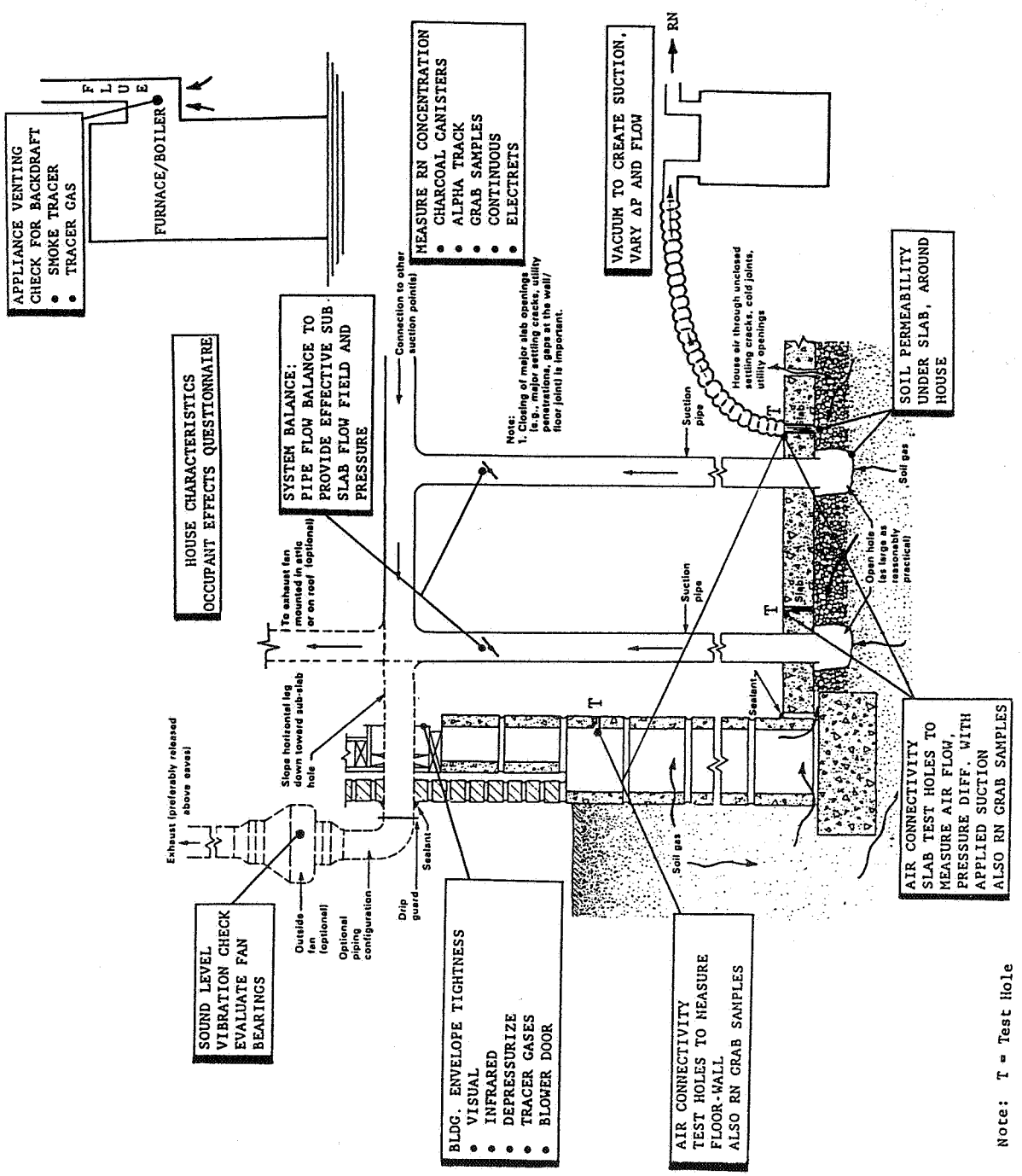

Figure 1. Subslab depressurization (SSD) system for radon mitigation. Gravel serves as a collection volume for the soil gas which contains radon. Holes through the slab are used in the diagnostic procedures[6,10] to specify the mitigation system. Diagnostic tests are specified in the blocks.

• Movement of the radon gas within the building determines which rooms exhibit the highest radon levels and how the radon reaches those rooms can be important. Tracer gas methods may be substituted for the radon to more readily evaluate the interior flow structure since the tracer gas detection equipment responds immediately to the tracer concentration. In our studies we have found two methods to be particularly useful: constant concentration tracer gas (CCTG) methods directed at evaluating local air infiltration and soil gas flows, and perfluorocarbon tracers (PFT) to map out the interroom flows as well as establish the tightness of the entire house over the longer term.

• The relationship of the radon mitigation system with the normal ventilation of the building is important. To answer the question of whether air that exhausts from a mitigation device is interior air requires that the interior air be properly identified. One approach that has proved to be very successful is using a constant concentration tracer gas system to maintain the interior air at a known tracer gas concentration. (If more than one zone is to be evaluated, multiple tracer gases need to be employed). Tracer gas levels in the exhaust air from the mitigation system is then measured and the percent indoor air evaluated from the concentration ratio (exhaust air concentrations are divided by interior air tracer concentrations). A typical trace of this concentration ratio is shown in Figure 2 and discussed in Reference 9. The flow of interior air can be a significant portion of the exhaust flow. The energy cost can easily exceed fan energy expenditure. PFT techniques may be used in a similar way to determine this important parameter.

Figure 2. Ratio of the tracer gas concentration in the exhaust versus the concentration in the house. The ratio determines the exhaust rates of the interior, conditioned air and hence the energy cost.

• Early diagnostic techniques make use of the blower door and pressurization/ depressurization to evaluate the building tightness. This has several implications to the radon mitigation team. Evaluating relative tightness of basement and living space and the degree of interaction between the two zones can indicate which mitigation approaches make sense. For example, only if the zones are relatively independent of each other could one consider pressurizing the basement to prevent the entry of soil gas. If good isolation doesn't exist, pressurization of the basement could force radon gas into the living space. A blower door can also be used to determine what volume of airflow is needed to pressurize the basement.

Greater tightness of the building structure, often associated with modern buildings, does not necessarily mean higher radon levels due to reduced dilution from air infiltration, rather it can mean reduced stack effect and less radon entering the building.

• Charting the path for radon gas is not limited to the living space. Prime pathways exist beneath the floor slab of the basement, crawl space and slab-on-grade construction. What happens in hollow walls and the soil just outside the walls can prove equally important. One of the key diagnostic tests is to determine the ability to communicate under the slab, so called "connectivity." Test holes are made through the slab as shown in Figure 1, and with an industrial vacuum cleaner supplying suction at one hole, pressure and flow measurements are made at the other test holes. Pressure values reveal the extent and magnitude of the pressure field, where pressure tends to equilibrate even when the soil is tightly packed. The flow values immediately reveal the degree of communication and point out that the flow path need not be simply radial but rather the flow seeks out that soil or gravel which offers the path of least resistance[6,7,10].

• One measurement of the durability testing that we are just beginning to interpret is the concentration of radon in the exhaust from the subslab mitigation system. When this information is combined with the velocity measurement at the same mitigation exhaust pipe location, we can then proceed to calculate the total flow of radon gas from the mitigation system.

One question to be resolved is: Can we compare the amount of radon exhausted from any given house and more fully understand the role that the mitigation system is playing? One such comparison involves the natural flow of radon through the same house. To make the calculation of the natural flow requires a knowledge of the average air infiltration rate for the house, the radon concentration upstairs and in the basement/crawlspace, as well as the volumes of those zones. Figure 3 shows data on these air exchange rates using the PFT technique. The calculation proceeds as follows:

$$R = AI \times 10^3 \times \frac{(C_u \times V_u + C_{b/c} \times V_{b/c})}{(V_u + V_{b/c})}$$

where R is the radon flow, pCi/h
AI is the air infiltration, m^3/h
C is the radon concentration, pCi/L
V is the volume, m^3
u is upstairs and b/c is basement/crawl space

Comparisons for five test houses are shown in the following table.

COMPARISONS OF RADON QUANTITIES EXHAUSTED BY MITIGATION SYSTEMS AND BY NATURAL MEANS BASED ON FIVE HOUSES

House No.	Rn Level (pCi/L)		House Volume (M3)		AI_{avg} (M3/h)	Rn Level Exhaust(pCi/L)	Exhaust Vel(M/S)	Rn Quantity (pCi/h)		Ratio: Mitigation/Natural
	Basement	Upstairs	Basement	Upstairs				Exhaust	Natural	
2	22	15	219	296	398	154	3.50	15,731,000	6,974,000	2.26
3	170	70	224	469	338	946	2.65	73,167,000	34,585,000	2.16
4	29	56	211	499	283	44	8.49	10,902,000	10,478,000	1.04
5	60	35	371	398	135	435	4.55	57,767,000	6,353,000	9.09
7	33	18	199	392	203	504	2.63	38,687,000	4,680,000	8.20

The ratio of the radon gas exhausted from each house via the mitigation system is compared to the radon natural flow value. Ratios vary from one to more than nine. We can ask, "what is special about house #4 which has the same radon gas flow via mitigation system or natural means, i.e., ratio one?" It is the home with the least porous soil -- that is basically pure clay. It is a home where high ventilation rates, e.g., using a blower door or opening windows will depress the radon levels, and then it takes many hours for the house to return to the previous elevated radon levels. Such behavior could be interpreted as evidence of a limited radon entry rate. However, just comparing the natural radon entry rate with those of the other homes would not single out this house. In fact, looking at natural radon entry rates, it is evident that house #3 stands out with a rate far above the others $\sim 35 \times 10^6$ pCi/h versus $7.5 \pm 3 \times 10^6$ pCi/L for all the rest. House #3 has a soil condition of high porosity, i.e., stone flour roughly 1/8 inch diameter and a good gravel bed, just the opposite of house #4.

The total amount of radon gas mechanically exhausted from the soil varies by a factor of seven in these homes. The lowest value is for house #4 with the clay soil. The highest value is for house #3 with the very porous soil. The two highest houses (#3 and #5) were the houses with reoccurring periods of above guideline levels of radon which is a critical durability characteristic. However, house #7 has a considerable amount of clay soil and still ranks third.

Again, this is a preliminary review of such radon exhaust data and it may possibly hold important clues to those homes most and least susceptible to reoccurring radon problems.

Some of the diagnostic techniques just described will encounter difficulty in below grade applications. Masonry construction tends to mask the temperature of the soil gas. The soil gas temperature may not be different enough from the basement temperature to make air leakage sites evident via infrared techniques. Sound sources, unless placed beneath the slab, would seem to have little chance of working effectively. Soil properties can vary from site to site and even from one house site to the other. To summarize, while there are similarities in the demands of the two applications there are enough differences that each application must be carefully considered.

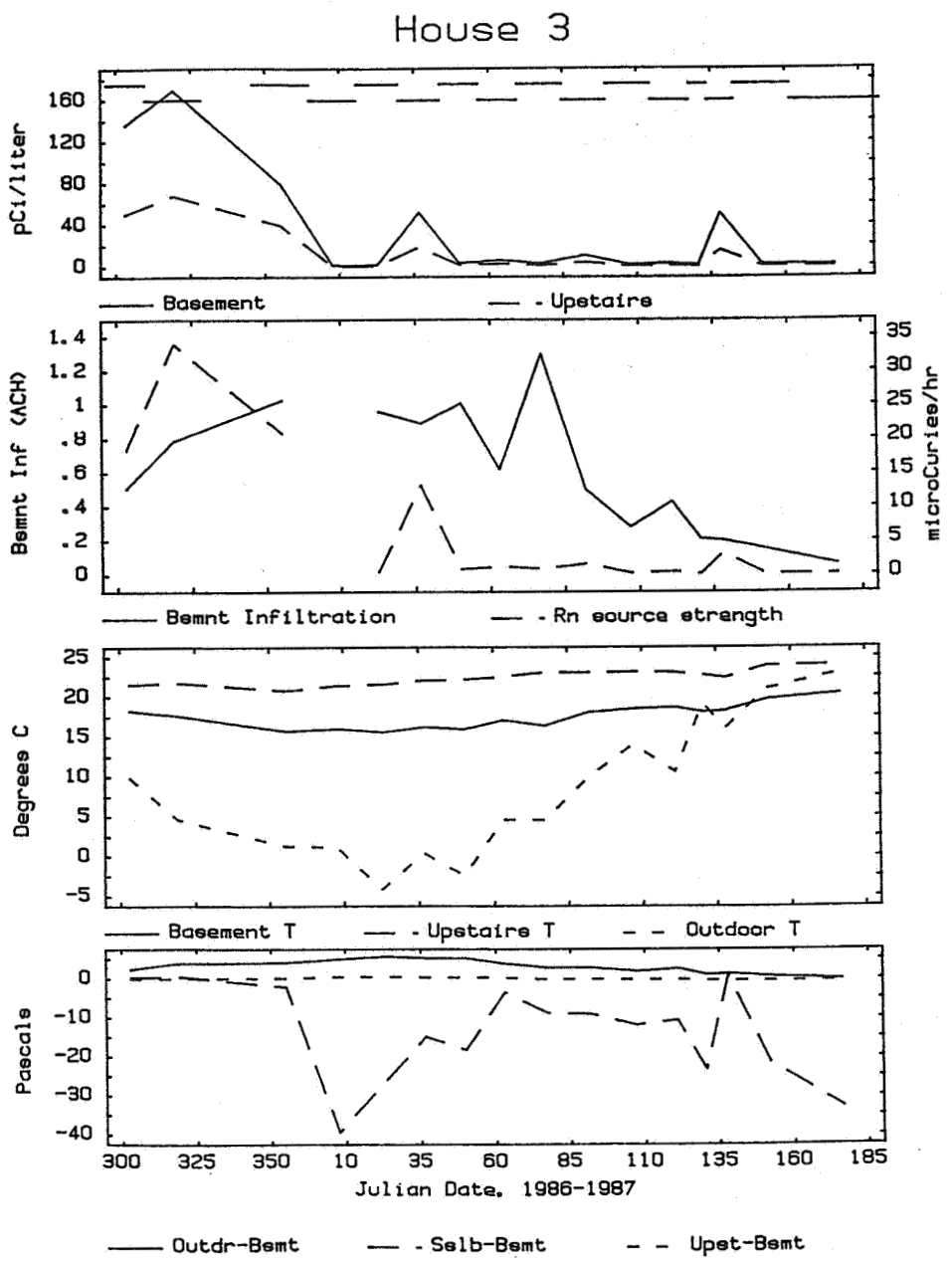

Figure 3. Profiles of radon concentration and air infiltration rates aid in the analysis of how the IAQ of the house is being affected by airflow patterns and radon sources. The top box in the figure shows the radon concentrations in the basement and upstairs. Also, at the top of the box, the dashed lines indicate the periods over which PFT measurements were taken. The second box shows the basement air infiltration rate (solid line) and the radon source strength (broken line). The third box shows the basement, upstairs, and outdoor temperatures. The fourth box shows the differences between the outdoor/basement, subslab/basement, and upstairs/basement pressures. The greater these differences, the greater the relative depressurization of the basement. The points from which each line is plotted are the parameter averages during the tracer gas time period. Each time period is 10 to 14 days long.

3.0 CASE STUDY

To illustrate the application of some of the techniques just discussed, we will use test home #21 in Princeton that has experienced basement radon levels in the 200 pCi/L range for significant parts of the year. Our task was to analyze the cause of the problem and propose solutions. Part of the evaluation of the solution is how much energy will be used and how does the mitigation system influence the air exchange rate by exhausting interior air.

The house plan is shown in Figure 4 and points out that only part of the house has a basement; the remaining substructure is made up of shallow crawl spaces, approximately 25cm high, above a concrete slab.

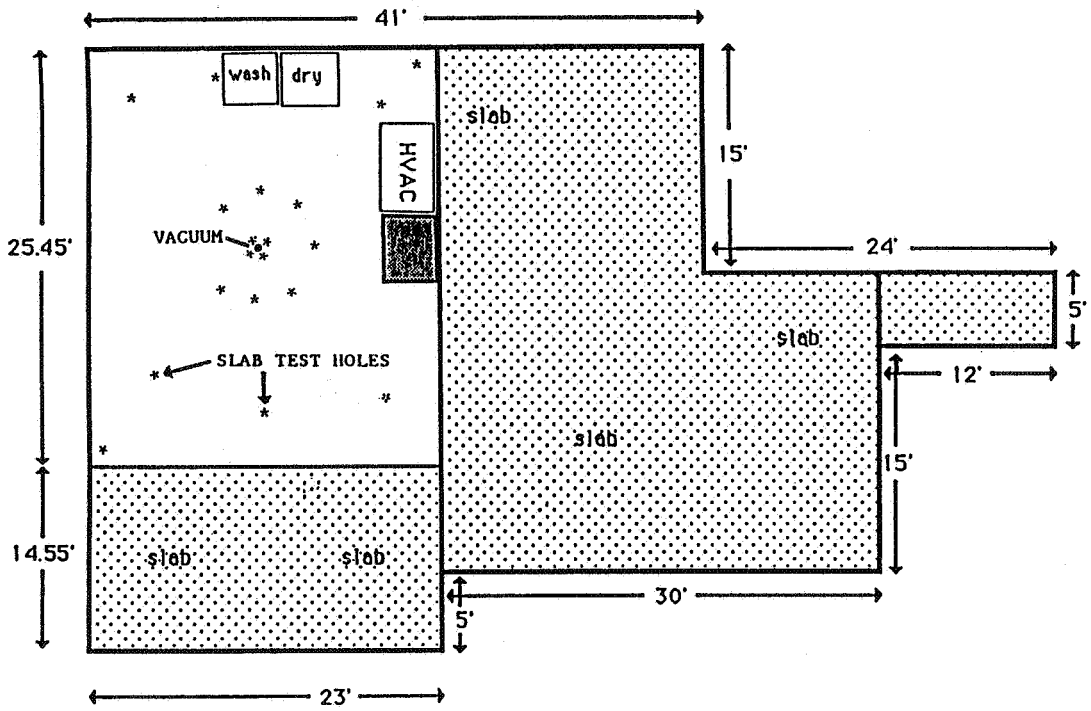

Figure 4. Plot plan of substructure of test house #21 pointing out basement and crawl space areas (noted slab) and details of where the suction is applied ●, and where pressure and velocity measurements are made *.

Tests of the soil immediately under the basement slab and in the hollow basement walls revealed radon levels no higher than 3,000 pCi/L, not exceptionally high for the geographic location and noticeably less than other test houses which exhibited much lower interior radon levels.

The blower door test revealed test house #21 to be very ordinary for its period of construction ~ 1960. The air exchange rates were shown to be approximately 13 ACH for 50 Pacals differential pressure whether or not the basement door is open. This is because of the warm air ducting system in the home. R^2 values are in the .999 range for each of the tests, indicating good repeatability. Clearly these results discourage one from being able to pressurize the basement as a mitigation scheme. ELA values also remain basically unchanged, thus yielding a similar diagnosis.

Influence of the heating method on interior radon concentrations can also be traced to the warm air ducts and the use of a central furnace fan that tends to mix the air in the house as well as generate a variety of pressures in different zones [10]. To point out these effects, experiments in test house #21 involved heating the house alternately with electric resistance heaters installed on the living level, and with a gas combustion furnace in the basement connected to a whole house air distribution system, driven by the furnace fan. The gas combustion heating system usually runs on an automatic setback mode, during which the thermostat automatically sets back to 55°F (13°C) at midnight and turns back up to its previous setting of 68°F (20°C) at 8:00 A.M. The data show that the furnace fan has a large effect on pressure differences across the building shell, and on the distribution of the radon indoors. These effects can be compared to the time periods when the furnace fan was not operating.

Figure 5 shows the radon concentrations, measured each half-hour, in the basement and in the subslab during gas combustion with automatic setback period along with the pressure differences between the outdoors and the basement and between the subslab and the basement, and the percent time the furnace fan is on during each half-hour. Figure 6 shows the same parameters for an electric heat period. The sharp rises in the pressure differences in Figure 5 coincide with the time the furnace fan is on. During the same periods, the basement radon decreases while the subslab radon increases. Increased mixing of the basement air with the upstairs air by the furnace fan causes the decrease in basement radon concentration. The variation in the upstairs radon during the furnace fan use, not plotted in Figure 5, closely parallels the pattern of the subslab radon concentration, and the upstairs radon increases by roughly the amount of radon the basement looses (considering the volumes involved).

Operation of the furnace fan is the main driving force for the variation in the radon concentration during the gas heating. The furnace fan depressurizes the basement compared to the outdoors by 1.8 Pa, and between the basement and the subslab by 0.9 Pa. The increased pressure difference increases the air infiltration into the basement. This increased air infiltration includes both soil gas and outdoor air. Each house will have a different ratio between the degree of leakiness to the soil gas and the degree of leakiness to the outdoors. This ratio determines whether increased air infiltration raises or lowers the indoor radon concentration. If, for example, the basement is very leaky to outdoor air but fairly well isolated from the soil gas, outdoor air will make up most of the increased infiltration and thus dilute the basement radon. It would be helpful to know how much this quantity varies among different houses. If it remains relatively constant among similar housing types built on soils with similar permeabilities, it may be possible to design a measurement to characterize the potential radon problem on a building site based on the soil permeability and radon content. With the limited data available to date there is no indication that generalization can be made at this time.

The pressure field can be established even if the soil is rather tightly packed. Flow measurements quickly reveal the degree of connectivity that is present. One researcher has referred to this

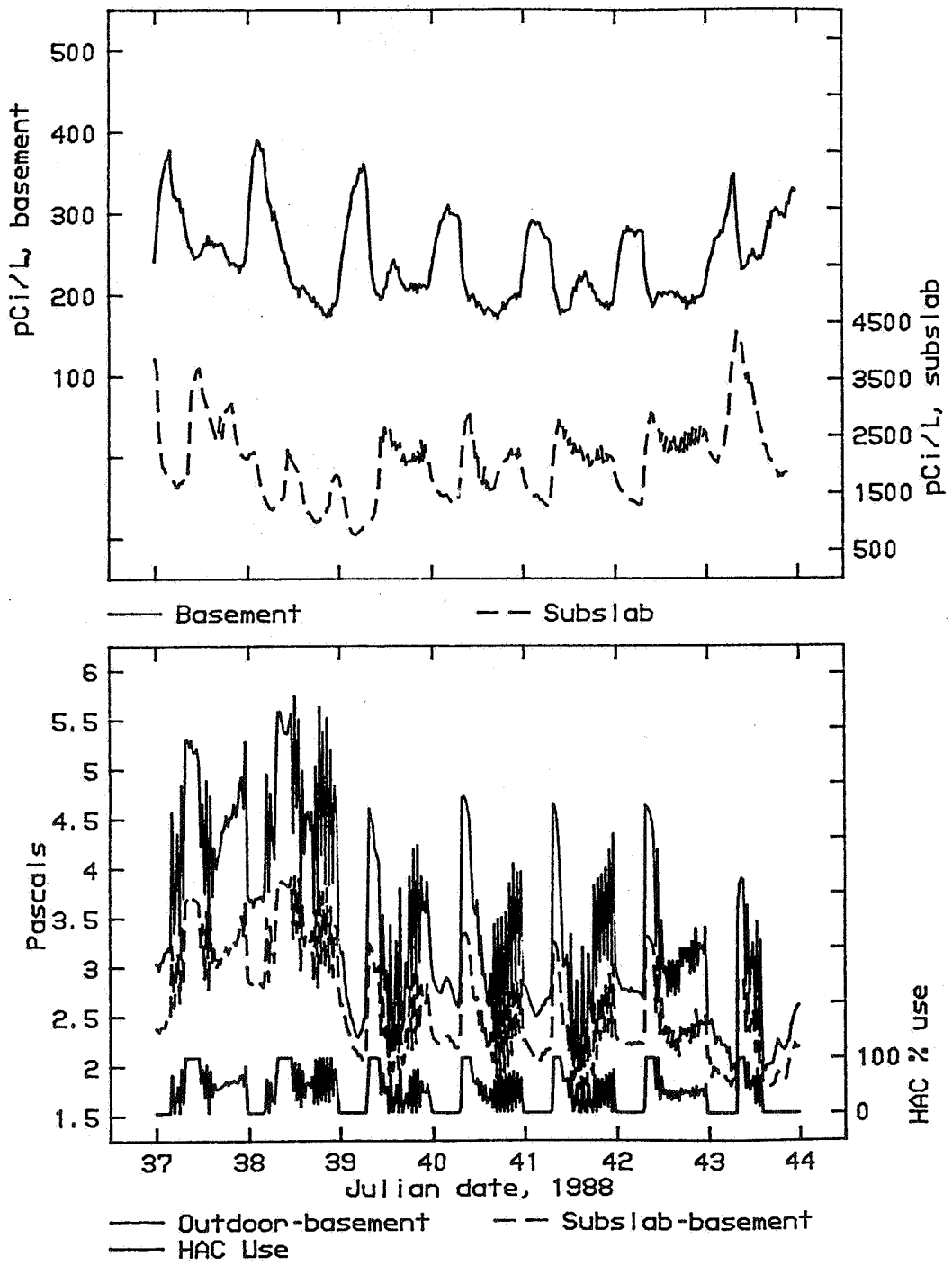

Figure 5. Half-hour radon concentrations in the basement and subslab for eight days in February 1988. Pressure differences between outdoors and basement, and subslab and basement are shown for the same period correlated to furnace fan use (heating, air conditioning, HAC) for the gas combustion form of heating.

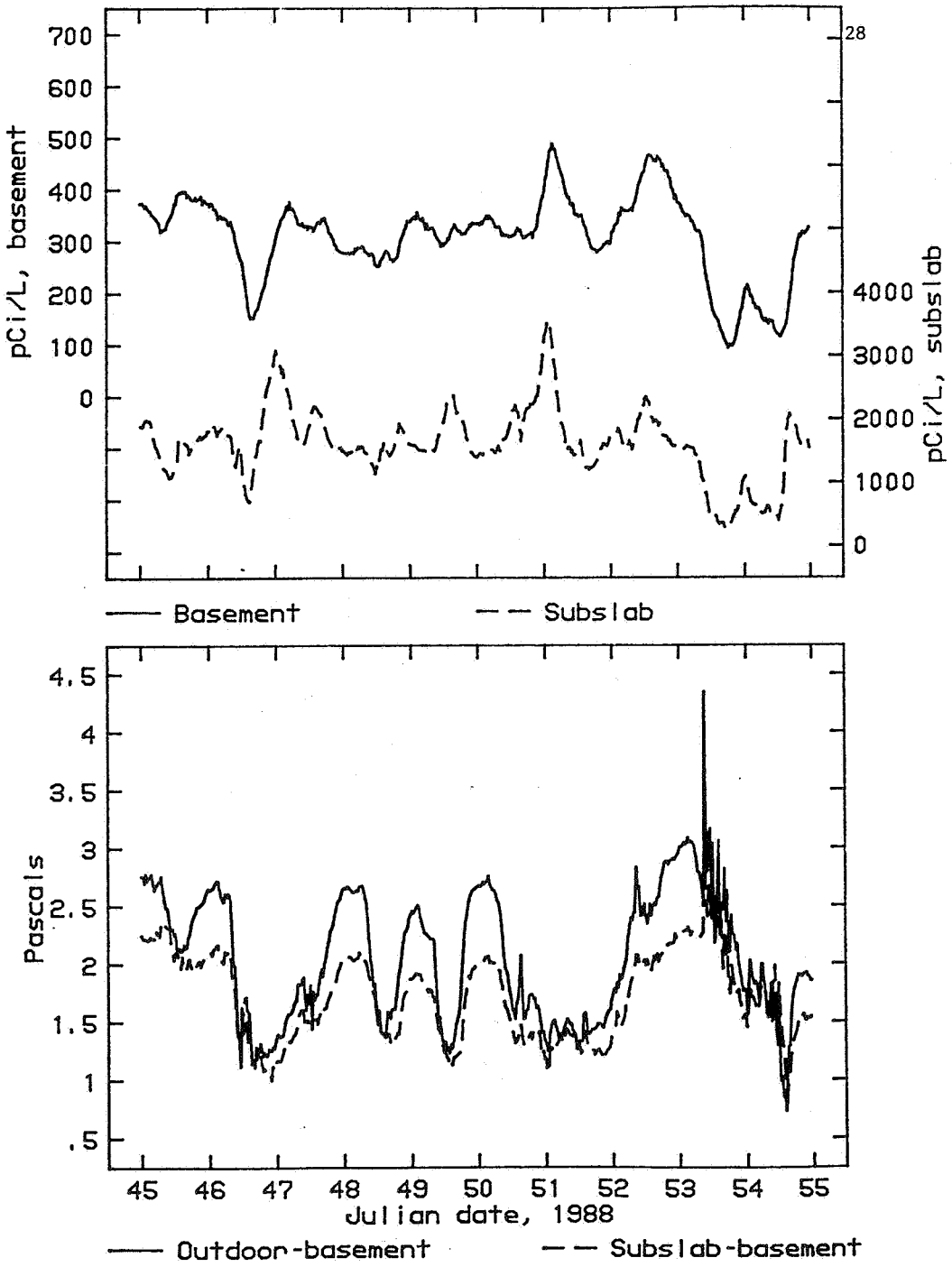

Figure 6. Electrical heating of the same home as in Figure 5 pointing out the lag between basement radon and subslab radon concentrations.

measurement technique and interpretations as a "blower floor" related to a blower door.[6] Typical of these measurements is the plot of data from house #21 shown in Figure 7. The relatively even radial distribution of pressure can be seen in the profile map, however, the wild variations in flow rates which are not shown appear to indicate no simple radial "highway" but rather the airflow under the slab is searching for paths of easier flow to the exhaust point.

Tests of soil porosity, connectivity, radon source strength, etc., all reveal key characteristics of a particular site and building. We are trying to finalize a rapid diagnostics protocol emphasizing what key measurements should be made. The problem is that the protocol should not extend beyond two hours if it is to have an impact in the market place. Unfortunately, it is difficult to stay within the two-hour constraint and supply all the needed information for the proper choice of mitigation system. The goal is to avoid the high failure rate, greater than 50%, of systems that fail to perform within the radon guidelines over the long term.

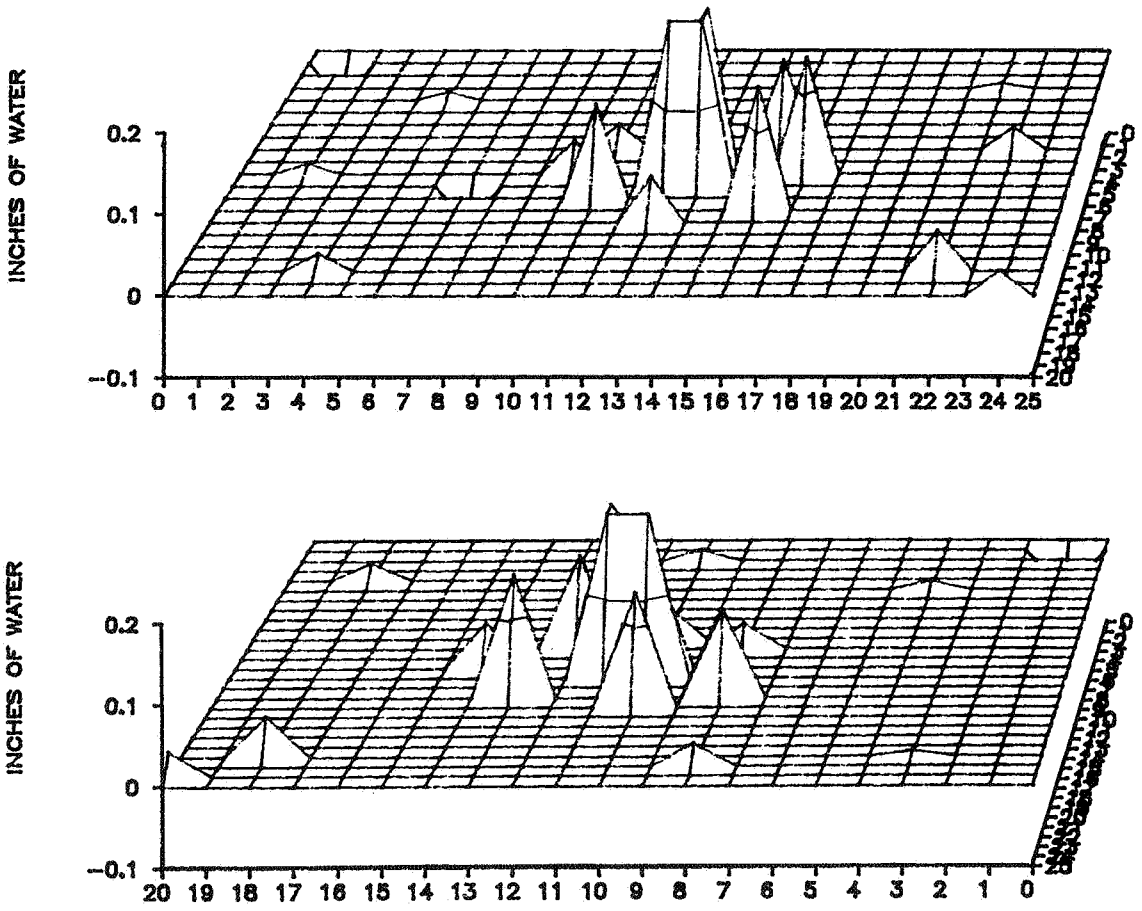

Figure 7. Graphical representation of the pressure profiles viewed from two directions in house #21. The individual points where the pressure measurements have been made are noted in Figure 4. These are negative pressures because of the industrial vacuum cleaner which has been used in this diagnostic procedure.

4.0 SUMMARY

We hope this exposure to the world of radon diagnostics and mitigation, with the realization of how closely many of the methods coincide with previous experiences in air infiltration measurement, will encourage you to pose new innovations in this discipline. The substructure of buildings can prove to be a very difficult test site. One desires to search out radon entry points, but one is confronted with the fact that any oversight of leakage area may mean no radon reduction. Small temperature variations between soil gas and substructure, as well as the presence of porous media such as block walls, encourages radon intrusion. Test procedures are not only concerned with airflow paths and therefore the paths of radon through the home, but also pathways beneath the structure can be assessed by methods using both pressure and flow indications. These methods evaluate connectivity and the ability to mitigate. Mitigation can take many forms but the efficient subslab depressurization system has been demonstrated to prevent more than 90% of the radon from entering the home. In the radon removal process, the system may be removing as much as ten times the natural flow of radon from the soil, possibly causing higher ambient levels of radon near the home. Interior conditioned air is normally removed as part of the mitigation procedure and these energy implications can outweigh the electrical costs for the mitigation system fan. With all of these factors in mind, well thought-out diagnostic procedures are essential if the job is to be done correctly. The radon research community welcomes new thinking on this subject as it works toward more cost effective and durable solutions to this indoor air quality problem which ranks very high in terms of human health risk.

ACKNOWLEDGMENTS

The authors wish to acknowledge the support of the Building Systems Division, Office of Building and Community Systems, United States Department of Energy which has funded advancements in PFT and CCTG technology so necessary for the research described here. We also wish to acknowledge the sponsorship of the U.S. Environmental Protection Agency, Air and Energy Research Laboratory whose responsibilities are directly related to radon mitigation.

REFERENCES

1. MATTHEWS, T.G. et al.,
"Investigation of radon entry and effectiveness of mitigation measures in seven houses in New Jersey: mid-project report," Oak Ridge National Laboratory Report, ORNL/TM-10671, 1988.

2. NAZAROFF, W.W., MOED, B.A., and SEXTRO, R.G.,
Soil as a source of indoor radon: generation, mitigation, and entry," Chapter 2 of Radon and Its Decay Products in Indoor Air (Editors Nazaroff, W.W., and Nero, A.V.), John Wiley and Sons, Inc., 1988.

3. SEXTRO, R.G., MOED, B.A., NAZAROFF, W.W., REYZAN, K.L., and NERO, A.V.,
"Investigations of soil as a source of indoor radon," Chapter 2 of Radon and Its Decay Products, (Editor Hopke, P.K.) ACS Symposium Series, American Chemical Society, Washington, DC, 1987.

4. DEPIERRO, N. and CAHILL, M.,
"Radon reduction efforts in New Jersey," Proceedings of the EPA Symposium on Radon and Radon Reduction Technology, Colorado, Oct. 1988.

5. Section 301 of the National Indoor Radon Abatement Act, U.S. Congress H.R. 2837, 1988.

6. HARRJE, D.T. and HUBBARD, L.M., Proceedings of the radon diagnostics workshop, April 13-14, 1987. EPA Document EPA-600/9-89-057, June 1989, also HARRJE, D.T., HUBBARD, L.M., and SANCHEZ, Diagnostic approaches to better solutions of radon IAQ problems, Healthy Buildings '88 - Planning, Physics and Climate Technology for Healthier Buildings, Vol. 2, Swedish Council for Building Research, Stockholm, Sweden, D20:1988, 1988 pp. 143-152.

7. HENSCHEL, D.B.,
"Radon reduction techniques for detached houses - technical guidance," (2nd Edition) Air and Energy Engineering Laboratory, Environmental Protection Agency, EPA/625/5-87/019, 1988.

8. "Standard practices for air leakage site detection in building envelopes," Standard E 1186-87, 1988 Annual Book of ASTM Standards, Section 4, Construction, Vol. 04.07, ASTM, Philadelphia, PA. 1988, pp. 885-889.

9. HARRJE, D.T., HUBBARD, L.M., GADSBY, K.J., BOLKER, B., and BOHAC, D.L.,
"The effect of radon mitigation systems on ventilation in buildings," ASHRAE Transactions 1989, Vol. 95, Pt. 1.

10. HUBBARD, L.M., BOLKER, B.M., GADSBY, K.J., HARRJE, D.T. and SOCOLOW, R.H.,
"Investigation of radon entry into dwellings and the effect of selected radon mitigation techniques - Final Report 1988," Princeton University Center of Energy and Environmental Studies, December 1988.

Discussion
Paper 14

Jorn T. Brunsell (Norwegian Building Research Inst.)

Have you tried to blow room air into the ground to make a "pillow" of radon free air under the house?

David Harrje (Princeton University, USA)

This method can be used to pressurize the basement/crawl space if there is a good preparation between basement and living space (i.e. an airtight floor). If air is blown under the slab, the results have been mixed. The danger is that while a higher pressure may be established under the slab to prevent radon entry, because of openings in the wall construction, radon may be forced into the building. Using depressurization, walls tend to be evacuated of radon at the same time the subslab is purged. Some studies in the Pacific Northwest, USA, have shown subslab pressurization to actually outperform depressurization when soil conditions and construction features were favourable.

PROGRESS AND TRENDS IN AIR INFILTRATION
AND VENTILATION RESEARCH

10th AIVC Conference, Dipoli, Finland
25-28 September, 1989

Paper 15

WIND PRESSURES ON LOW-RISE BUILDINGS AN AIR INFILTRATION ANALYSIS

Jan Gusten

Building Aerodynamics Research Group
Division of Structural Design
Chalmers University of Technology
Gothenburg
Sweden

ABSTRACT

The distribution of wind pressure on a building envelope is governed by the size and shape of the structure and the turbulence characteristics of the wind. Observation of the mean wind pressures shows that surfaces are divided into pronounced zones of positive and negative pressure. The turbulence gives rise to fluctuating pressure components of appreciable magnitude. This fact changes the prerequisites of the ventilation for a given volume.

The pressure in the cavity behind the facade materials depends on the external pressures over the facade. A levelling, or smoothing, of the pressure fluctuations can take place, depending on the cavity design and permeability distribution.

The wind pressure spectrum shows that the greater part of the turbulent energy is concentrated at frequencies below 1 Hz. Full–scale measurements have shown that the fluctuations, which are quantified by the calculated variance of the spectrum, are of the same order of magnitude as the mean pressure. The degree of correlation between fluctuating components of the wind pressure on different parts of the building envelope is low. Because of this, the interchange of air is at all times based on a varying pressure distribution, and the participation of different leakages is variable. In the case when air infiltration can be expected to account for a considerable part of the total air exchange rate, the methods of calculation used should take into account the real wind characteristics and the response of the building to wind fluctuations.

LIST OF SYMBOLS

$H(f)$	transfer function
$S_{cav}(f)$	the power spectrum for the pressure difference between the cavity pressure and the internal pressure (Pa^2/Hz).
$S_p(f)$	power spectrum for wind pressure (actually the spectrum for the difference between external pressure and internal pressure) (Pa^2/Hz).
$S_{p,cav}(f)$	cross spectrum between wind pressure and pressure in the cavity (Pa^2/Hz)
f	frequency (Hz)
$\gamma^2(f)$	coherence function
σ_p	standard deviation for wind pressure fluctuations (Pa)
τ	time lag (sec)

1 INTRODUCTION

The rate of air exchange is determined by the degree of air tightness, the distribution of the leaks on the surface of the building and the indoor and outdoor climatic conditions. Wind environment, temperature–based variations of air density and the driving mechanisms in ventilation systems give rise to pressure differences across the building surface, resulting in air flow through existing leakages. The interplay between climate and technical systems can sometimes result in undesirable consequences regarding hygiene, durability and damages.

The purpose of this paper is to elucidate the problem of air infiltration by considering air flow–structure interaction. Wind pressure distributions on low–rise buildings are exemplified especially for moderate wind speeds and the importance of pressure fluctuations is analysed.

The work is concentrated upon the wind, acting as a driving force for air infiltration. In this respect, special attention is paid to the influence of fluctuations in wind speed and direction. Methods of spectral analysis are used to describe the energy content of the fluctuating parts of the wind pressure at different frequencies and wavelengths. Comparisons between wavelengths and the dimensions of existing leakage areas can give information concerning the contributions of fluctuations to the rate of air infiltration. The transformation to the frequency domain makes it possible to study the effects on air infiltration due to variations of wind pressures. In addition, the analyses provide conditions for describing existing connections between pressures on different surfaces of the building.

2 FULL–SCALE MEASUREMENTS OF WIND PRESSURES

A measurement program, embracing full–scale measurements on four single –unit dwellings, has been carried out. The objects, which are comparatively newly built, comprise one one–storey building, two buildings of 1½ storeys, and one of 3 storeys. The insulation standard and the levels of air–tightness corresponds to the Swedish Code of Practice. The measurements include registration of pressure differences between external and internal pressure on facade units and roofs. Measurements have also been performed in cavities, attics and crawl spaces and pressure differences between different storeys were recorded. The measurements were carried out during relatively calm weather conditions.

A survey of problems related to low wind pressure registrations includes an assessment of the qualities of the equipment, the difficulty of calibration and choosing relevant reference pressures. Besides the qualities of the measuring system, the characteristics of the measurement points are of great importance. In a situation where measurement errors can be considerable, a well– hought–out strategy for the experiments and a careful design of the measurement method with regard to all possible influencing factors is required in order to improve the accuracy.

3 RECORDED WIND PRESSURE DISTRIBUTIONS BASED ON STATIONARY WIND PRESSURES

The distribution of pressure over a 1½–storey building is illustrated in Figure 3.1.

For steady flow conditions, the pressure distribution over the building can be described by mean pressures representing different periods of time and different elements of the building envelope. The pressure distribution on the building becomes that expected for a given wind direction. Definite zones with positive and negative pressures arise. The mean pressures on different parts of the building surfaces are correlated. Calculations show that there is a balance between the air volumes which move in and out of the building.

The internal pressure is determined by the pressure distribution, the outdoor and indoor temperatures, the air tightness of the building and the effect of a mechanical ventilation system, if present. The internal pressure of the building is estimated from the state of equilibrium for the inflow and outflow volumes, whereby differences in density for the flows are taken into consideration. This model for describing the air exchange is usually used for the calculation of energy losses through ventilation and it gives a simplified description of the air infiltration process.

There are several weaknesses inherent in the calculation procedure, which appear when it is applied with input data from full–scale measurements. There is a need for additional information about the pressure distribution for different climatic conditions and the distribution of leaks over the building envelope. Input data based on pressure coefficients obtained from the Swedish Code of Practice give, in comparison with data from full–scale measurements, a larger number of calculated air changes.

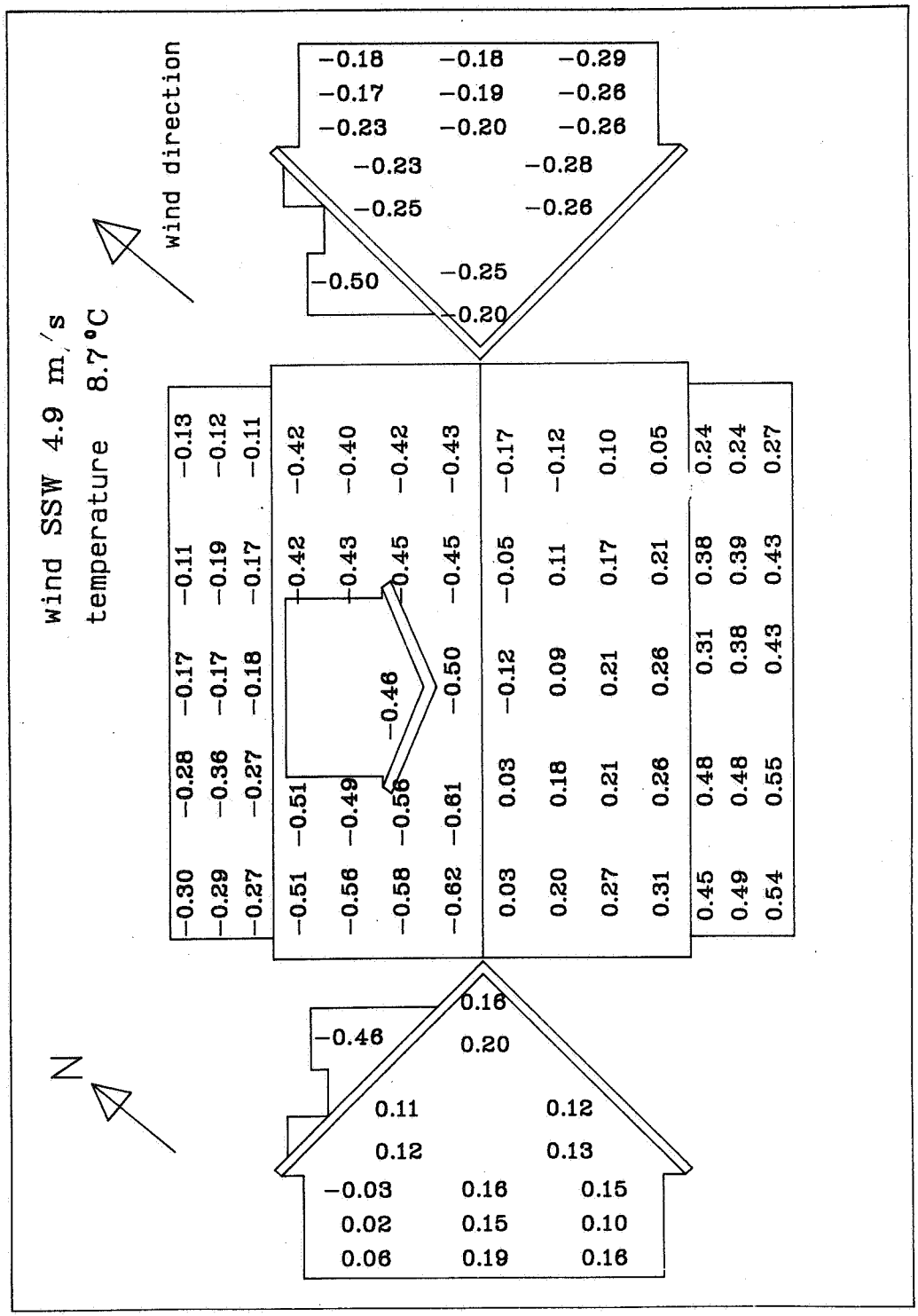

Figure 3.1 Pressure coefficients, example of pressure distribution.

4 REGISTERED FLUCTUATIONS OF PRESSURE DIFFERENCES

4.1 External pressures

The wind pressure distribution on a building is in reality characterized by large variations about the mean pressure. Changes in speed and direction give rise to a continually varying pressure distribution without any distinct zones of positive and negative pressure. The fluctuations of the wind speed and their relation to the wind pressures on a surface vary stochastically, like the wind pressure. Time–related and spatially–related fluctuations in wind speeds and direction characterize the level of turbulence, which can be described by means of fundamental statistical methods. The external pressure on a surface, for example, can be described by three quantities: mean value, variance, and the spectrum of the fluctuating component. The mean and the fluctuating pressure on the surfaces give rise to an exchange of outdoor and indoor air through leaks in the construction. Measurements show that magnitude of the fluctuations, can be of the same order as the mean pressure.

The degree of turbulence in the oncoming wind, together with the effect of the shape and size of the building, the surroundings and the terrain, determines the characteristics of the pressure fluctuations of the external pressure on a facade. A quasi–steady approach to wind loads gives adequate results only for pressures on the windward side. The separated flow on the roof and the leeward sides of the building can be described by eddies of different size. Their scale is generally less than that of the atmospheric turbulence. Large eddies give a comparatively uniform pressure distribution, while small eddies have a local effect.

If the variations in wind speed are known, it is possible, on the windward wide of a structure, to calculate pressure distributions by employing Bernoulli's equation. This situation cannot be applied to the leeward side. Because of friction, characterized by a broad, extremely turbulent boundary layer, the air flow separates from the building surface. Thus, the fairly simple relation between wind speed and wind pressure on the windward side becomes more complicated on the leeward side.

The degree of correlation between the pressures at any two arbitrarily selected points depends on the relation between the dimensions of the building and the length scales of the energy contained in turbulence eddies. The scale of turbulence is usually considerably larger than the size of the building. The building can be observed in a wind pattern of almost uniform structure of varying intensity. The pressure differences, caused by eddies acting on the windward and leeward sides, will be correlated. This is not so for the differences generated by the building. Because of this, the resulting wind pressures on the windward and leeward sides do not become fully correlated. A study of external pressures on different parts of walls, exemplified by the windward and leeward sides in Figure 4.1.1, gives for all cases a very low – in most cases an almost non–existent – degree of correlation.

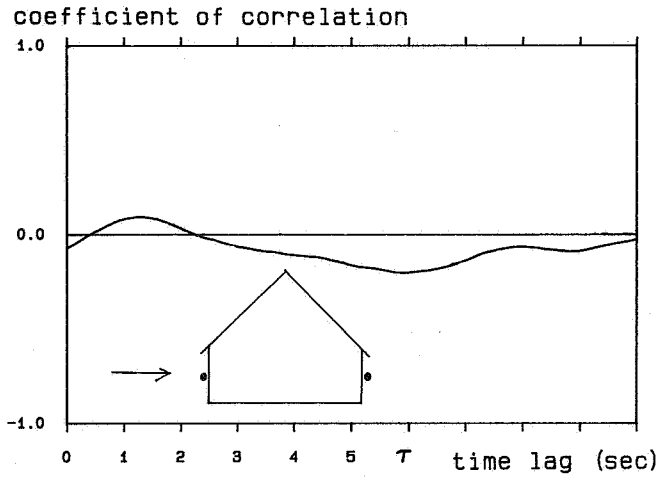

Figure 4.1.1 Coefficient of correlation between external pressures on windward and leeward sides

The low degree of correlation between windward and leeward sides is only of interest when the fluctuating parts of the wind pressure are taken into consideration. Mean pressures between different building surfaces are correlated, due to the long averaging period.

Pressures over a measurement object are exemplified in Figure 4.1.2 where density functions, based on measurement data, have been determined. The pressure differences are those expected with positive pressures on the windward side and negative pressures on the leeward side. The variation of the pressure differences is considerable. The random variation of wind in speed and direction with time indicates that the external wind pressure on facades and roof is a noisy process. The fluctuations are unequal in size on different parts of the building. The deviation from the mean value is, for example, larger on the windward than on the leeward side.

Spectra for wind pressures on the facades are exemplified in Figure 4.1.3. The dominating energy content is found in frequency intervals below 1 Hz. Shapes and amplitudes are comparable for spectra representing different surfaces. However, the coherence function for opposite facades has low values. For surfaces with similar orientation, for example facade and roof, the coherence rises.

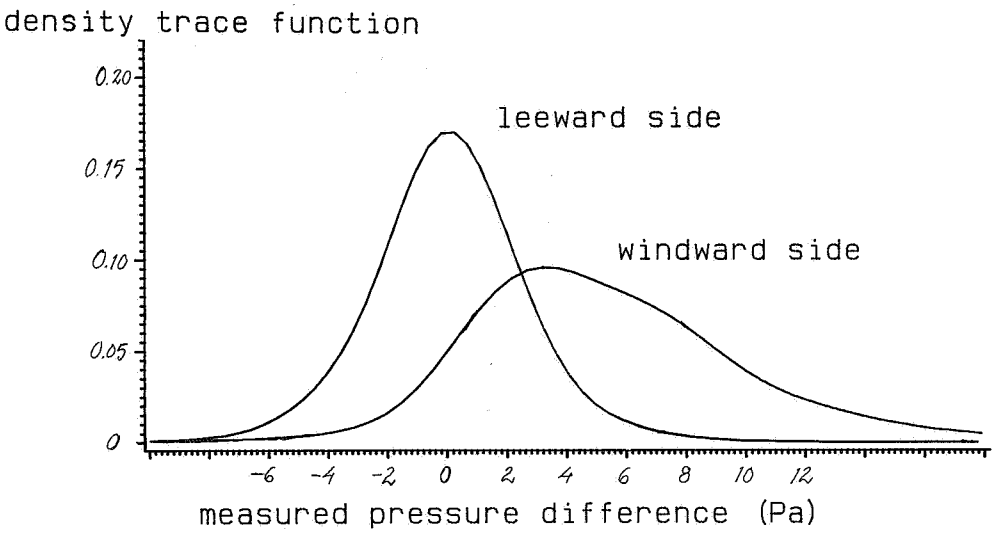

Figure 4.1.2 Probability density functions (density trace functions) describing wind pressure on windward and leeward sides

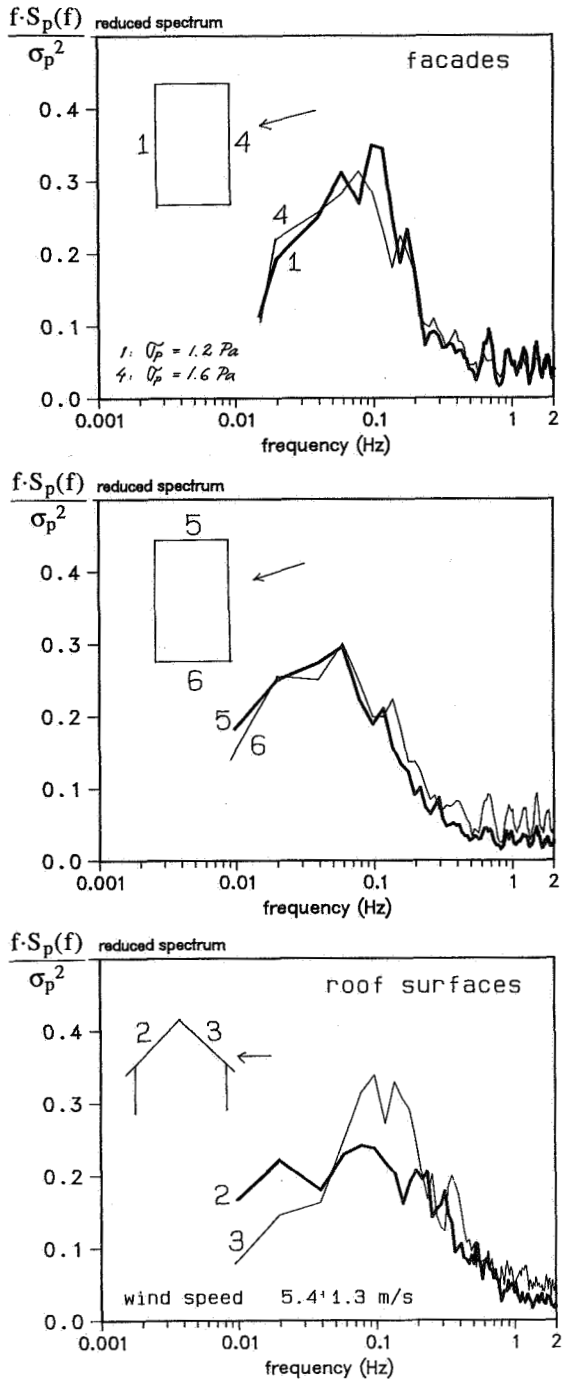

Figure 4.1.3 Comparisons between spectra of wind pressures on facades and roof

4.2 Ventilated cavities behind the external walls

Normally, external walls are designed with a cavity behind the facade material. The cavity is supposed to have an equalizing, and in most cases also a reducing, effect on the external pressures. The degree of smoothing is determined by the distribution of leakages on the facades and the design of the cavity, especially with respect to air intakes and exhausts. Hence, the cavity has an important influence when wind is acting as a driving force for air exchange.

Generally, the pressure is reduced and damped in the cavity. However, measurements show that this is not always the case. For a one–storey dwelling, the external pressures on facades have been compared with pressures in the cavity. The measurement point in the cavity is situated just behind the corresponding point on the facade. The construction of the cavity with horizontal nailing battens restricts the vertical air flow, see Figure 4.2.1. In practice the air layer is thereby divided into a number of bays.

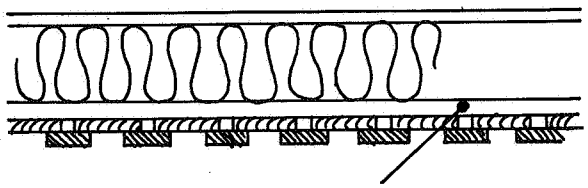

Figure 4.2.1 The appearance of the air cavity, horizontal section

On the windward side, the expected pressure reduction across the exterior facade material fails to appear. As a result of the design of the cavity, the pressure increases behind the facade. The mean value of the pressure difference between the pressures in the cavity and inside the building increases from 1 to 2 Pa compared with the difference between external and internal pressure. No appreciable damping of the fluctuations in the cavity is indicated.

On the leeward side, slightly negative pressure differences on the facade change into positive ones in the cavity, as shown in Figure 4.2.2. The curves indicate a smaller variation around the mean value in the cavity as compared to facade pressure.

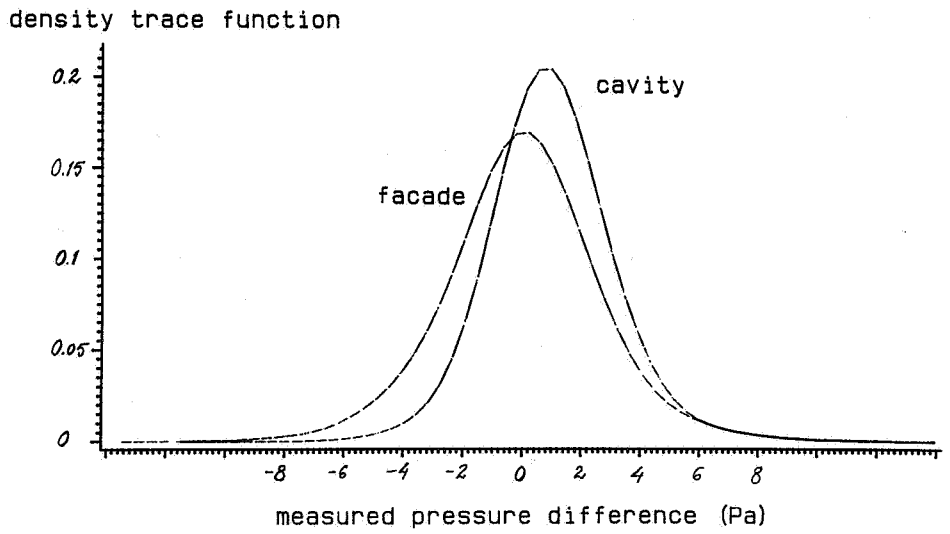

Figure 4.2.2 Probability density functions (density trace functions) describing wind pressure on the facade and in the cavity, leeward side.

Fluctuations of pressure differences are illustrated in the form of reduced spectra in Figure 4.2.3. On the windward side, the spectra for facade and cavity become almost equal. A peak is noted near to the frequency 0.1 Hz. A high degree of similarity between facade and cavity is also found on the leeward side. The shapes of the spectra are similar in character on the two sides.

The connection between facade and cavity is good for all facades, as can be seen from the degree of coherence exemplified in Figure 4.2.4. The coherence function, $\gamma^2(f)$, is defined as

$$\gamma^2(f) = \frac{|S_{p,cav}(f)|^2}{S_P(f)\ S_{cav}(f)} \qquad (4.1)$$

The relation between external pressure on the facade and the corresponding pressure in the cavity has also been estimated in terms of transfer functions, H(f). These functions, illustrated in Figure 4.2.5, make it possible to describe the pressure conditions as

$$S_{cav}(f) = |H(f)|^2 \cdot S_P(f) \qquad (4.2)$$

where

$S_P(f)$ is the spectrum for the pressure difference between facade and internal pressure,

$S_{cav}(f)$ for that between cavity and internal pressure, and

$S_{p,cav}(f)$ the cross spectrum between facade and cavity.

For the frequency range of interest, the magnitudes of the transfer functions are approximately $0.7 - 0.9$.

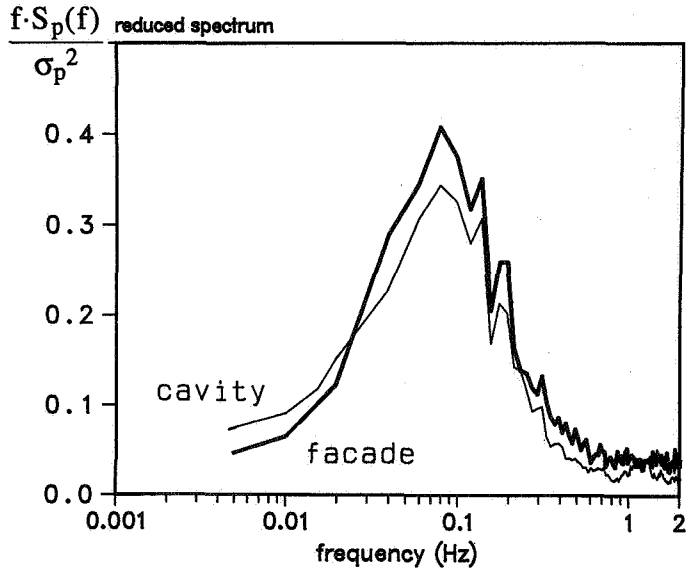

Figure 4.2.3 Spectra illustrating the variations in pressure difference for facade–cavity on the windward side.

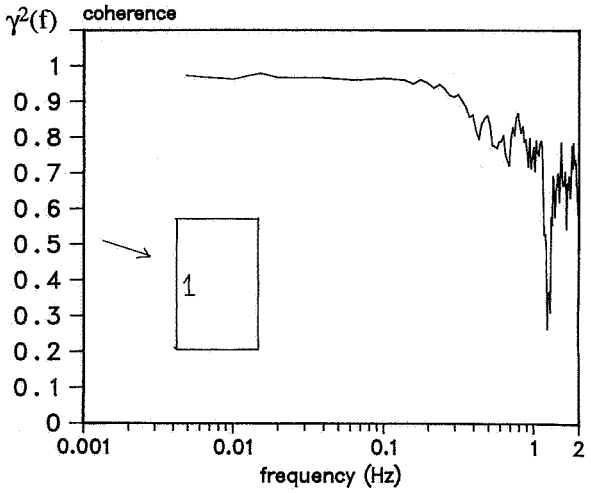

Figure 4.2.4 Coherence functions between facade and cavity for the windward side of the building

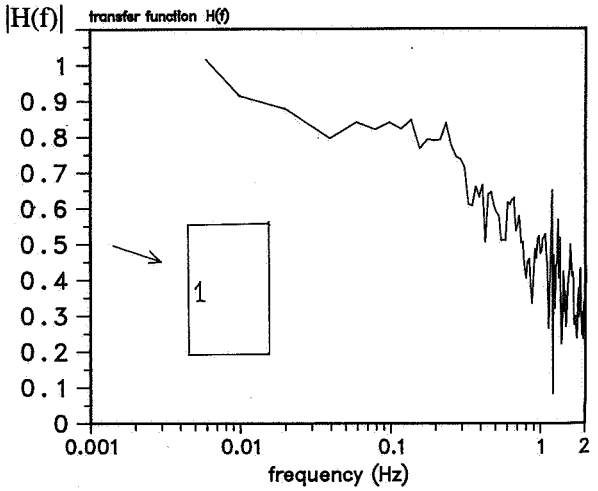

Figure 4.2.5 Transfer functions between facade and cavity, windward side

The strong relation between wind pressure on a facade and the pressure in a cavity just inside the wall is illustrated by the cross–correlation between the pressures. A sampling of recorded pressures at a sampling frequency of 50 Hz, i.e. equivalent to 0.02 seconds, shows that the cavity pressure on the leeward side of the building has a time delay of about 0.2 seconds with respect to the local external pressure (see Figure 4.2.6.). This delay is not observed on the windward side.

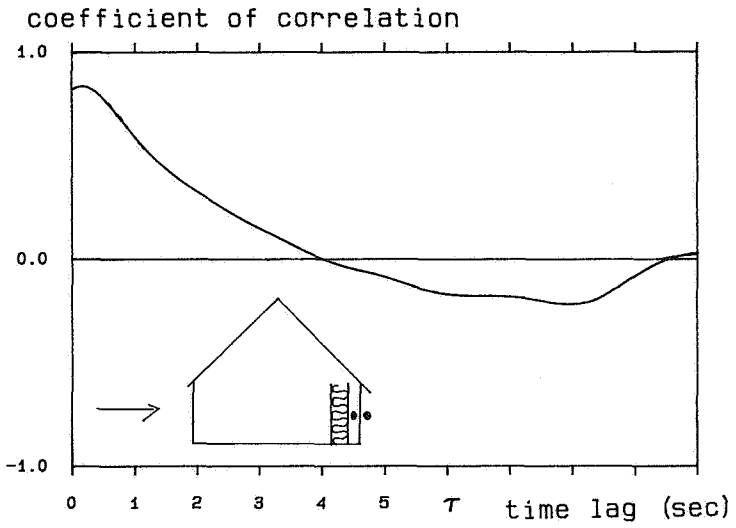

Figure 4.2.6 Coefficient of correlation between pressures on the facade and in the cavity, leeward side

The attic gives a marked smoothing and damping of the fluctuating parts of the pressure differences acting over the roof of the building. The energy content for the fluctuating wind pressure on the roof is greatly reduced in the attic, illustrated by spectra in Figure 4.2.7. The number of air changes in the space is in most cases large. The ventilation of the attic is to a large extent dependent on wind conditions with regard to both speed and direction.

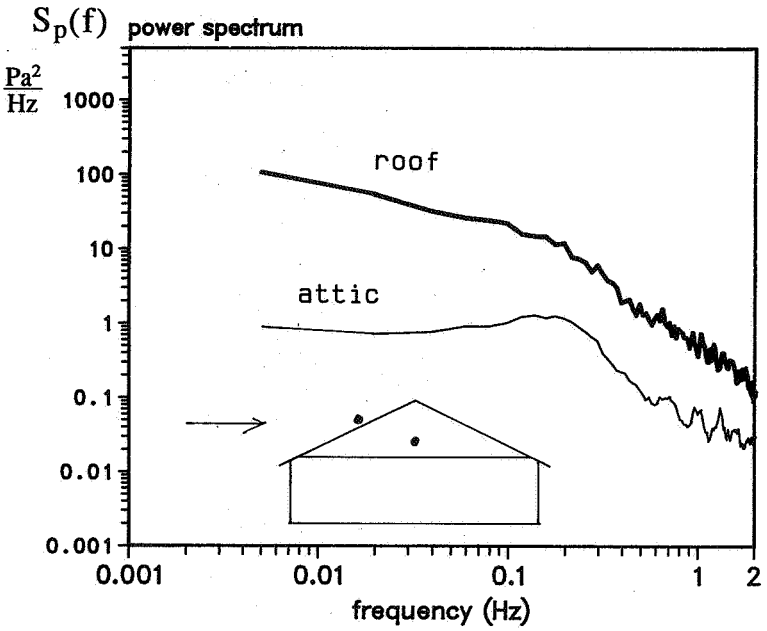

Figur 4.2.7 Spectra representing fluctuations in pressure on the roof and in the attic

5 AIR INFILTRATION CAUSED BY FLUCTUATING WIND PRESSURE, CONCLUSIONS

Low degrees of correlation and coherence between the pressure fluctuations on different parts of the building surfaces indicate a continually varying pressure distribution. A more exact assessment of the contribution from the fluctuating wind pressure to air infiltration requires information about the characteristics of the fluctuations of external pressures and the geometry of the leaks and current air flows in front of and through the leaks.

Spectral methods can be used to estimate the parts of the fluctuations of wind speed and wind pressure which contribute to the rate of air infiltration. Wind spectra describe the frequency interval containing the major part of the energy content. By means of spectra for the pressure differences across a wall, the extent of the fluctuations can be compared with the dimensions of the structure and the leaks. It thereby becomes possible to judge the degree to which the fluctuations have an influence on the air flow through leaks. The exchange of air through openings, for example round windows, is caused by a pulsating flow, which is complicated by the fact that air is transferred in and out simultaneously.

The majority of cracks in facades can be presumed to have a width of between 0.5 and 3 mm. For a wind speed of 2 m/s, the gust wave length has a magnitude of between 20 metres at 0.1 Hz and 2 metres at 1 Hz. A comparison with the size of a leak through an external wall indicates that a uniform field of pressure is built up over the leak (compare Figure 5.1). High frequencies are needed, e.g. a wavelength of 0.1 metres corresponding to the frequency 20 Hz, to obtain a number of local pressure fields developed over the leak, without any mutual relation or correlation.

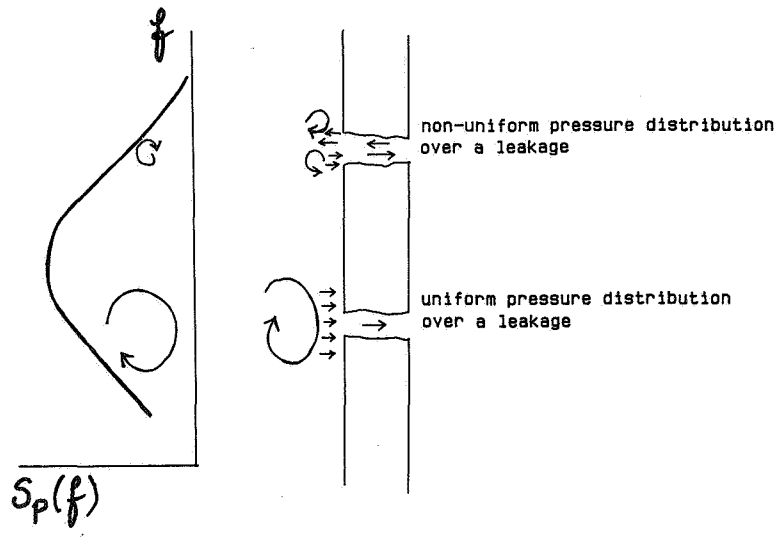

Figure 5.1 Illustration of local pressure fields

Full–scale measurements show that the pressure fluctuations can be characterized as extremely low–frequency, in the frequency range below 1 Hz, and the majority can therefore give contributions to air infiltration. The geometric form and dimensions of the leakages give the conditions for the air flow to penetrate through a construction and subsequently be mixed with the inside air. A part of the pressure fluctuations which are squeezed into the opening, or the leak, is not transmitted the whole way and does not take part in the exchange of air between the inside and the outside.

In the case where air infiltration can be expected to give rise to a considerable part of the total air exchange rate, the methods of calculation used should take into account the known characteristics of wind and the building's response to wind fluctuations.

REFERENCES

GUSTÉN, J *Wind pressures on low–rise buildings. An air infiltration analysis based on full–scale measurements.* Publication 1989:2, Division of Structural Design, Chalmers University of Technology, Gothenburg.

Discussion
Paper 15

Earle Perera (Building Research Establishment, UK)

1. Could you describe briefly your pressure measuring system including what you use as your reference back-off pressure?

2. What is the correlation between external windward pressure and internal pressure?

Jan Gustén (Chalmers University, Sweden)

1. The measuring system consists of electronic pressure transducers and anemometers for wind speed and wind direction, plastic tubes of length 25 metres and FM tape recorders. A transfer function H(f) has been determined for the tubes. The results are either related to the internal pressure and/or to a static reference pressure at the height of 10 metres.

2. For the objects measured the variations in the internal pressure are very small.

J-M Fürbringer (EPFL, Switzerland)

If you measure pressure difference you have the influence of the stack effect. How do you treat this point?

Jan Gustén (Chalmers University, Sweden)

Registrated pressure differences between the external and internal pressures include wind loads as well as variations in air density. During each measuring period the outdoor and indoor temperatures are constant. Consequently, the pressure fluctuations depend only on variations in wind speed and wind direction.

PROGRESS AND TRENDS IN AIR INFILTRATION
AND VENTILATION RESEARCH

10th AIVC Conference, Dipoli, Finland
25-28 September, 1989

Paper 16

VENTILATION AND AIRTIGHTNESS IN ENERGY BALANCE ANALYSES

Ake Blomsterberg

Dept of Building Science
Lund Institute of Tech.
Box 118
S-221 00 Lund
Sweden

Dept of Energy Systems
National Testing Inst.
Box 857
S-501 15 Boras
Sweden

SYNOPSIS

The air exfiltration part of ventilation is often difficult to determine and its part of the energy balance is therefore usually determined as a remainder or given a constant value.

This paper examines ventilation systems in six different modern houses. The constant concentration tracer gas technique tended to underestimate the total ventilation. A simplified theoretical one-zone model made accurate estimations of the air exfiltration. For detailed information on air flows a multi-zone network model was useful.

Different levels of airtightness should be required depending upon the ventilation system. It is recommended to couple predictions with tracer gas measurements. Determining the energy balance, e.g. using a constant air change rate for the mechanical and/or natural ventilation is in most cases inaccurate, unless the house is very tight.

1. INTRODUCTION

Ventilation in buildings occurs as a consequence of natural ventilation and through the use of purpose provided ventilation. The air exfiltration part of ventilation is often difficult to determine for different boundary conditions. The influence of ventilation on the energy balance of a residential building is therefore usually determined as a remainder together with internal gains from people and the sun or given a constant value.

This paper summarizes a report (Blomsterberg) on one-family houses, examining:
- the influence of ventilation and airtightness on the energy balance
- methods of separating out the ventilation heat losses from the energy balance
- the performance of different ventilation systems.

The results are based on performance monitoring and evaluation during two years of six modern one-family houses with different ventilation systems. Two of the houses are equipped with mechanical exhaust-supply ventilation and three with mechanical exhaust ventilation. The ventilation systems were studied during several one-week periods using the constant concentration tracer gas technique. The airtightness of the houses was examined using the fan pressurization technique. The ventilation was predicted with a simplified theoretical one-zone model (the LBL-model) and a multi-zone network model (MOVECOMP).

2. TEST METHODS

2.1 Airtightness

The standard method for finding the leakage function of a building is fan pressurization. According to the Swedish standard for fan pressurization (SS 02 15 51) all openings in the exterior envelope intended for ventilation purposes must be sealed before the test is performed. For the purpose of modelling air infiltration a test was also made with open supply vents part of an exhaust fan ventilation system and with open vertical shafts part of an unpowered ventilation system.

A door-leaf is replaced by a sheet of plywood. An air flow generating and metering system is connected through the sheet, and a sensing tube from the micromanometer continues through the sheet to the outside. The air flow rate is recorded at a number of pressure differences, positive and negative, and the test results presented in a diagram with pressure difference and air flow/air change rate on the axes. The requirement of the Swedish Building Code of 1985 is 3.0 air changes per hour at 50 Pa, for a detached house.

2.2 Ventilation

The most straightforward method of measuring total ventilation rate i.e. the combined effect of purpose provided ventilation and natural ventilation is to measure it directly. There are many ways of measuring total ventilation, and almost all of them involve a tracer gas, which permits the indoor air to be labelled so that air movement can be traced. If the purpose provided ventilation is mechanical with ducts, then the air flow in the ducts can be measured with different techniques for volume and mass flow rate measurements, without a tracer gas.

The tracer gas is injected into and mixed with the indoor air and its concentration is monitored. There are three different schemes; decay, constant concentration, and constant flow of a tracer gas. All measurements are governed by the continuity equation. The single-chamber continuity equation is given here:

$$V \, dC/dt + Q \, C = F$$

where
V is the effective (i.e. ventilated) volume, m3
dC/dt is the time rate of change of concentration,
Q is the infiltration, m3/s
C is the concentration and
F is the effective injected tracer gas flow rate, m3/s.

In all houses, examined in this paper, the constant concentration technique was employed, where a constant concentration of a tracer gas is maintained in the test space. One of the principle advantages with this technique is that it eliminates the problem of estimating the effective volume as the effective volume is eliminated from the continuity equation:

$$Q\ C = F$$

The field of application is to continuously monitor the supply of fresh air to individual rooms i.e. fresh air which enters an individual room directly instead of first passing through an adjacent room.

An automated air infiltration monitoring system (developed by the National Testing Institute) based on this principle was used. The system is capable of handling nine rooms simultaneously. Tracer gas is injected into each room and the concentration is measured in each room. After each measurement the tracer gas flow is updated. The same constant concentration is maintained in all rooms being tested. Air flows between rooms shouldn't affect the measurements i.e. air flows between rooms will never be measured, as all air flows between rooms contain the same tracer gas concentration. Other techniques have to be used to study the air flows between rooms.

3. MODELS

3.1 Multi-zone Network Approach

The multi-zone approach is recommended when the internal partitioning in a building presents a resistance to the movement of air and/or when information as to the supply of fresh air to individual rooms and air flows between rooms is wanted.

A multi-zone model, which has been developed at the Royal Institute of Technology in Stockholm (Bring), was used as a tool for further evaluating the measurements performed for this paper. In the program (MOVECOMP) the building and its ventilation system is modelled. The model consists of pressure nodes

connected to each other with flow paths. The nodes are different zones and duct components, while the flow paths are different leakage openings and ducts. The air flows are calculated by seeking a flow balance in each node. Mass balance has to be achieved.

The natural driving forces (i.e. wind and temperature) are determined by the pressure distribution on the building envelope and the pressure gradients within different rooms and inside the duct system. The stack effect is caused by differences in air density. In the model the pressure gradients are assumed to be linear, i.e. the gradients within a certain volume are calculated as if the density was constant. The wind pressure is related to the dynamic pressure of the free wind with a pressure coefficient.

The mass flow through leakage openings and ducts/ducts components, which is a function of the pressure difference, is throughout the model approximated with a power function. The flow through a leakage opening is calculated using the same flow exponent throughout the entire flow intervall. The Reynholds number correction of the air flow coefficient is done for the actual condition. Ducts/duct components are simulated in a conventional manner with the flow as a function of the squareroot of the pressure difference. The air flow coefficient is determined for the actual

Reynholds number.

The system of simultaneous equations describing the flow balance is solved with a modified Newton-Raphson method. The method avoids in most cases otherwise common problems with convergence. As a result of a simulation natural and mechanical ventilation air flows in a building between rooms, through a building envelope and in a ventilation system are given. The pressure conditions within the simulated building are also given. Almost any kind of combination of zones and leakage openings can be simulated.

3.2 Simplified Theoretical Approach

A number of "simplified" methods have been developed in order to reduce the computational effort of theoretical techniques. As of yet they are only applicable to single zone structures and only provide estimates of the total ventilation. The model, which is used in this paper, was originally developed at Lawrence Berkeley Laboratory (Sherman). The primary input to the model is the air leakage of the entire building envelope, which is given as an effective leakage area.

The forces that drive infiltration are pressure differences across the building envelope caused by wind forces and by indoor-outdoor temperature differences. The stack-induced infiltration and the wind-induced infiltration are calculated separately. The air flow resulting from the two driving forces must be combined to arrive at the total infiltration. If the expression for wind-induced and stack-induced infiltration are interpreted as effective pressure differences across the leakage area of the structure, the total infiltration can be determined by adding these two pressures. If the flow is proportional to the squareroot of the pressure, then two flows acting independently must add as the squareroot of the sum of the squared flows.

The ventilation through vertical shafts is combined with the the above flows using superposition. The same technique should apply if there is an exhaust fan. A balanced ventilation system should not affect the pressure drop across the envelope caused by the natural driving forces. The fan flow should therefore simply be added to the natural ventilation.

4. BUILDINGS

A number of experimental houses has been performance monitored and evaluated by the National Testing Institute with the author as project leader. All of them except one are energy efficient designs. Common features are a very high standard of the thermal insulation and a system for mechanical ventilation (see table 1). The energy inefficient house is an older conventional house, which was included in the study for the purpose of comparison.

Skultorp (Skul): Two experimental one-storey houses were built in 1982 in Skultorp, in southern Sweden. Both houses are very well insulated modern wood frame structures, employing boxbeams made of wood and masonite throughout the structure. Each house is 110 m2. Space heating is provided for by a warm air heating system. The warm air is blown into the individual rooms from inlets located in the partitions up by the ceiling.

Täby: A conventional 1.5-storey house was built in 1982 in Täby 30 km north of Stockholm in Sweden. The house is 146 m2 and was designed according to Sweden's National Building Code for energy conservation, but with windows with a better U-value than what's required. Space heating is provided for by a warm air heating system. The warm air is blown into the individual rooms from inlets located in the partitions up by the ceiling.

Table 1 Technical description. SBN80 = Swedish Building Code of 1980. ELAK = Building Code for houses with electric heating.

Project	Skul	Täby	L85	Karl	Svan
SBN80-insulation	-	x	-	-	-
ELAK-insulation	x	-	x	x	-
"Superinsulation"	x	-	x	x	-
Balanced ventilation	x	x	-	-	-
Extract ventilation	-	-	x	x	-
Unpowered vents	-	-	-	-	x
Warm air heating	x	x	-	-	-
Electric base-board heaters	-	-	x	-	-
Hydronic heating	-	-	-	x	x
Heat recovery	x	x	-	-	-

Lättbygg 85 (L85): A group of 18 identical 1.5-storey well-insulated experimental houses in Täby 30 km north of Stockholm, utilizing simple construction techniques, was built during 1984. All houses are modern wood frame constructions employing I-beams made of wood and masonite throughout the construction. Wall, ceiling, roof, and floor elements are prefabricated. Space heating is provided for with electric baseboards heaters. The houses are 119 m2.

The houses have an exhaust fan ventilation system, with special vents, in the exterior walls, for supplying fresh air. The ventilation rate can be controlled by the user by adjusting a conveniently located three-way switch: no one at home = 0.1 air changes per hour, at home = 0.3 air changes per hour, maximum = 0.5 air changes per hour.

Karlstad (Karl): Sixteen well-insulated townhouses, utilizing passive solar energy and attached sunspaces, were built in 1984 in Karlstad. There are two types of townhouses, a one-storey townhouse with a floor area of 90 m2 and a two-storey with 116 m2. All townhouses have a sunspace facing south. The three monitored townhouses are 116 m2.

The townhouses are modern wood frame constructions with structural elements of concrete. They are heated by an hydronic heating system incorporating only two radiators on the first floor and a towel-dryer on the second floor. There are fans in the intermediate floors in order to circulate the heated air within the apartment.

Svaneholm (Svan): A conventional house was built in 1972 in Svaneholm 15 km south of Boras in Sweden. The house is 135 m2. It is a one-storey building with full basement. The house was designed according to Sweden's standard for energy conservation of 1968. Space heating is provided for by a hydronic heating system. The heat is delivered by an oil fired boiler. The house is ventilated by unpowered vents i.e. vertical shafts where the air is mainly driven by the stack effect.

5. RESULTS AND DISCUSSION

5.1 Predictions of Ventilation

All measurements of ventilation rates using tracer gas are valid for the range of weather conditions, which prevailed during the measurements. The question is what happens if the weather conditions are changed, the building moved to another location or even the building itself modified. If we want to calculate the influence of ventilation on the energy balance we need to know the ventilation rate throughout the year, not only for certain weather conditions. For a house with mechcanical ventilation we need to know the air exfiltration part of the total ventilation as well. Heat can't easily be recovered from that part. To answer some of these questions the buildings were modelled using two different models:
- the LBL-model (single-zone simplified theoretical model)
- MOVECOMP-PC (multi-zone network model)

The first step for both models was to examine how accurately they predict ventilation rates during the actual tracer gas measurements. As inputs were used:
- the results from the fan pressurization tests
- the distribution of leakage openings according to infrared photography scans
- the actual local shielding conditions
- the building height
- the measured indoor and outdoor temperatures (hourly averages)
- the on site measured wind speed (hourly averages)
- the terrain roughness

- the measured mechanical ventilation rates (air flows in the ducts), which were assumed to be constant.

The following inputs only apply to MOVECOMP-PC:

- the on site measured wind direction (hourly averages)
- wind pressure coefficients from windtunnel studies
- the measured geometry of door openings, which was converted to a leakage function
- each room was a separate zone.

The second step was to make predictions for an entire heating season. Weather data was taken from the reference year 1971 of Stockholm. Using the LBL-model hourly calculations were performed. Predictions with MOVECOMP for one combination of wind speed and temperature difference i.e. for one hour requires half a minute of time on a PC. To simplify the calculations the reference year was condensed to relative frequencies of simultaneous values of outdoor temperature and wind speed. This way MOVECOMP could be used for estimating the ventilation rate for an entire heating season.

5.2 Predictions using the LBL-model

Predictions were made for all the houses and compared with tracer gas measurements. The main inputs for the modelled houses are presented in table 2.

Table 2 Inputs to the LBL-model. L = effective leakage area, cm2. Q = fan flow, m3/h. n = number of air changes per hour at 50 Pa (fan pressurization). Exhaust = the difference between the total exhaust and the supply.

Project	Skul	Täby	L85(3)	L85(14)	Karl	Svan
Lceiling	30	40	40	56	42	100
Lfloor	30	0	20	28	0	0
Ltotal	89	130	132	185	125	250
(n)	(1.1)	(2.0)	(1.3)	(2.2)	(2.0)	(5.0)
Qexhaust	33	9	80	70,90	140	0
Qsupply	109	160	0	0	0	0

Skultorp: The LBL-model overpredicts the ventilation rate with 10 % for a 21 hour measuring period (see table 3). The weather was rather typical for a inland winter day in southern Sweden, the wind speed varied between 0 and 5 m/s and the temperature between 0 C and - 2 C.

The measured total ventilation rate (135 m3/h) is even lower than the measured mechanical ventilation rate (142 m3/h). The inaccuracy in both measurements is however 5 to 10 %. The model predicts the relative variation in total ventilation fairly well for the measuring period. According to the prediction the average air exfiltration for the 21 hours is 7.5 m3/h, which is a reasonable number.

The predictions for an entire heating season show an average total ventilation rate of 151 m3/h. The average air exfiltration is 9 m3/h, while the maximum is 33 m3/h and the minimum 1 m3/h. Only 5 % of the total ventilation is "uncontrolled" i.e. doesn't pass through the mechanical ventilation system. There is no need to make the house tighter.

Täby: The predictions show similar results to the Skultorp house. This time the LBL-model overpredicts with 12 % for a 85 hour and a 23 hour period (see table 3). The weather was rather cold with an average value of - 6.5 C (85-hour period) and -3.4 C (23-hour period), while the wind speed was very low with an average value of .3 m/s (85-hour period) and .6 m/s (23-hour period). The lowest temperature was -13 C and the highest - 1 C. The wind speed didn't change very much, this is also a very well shielded house located inland and is therefore not likely to ever experience high wind speeds.

According to the measurements the air exfiltration is only 6 m3/h, but as mentioned before both measurements are experiencing inaccuracies in the order of 10 %. The LBL-model gives an air exfiltration of 27 m3/h. The truth must be somewhere in between.

The average total ventilation rate during the heating season will be 191 m3/h according to the LBL-model. This corresponds to an average air exfiltration rate of 22 m3/h with a maximum of 47 m3/h and a minimum of 6 m3/h. Approximately 12 % of the total ventilation doesn't pass through the mechanical ventilation system and isn't quite controlled. Although the envelope of the house meets the requirements in the Swedish Building Code it should preferably be tighter.

Lättbygg 85: The discrepancy between the LBL-model and the tracergas measurements is large. For house # 14 the model overpredicts with 60 % for a 108 hour period (see table 3). The overprediction for house # 3 is more reasonable with a value of 23 % for a 17 hour period. For house # 14 there was probably background leakage of tracer gas, which accounts for part of the large discrepancy between prediction and measurement. The air exfiltration is 7 m3/h in house #3 and between 14 m3/h and 19 m3/h in house # 14

according to the LBL-model for the measuring periods. The LBL-model tracks the variation in ventilation fairly well, but overstimates the air exfiltration rate.

The weather was rather cold during the 108-hour period with an average outdoor temperature of - 14 C. The wind speed was very low approximately 0.5 m/s. For the other periods the average outdoor temperature was close to the freezing point.

The total ventilation rate during the heating season in house # 3 varies between 82 m3/h and 100 m3/h, while the average value is 88 m3/h. The air flow through the exhaust fan was assumed to be at a constant rate of 80 m3/h, which is equal to the average measured rate. The average air exfiltration rate is then 8 m3/h. The maximum rate is 20 m3/h and the minimum rate 2 m3/h. Approximately 10 % of the ventilation rate isn't quite "controlled" i.e. doesn't pass through the intended ventilation system.

An estimation for an entire heating season was also made for house # 14. The result was an average total ventilation rate of 95 m3/h and air exfiltration rate of 15 m3/h. The maximum exfiltration rate was 36 m3/h and the minimum rate 3 m3/h. The "uncontrolled" air flow is thus 15 % of the total ventilation rate. The variation in this flow is also rather large. Although the house meets the requirement for airtightness of the Swedish Building Code, it isn't tight enough.

Karlstad: This is the only house that isn't a detached house, it is a two-storey townhouse with an attached sunspace. The LBL-model was primarily developed for detached houses. In spite of this fact the results from using the model on one of the townhouses in Karlstad (apartment B4), gave reasonable results. The overprediction was 10 % for a 24-hour winter period (see table 3). The air exfiltration is, according to the prediction, very low.

The Karlstad apartment has an average total ventilation rate of 146 m3/h during the heating season i.e. the air exfiltration is very low, 6 m3/h or 4 % of the total rate. The variation in air exfiltration is also very small. The maximum value is 16 m3/h and the minimum value 1 m3/h. There is obviously no need to make the house tighter.

Svaneholm: The LBL-model tracks the total ventilation rate fairly well, but with an average overprediction of 10 % for a 43-hour period (see table 3). The average wind speed was 2 m/s and the average outdoor temperature was 1 C.

The predicted average ventilation rate during the heating season for the Svaneholm house is 75 m3/h, which is only 0.23 air changes per hour. The maximum ventilation rate for the same period is 0.35 air changes per hour. The minimum is 0.10 air changes. The ventilation is always below the required rate of 0.5 air changes per hour, unless the house is made leakier or the occupants open windows. Even if the house was made leaky enough to obtain a correct average ventilation rate, there would be long periods when the ventilation would be inadequate and long periods when the ventilation rate might be uncomfortably high.

5.3 Predictions using MOVECOMP

All the predictions were performed using average weather conditions for the measuring periods (see previous chapter). If the weather conditions change over time the air infiltration prediction can then be in error. For all the measuring periods predictions were therefore made using the relative frequency of simultaneous values of outdoor temperature and wind speed.

Skultorp: The predicted total ventilation rate is very similar to the LBL-prediction i.e. the average predicted total ventilation rate is approximately 10 % higher than the tracer gas measurements (see table 3). The variation in total ventilation rate is similar for the prediction and the measurement.

The average air exfiltration rate during the heating season is 10 m3/h according to MOVECOMP. This value is very similar to the LBL-prediction (9 m3/h). The variation in air exfiltration rate during the heating season is according to MOVECOMP large, the maximum value being 42 m3/h and the minimum 1 m3/h. The spread according to the LBL-model is 33 m3/h to 1 m3/h.

Täby: The predictions of the total ventilation rate is very similar to the predictions using the LBL-model (see table 3). What this prediction also shows is that the fresh air supplied directly to the bathroom, the WC and the closet probably wasn't covered by the tracer gas measurement. This makes up for the discrepancy between measurement and prediction.

Lättbygg 85: The prediction of the total ventilation rate for house # 3 is closer to the tracer gas measurement than the LBL-prediction (see tabel 3). There is no air exfiltration according to MOVECOMP.

During the heating season the variation in air exfiltration rate is very large according to MOVECOMP. The maximum rate is 67 m3/h and the minimum rate 1 m3/h. The average rate is however very low, 4 m3/h. According to the LBL-model the average rate is higher, 8 m3/h, and the variation smaller, between 20 m3/h and 1 m3/h.

Predictions were also made for house #14. This house is identical to # 3 with a few exceptions, it is leakier, and the weather during the measuring period was much colder. There is a large discrepancy between prediction and measurement. The overprediction is close to 70 % (see table 3). This can partly be explained by the fact that there was presumably a constant background leakage of tracer gas from the equipment during the tracer gas measurements. This would mean that the measured ventilation rate would be too low with almost a constant factor, as the total ventilation rate is dominated by the exhaust air flow, which can be assumed to be constant over time.

The total measured and predicted ventilation rate varies almost to the same extent over time. During the 108-hour period the predicted rate varies between 116 and 155 m3/h, while the measured rate varies between 60 and 73 m3/h. As can be calculated from the prediction there is an air exfiltration rate of between 26 and 65 m3/h in house # 14, while there was no air exfiltration in house # 3. This can partly be explained by the fact that house # 3 is tighter and was subject to a milder climate.

The variation in air exfiltration rate during the heating season is larger for house # 14 than for house # 3. The main reason is that house # 14 is leakier. The maximum air exfiltration rate is almost two times higher, 117 m3/h compared with 67 m3/h. The average rate is four times higher, 18 m3/h vs. 4 m3/h. The average air exfiltration rate is 20 % higher than the LBL-prediction, and the maximum rate is 3 times higher than the LBL-prediction. The maximum values occur at high wind speeds and are therefore uncertain, as high wind speeds never occured during the tracer gas measurenments.

Karlstad: The overprediction of the total ventilation is very small for apartment B4 (see table 3). The discrepancy would be negligible if we take into account that the predicted air infiltration to the WC probably wasn't covered by the tracer gas measurements. Both prediction and measurement indicate that there is no air exfiltration during the measuring period. The prediction also shows that the total flow of air from the sunspace to the house is 34 m3/h, which is 1/4 of the total ventilation. The same

result was obtained from a separate tracer gas measurement, where the same concentration was kept in the sunspace as in the house itself. According to the design principles all air should have entered the house through the sunspace.

The average predicted air exfiltration rate during the heating season is reasonable. The rate is 9 m3/h, which is higher than the LBL-prediction of 6 m3/h. The maximum rate is too high, 110 m3/h (compare with Lättbygg 85). The result of the LBL-prediction is 25 % of that value 26 m3/h.

Svaneholm: The prediction overestimates the ventilation rate with 40 % (see table 3), which is not surprising taking into consideration the assumptions which had to be made in order to create the necessary inputs.

Table 3 Measured and predicted ventilation rates, m3/h.

Project	Skul	Täby	L85(3)	L85(14)	Karl	Svan
Measured, mechanical	142	169	80	90	140	-
total	135	174	71	69	131	71
Predicted, total LBL-model	149	196	87	109	144	78
MOVECOMP	152	198	80	118	140	101

5.4 Energy balance

For most houses the ventilation heat loss make up an important part of the energy balance. It may constitute between 20 and 50 % of the total energy loss. For all tested houses the ventilation heat losses were calculated using weather data from the heating season of the reference year 1971 of Stockholm (see table 4). The calculations are based on the average predicted ventilation rates, i.e. the average of the LBL-prediction and the MOVECOMP-prediction.

In the original energy balance the calculation of the air exfiltration heat loss was based on an estimation of the air exfiltration rate. For all houses (except Svaneholm) the rate was estimated to be 0.05 ach throughout the heating season. This gives a "correct" exfiltration heat loss for only one house, the L85(14). For the tight houses, the Skultorp house,

Table 4 Calculated ventilation heat losses for the heating season of the reference year 1971 of Stockholm, kWh. For the purpose of this calculation it was assumed that no heat recovery was installed.

Project	Skul	Täby	L85(3)	L85(14)	Karl	Svan
Total ventil. (MOVECOMP, LBL)	5100	6450	2900	3250	4950	2550
Exfiltr. (MOVECOMP, LBL)	300	700	200	550	250	2550
Exfiltr. (0.05 ach)	450	600	550	550	450	-

the L85(3) house and the Karlstad, the heat loss due to air exfiltration is overestimated using the simple approach. None of the above used averaging techniques shows directly the energy consumption for space heating due to air exfiltration. In the real building the air exfiltration will vary over time. There can then be periods when the space heating due to exfiltration is reduced by internal gains in a low energy house i.e. it is important to know when the air exfiltration occurs.

6. CONCLUSIONS

Six different modern Swedish one-family house with different ventilation systems were examined in this report. There is only one house that isn't quite modern and can't be considered a low energy house. If doors and windows are closed in this house, with unpowered vents and vertical stacks, it will be inadequately ventilated all year around. The house wasn't even as tight as is required by the Swedish Building Code. The ventilation rate can of course be increased by airing. Whether relying on airing or unpowered vents and vertical stacks or both of them, it is very difficult to recover any heat from the air leaving the structure.

The three houses with exhaust fan ventilation systems were all adequately ventilated. For two of them the air exfiltration rates were fairly low i.e. there is no need to make the houses tighter in order to better control the energy loss due to air exfiltration or to improve the total ventilation. All of them met the airtightness requirement of the Swedish Building Code. One of the ideas behind the ventilation system

was that the occupants should be able to control were the outdoor air entered the house. Vents which can easily be closed and opened were incorporated in the building envelope. Measurements and calculations show for these three houses that approximately 1/3 of the air enters through the vents if all of them are open. The remainder of the outdoor air enters through whatever cracks or openings there are.

Two houses were equipped with a balanced mechanical ventilation system. One of the two houses (2.0 air changes per hour at 50 Pa) should preferably have had a tighter building envelope. This would have reduced the air exfiltration heat loss substantially. The other house had a very low air exfiltration rate, due to the fact that the house is very tight (1.1 air changes per hour at 50 Pa).

The following conclusions are valid for the examined houses. The constant concentration tracer gas technique tended to underestimate the total ventilation. All air flows were probably not measured. A simplified theoretical one-zone model can be useful and makes accurate estimations of the air exfiltration in tight houses with mechanical ventilation. This is also a very straightforward kind of model to employ. It is necessary to know the airtightness of the building envelope, the mechanical air flow rates and the shielding. For detailed information on air flows a multi-zone network model can be useful. There are however two problems associated with a multi-zone network model: it is time-consuming to put together all the required inputs and there isn't enough data as to wind pressure and the location of leakage openings.

Whatever model is used it is recommended to couple predictions with tracer gas measurements. Determining the energy balance, based on a simple estimation of the air flows due to mechanical and/or natural ventilation by e.g. using a constant air change rate, is in most cases inaccurate, unless the house is very tight.

7. REFERENCES

1. BLOMSTERBERG, Å.
"Ventilation and Airtightness vs. Energy Balance and Indoor Climate in Residential Buildings"
Dept of Building Science, Lund Institute of Technology, Lund, Sweden (draft).

2. BRING, A., HERRLIN, M.
"User's Manual - MOVECOMP-PC(R) - An air Infiltration and Ventilation System Simulation Program"
Bris Data AB, Stockholm, Sweden, 1988.

3. SHERMAN, M.
"Air Infiltration in Buildings"
Ph.D. thesis, LBL-10712, Lawrence Berkeley Laboratory, Berkeley, California, U.S.A., 1980.

Discussion

Paper 16

Willem de Gids (TNO, Netherlands)

Did the natural ventilated houses have slot vents in the roof? Why did you come to the conclusion that natural ventilation fails? The flow rates given do not differ significantly from, for instance, mechanically exhaust systems as you showed by the model calculations.

Åke Blomsterberg (Lund Institute of Technology, Sweden)

The house with natural ventilation had five inlets (vents) which can be opened and closed. The calculations and measurements were made with all inlets open. During the heating season the average predicted ventilation rate, with all windows closed, is then 75 m^3/h, which is 0.25 ach. According to the Swedish National Building Code the required minimum ventilation rate is 0.5 ach. All the other tested houses meet this requirement.

Bjorn Kvisgaard (Bruel & Kjaer, Denmark)

One of your conclusions was that the constant concentration method underestimated the air exchange in the house. How did you come to that conclusion?

Åke Blomsterberg (Lund Institute of Technology, Sweden)

Our automated tracer gas system has nine channels. We were therefore not able to cover all rooms, i.e. in some rooms fresh air entered from the outside and used air was exhausted without being labelled with tracer gas. This we discovered in houses with mechanical ventilation. The total ventilation as measured by tracer gas was smaller than the air flows in the ventilation ducts (not measured by tracer gas). Both measurements have of course a certain inaccuracy.

Jorma Heikkinen (Technical Research Centre, Finland)

Is it acceptable, according to Swedish Building Codes, to design a ventilation system where only 1/3 of incoming air flow can be delivered into individual rooms?

Åke Blomsterberg (Lund Institute of Technology, Sweden)

I was referring to houses with exhaust fan ventilation where 1/3 of the fresh air enters through the vents if all of them are open. The remainder of the fresh air enters through whatever cracks or openings there are. The Swedish Building Code only specifies that the total ventilation should be 0.5 ach and certain minimum exhaust air flows from bathrooms and kitchen.

Willigert Raatschen (Dornier GmbH, Germany)

To get a reliable data input base for the network simulation you did blowerdoor and tracer gas measurements. Further you stated that background leakage is about 2/3 of the total leakage. How did you get around with the distribution of the background leakage into the different walls?

Åke Blomsterberg (Lund Institute of Technology, Sweden)

The air leakage sites were distributed according to the themography tests. The problem was to determine the size of the individual leakage paths. All paths were given the same flow exponent i.e. the exponent from the blower door test of the entire house. For walls the themography tests showed, in most cases, leakage sites at the lower and the upper edge and around windows. Half of the leakage for a wall was then considered to be around windows.

David Hill (Eneready Products, Canada)

Concerned by conflict of conclusions.

1. House with mechanical supply and exhaust should be tighter than 1.0 ach.
2. Houses with mechanical exhausts should be tighter than 2.5 ach.
3. Only 1/3 of the air passed through inlets.

Perhaps a good conclusion for building science/energy reasons, but 2) and 3) seem in conflict regarding ventilation effectiveness and exhaust in homes.

Åke Blomsterberg (Lund Institute of Technology, Sweden)

The required airtightess of 2.5 ach includes the air leakage through the inlets (all of them open). When only 1/3 of the fresh air enters through inlets, some rooms might not get enough fresh air. Ideally the air leakage through the building envelope is fairly evenly distributed i.e. the remainder of the fresh air (2/3). The overall aim is that the exfiltration rate should be less than 10% of the total ventilation for a home with mechanical ventilation.

PROGRESS AND TRENDS IN AIR INFILTRATION
AND VENTILATION RESEARCH

10th AIVC Conference, Dipoli, Finland
25-28 September, 1989

Paper 17

THE PERFORMANCE OF RESIDENTIAL VENTILATION SYSTEMS

R. RUOTSALAINEN, R. RÖNNBERG, A. MAJANEN, O. SEPPÄNEN

Helsinki University of Technology
HVAC-laboratory
02150 Espoo
FINLAND

1. SYNOPSIS

The indoor climate and ventilation were measured in 50 dwellings with various ventilation systems. The health and comfort of people living in the dwellings were studied with a simultaneous questionnaire. The ventilation rates measured with a tracer gas using the decay method varied from 0.1 to 1.2 m^3/hm^3, with an average of 0.5 m^3/hm^3. The ventilation rate in the bedroom was usually lower than the mean ventilation rate of the dwelling. The ventilation rates measured in a two-week period with the passive perfluorocarbon method varied from 0.2 to 1.9 m^3/hm^3, with an average of 0.8 m^3/hm^3.

There was a statistically significant correlation between the ventilation rate and the typical sick building symptoms expressed by people living in the dwellings. When the ventilation rate was low (below 0.3 m^3/hm^3), people had more symptoms than when the ventilation rate was high (above 0.6 m^3/hm^3). No such correlation was found between the various ventilation systems and health.

2. INTRODUCTION

People spend most of their time in residential buildings. Ventilation has an effect on the indoor air quality and people's health and satisfaction with the indoor climate. Residential buildings are often criticised for having poor ventilation, yet little information is available on the operation of various ventilation systems in practice. The aim of the study was to gather information on ventilation in residential buildings and compare ventilation systems in respect to health and satisfaction. 50 residential buildings were selected for the study, in which the operation of the ventilation system and the indoor climate parameters were measured.

3. METHODS

The sample consisted of 28 residences in detached or semi-detached houses and 22 apartments in the Helsinki area. The ventilation systems were: natural ventilation, mechanical exhaust and balanced ventilation. The measurements were carried out during the 1987-88 heating season and they covered the ventilation rates in each room, the carbondioxide concentration, the dust concentration, the level of noise from the ventilation system and the thermal climate. The ventilation rates were measured by the tracer gas technique using both the decay method and the passive perfluorocarbon method. The ventilation

rate was estimated as the inverse value of the nominal time constant.

A questionnaire on health, comfort and satisfaction was carried out with the measurements. People living in the dwellings were asked whether they had had any of the following symptoms during the last two months: skin, eye, nasal or respiratory symptoms, fatigue or headache. A summation score was calculated from the perceived symptoms as in previous studies [1, 2, 3]. The scale of the summation score of symptoms was from 0 (no symptoms) to 6 (suffering from all six types of symptoms).

4. RESULTS OF THE MEASUREMENTS

4.1. Ventilation rates in dwellings

The ventilation rates measured with a tracer gas using the decay method varied from 0.1 to 1.2 m^3/hm^3 when the ventilation systems were in normal operation, i.e. as they were operated most of the day [4]. The average was 0.5 m^3/hm^3. In over half of the dwellings the ventilation rate was between 0.3 and 0.6 m^3/hm^3. The distribution of the mean ventilation rate is shown in Figure 1.

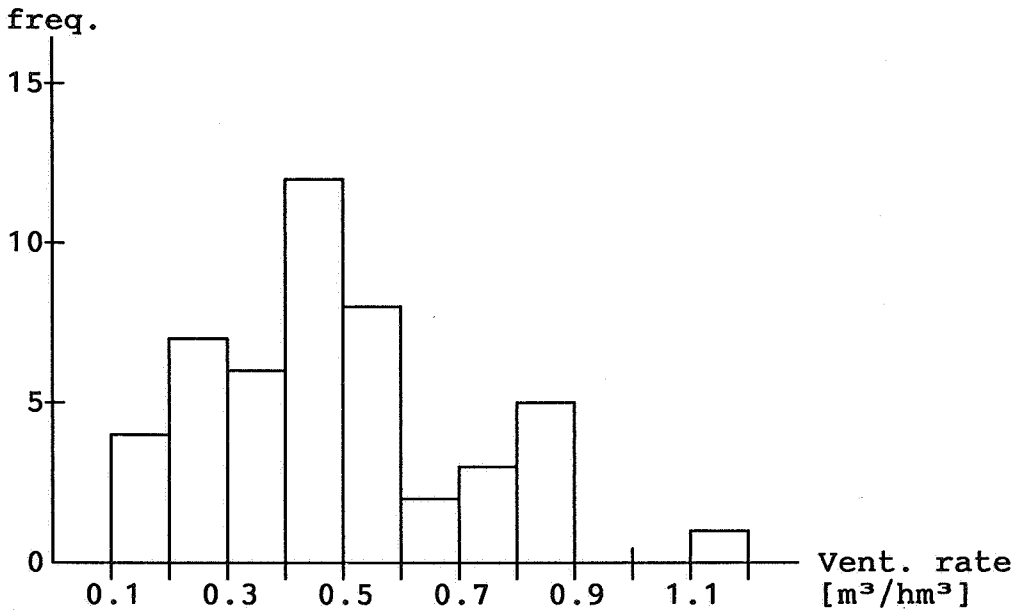

Figure 1. Measured mean ventilation rates in the dwellings.

The difference in the mean ventilation rates was not great between the various ventilation systems. The dwellings with natural ventilation had on average lower ventilation rates than the dwellings with mechanical ventilation. In these 15 dwellings the average ventilation rate was 0.40 m^3/hm^3. In the dwellings with mechanical exhaust (18 dwellings) the average ventilation rate was 0.55 m^3/hm^3. The lowest ventilation rates were usually in the dwellings where a mechanical ventilation system was installed but operated only during cooking and bathing, i.e. it was most of the time out of operation. In dwellings with balanced ventilation (17 dwellings) the average ventilation rate was 0.50 m^3/hm^3. The mean ventilation rates of the dwellings with various ventilation systems are shown in Figure 2.

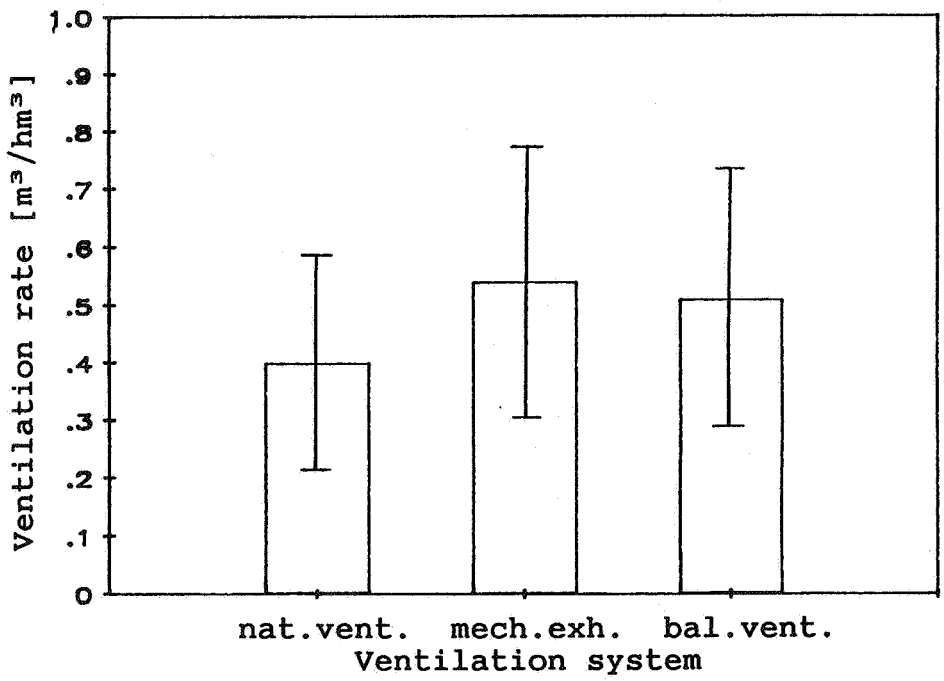

Figure 2. Measured mean ventilation rates and standard deviations in the dwellings.

4.2. Ventilation rates in bedrooms

The ventilation rate in the bedroom was usually lower than the mean ventilation rate of the whole dwelling. Closing the bedroom door especially decreased the ventilation rate if air was not supplied to the bedroom. On average the highest ventilation rate was in the bedrooms with balanced ventilation. On average the lowest ventilation rate was in the bedrooms with natural ventilation. The ventilation rate was most evenly distributed in the dwellings with mechanical air supply to each room. The mean ventilation rates

of the bedrooms with various ventilation systems are shown in Figure 3 and the correlation between the ventilation rate of the bedroom and the mean ventilation rate of the dwelling is shown in Figure 4.

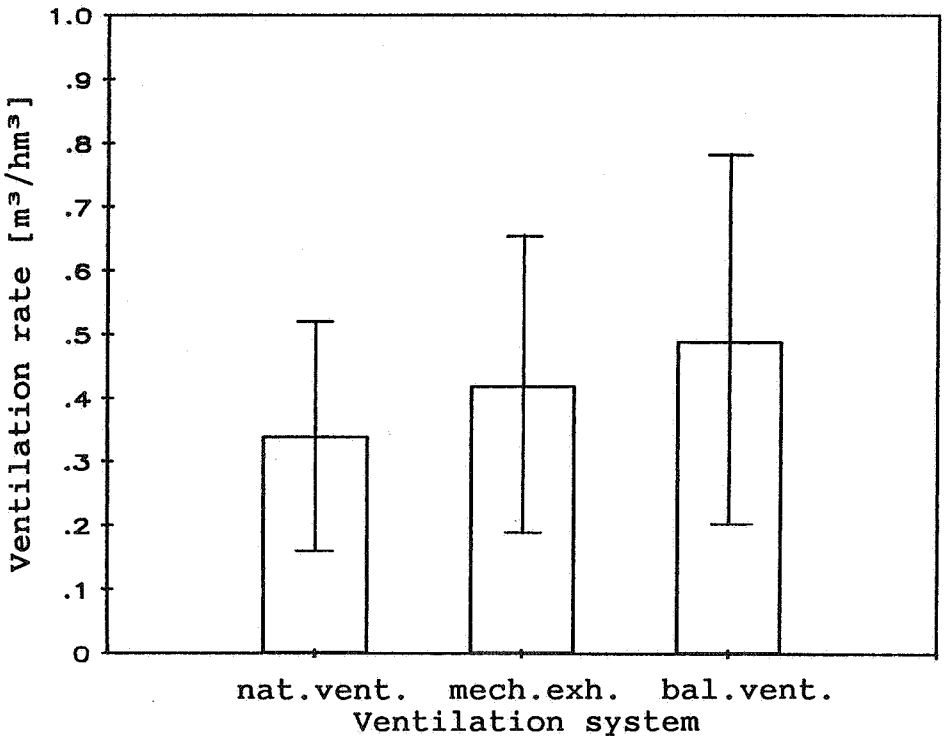

Figure 3. Measured mean ventilation rates and standard deviations in the bedrooms.

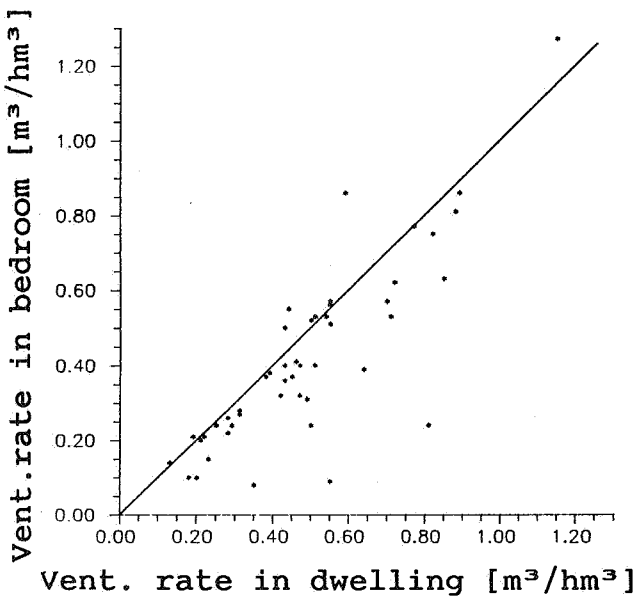

Figure 4. The correlation between the mean ventilation rates of the dwellings and the ventilation rates in the bedrooms.

4.3. Long term ventilation rates

The ventilation rates measured with the passive perfluorocarbon method varied from 0.2 to 1.9 m^3/hm^3, with an average of 0.8 m^3/hm^3 [5]. During the two-week period people lived normally and used the ventilation system and windows as usual. In these measurements the differences in the mean ventilation rates were not great between the various ventilation systems, being less than 0.2 m^3/hm^3. The distribution of the mean ventilation rate measured by the PFT-method is shown in Figure 5.

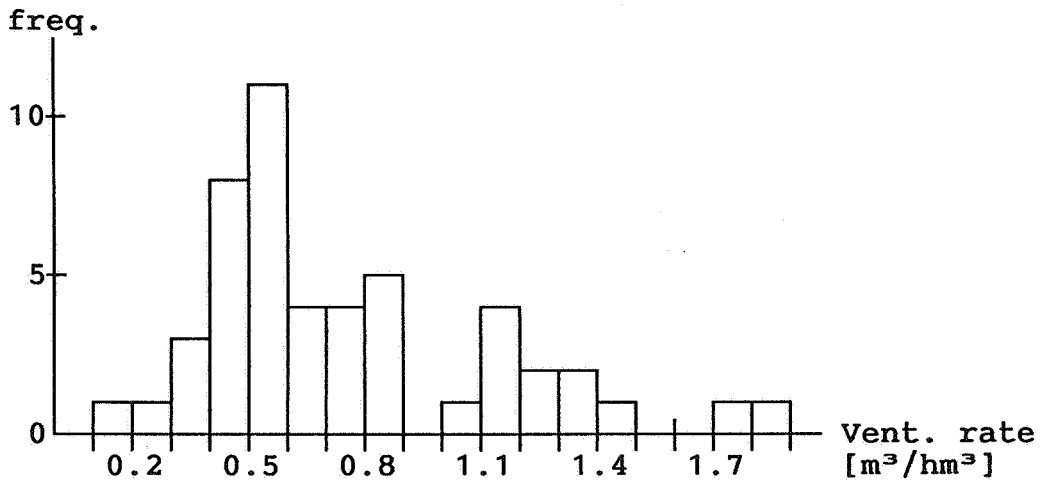

Figure 5. The mean ventilation rates in the dwellings measured by the PFT-method in a 2-week period.

The ventilation rate measurements using the passive perfluorocarbon technique were carried out twice in spring 1988. The mean ventilation rates in the second period (in April) were on average lower than in the first period (in January). The averages were 0.78 m^3/hm^3 (first period) and 0.61 m^3/hm^3 (second period). Airing and outdoor temperature may explain the difference between these two periods. The outdoor temperature was 7 °C higher in the second period (-3 ° and +4 °C). The differences between these two periods are shown in Figure 6.

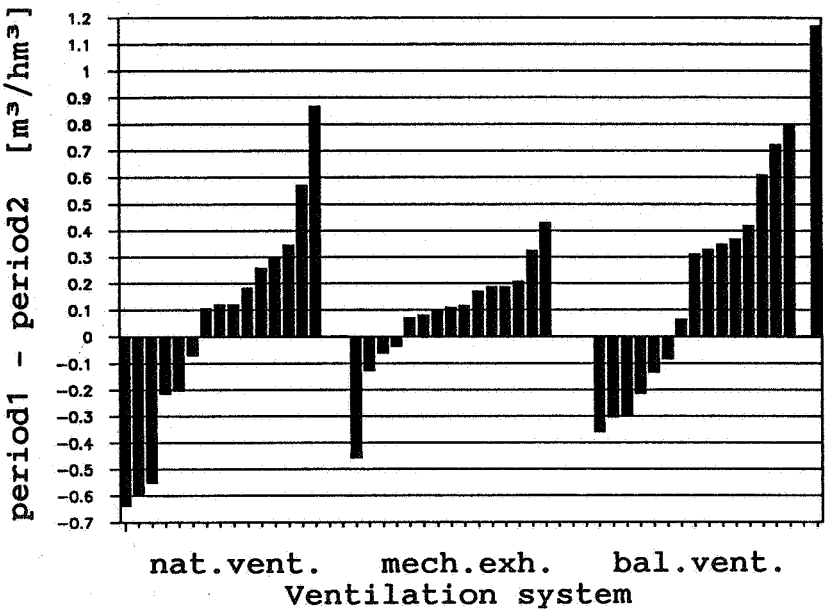

Figure 6. The differences in the mean ventilation rates between two measuring periods.

The ventilation rates measured with the PFT-method were higher than those measured with the decay method. The averages were 0.78 m³/hm³ (PFT-method) and 0.49 m³ /hm³ (decay method). In the decay measurements the ventilation fans ran at normal capacity and the windows were closed. The differences between these two methods are shown in Figure 7.

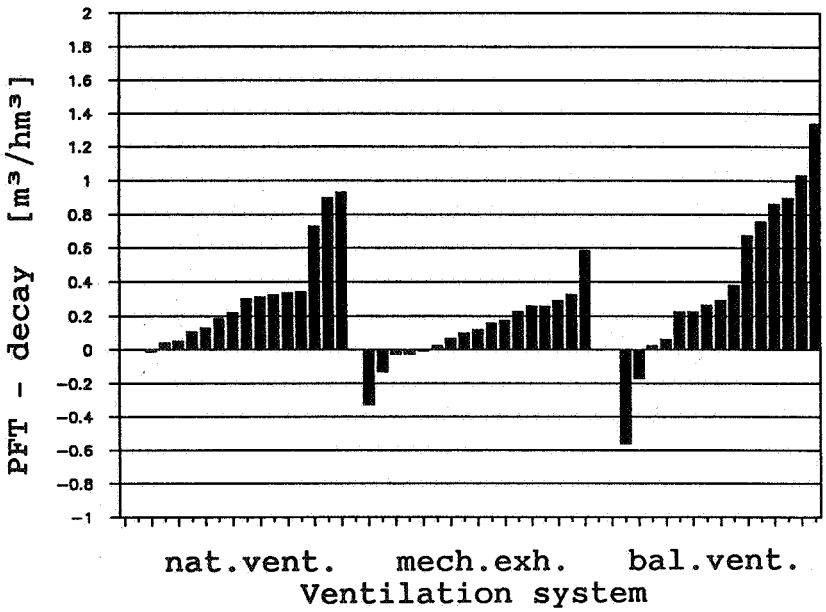

Figure 7. The differences in the ventilation rates between the PFT and decay methods.

4.4. Carbondioxide concentration

The steady-state carbondioxide concentrations measured at night in master bedrooms varied from 500 to 3700 ppm with an average of 1300 ppm. Typically two adults slept in the bedrooms. The difference in the CO_2-concentration was not great between the various ventilation systems. The distribution of the CO_2-concentration is shown in Figure 8.

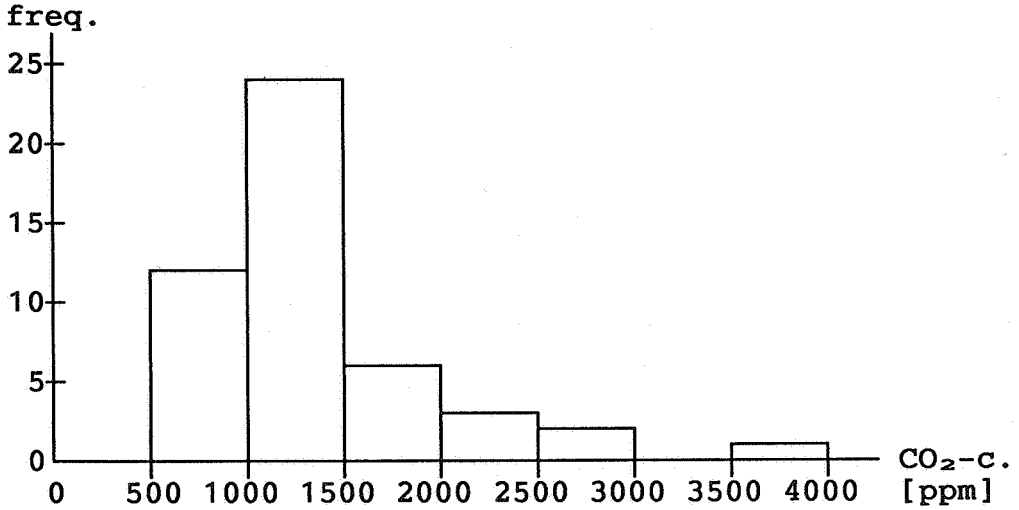

Figure 8. Measured steady-state carbondioxide concentrations during the night in master bedrooms.

4.5. Dust concentration

Dust concentrations in the dwellings were measured using the deposition method: a dust sample passively collected settling dust on a greasy surface. Measured dust concentrations were collected in bedrooms on a horizontal plane at a height of approximately 1.4 m for 100 hours. The dust concentrations varied from 7 to 70 µg with an average of 20 µg. In the dwellings with natural ventilation the dust concentrations were on average lowest. In the dwellings with balanced ventilation the dust concentrations were on an average highest. But the differences were small. The highest separate dust concentrations were also in the dwellings with mechanical ventilation. The people living in the dwellings and their activities influence the dust concentration more than the ventilation system and the ventilation rate. The dust concentrations in the bedrooms with various ventilation systems are shown in Figure 9.

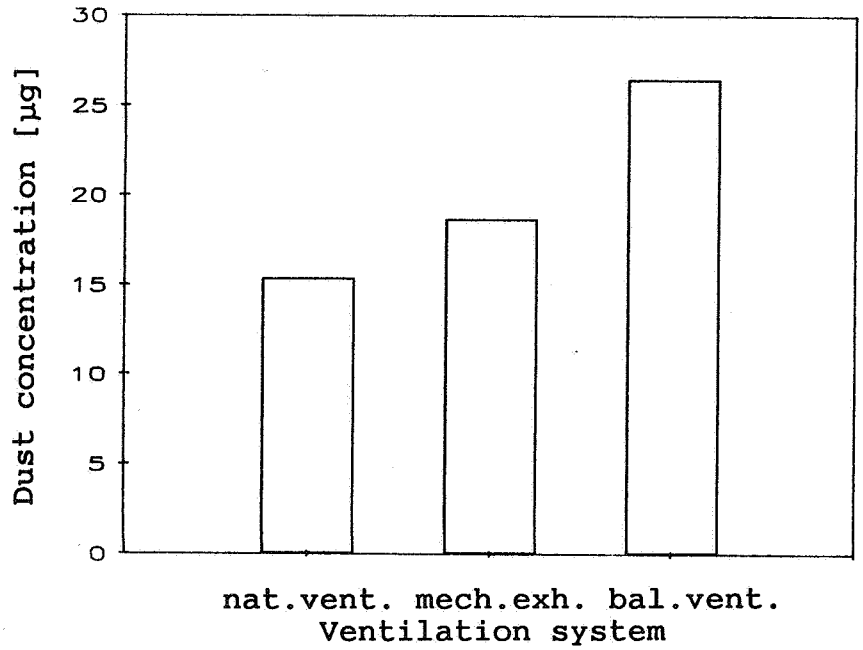

Figure 9. Measured dust concentrations in the bedrooms.

5. RESULTS OF THE QUESTIONNAIRE

5.1. Ventilation

The people living in the dwellings felt that the most common defects of the ventilation in the heating season were the non-uniform air-exchange in the dwelling, and the fact that they were not able to control the ventilation system. Some people also felt that the ventilation system caused noise and draught.

Almost one third were dissatisfied with the ventilation system during the heating season. Most dissatisfied were the people living in the dwellings with natural ventilation (half). The people living in the dwellings with mechanical ventilation were generally more satisfied with the ventilation.

There were differences in airing habits between the ventilation systems. In the dwellings with natural ventilation people aired more often than in the dwellings with mechanical ventilation. The proportion of people who seldom aired was biggest in the dwellings with balanced ventilation.

5.2. Ventilation and symptoms

A statistically significant correlation was found between the measured ventilation rate and the summation score of symptoms (chi-square test: $p < 0.01$). When the average ventilation rate in a dwelling was below 0.3 m^3/hm^3, people expressed several symptoms. When the ventilation rate was above 0.6 m^3/hm^3, people expressed only few or no symptoms. The connection between the ventilation rate and the summation score of symptoms is shown in Figure 10.

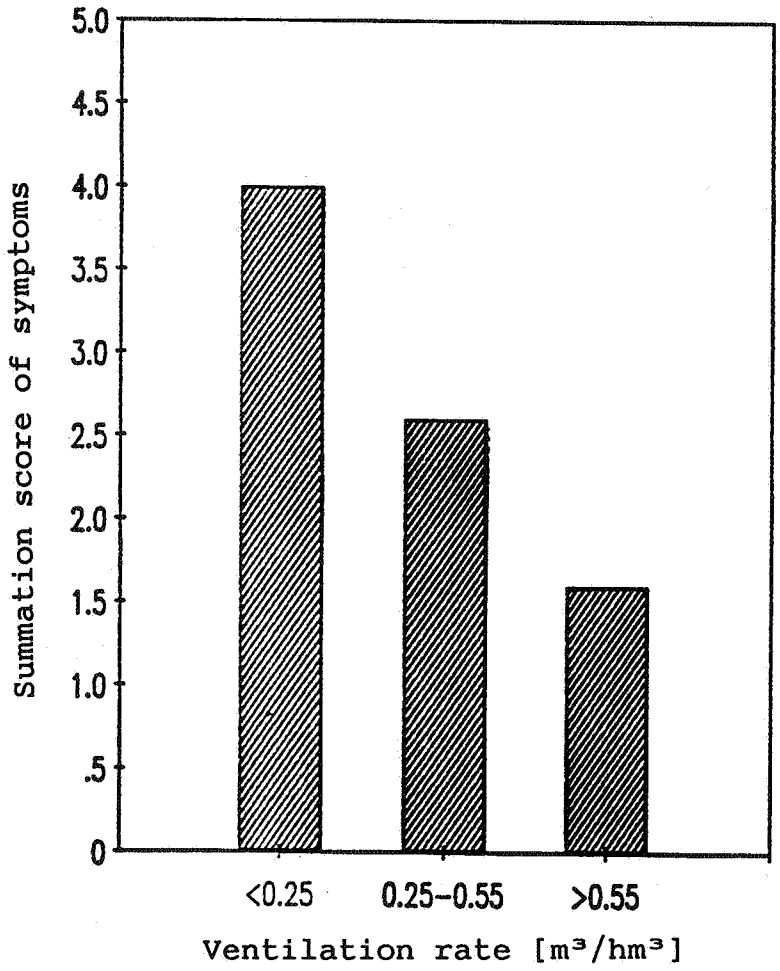

Figure 10. The connection between the ventilation rate and the average of the summation score of symptoms (n = 98).

A correlation was also found between common colds and the measured ventilation rate. When the ventilation rate was above 0.5 m^3/hm^3, 25 % of the people living in the dwellings had flu more often than once a year; when the ventilation rate was below 0.3 m^3/hm^3, the percentage was 60.

A correlation was also found between the sensation of sufficient ventilation and the ventilation rate ($p < 0.05$). When the ventilation rate was low (below 0.3 m^3/hm^3), the majority of the people often felt the ventilation in the bedroom insufficient. When the ventilation rate was high (above 0.6 m^3/hm^3), the majority of the people felt the ventilation in the bedroom was usually acceptable.

A statistically significant correlation was found between the steady-state carbondioxide concentration during the night and the sensation of the freshness of the air ($p < 0.01$). When the CO_2-concentration was below 1000 ppm, the majority of the people did not feel the air was stuffy. When the CO_2-concentration was above 1500 ppm, the majority of the people felt the air was stuffy sometimes or often.

The summation score of symptoms did not correlate with the ventilation system, i.e. the values of the summation score were distributed randomly within three ventilation systems.

6. DISCUSSION

The ventilation rates of dwellings vary a lot. The ventilation rates in the bedrooms are often too low, although people spend much of their time in the bedroom.

The ventilation rate of a dwelling has an effect on health. A low ventilation rate increases the number of the symptoms expressed by people; and the number of symptoms decreases as the ventilation rate increases. No statistically significant correlation was found between various ventilation systems and the number of symptoms expressed by people.

A sample of 50 dwellings is relatively small, so in order to increase the statistical reliability the study is to be expanded to cover a larger group of dwellings. People's satisfaction with the ventilation and the effect of the ventilation and heating systems on their health and comfort is being studied with a questionnaire mailed to over 2000 dwellings with ventilation systems similar to those in this study. 300 of these dwellings have been selected for detailed analysis during the 1988-89 heating season. The analyses of these measurements will be complete by the end of 1989.

7. REFERENCES

1. Jaakkola, J. Indoor air in office building and human health. Experimental and epidemiologic study of the effects of mechanical ventilation (in Finnish). Helsinki 1986. Nat. Board of Health in Finland. 127 p.

2. Jaakkola, J. et al. The effect of air humidification on different symptoms in an office building. An epidemiological study. Healthy Buildings '88, Vol. 3. Stockholm 1988. pp. 207-215.

3. Finnegan M. et al. The sick building syndrome: prevalence studies. 1984. Br. Med. J. 289: pp. 1573-1575.

4. Ruotsalainen, R., Majanen, A. The performance of ventilation in some experimental residential buildings (in Finnish). Espoo 1987. Univ. of Tech., HVAC-lab. 103 p.

5. Säteri, J. et al. The performance of the passive perfluorocarbon method. 10th AIVC Conference. Espoo 1989.

Discussion
Paper 17

Peter Jackman (Building Services Research & Information Association, UK)

If the lowest ventilation rates occurred in those houses where the mechanical ventilation was switched off, how do you explain the fact that people were prepared to put up with unpleasant symptoms when they could have been alleviated simply by turning on the ventilation system?

R. Ruotsalainen (University of Technology, Helsinki)

People do not realize that the ventilation rate really has an effect on symptoms and comfort. Also they do not always know how the ventilation systems are designed to be operated.

Mike Holmes (Ove Arup, London, UK)

You said that you measured noise. Is there any evidence that people prefer to switch the system off and suffer the consequences of a low air exchange rate rather than live in a noisy environment?

R. Ruotsalainen (University of Technology, Helsinki)

The noise of the ventilation was not a major reason to turn off the mechanical ventilation system. Approximately 10% of people expressed that ventilation causes noise.

Willigert Raatschen (Dornier GmbH, Germany)

You showed the comparison between PFT results and tracer gas decay results. There was a very poor agreement. Are PFT's not reliable or did you compare average values with point measurements?

R. Ruotsalainen (University of Technology, Helsinki)

The measurements with the decay method are point measurements and the measurements with the PFT-method are average values during a 2-week period. The ventilation rates measured with the PFT-method were in average 0.3 ach higher than measured with the decay method. The main reasons for this were that during the decay measurements the ventilation systems were in normal operation and windows were closed. So the agreement was not so poor.

Jorma Heikkinen (Technical Research Centre, Finland)

What do you mean by ventilation rate in a bedroom? Is it the air coming from outside or does it include the air flow from other rooms?

R. Ruotsalainen (Technical University of Helsinki)

The ventilation rate in the bedroom includes both the air flow from outside and the air flow from other rooms.

N. Bergsoe (Danish Building Research Inst.)

What were the criteria for selecting houses and apartments?

R. Ruotsalainen (University of Technology, Helsinki)

We selected some dwellings from blocks of flats and from small houses; and from these two groups we selected the same amount of dwellings with three different ventilation systems.

David Hill (Eneready Products Ltd, Canada)

Health and air change correlated.

Health and ventilation technology independent.

Can you correlate occupancy and ventilation in M^3/hr (not ach)

R. Ruotsalainen (University of Technology, Helsinki)

When the outdoor air flow rate per person was below 7 l/s person, 66% of people expressed several symptoms. When the outdoor air flow rate per person was above 11 l/s person, only 22% of people expressed several symptoms.

Martin Liddament (AIVC, UK)

I am very interested in your presentation on the performance of residential ventilation systems. I would be pleased if you could supply the following additional information.

Average CO_2 concentration	?	?	?
Average dust concentration	?	?	?
Cold symptoms	60%	?	25%
Ventilation rate	< $.3m^2/hm^3$	> $.6m^3/hm^3$	

Also how many tracer decay measurements were made in each dwelling?

Risto Ruotsalainen (University of Technology, Helsinki, Finland)

Here are the average values you asked, shared by the ventilation rates. In each of the 50 dwellings was made one measurement using the decay method.

VENTILATION RATE (ach)	<0.3	0.3-0.5	>0.5
Several sick building symptoms (3-6) (%)	65	55	20
Common cold more often than once a year (%)	60	40	25
Dust concentration (μg)	14	24	21
Steady-state CO_2-concentration (ppm)	1800	1200	1300

PROGRESS AND TRENDS IN AIR INFILTRATION
AND VENTILATION RESEARCH

10th AIVC Conference, Dipoli, Finland
25-28 September, 1989

Paper 18

TESTING OF HEATING AND VENTILATING EQUIPMENT WITH THE DUCT TEST RIG

Don Fugler

Canada Mortgage and Housing Corporation
Research Division
682 Montreal Road
Ottawa, Ontario
K1A 0P7
Canada

SYNOPSIS

Canadian research into residential ventilation and combustion venting revealed that the installed performance of exhaust equipment, ducting passages, and site-built chimneys was largely unknown. It became necessary to establish actual characteristics in order to be better able to predict the safety and effectiveness of various ventilation measures.

For this reason, Canada Mortgage and Housing Corporation (CMHC), the federal agency responsible for housing policy, had a research device designed and fabricated. The duct test rig (DTR) can be used for taking a wide variety of field measurements. It uses the principal of a zero-pressure difference across the duct opening to negate the effects of the measurement device. There is an internal fan capable of creating flows in a measurable range of 2-390 L/s, and both heat-generating and temperature-sensing attachments to assess duct thermal performance. The fan can be used to generate the pressure-vs-flow characteristics of passive devices, or to aid in fan system flow measurement.

Contractors across Canada used the DTR to test 205 houses in the winter of 1988-1989. Preliminary analysis is available on the installed flows of exhaust equipment. Data analysis is ongoing on the areas such as the following: chimney performance, chimney and duct leakage areas, and the comparison of installed exhaust and intake flows.

1. INTRODUCTION

The flow of air through ducts, fans, and chimneys has always been somewhat mysterious to most householders, and unfortunately also to many of the tradespeople installing or maintaining these systems. Canada Mortgage and Housing Corporation (CMHC), the federal agency responsible for housing policy, has been investigating both combustion venting and house ventilation issues through the 1980's. The CMHC Research Division looked at the conditions under which chimneys must function, the venting characteristics of the chimney itself, and the interplay between these factors. The field research quickly proved that the designed characteristics of air-moving devices and their actual installed performance were very different.

For example, an early survey of the airtightness of

Canadian houses allowed CMHC to predict the number of dwellings where the backdrafting of furnace chimneys would occur [1]. This could be calculated from the interaction of the envelope leakiness area and the capacity of exhaust devices, a combination that could produce excessive house depressurization. The field-tested incidence of spillage was lower than these predictions. Upon further inspection of test houses, it became apparent that the exhaust flows of fans in the houses were far below the rated values used in the estimations. This was proven again when provincial authorities in British Columbia started to insist upon well-installed exhaust fans. They found that this increased the incidence of combustion spillage in their vicinity [2].

New codes and standards in Canada are specifying levels of house ventilation and limits to house depressurization. In order to justify or design such levels, an accurate means of estimating airflow in houses is required.

CMHC has just completed a two part research project to this end. In the first stage, a consultant designed, constructed, and calibrated a test device. This is called the "duct test rig", and is suitable for testing the flow and thermal characteristics of ducts and chimneys, both active and passive [3]. It was designed to provide the same ease of use and accuracy that blower doors have accomplished in the testing of house airtightness. The second stage involved the use of two duct test rigs to monitor the performance of ducts and chimneys in a wide sample of Canadian houses [4].

2. PROCEDURE

The duct test rig (DTR) uses the pressure drop across calibrated orifices to calculate airflows. The flow range that can be measured is 2-390 L/s. The DTR has a built-in axial fan which can be used to create pressures and flows in passive devices, such as chimneys and air intake ducts. Comparing the flow response to the imposed pressures across a system allows the calculation of its aerodynamic characteristics. The controllable fan also permits the DTR operator to adjust the pressure across the inlet of an active device being measured (eg. a kitchen exhaust fan). By setting this pressure to zero, the DTR operator ensures that the measurement device does not significantly change the normal flow of the fan by increasing the flow resistance at the fan face. The Dutch Flow Finder uses much the same principal [5]. A diagram of the DTR construction is shown in Figure 1; a

photo of the DTR in field use is shown in Figure 2.

Figure 1: Duct Test Rig Components

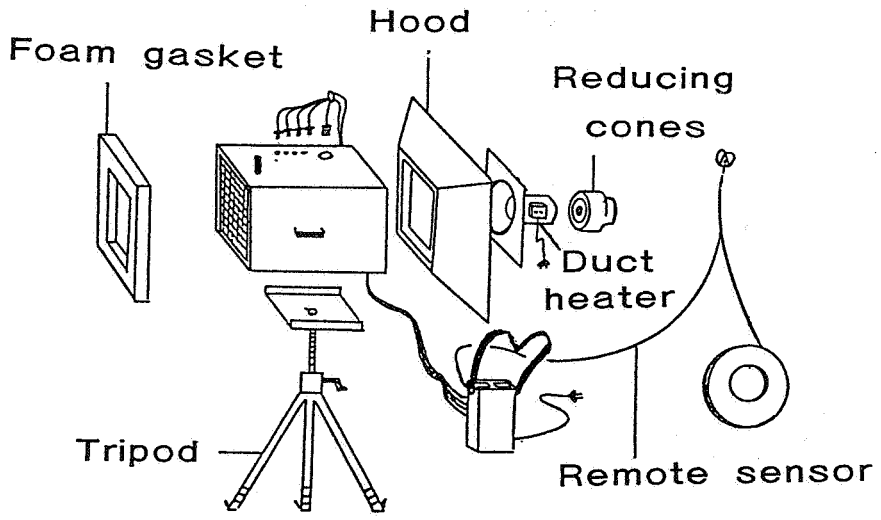

The DTR comes with a number of attachments and accessories. There is a fabric hood to facilitate attachment to open fireplaces as well as spun aluminum cones to reduce the opening size to various duct diameters. For thermal testing, a duct heater can be mounted directly on the DTR to produce a measured heat input to a duct or chimney. A remote sensor is used to measure the temperature at a distance from the DTR. Airflows can be calculated on-site using a programmed calculator mounted on a control module. A photographic tripod permits the operator to elevate the DTR and operate it without having to support the weight. The control module contains fan speed controls, pressure transducers, and a temperature readout.

There is a wide range of tests that can be undertaken using the DTR. In a typical house in the Duct and Chimney Survey, the technician would measure the free flow of all exhaust devices, such as bathroom and kitchen exhaust fans, clothes dryers, and central vacuum systems vented to the outside. Frequently the DTR was also used to establish the ability of the fan to vent when aided or impaired by various levels of pressure across the fan. For instance, is the fan flow severely degraded by a house depressuization of 10 Pa? By blocking the fan outlet at the outside wall, the leakage area of the ducting system could also be measured.

Technicians employed the DTR to measure chimney characteristics as well, including pressure-vs-flow, leakage area, and the thermal characteristics of the chimneys. Passive inlets could be measured in the same way. When a house was equipped with a forced air heating

Figure 2: Testing with DTR

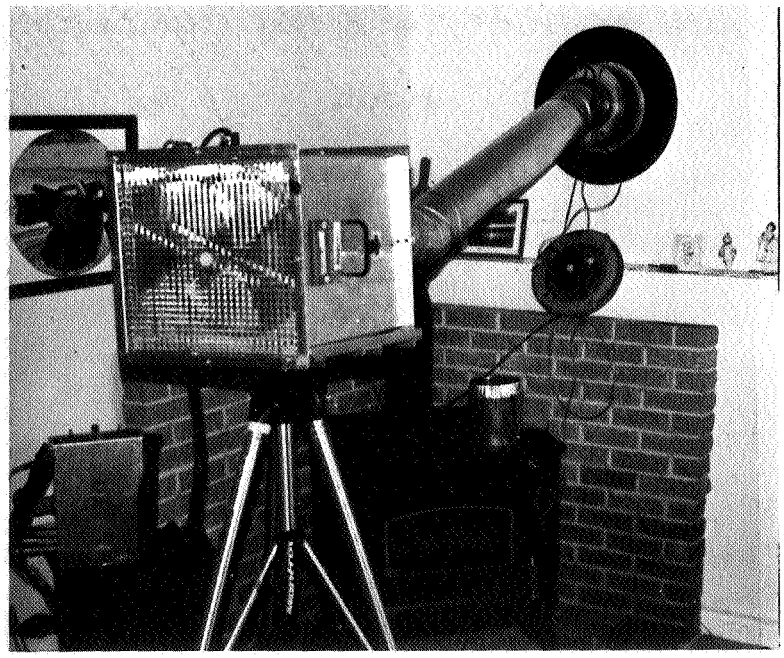

system, technicians measured the total flows from the supply air registers, and compared the results to the estimated furnace output, to determine the effectiveness of the distribution system.

The above is a list of the potential test array. In the Duct and Chimney Survey project, it was not possible to perform all tests in all houses due to limitations of time and money. A full spectrum of tests would also endanger the generally cooperative attitude of the people who had volunteered their houses for testing, as a well-equipped house might take days to test thoroughly. Due to these restraints, only a selection of the possible tests was performed in any given house.

Contractors eventually inspected 20 houses in each of 10 cities, and 5 houses in an eleventh, for a total of 205 dwellings. Each city sample was designed to be representative of the existing stock in terms of house size, design, age, appliance usage, etc. While there is little statistical basis to the house selection, the results of the survey should be typical of the housing stock in and around the cities sampled. A rough quota system was used to ensure a minimum sampling of all desired air-moving devices.

In each region, the main survey contractor trained the local contractor and his aid, a mechanical contractor,on the usage of the DTR and the testing protocol, during the first 6 houses of their 20 house sample. A normal site visit would start with a homeowner interview and building inspection. The DTR would generally be assembled first on the furnace chimney (if available) to

measure the chimney flows and thermal characteristics. The forced air ducting system, if present, would be tested subsequently. Fans, fan ducting, and air intake ducting would be completed before departure. Such testing would typically take three hours, permitting data gathering from two houses daily for each crew of two. The field testing took place from December 1988 through May 1989.

3. RESULTS

The DTR generally performed as expected during the Duct and Chimney Survey and there is a wealth of information now available from the study. Some of the results are usable in their present form, while others require extensive data analysis and manipulation.

Table 1 presents a summary of the exhaust flows found in the survey. The flows cited for bathroom and kitchen fans, clothes dryers, and central vacuum systems were all measured at neutral pressure: that is, they reflect the installed flow rates of those devices. As mentioned previously, there are data on the ability of these devices to function under other pressure levels. Figure 3 illustrates the response of two bathroom fans, one relatively unaffected by house pressure and a weak one that stalls at about 5 Pa house depressurization, a level readily achievable in many new Canadian houses.

Table 1: Exhaust Flow Results

Device	Number Tested	Mean Flow (L/s)	Range (L/s)
Bathroom Fans	103	17	2 - 98
Kitchen Fans	62	59	3 - 155
Clothes Dryers	61	37	10 - 83
Central Vacuums	24	24	10 - 41
Chimneys at 10 Pa			
- Furnace	120	43	10 - 176
- Fireplace	35	104	23 - 229
- Woodstove	28	50	9 - 160

The data for all devices can be further analyzed in terms of flow vs duct diameter, equivalent duct length, appliance age, make and model, etc. Some of this work has been done, or is in progress. Figure 4 gives a graphical representation of the flows found from clothes dryers, with the data from one manufacturer superimposed

on the bar graph.

This data can be used by researchers or designers who want to determine the exhaust flow rates from Canadian (or to some extent, North American) houses. For comparison, the flow rates of the intake or make-up air ducts in the survey averaged about 15 L/s at the maximum recommended house depressurization of 5 Pa. These intake flows fall far short of the exhaust flow rates.

Figure 3: Flow vs. Pressure for Two Bathroom Fans

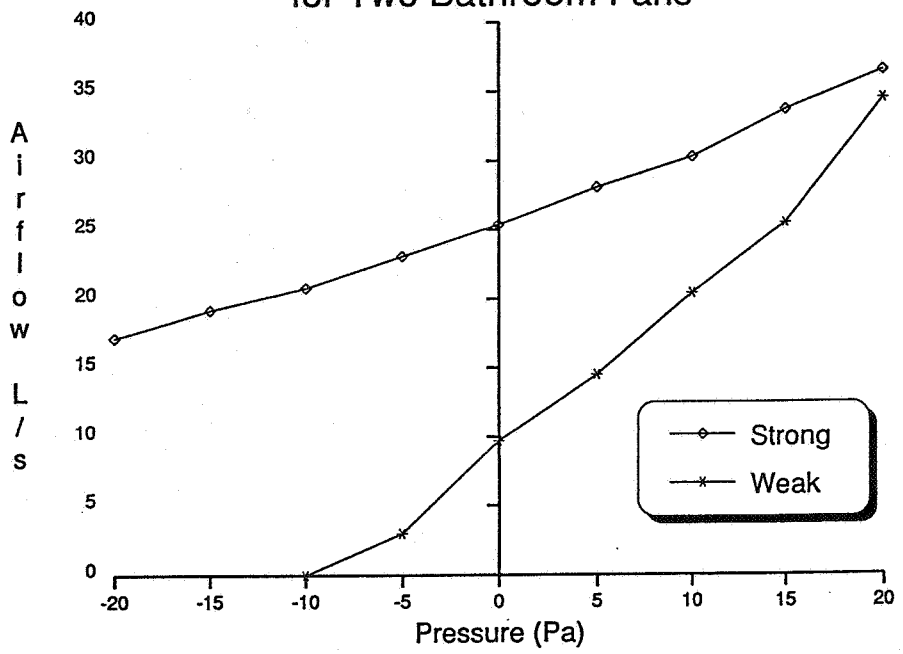

The chimney exhaust flow rates are somewhat artificial, in that they represent the flow through the chimney measured under a 10 Pa pressurization of the chimney or vent connector base. This has been calculated as roughly equivalent to the flows found due to normal operation of the combustion devices. Since the DTR could not test a chimney with a combustion device in operation, this level of chimney base pressurization has been used as a rough surrogate. In abnormal conditions (eg. very high firing rates, high wind, etc.), these flows will be an underestimate of the true flows but, for most conditions, the listed flows will be reasonable estimates. As with the fan data, the chimney flow rates can be further broken down in terms of chimney size, height, material, etc. from the survey data.

Table 2 shows some results of duct leakage calculations for chimneys and forced air heating ducts. They were tested by pressurizing the chimney or duct with the DTR with the other end blocked. The leakage is quoted in terms of litres per second of flow at 50 Pa of positive pressure, normalized by the internal surface area of the chimney or duct. The leakage measurements were not

Figure 4: Clothes Dryer Performance

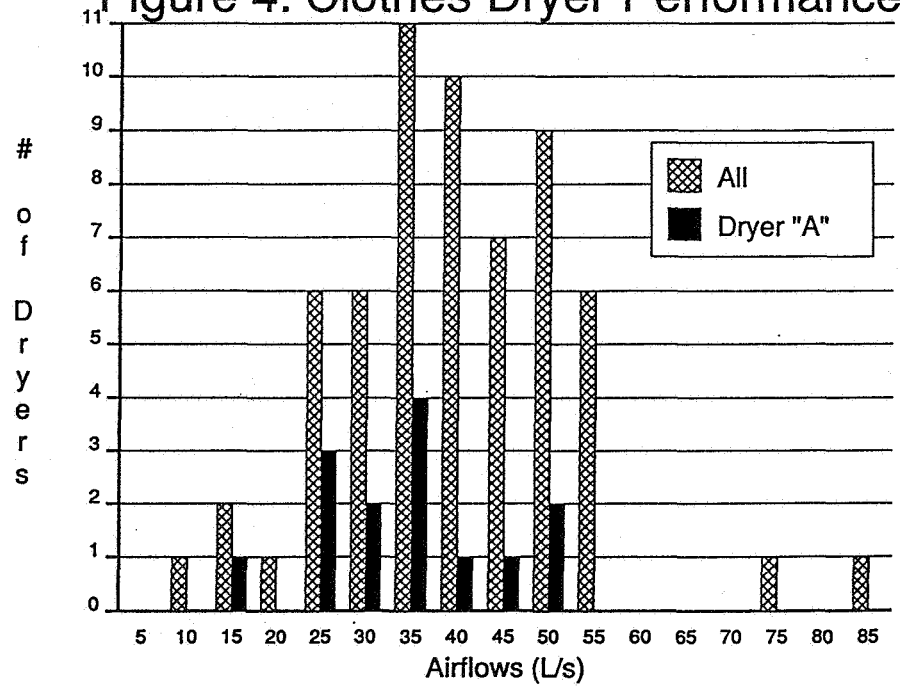

performed on every device in the survey.

Observations by the field testers may prove as valuable as the numerical data collected. They suggest that the typical Canadian exhaust fan installations are largely ineffective, but that this ineffectiveness cannot be readily perceived. There are several instances where the proud homeowner waited for test results on their exhaust fan, only to find that it was not creating any flow. Exhaust outlets were plugged or inoperative, ducting was incomplete or too constrained, or the fans had no ability to move air against any depressurization. Forced air ducting systems distributed only a portion of the furnace output through the supply registers, making it difficult to properly adjust or balance the circulation system. In the 205 houses, there were a great number of blatant heating and ventilating deficiencies. For instance, in one house the barometric damper on the oil furnace chimney had been installed backwards and maintained that way for years. This caused the damper

Table 2: Leakage Testing Results

Device	Number Tested	Leakage Area(cm^2 per m^2 of chimney surface)
Furnace Chimneys	62	4.8
Fireplace Chimneys	19	15.4
Heating System Ducts	29	13.3

only to open under pressurization, producing smoke spillage into the house. When the chimney demanded more air, the damper would shut tightly. It is clear that current inspection and maintenance practices often do not catch such dangerous and obvious deficiencies.

4. DISCUSSION

One of the prime purposes of this project was to establish the exhaust flow rates found in Canadian housing, in order to aid in ventilation system design. This has been successfully completed, and the data is now available on such devices as kitchen and bathroom exhaust fans, clothes dryers, central vacuum cleaners, etc. The database is large enough to isolate the effects of duct construction, duct size, fan type, etc. and is available from CMHC for further analysis.

A second project objective was to determine the characteristics of chimneys so that combustion appliance design and modeling could be accomplished with some knowledge of the venting system performance over time. Once again there is a sizeable database which can be manipulated to isolate the effects of chimney size, height, material of construction, etc. At the time of writing this paper, some of this analysis has been done (eg. see Table 2). One question that remains is the true form of the flow-vs-pressure and thermal characteristics.

The DTR generated specified pressure differences during the flow vs pressure testing, at 10 Pa intervals. Refer to Figure 5 for an illustration of the test conditions. For instance, at the first interval, the hood pressure (P_h) minus the basement (or appliance room) pressure (P_b) equals 10 Pa. This does not translate to 10 Pa across the chimney, as the basement pressure varies significantly from the chimney top pressure (P_t). To find the actual pressure difference affecting the chimney flow, it would be necessary to relate P_b and P_t, which involves knowing outside weather conditions (wind and temperature) plus the location of the neutral pressure plane of building tested. Some of this can be gathered or assumed from the test data, but all assumptions affect the accuracy of the calculated characteristic.

During parallel testing using the DTR on an Ottawa chimney study [6], the effects of wind and stack effect on the chimney chracteristic measurements became apparent. From previous experience on leakage flows, the researchers expected the flow vs pressure characteristic

to assume the form of Q = C*P^n, where:

Q is the flow in L/s,
C is a constant in L/(sPa^n)
P is the pressure difference in Pa, and
n is the non-dimensional exponent.

The exponent value was expected to vary between 1 for laminar flow and 0.5 for fully turbulent flow. The results in the chimney testing showed that the exponent

Figure 5: Chimney Testing

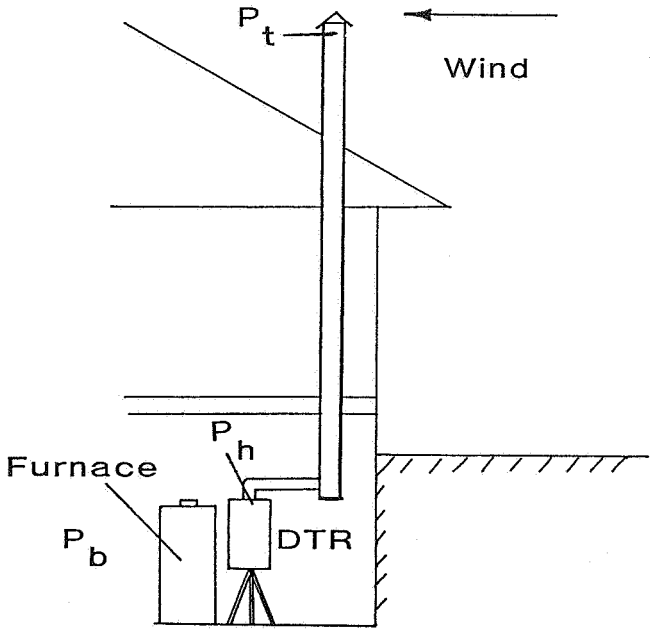

values often ranged between 0.4-0.5, especially when testing bigger chimneys and during windy conditions. Wind and natural draft effects were causing an additional pressure difference across the chimney that was not included in the above calculation. The contractors have suggested two alternatives: accept that the calculated characteristics reflect the actual working conditions of chimneys, or use data available from chimney thermal testing to remove the wind and stack effects. At the time of writing this paper, these calculations have not been completed.

Similarly, the thermal characteristics of chimneys are affected by their time response. Chimneys were heated using 1-2 kW heaters (in addition to the DTR fan heat). The contractor argued from preliminary testing that a chimney-top steady-state temperature was obtained within five minutes, using even such low power inputs during cold weather. (This is not as unlikely as it first appears. This input heat should be compared to the typical heat contained in the flue gases, not to input rating of the appliance.) Although householders were asked to refrain from using the furnace immediately

prior to the testing, it is also likely that the relative amount of cooldown time, from the previous furnace firing, will also bias the results. More definitive answers will be known after further analysis.

5. CONCLUSIONS

While much of the analysis of results from the Duct and Chimney Survey remains to be done, there are some preliminary conclusions available.

1) The duct test rig generally performed as designed. It proved to be relatively easy to measure the flows due to active devices and to establish the pressure-vs-flow characteristics for passive ducts. Some additional theoretical work is necessary to translate the data from fan-forced testing of chimneys.

2) An adequate library of installed exhaust flows in Canadian housing now exists for accurate estimation of house ventilation rates or depressurization limits.

3) The performance of the kitchen and bathroom fans, and the make-up air ducts used in Canadian housing, is far below the designed and required flows. In a significant number of cases, they moved almost no air.

4) There are many chimneys in Canada with high air leakage rates that will affect their ability to vent.

6. ACKNOWLEDGMENTS

The author would like to thank Wayne Pushka for his help in the preparation of this paper.

7. REFERENCES

1) WHITE, J.H. "Identifying Ventilation Troubled Houses" Canada Mortgage and Housing Corporation (CMHC), 1984.

2) FUGLER, D. "Canadian Research into the Installed Performance of Kitchen Exhaust Fans" ASHRAE Transactions 1989, V. 95, Pt.1.

3) SHELTAIR SCIENTIFIC LTD. "Duct Test Rig" for CMHC, 1988.

4) SHELTAIR SCIENTIFIC LTD. "Duct and Chimney Survey" for CMHC, in preparation.

5) PHAFF, H. "Measurement of low air flow rates using a simple pressure compensating meter" Air Infiltration Review, August, 1988.

6) INSTITUTE DE RECHERCHE EN TECHNOLOGIE APPROPRIE "Field-testing of Various Chimneys and Fluepipes" for CMHC, in preparation.

PROGRESS AND TRENDS IN AIR INFILTRATION
AND VENTILATION RESEARCH

10th AIVC Conference, Dipoli, Finland
25-28 September, 1989

Paper 19

THE H,X-DIAGRAM AS A REPRESENTATION OF MEASUREMENTS OF RANGES OF COMFORT IN A LONG DURATION TEST

Prof.Dipl.-Ing.H.Trumper, Dipl.Ing.W.Jansen

Universitat Dortmund (FRG)
Abteilung Bauwesen
Fachbereich Technische Gebaudeausrustung
Postfach 500500
August- schmidt-Strasse 6
D-4600 Dortmund 50
FRG

SUMMARY

A new visual method is yielded by a particular application of Mollier's h,x-diagram. Point fields (temperature and humidity) lead to a significant improvement upon previous graphic methods.

Flats with mechanical balanced ventilation are drier and more influenced by the exterior climate than are with shaft ventilation system ventilated flats ("Berlin ventilation").

The evaluation of the graphic representation of the experimental results in the form of curves permits rapid assessment of the experimental results.

When the experimental data is plotted in Mollier's h,x-diagram, the comparison with fields of comfort published in the literature becomes possible.

The display of the experimental data in Mollier's h,x-diagram further allows both differences between individual flats and seasonal behavioural changes of the occupants to be displayed in a small number of diagrams.

1. INTRODUCTION

Problems with moisture in dwellings always occur whenever the air humidity in inhabited rooms exceeds a certain value and causes damage to buildings or health.
At the present time, when much housing is planned with closely-fitting windows and other structural measures to minimize consumption of energy, low air-exchange coefficients (/7/, p.1193) often lead to moisture damage (/1/, /3/, /5/, /8-12/).

Particularly in winter, it is difficult from the energy-saving point of view to introduce outside air into a dwelling in such a manner that the minimum quantity of energy is needed to heat this air.
On the other hand, especially in winter, a continuous flow of outside air into the dwelling tends to dry the air inside.
The attempt must therefore be made to find a compromise: draughty dwellings have energy costs, whilst well-insulated and tight dwellings may have

such low air-exchange coefficients that the health of the inhabitants suffers.

Consideration of these aspects has led to the emergence of various test buildings which should make it possible to determine the relationships between temperature, humidity, energy and ventilation systems (/5/) in inhabited dwellings. In the investigations, particular attention is paid to the ventilation systems since these significantly influence the interior humidity (/8/, /11/).

2. THE VENTILATION SYSTEMS

The experimental building which yielded the experimental results and thus the h,x-diagrams was approved by the BMfT (Federal Ministry for Research and Technology) in Bonn as an experimental building, and was put into operation in 1983 in Duisburg, in order to investigate various ventilation systems (/10/).
Some of the flats were provided with mechanical balanced ventilation via air-ducts whereby the energy of the exhaust air is transferred to the supply air via a heat-exchanger. The supply air is led into the living area and the discharge air is exhausted from bathroom and kitchen.

The second research house is an equivalent block of flats in the same housing estate; this building has another ventilation system: conventional shaft ventilation which is also known as "Berlin ventilation". Here the air is coming through the window rabbet or the opened window.
Temperature and humidity were detected by four sensors (bedroom, children's-room, dining-room, living-room).
Initial results from the Duisburg experiment are listed in /9/.

Numerous measurements in the experimental flats yielded experimental curves with which visual comparison was used in an attempt to discover the positions at which condensation was favoured: these points were above all windows and outside walls. The surface temperature of these building elements is determined on the one hand by constructional factors (e.g. U-value (/7/, p.128))and on the other hand by the interior air temperature which the occupants can regulate with the aid of the heating system.
Further, initial conjectures on the influence of the

ventilation system were made: "The highest humidity values were measured in flats with tightly-fitting windows but without mechanical ventilation" (/9/, p.112).

3. METHOD OF THE APPLIED H,X-DIAGRAM

A new manner of representing the measured values is indicated by the h,x-diagrams of Mollier (/7/, p.100ff.).
The values of temperature and relative humidity measured hourly during one month are plotted in the h,x-diagram. This yields experimentally-measured comfort fields which are contrasted to the comfort fields according to DIN 1946 (/2/) and Leudsen-Freymark (/5/, p.130 ff.; /8/, p.14).

Comparison of the experimentally-measured comfort fields with e.g. DIN 1946 reveals agreement during the summer months only, whilst the experimental data is most nearly approached by the Leudsen-Freymark comfort field during the other months.
In comparison to both comfort fields, however, the measured values are concentrated towards the right-hand edge of the comfort limits (to higher relative humidity).
The following mean values define the comfort field:

Summer:	temp.:	24	°C at	11	g/kg abs. humidity
Autumn:	temp.:	21	°C at	10	g/kg abs. humidity
Winter:	temp.:	20	°C at	8	g/kg abs. humidity
Spring:	temp.:	21	°C at	7	g/kg abs. humidity

If a new comfort field is defined by the experimental values, this does not lie parallel to a constant temperature as is the case for the above-mentioned fields, but rather lies along a relative humidity of approx. 55 %.
The course at constant relative humidity is especially conspicuous for measurements made during the winter months. It becomes clear that the interior relative humidity remains approximately constant despite fluctuating interior temperatures, whilst the absolute humidity varies with the temperature.

This does not however mean that the flat becomes absolutely dryer when it is heated more, but that the water content of the air increases, and the relative humidity remains almost constant. A possible cause is absorption and desorption from walls and furniture.

The h,x-diagrams for the summer (Figs. 1.1 and 2.1) show that the values for all interior rooms are concentrated around a nucleus at about 25 °C and 50 % - 60 % relative humidity, similar to the exterior weather data. According to the number of occupants it is more humid or drier.

In autumn (Figs. 1.2 and 2.2), the temperatures are lower. The relative humidity increases significantly, and decreases somewhat as winter approaches.

In winter (Figs. 1.3 and 2.3), different comfort fields are found for different rooms, which will certainly be the result of attempts by the occupants to save energy by keeping the room doors closed as far as possible.

Towards spring (Figs. 1.4 and 2.4), the comfort fields are less dispersed. The bedrooms are still cold, whilst the first rays of the sun raise the living-room temperatures somewhat (south-facing living-rooms). Since heating continues to be required, the living-rooms remain warmer. The zone of comfort follows a constant relative humidity in this case too.

The high relative humidity - about 85 % - in autumn (Fig. 2.3) of flats with "Berlin ventilation" is of interest. Although walls and furniture store moisture, this property has only a short time-span of one or two days.

The main proportion must therefore arise from exterior humidity. As soon as the sun shines, the occupants open the windows, and exterior air streams into the flats. When the weather deteriorates, the windows are at once shut, and the moisture remains in the flat because the "Berlin ventilation" cannot transport so much exhaust air.
Since the autumn weather is generally very changeable, and the flats are heated irregularly, the high humidity remains in the flat until winter when heating is continuous.

The method of applied h,x-diagrams permits a rapid and simple visual comparison of flats throughout the year, whereby the influence of the occupants' lifestyle too (e.g. the closing of doors) can clearly be recognized.

h,x-diagram: representation for flats with balanced ventilation

Fig. 1.1

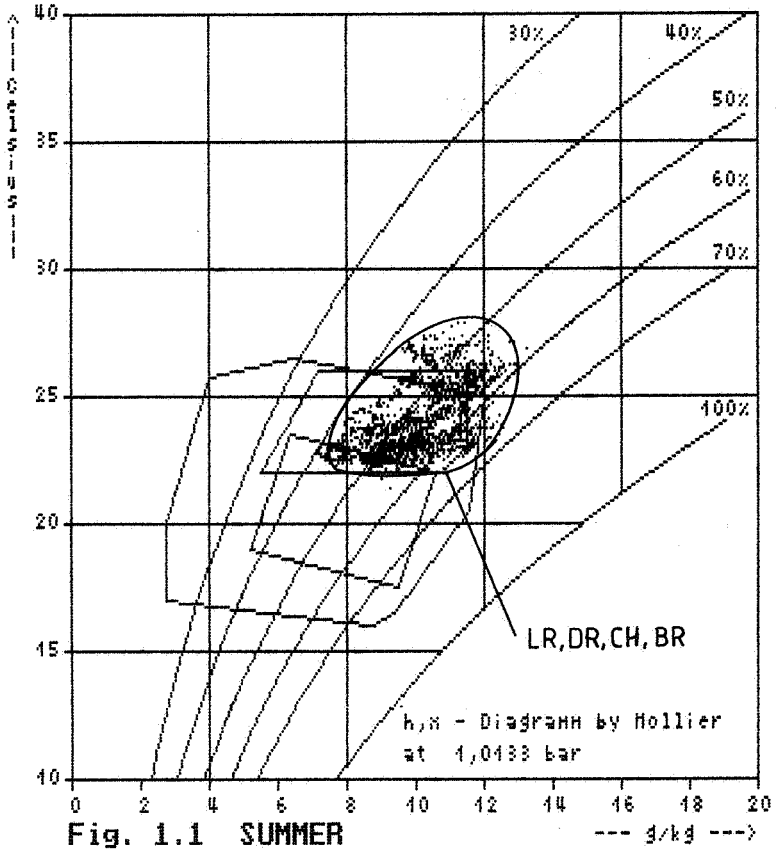

Fig. 1.1 SUMMER

Fig. 1.2

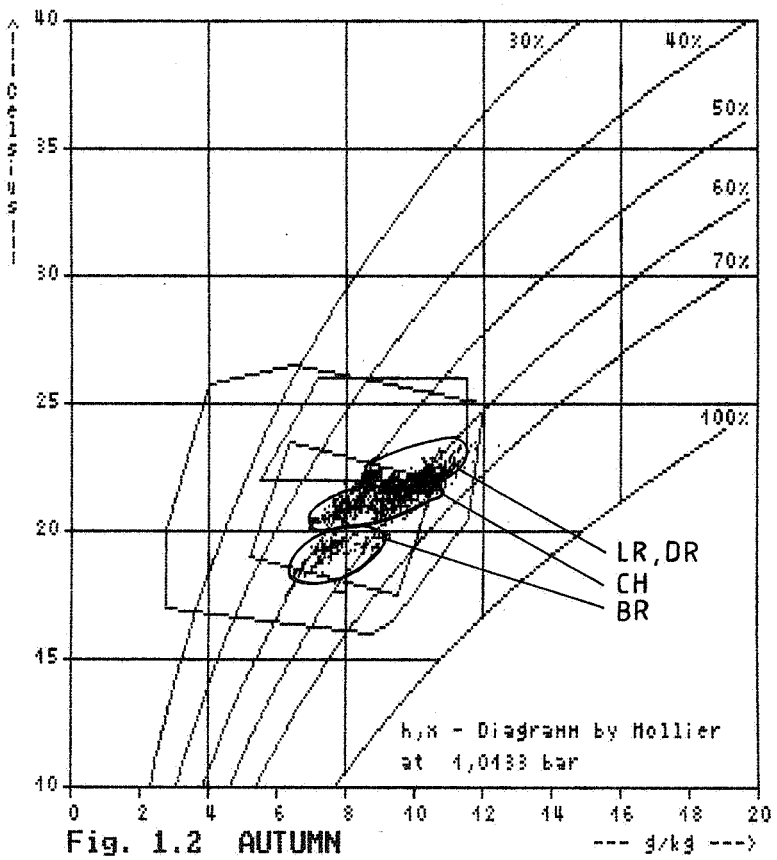

Fig. 1.2 AUTUMN

h,x-diagram: representation for flats with balanced ventilation

Fig. 1.3

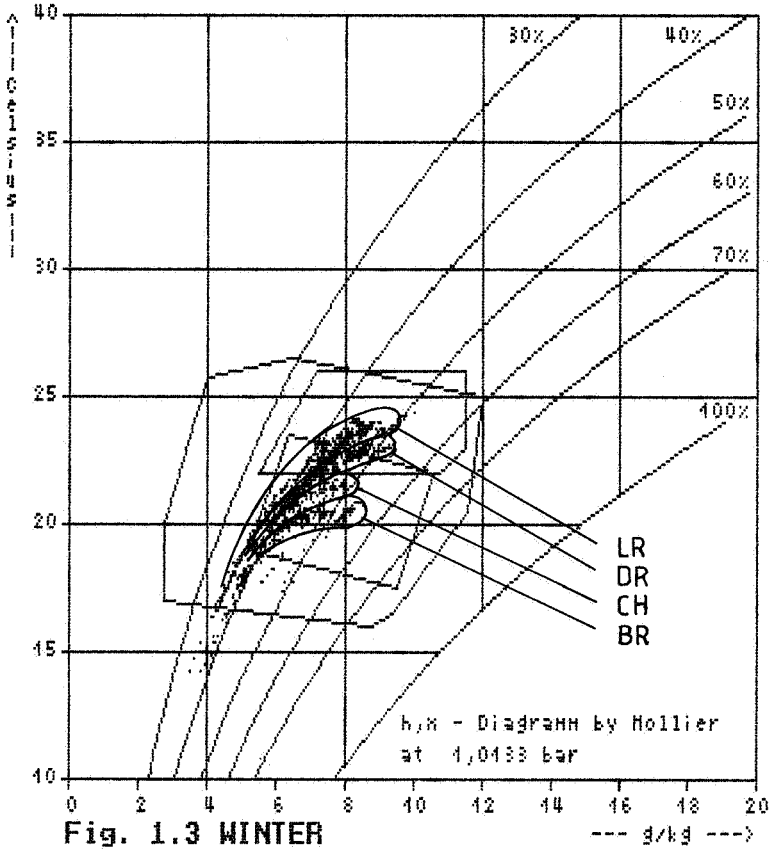

Fig. 1.3 WINTER

Fig. 1.4

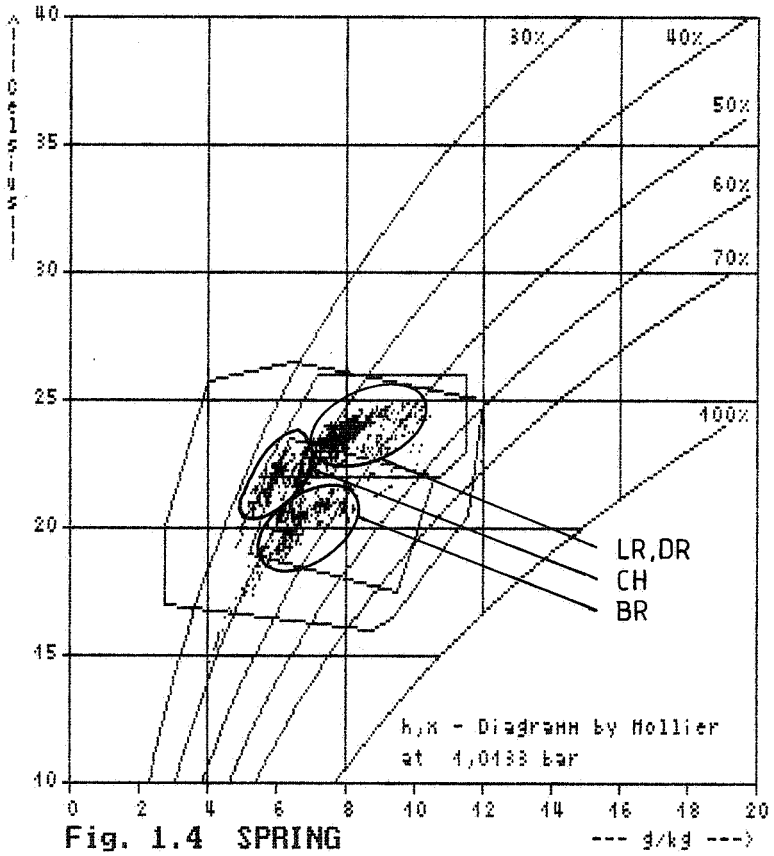

Fig. 1.4 SPRING

h,x-diagram: representation for flats with Berlin ventilation

Fig. 2.1

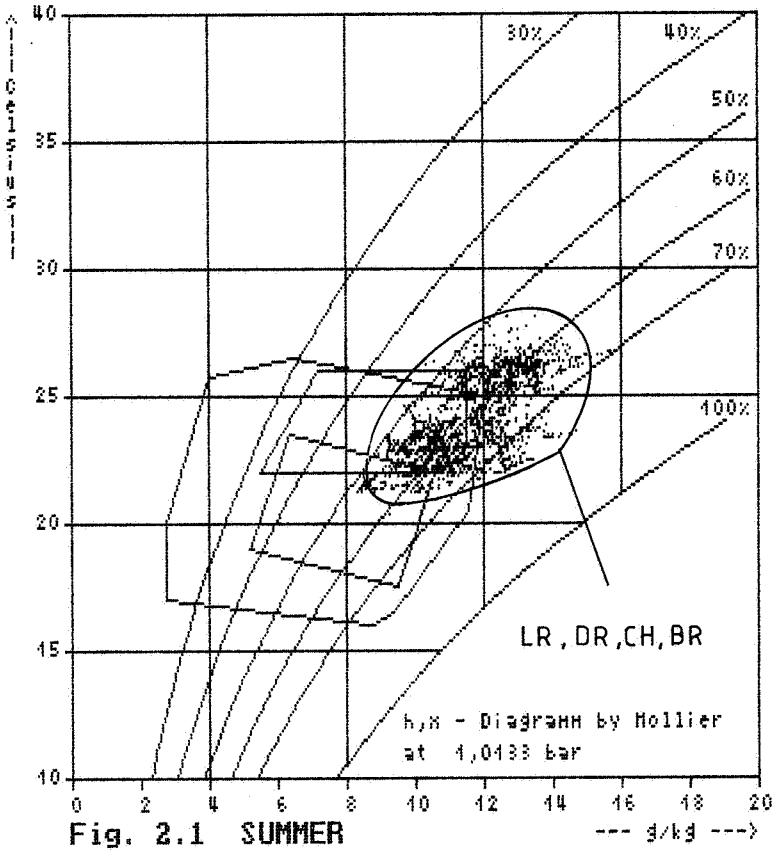

Fig. 2.1 SUMMER

Fig. 2.2

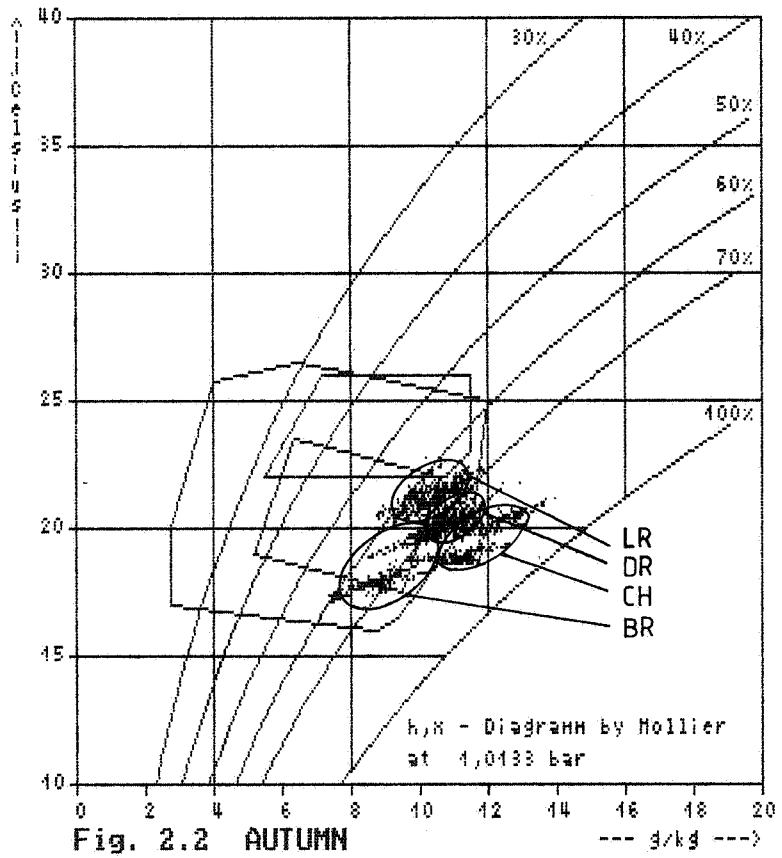

Fig. 2.2 AUTUMN

h,x-diagram: representation for flats with Berlin ventilation

Fig. 2.3

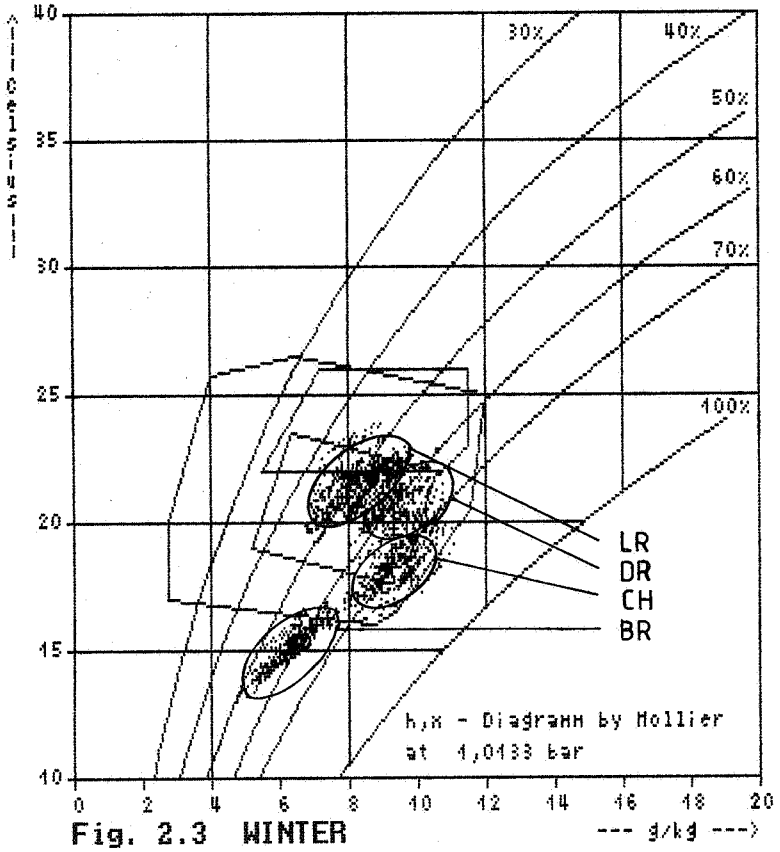

Fig. 2.3 WINTER

Fig. 2.4

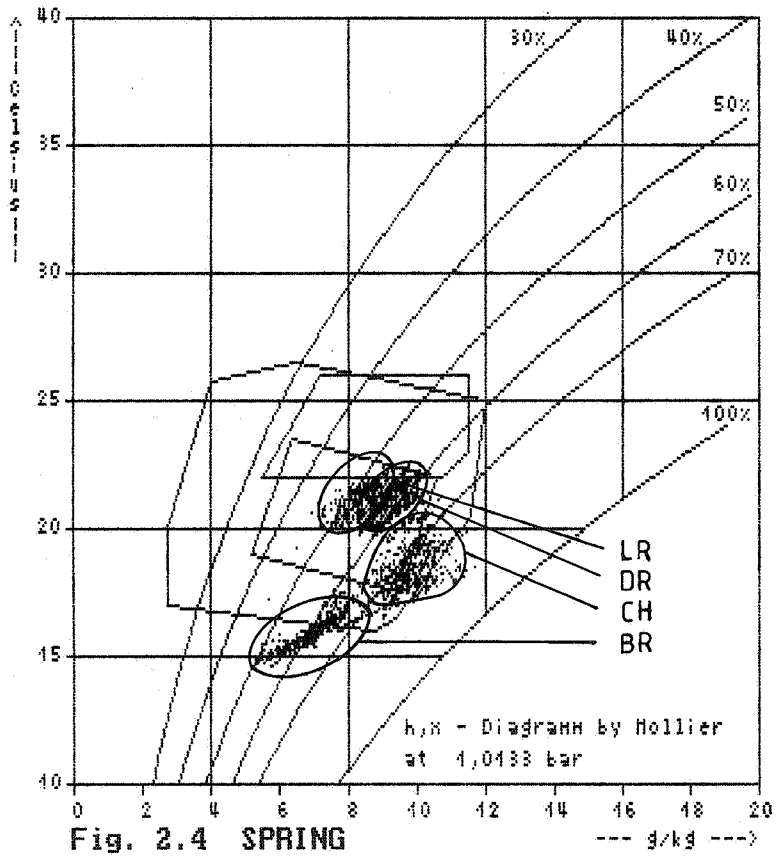

Fig. 2.4 SPRING

LITERATURE

/ 1/ Bley: Untersuchung über Feuchte- und Temperaturverhalten in fensterlosen Innenküchen
Dissertation Universität Dortmund

/ 2/ DIN 1946: Raumlufttechnik E9/86

/ 3/ Erhorn, Gertis: Wohnfeuchte und Wärmebrücken
Heizung, Lüftung, Klimatechnik
Haustechnik HLH 38 1985 Nr.3 S.130-135

/ 4/ Fanger: Thermal Comfort
Mc Graw-Hill Book Company
New York 1972

/ 5/ Jansen W.: Statistische Untersuchungen über Abhängigkeiten von Temperatur, Feuchte und Energieverbrauch in Wohnungen mit verschiedenen Lüftungssystemen
Dissertation Universität Dortmund

/ 6/ Künzel, H.: Die klimaregelnde Wirkung von Innenputzen, Gesundheits Ingenieur 81 (1960), Nr. 7, S. 196-201

/ 7/ Recknagel; Sprenger; Hönmann: Taschenbuch für Heizung und Klimatechnik
München, Wien 1988/89

/ 8/ Schmickler F.-P.: Untersuchungen über die Luftfeuchte in Wohnungen in Abhängigkeit von unterschiedlichen Lüftungssystemen unter Verwendung einer neuen Kennzahl
Dissertation Universität Dortmund

/ 9/ Trümper H., Hain K., Gorißen N.: Zusammenhänge zwischen Energieeinsparung und Raumfeuchtigkeit
Forschungsauftrag BMFT Bonn 1985-1988
Demonstrationsvorhaben Duisburg

/10/ Trümper H., Schmickler F.-P.: Demonstrations- und Forschungsprojekt Duisburg, Vortrag auf dem Kongress CLIMA 2000,
Kopenhagen 1985, VVS Kongres - VVS, Messe ApS, Odrup Jagtvej 42 B

/11/ Trümper H., Hain K., Schmickler F.-P.: Vergleichende Untersuchung verschiedener Lüftungssysteme in bewohnten Mehrfamilienhäusern
Forschungsauftrag BMFT Bonn 1986
Demonstrationsvorhaben Duisburg

/12/ Trümper H., Hain K., Jansen W.: Veröffentlichung auf dem 12. internationalen Kongress für Technische Gebäudeausrüstung
Vergleich verschiedener Wohnraumfeuchten
Demonstrationsvorhaben Duisburg
Berlin 1988

LIST OF SYMBOLS

Fig. - figure

°C - degree Celsius
g - gram
kg - kilogram

LR - living-room
DR - dining-room
CH - children's-room
BR - bedroom

PROGRESS AND TRENDS IN AIR INFILTRATION
AND VENTILATION RESEARCH

10th AIVC conference, Dipoli, finland
25-28 September, 1989

Paper 20

VENTILATION BY DISPLACEMENT: CALCULATION OF THE FLOW IN A THREE-DIMENSIONAL ROOM

Lars Davidson and Erik Olsson

Dept of Applied Thermodynamics and Fluid Mechanics
Chalmers University of Technology
S-412 96 Gothenburg
Sweden

ABSTRACT

Displacement flow systems are becoming popular, especially in Scandinavia, for comfort ventilation. In these systems air is supplied near the floor at low velocity (see Fig. 1); the temperature of the supply air is a few degrees below that of the air in the room. The supply air is heated by persons and/or machinery in the room. Turbulent plumes are formed above these heat sources. Apart from the plumes, the flow in the room is divided into two zones: a lower zone (the occupied zone) to which clean cool air continuously is supplied, and an upper zone (above the occupied zone) where contaminated warm air is recirculating.

In the present study, the flow in displacement flow systems (a water box model) has been calculated using finite difference methods; the results have been compared with experimental data, and the agreement is reasonably good.

NOMENCLATURE

$C_{1\epsilon}$, $C_{2\epsilon}$, C_{μ}	constants in the turbulence model
G	turbulence generating source term in the k and ϵ-equations
G_B	turbulence generating source term due to buoyancy in the k and ϵ-equations
g	acceleration due to gravity
k	turbulent kinetic energy
L	length of a side of the cubical room (see Fig. 2)
n	nominal time constant (= number of air changes/hour)
p	pressure
Q	heat source
S_{ϕ}	source term of general variable
t	temperature in ^{o}C
U, V, W	mean velocity in x, y and z-directions, respectively
U_i	mean velocity in x_i- direction
$\dot{V}$	volumetric flow rate
x	horizontal Cartesian coordinate (see Fig. 2)
x_i	Cartesian coordinate in the i-direction
y	horizontal Cartesian coordinate (see Fig. 2)
z	vertical Cartesian coordinate (see Fig. 2)
z_{front}	the z-level of the front (see Fig. 1)

Greek symbols

β	coefficient of thermal expansion
τ	time
$\Delta\tau$	time step
Γ_{ϕ}	exchange coefficient of dependent variable

ϵ	dissipation of turbulent kinetic energy
μ, μ_t, μ_{eff}	dynamic viscosity (laminar, turbulent and effective, respectively)
ρ	density
σ_ℓ	laminar Prandtl number
σ_k, σ_t, σ_ϵ	turbulent Prandtl number for k, t and ϵ, respectively
ϕ	dependent variable

Subscripts

in	inlet
out	outlet
ref	reference value for the room

1. INTRODUCTION

Displacement flow systems have been used for industries with heavy heat loads for many years [1,2]. In Scandinavia this type of ventilation system has also become popular for comfort ventilation in rooms; here persons, machinery, lighting etc. constitute the heat loads. The features of this new displacement flow system and the traditional mixing ventilation are given below.

Mixing flow systems

In these systems the air is supplied through a small inlet device near the ceiling (or in the ceiling) at relatively high velocity. A jet, or wall jet, is formed and it entrains the air in the whole room. This gives a nearly uniform distribution of temperature and contaminant throughout the room.

Displacement flow systems

The air is supplied at low velocity through a large inlet device near the floor; the temperature of the supply air is cooler than that in the room. The cool air is heated by the heat source (see Fig. 1). A plume is formed above the heat source due to the higher temperature there (the density is lower) than in its surroundings. The volume flow rate in the plume entrains the surrounding air, and the flow rate in the plume increases with height. At the vertical level z_{front} (the z-level of the front, see Fig. 1) the flow rate in the plume is equal to total ventilation flow rate. The flow in the room is divided into two zones at the front: a lower zone with clean cool supply air, and an upper zone where contaminated heated air is recirculating (for further details, see Section 3).

As displacement flow systems are now increasingly replacing the traditional mixing flow systems, it is of great interest to perform a numerical study of the flow in a displacement system. The object of

the present study is to calculate the flow in such a configuration using finite-difference methods, and to compare the calculated results with experimental data [3] in order to investigate how well such flows can be predicted using finite-difference methods. No such investigation has, to the best of the author's knowledge, previously been carried out.

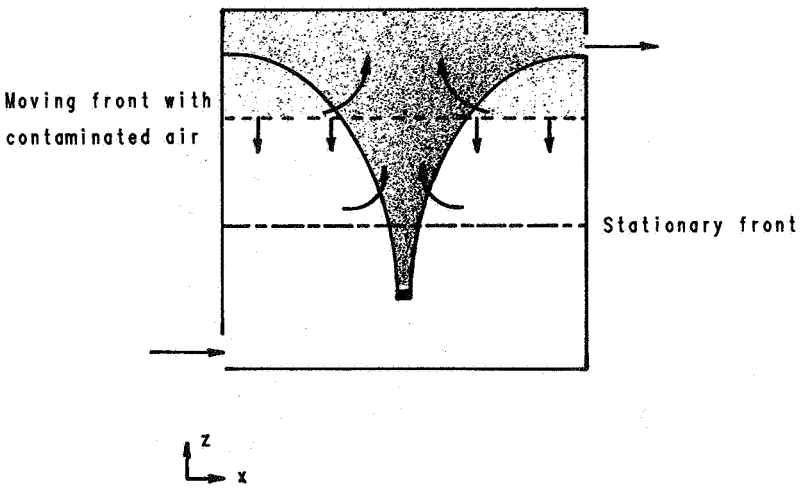

Figure 1. A schematic figure for a displacement flow system.

The experiments (and the calculations) were carried out in a water box model; water was chosen as medium because it is easier to carry out visualization experiments in water.

The finite difference method used is briefly presented in Section 2, and in Section 3 the function of displacement flow systems is described. Results are given in Section 4, and conclusions are drawn in Section 5.

2 SOLUTION PROCEDURE

The computer program by Davidson and Hedberg [4] has been used. The program solves equations of the type

$$\frac{\partial}{\partial \tau}(\rho\phi) + \frac{\partial}{\partial x_i}\left(\rho U_i \phi - \Gamma_\phi \frac{\partial \phi}{\partial x_i} \right) = S_\phi \qquad (1)$$

by expressing them in finite difference form. The finite difference equations are solved by a method which is based on the SIMPLEC procedure by Van Doormal and Raithby [5]. The four main features are [6]:

Table 1. Definition of Γ_ϕ and S_ϕ for conservation equations

Equation	ϕ	Γ_ϕ	S_ϕ
Continuity	1	0	0
Momentum	U	μ_{eff}	$-\partial p/\partial x$
Momentum	V	μ_{eff}	$-\partial p/\partial y$
Momentum	W	μ_{eff}	$-\partial p/\partial z + \rho\beta g\ (t-t_{ref})$
Temperature	t	$\mu/\sigma_\ell+\mu_t/\sigma_t$	0
Turbulence energy	k	μ_{eff}/σ_k	$G - \rho\epsilon + G_B$
Turb. dissipation	ϵ	$\mu_{eff}/\sigma_\epsilon$	$\epsilon/k[C_{1\epsilon}(G+G_B) - C_{2\epsilon}\rho\epsilon]$

Notes:

1. $G \equiv \mu_t \frac{\partial U_i}{\partial x_j}\left(\frac{\partial U_i}{\partial x_j} + \frac{\partial U_j}{\partial x_i}\right)$; $\mu_{eff} = \mu + \mu_t = \mu + C_\mu \rho k^2/\epsilon$

   $G_B \equiv -\frac{g\beta}{\sigma_t}\mu_t \frac{\partial t}{\partial z}$

2. Turbulence constants [7]

   $C_\mu = 0.09$; $C_{1\epsilon} = 1.44$; $C_{2\epsilon} = 1.92$; $\sigma_k = 1.0$; $\sigma_\epsilon = 1.3$

   $\sigma_t = 0.9$

i) use of staggered grids for the velocities;

ii) formulation of the difference equations in implicit, conservative form, using hybrid upwind/central differencing;

iii) rewriting of the continuity equation into an equation for pressure correction, where the latter is used to correct the pressure and the velocities; and

iv) iterative solution of the equations.

A transient formulation was adopted as a convenient means of introducing relaxation into the iterative solution. When only the steady-state solution is of interest, the time step, $\Delta\tau$, is used as a free parameter through which the convergence rate may be optimized.

In the present calculations the dependent variable in Eq. (1) takes the following forms: U, V, W, t, k, ϵ and 1 (continuity equation). The corresponding coefficients, Γ_ϕ, and sources, S_ϕ, are defined in Table 1. The Boussinesque approximation was used for the gravitation term in the W-momentum equation.

2.1 Boundary Conditions

The xz-plane y = L/2 is a symmetry plane (see Fig. 2), and the calculations were consequently carried out in one half of the room only (0<y<L/2). At the symmetry plane zero gradient was imposed for all variables except for the V-velocity, which was set to zero.

Constant profiles were used at the inlet. The inlet velocity and temperature were set according to the experiments; the turbulent quantities were set to zero since the flow through the inlet was considered to be laminar (for n=2 the Reynolds number based on the inlet velocity and height of the inlet was 280).

Conventional wall-functions [7,8] were used for velocity components parallel to the walls, k and ϵ at all walls; zero heat flux (adiabatic walls) was applied for the temperature.

At the outlet the exit velocity was set according to mass balance and zero stream wise gradient was imposed for the remaining variables.

The heat source in the middle of the room (see Fig. 2) was evenly distributed in the volume bounded by the dotted lines.

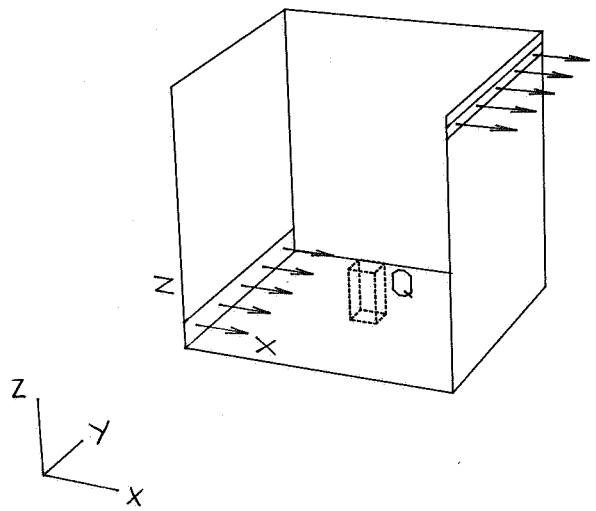

Figure 2. Configuration. The room is cubical with side-length L (=0.5 m). The height of the inlet is 0.2L. xz-plane y=L/2 is a symmetry plane. A heat source, Q, is introduced (uniformly distributed) in the region bounded by dotted lines in the middle of the room (0.48<x/L<0.52, 0.48<y/L<0.52, 0<z/L<0.22)

3. VENTILATION BY DISPLACEMENT

In displacement flow systems the clean air is supplied through a large inlet near the floor, and the air is extracted near the ceiling; the temperature of the incoming air is a few degrees below that of the room temperature. Figure 1 shows schematically how ventilation by displacement works. The incoming air is heated by persons and/or machinery in the room, and the heated (and contaminated) air rises due to buoyancy. Above the heat source a turbulent buoyant plume is formed which entrains surrounding air on its way upwards; thus the air flow rate in the plume increases with height. When the air in the plume reaches the ceiling it spreads laterally. As the air flow rate in the plume ($\dot{V}_{plume}$) is normally much greater than the total ventilation flow rate ($\dot{V}_{in}$), a fraction ($\dot{V}_{plume} - \dot{V}_{in}$) cannot, due to continuity, be extracted through the outlet, but it must turn downwards. At each horizontal plane above the heat source the upward directed air flow rate in the plume must, due to continuity, exceed the downward directed flow rate by the total ventilation flow rate, $\dot{V}_{in}$. At the z-level where the air flow rate in the plume is equal to the total ventilation flow rate, the downward directed flow will turn upwards again; this z-level is called the <u>front</u>.

In this way the flow in the room is divided into two zones:

i) the lower zone to which clean air is supplied (except in the plume where contaminated air is moving upwards);

ii) the upper zone where contaminated air is recirculating.

The plane which divides these two zones is called the <u>front</u>. It is, of course, desirable that the front is located above the occupied zone.

When ventilation by displacement is compared with traditional mixing ventilation, the following points are worth noting.

i) In mixing ventilation the contaminants are dispersed evenly in the whole room. This implies that, when the flow is stationary, the conditions in the room are the same as at the outlet. The aim of ventilation by displacement is to keep the contaminants isolated by quickly <u>displacing</u> (transporting) them to the region above the occupied zone. In the ideal system this means that the conditions in the occupied zone are the same as in the supplied air.

ii) Stagnation zones with low ventilation efficiency are often formed in mixing ventilation, whereas in ventilation by displacement this does not usually occur.

iii) For a given ventilation air flow rate the z-level of the front is strongly dependent on the heat load, and the higher the heat load is, the lower the z-level of the front will be. The location of the front is a crucial parameter for the performance of the displacement flow system. It may happen that the front is located in the occupied zone [9], which, of course, is not desirable.

iv) In office buildings cooling is needed almost throughout the year (even in Scandinavia!). Since, in displacement systems, the cool air is in the occupied zone (and the heated air above) less cooling effect (less under-temperature on the supply air) is needed in these systems compared with mixing flow systems.

4. RESULTS

The flow in a three-dimensional room is calculated, see Fig. 2. The width of both the inlet and the outlet is equal to the width of the room. In the middle of the room near the floor a heat source is introduced (dotted region in Fig. 2). The medium is water, and the inlet temperature is around 13°C. Sandberg and Lindström [10] and Sandberg [3] have carried out a number of experimental investigations on this configuration in which vertical temperature profiles have been measured; the calculated results are compared with these data. More details can be found in [8,11].

Table 2. Data for five different cases.

Case	Q^* [W]	n [1/h]	U_{in}[m/s]
Q200	200	2	0.00277
Q300	300	2	0.00277
Q400	400	2	0.00277
Q600	600	2	0.00277
n4	600	4	0.00544

*Note that only Q/2 is introduced in the calculations, since the calculations are carried out in one half of the room only (y = L/2 is a symmetry plane).

Calculations are carried out for five steady flow cases, see Table 2. All cases have been calculated using a rather coarse numerical grid with 19x11x18 nodes. Case Q200 has also been calculated using a finer grid with 35x19x38 nodes. In all figures presented below, the coarse grid has been used unless otherwise stated.

The calculated velocity vectors for Case Q200 are shown in Figs. 3-5. It can be seen that the flow goes from the inlet towards the opposite wall. Near the heat source ($x/L \approx 0.5$, $y/L \approx 0.5$), the flow is, due to buoyancy, lifted up towards the ceiling, and a turbulent buoyant plume is formed. At the xz-planes where the heat source is introduced ($y/L \approx 0.5$, see Fig. 3b), the direction of the flow is changed from horizontal in the positive x-direction to vertically upwards; in the other xz-planes the direction of the flow is not changed so much, see Fig. 3a.

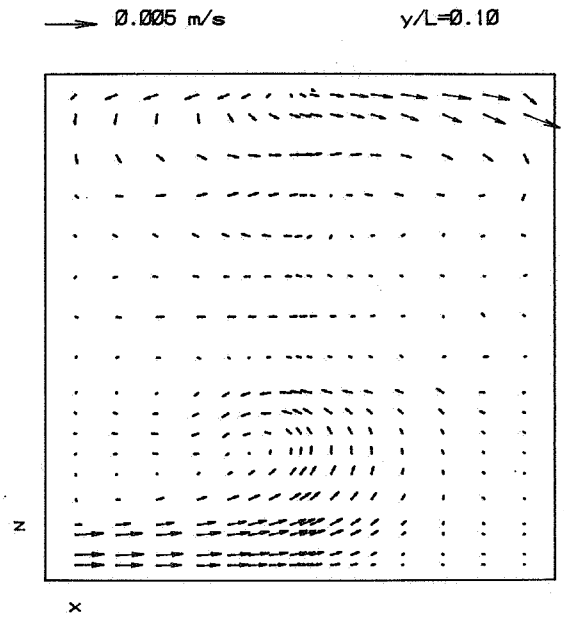

a)

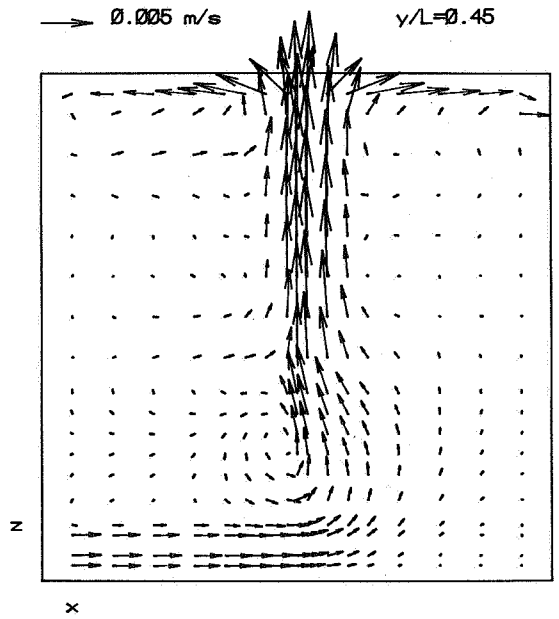

b)

Figure 3. Calculated velocity vectors. Case Q200. xz-plane. a) y/L=0.1, b) y/L=0.45.

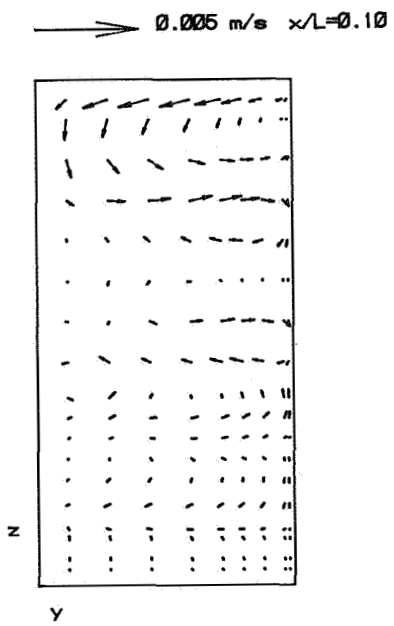

a)

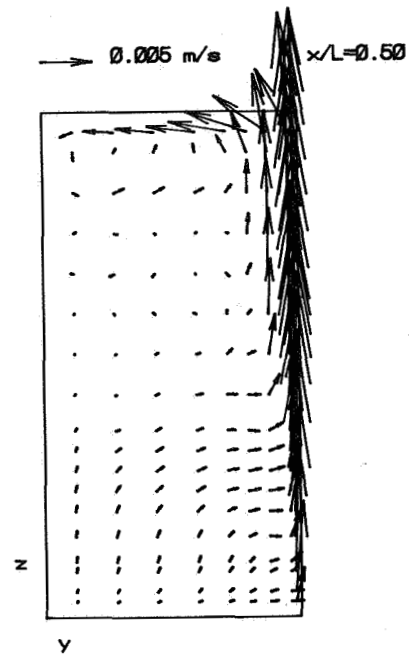

b)

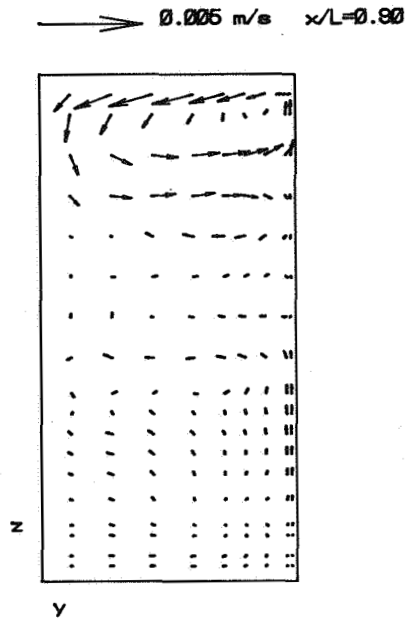

c)

Figure 4. Calculated velocity vectors. Case Q200. yz-plane. a) x/L=0.1, b) x/L=0.5, c) x/L=0.9.

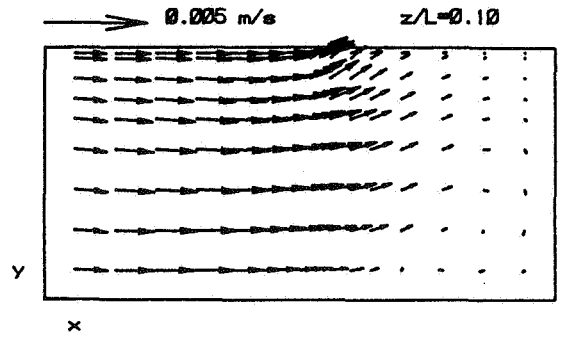

a)

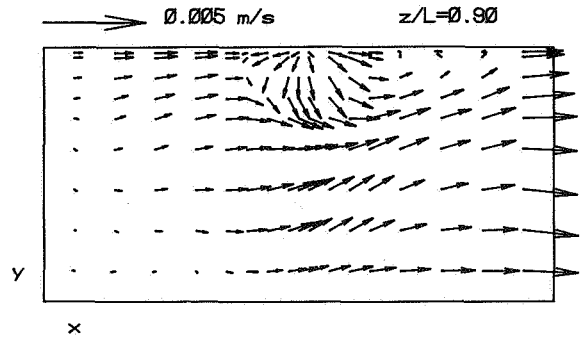

b)

Figure 5. Calculated velocity vectors. Case Q200. xy-plane. a) z/L=0.1, b) z/L=0.9.

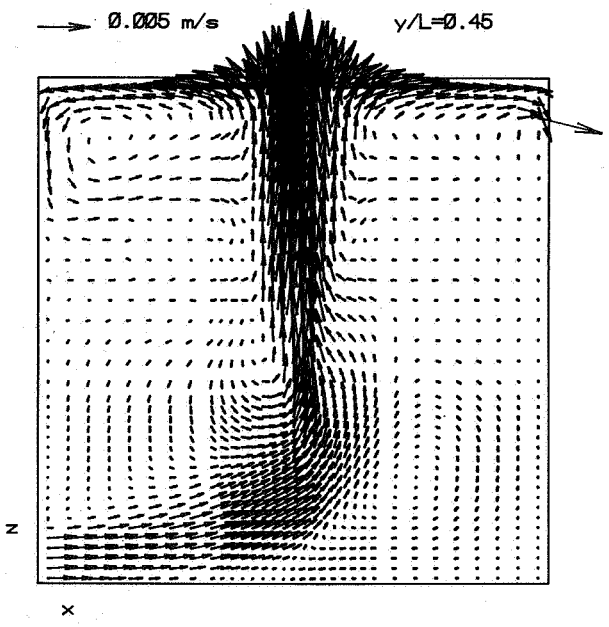

Figure 6. Calculated velocity vectors. Case Q200, fine grid. xz-plane, y/L=0.45.

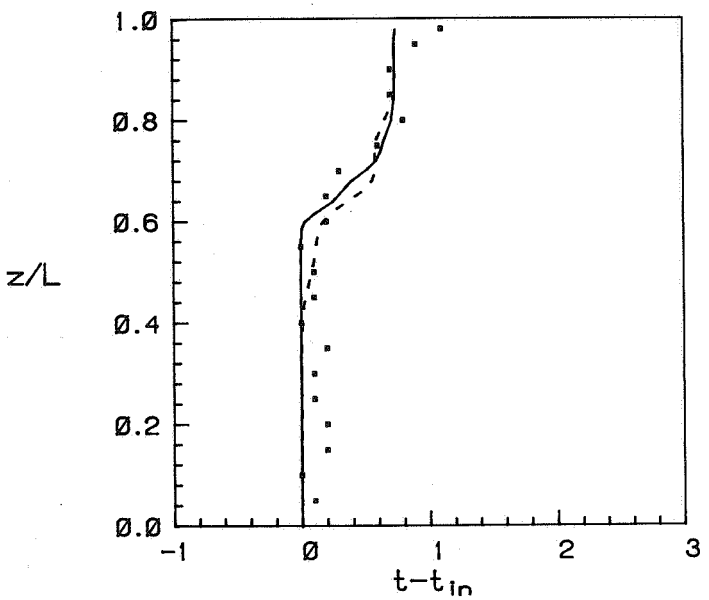

Figure 7. Temperature profiles along a vertical line at x/L=0.5, y/L=0.1. Case Q200. Solid line: calculations, fine grid; dashed line: calculations, coarse grid; markers: experiments [3].

The calculated velocity vectors shown in Fig. 6 were obtained using the 35x19x38-node grid. When these results are compared with those obtained using the 19x11x18-node grid (Figs. 3-5), it can be seen that the flow patterns are very similar. The calculated temperature profile along a vertical line, obtained with the fine grid, is compared with that obtained with the coarse grid in Fig. 7, and, again, the results predicted using the two grids are very similar.

The calculated temperature profiles along four vertical lines for Case Q200 are compared with experimental data in Fig. 8a. It can be seen that the calculated results agree well with the experimental data; the experimental temperatures near the ceiling are, however, somewhat higher than the calculated ones. The reason for this may be that in the experiments warm water is trapped at the ceiling because the outlet is situated at some distance below the ceiling, or it may be that the ceiling is insuffiently insulated (the surrounding room temperature in the experiments was approximately 20^{o}C [3]).

In Fig. 8b the calculated temperature profiles for Case Q600 are compared with experiments. Here the experimental values are larger than the calculated ones. It should be noted that this already is the case already near the floor, which might be due to the possibility that in the experiments the water has been heated on its way from the inlet to the measuring points (which are located near the wall opposite the inlet). This heat may come from outside the water box model due to insufficient insulation of the walls, or it may be that heat diffuses from the plume or from the upper part of the room to this region. The question of how well the walls are insulated in the experiment is easily answered by checking how well the global heat balance is satisfied [heat source=$\rho\dot{V}_{in}$ (t_{out}- t_{in})]. In Case Q200, 68 Watt is leaking through the walls, and in Case Q600 90 Watt. In the former case most of the heat seems to come through the ceiling. The diffusion from the plume and/or from the upper part of the room is probably more important in Case Q600 than in Case Q200, since the turbulent diffusion is larger in Case Q600, due to the velocities and the velocity gradients being larger. Another problem in the experiments for Case Q600 is that the inlet temperature drifts between 12.5 and 12.8^{o}C; t_{in}= 12.6 has been used in Fig. 8b (as well as in Figs. 14-15, see below). This drift of the inlet temperature can also be the reason for why the experimental temperatures near the floor are higher than the calculated ones. Despite the discrepancies between the experimental and the calculated temperature profiles, their <u>form</u> is very similar.

It is further seen in Fig. 8 that the calculated temperature profiles are all very similar, which shows that the temperature is nearly a function of z only, i.e. t = function(z).

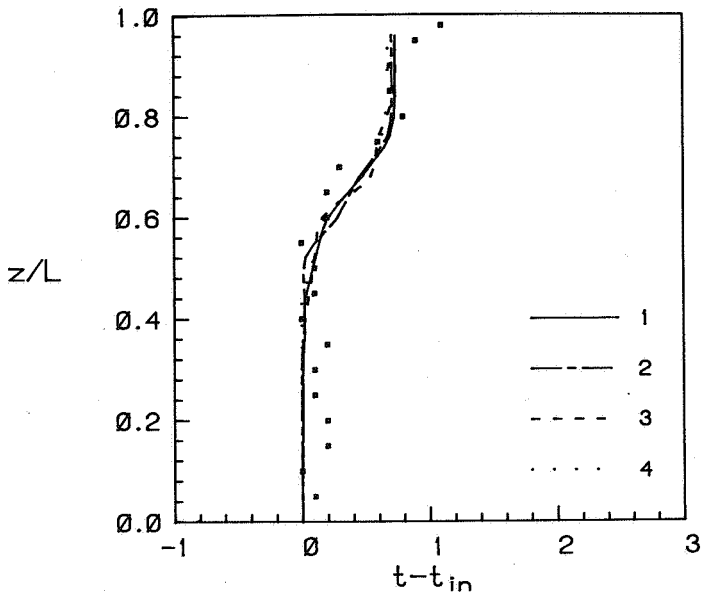

a)

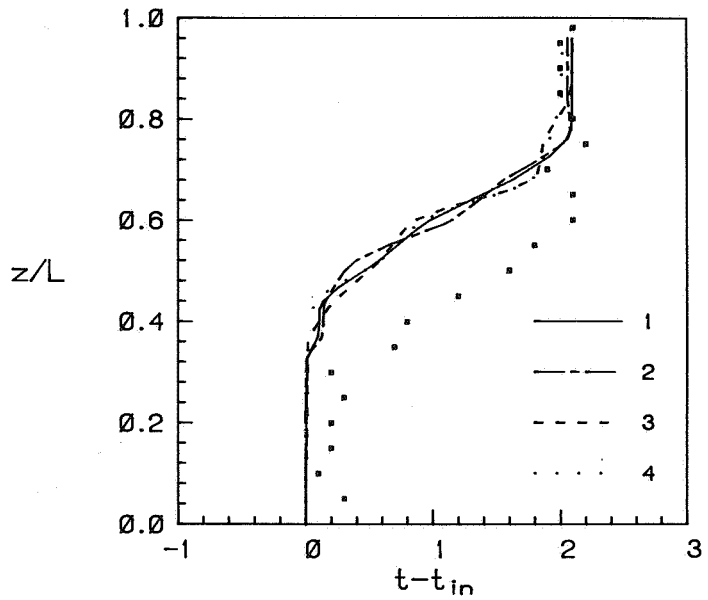

b)

Figure 8. Temperature profiles along vertical lines. Line 1: x/L=0.1, y/L=0.1; line 2: x/L=0.9, y/L=0.1; line 3: x/L=0.1, y/L=0.4; line 4: x/L=0.9, y/L=0.4. Markers: experiments [3]. a) Case Q200. b) Case Q600

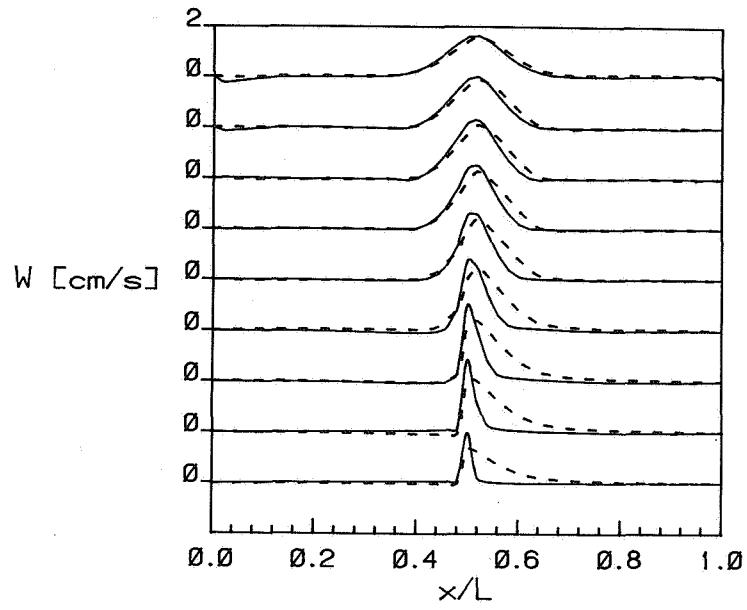

a)

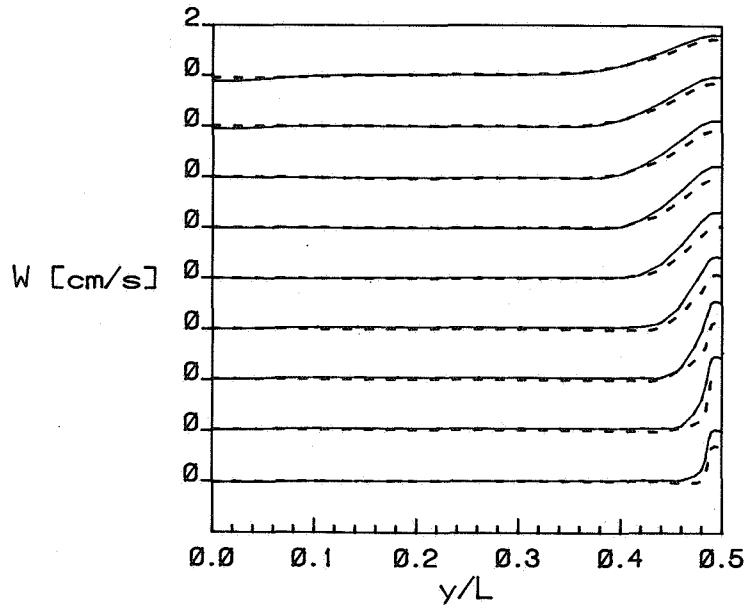

b)

Figure 9. Calculated horizontal W-velocity profiles. z/L=0.1,0.2,..., 0.9. Case Q200. Solid lines: fine grid; dashed lines: coarse grid. a) xz-plane, y/L=0.5, b) yz-plane, x/L=0.5.

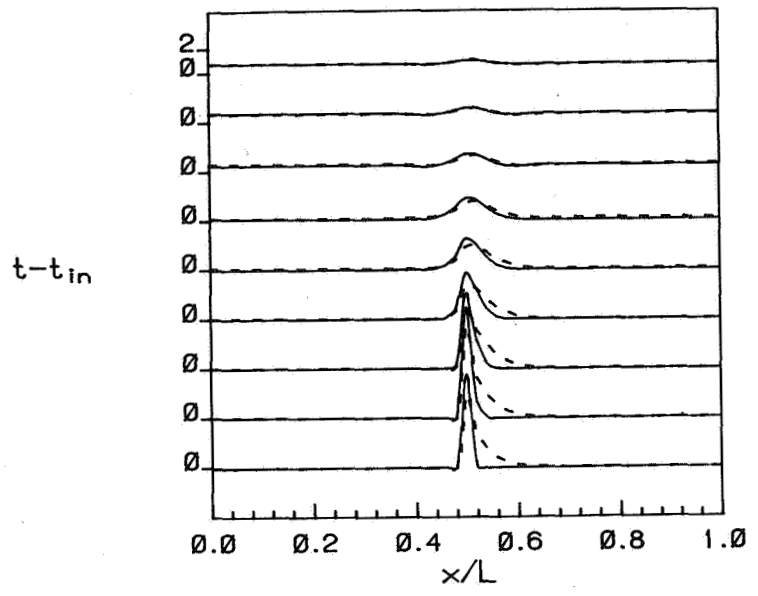

a)

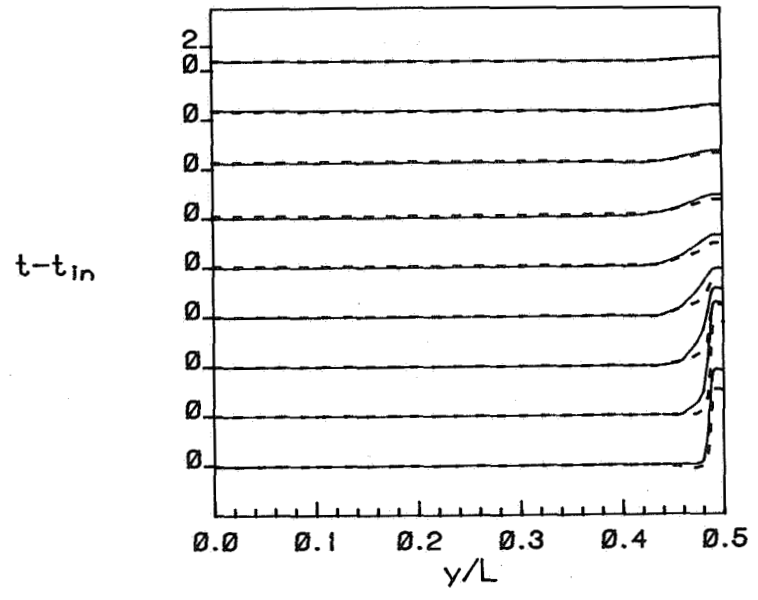

b)

Figure 10. Calculated horizontal temperature profiles. z/L=0.1,0.2, ...,0.9. Case Q200. Solid lines: fine grid; dashed lines: coarse grid. a) xz-plane, y/L=0.5, b) yz-plane, x/L=0.5.

Horizontal W-velocities and temperature profiles for the planes x/L = 0.5 and y/L = 0.5 are presented in Figs. 9-10. Outside the plume, it is striking how constant both the W-velocity (which is close to zero) and the temperature are. The flow is very stratified outside the plume, and moves horizontally along the isothermals; this was also found by the author [12], where the flow in three-dimensional thermally ventilated rooms was calculated. Further it can be seen (in Figs. 9-10) that the profiles predicted with the two different grids differ rather much from each other. The profiles predicted with the coarse grid are somewhat asymmetrical around the mid-plane x/L = 0.5, which shows that the plume is affected by the inlet wall jet, and that the plume is pushed away from the inlet by the wall jet. This phenomenon is, however, caused by the coarseness of the grid. Despite these differences between the predictions with the two grids, the predicted values of the z_{front} differ not more that 5 percent (see below).

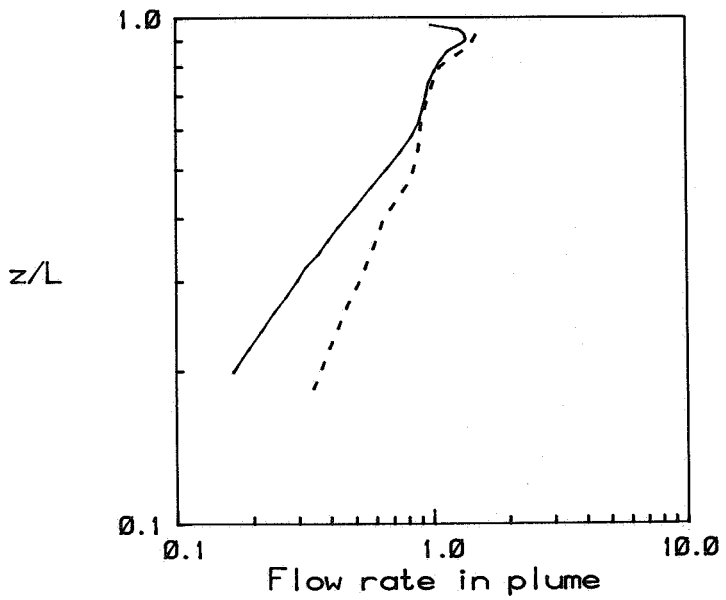

Figure 11. Calculated flow rate in the plume scaled with the total ventilation flow rate. Case Q200. Solid line: fine grid; dashed line: coarse grid.

A parameter which is of great interest to an engineer who is designing a displacement flow system is the flow rate in the plume; when this parameter is known the value of the z_{front} is easily obtained ($z=z_{front}$ where $\dot{V}_{plume} = \dot{V}_{in}$). The flow rate in the plume as a function of the vertical coordinate, z, is shown in Fig. 11, and, as can be seen, the discrepancy between the flow rate predicted with the two grids is rather large; this was to be expected, as the W-velocities in Figs. 9a and 9b are rather different. The flow rate in the plume as a function of z was calculated as

$$\dot{V}_{plume}(z) = \int_{\delta A(z)} W(x,y,z)dA, \quad W(x,y,z) > \lambda W_{max}(z)$$

The area of the plume, $\delta A(z)$, in the integral is thus defined as the region where the W-velocity at the z-level in question is larger than $\lambda W_{max}(z)$ [$W_{max}(z)$ is the maximum W-velocity at level z]. The factor λ was chosen as 0.05; an increase of λ to 0.1 altered the calculated flow rate less than 5 percent. According to Chen and Rodi [13] the flow rate in a plume varies as z^m where m = -5/3; the flow rate predicted with the fine grid gives m = -1.52 for z/L<0.6. For larger z the flow rate increases at a much lower rate, because the temperature difference between the plume and its surroundings (which is the driving potential for the plume) decreases.

From the flow rate in the plume the value of the z_{front} is, as mentioned above, easily calculated. For the coarse grid $z_{front}/L=0.74$ is obtained, and for the fine grid, $z_{front}/L=0.68$ (Case Q200); for Case Q600 the value 0.62 is obtained.

It is not clear how to define the experimental value of the z_{front} from temperature profiles; if the z_{front} is defined as the average of the two levels where:

i) the temperature exceeds the inlet temperature by Δt; and

ii) the temperature is Δt below the temperature at the ceiling or, rather, below the outlet;

where Δt is, say, 0.1^oC, then the experimental values $z_{front}/L \approx 0.45$ for Case Q600, and $z_{front}/L \approx 0.7$ for Case Q200 are obtained. The calculated value thus agrees well for Case Q200, but less well for Case Q600. It is hard to tell whether this discrepancy is due to inaccuracies in the experiments or in the calculations, and it should be remembered that the front is not very distinct for this case, since the temperature increase from minimum to maximum occurs over a very long distance ($\approx 0.4L$).

What happens when the heat load is increased? The velocity and the flow rate in the plume should increase and, consequently, the value of the z_{front} should decrease. This is because the larger the heat source is, the larger the flow rate in the plume, and the lower the z-level where the flow rate in the plume is equal to the total ventilation flow rate, i.e. where $z=z_{front}$ (see Section 3). In Fig. 12. the calculations with different heat loads (Q200, Q300, Q400, Q600) are presented. It is seen that the value of the z_{front} does decrease with increasing heat load as expected.

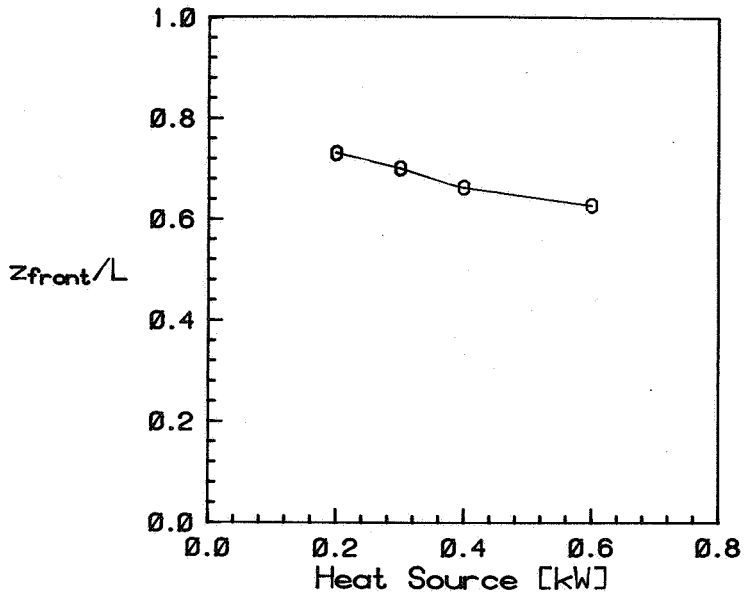

Figure 12. Calculated z_{front}/L as a function of the heat load. Cases Q200, Q300, Q400, Q600

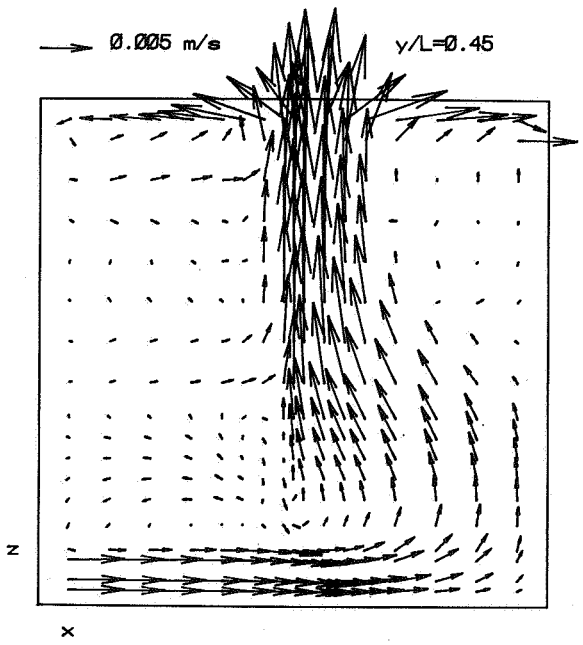

Figure 13. Calculated velocity vectors. Case n4. xz-plane, y/L=0.45.

Whereas a higher heat load gives a lower value of the z_{front}, a larger total ventilation flow rate (higher inlet velocity) gives the opposite result: a higher position of the front. Calculations with different inlet velocities were carried out in order to plot the position of the front versus the number of air changes/hour, n. It was found, however, that the inlet wall jet disturbs the plume for high velocities, see Fig. 13. It can be seen that near the floor the wall jet passes the heat source (at x/L=0.5) without being lifted (compare Figs. 3b, 6).

4.1 Computational Details

All calculations have been performed on a VAX 2000, which is about half as fast as a VAX 785 for this type of application. The CPU time required for a convergent solution varied between 26 hours (Case Q200) and 48 hours (Case Q600) using the coarse grid. The CPU time using the fine grid was approximately 80 hours. Time steps of five seconds were used, and two to four thousand time steps were needed in order to get a convergent solution.

It is well known that for buoyancy driven flows (as in displacement flow systems) it is hard to get convergent solutions [14,15]. For Case Q600 no steady solution could be obtained, but the flow had to be calculated transiently. The time variation of the flow was, of course, very small after 60 minutes in real time.

5. CONCLUSIONS

The flows in displacement flow systems have been calculated and compared with experimental data. The predicted flow pattern was shown to agree reasonably well with experiments. The calculated results show the typical, for displacement flow systems, division of the flow into two zones: one lower well ventilated zone, and one upper zone where warm fluid is recirculating. The calculated temperature profiles have been compared with experimental ones, and the agreement was good in one case (Case Q200), but less good in Case Q600. It is hard to tell whether the reason for this discrepancy is inaccuracies in the experiments or in the calculations.

The z-level of the front (see Fig. 1) was well predicted in Case Q200 (it differed less than 5 percent from the experimental value), but it was less well predicted in Case Q600 (25 percent lower than the experimental value). The front is, however, not very distinct for this latter case, since the temperature increase from minimum to maximum occurs over a very long distance ($\approx$0.4L).

The present calculations have been carried out in a water box model [3], which has different Reynolds numbers and Archimedes numbers than a full scale room with air as medium. There is a need for more numerical studies of the flow in full scale rooms in order to further investigate the feasibility of finite-difference methods in calculating the flow in displacement flow systems; in such calculations, heat radiation effects should be taken into account.

ACKNOWLEDGEMENTS

The author wishes to thank Dr. Mats Sandberg at the National Swedish Institute for Building Research, who has been very helpful. The author is also grateful to Professor Erik Olsson for his help and support. The Swedish Council for Building Research has sponsored this work.

REFERENCES

1. BEIER, R.A. and GORTON, R.L., "Thermal Stratification in Factories - Cooling Loads and Temperature Profiles", ASHRAE Trans., Vol. 84, Part 1, 325-338 (1978).

2. KREICHELT, T.E., KERN, G.R. and HIGGINS Jr, F.B., "Natural Ventilation in Hot Process Buildings in the Steel Industry", Iron and Steel Engineer, 39-46 (1976).

3. SANDBERG, M., Private communication, National Swedish Institute for Building Research, Gävle, Sweden (1988).

4. DAVIDSON, L. and HEDBERG, P., "A General Computer Program for Transient, Three-Dimensional, Turbulent, Recirculating Flows", Rept. 86/13, Dept. of Applied Thermodynamics and Fluid Mechanics, Chalmers University, of Technology, Göteborg (1986).

5. VAN DOORMAAL, J.P. and RAITHBY, G.D., "Enhancements of the SIMPLE Method for Predicting Incompressible Fluid Flows", Numer. Heat Transfer, 7, 147-163 (1984).

6. PATANKAR, S. V., "Numerical Heat Transfer and Fluid Flow", McGraw-Hill, New York (1980).

7. RODI, W., "Turbulence Models and Their Application in Hydraulics", International Association of Hydraulic Research, Monograph, Delft, The Netherlands (1980).

8. DAVIDSON, L., "Numerical Simulation of Turbulent Flow in Ventilated Rooms", PhD thesis, Dept. of Applied Thermodynamics and Fluid Mechanics, Chalmers University of Technology, Göteborg (1989).

9. SANDBERG, M. and BLOMQVIST, C., "Displacement Ventilation Systems in Office Rooms", ASHRAE Trans. (1989).

10. SANDBERG, M. and LINDSTRÖM, S., "A Model for Ventilation by Displacement", Proc. Room Vent 87, International Conference on Air Distribution in Ventilated Spaces, Stockholm, Sweden (1987).

11. DAVIDSON, L., "Ventilation by Displacement in a Three-Dimensional Room: A Numerical Study", accepted for publication in Building and Environment, March, 1989.

12. DAVIDSON, L. and OLSSON, E., "Calculation of Age and Local Purging Flow Rate in Rooms", Bldg. Environ., 22, 111-127 (1987).

13. CHEN, C.J. and RODI, W., "Turbulent Buoyant Jets - a Review of Experimental Data", Pergamon Press (1979).

14. JONES, I.P., "The Convergence of a Simple Iterative Strategy for Strongly Stratified Flows", Proc. 4th Int. Conf. on Numerical Methods in Laminar and Turbulent Flow, Swansea, 1, 733-740 (1985).

15. GALPIN, P.F. and RAITHBY, G.D., "Numerical Solution of Problems in Incompressible Fluid Flow: Treatment of the Temperature-Velocity Coupling", Numer. Heat Transfer, 10, 105-130 (1986).

Discussion
Paper 20

B. Fleury (ENTPE LASH, France)

1. Did you use free boundary conditions at the outlet?
2. What type of computer did you use and how long does it take to converge (CPU)?

Lars Davidson (Chalmers University of Technology, Sweden)

1. Boundary conditions at outlet is unigradient conditions.

2. Vax 2000 workstation CPU-time 26-80 hours depending on case. Q600 longest. With Dec3100 workstations which are used today the corresponding CPU-time would be 2-3 hours.

G Gottschalk, (ETH Zurich, Switzerland)

You have presented the solutions for vertical location of the front for powers 200 and 600 W in water experiment. What figures would you propose for thermal loads equivalent to their experimental date if recalculated to reality i.e. air/full scale and expressed in W/m^2 of the floor?

Lars Davidson, (Chalmers University of Technology, Sweden)

I do not know since in a full scale room (with air as medium) the Reynolds number is two orders of magnitude larger thin the water box model and the Archimedes number is three orders of magnitude larger.

Mike Holmes (Ove Arup , London, UK)

Did you use the properties of water in your simulation or assume the water model represented air? The thermal conductivity is significant so if temperature difference is used as the driving force it is unlikely to represent the performance of real systems. Have you considered the use of saline solutions to generate density differences? Much work has been done in the Department of Applied Mathematics, Cambridge, England by Paul Linden.

Lars Davidson (Chalmers University of Technology, Sweden)

I did use the properties of water; laminar Prandtl number, and coefficient of thermal expansion. I have not considered use of saline solutions but I would be interested to learn about your experiences.

David Harrje (Princeton University, USA)

To model a room situation, in our case with solar heating, we have used ethylene glycol and color schlieren to thermally map flow. At MIT, they have explored such modelling as well. Both studies were concerned with nondimensional factors, Re, Nu, etc. Perhaps those studies can help you in your research, and I will send you those reports.

Lars Davidson (Chalmers University of Technology Sweden)

That sounds interesting. I would be glad to have some of your reports.

PROGRESS AND TRENDS IN AIR INFILTRATION AND VENTILATION RESEARCH

10th AIVC Conference, Dipoli, Finland
25-28 September, 1989

Paper 21

DISPLACEMENT VENTILATION FOR OFFICE BUILDINGS

B. KEGEL AND U.W. SCHULZ

Sulzer Brothers Limited
CH-8401 Winterthur
Switzerland

DISPLACEMENT VENTILATION FOR OFFICE BUILDINGS

Synopsis

A test room with a Displacement Ventilation System has been built. Air velocity and temperature profiles were measured at different places in the room under summer and winter conditions.

Additional numerical simulations for the same conditions as in the experiment were performed. The measured and calculated values showed good correspondence.

An office room is normally not occupied permanently, therefore its transient behaviour was also investigated.

1. INTRODUCTION

The idea of using the Displacement Ventilation System for the air conditioning of office buildings is becoming more and more popular nowadays. Nevertheless, many building owners and designers have reservations in applying it.

On the other hand, numerous results from R&D projects and field measurements relating to displacement systems are already available. Performance has been good, and according to the application the system presents advantages compared to Mixing Ventilation-Systems.

The demand for better and more efficient systems is growing with our increasing comfort requirements in buildings.

It is not only the behaviour of the room with a displacement system that is not yet exactly known. Human perception and its effect on the momentary requirement for comfort also are not sufficiently understood.

Thus today's investigations on displacement ventilation have to deal with the air flow patterns and temperature distributions in the room, as well as with the sensation of comfort of human beings, a rather complex situation, as the comfort problem does not have a simple solution.

To find some practical solutions, we tested two typical cases:

a) a winter condition, with and without additional heating

b) a summer condition with two different local distributions of the solar heat load.

For both, the measurements and their impact on comfort were discussed.

In addition, both cases were calculated with the AIRCOND numerical simulation program. Simulation was performed before the experiments.

These experiments describe the situation for steady state conditions. As the time constant of an office room is of the same order of magnitude as the daily working hours, the transient behaviour of the room was also investigated.

2. TEST ROOM

An office for two persons (15 m^2/person) was built as a test room in our laboratory. Floor plan and measuring points are shown in Fig. 2.1.

The room represents a typical office having one outside wall with windows.

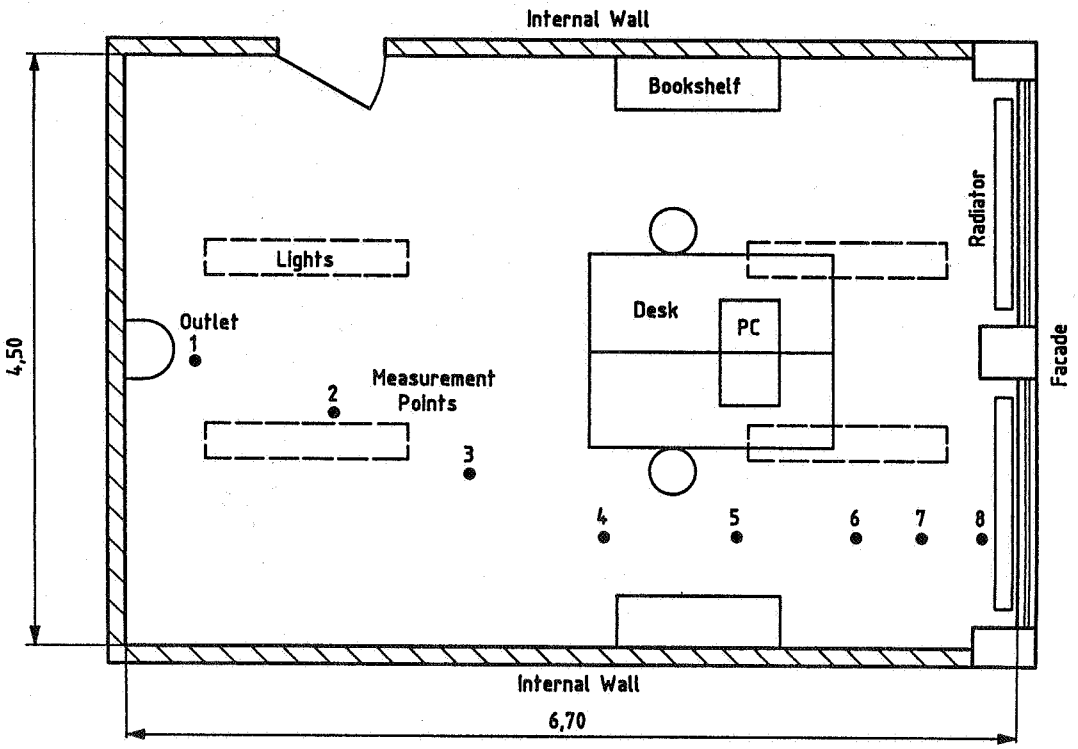

Fig. 2.1 Floor plan of the test room with furniture and location of the internal loads. In addition the measurement points for the temperatures and air velocities are indicated.

Dimensions	:	6.70 x 4.50 x 2.65 m
Room volume	:	80.0 m^3
Floor heating	:	20..33°C
Radiators	:	2 x 0..600 W Below the window
Ventilation system	:	Displacement outlet REPUS RAC 25-10 Surface area 0.95 m^2 Air volume 0..820 m^3/h Temp. 12..20°C

Internal load	:	2 persons 2 x 80 W 2 PCs 2 x 120 W Lights 464 W Extract light fittings
Windows	:	2 x 3.1 m^2 Temp. 8..20°C
Walls	:	U value 0.25 W/m^2K M* (spec. mass) 50 kg/m^2
Temperature measurement	:	Fe/CuNi elements Time const. 1 sec Range -200..900°C
Air velocity measurement:		Sulzer Low-Velocity Hot-Wire Anemometer Time const. 0.1 sec Range 0.04..0.50 m/s

3. EXPERIMENTAL INVESTIGATIONS

Related to displacement systems, mostly the maximum internal heat load is mentioned. For all-air systems, it will be around 30 W/m^2, for certain situations even as high as 40 W/m^2.

Since in practice lower heat loads often occur, the measurements were taken for different conditions. For the maximum internal load during summer condition, the temperatures and air velocities were measured at different locations in the room. The same measurements were taken for winter conditions, where the internal load compensates for the transmission heat loss of walls and windows.

The aims in both cases were to:

1. investigate the stability of the air flow in the room and

2. measure and assess the temperatures and air velocities with regard to comfort criteria.

3.1 Winter Conditions

For comfort reasons, the cold air downdraft from windows is often compensated with radiators below the window.

With new windows having a U value between 1.3 and 2.1 W/m^2K and mixing ventilation, radiators do not necessarily have to be underneath the window. Whether this would apply also for rooms with a displacement system was tested in two similar cases: with and without radiator. Details for both cases are listed in Table 3.1.

All the measurements were made at steady state conditions with a constant air inlet temperature. No control for the room temperature was used.

		Winter without heating	Winter with heating
Persons	[W]	2 x 80	2 x 80
PCs	[W]	2 x 120	2 x 120
Lights	[W]	-	-
Radiator	[W]	-	270
Window	[W]	-250	-280
Tot.int. spec. load	[W/m^2]	13	22
Air change rate	[1/h]	4	4
Air inlet temp.	[°C]	19,3	19,5

Table 3.1 Internal load, transmission losses and key data of the ventilation system for winter conditions.

Air velocity and temperature profiles for both winter cases are shown in Fig. 3.2. The most impressive result is the small temperature gradient within the occupied zone. This was found to be true even when the radiator was used, thus the assumption was disproved that the air rising from the radiator would induce so much room air that stable air stratification is disturbed.

Both winter cases have similar air velocity and temperature profiles in the occupied areas. Most critical for the comfort are the first few centimetres above the floor (supply air layer). There the velocities are below 12 cm/s and the temperature is 20,5 °C, leading to a FANGER PPD rate of less than 10 %.

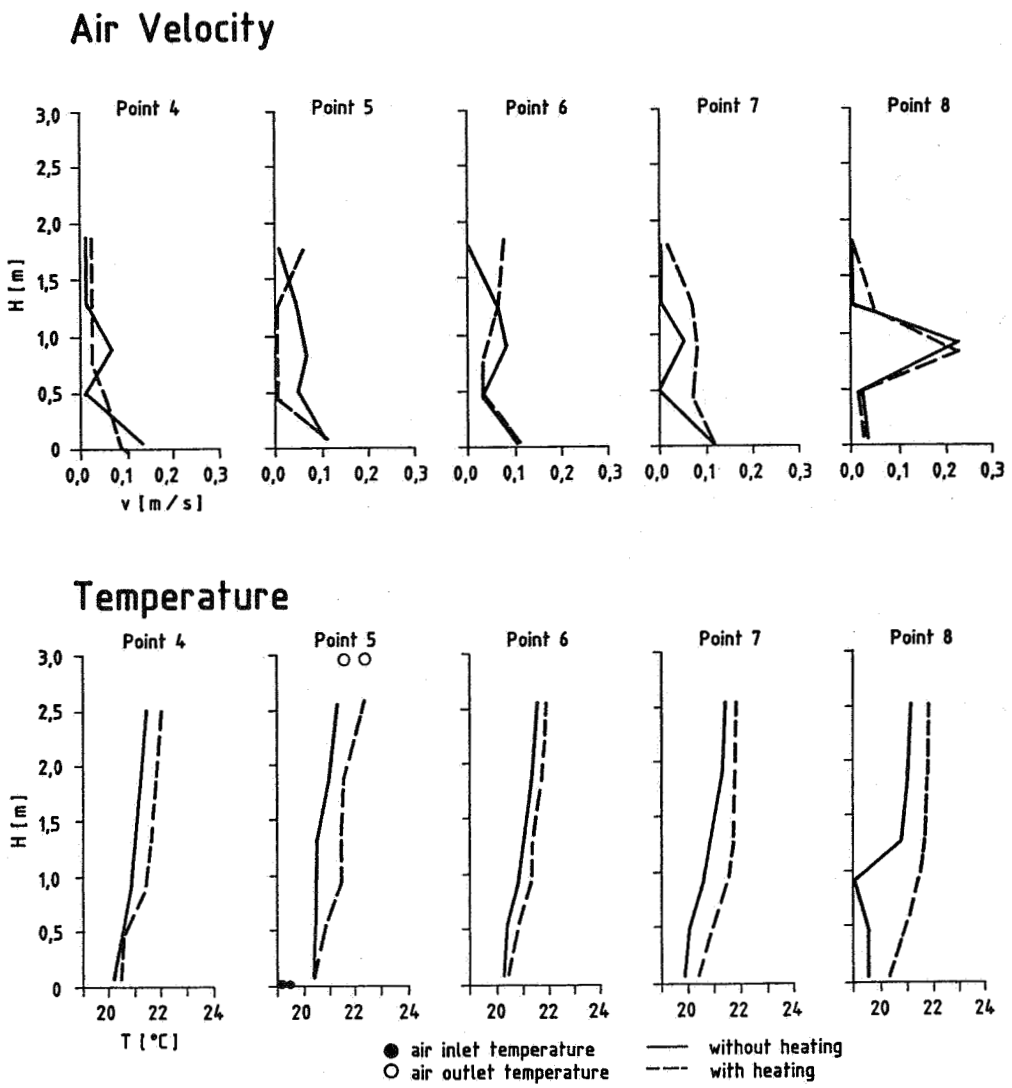

Fig. 3.2 Air velocity and temperature profiles for the winter case with and without radiator heating.

The two experiments were made with low values of internal loads (13 W/m^2 and 22 W/m^2). Additional experiments with lighting showed that the characteristics of the air velocity are not influenced. The room temperature increases by 1.0 K below the ceiling and by 0.2 K at foot level, corresponding to 25 % of the installed electrical power.

The above results apply only for walls and fenestrations with low U values. The U values we simulated were:

Wall : 0.3 W/m^2K

Fenestration : 1.4 W/m^2K

For offices with more than one exterior wall, further investigations are necessary.

As it is not possible to provide space heating with a displacement system, an additional heating system would always be necessary providing heat during nights and weekends. If the internal heat load compensates for the transmission losses, it is possible to shut off the heating without any loss of comfort.

For buildings with less insulated windows, the radiator heat load may be reduced in accordance with the internal load during occupation. In this case the window sill construction has to be optimized to obtain the best possible configuration of the downward and upward air flows along the window.

3.2 Summer Conditions

During summer, the transmission heat for well insulated facades is of minor importance. However the heat gained by solar radiation through the windows may represent a substantial addition to the internal load of the room.

The temperature gradient in the room is affected by the capability of the walls to absorb the solar radiation. Surfaces having a slightly higher temperature than the room air emit their energy mainly through radiation. In cases where the temperature is increased, the convection heat exchange becomes more intense. And with more convection, the temperature gradient in the room also becomes bigger.

The designer has some influence on the effect of the heat gains from solar radiation in the space by selecting proper materials and colours. Having for example a light coloured floor, the reflectivity is increased, thus a uniform distribution of the heat within the space and a small temperature gradient may be achieved. On the contrary, internal heat gains from people, PCs etc. are independent of the colour of the sufaces, as the absorbtion coefficient for long wave radiation is constant.

In the summer case 1, solar radiation of 1010 W (34 W/m^2) was distributed over the entire floor.

In the summer case 2, 530 W (18 W/m^2 for the entire floor area) was distributed over one quarter of the floor area near the window; a somewhat more realistic case, as during summer the solar radiation does not reach the far end of the room. A comparison of both cases demonstrates the important influence of the heat distribution on the temperature and velocity profiles within the room.

Details of both cases are listed in Table 3.3.

		Summer 1	Summer 2
Persons	[W]	2 x 80	2 x 80
PCs	[W]	2 x 120	2 x 120
Lights	[W]	-	-
Solar radiation	[W]	1010	530
Tot. spec. load	[W/m^2]	47	31
Air change rate	[1/h]	6	6
Air inlet temp.	[°C]	16,9	19,3

Table 3.3 Internal load, solar radiation heat load and key data of the ventilation system for summer conditions.

With regard to the comfort requirement the situation with the heat load over the entire floor (summer case 1) was found to be better than the case where the heat is only emitted in the window area.

The characteristic values at the desk area are:

	Summer 1	Summer 2
Temp. gradient	: 2.0 K/0.1-1.3 m	2.9 K/0.1-1.3 m
Velocity at 0.1 m:	0.15 m/s	0.20 m/s

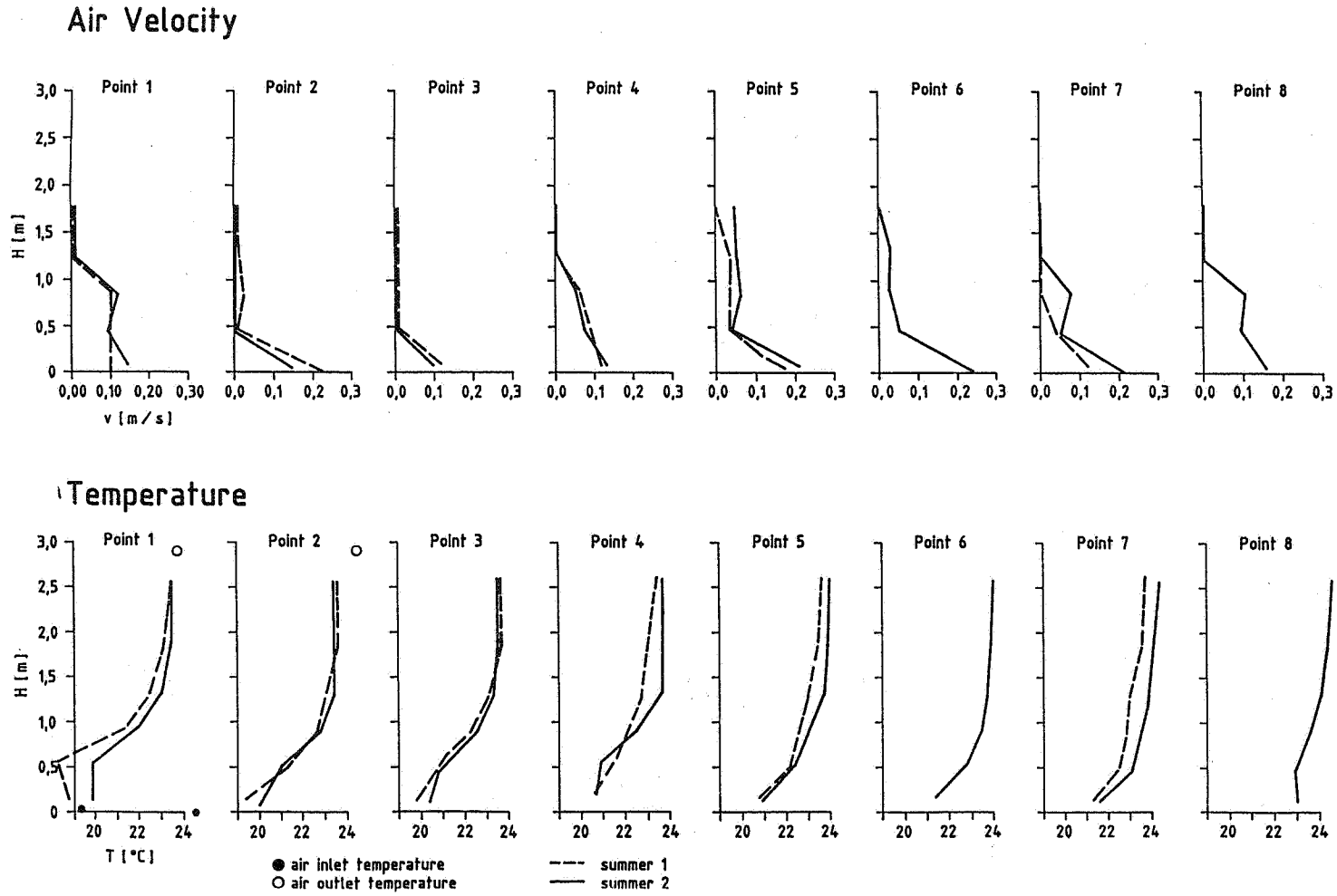

Fig. 3.4 Air velocity and temperature profiles for summer cases 1 and 2

Figure 3.4 shows how the air temperature rises over the heated floor area in case 2. The heated air causes high air velocities in the window area. On the other hand, the air velocity near the outlet is higher in case 1. This is due to the increased temperature difference between the supply and the room air.

For the influence of the outlet construction on the air velocity distribution, see H.M. MATHISEN 1988 and P.V. NIELSEN et.al. 1988.

The major differences between the two summer cases were in the energy density and the area of the heated floor.

With 70 W/m^2 in the window area of case 2, the floor temperature was higher and therefore the convective heat exchange more intensive than for case 1. This convective heat flow caused the high temperature gradient in case 2, although the solar heat gain of case 1 was twice that of case 2.

As a design guideline it can be said that surfaces impinged by solar radiation should be of light colour and of a material with a high energy absorbtion capacity, so that the surface temperature can be kept as low as possible.

In addition to the above-mentioned recommendations, solar protection devices should be installed on all sun-orientated windows, as the unprotected solar radiation often exeeds the allowed internal load.

4. NUMERICAL SIMULATION OF TEMPERATURES AND AIR VELOCITIES

The experiments as described above were simulated with the numerical program AIRCOND.

The characteristics of AIRCOND are as follows:

- finite volume method
- 3-dimensional
- nonsteady flow
- incompressible flow
- laminar / turbulent flow
- logarithmic wall function
- Newtonian fluids
- cartesian coordinates, orthogonal grid
- boundary conditions on walls fixed for either temperature or heat flux
- turbulence : k-ε model

The results of the simulation and the experiment for summer case 2 are compared in Fig. 4.1. This example is also representative for the other cases, as the results are similar.

It is interesting to observe the similar shape of the computed and measured velocity and temperature distribution shown in Fig. 4.1.

The velocity profiles coincide extremely well. Most of the differences of 1 to 3 cm/s are caused by having only 6 measurement points in the height of the rooms, whereas with the simulation 18 points were calculated.

For the measuring points 5 to 8 at floor level, the calculated velocities are up to 4 cm/s below the measured ones. The reasons for this are not yet completely understood.

The deviations of the temperatures exceed those of the velocities. All the calculated values are systematically about 1 K lower than the measured ones. Nevertheless the shapes of the curves correspond to each other.
The reasons for these differences are as follows:

1. The air inlet temperature is 0.3 K lower for the simulation than for the experiment.

2. The measured temperatures are global, not air temperatures. For our room configuration the global temperatures are 0.2 to 0.3 K higher than the air temperatures.

3. The simulation program does not consider the radiation within the room.
   The radiant heat transfer between internal loads and walls was estimated. These values were then used as boundary conditions for the simulation.
   If the radiant heat exchange is estimated too high, then the calculated air temperature is lower than the measured values.

Generally it can be said that the results for the air velocities are reasonable. The absolute temperatures have some deviations, but the shape of the temperature distribution (relative temperature) is correct.

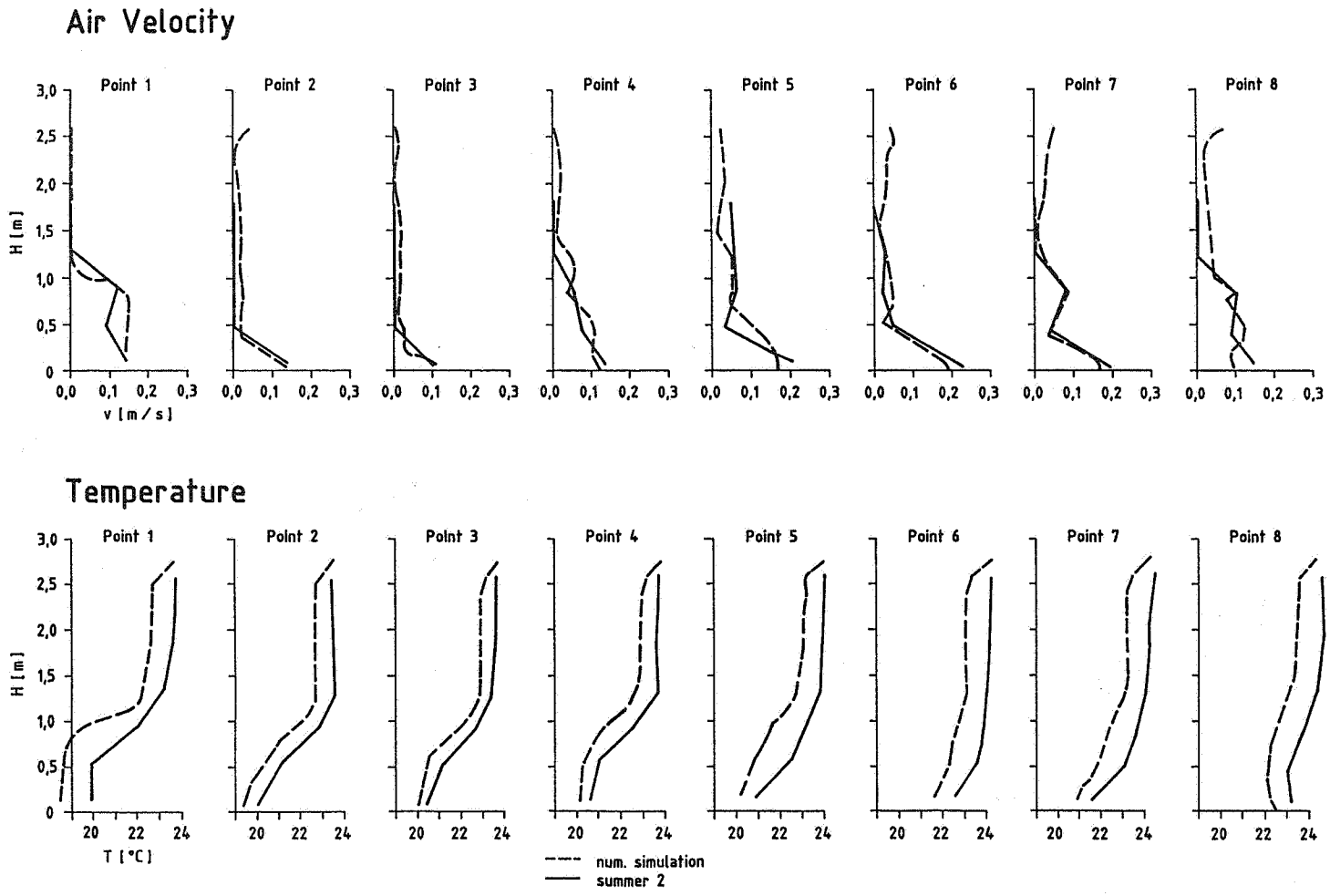

Fig. 4.1 Air velocity and temperature profiles for summer case 2.
Results from the numerical simulation and the experiment.

A

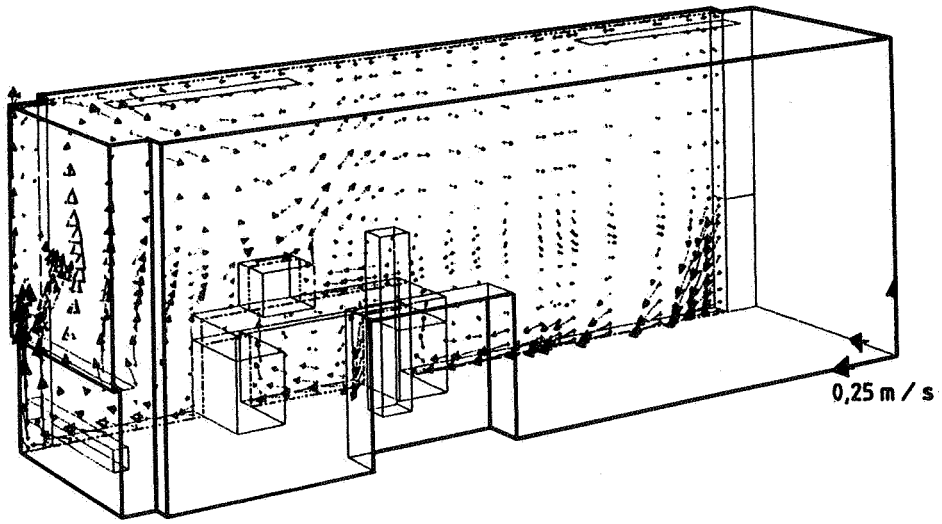

B

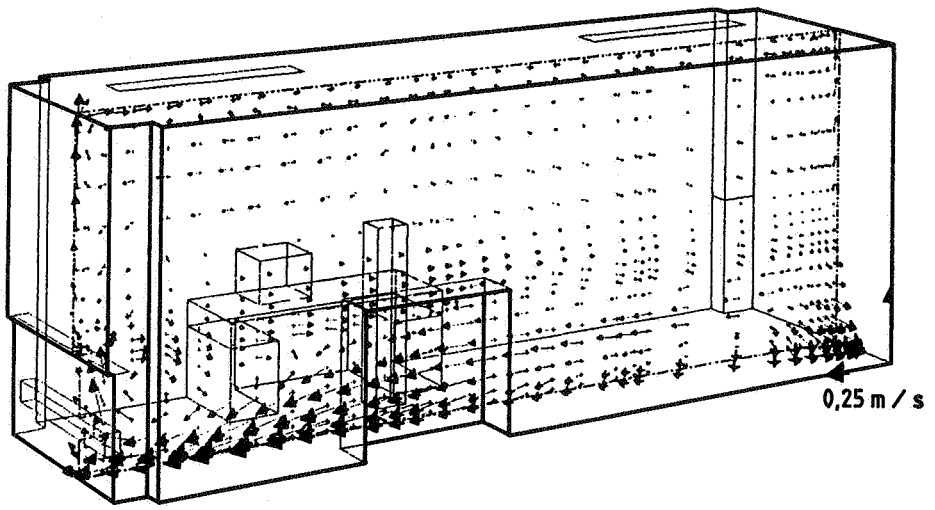

Fig. 4.2 Calculated air velocities for the summer case. Fig. A shows the velocities in the center of the room; Fig. B those in the middle of the free section between the desk and the bookshelf.

In addition to the experimental results, the simulation shows some interesting results:

1. A reduction of the free floor area causes a substantial increase of the air velocity above the floor. In our test room the free floor area was reduced by 66 % due to two desks, bookshelfs and cylinders (simulating persons). Fig. 4.2 B shows the increase of the thickness and velocity of the supply air layer.

   This effect can be reduced by increasing the cross section area, e.g. moving the bookshelf away from the narrow zone of the desks.

2. Rooms with displacement ventilation normally have a very little horizontal temperature gradient (such as the rear side of the room in Fig. 4.3).

   The high and local internal heat load of summer case 2 caused a temperature difference of 2 K between the window area and the back of the room. The two desks and the high load of 70 W/m^2 in the window area prevented a uniform temperature distribution in the occupied zone.

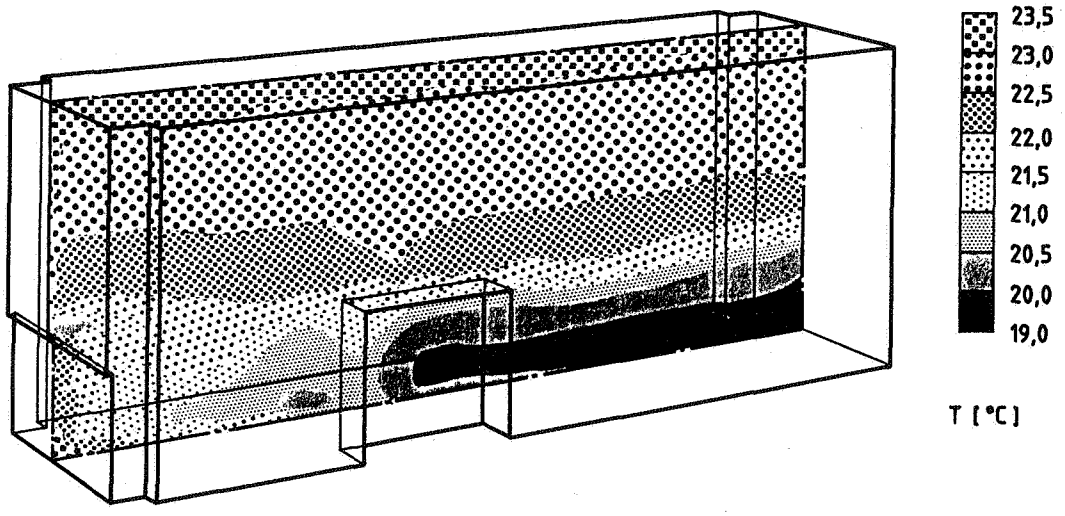

Fig. 4.3 Calculated air temperatures for summer case 2. The temperatures apply for a cross section through the center of the simulated person. Note how the lower part of the room is divided into two sections by the "wall" of desks, bookshelves and persons.

It would have taken a lot of time to measure the same number of points that were numerically calculated. Having the temperatures and velocities for many points all over the room allows much better interpretation than with the few values of the measurements. This is another important advantage of the numerical simulation.

5. TRANSIENT BEHAVIOUR OF THE TEST ROOM

In a room with a mixing ventilation system, the kinetic energy of the supply air is always higher than the kinetic energy of the buoyancy airflow from internal loads. This means the temperature gradient is small and internal surface temperatures are equalizied with such a system.

In a room with a displacement ventilation system, the buoyancy airflow is the only motor of the air movements. For this reason the air temperature is not uniform. As a consequence, the influence of the building structure on the transient behaviour of the room is increased.
The utilization of a room featuring a displacement ventilation system causes its temperature to rise. In the upper part of the room (1,0 to 1,5 m under the ceiling) the temperature rise is up to 3 K, over the floor it is around 1 K. (Experimental values for internal loads of 20 to 30 W/m^2 and an air change rate of 4 to 6 per hour).

In such a room (with an air temperature gradient), the upper parts of the surfaces (ceiling, wall) are cooler than the air, and the lower parts (mainly the floor and the first metre of the wall) are warmer than the air. The air temperature difference between floor and ceiling is more than twice the difference between the corresponding surface temperatures. This has to be taken into account using the comfort equation.

As the surface temperatures of the room are not equal,there is an intensive radiation heat exchange between the surfaces. For an internal load of 400 W, the radiation heat exchange from the ceiling to the floor is 64 W in our test room. This energy heats up the supply air and improves the comfort condition at floor level.

In rooms with cooling panels on the ceiling, this radiation is missing at floor level, and the heating effect of the supply air is reduced. In addition, the cooled ceiling keeps the surface temperatures constant, so that the storage effect of the walls is not used in such room.

For comfort reasons, it is also important to know that the air velocities do not change during the transient time.

In our test room, it took between 20 and 35 hours until we reached the steady state condition. During the first 10 to 12 hours, a constant energy flux of 0,5 to 1 W/m^2 was stored in the room structure, thus reducing the load of the ventilation system by 15 to 30 %.

The temperature gradient in the room depends on the internal load and the air change rate:

The higher the air change rate, the lower the temperature gradient becomes, but as soon as a temperature gradient has been established it cannot be reduced by means of an increasing air change rate. This means the entire room is cooled at a constant gradient if the air volume is increased.

Further experiments on the storage effect and the temperature control in the room are in progress.

As a result, it can be said, that for displacement systems the transient behaviour represents an additional important parameter. Though it complicates the system, a proper application can reduce the energy consumption and improve comfort conditions at the same time.

6. SUMMARY

The experiments in the room with a displacement ventilation system showed that for winter and summer conditions, comfortable conditions can be obtained.

In a well insulated building, heating can be shut off during the time of occupation. For summer conditions and intensive solar radiation through the windows, Venetian blinds are necessary.

The result from the numerical simulation of the test cases showed a good correspondance with the measurements. The values for the air velocity coincide better than those for the temperature.

It is a feature of displacement systems that the room temperatures vary within a few degrees during occupation. The transient behaviour of the building structure contributes therefore considerably to the resulting indoor climate.

7. ACKNOWLEDGEMENTS

I would like to thank Mr. Durrer and Mr. Puippe of the Sulzer Research and Development Department for their work on numerical simulation and their cooperation.

The simulation project is supported by the "Schweizerischer Nationalfonds zur Förderung der wissenschaftlichen Forschung".

8. REFERENCES

M. SANDBERG
Displacement Ventilation in Office Rooms
ASHRAE Conference, Vancouver 1989

E. SKARET
Displacement Ventilation
Roomvent 87, Stockholm 1987

H.M. MATHISEN
Air Motion in the Vicinity of Air-Supply Devices for Displacement Ventilation
9th AIVC Conference, Genf 1988

D.P. WYON, M. SANDBERG
Thermal Manikin Prediction of Discomfort due to Displacement Ventilation
The National Swedish Institute for Building Research

A. MELIKOV, B. DERBISZEWSKI, G. LANGKILDE
Draught Risk in Rooms with Displacement Ventilation
The Technical University of Denmark 1989

P.V. NIELSEN
Displacement Ventilation in a Room with low-level Diffusers
Indoor Environmental Techn. Nr. 10, Aalborg 1989

P.V. NIELSEN et.al.
Displacement Ventilation by Different Types of Diffusers
Indoor Environmental Techn. Nr. 8, Aalborg 1988

CH. MOSER
Empfindlichkeit der Quellüftung
Diplomarbeit, Federal Inst. of Techn. Zürich 1989

M. FANKHAUSER
Quellüftung
Semesterarbeit, Federal Inst. of Techn. Zürich 1989

Discussion
Paper 21

E. Olsson (Chalmers University, Sweden)

1. Have you tried to change the level of the front by balancing heating and ventilation flow?
2. What kind of turbulence and radiation models were used?

Beat Kegel (Sulzer Bros, Switzerland)

1. No, the aim of the experiments was to measure a characteristic office room not an optimisation of the front.

2. Turbulence: k-e

radiation: rough estimation of the radiative and convective heat flows used as boundary conditions.

Marco Masoero (Politecnico di Torino, Italy)

If the major problem in summer operation is the heating of the floor surface due to incident solar radiation, would it make sense to use cool water pipes buried in the floor slabs as the cooling system?

Beat Kegel, (Sulzer Bros, Switzerland)

Maybe, but the time constant of such a system is too high so it would be very difficult to control such a configuration.

Charles Filleux, (Basler & Hofmann, Switzerland)

a) Do the air change figures you give include recirculation air? They seem very high.

b) Did you try to run lower air change rates and simultaneously lower the inlet temperature?

Beat Kegel (Sulzer Bros, Switzerland)

a) The experiments did not deal with the way the air comes from; quantity and temperature were the important parameters.

b) Yes, but we did not meet the comfort criteria anymore.

B. Fleury (ENTPE/LASH, France)

Can we get the turbulence intensity from the numerical results?

Beat Kegel (Sulzer Bros, Switzerland)

Yes, you can get the 50 and 84% time value of the velocities.

PROGRESS AND TRENDS IN AIR INFILTRATION AND VENTILATION RESEARCH

10th AIVC Conference, Dipoli, Finland
25-28 September, 1989

Paper 22

ENVELOPE LEAKINESS OF LARGE, NATURALLY VENTILATED BUILDINGS

M D A E S Perera and R G Tull

Building Research Establishment
Garston
Watford
Herts WD2 7JR
UK

SYNOPSIS

Whole-building pressurisation tests can quantify the air-leakiness of a building's external envelope. The resulting information can be used in assessing the quality of the building fabric. At present there is little information regarding the leakage characteristics of large, non-domestic UK buldings. As a step towards providing more information, the Building Research Establishment (BRE) has developed and constructed a multifan pressurisation system known as BREFAN to pressurise large buildings like offices and hangars.

This paper presents results from field measurements in five large and naturally ventilated buildings. Using BREFAN, measurements in a medium-sized building specifically designed and constructed as a low-energy office (LEO), showed a reduction of 9% (at a pressure difference of 25 Pa between inside and outside) in its envelope leakiness after new and improved windows were installed as part of a programme of modifications. Using Q_{25}/S (whole building leakage rate at a 25 Pa pressure differential per unit permeable surface area) as an index of the leakiness of the building envelope, these results, when compared with measurements made previously in a conventional UK office, showed that the LEO building was twice as tight as the more conventional building. Comparison with measurements made in North American showed the LEO building was as tight as buildings found there.

BREFAN measurements in a second building, a conventional hangar built in the early 1960's, showed it to be very leaky. At 25 Pa pressure difference, the opening of a roof vent increased the leakiness by 17% and unsealing a large folding door increased it by 8%.

The envelope leakiness of the hangar was compared with measurements in three other large single-cell factory buildings using a different system of fans to pressurise the buildings. One of these, built 35 years ago, was as leaky as the hangar building. The other two buildings, built within the last decade under current UK Building Regulations, were shown to be twice as tight.

KEYWORDS: pressurisation, fan pressurisation, pressurisation testing, air leakage, leakage area, air tightness, large building, nondomestic building, commercial building, office building, multistorey building.

1. INTRODUCTION

Air enters a naturally ventilated building either through purpose-built openings like windows or by uncontrolled leakage (infiltration) through cracks and gaps in the building envelope. In most circumstances, this adventitious leakage through the building fabric is a source of excessive ventilation which can lead to energy waste and, in some cases, to discomfort.

The leakiness of the building envelope can be quantified by measuring the whole-building air leakage rate at an appropriate applied pressure differential between inside and outside. This is done by sealing a portable fan into an outside doorway and measuring the airflow rates required to maintain a set of pressure differences across the building envelope. Although the technique, equipment and protocol to carry this out are well established for dwellings[1], this is not the case for large and complex buildings like offices.

In North America, where most office-type buildings are mechanically ventilated, the ventilation system can be used[2] to pressurise the building. For the UK, this is not a fully viable method since most buildings are naturally ventilated. In Canada, an alternative approach[3] has been to use a large diameter trailer-towed fan with its own power generator.

To avoid using a large, cumbersome fan, the Building Research Establishment (BRE) has developed a multiple-fan pressurisation system[4,5] called BREFAN. Novel features of this system include portability, ability to be powered from conventional 13 amp sockets and stable fan-speed control during multiple-fan operation.

This paper presents results obtained from field measurements in five naturally ventilated non-domestic buildings comprising one office and four single-cell industrial units. Measurements in the medium-sized office building located at BRE are compared with earlier measurements[4] to assess the effect of installing improved windows throughout the building.

Measurements in a hangar, also at BRE and one of the four single-cell buildings tested, show the reduction in the overall envelope leakiness when a folding steel door is sealed or the increase when a roof vent is opened.

Finally, to place the results in some context, a leakage index is used to compare the leakiness of these two buildings at BRE with similar buildings elsewhere. This comparison includes measurements from the other three industrial buildings which were pressurised with a different system of fans.

2. EXPERIMENTAL ARRANGEMENTS

2.1. BREFAN System

The design and construction of the BREFAN pressurisation system is fully described fully in the earlier papers[4,5] but, for completeness, the essential features are as follows. The system consists of three identical fan pressurisation units. Each unit is fully portable, powered from conventional 13 amp sockets and operated using a single- to three-phase speed controller to stabilise its speed during multiple-fan operation.

Airflow through each fan is measured using a conical inlet [6]. Each fan unit is capable of providing a flow rate of 5.5 m^3/s against a building envelope pressure difference of 50 Pa. The number of fans used in any building is set by that required to achieve a target pressure difference. Short lengths of flexible ducting are used to connect the fans to 'false' plywood door panels which are temporarily sealed onto an outside doorway of the test building.

2.2. Test Buildings at BRE

Two of the naturally-ventilated test buildings are located at the BRE site in Garston. One is a three-storey building built as a 'low-energy' office (LEO)[7] and the other is a conventional single-cell hangar built in the mid-1950s.

The outside walls of the LEO consists of 9 mm thick clay tiles on the outside face followed in succession by 125 mm thick precast concrete panels, a 300 mm void filled with blown polystyrene beads and plasterboard (12.5 mm thick) with an aluminium foil vapour barrier. The building volume is estimated as 5315 m^3 and the external surface area as 1750 m^2.

Although the LEO building was formerly mechanically ventilated, the ventilation system is now disabled and the duct openings of its air handling unit (located on the roof) are blanked off. As part of a program to improve thermal insulation levels, the older double-glazed windows (with 6 mm air gaps) have now been replaced with new tighter units incorporating Argon fill.

The hangar-type building is known in the UK as a 'Marston' shed. Originally a single building, its southern end was extended in the mid 1960's and joined to a similar building. A brick partition separates the two buildings with access between them via a horizontally-sliding folding shutter door. During the field tests, all measurements were carried out in the northern hangar of the combined building.

The walls and roof of the hangar consist of corrugated asbestos cement sheeting fixed to a steel frame with hook bolts and lined internally with plasterboard. The volume and external surface area are estimated as 4690 m^3 and 1400 m^2 respectively.

The other three single-cell factory units tested were all located outside BRE and represented some of the UK stock of industrial buildings. Table 1 gives summary details of these test buildings,

2.3. Test Conditions

After the new windows were installed, a whole-building pressurisation test was carried out in the LEO using two of the fan units (Figure 1). During the test, all outside doors and windows were kept closed while all internal doors were wedged open. Using a nearby meteorological site, wind speed during the test was measured to be about 2 m/s at a height of 10 m. Inside and outside air temperatures were 6 ^{o} and 17 ^{o}C respectively.

Three pressurisation tests (Tests A1, A2 and A3) were made on the hangar. Three fan units were placed (Figure 2) in a gap created by raising the vertical sliding door at the north end. For test A1, the folding shutter door between the test hangar and the adjoining hangar was sealed with polyethylene sheeting. In test A2, a roof vent (measuring 1.5 m by

0.35 m) was opened. In test A3, the roof vent was closed but the polyethylene sheet was removed from the door. Wind speed was about 2 m/s during the test and the inside and outside air temperatures were similar at about 22 °C.

3. RESULTS

Figures 3 and 4 show the airflow rates, Q, plotted against applied pressure differential, ΔP, across the outside wall envelopes of the LEO and the hangar respectively. For comparison, Figure 3 includes a best-fit pressurisation profile obtained previously[4] for the LEO before the new windows were installed.

Best-fit power-law profiles of the form,

$$Q = K \Delta P^n$$

where the coefficient K and the exponent n (lying between 0.5 and 1.0) are constants, were fitted to the data. This was done by transforming the above equation to the form,

$$\log_e(Q) = \log_e(K) + n \log_e(\Delta P)$$

and fitting a linear regression line on the transformed variables. The computed coefficients and exponents (with associated 95% confidence intervals), together with the correlation (r^2) for the goodness-of-fit, were evaluated and are as follows:

Building	*Test*	*Ln(K)*	*Coeff. K* $(m^3/s)/Pa^n$	*Exponent, n*	*Corr.* r^2
LEO		-0.888 ± 0.026	0.412	0.58 ± 0.01	0.999
HANGAR	A1	0.713 ± 0.143	2.041	0.64 ± 0.06	0.976
HANGAR	A2	1.125 ± 0.098	3.081	0.56 ± 0.04	0.986
HANGAR	A3	0.913 ± 0.088	2.492	0.61 ± 0.03	0.992

Note that no confidence interval has been ascribed to the coefficient K since the regression analysis was carried out on the log transform of this coefficient.

4. DISCUSSION

4.1. Leakiness of the LEO Office Building

Using the coefficient and exponent given above, the whole building air leakage rate can be calculated for any applied pressure differential over the measured pressure range. For dwellings, it is usual[8] to quote the leakage rate, Q_{50}, at an applied pressure difference of 50 Pa.

For some buildings, which are either large or excessively leaky or a combination of both, it is not always possible to achieve this target pressure. In such an instance, extrapolation to 50 Pa is considered acceptable[9] if the maximum achieved pressure is greater than 35 Pa and the correlation, r^2, of the best-fit line is better than 0.990. In

large building pressurisation testing, it is not always possible to fulfill these conditions and a leakage rate of Q_{25} at a lower target pressure of 25 Pa can be used[4].

At 25 Pa, the leakage rate of the LEO with new windows is 2.67 m^3/s. This is a 9% reduction from the 2.93 m^3/s obtained a year before the modification programme. Because of this time gap between the two tests, it is difficult to state categorically that this small reduction is due to the new windows since it is known that, for dwellings, seasonal variations do occur[8] in their leakage rates. Measurements will therefore be repeated during the coming heating season to clarify this aspect.

4.2. Leakiness of the Hangar Building

The Q_{25} leakage rate for Test A1 with the partition door sealed was calculated as 16.0 m^3/s. Opening a roof vent (Test A2) or unsealing the partition door (Test A3) increased this to 18.7 and 17.2 m^3/s respectively representing increases of 17% and 8%.

Using the roof-vent open area of 0.53 m^2 and a measured partition door periphery length of 18.8 m, a first-order approximation indicates a nominal door crack width of 1.3 cm for this type of horizontally-sliding folding steel door. It should, however, be noted that in reality the cracks are not only distributed around the perimeter of the door but also between each leaf of the door.

4.3. Comparison with Buildings Elsewhere

It has been shown previously[4] that the index Q_{25}/S (where S is the total permeable external surface area) is a suitable measure of a building's constructional quality with regard to the leakiness of its envelope. In Figure 5, the envelope leakiness of the LEO and hangar buildings are compared with other office and single-celled buildings found elsewhere. Relevant leakage and physical characteristics of these buildings are tabulated in Table 1.

Office buildings

As mentioned earlier, data on office leakage is scarce. Apart from the LEO, only one other UK building (a conventional office built in 1963) has been tested[4]. Other available data is limited to the USA (6 offices) and Canada (12 offices). The leakage for each of these two North American data sets have been aggregated[4] and are given in Table 1.

Figure 5 shows that whereas the LEO is as tight as the North American buildings, the conventional UK office is twice as leaky. Although it is not possible to generalise these findings to the majority of conventional UK office buildings, this comparison shows the tightness of a building designed to be relatively tight by current UK standards.

Single-celled buildings

It is useful to compare the leakiness of the hangar building with the following single-cell buildings elsewhere:

(a) A 35-year old conventional masonry building in the UK.

(b) Two factories built within the last decade to contemporary *UK Building Regulations* standards. (It should be noted that the Regulations do not give guidance on air leakage but on thermal performance).

(c) Three large buildings in Sweden.

The measured air leakage characteristics [Jones and Powell, personal communication] of these three Uk buildings are tabulated in Table 1 together with similar details[10] for the Swedish buildings. Using the tabulated values, the leakage index Q_{25}/S for each of the buildings have been calculated and shown graphically in Figure 5.

It can be seen that the two older UK buildings, the asbestos-walled hangar and the masonry building, have similar high leakage indices of 41 and 45 m^3/hr per m^2 respectively. A leakage of about 20 m^3/hr per m^2 for the other two UK buildings built to current *Building Regulations Standards* show a halving of the leakage rates. However, the three Swedish buildings with leakage indices between 2 and 5 m^3/hr per m^2 show that it is possible to reduce the envelope leakage of UK buildings much more with suitable construction techniques.

5. CONCLUSIONS

Whole-building pressurisation tests can quantify the air-leakiness of a building's external envelope. The resulting information can be used in assessing the quality of the building fabric. At present, there is only limited information regarding the airtightness of large, naturally ventilated non-domestic buildings in the UK. As a step towards obtaining this information, this paper presents results from measurements made in a small sample of office and single-cell industrial buildings in the UK.

Measurements in a building, built specifically as a low-energy office, shows this building to be as tight as those found in North America whereas a more conventional UK office building was twice as leaky. Installing improved windows appears to have increased the tightness of the low-energy building by about 9% but further tests will be made to ensure that this increase is not caused by a seasonal variation.

Measurements made in older conventional hangars show these to be twice as leaky as those built according to current UK *Building Regulations Standards*. There is, however, interest currently in the UK to improve the design of 'new-builds' and build tighter, low-energy factory units[11]. Published measurements in large Swedish single-celled buildings show that a further 10-fold increase in tightness is possible with known construction techniques.

ACKNOWLEDGEMENTS

Field measurements of the air leakage of the three factory buildings tested in the UK were carried out by University of Wales College of Cardiff for the Building Research Establishment under an Extra-Mural Contract BRE F3/2/338.

The work described here has been carried out as part of the research programme of the Building Research Establishment of the Department of the Environment and this paper is published by permission of the Director.

REFERENCES

1. International Standards Organisation, Draft Proposal: DP 9972 - Measurement of building airtightness using fan pressurisation, Presented at the Air Infiltration and Ventilation Centre Workshop on Measurement Techniques, Denmark, (1988).

2. Persily, A K and Grot, R A, Pressurization testing of federal buildings, ASTM STP 904 'Measured Air Leakage of Buildings' (Edited by Treschel, H R and Lagus, P L), publ. ASTM, Philadelphia, (1986).

3. Tamura, G T and Shaw, C Y, Experimental studies of mechanical venting for smoke control in tall office buildings, ASHRAE Trans., Vol 84(1), pp 54-71, (1978).

4. Perera, M D A E S and Tull, R G, Air tightness measurements of two UK office buildings, Paper presented at the ASTM Symposium on Airchange Rate and Air Tightness in Buildings held in Atlanta, U.S.A., (April 1989).

5. Perera, M D A E S, Stephen, R K and Tull, R G, Use of BREFAN to measure the airtightness of non-domestic buildings, BRE Information Paper IP 6/89, Building Research Establishment, U.K., (April 1989).

6. British Standards Institution, Fans for general purposes. Part 1. Methods of testing performance, British Standard BS 848;Part 1;1980, London, BSI, (1980).

7. Crisp, V H, Fisk, D J and Salvidge, A C, The BRE Low-Energy Office, BRE, Garston, (1984).

8. Warren, P R and Webb, B C, Ventilation measurements in housing, Proceedings of the CIBS Symposium on Natural Ventilation by Design held at the Building Research Establishment, Watford (December 1980).

9. Stephen, R K, Determining the Airtightness of Buildings by the Fan-Pressurisation Method: BRE Recommended Procedure, BRE Occasional Paper, Garston, BRE, 1988.

10. Lundin, L, Air leakage in industrial buildings - preliminary results, Proceedings of the 4th AIC Conference on Air Infiltration Reduction in Existing Buildings held in Switzerland, (1983).

11. Hughes, D, Low energy factory buildings, CIBS Building Services, p. 61, (February 1989).

CODE	BUILDING DESCRIPTION	PERMEABLE AREA (m^2)	VOLUME (m^3)	TEST CONDITION	LEAKAGE COEFFICIENT, K $(m^3/s)/Pa^n$	EXPONENT n
Offices						
LEO	Low energy office at BRE	1,750	5,315	Before new window	0.424	0.60
				After new windows	0.412	0.58
UK	Conventional UK office	2,195	6,254	as-built	1.388	0.51
USA	Six USA office buildings	Ref 4	Ref 4	as-built	0.72 (*)	0.60
CANADA	Twelve Canadian office buildings	Ref 4	Ref 4	as-built	0.64 (*)	0.65
Single-cell buildings						
UK #1	25-year old hangar at BRE	1,400	4,690	door sealed (A1)	2.041	0.64
				roof-vent open (A2)	3.080	0.56
				door unsealed (A3)	2.492	0.60
UK #2	10-year od factory unit (current UK standard)	3,459	15,000	as-built	4.162	0.50
UK #3	5-year old factory unit (current UK standard)	1,100	3,050	as-built	1.052	0.54
UK #4	35-year old UK unit	1,694	4,955	as-built	3.936	0.52
SW #1	Swedish industrial building (Code A in Ref 10)	6,796	36,373	as-built	Ref 10	Ref 10
SW #2	Swedish store (Code B in Ref 10)	9,876	61,127	as-built	Ref 10	Ref 10
SW #3	Swedish sports hall	5,809	31,622	as-built	Ref 10	Ref 10

(* USA/Canadian office leakage coefficients in units of $(m^3/hr)/Pa^n$ pr unit permeable area)

TABLE 1 - Building Characteristics

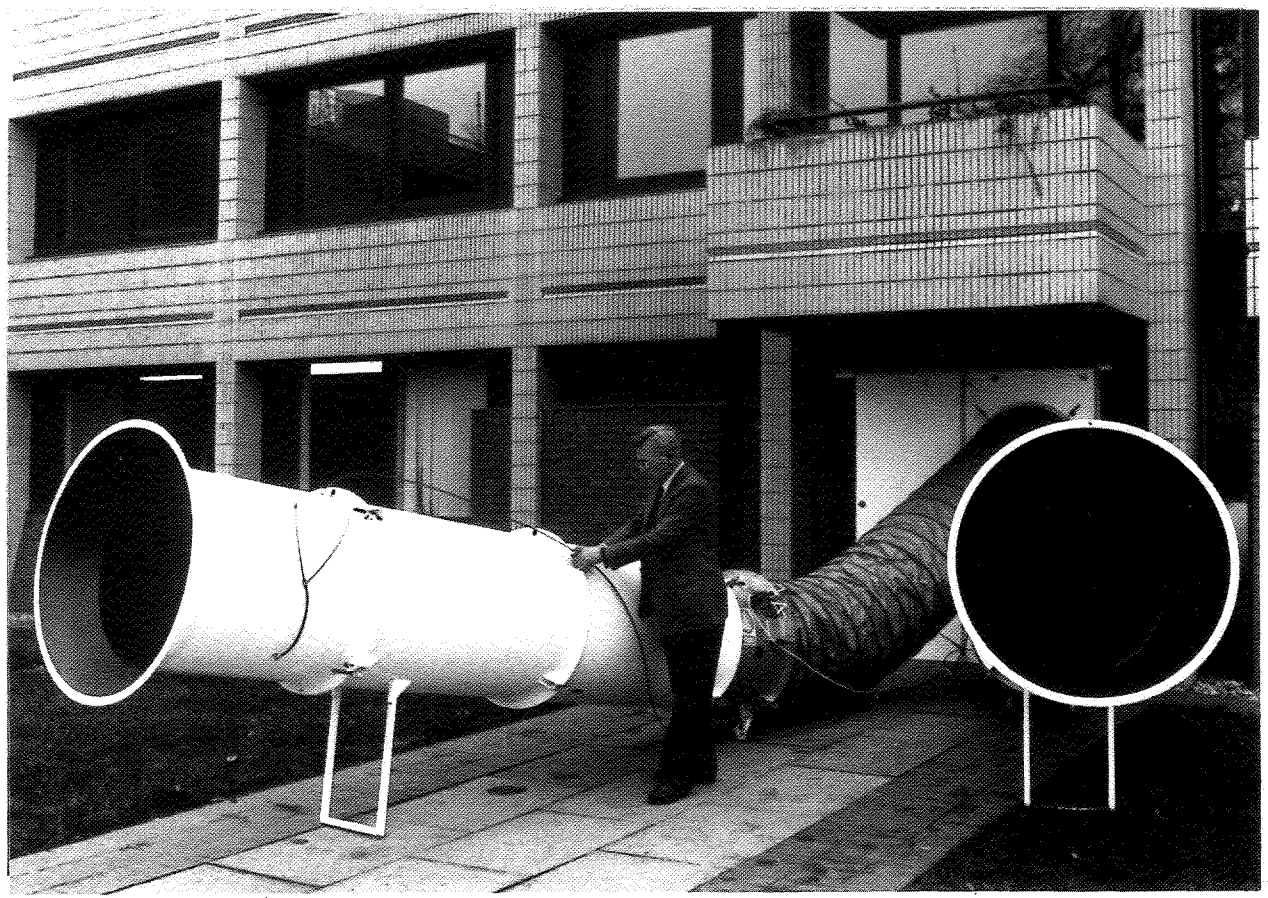

FIGURE 1 – BREFAN installed at the main entrance to the Low Energy Office

FIGURE 2 – BREFAN installed for testing the hangar building

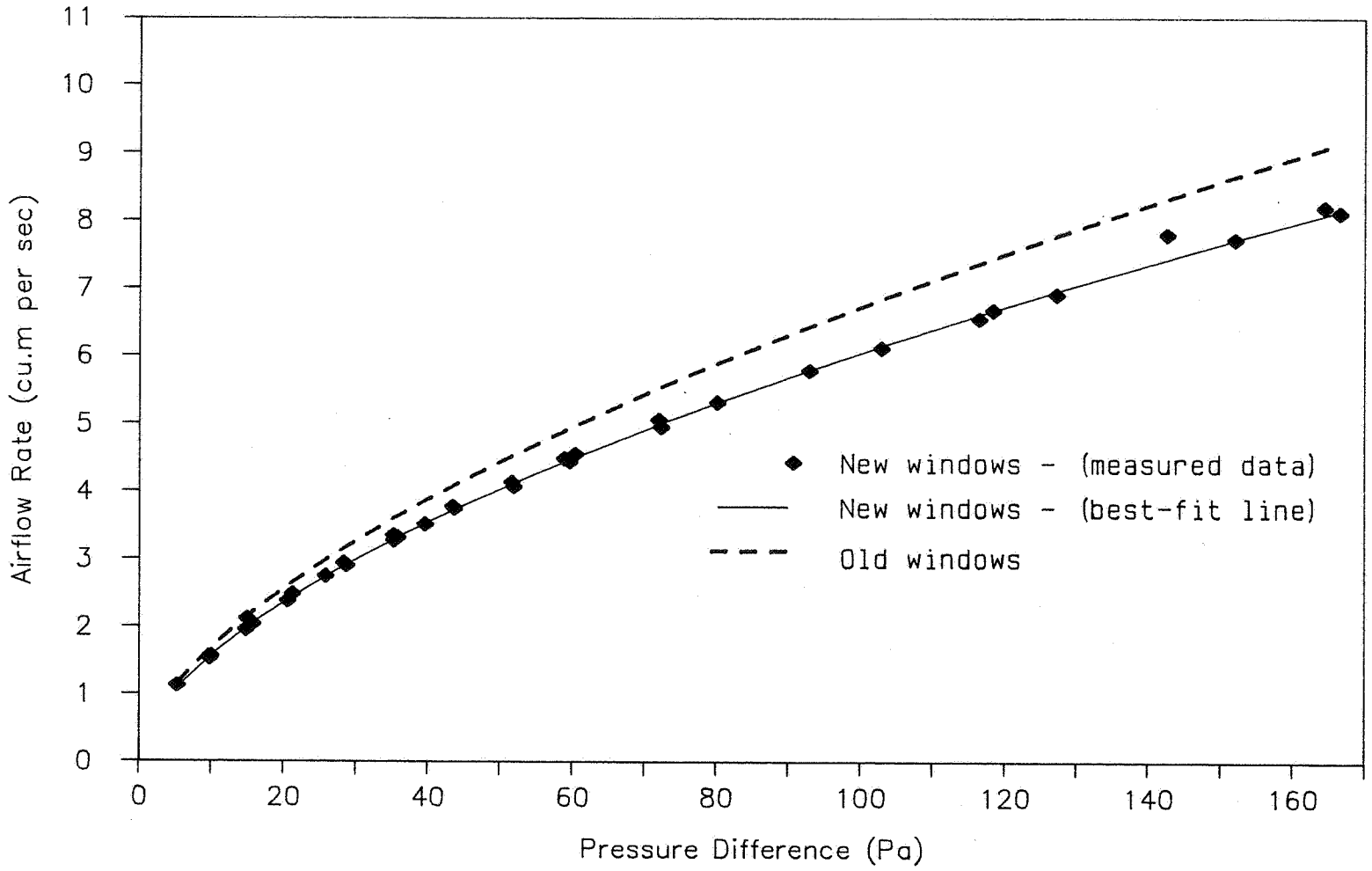

FIGURE 3 – Pressure tests in the low energy office (LEO) building

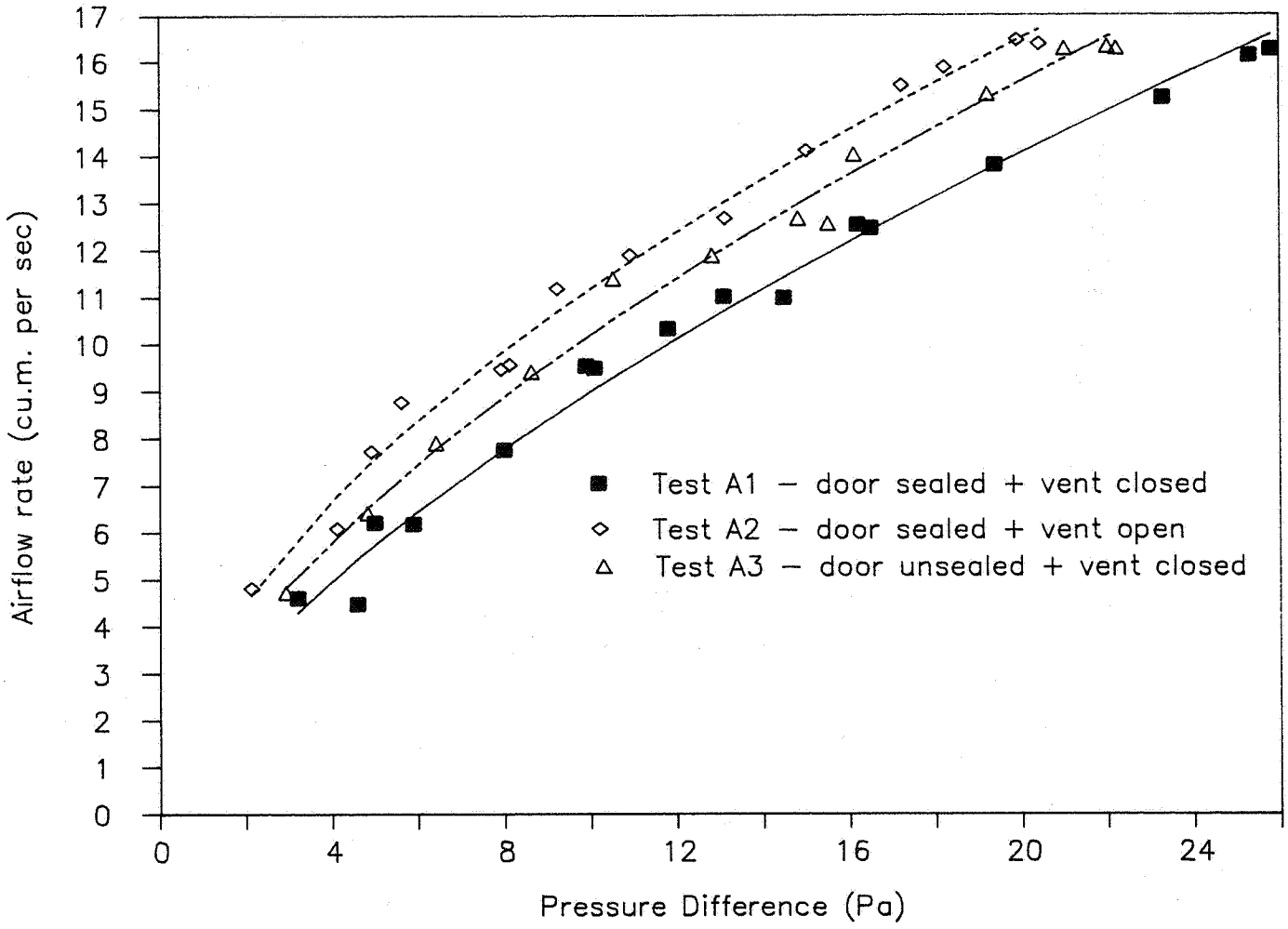

FIGURE 4 – Pressure tests in the hangar building

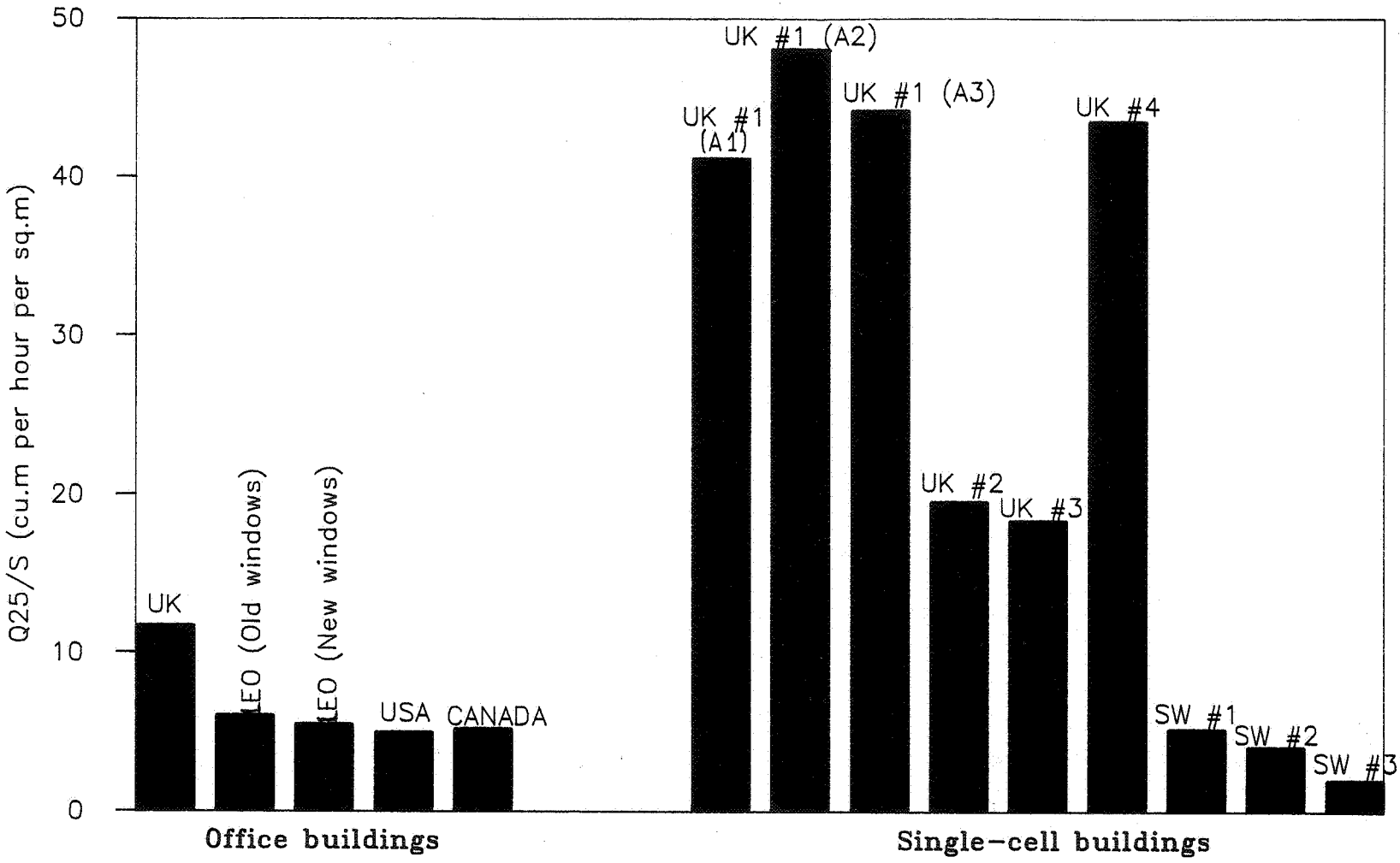

FIGURE 5 – Envelope leakage index of buildings

Discussion
Paper 22

J-M Fürbringer (EPFL, Lausanne, Switzerland)

a) In the measurements you present (pressurization) where do you measure the pressure difference across the envelope of the building?

b) You present results for 4 Pa pressure difference, but a wind of 3m/s can easily produce a higher pressure difference between leeward and windward side.

Earle Perera (Building Research Establishment, UK)

a) We measure both at ground level and also at an upper location - especially in a multi-storey office building. There is usually a measureable difference between the two (~ 4Pa) but results presented in the paper relate to difference measured at ground level.

b) Agreed, however measurements at the lower levels are carried out during calm periods - otherwise they are not used.

W. Raatschen (Dornier GmbH, Germany)

How did you get to the total permeability of the building or hangar?

Earle Perera (Building Research Establishment, UK)

A power law of the form $Q = k(P)n$ is fitted by the least squares method to the measured values of $Q(m^3/hr)$ and pressure difference $P(Pa)$. From this best fit law we compute the leakage rate at 25 Pa pressure difference as $Q25 = k(25)n$.

By studying dimensional drawings of the building we calculate the total external surface area $S(m^2)$ of the building envelope which was subjected to pressure differences and permeable to air flow. The permeability index of the building is then quoted as $Q25/S\ m^3/hr/m^2$.

PROGRESS AND TRENDS IN AIR INFILTRATION
AND VENTILATION RESEARCH

10th AIVC Conference, Dipoli, Finland
25-28 September, 1989

Paper 23

BUILDING DESIGN AND MAINTENANCE AND INDOOR AIR POLLUTION

R.H. Ferahian

Consulting Engineer
4998 de Maisonneuve Blvd #1416
Westmount
Quebec
Canada H3Z 1N2

SYNOPSIS

This paper examines some designs which lead to indoor air pollution and exhorts mandatory maintenance of all building services which determine the health and safety of the building occupants as an integral part of our city bylaws. Effect of poor maintenance of some of these systems on the indoor air quality is examined together with the effect of the interruption of the ventilation fans for energy conservation purposes, not always done legally. Among the examples considered are the effect of underground parking and its ventilation system, proximity of the fresh air intakes to exhausts of the building and/or adjacent buildings and the drains of the plumbing system. The author's denied appeals to ASHRAE committies regarding adotion of ASHRAE Standard 62-1981R, done to ensure that the ventilation fans are not turned off when such buildings are occuppied are discuused together with the City of Westmount's maintenance bylaw for apartment buildings adopted June 1989 which incorporates such a requirement. Our laws must ensure good air quality in our habitat as an environmental human right with the citizens' right of access to the information necessary to determine the quality of their indoor air environment for their health and safety. Examples from present Québec legislation are presented.

1. INTRODUCTION

This paper is a sequel to the author's summary[1],"Building Codes designed for ensuring good indoor air quality" presented at AIVC's 8th Anniversary Conference, an expanded and updated version of which was presented at the "Healthy Buildings '88" Conference held in Stockholm last year[2].

Naturally building codes can not encompass all the complex system of multi-disciplinary parameters that determine the indoor air quality in buildings, namely: quality of the outdoor air, percentage of the outdoor air in the ventilation air, design characteristics of the Heating, Ventilating, and Air Conditioning (HVAC) system structural and nonstructural materials used in the building, its furnishings, the use and activities within the building, and the age, maintenance and management characteristics of the building. Other bylaws and education must do their share to ensure good air quality indoors. And up-to-date codes are not much use if they are not respected or enforced. These papers[1,2] presented what the codes can and must do to guard against indoor air pollution.

That "Buildings like people can be sickly" and the "Sick Building Syndrome" has become a recognized and accepted fact is evidenced by its' recent coverage in the staid "The Economist"(May 13) in an article entitled "Architect, heal thyself." Therein, the "most radical building doctors" are reported recommending that "buildings should be designed for the people who work in them not for developers or design awards". To qualify as "most radical" such a requirement is most revealing. More often than not the architect considers

the office building as an investment for his client. Maximizing profits would require maximizing the rental floor area thus dictating as limited as possible vertical and horizontal space be allocated to the HVAC system. Such restrictions do not lead to the best HVAC systems and can lead to minimum seperation, if that, between the building's air intakes and exhausts & possibly contamination of the fresh air intakes[3,4].

Grant it, healthy buildings with spacious, well lit and well ventilated offices, preferably with openable windows, do cost more money than the conventional, sealed rectangular boxes we call our work place. But the health and welfare of the building users throughout the life-time of the building and its maintenance ought to be considered in the cost analysis of the building at the design stage. And advertised as such, because healthy buildings improve productivity of their users and that can save their employers more than the additional cost of the building. Judging by the response to the Healthy Buildings Conference in Stockholm last year[1] and in London, as noted in The Economist article cited, earlier this year, there is increasing realisation that such buildings are good business too.

Building codes and ASHRAE Ventilation Standards are deemed to apply only to the design and construction of the building but not its maintenance[1,2,4,5]. Ironic indeed, considering the building codes and the ventilation standards have their very raison-d'être in protecting the heallth safety and welfare of the building users. Many indoor air pollution problems arise from the bad maintenance of the essential building services especially the HVAC system. That is why the author has been advocating since 1981 that good maintenance of such services ought to be an integral part of our building codes and city bylaws[6]. This is among the major areas of emphasis in this paper, introducing the relevant clauses of Westmount's such bylaw[7].

It is apropos to mention here that concurrently with our conference, "Building Pathology 89" Conference is taking place at Trinity College, Oxford. According to its advertising pamphlet, it is the first international scientific conference on the inter-relationship of the building structure and materials with their environments and the living organisms within them concentrating on the environmental control of biodeterioration in building materials and aspects of the building environment affecting the health of the occupants". Thus although some aspects of building pathology were known to certain specialists, it is only now that the first such multidisciplinary scientific study of building performance inorder to improve design is taking place. There is still much to do to reap the benefits in practice.

2. BUILDING DESIGN AND INDOOR AIR POLLUTION

The Sick Building Syndrome is sometimes called "OPEC's Revenge" by those who believe it is mainly the result of our buildings being built increasingly more airtight than before to prevent heat loss through air infiltration and thus saving fuel costs. But the matter is even worse because this trend was accompanied by a reduct-

ion of the fresh air intake in the ventilation requirements when ASHRAE Standard 62-81 replaced ASHRAE Standard 62-73, a trend strongly objected to by the author[1,2,4-6] and reversed with the recent adoption of ASHRAE Standard 62-1981R. Thus under these circumstances, it was more important than ever before that the fresh air intake be really that, an indispensable first step.

2.1 Contamination of the Fresh Air Intake

Short-circuiting contamination of the fresh air intakes with exhausts of the building or adjacent buildings or contamination of the fresh air intakes due to their badly chosen locations, warned against in most codes[8-10] is more common cause of indoor air pollution than is suspected or admitted. Yet, as noted for one in the author's earlier paper[1], many papers on indoor air quality in buildings with prolonged complaints from the occupants, information is lacking on the location of the fresh air intakes and exhausts of the building and the nature of the exhausts. This is especially important in hospitals and university medical, science or other buildings where exhausts from research laboratories or other rooms may contain toxic chemicals and/or microbes or viruses not to mention organic or inorganic wastes' emanations.

Aerodynamic interaction of winds with the building may cause such contamination of the fresh air intakes with the exhausts under unfavourable atmospheric conditions-is not specifically warned against in the codes and needs to be. Earlier this year in the Feb-1st, The McGill Reporter published by the McGill University Relations Office, in an article,"Making the McIntyre Medical Building Well Again- Complaints finally bear fruit", it was reported this building occasionally suffers from this phenomenon during "air inversions" peculiar to Montreal because the site being next to the mountain, downward wind around the building brings exhausted air back through the air intakes. The article also noted that the same problem was so severe at the Stewart Biology Building that its exhaust stacks were recently extended to increase the distance between them and the air intakes, adding that the feasibility of doing the same for the McIntyre building was still being studied.

A critical analysis of this cause of indoor air pollution and requirements of the Canadian and ASHRAE Standards is given elsewhere[3,4]. Important buildings like the ones noted above especially at sites near mountains or downtown surrounded by other buildings would greatly benefit from model testing in boundary layer wind tunnels to determine the optimum design of their fresh air intake and exhausts and their locations[3]. An example of such testing to determine air infiltration in multi-storey buildings was given elsewhere[11]. Such tests could also give additional information for more economical structural design for the wind loads and the savings could well pay for the tests, if not more over the lifetime of the building.

Buildings housing PCB-filled transformers and/or capacitors. For such buildings as already noted ealier[1], contamination of the fresh intakes with the exhausts takes a special dimension of urgency when

the exhaust is from an area housing PCB-filled transformers and/or capacitors, because in case of a fire due to incomplete combustion of the PCBs, dioxins and furans are produced among which are some of the most toxic compounds created by man. Recent examples and recommendations are give elsewhere[4]. Suffice it to mention here that the sooner they are removed from our buildings the better as the total cost of fires involving such units can be catastrophic especially if they occurred when such buildings were occuppied. For the now famous 1981 Binghampton, N.Y. fire, the cost of the cleanup and rennovations for the building - still unfinished- is almost three times the original $17 million cost of the building- still higher than reported last[2]. Fortunately, that building was unoccuppied at the time of the fire. How often can we be as lucky as that?

For this section, the following example is apropos. The building, to be refered to later on[2-6], is an air conditioned 16-storey office apartment complex built in the midsixties with three levels of underground parking and capped with rooftop mechanical room, laundry room and swimming pool. The "Bylaw Concerning Health and Sanitation in Buildings" governing the design of buildings then, and operative till 1987 when updated[1,2], for the City of Westmount, Québec, Canada where the building is located, stipulated,

> "All air sources for ventilating purposes shall be drawn from the exterior of the building, any intake being so located that the air entering the system will contain no more bacteria, dust, odors, toxic substances or moisture than the normal exterior air for the locality in which the building is situaited."

But one fresh air intake of the building was located practically immediately adjacent to the kitchen exhaust of a public restaurant in the complex and the ventilation pit of the garage levels which also was the recipient of the exhaust from the electrical room, on the second garage level, housing a PCB-filled transformer and four capacitors. Moreover the building overhang of about 1½ metres covered the restaurant kitchen exhaust and the fresh air intake, the centre of which was within 6 metres from where the building's garbage was collected. To boot, this fresh air intake was next to the loading backdoor where trucks used to idol, for one, collecting the garbage thus additionally contaminating the fresh air intake with their exhausts. The restaurant was closed in 1980. This has been used as a classical example[2-6] where not to put a fresh air intake.

2.2 Underground Garages as Air Pollution Sources

That pollutants generated by automobiles can infiltrate into the floors above the underground garages through the stairwells and the elevator shafts of the building is well known. Often they are among the contributers to the sick building syndrome as noted in the examples given elsewhere[12], where levels of Carbon Monoxide as much as ten times the outdoor ambient levels and well above the accepted norms had been recorded. And Carbon Monoxide is not the only toxic pollutant generated in car exhausts!

That is why it is imperative that the garage ventilation system efficiently and continuously ventilate the pollutants to the out-

side. Not only for the automobile exhausts but also because the underground levels, depending on the site, if the basement floors and walls are not properly designed, can be traps for radon and its progeny,infiltrating from the foundation soils, whose levels must be kept through ventilation to the outside to acceptable minimum levels[1,2,13]. Exhausts from garages ought to be as far removed from fresh air intakes of buildings as possible to ensure against contamination and indoor air pollution.

For the building quoted as an example in the preceding section, alterations were carried out to improve indoor air quality[2,4]. For one, all the ventilation pits were fitted with metallic caps that had flow grills in the vertical plane in compliance with the building code. For the specific garage ventilation exhaust pit mentioned there, a further improvement was effected when its cap was replaced with another whose exhaust grill was so oriented so as to be the furthest from the fresh air intake. This latter change came after the author's official application under Québec's Access to Information Act to examine the engineering drawings of the building's ventilation system to determine the locale of the fresh air intakes and exhausts,including their nature, of the building - and some months after the event described below.

Careless Construction and Inadequate Inspections can also lead to indoor air problems and even deaths. Complaints from the offices on the second floor of the building mentioned above with the occupants of one taken to hospital because of dizziness and nausea and the Westmount's Firemen's measurements of high levels of Carbon Monoxide (CO) lead to evacuation of the offices till the CO levels had subsided to acceptable levels that same day. The blood tests of the persons affected had also confirmed the CO exposure. It was reported that an unblocked opening in the concrete structure had provided direct access of the CO from the garage ramp to the offices. The fatal potential for such carelessness can not be overemphasized. How often and for how long had the occupants of these offices been sufferring ill-health and malaise due to this carelessness till its correction?

Faulty Design and/or Poor Maintenance of Systems other than the HVAC System can be the cause of serious and even catastrophic indoor air pollution. While on the subject of pollution emenating from garages two further examples are apropos. Until the middle of last year, the Saturday test runs of the diesel-fueled emergency generator caused fumes to infiltrate the underground garage area of the same building and its ventilation system because of bad maintenance and- as was found by the fire inspectors after a power outage then- faulty design. The garage ventilation fans were not connected to the emergency generator.

Another example concerns uncorrected water leaks due to faulty design and/or poor maintenance that lead to short-circuiting fires in circuit breakers housing PCB-cooled transformers, for example, with potentially catastrophic consequences as noted earlier.

3. ENERGY CONSERVATION AND INDOOR AIR QUALITY

The strong objections to the energy conservation measures in our buildings presented earlier at the start of section on building design and indoor air pollution and voiced for long now by the author[1-6] need not be repeated here. This was accompanied by objections to outdated building codes[1,2,4-6] and inaction of the author's City to act against the shut-off of the ventilation fans at night in his apartment building based on the premis- never accepted by the author- that the City's relevant bylaw governing ventilation was for design and construction but not maintenance of the building[4-5,1-2].

That these strong objections bore fruit is evident because now the City of Westmount has one of the most up-to-date building design and construction bylaws[14] and also maintenance bylaw for apartment buildings[7] which prohibit such ventilation fan shut-off. Also with the adoption of ASHRAE Standard 62-1981R, the trend towards reducing the fresh air intake in our buildings has been reversed as this Standard has gone back to requiring mean values of the recommended outdoor air intake specified in ASHRAE 62-73. In this latter, for offices,for example, the minimum outdoor air intake was specified as 7½ L/sec.person, it was reduced in ASHRAE 62-81 to 2½ L/sec.person when no smoking was observed even though that standard had noted that the "supply of outdoor air shall never be less than 2.5 L/sec.person" because this was "supply of the outdoor air necessary to dilute the CO_2 produced by metabolism and expired by the lungs". In Scandinavia and W. Germany such low fresh air intakes as 2.5 L/sec.person were not even contemplated on basis of preserving Acceptable odour conditions[5].

It appears that the battle cry of the seventies- "Energy Conservation is the moral equivalent of war" was taken too literally as horror stories abound. For one, ventilation fans are sometimes turned-off under the guise of energy conservation to cover up malfunctions in the HVAC system and/or poor maintenance such as inadequate temperature control at peak loads[1-3,5,6]. The two following horror stories, the first in the U.S. and the second in Canada illustrate its geographic scope and democratic strike:

The first occurred in Birmingham, Alabama in a three storey office building with non-openable windows. After continued health complaints from the occupants, investigations revealed "to conserve utility costs the building owner had elected not to install outside make-up air ducts on the building's HVAC system" without having contravened the local building bylaws![15] Unfortunately, not all cities in the U.S. require compliance with the most recent ASHRAE recommendations, if at all. Private enterprise or criminal negligence?

The second as reported by the April 1987 issue of "Québec Science" in an article entitled "Ces Immeubles Qui Nous Etouffent", hit no less than the offices of the Prime Minister of Québec in 1985. Apparently then, smell of "latrines" filled these offices to the embarrasement of the occupants. For a month and in vain, the search

went on in vain for the source of the emanations. Finally, an inspector was called in from'Commission de la santé et sécurité au travail' and a major fault in the ventilation system was identified:the fresh air intake was practically nil. Previously where the fresh air met the exhaust air, a drain pipe had been installed to discharge the resultant water condensation through a double-goose neck "S" connection into the sewers ("vers les égouts"). The "S" neck connection was to prevent the odours feeding back indoors. This worked as long as there was enough condensation flowing through the drain pipe to fill the"S" neck. But as there has been practically no fresh air intake, the water in the "S" neck had dried up, and thus a free passage had been produced for the unwelcome odours not to mention the pollution into the Prime Minister's offices!

3.1 SWITCH-OFF OF THE VENTILATION FANS

Complaints to the City of Westmount in November 1985 concerning turning off at night till the early hours of the morning the exhaust fans servicing the bathrooms and also the air intake fans servicing the public corridors-and thus the apartments-for the apartment-office complex discussed earlier, revealed that the City's then applicable 'Bylaw concerning Health and Sanitation in Buildings'"are complied with when the ventilation equipment having certain capacity is installed in the premises in question"- but that the "Bylaw regulates design rather than maintenance".

On January 20th, 1988, this switch-off of the fans was brought up by the author at the Québec Rental Board- Regie du logement- as being detrimental to the health and safety of the occupants and in contravention of the provisions of Québec's Act respecting the conservation of energy in buildings[16], where it is clearly specified that the reduction in the ventilation requirements shall be allowed only when the building is not occuppied. Thus according to this regulation which is based generally on the provision of ASHRAE Standard 90 "Energy Conservation in New Building Design" and the minimum ventilation requirements of ASHRAE 62-1981[9], while the fans' shut-off could be acceptable for the first five office floors, it is not for the top eleven apartment floors, especially at night when all the tenants are sleeping.

The fans were not turned back on 24 hours a day till February 3rd 1988 that being two days before a hearing at Québec's Commission d'accès à 1'information where the author was contesting the City's decision to deny him access- in compliance with the building's owner's instructions- to the reports based on which the daily schedule of the fans' shut-off was approved.

At that hearing however, the City's Director of Services claimed that they did not have "the" reports in question but "a" report - comprising of extracts of the reports-supplied to them by the owner of the building. The Commission accepted the City's claim and after a further hearing and almost a year after the first,the Commission ruled in may favour indicating that the documents sought were not proprietory technical information but proof of compliance with the relevant Bylaws. But the extracts received showed results of CO

and CO_2 measurements prior the period of the fan switch-off! These two pages of measurements were CO records of less than 2 ppm for the second floor offices referred to earlier in section 2.2 & after that CO-scare-evacuation described therein. The second sheet showed CO and CO_2 measurements for "Etages résidentiels" and"Air extérieur" for another day:with the CO levels given as a stark zero and and 1-2 ppm respectively and the CO_2 levels given as 400 and 300ppm respectively without giving information as to where exactly they were measured nor the duration of the sample. Thus it is hard to imagine how based on this scant information the shut-off of the fans at night as described earlier was allowed for more than two years in the apartment building!

Westmount's Bylaw 1031[7] Concerning Safety and Sanitation in Apartment Buildings adopted June 19, 1989 specifies that the "ventilation system(s) in such apartment buildings is (are) maintained in good working order and is (are) in operation at all times". One wonders why it was not inacted years earlier when asked for by the author? But this still leaves office workers unprotected. The City officials noted that under Québec Cities and Towns Act, the City Council is not empowered to apply the same law to office buildings!

The effect of interrupting ventilation fans is not well known and, even less, documented[1,2,5,6]. Both ASHRAE 62-1981 & ASHRAE 62-1981R provide guidance for interrupting the use of the outdoor air when the buildings are used intermitently. The nature of the contaminants must be known. If they are result of outgassing of material or other sources within the building, it must be ventilated prior to occupancy. How often is there recorded reliable proof that the ventilation fans' switch-off after business hours has not compromised the indoor air quality on return of building occupants?

Appeal to ASHRAE: Following his presentation at the IAQ 86 Conference in Atlanta Georgia[4] and based on his bitter experience with the ventilation fans' switch-off in his building, on Dec.3,1986, the author recommended on the official"Form For Commentary"on the Proposed ASHRAE 62-1981R that "the outdoor air requirements specified therein be qualified as continuous supply when the tennants and /or building users are therein. And that the ventilation fans be maintained and operated capable of this need". Contrary to expected and inspite of my subsequent letters for response, I did not get it till June 5, 1988 and then to be informed by Mr. John E. Janssen, Chairman of SPC 62-1981R that my request will be reported as "an unresolved issue". My appeal against publication of the Standard without such a qualification was denied by both the Standards Committee and the Board of Directors Appeal Panel on the grounds that, "There is no indication that that any ASHRAE Standards' Committee Procedures were violated" and this was finally confirmed by the vote of the BOD on June 25, 1989, even though on "substantive grounds" there was good reason behind my appeal.

4. BAD MAINTENANCE AND INDOOR AIR POLLUTION

The author has for long advocated the need for maintenance bylaws to ensure the good maintenance of all essential building services

necessary for the health, safety and wellbeing of the tenants and/or users of our buildings[1-6]. The new Westmount maintenance bylaw[7] for apartment buildings ensures that they are maintained "in a clean and sanitary condition at all times" including as presented earlier that the ventilation system be in operation at all times. Inadequate maintenance and nonchalant attitude of some building managers regarding the needed good air quality can be a serious cause of indoor air pollution. In the early eighties, the ventilation of the corridors supplying the apartments in the building referred to earlier was often swictched off for several weeks, due to among others, inadequate temperature control and chemical smells caused mainly by a defective oil-fired boiler whose exhausts on the roof also contaminated the fresh air intake there under unfavourable winds[1,2,6].

Legionaire's disease and humidifier fever are well known now. It was only recently,however,that a conference was convened to treat the maladies caused by poor maintenance of air-conditioners and humidifiers[17].

Other examples are not well known as noted elsewhere[1,2] and the examples given here. A badly maintained swimming pool, especially one on the roof of a building, or an incorrectly designed and/or badly maintained plumbing systems- witness the experiences in 1985 in the offices of the Prime Minister of Québec- can result in serious problems. Water leaks can become host to algae and fungal growth in places unknown to the tenants but that effect their indoor air quality and health and even lead to deaths. So can badly maintained saunas or poor drainage of roofs cause such growths in partition walls, among others. And if such microorganisms are carried by the ventilation system other areas can be affected.

Infact, it is only recently that the consequences of these microorganisms on our indoor air have received the inter-disciplinary examination needed in order to improve building design[18]- witness, for one, my comments on the"Building Pathology 89" Conference in the introduction. An extensive study on mycotoxins and extreme fatigue syndrome for St. François d'Assise hospital in Québec City is given elsewhere[19]. But no doubt good building design and good maintenance of,among others, the HVAC system is a first essential to "Healthy Buildings".

5. ACCESS TO INFORMATION ON VENTILATION SYSTEMS

In order to determine the locale of the fresh air intakes and the exhausts of the building referred to in the examples earlier, the owners were subpoenaed three times in 1979 by the Québec Rental Board to bring the relevant engineering drawings,but they were not. In 1985, the author tried again this time through Québec's "Commission d'accès à l'information" after the City of Westmount denied the access on the premis that the owner's permission was not granted. The Commission in a 16 page June 6,1986 ruling concurred with the city's decision noting that its governing "Act respecting access to documents held by public bodies and the protection of personal information" takes no account of the applicant's status, as a tenant that is, and that these drawings being"technical information

supplied by a third person and ordinarily treated by a third person as confidential" can not be released"without his consent" unless the information"reveals the existence of an immediate hazard to the health or safety of persons or a serious or irreperable impediment to their right to a healthy environment". Our present laws are heavily lopesided towards protecting the rights of property owners and the permit granting cities vis à vis the tennants' environmental right to know[5,2].

The Commission interpreted "immediate hazard" as excluding- to my strong objections- potential and probable ones. When the author had countered that such interpretation would even exclude the risk of earthquakes even though the National Building Code requires design for them, the retort was that that was outside the expertise of the Commission. Moreover,that interpretation also excluded immediate risk whose cummulative effects over time could cause "serious or irreparable impediment". Why should demonstartion of only"irreparable" impediment to one's right to a healthy environment be required for relaease of the information sought?(And let it not be forgotten that the Act grants access to only "documents held", which may not contain - even by design- the information sought.) How many"reparable" environmental damages can our physical and social systems withstand? And how is this "reparable" damage defined? Prudence - and yes humility- pays multifold in the long run in environmental protection and our laws must reflect it.

Thus the Act's "right to a healthy environment" must include the citizens' "right to know" about contaminations in their habitat and the tenant's right to know about the design and operation of the building systems that determine his health and well-being, including information necessary- not just any conjured-up documents to comply with the word but not the spirit of the law- to determine the acceptability and legality of the energy conservation measures that affect his indoor air environment. Such were the author's arguments presented in his brief[20] submitted to Québec's legislative Committee examining the Access-to-Information Act's mandate.

6. CONCLUSIONS

After the bombing of the House of Commons in 1943, Sir Winston Churchill urging that the Chambers be rebuilt exactly as they were before,because their physical characteristics have formed the very structure of British democracy, dramatically noted, "We shape our buildings, and afterwards our buildings shape us". Yes indeed. Some of our buildings are making us sick now. Not only architect, but also law maker heal thyself! The jurisdiction of our Clean Air Acts must be extended to cover the air indoors which may often be more polluted than that outdoors. And good maintenance of the building systems that determine the health and safety of the occupants must be mandatory part of our codes and part of the initial planning and dessign of buildings.[21]

7. ACKNOWLEDGEMENT

The author gratefully acknowledges that this paper incorporates, expands, and updates parts of his earlier paper given in ref. (2).

REFERENCES

1. FERAHIAN, R.H.
"Building codes designed for ensuring good indoor air quality" Proceedings of the 8th AIVC Conference, Ventilation Technology Research and Application, Uberlingen, Federal Republic of Germany Publishers- Air Infiltration Centre, Bracknell, G.B.,1987, pp. 23.1 - 23.6.

2. FERAHIAN, R.H.
"Building codes designed for ensuring good indoor air quality" Proceedings of the "Healthy Buildings '88" Conference, Volume 3, Systems, Materials and Policies for Healthier Indoor Air, Published by Swedish Council for Building Research, Stockholm, 1988 pp. 671-678.

3. FERAHIAN, R.H.
"Indoor air pollution caused by short-circuiting of fresh air intakes with exhausts of buildings". Proceedings of CLIMA 2000 World Congress on Heating, Ventilating and Air Conditioning, Vol.4, Indoor Climate, VVS Kongres-VVS Messe, Copenhagen, 1985 pp. 307-312.

4. FERAHIAN, R.H.
"Contravention of Building Bylaws for HVAC systems and bad maintenance as causes of indoor air pollution". Managing Indoor Air for Health and Energy Conservation- Proceedings of ASHRAE-IAQ 86 Conference, ASHRAE, Atlanta, Georgia, 1986, pp.251-257.

5. FERAHIAN, R.H.
"Violation of Building Bylaws, energy conservation and bad maintenance as causes of indoor air pollution". Proceedings of the 4th International Conference on Indoor Air Quality and Climate, Institute of Water, Soil and Air Hygiene, Berlin, 1987,pp.23.1 to 23.6.

6. FERAHIAN, R.H.
"Indoor Air Pollution - Some Canadian Experiences" Proceedings of the Third International Conference on Indoor Air Quality and Climate, Volume 1, Recent Advances in Health Sciences and Technology, Swedish Council for Building Research, Stockholm, 1984, pp. 207-212.

7. City of Westmount, Bylaw 1031, "Bylaw Concerning Safety and Sanitation in Apartment Buildings", adopted June 19, 1989.

8. ASHRAE Standard 62-73, "Standard for Natural and Mechanical Ventilation", American Society for Heating, Refrigerating and Air Conditioning Engineers, Inc. Atlanta, Georgia 1973.

9. ASHRAE Standard 62-81, "Ventilation for Acceptable Indoor Air Quality", ASHRAE, Atlanta, Georgia, 1981

10. ASHRAE Standard 62- 1981R, "Ventilation for Acceptable Indoor Air Quality", ASHRAE, Atlanta, Georgia, adopted June 25, 1989.

11. GRABAU, P. and DAVENPORT, A.G.
"Estimstion of Air Infiltration in multi-storey buildings using wind tunnel tests", Supplement to Proceedings of the 8th AIVC Conference, Ventilation Technology Research and Application, Uberlingen, Federal Republic of Germany, Publishers- Air Infiltration and Ventilation Centre, Bracknell, G.B.,1987,pp.81-93.

12. STERLING, E.M., McINTYRE, E.D., COLLETT, C.W., STRELING, T.D. and MEREDITH, J.
"SICK BUILDINGS: Case studies of Tight Building Syndrome and Indoor Air Quality Investigations in Modern Office Buildings", Environmental Health Review, September 1985, pp. 11-19.

13. U.S. Department of Energy,
"Indoor Air Quality Environmental Information Handbook:Radon. January 1986, U.S. D.O.E. Washington, D.C. U.S.A.

14. City of Westmount,
"Bylaw 994 Concerning Building and Building Construction", Westmount, Québec, Canada 1985.

15. SALISBURY, S.A.,
"Measuring Carbon Dioxide levels as indicator of poor building ventilation: a case study.", Proceedings of the ASHRAE IAQ 86 Conference- Managing Indoor Air for Health and Energy Conservation, ASHRAE, Atlanta, Georgia, 1986, pp.78-82.

16. Government of Québec,
"Regulation respecting energy conservation in new buildings" Order in Council 89-83, 19 January 1983, 117 Gazette Officiel of Québec 2, 775.

17. MOLINA, C., Editor
"Maladies des Climatiseurs et des Humidificateurs- Humidifiers and Air-Conditioners Diseases", Editions INSERM (Institut National de la Santé et de la Recherche Medicale), Paris 1986.

18. Health and Welfare Canada:Working Group on Fungi and Indoor Air.
"Significance of Fungi in Indoor Air", Special Supplement, Canadian Journal of Public Health, Vol. 78, March/April 1987,S1-32

19. MANVILLE, C., AUGER, P.L., SMORAGIEWICZ, W., NECULCEA, D., NECULCEA, J., and LEVESQUE, M.,
"Mycotoxines et Syndrome d'extreme fatigue dans un hôpital" Proceedings of the "Healthy Buildings '88" Conference, Vol. 2, Planning, Physics and Climate Technology for Healthier Buildings, Swedish Council for Building Research, Stockholm 1988, pp. 309-317.

20. FERAHIAN, R.H.
"In Search of Access-to-Information Act", Brief submitted on Feb. 26, 1988 to Committee on Culture,Québec National Assembley.

21. FERAHIAN, R.H., Letter to The Economist in response to its article "Architect, heal thyself" of its May 13, 1989 issue.

PROGRESS AND TRENDS IN AIR INFILTRATION AND VENTILATION RESEARCH

10th AIVC Conference, Dipoli, Finland
25-28 September, 1989

Paper 24

A PERSPECTIVE ON THE AIVC

Willem F. de GIDS

MT-TNO
P.O. Box 217
2600AE Delft
The Netherlands

1. Introduction

The AIVC nowadays is an established "Centre" on infiltration and ventilation research. It is well known throughout the world. This position has not been reached easily. But years of hard working and critical managing of the Centre was a necessity. The Centre, operating agent, staff and steering group, has to think about the future. Resting on your wings is dangerous and finally will lead to abolition.
The question is:
What can a centre like this really mean for society in the future ?
To answer this question one has to go back in time and follow the developments till to day.

2. Past and present

2.1 Past

The centre has started as a result of discussions in the energy load calculation annex (Annex1) about the role of infiltration in the energy load of a building.
The specialists at that time did use codes mostly taking into account a constant ventilation rate. Infiltration was in most cases not taken into account. Many comparisons of measured and calculated data failed.
The specialists at that time thought that infiltration was an important missing factor. From that moment on a group of experts in infiltration started to discuss about the level of knowledge on infiltration processes in buildings.
They recognized big differences in the knowledge and understanding in the different countries. One country had a lot of experimental work done, while others did more on explaining the process of infiltration. They found many aspects on which infiltration was based where data and knowledge was missing.
The conclusion was that answering the question on energy load of infiltration could only be attacked by a close internatinal cooperation. And after some time of preperation the Centre was inaugurated.

Eight countries (U.K., U.S.A, Denmark, Sweden, Italy, Switzerland, Canada and the Netherlands) from 1979 on worked together in a joint funded project.
The main objectives of the Centre were very roughly summerized:

- gathering all available published work
- evaluation of that work
- stimulate new research
- disseminate information.

The means to reach the goals were:

- production of technical notes
- producing handbooks
- distribution of a newsletter (Air Infiltration Review)
- organisation of conferences and workshops.

A staff of about five people was trying to reach the goals. They were guided by a steering group, while the operating agent was managing all administrative and financial aspects.
To give some examples of the results:

- Yearly conferences with published proceedings
- Handbook Air Infiltration Control in Housing
- Air Infiltration Calculation Techniques Guide
- Air Exchange Rate and Air Tightness Measurement Techniques Guide
- Technical notes:
  * Air infiltration Glossary
  * Validation and Comparison of Mathematical Models
  * Windpressure Data
  * Ventilation Strategy
  * Survey of Current Research
  * Airborne Moisture Transfer
  * Standards on Ventilation and Air Tightness

The aim to improve the understanding of the complex air infiltration processes and at the same time reduce infiltration in buildings became a reality.
The success of the Centre was there.

2.2 Present

Many countries then began to realize that not being a member of this centre became a problem. They did not get all the avaivlable knowledge. Moreover the member countries made a lot of progress due to internatinal cooperation in research and in the application of it. Five new countries became member of the centre.
At this moment the Centre is funded by thirteen member countries. West Germany, Finland, Norway, Belgium and New Zealand joint the centre since the inauguration as members. There are a few countries at this moment interested to become a member of the centre, for instance France and Japan.
The role and work of the centre was not "steady state" but can be described as "dynamic". After some years focussing on infiltration the scope was broadened to ventilation.
The centre got its present name:
Air Infiltration and Ventilation Centre.
Since a few years the air transport related indoor air quality and comfort aspects became part of the workprogram of the centre. Also the flow in the room and efficient ways of ventilation and removal of contaminants needed to be studied.
The scope of the centre is growing and becomes wider.
Some other annexes had finished their work. Interesting results had to be published. The centre could easily carry out this type of work because of their experience in writing technical notes. The summary report of "Inhabitants behaviour with regard to ventilation" was published by AIVC.

Some new technical notes:

* Multizone Simulation Study
* Building Air Flow Simulation
* Air Change Efficiency
* Infiltration and Ventilation/ Comfort and Indoor Air Quality
* COMIS Fundamentals

are planned to be published in the near future.

The work-power of the centre is at this moment about seven people. New is that people from other countries come to the centre to work there on special items for several months. This is an old wish which becomes reality at this moment. This is a new way to improve international cooperation.

3. Perspective

Past and present may be seen as successful international cooperation between countries in the centre.
The real question for the members of AIVC is :
What new facts can we deliver as a result of our work to the society. Moreover, is the money invested to reach that available and well spend.
One has to realize that there is more than infiltration and ventilation research. The enourmes environmental problems in the world put also a pressure on us. We have to consider our contribution on solutions. Taking that as a starting point for our perspective, it seems to me that a variety of new items comes to us.
The importance of infiltration and ventilation as a key parameter for indoor air quality and comfort must be our motivation to undertake new projects. Specially where the interaction between other specialists play an important role. Interdisciplinery work has to be undertaken.
Hygienists, medical doctors, designers of new building and installations need our special attention.
Infiltration and ventilation must be a normal partition in the education of all types of professions. We still have a lot of existing knowledge which did not really found their way to practice.
On the other hand new research has to be started. There are still questions which cannot be answered with the existing knowledge.
For instance the questions :

- What is the overal exposure of a housewife, a young child, an elderly due to typical indoor air pollutants during their stay in our existing housing stock.

-What effect can infiltration and ventilation have on that exposure.
-Can we improve our ventilation systems in that way that a positive effect of it can be reached.

The questions given have to do with indoor air quality. But at the same time we cannot have the situation that we waste energy and moreover are misusing energy and put an extra burden on the quality of our outdoor environment.
From that standpoint one can easily see new investigations for our future.
To give answers on the questions mentioned above, we need tools te evaluate situations in buildings. This tools will be mainly models. To be more specific, my opinion is that there will be a need for all kind of models coupled to eachother.
Our models are far from adequate to answer all questions.

Some items which need to be studied :

-The interaction between multizone flow and room air flow. Specially when the connection between the two is a large opening ore even large openings. The flow through large openings (for instance the turbulence effects) is not quit well known and play on the other hand an important role in the transport of pollutants through the building.

-The existing models must have the possibility to communicate with eachother. Again the flow over large openings is highly dependent on the temperature difference. If this will be only estimated in the ventilation models, we might miss a good insight in this effect.

-Input data such as pressure coefficients and air leakage data need to be gathered and studied. The availability of it must be in the form of data- bases.

-Absorption, desorption, condensation etc. are factors who strongly influence the pollutant levels in the rooms. Data from experiments is lacking at this moment. Models has to be modified on this point

-The behaviour of occupants need to be studied in more detail than till now. Occupants spent their time in different rooms. They have a significant influence on the production of some pollutants and they are the predominant factor in the proper use of the ventilation systems.

-Development of good design procedures controlling infiltration to minimize the use of energy is still not a fulfilled item.

-The development of ventilation strategies depending on building style, behaviour, local circumstances like weather and concentrations of pollutants ouside the building is necessary.

-Since energy is not any longer an economic but also an ecologic factor, we have the task to develop new ventilation systems which also for the transport of air use the real minimum of energy. Better fan efficiencies, grids and ductwork with lower pressure losses, better control systems need to be developed.

4. Conclusions

Looking to the past we can conclude that the centre has fulfilled a very positive role in the internatinal cooperation on infiltration and ventilation research.
We have made good progress, the centre is running well, but we have to be carefull not to be apathic.
The centre must try to achieve a permanent position in the dissemination of results in the field of infiltration, ventilation, air transport related aspects of indoor air quality and indoor environment.
The centre must play a major role in initiating new research on items which are important to answer questions for the future.
The means they use at this moment are adequate to reach that goals.
The groups to be reached need to be wider than the group of infiltration and ventilation research people.